Understanding Satellite Navigation

Second Edition

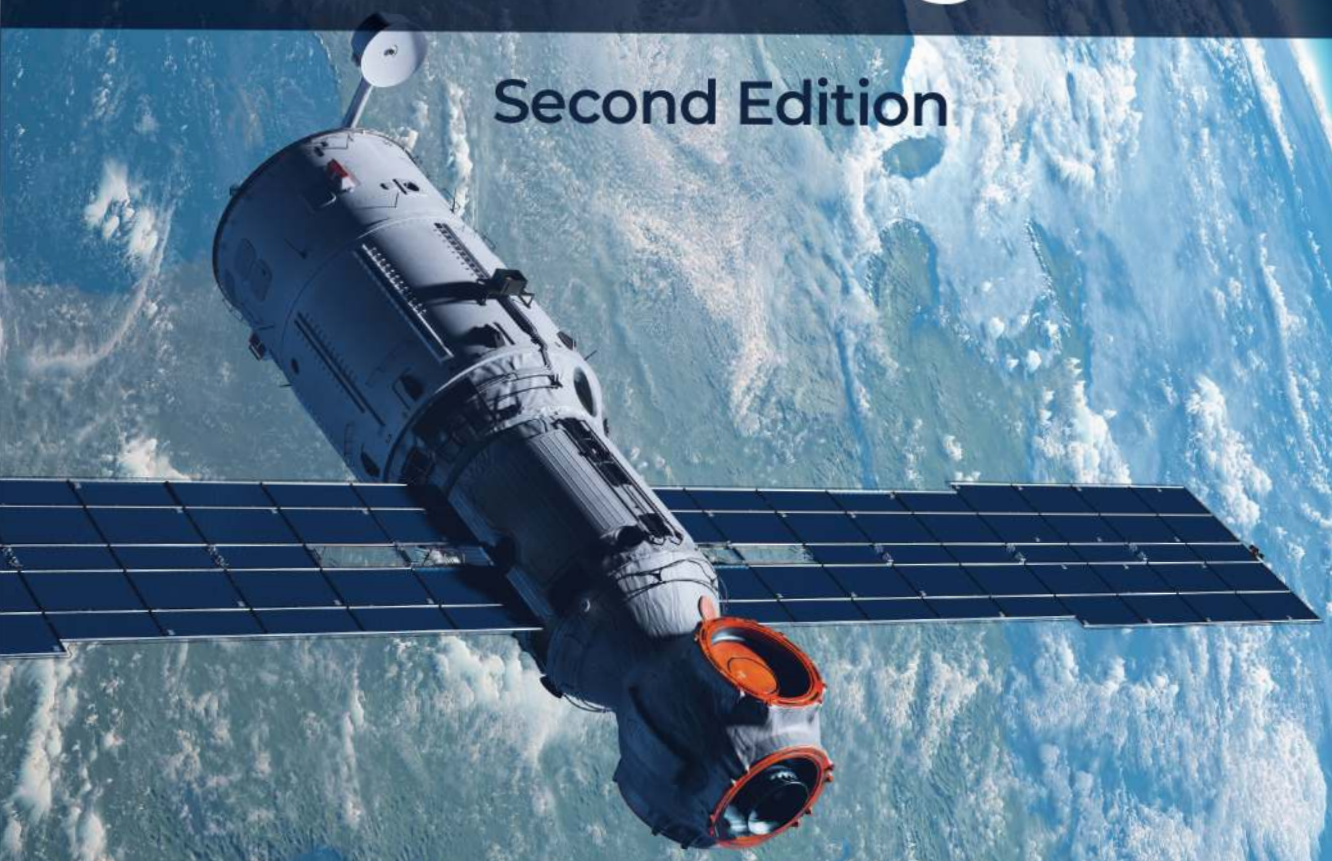

Rajat Acharaya

Understanding Satellite Navigation

Understanding Satellite Navigation

Second Edition

Rajat Acharya

ACADEMIC PRESS
An imprint of Elsevier
elsevier.com/books-and-journals

Academic Press is an imprint of Elsevier

125 London Wall, London EC2Y 5AS, United Kingdom
50 Hampshire Street, 5th Floor, Cambridge, MA 02139, United States

Publisher's note: Elsevier takes a neutral position with respect to territorial disputes or jurisdictional claims in its published content, including in maps and institutional affiliations.

Books and Journals published by Elsevier comply with applicable product safety requirements. For any product safety concerns or queries, please contact our authorised representative, Elsevier B.V., at productsafety@elsevier.com.

For accessibility purposes, images in electronic versions of this book are accompanied by alt text descriptions provided by Elsevier. For more information, see https://www.elsevier.com/about/accessibility.

Notices

Knowledge and best practice in this field are constantly changing. As new research and experience broaden our understanding, changes in research methods, professional practices, or medical treatment may become necessary.

Practitioners and researchers must always rely on their own experience and knowledge in evaluating and using any information, methods, compounds, or experiments described herein. In using such information or methods they should be mindful of their own safety and the safety of others, including parties for whom they have a professional responsibility.

To the fullest extent of the law, neither the Publisher nor the authors, contributors, or editors, assume any liability for any injury and/or damage to persons or property as a matter of products liability, negligence or otherwise, or from any use or operation of any methods, products, instructions, or ideas contained in the material herein.

ISBN: 978-0-443-36432-7

Publisher: Matthew Deans
Acquisitions Editor: Ritika Manhas
Editorial Project Manager: Abhinav Singh
Production Project Manager: Kamesh R
Cover Designer: Greg Harris

Typeset by Aptara, New Delhi, India

Dedicated to my loving wife Chandrani and son Anubrata.

Contents

Preface

Over the past decade, satellite navigation has become deeply embedded in everyday life.It now stands as a keystone across diverse domains of human activity, shaping countless tasks we perform daily. Significant of change has taken place in both technology and applications, since the publication of the first edition of this book. Therefore, it was essential requirement that this book be updated to a new edition. This second edition of the book will not only carry all the foundation of the first, but will also incorporate the latest developments in satellite navigation. With advancements in technology, newer services and applications have been introduced. Precision techniques like RTK and PPP are being increasingly employed in innovative ways. This extensive usage demands greater accuracy and precision, enhanced security, improved reliability, and above all, uninterrupted coverage. You will find this edition to cover all these topics comprehensively. A whole new chapter related to the reliability and security of the GNSS has been introduced. It explores the reliability challenges, like jamming and spoofing, and the new approaches to counter the threats. Technical insights into PPP have been added, while the existing services are also updated. The requirement of enhanced availability can be fulfilled reliance on multiple systems. In this direction, use of multifrequency and multiconstellation receivers are now widely adopted. This makes compatibility and interoperability critical topics, which are also discussed here.

In all incorporations in this new edition, the idea of easy accessibility and readability remained the guiding principle. The main feature of the first edition of explaining complex concepts ground up right from a foundation level with just the essential mathematics is still maintained in this edition. This edition continues the use of MATLAB as a visualization tool for every important new concept that is introduced.

I hope the simple and straightforward approach of the book to develop advanced technological concepts right from the first principle will still keep this book popular amongst the new learners and resonate with readers from different backgrounds.

Finally, I wish to emphasize that the views and the opinions presented in this book are solely mine and do not necessarily reflect the views of my employer or the Government of India.

Rajat Acharya

Acknowledgment

"Om Saraswatvai Namoh." At the very outset, I bow to Devi Saraswati, the Goddess of Knowledge, for listening to my humble prayer and blessing me with the opportunity to write this book.

As the second edition of my book "*Understanding Satellite Navigation*" is being published, I feel a profound sense of gratitude for all the support and contributions that have made this work possible.

First and foremost, I extend my heartfelt thanks to the readers of the first edition. Your feedback, comments, and constructive criticism have been instrumental in shaping this updated and improved edition. Your engagement and appreciation have been a source of motivation and inspiration.

I owe a great debt to my parents for instilling in me a love for learning. My heart is full of thankfulness towards my extended family for their unwavering support and encouragement, especially for Didi, Pinaki da, and Sandhya di. My niece Purbita Chatterjee also deserves a special mention for the unconditional support she has always extended to me. I am also deeply grateful to my wife and son for their patience and understanding during the countless hours spent researching and writing—thank you.

I would also like to acknowledge the expertise and guidance of my colleagues and mentors in the field of satellite navigation. The knowledge and insights you have shared enriched this book and ensured its accuracy and relevance. Dr. M.R. Sivaraman, Dr. Ashish Dasgupta, Dr. Kalyan Bandyopadhyay, Dr. Apurba Datta, Dr. Bijoy Bandyopadhyay, and Shri Vilas Palsule need special mention amongst them. I am equally grateful to to Dr. Bijoy Roy, and Shri Prasun Jha for reviewing this updated edition upon my request despite their busy professional schedules. Their meticulous review and invaluable feedback have greatly enhanced the quality of this edition. I also hold heartfelt gratitude to Ms. Ananya Dasgupta for her thoughtful review and gentle refinement of the book's literary content, which added grace and clarity to these pages.

I thank all my friends and well-wishers, whose trust in me and in my work has been the cornerstone of this journey. Their belief added tremendously to my energy throughout the process.

I am particularly grateful to the publishing and editing staff at Elsevier for their meticulous attention to detail and commitment to excellence. Your editorial skills have been crucial in refining the manuscript and ensuring its clarity and coherence. Last but not least, I would like to express my appreciation to the whole team at Elsevier and Academic Press for their continued support and professionalism. Your dedication to bringing this book to life is truly commendable.

Thanks to everyone who has been a part of this venture. I hope that this second edition will continue to serve as a valuable resource for those seeking to understand the complexities of satellite navigation.

CHAPTER

Introduction to navigation 1

1.1 Introduction

Navigation is a basic need for anyone who wants to move with a purpose. Navigation is the art of moving in a suitable direction in order to arrive at a desired location. Even in prehistoric times, when the most primitive form of animals started moving on Earth, the art of navigation existed in its most ancient form. Even today, when humans, the most evolved species on Earth, move by flying in the most technologically advanced aircraft, or by driving a car, or by riding a bicycle, or simply walking, with a desire to reach somewhere, we perform some sort of navigation.

You may have noticed that when we move without the aid of instruments and the route to our destination is known to us, we generally use some sort of mental map, which is mostly pictorial in the form of landmarks and connected paths. On this map, we identify our positions and apply our previous experience to guide us and decide the course of our movement. However, this method does not work for a new destination or for places where such landmarks are not present. This is the reason why people get lost in new places, in deserts or in the oceans. In such situations, we use paper or digital maps, which give us necessary information to guide ourselves. However, whether paper or digital, or as mental pictures including other geographical information, these maps are aids to navigation. They only enable us to locate and relate our positions with respect to our destinations and show different possible ways to reach there. The decisions we make in choosing the course of our movement by comparing our position with the available information on these maps is actually an art, called navigation.

To carry out the activity of navigation, we first need to know our position, to identify correctly where we are, and that of our destination. Only then can we make an appropriate decision about how to move to reach the latter. *Satellite navigation* is a technology that provides us with the correct position and its derivatives, on or off the Earth's surface. Here, the signals transmitted from navigation satellites are used to derive the required set of position coordinates. This is done in a navigation receiver. In turn, and in conjunction with the additional information, these parameters are used to decide the further course of movement or are utilized in other position-based applications.

However, positions are not sought only for movement. Sometimes our exact position is also required to be correlated with other facts or to derive ancillary information. For example, if we know our position on the Earth's surface, we can easily figure out the kind of climate we should expect. Knowing precise positions of

Understanding Satellite Navigation, Second Edition. DOI: https://doi.org/10.1016/B978-0-443-36432-7.00003-1

a network of points on the Earth surface will also let one obtain the exact shape of the Earth. Its derivatives may provide information such as tectonic or crustal movements. There are many other interesting applications of navigation, in which the knowledge about position and its derivatives are used for useful and exciting outcomes. We shall discuss them in Chapter 11.

The typical requirement of the estimation of position is global; for that, we need to represent positions uniquely. Positions are hence represented in terms of a common global reference such that the location of all the points on and near the Earth can be expressed by distinct and unique coordinates. It is like the unique identity of that position on the globe. Thus, finding the position of a person is simply a matter of determining the unique identity of the location where he or she currently is. These coordinates are hence so chosen that they can be used conveniently to specify the positions. In later subsections of this chapter, we will learn about the reference frames and different coordinate systems, which form the basis for representing positions.

1.1.1 Organization of this book

Philosopher Socrates said, "Know thyself." At the outset of learning navigation, we can use his quote and say, "Know (the position of) thyself." Thus, our entire endeavor throughout this book will be to understand the fundamentals of how modern space technology is used to fix our position, aided by advanced techniques and effective resources. Details about existing systems currently being used for this purpose will be discussed post hoc.

It is also important to know how the information is organized in this book. More logically things are developed here, easier it will be to understand them. Thus, it is a good idea to first have a holistic view of how the different aspects of a satellite navigation system are gradually introduced in different chapters in this book. We therefore suggest that readers continue reading this section describing the overall organization of this book, though many of us have a general apathy toward such explanatory material and a tendency to skip it.

The first chapter of this book is informative. We will start by introducing the term 'navigation' and understanding how the navigation technology evolved over time through a chronological description from its inception up to the current state of the art. We will therefore learn about the historical development of the navigation system. Whilst to some, history may sound boring, but according to English philosopher and statesman Sir Francis Bacon, "Histories make men wise." We will therefore not lose this opportunity to enhance our wisdom. So, first a brief introduction to the predecessors of satellite-based navigation will be discussed. Then, we shall have a quick look at the history of satellite navigation, before we gear up to understand the technological aspects of the subject. All of these will be covered in this chapter, and reading it, we hope, will be as interesting as the technology in subsequent chapters. Chapter 2 is also information-based, primarily regarding the overall architectural segments of the whole satellite navigation system. We will only learn in detail about the control

segment in this chapter, while other segments will be discussed in the following chapters. You will really feel the enjoyment reading this book in Chapter 3, where we describe the space segment of the architecture. From this chapter onward, there will be frequent MATLAB activities illustrating the ongoing topic. We suggest that readers attempt these activities as they come across them, rather than leaving them to be done at the end. Chapter 4 details the satellite signals used for navigation purposes and transmitted by satellites. Their characteristics will be described, and the rationale for their use explained. The recent new features introduced in the navigation signals will also be described. Chapter 5 describes the user segment. It provides the working principles of a navigation receiver including its different functional units and their technical aspects. This chapter explains how signals are used in receivers to derive the parameters required to fix a position. Chapter 6 explains the algorithms for the derivation of the navigation parameters, that is, position, velocity, and time (PVT), by using the measurements and estimations performed in the receivers. Errors incurred in such estimations, with their sources and effects, are discussed in detail in Chapter 7. Chapter 8 contains the topic of differential navigation systems. It is a vast subject that could easily fill a book the same size as this or even bigger. However, we have adapted it here into a single concise chapter of only a few pages, illustrating the most important aspects of it. Chapter 9 contains some special topics such as the Kalman filter, the ionosphere, and the space weather, each of which has large implications for navigation systems. Readers may skip reading this particular chapter if they wish, without loss of continuity. However, that would be at the cost of losing some very interesting facts and information. Chapter 10 is a new addition in the book in this edition that deals with the trending topics of the reliability of the GNSS system. Finally, Chapter 11 provides details of some important and interesting applications of satellite navigation.

1.2 Navigation

Navigation is related to the art of one's movement to reach the destination, safely and efficiently. The word "navigation" stems either from the Latin word "*Navigare*," which means 'to sail or drive a ship', or from the Sanskrit word "*Navgati*," meaning the "motion of a ship." Its contemporary meaning, is the art of providing position and/or direction to anyone on land or sea or in space (Elliot et al., 2001)

1.2.1 History of navigation

The art of navigation predated the advent of mankind. Prehistoric animals moved in search of food using their innate navigation skills. Fig. 1.1, however, is only indicative. Marine animals navigate by sensing the water temperature and the ocean currents, while some migratory birds use the aid of the geomagnetic fields to find their path.

Humans have been using different techniques of navigation since the early ages of civilization. Primitive people living in caves had to hunt deep in the forest in search

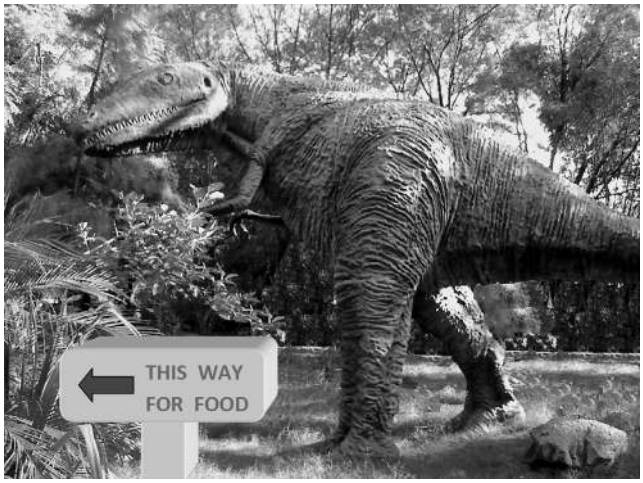

FIGURE 1.1

Primitive navigation.

of food when geographical movement was not easy, and finding their way back was difficult. Thus, they made special marks on trees or erected stone pillars to create landmarks in order to navigate back home. The use of sound or smoke signals was another common means of finding their way back. We will look more at the formal classifications later, but it is worth mentioning here that these *guidance* methods were the most primitive methods of navigation.

Navigation was developed at sea, with most developments in the modern navigation system occurring in the process of guiding sea vehicles. In ancient times, seafaring explorers started traveling across the oceans in search of new lands in order to increase trade and to colonize. Development in the field became necessary in order to cater to the increasing needs of voyages.

The first kind of sea navigation was probably done by skirting around the coast, and thus by staying in sight of land. Pictorial maps were created during this time by sailors who would draw what they could see along the coast and mark their routes. Using these, they could return or retrace their course on subsequent journeys. The activity of mapping the sea along its coasts is not navigation, but finding one's own position from it and thus deciding the direction of movement, is certainly what navigation is. However, both systems were developed simultaneously and are sometimes treated as the same thing. The first known coastal and river maps were prepared in China around 2000 BC and indicated sailing directions (Wellenhof et al., 2003). When voyages ventured further out into the sea, the only means of navigation was by observing the position of the sun and stars. This kind of navigation is termed celestial navigation. Some experienced sailors could also navigate by understanding the winds or determining the depth of the seabed, from which they could estimate

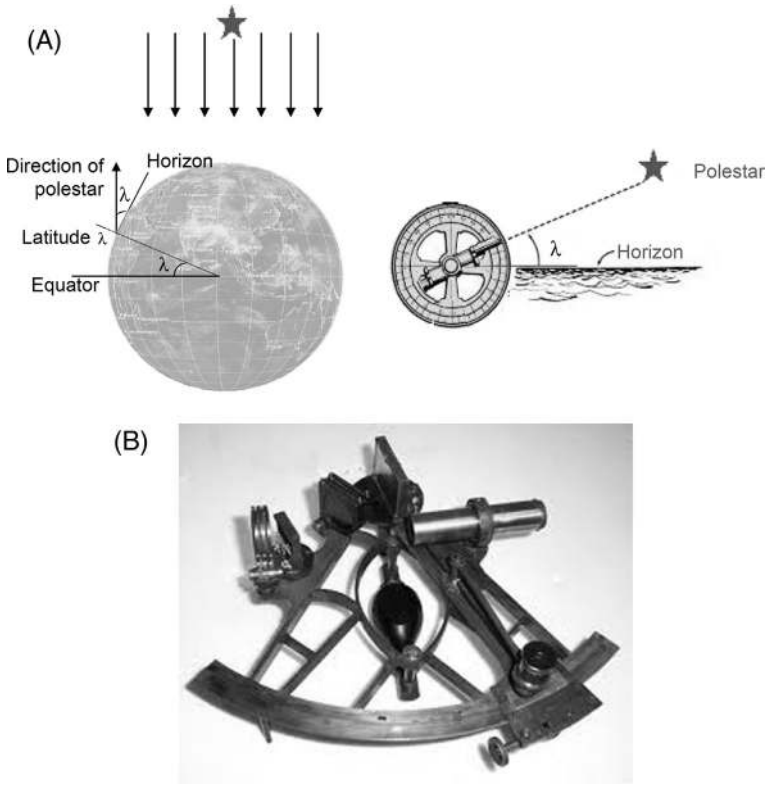

FIGURE 1.2

(A) Working principle of Astrolabe. (B) Sextant.

their distance from land. The latter was probably the earliest form of bathymetric navigation.

Written records of celestial navigation date back to the third century BC. Some of these accounts are available in Homer's epic, *The Odyssey* (History of navigation, 2007). The Indian epics Ramayana and Mahabharata also contain accounts of using celestial navigation. The astrolabe, which measures the elevation of the sun and the stars, as shown in Fig. 1.2A, became the main instrument for positioning and was apparently used even before 600 BC (Kayton, 1989). Heron and Vitruvius gave a detailed description of the odometer, an instrument to measure distance (Wellenhof et al., 2003). During this time, Greek and Egyptian sailors started using the polar stars and constellations to navigate, because they did not disappear below the horizon throughout the night. Measurement done by the instruments were aided by nautical charts. Ptolemy produced the first world map, which remained in use for many years during sea voyages. Textual descriptions for sailing directions have been in use in one form or another since then.

The Middle Ages in navigation were marked by the discovery of lodestone. With this, navigation became easier for sailors, who started to use it for its magnetic properties. Comparing it with detailed maps of that period, they could find their way easily even with unfavorable sky conditions, allowing sailors to navigate even with limited visibility. The first true mariner's compass was invented in Europe toward the beginning of the 13th century AD. Thus, when Christopher Columbus set out on his transatlantic voyage in 1492, he had only a compass, a few dated measuring instruments, a method to correct for the altitude of Polaris, and some rudimentary nautical charts as tools for navigation.

From the middle of the 16th century, navigation saw a rapid development in related technology when a number of instruments and methods were invented. This was when the Europeans started to settle colonies in different countries, and they used sea routes to navigate to these new lands. The improvement of navigational techniques became a necessity, and the mathematical approach toward navigation made it a scientific discipline. By the 17th century, the quadrant had become one of the dominant instruments. Magnetic variations were studied, and the magnetic dip, the angular inclination of the geomagnetic lines of force at a location, was discovered, which gave enormous support to position finding. The defined nautical mile could also now be measured with much greater accuracy. By the middle of the 18th century, the invention of instruments such as the sextant and the chronometer marked the onset of modern times in navigation. The sextant, as shown in Fig. 1.2B, could measure the elevation of the sun, moon, or a star by aligning its reflection from a semireflecting surface with the visible horizon seen directly through it. In the process, its own relative position could be estimated when the position of the star or the sun was known.

Time always remained an important parameter when finding a position. The sundial was a primitive clock, the oldest of which was found in Egypt at Karnak. It was also used in ancient Greece and China (Kayton, 1989). Later, the pendulum clock was invented and was used to keep time on land, but it was not suitable for marine platforms. Thus, for the seagoing vehicles and mariners, the best devices were still water and sand clocks. This put a serious constraint on the accurate determination of longitude, which requires precise knowledge of time. Around the middle of the 18th century, a huge sum of prize money was offered to anyone who could provide a precise method of measuring longitude. In 1759, John Harrison invented a clock that was accurate within a few seconds over a period of around 6 months. Captain Cook used the Harrison Clock for his expedition to the Antarctic. Another remarkable event that took place in the determination of longitude was the landmark decision to adopt the prime meridian (0 degree longitude) in 1884. It remains the basis of positioning even today.

In the last decade of the 19th century, radio communications started in the form of wireless telegraphs. For seagoers, signals started being sent to ships not only in the form of messages, but also to allow navigators to correct their chronometers. Radio communication between ships also helped sailors to make navigational decisions.

Radio-based navigation systems advanced rapidly during World War II. By this time, the quartz clock became available, and microwaves were used extensively with

navigational devices. British physicist Robert Watson first demonstrated the radio detection and ranging system (RADAR) as a warning system against air attacks. This technology was readily implemented in ships as a navigation aid. Soon after this, Alfred Loomis suggested a radio-based electronic navigation system, which was later developed into the long-range navigation (LORAN) system.

Radio navigation was ushered into a new era in October 1957, when the former Soviet Union (USSR) launched the world's first artificial satellite, Sputnik. Scientists used the Doppler shift of Sputnik's signal to obtain the satellite's position and velocity. Subsequently, a series of satellite-based navigation programs was undertaken and established by both the United States of America and the USSR. During this time, satellite constellations for navigation based on both Doppler and ranging came into use. The Transit satellites that started operating in 1964 were Doppler-based navigation systems, whereas the SECOR (Sequential Collation of Range) system was based on ranging. These were followed by the Russian Tsikada and American Timation (Time and Navigation) systems. Timation was planned for time transfer by sending precise clocks into space. The results of these precursor programs formed the basis of today's global positioning system (GPS) of NAVSTAR (Parkinson & Spilker, 1996) by the USA and GLONASS (Globall Navigation Satellite System) by Russia. Currently, many countries and groups of nations use their own satellite-based navigation system: the Galileo system of the European Union, BeiDou of China, and NavIC (Navigation using Indian Constellation) of India are some of them. We shall learn about the basic working principles of these systems in later chapters.

1.2.2 Types of navigation

A modern navigation system is typically a radio navigation system that is nonautonomous in nature. It means the system operates only when an appropriate external signal is received by a receiver (Wellenhof et al., 2003). It provides PVT in a three-dimensional system. However, there are certain autonomous forms of navigation, too. Based on the nature of parameters and how they are derived, modern navigation systems can be divided into three broad types.

1.2.2.1 Guidance

Guidance is a type of navigation that provides only a course to a destination for the user, but with no information about its exact current position. Thus, the user only knows the route that should be followed to lead him or her to the destination, with no knowledge of the present position coordinates.

Guidance is the oldest type of navigation. The movements of early travelers finding their way to their destination by observing the rising and setting of the sun and the moon, and orientation of the constellations, were navigation of guidance type. In modern times, when you follow the markers in a big airport directing you to reach

your designated terminal, or when you decide your route on the basis of displayed signs on a highway, this is navigation of the guidance type. Thus, we frequently utilize guidance navigation throughout our lives, sometimes without even realizing it.

Some modern radio navigation systems are in this group, such as the instrument landing system (ILS) and microwave landing system, which are used for aircraft.

1.2.2.2 Dead reckoning

Sometimes it is difficult to use guidance navigation, especially for long-range movement. In such cases, it is more convenient to know one's current position rather than be guided from origin to destination. But how do we update our position with time? Position at the current instant can be determined from the positions at any prior time, using the value of time elapsed since then and some simple dynamic parameters obtained through measurements. Thus, the current positions of any moving entity can be deduced in relation to any prior position, or even with respect to the point of its origin of movement. One of the easiest methods of doing this is by using the basic principles of Newton's laws of motion. From these laws, we derive the current position and velocity of the body as

$$V_k = V_{k-1} + a_{k-1}(t_k - t_{k-1}) \tag{1.1}$$

$$s_k = s_{k-1} + v_{k-1}(t_k - t_{k-1}) + \frac{1}{2} a_{k-1}(t_k - t_{k-1})^2 \tag{1.2}$$

where s_k and s_{k-1} are the positions at time t_k and its previous instant t_{k-1}, respectively. v_k and v_{k-1} are the corresponding velocities, and a_{k-1} is the acceleration at instant t_{k-1}.

Therefore, the position s_k and velocity v_k at any instant t_k may be derived from those at the previous instant t_{k-1}, just by knowing the acceleration, a_{k-1}, and from their previous values s_{k-1} and v_{k-1}, respectively. Similarly, the values of s_{k-1} and v_{k-1} can be derived from parameters at an instant even before them. Therefore, extending this logic backward, we can say that if we know the position s_0 at any starting point with a standstill condition, that is $(v_0 = 0)$ at any time instant t_0, we can find out its position and velocity at any later time t_k just by measuring acceleration "*a*" at the initial and all intermediate instants. Because the present position is deduced from an initial *standstill* condition (i.e., the "dead" condition of the body) from which we start reckoning (i.e., calculating the position), this kind of navigation is called dead reckoning. The term is also sometimes said to be derived from the word "deduced" (Meloney, 1985).

There are six degrees of freedom for any rigid body. Degrees of freedom are the set of independent dimensions of motion of the rigid body that completely specify the movement and orientation of the body in space. They indicate the independent directions in which a body can exhibit linear or rotational motion without affecting its similar movement in any other direction. In accounting for such motions, the three directions of translational motion defining the position of the body are considered. Along with them, the three orthogonal rotational directions of the body provide its orientation. Thus, in addition to position, dead reckoning can also be used to find the

orientation, that is, the attitude of the body by measuring the angular acceleration of the body about these three rotational axes.

Navigational systems based on these inertial properties of a dynamic system belong to the category of Dead Reckoning. The inertial navigation system (INS), which most commercial aircraft use as their primary navigational system, is an example of this type.

1.2.2.3 Piloting

In the piloting or pilotage type of navigation, the user derives navigational parameters (PVT), which are updated at each observation. New measurements are performed over the update interval, which leads to new position estimates for every update.

Satellite-based navigation, which is the subject of this book, belongs to this category. Other systems of this kind are hyperbolic terrestrial radio positioning systems such as the Long Range Navigation (LORAN), etc. (Loran, 2011).

1.3 Referencing a position

We fix our positions using different navigation systems. But the question is, *with respect to what?* A more fundamental question that may arise is, *do we always need to represent our position with respect to something?* If yes, then what should that "something" be?

To answer these questions, let us start by using a simple analogy. How do we typically communicate our positions in everyday life? Verbally, we actually tell our location to someone in a fashion like, "I am on Parallel Boulevard, about 100 yards right from the old lighthouse," or "I am at Copley Plaza, about 50 m south of the city library," or "I have come across the NSCB airport by half a kilometer due east." Notice the common features we use in these statements. In all cases, we refer to our position in terms of distance with respect to some specific reference landmarks such as the lighthouse, the city library, or the airport. Furthermore, we mention the distance from them in definite directions. We also assume that the person to whom the position is being described already knows these landmarks used as references. The description is useless if he or she is new to these places and does not know where the references are. Thus, what we deduce from these examples is that we need a fixed (or apparently fixed) and defined reference to describe our position, and a distance from these reference points with directions. Fixed and known references, defined directions, and definite distances are thus the elements required to describe positions.

The reference used should be universally accepted and understood, and should be convenient for referring to any position of interest. We have talked about specific landmarks as references in our example. These references are local and cannot be used to describe positions of any location across the globe. Therefore, to perform pragmatic position fixing, what should be the nature of these references? The obvious answer is that the reference point itself must be located with approximate equal nearness to all points whose positions are to be described so that any point in question may be represented with equal convenience.

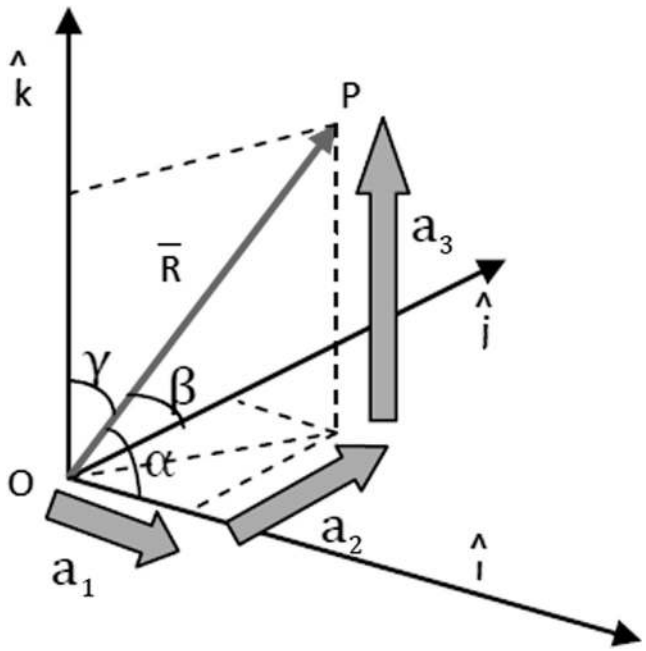

FIGURE 1.3

Orthogonal bases in a three-dimensional space.

Then, once the reference is set, the next requirement is to represent the distances of our position in the best possible way. From any pragmatic reference point O, as in Fig. 1.3, there will be a shortest radial range, moving along which the point in question, P, may be reached. The distance is shown as R. However, in our three-dimensional space, this range may be in any arbitrary direction from the reference, O. Describing any arbitrary direction is impossible unless we make use of some predefined standard direction for specifying it. In a three-dimensional space, there can be a *maximum* of three mutually independent orthogonal directions. We may fix three such directions in space, each referred to as an axis. The direction of radial range may be described by the angle it makes with such directions. The angles are represented by α, β, and γ, which are such that the relation $\cos^2\alpha + \cos^2\beta + \cos^2\gamma = 1$ is always maintained. The same point P may also be reached by moving vectorial distances along these axes. These paths are nothing but projections of the radial vector distance R on the defined axes shown as a_1, a_2, and a_3 in Fig. 1.3.

Thus, we can express vector **R** as

$$\mathrm{R} = a_1\hat{\mathrm{i}} + a_2\hat{\mathrm{j}} + a_3\hat{\mathrm{k}} = |\mathrm{R}|\left(\cos\alpha\,\hat{\mathrm{i}} + \cos\beta\,\hat{\mathrm{j}} + \cos\gamma\,\hat{\mathrm{k}}\right) \tag{1.3}$$

where i, ĵ, and k are the unit vectors along these three axes and form the basis.

In general, we equivalently move three orthogonal vectorial distances along the axes to move effectively from the reference point to reach any other point of choice.

Any mutually orthogonal vectors can be used to represent the axes for movement. But depending on the need, we use some standard predefined fixed directions of these vectors. This is because it serves no purpose toward convenient representation if these three directions are always chosen arbitrarily.

So, to represent the position of a point, we first need to fix a reference point. Then, with respect to this reference, the positions of all other points in question may be described in terms of distances along three fixed, predefined orthogonal axes.

1.3.1 Reference frame

Reference frame: Any predefined reference point and associated definition of three orthogonal axes, with respect to which the position of all other points may be represented, constitutes a reference frame. It is typically established by specifying the position of the reference point and direction of the axes. The reference point is specified by attaching it to any physical system and is referred to as the origin of the frame.

Accordingly, there may be two types of reference frames, described below.

Inertial: An inertial frame of reference is one that is not itself accelerating, and hence one in which the laws of inertia are valid.

Noninertial: A noninertial frame of reference is one that is itself accelerating, and hence the laws of inertia are not valid.

We mentioned that the positions of other points are defined in terms of distances along the defined orthogonal directions from this reference point. The unit vectors along these three orthogonal vectors thus form the basis for describing distances with respect to the reference. There can be different orthogonal sets of such basis vectors, and each set can constitute a coordinate system.

Coordinate system: A defined set of three orthogonal basis vectors associated with each axis of a reference frame, using which the position of any point in space may be described in terms of distances along the axes from the origin.

Different types of coordinate systems, such as Cartesian, spherical, and cylindrical, are used for different applications. However, for navigation on Earth, geocentric reference frames with Cartesian or spherical coordinate systems are typically used.

1.3.1.1 Heliocentric reference frame

Helios was the Greek Sun God, whose name was later Latinized as *Helius* to represent the Sun. Thus, from the name, it is evident that heliocentric reference frames are those in which the origin of the reference frame is fixed at the center of the Sun. These references are used to represent the positions of the celestial bodies or the positional elements in the solar system. However, it is not suitable for representations of positions over the Earth or near it.

1.3.1.2 Geocentric reference frame

We have seen that the location of points in three-dimensional space is most conveniently described by coordinates with an origin around the points. Therefore, to suitably represent positions on the Earth and around it, the chosen reference frames

are typically geocentric. The origin coincides with the center of the Earth, and the axes align with the Earth's conventional axes or planes. Geocentric reference frames can be naturally divided into different classes, as described subsequently.

To represent positions on the Earth and its surroundings, a geocentric reference frame may be defined with Cartesian coordinates. But how are the axes of this frame defined? For an inertial system, the axes should not linearly accelerate or rotate, because rotation is always accompanied by acceleration.

We know that the Earth is spinning about its own axis and is revolving around the sun as well. Thus, what appears to us to be fixed and stationary on the Earth when we look at it standing on the Earth is not actually so. We can find that everything on Earth is rotating with it, if we look at it from a fixed point in space. Thus, no frame fixed with the Earth can be stationary. Furthermore, as the Earth revolves around the sun, so too is everything that appears to be fixed upon it.

Then what can we use as a stationary reference frame? Truly speaking, nothing has yet been found that can be treated as absolutely stationary. No reference may be truly considered inertial. Therefore, we use relative stationarity, that is, those references that are approximately stationary, compared with the motion of the Earth. Distant stars or constellations can be used for this purpose. When we look toward the sky from the Earth, the distant stars appear to surround us in all directions. These stars apparently remain fixed at their positions throughout the year, whatever be the position of the Earth around the Sun. These stars are at such a great distance that the range of the Earth's movement is proportionately negligible compared to it. These distant stars may be assumed to form a hollow sphere of infinite radius, with the Earth at the center, called the celestial sphere. The deviations of these stars, as observed over the entire movement of the Earth, are trivial and hence can be considered stationary. A geocentric frame with axes pointed towards fixed points of this celestial sphere may be considered as an inertial frame. However, the Sun appears to move in this geocentric frame on an elliptical path called the ecliptic. The direction toward the distant stars on the celestial sphere from the geocenter through the point where the ecliptic crosses the Earth's equatorial plane with the northward motion of the Sun is called the direction of the vernal equinox or the first point of Aries. The angular distances of the distant stars as observed from the Earth are reckoned with respect to this fixed direction that marks the beginning of the Aries constellation (Fig. 1.4).

1.3.1.2.1 Earth-centered inertial

The Earth-centered inertial (ECI) is a geocentric reference frame that does not rotate with the Earth, and hence, the axes retain their orientation relative to these fixed distant stars.

In the ECI frame, as illustrated in Fig. 1.4A, the origin of the frame is at the center of the Earth, and the three axes of the right-handed orthogonal frame are attached to it. The X and Y axes of the Cartesian coordinates remain on the equatorial plane of the Earth, mutually perpendicular to each other. The X axis remains always directed toward the first point of Aries, whatever the position of the Earth is. The Z axis remains perpendicular to the equatorial plane and aligned along the mean

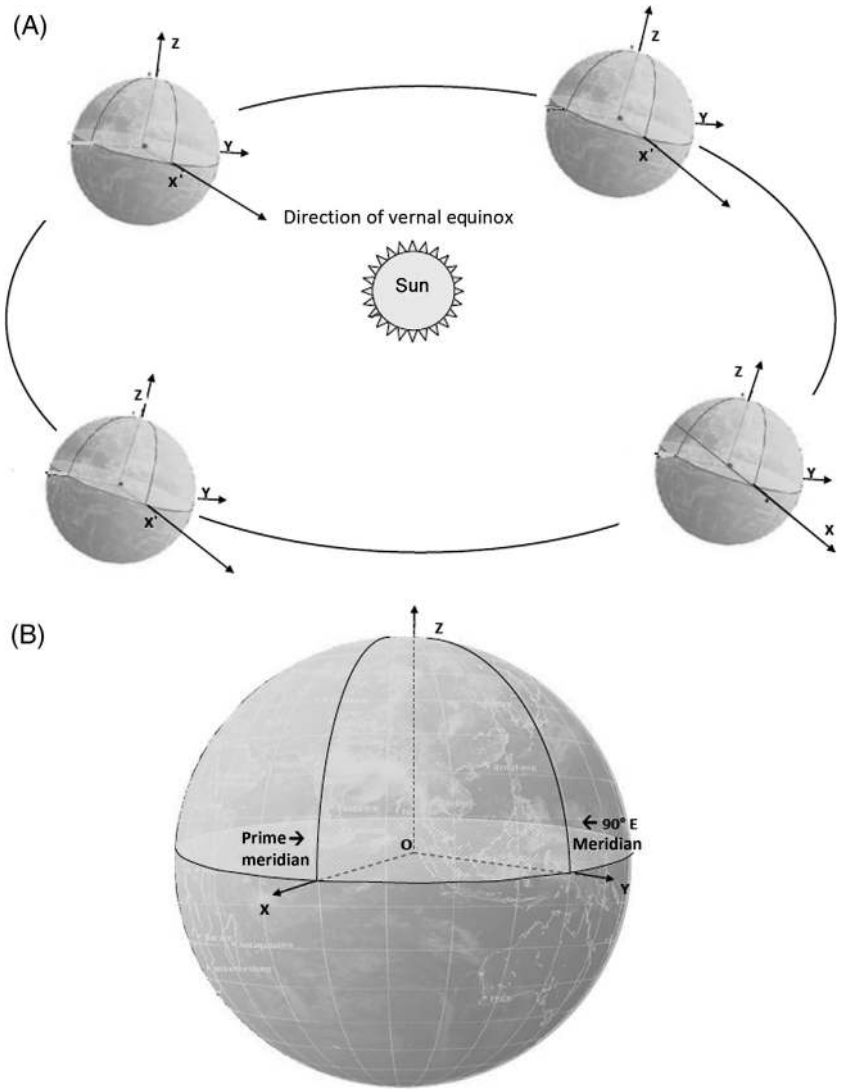

FIGURE 1.4

(A) ECI reference frame. (B) Earth-centered, Earth-fixed reference frame.

rotational axis of the Earth and points toward the North Pole. Although the frame is geocentric, the reference frame does not rotate as the Earth rotates about its axis. Thus, the coordinate system has a fixed orientation in space and hence may be called an inertial system as long as other perturbations of the axes are considered trivial. However, the perturbations cannot be totally neglected for precise applications. To

alleviate this problem, the directions are redefined at a fixed epochs. For example, the direction that these axes made on January 1, 2000, is taken as the current standard (Leva et al., 2006). Satellites revolving around the Earth experience gravitational pull effective from the point of its mean center but are not affected by the rotation of the Earth. Therefore, to represent the positions of satellites revolving around the Earth, ECI acts as a suitable reference system. Since the Earth rotates but the frame does not, the position of the points fixed on the Earth's surface changes with time in this reference frame.

1.3.1.2.2 Earth-centered, earth-fixed

We saw in the last section that in an ECI frame, the position of locations fixed on the Earth's surface changes with time. This is inconvenient for conventional positioning uses. So, if we define a geocentric reference frame in which the axes are fixed with the Earth and rotate with it, the coordinates of any fixed position on the Earth remain fixed over time. Hence, this problem can be avoided.

Earth-centered, Earth-fixed (ECEF) is a geocentric reference system in which the axes are attached to the solid body of the Earth and rotate with it. This is shown in Fig. 1.4B. In this kind of system, the origin of the frame is again at the center of the Earth, and a right-handed frame of axes is attached to it. The distances are primarily represented in Cartesian coordinates, XYZ. The X and Y axes remain on the equatorial plane and perpendicular to each other. The X axis is fixed along the prime meridian (i.e., 0 degree longitude), and the Y axis is accordingly placed on the equatorial plane along 90 degree E longitude. The Z axis remains pointing toward the North Pole. As the Earth rotates about its axis, the coordinate system also rotates with it, rendering the frame noninertial. It is suitable for indicating positions located on the Earth's surface and consequently moving with the Earth.

1.3.1.2.3 Geographic and geodetic coordinates

In describing these reference frames, we have mentioned nothing about the shape of the Earth. You may argue that one should not be concerned with the Earth's shape while defining the frames. It suffices to consider the origin at the center of the Earth and align the axes correctly. But then, how can one place the origin of the frame at the Earth's center unless you know where the center is? Obviously, we do not have access to the center of the Earth, and what is available to us are only measurements of the Earth. Therefore, from these measurements, we can fix the frame correctly. Fixing the frame correctly with the origin placed at the centre of the Earth, is equivalently, is equivalent done by representing a few specific points on the Earth by the correct coordinates with respect to that frame with geocentric origin. These measurements may also be used to generate a regular surface on which we can represent the position coordinates on the surface of the Earth.

First, assuming simplistically that the Earth is a perfect sphere, the ECEF frame may be considered with spherical coordinates for positioning. This constitutes the geographic coordinate system (Heiskanen & Moritz, 1967). Here, the orthogonal

coordinates are the radial distance of the point from the origin at the center of the earth: i.e. the radius (R); the angular distance of the point at the origin from the predefined equatorial plane, called the latitude (λ); and the angular separation of the meridian plane of the point from the meridian plane of the prime meridian, called the longitude (φ). This exempts the use of large Cartesian coordinate values for positions on the Earth's surface, except for the radius value R. For locations on the Earth's surface, R is approximately a constant.

However, the Earth is not a perfect sphere. The true surface of the Earth is too irregular to be represented by any geometric shape. Therefore, this topographic irregularity may be regarded as the variation over a smooth surface. This smooth surface is known as the geoid and is a model of the Earth that has a constant gravitational potential. Thus, it forms an equal gravito-potential surface such that its gradient at any point represents the gravitational force at that point in a direction perpendicular to the surface. In other words, the geoid is always perpendicular to the direction of the gravitational force. This is the direction pointed to by the free vertical plumb lines at any point. Considering that the water surface always remains at the same potential, the mean sea level is used as a physical reference to obtain a geoid shape. It is extended to the land surface, below, above, or on its normal topology to get a complete geoid shape (Ewing & Mitchell, 1970).

The geoid is also not a defined geometric shape. Therefore, the surface needs to be approximated to a regular geometric shape, fitted in the best possible way to this geoid, so that any position may be sufficiently estimated and represented by easy mathematical calculations pertaining to that shape.

The regular shape that best fits the geoid is the ellipsoid of revolution. This is obtained when an ellipse is rotated about its minor axis. Thus, a reference ellipsoid is chosen that represents the Earth's geoid shape in the least square error manner. This ellipsoid is typically described by its semimajor axis (equatorial radius) "a" and flattening "f" = (a − b)/a, where b is the semiminor axis (polar radius). The reference ellipsoid must have a definite orientation with respect to the true Earth shape in the closest possible way. Fixing the orientations in a three-dimensional space is equivalent to fixing the positions of a few selected points on the Earth's surface with respect to the right-handed ECEF coordinate frame positioned at the center of this ellipsoid model of the Earth. Conceptual descriptions of these surfaces are illustrated in Fig. 1.5.

Realizing the ellipsoidal model in practice requires positioning a large number of points on the Earth's surface to be measured, including their gravimetric parameters. Hence, it is much more practical to define the ellipsoid that fits best to the smaller regions in question. This has, therefore, been mostly done on a regional basis.

To determine the proper shape of the Earth and the associated parameters, the measurements performed are called geodetic measurements, a wide and complex scientific discipline. The basic parameters determined from these measurements are called the geodetic datum.

The formal meaning of datum is something that is used as a basis for calculating or measuring. In the case of geodesy, these are the data defining the dimensions of the

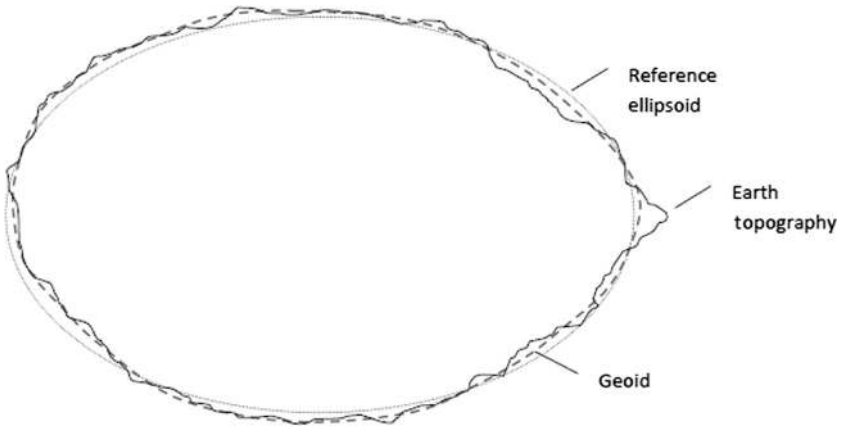

FIGURE 1.5

Ellipsoid reference.

Earth. For this, geodesists generate data, local or global, constituting the parameters of this reference ellipsoid, which they empirically estimations of as the best geometric fit for the Earth's surface.

Before the satellite geodesy era, the coordinate systems associated with a geodetic datum attempted to be geocentric, but all parameters were obtained by empirically fitting the local measurements with an ellipsoid surface. These were regional best fits to the geoids within their regions of validity, minimizing the deflections over these local areas. The origin being computed on a local basis differed from the true global geocenter by hundreds of meters, owing to the region specific features of the geoid. Some important regional geodetic datums are:

- Everest Datum (ED 50)
- North American Datum (NAD 83)
- Ordnance Survey of Great Britain (OSGB 36)

With the advent of space-based measurements using satellites, a specific geocenter could be defined because the satellites orbit about the natural geocenter. This point becomes the obvious choice of origin of a coordinate system because the satellite positions in space are themselves computed with respect to this point.

World Geodetic System 1984 (WGS 84): The WGS 84 is composed of a set of global models and definitions with the following features:

- An ECEF reference frame.
- An ellipsoid as a model of the Earth's shape.
- A consistent set of fundamental constants.
- A position referred to as WGS84-XYZ or WGS84-LLA (latitude, longitude, and altitude).

- An ellipsoid semimajor axis taken as 6378137.0 m, and semiminor as 6356752.3142 m.

The height of the geoid measured normally above the ellipsoid is called the *geoid height*. Similarly, the height of the terrain measured above the geoid is called the *orthometric height* and is expressed as the height in meters above mean sea level.

Detailed information on this subtopic can be obtained from references such as El-Rabbani (2006), Larson (1996), Leick (1995), Leva et al. (2006), and Torge (2001).

1.3.1.3 Local reference frames

A local reference frame is constituted when the reference point (i.e., the origin of the reference frame) is located at a point local to the observer, generally on or near the surface of the Earth instead of at the center of the Earth. Because these frames are used to specify positions of objects local to the observer, they are so named.

1.3.1.3.1 East-north-up

One of the most useful local reference frames is the East-North-Up (ENU) system. It is a local Cartesian coordinate system in which the E axis of a right-handed system is directed toward the local east, the N axis is along the local north, and the U axis is vertically up. These axes are suitable for representing the position of objects on and above the Earth's surface, such as a flying aircraft or a visible satellite. By local east, we mean that the axis originating from the reference point on the Earth's surface is contained on the latitudinal plane and is tangential to it at that point toward East. Similarly, by local north, we mean that the axis is tangential to the meridian plane at that local point of reference. Thus, the E and N axes both lie on the local horizontal reference and is directed towards the local North. The description is illustrated in Fig. 1.6. A similar local frame is North-East-Down (NED).

1.3.1.4 Conversions between coordinate systems

Conversion of the coordinates from one system to another is essential for navigational purposes. Navigational estimations are typically (although not essentially) done in ECEF Cartesian coordinates, whereas application requirements may use other systems. Therefore, the estimated coordinates are converted to geographical, geodetic, or other coordinates, as necessary. However, it may become necessary to convert them into local coordinates. Here, we discuss only the conversion between the Cartesian ECEF and ENU coordinates with a spherical Earth. For conversion from ECI to ECEF geodetic coordinates, see Fig. 1.7 and refer to focus 3.1.

1.3.1.4.1 Earth-centered, earth-fixed cartesian to geodetic latitude–longitude

Refer to Fig. 1.7. The Cartesian coordinates x, y, z in ECEF can be expressed in terms of the geodetic latitude λ ($-\pi/2 \leq \lambda \leq \pi/2$), longitude φ ($-\pi \leq \varphi \leq \pi$) and height

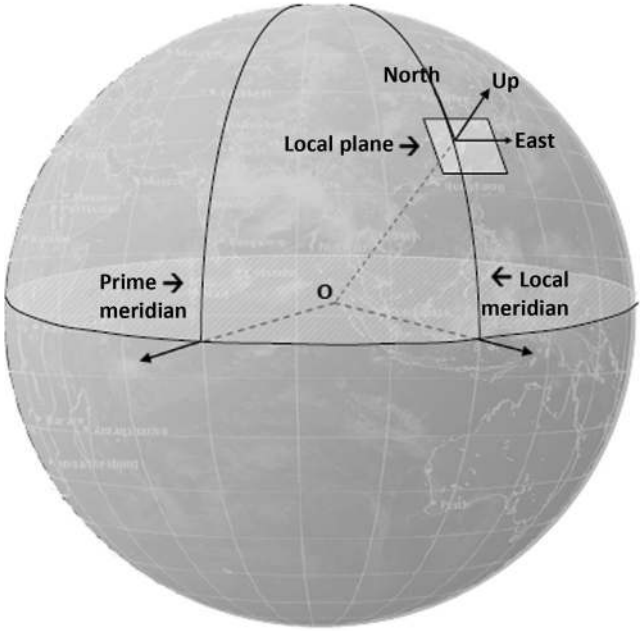

FIGURE 1.6

Local ENU coordinates.

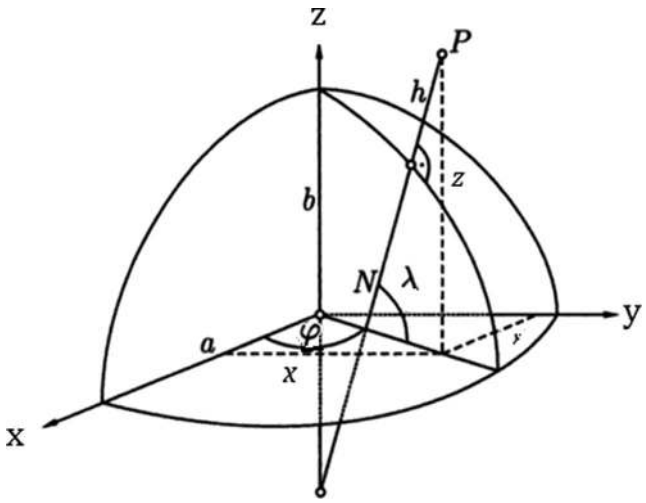

FIGURE 1.7

Conversion of Ellipsoid to ECEF coordinates.

h as

$$\begin{aligned} x &= (N + h)\cos\lambda\cos\varphi \\ y &= (N + h)\cos\lambda\sin\varphi \\ z &= \left(N\left(1-\varepsilon^2\right) + h\right)\sin\lambda \end{aligned} \tag{1.4}$$

where ε is the eccentricity of the ellipsoid and is given by $\varepsilon = (1 - b^2/a^2)^{½}$. a and b are the equatorial radius (semimajor axis) and the polar radius (semiminor axis), respectively, of the ellipsoidal Earth and h is the ellipsoidal height. N is the radius of curvature in the prime vertical. It is the portion of the line drawn from the point to the Z axis lying between the Earth surface and Z axis intersecting the ellipsoid normally. N is given by

$$N = \frac{a^2}{\sqrt{a^2\cos^2\lambda + b^2\sin^2\lambda}} \tag{1.5}$$

where a and b are already defined above. Similarly, the conversion from the Cartesian coordinates to the geodetic coordinates may be done using the following equations:

$$\varphi = \tan^{-1}(y/x) \tag{1.6a}$$

It is important to remember that, for the same value of the ratio (y/x), the angular value of φ may lie on different quadrants depending upon the positive or negative signs of x and y. The value of the longitude has to be chosen accordingly.

The conversion for the latitude λ and height h involves a circular relationship involving N, which again is a function of latitude λ. Denoting $(x^2+y^2)^{1/2} = p$, they can be expressed as

$$\frac{z}{p}\cot\lambda = 1 - \frac{\varepsilon^2 N}{N+h} \text{ and } h = \frac{p}{\cos\lambda} - N \tag{1.6b}$$

The parameters can be solved iteratively or by using more elaborate methods (Geographic coordinate conversion, 2024).

1.3.1.4.2 Cartesian earth-centered, earth-fixed to earth-centered inertial

To convert from conventional Cartesian ECEF to ENU coordinates of a point location with a spherical model of the Earth, we need to conduct some coordinate transformation exercises. Let a point in space be represented as x, y, and z in the ECEF and E, N, and U in the ENU coordinate system, with the origin located at latitude λ and longitude φ for a spherical earth of radius R. The corresponding ECEF coordinates are x_L,y_L,z_L. Therefore, the differential coordinates in ECEF frame of the point in question with respect to the ENU origin are given by $x_r = (x - x_L)$, $y_r = (y - y_L)$ and $z_r = (z - z_L)$, respectively. To obtain the coordinates of the same point in ENU, first let us rotate the ECEF axes about the Z axis by an amount φ to an intermediate coordinate system X′Y′Z′ that has the same origin but with the x axis directed along the φ instead of the prime meridian. Thus, in this coordinate, the coordinates x′, y′, and z′ may be

represented as

$$\begin{aligned} x' &= x_r \cos\varphi + y_r \sin\varphi \\ y' &= -x_r \sin\varphi + y_r \cos\varphi \\ z' &= z_r \end{aligned} \tag{1.7}$$

Now, rotate the axes about the Y′ axis by an amount of λ to another frame X″Y″Z″. This turns the X′Z′ plane in such a way that the new X″ axis directs vertically up at the selected point. In this frame, the x″, y″, and z″ become

$$\begin{aligned} x'' &= x' \cos\lambda + z' \sin\lambda \\ y'' &= y' \\ z'' &= -x' \sin\lambda + z' \cos\lambda \end{aligned} \tag{1.8}$$

This coordinate system is aligned with the ENU system with the X″ axis aligned along the Up direction, Y″ along East, and Z″ along local North of the ENU origin. Thus, we get the required set of ENU coordinates as

$$\begin{aligned} E &= y'' = -x_r \sin\varphi + y_r \cos\varphi \\ N &= z'' = -x_r \cos\varphi \sin\lambda - y_r \sin\varphi \sin\lambda + z_r \cos\lambda \\ U &= x'' = x_r \cos\varphi \cos\lambda + y_r \sin\varphi \cos\lambda + z_r \sin\lambda \end{aligned} \tag{1.9}$$

The conversion from ENU to ECEF can be easily obtained by inverting the transformation matrix. The relation becomes,

$$\begin{aligned} x &= -E \sin\varphi - N \sin\lambda \cos\varphi + U \cos\lambda \cos\varphi + x_r \\ y &= E \cos\varphi - N \sin\lambda \sin\varphi + U \cos\lambda \sin\varphi + y_r \\ z &= N \cos\lambda + U \sin\lambda + z_r \end{aligned} \tag{1.10}$$

1.4 Radio navigation system

Radio signals can traverse a long range within which they can be received by suitable receivers, and the information within can be used for different purposes, including navigation. Radio navigation has advantages in that the signals necessary to derive positions can be communicated under all weather and visibility conditions, and a lot of information required for both basic navigation as well as ancillary uses can be transferred with it reliably and with high accuracy. However, all of these advantages come with the price of more complex instruments.

Here, we shall briefly look at the working principles behind each of a piloting, guidance, and dead reckoning types of navigation systems. In all of these discussions, we purposefully avoid any mathematical descriptions to make it as simple as possible. However, the related basic concepts will be mentioned so that interested and enthusiastic readers may relate them to further reading.

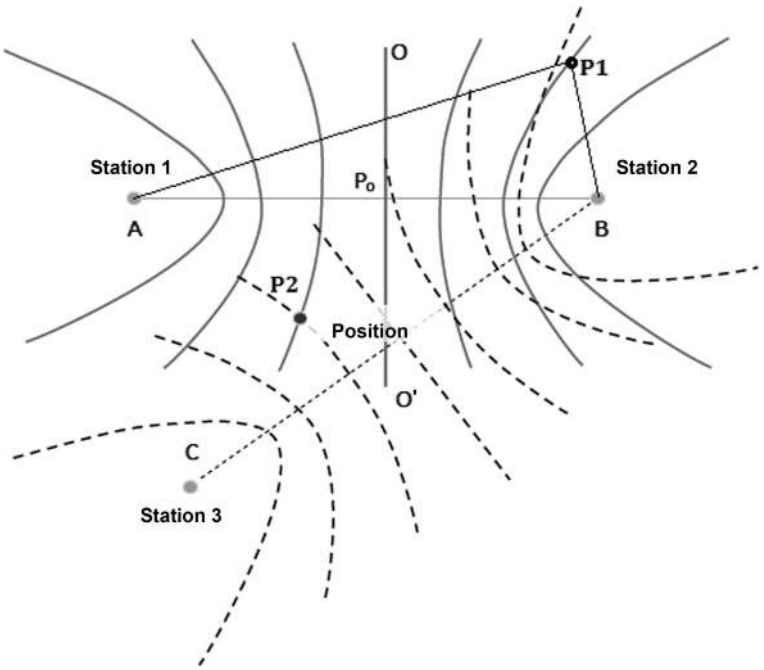

FIGURE 1.8

Hyperbolic lines of equivalent TDoA.

1.4.1 Piloting system

Hyperbolic terrestrial radio navigation is a *piloting* system, based on the principle of finding the position from the time difference of arrivals of signals to a receiver from a pair of radio transmitters located at known positions. These two transmitting stations, say A and B, can be joined by a straight line called the principal line.

As shown in Fig. 1.8, at any point, say P1, the signals issued simultaneously by the two transmitters will arrive with a finite time difference. As the radio waves move with a constant velocity 'c' in all directions, the time difference of arrival (TDoA) is proportional to the path difference between stations at the receiver location P. Let R_A and R_B be the ranges of P from stations A and B, respectively. Therefore, if two signals are transmitted simultaneously from these two different stations and are received by the receiver at P at the point at a time difference of Δt, the range difference of these two transmitting stations from the receiver is $(R_A - R_B) = c\ \Delta t$

The locus of all points having the same time difference of arrival will form the geometrical shape of a hyperbola. Different such hyperboloids can be obtained for different values of TDoA. A quadratic equation corresponding to this TDoA will be formed. This equation will be constituted by the known positions coordinates of A and B, that is, the origin of the signals, the known time difference of arrival, and the

unknown position coordinates of the point in question, P1. For the special case, when this time difference of arrival is zero (i.e., the ranges are equal), it will be equidistant from both A and B, as is point P_0 in the figure. All such possible points will construct a straight line normal to the principal line and pass through its midpoint, as shown as OO′ in the figure.

If the positions of the two synchronized stations are known, the locus of the possible positions of the receiver can be determined from hyperbolic geometry. However, the exact coordinates of the receiver are yet to be fixed. In two-dimensional space, the position of the receiver can be explicitly obtained by generating a similar locus from another pair of stations. With A and another transmitter C, the TDoA for the same point P1 will be different. Hence, another set of hyperbolic equations can be obtained, having the same unknown position coordinates of P1. The exact position can be obtained by solving these two hyperbolic equations.

This is illustrated in the figure for point P2, where the two sets of transmitters have formed two sets of hyperbolae, one denoted by solid lines and the other by broken lines. The crossover point of the two loci for the two time differences, gives the position P2, as shown in the figure (Loran, 2011).

1.4.2 Guidance system

An ILS is a *guidance* type of navigation that provides an instrument-based technique for guiding an aircraft to approach and land on a runway. It uses a combination of two different radio signals to enable a safe landing even during challenging conditions such as low visibility.

The ILS provides the aircraft with a recommended path it should follow so that it maintains its horizontal position at the center of the runway and the vertical position most appropriate for a smooth landing. Thus, an ILS consists of two independent subsystems. The first, which provides lateral guidance, restricting the aircraft approaching a runway to shift laterally from the recommended path, is called the localizer. The second, which gives vertical guidance and hence restricts vertical deviation of the aircraft from the recommended path of descent, is called the glide slope or glide path. Guidance in both of these is provided by transmitting a pair of amplitude-modulated signals from two spatially separated transmitters. A similar pair of signals is available in both lateral and vertical directions. Fig. 1.9A and B illustrate the condition. This signal is received by ILS receivers in the aircraft and is interpreted to obtain guidance information. This is done by comparing the modulation depth of the modulating signals within a particular pair through differencing. The pair of signals is spatially separated in such a way that exact cancellations of the modulating signal happen only along the recommended path of the movement of the aircraft. Once the aircraft deviates from this path, one of the components exceeds the other, and there appears a nontrivial resultant value of the difference signal. Then, the aircraft positions are adjusted accordingly to bring them back to the positions of exact cancellation (Kayton, 1989; Meloney, 1985; Parkinson & Spilker, 1996).

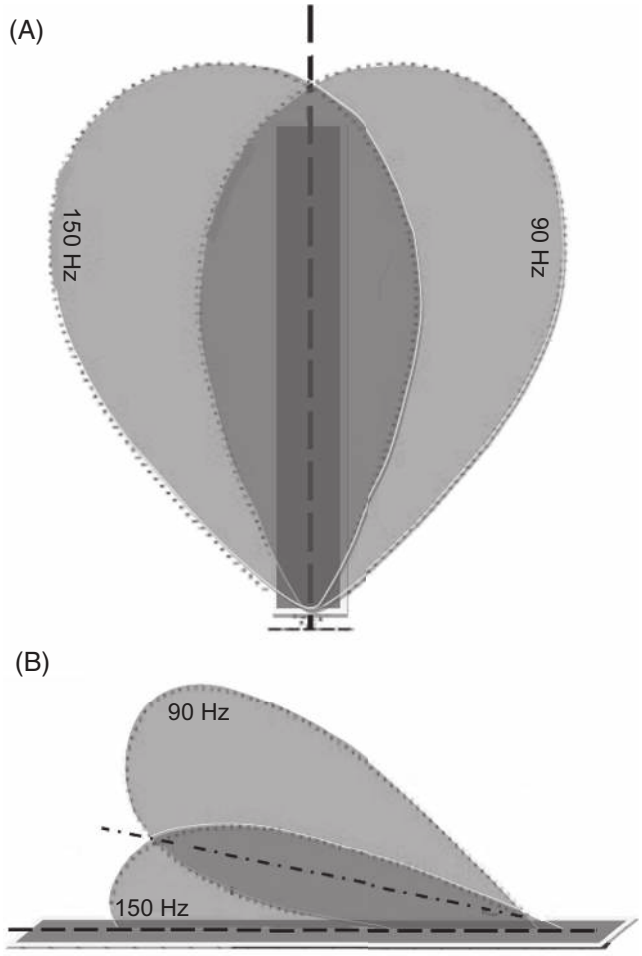

FIGURE 1.9

Radiation pattern of ILS for (A) plan view of localizer, (B) lateral view of glide scope.

1.4.3 Dead reckoning system

An INS is a type of dead reckoning system. It is used by most commercial aircraft for navigation en route and consists of inertial navigation instruments. The instrument that measures translational acceleration is called the accelerometer. It is typically a piezoelectric transducer whose mechanical equivalence is shown in Fig. 1.10. The other instrument, measuring the rotational motion, is called the gyroscope. At any instant, these instruments provide the dynamic parameters of the vehicle. These instruments give the linear and angular accelerations from which, in conjunction with

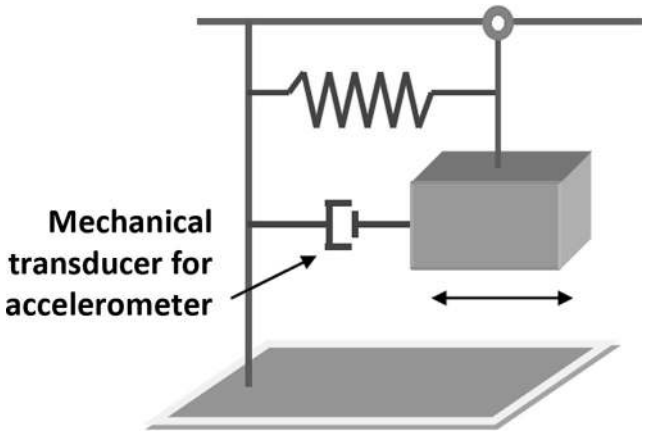

FIGURE 1.10

Schematic of the mechanical equivalent of an accelerometer.

the position derived at any definite time, the subsequent positions of the vehicle may be derived, as described in Section 1.2.2. An INS can provide continuous and reliable position determination, but errors continue to accumulate over time owing to the integration algorithm used (Grewal et al., 2002) (Fig. 1.10).

Conceptual questions

1. What features should a reference frame contain that can be used to conveniently represent the positions of objects on the ground, as seen from an aircraft?
2. When do the ECI and the ECEF coordinate axes coincide? Do they coincide again after every interval of a solar day (i.e., after every 24 h) from that instant? Give reasons for your answer.
3. Is the phase information relevant for signals provided by the glide scope and the localizer of an ILS to keep the aircraft in a fixed locus?
4. How many reference transmitting satellites are required to employ hyperbolic navigation using signals from space? Give reasons for your answer.

References

Elliot, J., Knight, A., & Cowley, C. (Eds.). (2012). *Oxford Dictionary and Thesaurus*. New York: Oxford University Press.

El-Rabbani (2006). *Introduction to GPs* (2nd ed.). Artech House.

Ewing, C. E., & Mitchell, M. M. (1970). *Introduction to geodesy*. American Elsevier Publishing Company.

Geographic coordinate conversion (2024). *Wikipedia*. Available at https://en.wikipedia.org/wiki/Geographic_coordinate_conversion. Retrieved on 16 December 2024.

Grewal, M. S., Weill, L. R., & Andrews, A. P. (2002). *Global positioning systems, inertial navigation, and integration*. Wiley. doi:10.1002/0471200719.

Heiskanen, W. A., & Moritz, H. (1967). *Physical geodesy*. W.H. Freeman and Company.

History of navigation (2007). Available at https://en.wikipedia.org/wiki/History_of_navigation. Retrieved on 19 January, 2014.

Kayton, M. (1989). *Navigation—land, sea and space*. IEEE Press.

Larson, K. M. (1996). In B. W. Parkinson, & J. J. Spilker Jr. (Eds.), *Global Positioning Systems, Theory and Applications,* Vol. II. AIAA, Washington DC, USA.

Leick, A. (1995). *GPS satellite surveying*. Wiley and Sons.

Leva, J. L., Kaplan, E. D., Milbet, D., & Pavloff, M. S. (1995). Fundamentals of Satellite Navigation. In E. D. Kaplan, & C. J. Hegarty (Eds.), *Understanding GPS: Principles and Applications,* second ed. Artech House, Boston, MA, USA.

Loran (2011). *Wikipedia* Available at https://en.wikipedia.org/wiki/LORAN. Retrieved on 17 October, 2024.

Meloney, E. S. (1985). *Dutton's navigation and piloting*. Naval Institute Press.

Parkinson, B. W., & Spilker, J. J. (1996). *Global positioning system, theory and applications*. AIAA.

Torge, W. (2001). *Geodesy. 3*. Walter de Gruyter.

Wellenhof, B. H., & Legat, M. W. (2003). *Navigation: Principles of positioning and guidance*. Springer-Verlag Wien.

CHAPTER

Satellite navigation 2

2.1 Introduction to satellite navigation

From general navigation, which we have discussed in chapter 1, we now move on to our specific topic of *satellite navigation* and introduce its basic concepts. Our approach in this book is to explain the fundamental principles of the generic satellite navigation system, instead of concentrating on any particular existing system. This chapter starts by formally defining satellite navigation and describing it as a service. It discusses the important aspects of a navigational service and its formal categories. Then the different architectural components of a typical satellite navigation system are elaborated with particular focus on the control segment.

2.1.1 Definition

Any type of Navigation involving a satellite that sends reference information to users, from which either the navigational parameters, such as position, velocity, and time (PVT), can be directly derived, is called satellite navigation.

The advantage of using satellites for the purpose of navigation is that the satellites have wide spatial coverage, which makes the service available to many users at a time. However, the associated limitations are the propagation impairments that the navigation signals experience while passing through the medium, and also the resulting weak signals at the receivers.

Satellite navigation systems provide navigation services to their valid users by offering them enough information such that, with appropriate resources and through proper processing, they can derive an estimate of their own position and time at all locations within the extent of the service area of the system and all times.

Satellite navigation is basically a piloting system in which the positional parameters are derived afresh every time. Unlike the other piloting system like LORAN, which works on the basis of "time difference of arrival" of the signals from two sources here, the positions are mainly derived on the principle of "time of arrival" of the signal. The satellite acts as the reference in this case, whose positions are precisely known in advance. The derived positions are represented in a suitable global reference frame.

Understanding Satellite Navigation, Second Edition. DOI: https://doi.org/10.1016/B978-0-443-36432-7.00019-5

2.1.2 Navigation service

We shall start this subsection with the definition of "service." However, we shall only define the term from the perspective of satellite navigation. Then, we shall quickly move on to its technical aspects. Brevity is necessary because the term "service" has enormous economic implications, and explaining this subject is not only extremely difficult but also beyond the natural capacity of the author of this book. Thankfully, that does not affect our objective, which is to understand the technical foundations of satellite navigation and not the implications of using it as a service.

Defining the term "service" is not simple. It is one of those words for which it is easy to understand the idea, yet difficult to create a crisp, clear definition that covers all of its aspects. Although, for our purposes, a lay person's understanding of the concept is adequate. In the most simplistic words, service is defined as an intangible economic activity that delivers commercial value to its users by facilitating outcomes that the users of the service want to achieve or experience, without exercising ownership of the service (Service, 2003).

Examples of services are the utilities like delivering cooking gas to our houses through pipelines, or providing power or internet connectivity through a cable, or providing mobile phone connectivity. Rail services offer trains to commute, tutors provide services by sharing knowledge, and physicians provide medical services. Each of the services has a commercial value. The user can take the benefit of the outcomes, like cooking food using the gas, talking on a mobile phone, or getting healthy using the doctor's by spending money. But for this, the user does not need or cannot claim to own the service.

Broadly, the users execute a process on the offerings to fulfill the need for which they opted for the service, without having to care about the processes that run in the background to offer the services. Users, however, typically expect a certain quality of service to be delivered to them. The quality of the service is important to the users and specifies whether the service can satisfy their requirements.

This is a very brief and simplified description of what a service is, but it is sufficient for our needs at this point. Satellite navigation is also a service, and as a service, it delivers all the necessary information for deriving PVT estimates to users through radio waves transmitted from satellites as signals. The delivery of these signals, which carry enough information so that the user's position may be derived, is the service that is provided. Users interact with these signals using their receivers and perform the process of estimation to obtain their positions. The users are the recipients of this service and obtain the value of the service, without bothering about the background processes necessary to provide the same.

2.1.3 Service parameters

The parameters that define the quality of the navigation service are its accuracy, availability, continuity, and integrity (Conley et al., 2006). These service parameters are further defined below:

2.1.3.1 Accuracy

Accuracy is the measure of the correctness of the position and other estimates carried out by the user with respect to their true values. In plain words, it describes how close to the true values the estimations are, using the service. Accuracy depends on many technical factors, such as the signal quality, correctness of navigational data and propagation effects, satellite geometry, and receiver goodness, etc. We shall discuss these in more technical detail in Chapter 7. These factors determining the accuracy are required to be assessed to provide a quantitative figure of the expected quality of the service offered.

It is also important to discuss the difference between the terms "accuracy" and "precision." Although we sometimes use them interchangeably, these two terms are entirely different in meaning. Accuracy is the conformity to truth, with the technical definition being the degree of closeness of the measure or estimate of a quantity to its actual value. The navigational service's position accuracy is given by the difference between the true position of the user to the estimated position. The smaller the difference, the better the accuracy. For any ensemble process, it is typically represented by the average absolute error of estimation.

On the other hand, precision is the measure of repeatability of a value, and it represents how well you adhere to the same value of your estimates for different tests under the same conditions. This is defined by the deviation of the estimates from the most expected value over the ensemble. It, thus, provides an idea of the distribution of the estimates about the mean and is represented by the standard deviation of the estimates, which is also the standard deviation of the estimation errors.

A measurement system can either be accurate but not precise or precise but not accurate; it can also be neither or it can be both. For example, a measurement carrying a constant bias, along with a large random error like Gaussian white noise, is neither accurate nor precise. If the samples are obtained through averaging several measurements, the random noise is removed, but not the bias. Then the measurement is precise but still not accurate. Otherwise, if the bias is removed only and the Gaussian noise remains, it becomes accurate but not precise. If, after removing the bias, we get averaged samples, the measurement becomes both accurate and precise (Box 2.1).

BOX 2.1 MATLAB EXERCISE

The MATLAB program accuracy_precision.m was run, representing the measurement of a value $x_0 = 0$ and $y_0 = 0$, where the measurements are done under two different conditions, (1) with random error only and (2) with bias and random error. The plots thus obtained will be given later. The bias values were taken as 2 and 3 for x and y, respectively, and the value of the standard deviation σ was assumed as 2 (Fig. M2.1 A and B). Run the program with different biases and for different values of σ and observe the nature of the points representing the measurements.

(*continued*)

BOX 2.1 MATLAB EXERCISE — *cont'd*

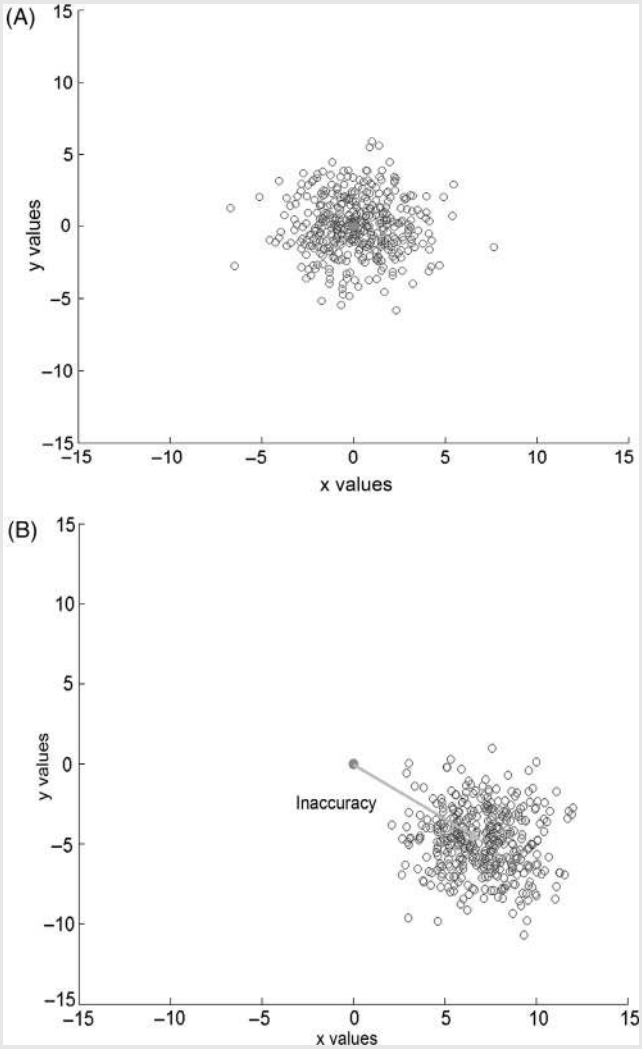

To explain this, refer to Fig. 2.1, which consists of a true position T of a body and its estimates represented by scattered points around it. For the estimates there is a radial error that exists, which is randomly scattered. Accuracy describes the closeness of the points to the true position, T. Points that are located closer to T are considered more accurate. The accuracy of all the estimates as a whole is the mean radial distance of the points from T.

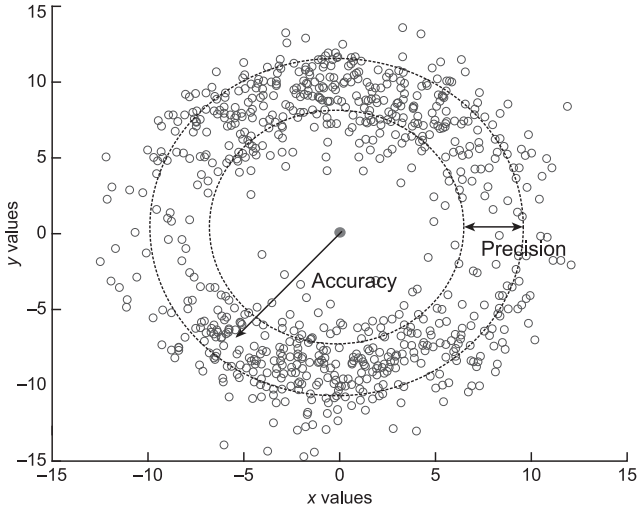

FIGURE 2.1

Difference between accuracy and precision.

Considering the many points representing the estimations under the same condition, precision is the width of the distribution of points. The ensemble of all points is considered precise when they all have the same radial error. So, when the estimates are precise, although not necessarily accurate, the points form a well-defined geometry, with its radial distance from the true position defining the accuracy. The more these points are scattered, the lower the precision of the estimate and vice-versa. However, it is not possible to reliably achieve good accuracy in individual measurements without precision.

2.1.3.2 Integrity

Integrity is the capability of the system to continue with the promised performance in terms of quality under all conditions, and also to indicate when it fails to do so. Any service is adhered to with some minimum quantitative specification of the quality of service. So, it is necessary for the system to disseminate information on whether the performance parameters are within the specified warranted limits at any *time* or not. It also includes the ability to provide a timely warning of any failure to do so, the latency being of importance here. This is an important concept in navigation because the user, on the basis of the integrity values, may decide on the usability of the service.

2.1.3.3 Availability

Availability is defined by the probability that the navigation system will make the navigation signal accessible to the user within a specified coverage area with warranted quality, such that the user can find his or her position and time. So, the time

that simultaneously meets the condition of signal accessibility and service quality and integrity is accounted for in calculating the availability of a system. Availability is a function of both the physical characteristics of the environment and the technical capabilities of the service provided (Conley et al., 2006).

2.1.3.4 Continuity

Continuity is the probability that a service, once available, will continue to be available and perform during the period of a phase of operation. It is, thus, the ratio of the period of time that the service sustains to the total intended period of use of the service after the user starts using it.

2.1.4 Categories of satellite navigation

The satellite navigation may be categorized on different basis. For most of the categories, this basis is one of the characteristic parameters of the navigation service. To classify this, we mention briefly just some prominent categories of the satellite navigation system.

2.1.4.1 Primary and augmented navigation

Evident from the name itself, this category of navigation system is based on the elementary characteristics of the service in terms of the essential contents of its signal. A primary navigation service is one in which the basic signal, containing the necessary and sufficient information for estimation of absolute positions, time, and their derivatives, is offered to the users.

In contrast, an augmented navigation consists of additional infrastructure, processing, and signals over the primary services so that combinedly they can provide improved position and timing estimates over the primary services in terms of accuracy and reliability.

2.1.4.2 Global and regional services

The navigation service can also be categorized on the basis of the area of available service. On the basis of availability, which also defines the extent of the service, it can be categorized into global or regional services. For global service, the navigation signals from the systems are available across the globe at any point in time. For regional satellite navigation services, the availability of the signals is restricted only within a limited geographical region over the Earth. However, for regional services, the signals may be accessed beyond the defined area of service, but the specified quality of the service is not guaranteed there.

2.1.4.3 Open and restricted services

This category is based on the accessibility of the signals. A satellite navigation system may be termed an open service when its signal can be accessed by anybody, typically free of any direct charge. It is thus suitable for mass market applications and is generally popular in terms of use. Restricted service, on the other hand, is the service

where access to the usable signal is restricted to a certain closed group of users. It generally has some additional advantages over open services, in terms of accuracy, availability, and integrity. That is why, it normally has more protection against viable threats and unauthorized uses.

2.1.4.4 Standard and precise services

This division of the navigation system is based on the accuracy and precision of the navigational solutions offered by the service. Standard navigation services offer a fair value of accuracy and precision with the best possible estimation of positions and times. The performance is suitable for general navigational applications and is meant for the general use of the mass application. The precision services, as the name suggests, offer much higher precision, as well as accuracy, to the position and time solutions to their users and are typically meant for critical applications and strategic uses. That is why, precision services are restricted, whereas the standard services are open and free. A single system can offer two different services distinguished by their accuracy (Spilker & Parkinson, 1996).

2.2 Architectural components

The architectural components of a typical satellite navigation system consist of the following three segments (Spilker & Parkinson, 1996):

Space segment: This consists of a constellation of satellites orbiting the Earth in space and transmitting the necessary navigation signals, from which the user can derive his or her position.

Control segment: Consists of infrastructure, resources, and assets that monitor, control, and maintain the space segment satellites from the ground, and derive the necessary information to produce the navigation signal. It also keeps the system time.

User segment: This consists of the users who, upon receiving the signals from the satellites, derive their own position, thus availing the navigation service.

The schematic of the segments and their interactions is shown in Fig. 2.2.

To understand why we need such architecture, we have to start from the user segment. Although we shall discuss the user segment in greater detail in a later chapter, we need this preamble to understand the design of such architecture at this point. In navigation service, the user, as mentioned in Section 2.1, should be completely able to derive his or her position upon receiving the signal transmitted from the satellite. For deriving his or her own position, the user is required to know the position of the reference, which, in this case, is the satellite, and the receiver's range from it. Moreover, the user receiver needs to get this from more than one satellite. The range is calculated using the propagation time, and the latter is obtained by comparing the signal transmission time from the satellite with the signal receiving time at the receiver. So, the satellite clock, from which the transmission time is derived, is also required to be highly stable and accurate. Even a trivial clock shift at the satellite needs to be corrected at the receiver during estimation.

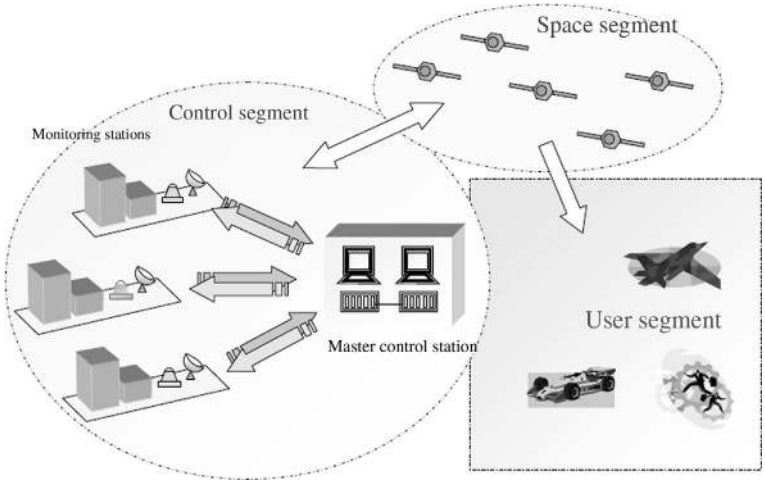

FIGURE 2.2

Segments of a Satellite Navigation System.

All these data, including the satellite position, transmission time of the signal, satellite clock correction factor, and much more similar information, need to be disseminated using radio aids to the user wherever the user is within the service area. Information should be transmitted in such a form that it may be directly obtained from the signal or derived from it through proper processing. This dissemination of information is necessary to be done synchronously from multiple satellites over the whole service area around the clock. This necessitates the use of a constellation of satellites and justifies the establishment of the space segment consisting of a constellation of satellites.

However, there must be some definite setup to control, maneuver, and monitor these satellites. The derived position, being a sensitive function of the position of the satellite, the latter needs to be precisely known. The positions of these satellites are hence required to be derived through proper monitoring of their dynamics and ground-based ranging. Any anomaly in the dynamic behavior of the satellite is to be corrected at the appropriate time. Similarly, a system time is required to be maintained, while any aberration in the satellite clock with respect to the system time is to be estimated for corrections. This is done by the ground-based control segment. The salient features of the three segments may be listed as follows:

Control segment:

- Situated on the ground.
- Multiple entities are connected through a network.
- Monitors the dynamics and behavior of the satellites in the space segments and their clocks.

- Predicts, updates, and uplinks data to be transmitted by the satellites.
- Commands maneuvers of satellites if necessary.

Space segment:

- Transmits the necessary data to the users for deriving the PVT information correctly.
- Orientation of satellites designed to serve the service area continuously.
- Design of space segment may be for serving local, regional, or global areas.
- Frequency and power levels are judiciously chosen for optimal performance.

User segment:

- Consists of the users of the service.
- User receive-only terminals to receive the transmitted data and compute their PVT.
- Receivers of different capabilities and accuracies are used.

Out of the abovementioned three segments, we shall take up and explain the Control segment in this chapter under Section 2.3. Chapters 3 and 4 will constitute the Space Segment and its aspects, including the signals, while Chapter 5 will contain the Receiver details and other aspects of user segments.

2.3 Control segment

We started with the notion of understanding the satellite navigation system with a system-independent perspective, covering all theoretical possibilities. Theoretically, the individual architecture of the different segments may vary, and the variations may depend on the nature of services offered and the area of service. Likewise, the control segment architecture is also determined by various factors. However, describing the architectural possibilities in a wide spectrum at this point will not be helpful in understanding, but will invite unnecessary complexity. So, instead of encompassing all such variants, we shall only concentrate on the commonality of the architectural features and discuss only these features in detail. It would be rather helpful if the reader, after completing the book, revisits this chapter once again to find any alternative possibilities of the architecture, which, I am sure, he or she will be capable of doing at that point.

The control system consists of assets and resources of the satellite navigation system situated on the ground, which are used to monitor, control, maneuver, and update the satellites in the space segments. These units of the complete architecture remain distributed over the entire service area and carry the necessary intelligence to perform the processes that help in the functioning of the system in an appropriate manner. Proper functioning of the system has the implicit meaning that the service requirements must be fulfilled effectively in their entirety.

First, let us find out what elements need to be present for the proper functioning of the service. The offerings of the service are the information-laden signal. This

must be made available to users via the navigation satellites. This, in turn, requires (1) knowledge of the proper location and dynamic behavior of the satellite and (2) proper generation of the signal. Therefore, a major objective of the control segment is to monitor the satellites in the space segment for their proper dynamic behavior, including their positions and attitude orbit, proper functioning, health, and the necessary station keeping. Any inconsistencies therein should be handled such that they do not affect the service. Second, the mandatory signal elements must be made available to the satellites to be successively transmitted to the user through the via the satellite. The ground control segment is also responsible for the important job of system timekeeping. For this purpose, it maintains the clock resources on the ground. Finally, it performs an overall management of ground assets.

The control segment architecture has the key driving requirements, such as the following:

- Proper provision of the control resources.
- Adequate redundancy of the resources commensurate with the system requirements.
- Appropriate location of ground elements to meet the overall objective.
- Generation of an independent timescale and achieving time synchronization across the system.

Architecturally, it is not a single entity but a collection of distributed resources, dispersed over the total service area of the system. The individual units that compose the control segment are the monitoring (and ranging) stations (MS), master control station (MCS), ground antenna system, system time keeping unit, and associated processing resources (Francisco, 1996).

2.3.1 Monitoring station

The monitoring station are the components of the ground segment used for the purpose of continuously ranging and tracking the navigation satellites and continuously receiving their signals for further utilization. To accomplish this end, these stations, comprising rugged reference receivers, are distributed over a diversified geographical region. Therefore, we shall discuss two aspects of MS, their receiver characteristics and their geographical locations, for effectively performing this job.

2.3.1.1 Receiver characteristics

The task of tracking the navigation satellites is accomplished by continuously receiving the signal and data they send. It is done by the reference receivers installed at these MS. From the received signal, the range measurements are done. These data also form the basis from which the performance of the satellites can be analyzed. The information derived from the navigation signal and the data, along with the local ground meteorological information, is communicated by the MS to the MCS for analysis. The information collected at these MS is processed at the MCS. The derived

parameters are required for the control of the system, to derive the future positions of the satellites and for the clock and other corrections.

Because the measured ranges are affected by the propagation impairments, such as the ionospheric delays, the measurements from these receivers are adequate to estimate and remove them from the ranges. Dual-frequency receiver data collected at the MS are used at the MCS for executing this correction. Furthermore, these channels are required to be calibrated to remove any interchannel bias. Likewise, all possible corrections to the signals are made.

The receiver, in general, continuously receives the profile signal which are used to obtain the profiles of the individual error components. The measurements are also used to derive the integrity of the signal. For such monitoring receivers, it is also important that any anomaly in the data is observed and identified. So, it is required to track the signal even if the signals are not consistent. Therefore, the MS are required to be equipped with receivers that can continue tracking the satellite signals even when they are heavily impaired. The receivers are expected to be adaptive enough to be able to accommodate such aberrations or abnormal data from satellites to the maximum extent possible. Moreover, the number of active channels should not limit the tracking of any visible satellite. To provide the necessary redundancy, the monitoring station receivers are installed in duplicate or even in triplicate, thus giving the system enough robustness against the loss of track by any of the stations.

Another requirement of the receivers at these monitoring stations is that they must have a stable clock. So, an atomic frequency standard with a precision counter is necessary to be running in these receivers. Besides, all such reference stations are required to be synchronized.

In addition to the satellite ranging data and other satellite data, the local meteorological data are also required to be collected at these sites to remove any signal ranging error due to the effects of tropospheric elements. For this, the receiver is collocated with meteorological sensors. The parameters of interest include the surface pressure, surface temperature, and relative humidity. The schematic of the monitoring station instruments is shown in Fig. 2.3.

2.3.1.2 Suitable positions

Because the monitoring station has to track the satellites around the clock, these stations are required to be distributed in such locations that the combined set of stations does not lose the visibility of any of these satellites. That is why the selection of the station locations across the whole service region is to be done in a manner so that all the satellites are visible to some of the MS at all times throughout the period of operation.

To serve the objective of deriving future satellite positions, their current positions are required to be estimated. This is done by measuring the satellite ranges by more than one monitoring station and deriving the satellite positions from them. The position estimation solutions are better when the MS are maximally dispersed. So, these stations are most often distributed across the globe for a global system. For regional systems, they are widely spread across the

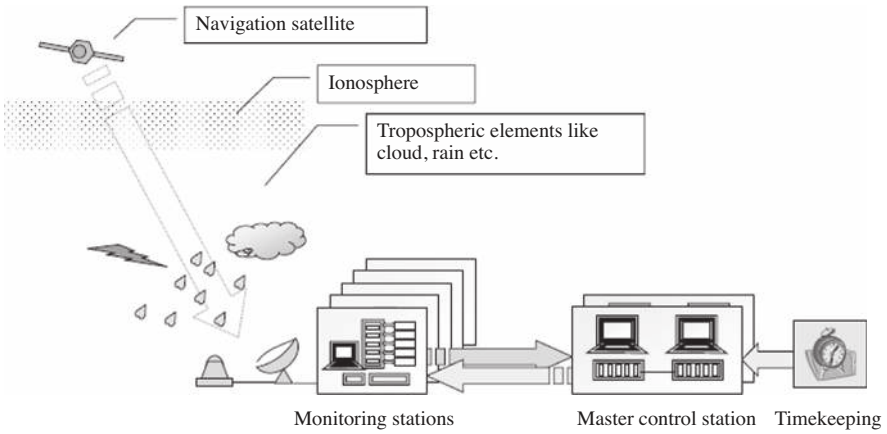

FIGURE 2.3

Schematic of Monitoring Station Instruments.

service area. The station locations must permit multiple stations to range simultaneously from multiple stations at any instant of time, and for each of the satellites.

To maximize the period that a monitoring station sees a particular satellite, their locations must be such that the satellite visibility is not restricted, even for low elevations of the satellite. Accordingly, the locations of the MS may be selected where there is clearance up to this lower elevation angle. A suitable elevation cutoff is kept to avoid large propagation through the troposphere and multipath. However, performance monitoring of satellites can still be continued to even lower elevations. So, locations near the coasts over the oceanic islands are deemed suitable, particularly for global services. This is because when the receivers are installed at well-planned positions here, they do not have the issue of blockage of lower angles, and the horizon-to-horizon visibility extent is large.

The finite inclination of the satellite orbits allows the satellite to traverse equally to both hemispheres. For the purpose of even vision of the satellites during their excursion on both hemispheres, equatorial locations are suitable for global operations. This allows viewing of the satellite up to the extreme ranges of the satellites in both hemispheres. With a large part of the equator being on the oceans, it facilitates both of the previous criteria. However, this may not be possible for regional services where the MS are required to be restricted within a limited geographical boundary, typically, but not necessarily, within the service area.

The precise location of the MS receiver may be identified through precise surveying, on which the accuracy of the satellite position estimation is dependent. Moreover, a noise survey is also needed to eliminate the influence of any external noise on the measurement system of these stations.

Individual MSs, located across the service area, must be connected with the central MCS to form a network. Therefore, there must be secure communication channels connecting these units with proper redundancy. This provides the required digital communication with the highest order of availability. High-speed optical or microwave data links are preferred options for establishing such networks. However, VSAT communication systems may also be used as a standby.

These MSs, although geographically separated, operate under the control of the MCS. It is from the MCS that the tracking orders and configuration commands come. It is also necessary to synchronize the clocks of the MS.

2.3.2 Ground antenna

The ground antenna is required for communication of data and commands between the satellite and the control segment. It should have a full duplex channel. Through its uplink channel, the satellite commands and navigation data are uploaded to the satellite. The telemetry, containing the satellite status information, and the satellite's response to the ground commands, satellite health, status and other related data are received from the satellite through the downlink.

Because this is entirely meant for communication, suitable lower bands and larger antenna sizes are used. It provides a large signal-to-noise ratio for reliable communication even at lower elevations, where the noise is naturally large.

Because of the similar criterion of visibility of the satellites like the MS, the locations of these antennas are also required to be globally distributed or across the regional area of service. Data upload can take place without any problem at any selected time. Moreover, these antennas also need to be always connected to the MCS and controlled by it in the same way as the MS. So, despite the ground antennas being a separate architectural entity of the control segment, they can be physically collocated with the MS. Over and above, collocation of these two resources helps in managing them efficiently.

The ground antenna can also support additional ranging in this communication band if necessary, using two-way techniques.

2.3.3 Master control station

Master control station is the site of processing measured data for deriving the navigation data, for assessment of the system, for taking decisions, also for generating and executing commands for the control and maneuvering of the system.

The MCS is a central element of the system, consisting of the computational resources and decision-making facilities for the proper management of the system. It analyzes the data received from the navigation satellites through the MS and, from the same, it derives and monitors the health and performance of the individual satellites. It also takes requisite decisions for necessary actions with consequent issuance of appropriate commands. In addition, it also generates the input to the navigation

message. Moreover, it manages the proper functioning of the different units of the control segment, including the monitoring station and the ground antenna. Besides, the MCS also keeps the system clock ensemble from which it derives the system time using a definite algorithm. So, the MCS is responsible for all aspects of constellation command and control, including routine satellite monitoring and maintenance, and also for any anomaly resolution. In addition to its scheduled job of navigation message generation and upload, it also performs the management of signal performance and timely detection of failures. In a word, it is the brain of the whole system.

2.3.3.1 Data processing

As discussed in the previous section, the MCS is connected with the MS that tracks the individual satellites and dispenses them with the data. The processing done at the MCS on this data forms the basis of all further actions and decisions taken here.

These data, received in almost real time from the different MSs, are passed on to the processing facility of the MCS. Here, all the processing resources are available, so that both the regular and the critical data are continually and simultaneously processed. The centralized processing architecture not only makes the best processing resources available to the data but also makes the distribution of the processed products through various distributed units easier.

The total process to convert the raw data collected at the monitoring station to a packaged database in a specific message format consists of the following steps (Dorsey et al., 2006; Francisco, 1996).

a) Measured data preprocessing.
b) System state estimation.
c) Navigation data frame generation.

2.3.3.1.1 Measured data preprocessing

The raw input data to MCS consists of satellite ranges and auxiliary data. The preprocessing of the data consists of correcting the measurement errors that remain in the measured ranges and other auxiliary data. It includes ionospheric error correction, tropospheric error correction, and other propagation error corrections, required to remove the excessive range estimates of the satellites. It also includes flagging and filtering of doubtful and inconsistent data, respectively. The ranges of the satellites measured at each of the MSs in two different frequencies are available to the MCS. From this, the ionospheric delay for the range measurements may be derived with precision. The derived delay is then used for the correction of the ranges. The meteorological measurements coming from these stations serve as auxiliary input. They are used to correct the range errors that occur as the satellite signal passes through the tropospheric regions of the atmosphere. The correction values may be derived using the standard models available for the purpose. Effects of the Earth's rotation during the propagation time also need correction. Hence, the Earth's orientation relative to the inertial scale also forms an important parameter for consideration. The range rate errors are also corrected. Thereafter, relativistic corrections and overall smoothing of

measured data are also performed. The carrier-aided smoothing is done to make the data ready for all further processing.

2.3.3.1.2 System state estimation

A planet in deep space follows a fixed path around its parent body in accordance with Newton's laws of motion. Its orbit is Keplerian or perfectly elliptical, and its position can be predicted exactly for any given future instant of time. A navigation satellite moves around the Earth under the Earth's gravitational field in accordance with the same laws. We shall learn about their motion in our next chapter in much more detail.

The navigation satellites, however, operating at an altitude of about 20,000 Km from the Earth's surface or even higher, are subject to external forces that produce orbital irregularities or perturbations. To improve the accuracy of the system, these perturbations must be accurately predicted such that the satellite positions are determined exactly at any instant of time. Measurements done at the MS are analyzed, and the estimation of different necessary dynamic parameters of the satellites is done using an advanced estimation algorithm. Estimation comprises position estimation to ephemeris generation. The required parameters are derived as system states in the presence of noise, for which a Kalman filter is typically used and provides excellent performance.

The current positions of the satellites are definitely one of the required states because, from this information, the trajectory will be derived and the future ephemeris of the satellites will be predicted. The measured range being a function of satellite and monitoring station positions, the range residuals from the values derived from surveyed MS position and approximate satellite position are attributed to the position error of the latter and timing inaccuracy based on their relative confidence. From this, the true positions and satellite clock aberrations are simultaneously estimated by the Kalman filter. The other parameters simultaneously derived are the clock drifts and sometimes the propagation delays. A consolidated filter using the inputs from all the MSs is used to give a better solution. Then, the total number of states derived is the solution of one large filter implementation.

Once the precise positions of the satellites and their temporal variation up to the current instant are derived, the trajectories of the satellites, including the perturbation effects, are determined. Subsequently, this up-to-date trajectory of the satellite is used to compute an orbit that best fits the same. The orbital Keplerian parameters are then obtained, which gives satellite positions for regular future time intervals (e.g., every minute for the following few hours). The geometry thus formed is also used to derive the expected perturbations from it.

However, there are many parameters other than the satellite parameters and clock corrections that need to be estimated. Because the MSs are located at well-surveyed positions and fixed, their locations are well known. But their relative clock offset and drift with respect to the system time may also be required to be established using the same filter. Furthermore, tropospheric wet delay correction values are also required to be estimated. The ionospheric corrections are already done using dual-frequency

measurements and dry tropospheric errors from the meteorological parameters during the preprocessing. Hence, these parameters need not be derived again.

The recursive estimates of the Kalman filter are comparatively efficient and provide numerical robustness to the systems (Francisco, 1996; Yunck, 1996). The state errors are to be kept at a minimum to a submetric level to support performance compliance. Errors add up when unmodeled components get included in the measurements or when the true temporal dynamics largely violate the assumed ones. So, to reduce these effects, any measurement blunders are blocked by fixing the range of possible measurement values and measurement variances. Periodic regeneration of output is performed whenever a force event is introduced that invalidates the model or when the residual for the filter indicates large nonlinearity.

2.3.3.1.3 Navigation data generation

The processed products at the MCS are used for generating the navigation message parameters. In fact, the derived parameters are used as input to the navigation data. To permit continued services, many advanced data sets may be generated a priori. Because the raw measurements are used for predicting the future orbits of satellites, the quality improves with an increase in measurement accuracy and number of MS. Typically, each set of the derived ephemeris is valid for a few hours, with the quality of prediction deteriorating with time. This is called the aging effect of the ephemeris. For this reason, it could be better if new sets of ephemeris had been available at smaller intervals. But the practical constraint is that this would require frequent estimations and uploads, increasing the load of the ground system. A greater concern is that a larger volume of data would be required to be uploaded to and stored at the satellite, which is preferably kept modest for various reasons.

The MCS needs to estimate parameters with stringent consistency to generate a high-quality navigation message with integrity. The message generation facility is important for reducing the computational load on the satellite. However, some functionalities may be housed in the satellites as the space technology evolves and advances through time.

The messages generated at the MCS are uploaded to the satellites for broadcasting to the user. To do this, the total navigation data sets are generated and arranged for regular uploading. Data sets transmitted are updated at periodic intervals to befit the accuracy requirements.

2.3.3.2 Telemetry and telecommand

The master station also requires the generation of a command for the configuration of MS and the satellites. These commands should reach the respective units for execution. However, the command generation, data transfer, and procedures should be highly secured and must be encrypted for the reason of security and authenticity, with the protocol being preestablished.

Analyzing the telemetry signal and generating telecommands are the responsibility of the MCS. The telemetry signals are continuously received at the ground antenna system. These signals are then required to be transmitted to the MCS through

secure channels. The collocation of the ground antenna with the MS gives the added advantage of transmitting this telemetry information through the same channel that delivers the ranging data to the MCS. The information thus received at the MCS may be used to generate activities.

When the information contained within the telemetry data is analyzed at the MCS, the analysis result, verifying whether values of different parameters inside the operable range, the operational state of the satellite, the operation of equipment, and verification of execution of commands, is used to make decisions on subsequent necessary actions. The decisions taken lead to the issuing of the telecommands, which are then required to be transmitted back through the command channels.

The MCS may also need to perform planned and unplanned station-keeping maneuvers. Communicating control signals to the satellite to initiate maneuvers and to change the state of operation, etc., are important tasks to be handled by the MCS.

The communication links thus require high availability and reliability in addition to security. Reliability and security may be achieved simply through encryption of the data and commands or by adding digital signatures to them. On the other hand, the onboard command handling facility and computing power enable information processing and execution of the command. The onboard processor can also make some decisions by itself. It reduces the load of the control segment to certain extent. But hierarchically, these autonomous controls must be much simpler and should not affect the system's operation.

2.3.4 Navigational timekeeping

2.3.4.1 International timekeeping

The Bureau International de Poids et de Mesures (BIPM), located in Paris, France, has the prime responsibility of global timekeeping. They compute and distribute the International Atomic Time (TAI) timescale, which is obtained by properly using and controlling data from more than 200 clocks distributed around the world (Lombardi, 1999; Petit et al., 2008).

However, TAI is an atomic clock time and has no relation to the solar day observed due to the spinning of the Earth, to which our conventional perception of time is related. So, they do not take into account the correction factors like the deceleration of Earth's rotation for correction and strictly adhere to the atomic definition of time. This makes TAI unsuitable for public time coordination.

To overcome this aspect, BIPM generates another timescale, called Universal Time Coordinated (UTC). This time is equivalent to TAI in terms of time progression. However, it accommodates corrections due to Earth rotation factors by keeping provision of the so-called "leap seconds," which are accordingly added to the TAI as necessary to ensure that the Sun crosses the Greenwich meridian precisely at 1200 h noon UTC with a precision of within 0.9 s when averaged over a year.

So, UTC is the reference timescale for the worldwide time coordination, providing the basis for the standard time in different countries and for different services.

2.3.4.2 System timekeeping

In navigation, time is the most important factor to be used for providing the services and to be disseminated to users. All derivatives are necessarily dependent on it. The control segment, therefore, needs to maintain the system timekeeping facility to generate, maintain, and distribute the reference system time. An ensemble of atomic clocks is used to keep the system time, and it may consist of a highly stable active hydrogen maser (AHM) and a cesium atomic clock, with appropriate time and frequency measurement equipment. The AHM clocks exhibit the best short-term stability, whereas cesium clocks exhibit good long-term stability. Hence, the combination of the maser and cesium clocks provides excellent short- and long-term stabilities. Appropriate algorithms are used for combining the individual times of the clocks in the assembly and hence may generate the best system time.

For the realization of clock timings, the employed algorithms may assimilate individual measurements of atomic clocks through their weighted combinations. Weights are derived using some statistical techniques based on the standard deviation of variations of the individual clocks. In other words, the clocks are weighted based on their stabilities. Thus, the ensemble clock, which is now a weighted average of all the clocks, ensures high stability and accuracy of the resulting timescale. The master control center thus derives the system time, which is a statistical output. Therefore, the effective system clock is a "Paper Clock," rather than being a physical one. This system time, like TAI, is atomic and not related to geodynamics. Hence, the difference between the system time and UTC is always monitored, and a correspondence with UTC is maintained and provided to the users for correcting and converting the system time to UTC, as required.

For the sake of completeness of our discussion on clocks and timing, it is recommended that, before concluding the chapter, we briefly mention the basic physics of an atomic clock. This will help us in understanding how it acquires such enhanced accuracy and what makes even these atomic clocks drift. An atomic clock is a combination of an arrangement of atomic emission and electronics to probe the same. It works on the principle of *tuning* an ordinary oscillator with a precise reference. The reference is the emission due to an atomic electron transition from an excited state to a lower state of energy. When enclosed in some definite magnetic field, a particular atomic energy state of some specific atoms shows a hyperfine spectral splitting. If the emission from the ordinary oscillator is used to excite the electrons, the latter will absorb the incident energy and will jump from the lower to the higher of the states obtained as a result of splitting. These excited electrons, on transitioning back to the normal level, emit the radiation of energy equal to the energy level difference. This radiation has a frequency proportional to the energy difference. If the frequency of the incident energy derived from the ordinary oscillator used for excitation is gradually changed and the corresponding emission with the targeted energy difference measured, it will show a resonating effect when the frequency of the oscillator is exactly equal to the frequency corresponding to the energy difference of the transition states. If δE is the energy difference, then the frequency of the illuminating signal at which this occurs will be ν, where $\delta E = h\nu$ and h is Planck's

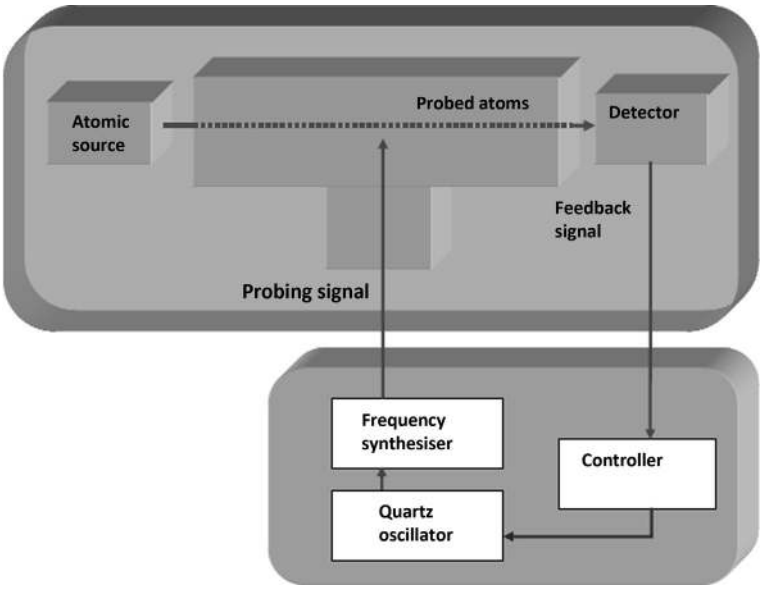

FIGURE 2.4

Schematic of an atomic clock.

constant. The emission may be observed by some well-responsive sensors to identify the maximum characteristic emission for resonance with maximum count of excited atoms. Once it is identified, the oscillator is fixed to the corresponding frequency that created the resonance. Thus, the ordinary oscillator is tuned precisely to the frequency, ν.

The activity of searching for the resonance frequency for the transition is called *probing*. The hardware used to probe the atoms consists of highly sensitive electronics with adequate protection from the external magnetic fields. The resonating condition is more accurately identified when the interaction time of the probe with the atoms is higher. The atoms thus need to be sloth, and the condition may be created by retarding the atoms and reducing their dynamicity. This can be done using lasers, a technique known as *laser cooling*. But this is possible only in large fountain clocks.

For an atom whose split levels of energy correspond to a frequency of ν, the time taken for ν numbers of oscillations to occur in such an emission is considered as 1 s. For different atomic sources, δE values are different. Consequently, ν is also different, making the numbers of oscillations that defines 1 s different for different atoms. The standard is defined for Cesium atoms, for which the frequency is 9,192,631,770 Hz.

A lucid elaboration of time and frequency measurements can be found in (Lombardi, 1999) and (Jespersen & Fitz-Randolph, 1997). A schematic figure of the arrangement of an atomic clock is shown in Fig. 2.4.

Conceptual questions

1. What could be the advantages and disadvantages of eliminating the control segment by adding all its functionalities in the space segment?
2. What methods can you devise to identify whether an anomaly detected in the measurements by MS is actual or measurement defects?
3. What are the alternatives to correcting the effects in the measurements when the clocks of the MS are not synchronized?
4. Assuming that the physical package performs identically, what are the features of the constituent atomic resonance cavity on which the accuracy of the clock is dependent? How is the reference set with respect to which the accuracy of the clock can be defined?

References

Conley, R., Cosentino, R., Leva, J. L., Haag, M. U., & Dyke, K. V. (2006). In: Hegarty, C. and Kaplan, E. (Eds.), *Performance of standalone GPS. Understanding GPS: Principles and applications (2nd Ed.)*. Arttech House, Boston, MA, USA.

Dorsey, A. J., Marquis, W. A., Fyfe, P. M., & Weiderholt, L. F. (2006). GPS system segments. In: Hegarty, C. and Kaplan, E. (Eds.), *Understanding GPS: Principles and applications. 2nd ed.* Artech House, Boston, MA, USA.

Francisco, S. G. (1996). GPS operational control segment. In B. W. Parkinson, & J. J. Spilker, Jr (Eds.), *Global positioning system: Theory and applications (1st ed.)*. AIAA. 435-465.

Jespersen, J., & Fitz-Randolph, J. (1997). *From sundials to atomic clocks: Understanding time and frequency*. National Bureau of Standards. Available at: https://digital.library.unt.edu/ark:/67531/metadc70421 Retrieved on 11 July 2013

Lombardi, M. A. (1999). *The measurement, instrumentation and sensors handbook*. CRC Press.

Petit, G., Jiang, Z., & Matsakis, D. (2008). Precise point positioning for TAI computation. *International Journal of Navigation and Observation, 2008*(1), 1687–5990. doi:10.1155/2008/562878.

Service, Wikipedia (2003) Available at: https://en.wikipedia.org/wiki/Service_(economics) Retrieved on 21 September, 2013.

Spilker, J. J., & Parkinson, B. W. (1996). Introduction and heritage of NAVSTAR, the global positioning system. In B. W. Parkinson, & J. J. Spilker, Jr (Eds.), *Global positioning system: Theory and applications* (1st ed.). AIAA. 3-28.

Yunck, T. P. (1996). Orbit determination. In B. W. Parkinson, & J. J. Spilker, Jr (Eds.), *Global positioning systems: Theory and applications*. AIAA, 559-589.

CHAPTER

Satellites in orbit 3

Preamble

This chapter is dedicated to describing the space segment of a satellite navigation system, particularly in terms of the positioning of the satellites. We learned in Chapter 2 that the space segment consists of satellites in their respective orbits that transmit navigation data to users. In this chapter, we shall learn about the important orbital parameters of these satellites and how to estimate their position using these parameters. Finding satellite positions, also known as reference positioning, is a mandatory task for final user position fixing. Here, we shall start our discussion with Kepler's laws that define the dynamics of satellites moving around the Earth. These laws and a few derivatives obtained from it will help us to obtain insight into the dynamics of satellites moving around the Earth and will also assist in finally deriving the satellite's position. We shall also learn about the different factors that perturb the satellite's motion. Finally, a few important orbits will be discussed, along with the rationale for selecting orbital parameters for different navigation purposes.

3.1 Kepler's laws and orbital dynamics

In Section 1.3, we learned that to define the position of a point, all we need is a predefined reference and the distances of the point from this reference along three definite axes. In a satellite navigation system, the position is described with respect to the geocentric reference frame, and the satellites act as the secondary reference points defined therein. Thus, to fix the position of any point in a designated coordinate system, the position of the satellites in that frame and the radial distances of the point from these satellites are needed. Therefore, these two parameters are extremely important and need to be readily available for the purpose of user positioning.

To know the position of the satellites, one must understand the dynamics of the satellites in orbit, and for that, it is necessary to know Kepler's laws. Johannes Kepler (1546–1630) was a German mathematician who examined the observational data of the planets moving around the Sun, prepared by his predecessor, Tycho Brahe (1546–1601), and formulated simple but useful laws. These laws are equally true for satellites moving around the Earth or for any other celestial bodies moving around another. Kepler's laws state that (Feynman et al., 1992):

Understanding Satellite Navigation, Second Edition. DOI: https://doi.org/10.1016/B978-0-443-36432-7.00018-3

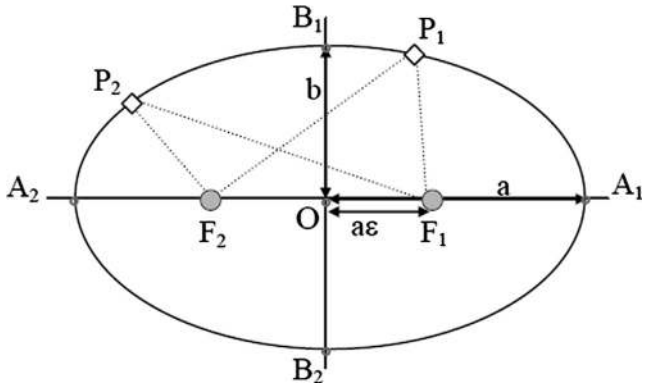

FIGURE 3.1

Geometry of an ellipse.

1. Every planet revolves around the sun in an elliptical orbit with the Sun at one of its foci.
2. A line joining a planet and the sun sweeps out equal areas in equal intervals of time.
3. The square of the orbital period of a planet is directly proportional to the cube of the semimajor axis of its orbit.

Why are these laws valid for any two celestial bodies? It is because these laws are basically derivatives of the fundamental gravitational laws, which are universal.

Our objective here is not to prove Kepler's laws. Rather, we shall see how, by using these laws, we can conveniently find the position of the satellites. For this, we require some elementary knowledge of geometry and will need to recall the law of gravitation.

3.1.1 Ellipse

We start with the geometry of an ellipse, which, according to Kepler's first law, is the shape of the orbit. An ellipse is a variation of a circle in which the radii along two orthogonal directions are different. Thus, it is like a circle compressed along one direction, as in Fig. 3.1. The greatest diameter, A_1A_2, is called the major axis, whereas the shortest diameter, B_1B_2, is called the minor axis. These two axes normally intersect at the center of the ellipse, O. There are two points, F_1 and F_2, equidistant from the center on the major axis, each called the focus of the ellipse. Their significance follows from the standard definition of the ellipse. It states that an ellipse is formed by the locus of a point that maintains a constant sum of distance from two fixed points on the major axis. These two fixed points are the foci of the ellipse, F_1 and F_2. A simpler way to say the same thing is that if you take any point on an ellipse and find that the sum of its distances from the two foci is C, then for any other point on the ellipse, the sum will also be C. Therefore, referring to Fig. 3.1,

$F_1P_1 + P_1F_2 = F_1P_2 + P_2F_2 = C$. The greatest radius of the ellipse, $OA_1 = OA_2 =$ "a," is called the semimajor axis, whereas the shortest radius, $OB_1 = OB_2 =$ "b," is the semiminor axis.

3.1.1.1 Eccentricity (ε)

The ellipse has two-dimensional geometry; hence, its shape can be represented by two independent parameters. Typically, semimajor axis "a" and semiminor axis "b" are used for this purpose. But here, we shall use the semimajor axis and the eccentricity. Eccentricity, ε, has a definite relation with "a" and "b," given by:

$$\varepsilon = \sqrt{1 - \left(\frac{b}{a}\right)^2} \tag{3.1A}$$

or,

$$b = a\sqrt{1 - \varepsilon^2} \tag{3.1B}$$

Therefore, it relates between the two parameters, "a" and "b," one of which can be derived from the other. The distances of each of the foci from the center (i.e., OF_1 and OF_2) of the ellipse are equal and are given by:

$$f = a\varepsilon \tag{3.2}$$

Thus, eccentricity indicates how far the focus is away from the ellipse's center. It is much like the way it is used in literary terms. Zero eccentricity refers to the state in which the semimajor and semiminor axes are equal, i.e., $a = b$. Then $f = 0$, with the foci coinciding with the center. Consequently, the ellipse is converted into a circle. The larger the value of ε is, the further the focus is from the center, with a larger difference between "a" and "b." The geometry tends toward a straight line as ε approaches unity.

Taking any focus—say, F_1 in Fig. 3.1—the distance to the vertex A_1, shown in the figure as F_1A_1 is the shortest range of any point on the ellipse from F_1. Since we shall relate this to the elliptical orbit of the satellite around the earth, we shall call this vertex point A_1 as the point of perigee, or simply perigee, for the focal point F_1. Similarly, F_1A_2 is the longest range, with A_2 known as apogee. These perigee and apogee distances may be obtained by subtracting and adding the focal length, respectively, to the length of the semimajor axis. Therefore, we get

$$F_1A_1 = F_2A_2 = a(1 - \varepsilon) \tag{3.3A}$$

$$F_1A_2 = F_2A_1 = a(1 + \varepsilon) \tag{3.3B}$$

and

$$F_1A_1/F_1A_1 = (1 - \varepsilon)/(1 + \varepsilon) \tag{3.3C}$$

From the above equations, we get that the sum of the distances of A_1 from F_1 and F_2 is $a(1 - \varepsilon) + a(1 + \varepsilon) = 2a$. Similarly, the sum of the distances of A_2 from F_1 and F_2 is 2a. With A_1 and A_2 as points on the ellipse, this corroborates the fact of the equal

sum of the distances from the foci to the point on the ellipse. Extending this, we can conclude that the sum remains 2a for all other points on the ellipse.

3.1.2 Elliptical orbit

From Kepler's law, we know that the orbit of the satellites revolving around the earth is elliptic. However, this includes the possibility that the orbit is circular, because a circle is a special case of an ellipse with zero eccentricity.

Before proceeding further, we need to discuss how the shape of the elliptical orbit of a satellite is realized and maintained in space. This can be obtained by considering that in such a two-body problem, the forces acting on the orbiting satellite are gravitational, attracting the satellite toward the Earth, and centrifugal, directed radially outward, owing to its cross-radial velocity. Furthermore, if no external forces are acting and the Earth is relatively fixed, then by virtue of a law of physics, a dynamic variable of the satellite called angular momentum remains unchanged. This is called the conservation of angular momentum. Angular momentum is given by

$$L = m\,\mathbf{v} \times \mathbf{r} \tag{3.4A}$$

Here, v is the linear velocity of the satellite with mass "m," and "r" is its radial distance from the center of the Earth. By virtue of Kepler's law, the center of the Earth is the focus of the orbit of the satellite. The cross-product $v \times r$ multiplies "r" with the component of v perpendicular to r only. Thus,

$$L = mv_\theta r \tag{3.4B}$$

where, v_θ is the cross-radial component of the velocity of the satellite. For circular orbits, v_θ is equal to the total velocity, v. If the satellite mass m is fixed, the term $v_\theta r$ is a constant.

You may have recognized that this is synonymous with Kepler's second law. From Fig. 3.2, we can see that the area swept by the satellite at the center of the Earth is

$$A = \frac{1}{2}\int_s r \times ds \tag{3.5A}$$

where, r is the radial distance of the satellite from the center, and s is the linear path traversed by the satellite. Thus, the area traversed per unit time by the satellite is

$$\frac{dA}{dt} = \frac{d}{dt}\left\{\frac{1}{2}\int_s r \times ds\right\} \tag{3.5B}$$

Assuming "r" to be invariant over the infinitesimal time dt, this can be written as (Roychoudhury, 1971).

$$\begin{aligned}\tfrac{dA}{dt} &= \tfrac{1}{2} r \times ds/dt \\ &= \tfrac{1}{2} r \times v \\ &= \tfrac{1}{2} r v_\theta\end{aligned} \tag{3.6}$$

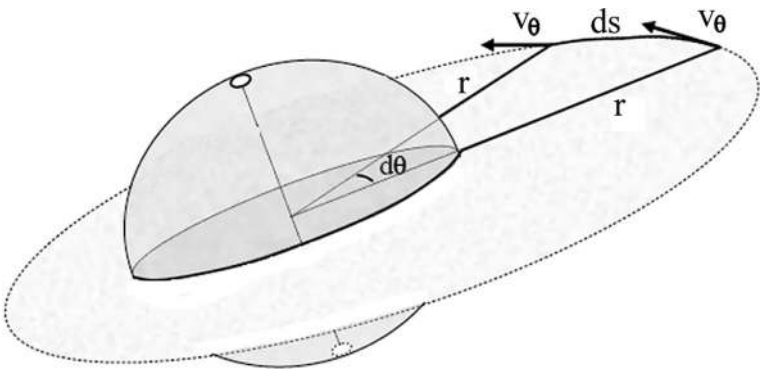

FIGURE 3.2

Area swept by satellite.

Because we have seen that the angular momentum, rv_θ, is a constant, half of it must also be so. This makes dA/dt a constant. Thus, Kepler's second law is an alternate way of stating the basic physical law of conservation of angular momentum for the planets and satellites.

To understand the formation of an elliptical orbit, let us start with the hypothetical condition that the satellite is at an infinite distance from the Earth. At this distance, it will remain out of the influence of the Earth, with no gravitational force acting upon it. Therefore, with no mutual force existing, the potential energy, PE, of the Earth–satellite system under this condition is zero.

However, as the satellite comes within a finite range, owing to the Earth's gravitational pull, the satellite starts moving toward Earth. This force is given by $F = -\mu/r^2\mathbf{r}$, where $\mathbf{r}$ is the unit vector directed radially outward from the center of the Earth and $\mu = GM$, where G is the gravitational constant of the Earth, and M is its mass. r is the distance of the satellite from the center of the earth. Because most orbital parameters are independent of mass, in the expressions here and in all subsequent derivations, we shall consider unit mass. We will mention at the appropriate place where the mass of the satellite is to be multiplied for generating the pragmatic conditions. As the satellite moves under the influence of the Earth's gravitational force, work is done on the satellite by the force; this work amounts to

$$\begin{aligned} W(r) &= \int_{\infty}^{r} -\frac{\mu}{r^2} \cdot dr \\ &= \mu/r|_{\infty}^{r} \\ &= \mu/r \end{aligned} \tag{3.7A}$$

where, the satellite is at any finite distance r from the center of the Earth. The potential energy of the system, which by definition, is the work done "by the body against the force," is thus $-W$. This was initially zero, but now it turns negative and is

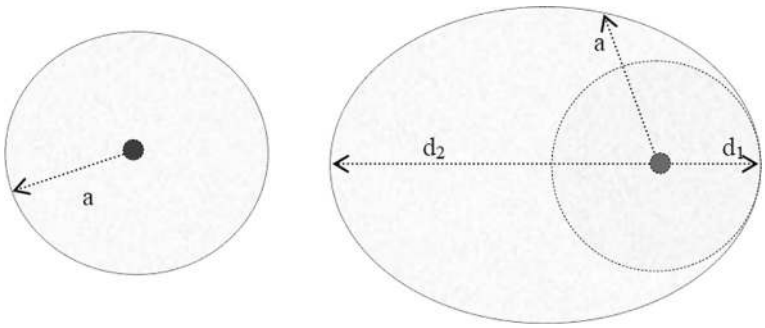

FIGURE 3.3

Circular and elliptical orbit.

equal to

$$\begin{aligned} PE(r) &= -W \\ &= -\mu/r \end{aligned} \tag{3.7B}$$

The negative value of potential energy indicates that effective work has been done on the body along the force. Hence, the potential energy of this two-body system has been lost to reach a final negative value, and the satellite has come under the influence of the gravitational force. Therefore, it will eventually fall to the earth unless some opposite force acts upon it. Such a force can be imparted to the satellite if it revolves around the Earth. The cross-radial motion during the revolution creates a centrifugal force opposite the gravity. The force amounts to v_θ^2/r at a range r from the Earth's center, where v_θ is the cross-radial component of the linear velocity of the satellite. For circular orbits, this velocity is always equal to the total velocity, v. For other shapes of orbit, v_θ is only a component of v while a finite radial component, v_r, exists. This velocity v required for the condition of force balance adds some positive kinetic energy (KE) to the satellite.

Now, consider the left of the Fig. 3.3. For a satellite at a distance "a" from the earth's center, if the velocity v is always cross-radial in direction and "just appropriate" in magnitude such that the resultant centrifugal acceleration v^2/a balances the gravitational acceleration μ/a^2, then in absence of any net acceleration on the satellite, the radius is maintained at the constant value "a." Therefore, we obtain circular orbits with a constant radius. The required condition is thus

$$\begin{aligned} v^2/a &= \mu/a^2 \\ v &= \sqrt{\frac{\mu}{a}} \end{aligned} \tag{3.8A}$$

Replacing the velocity with the constant angular momentum for unit mass, $L = va$, we get

$$\begin{aligned} L^2 &= \mu a \\ \text{or, } L^2/\mu &= a \end{aligned} \tag{3.8B}$$

Here, the term μ is a physical constant already defined before. Now, for the term L, although it remains constant for a closed system, we can adjust its value for a satellite by imparting a definite cross-radial velocity at a definite radius. Thus, the value of L determines its equilibrium radius "a" for a circular orbit. Remember that this L is the angular momentum of the satellite per unit mass. Therefore, when the satellite mass is "m," the total angular momentum must be divided by "m" to get the corresponding value of "L." Thus, to provide a definite circular shape to an orbit of any arbitrary radius "a," the satellite at distance "a" from the Earth's center should be given and maintained with a cross-radial velocity of $v = \sqrt{\mu/a}$, as in Eq. 3.8A. The corresponding L thus produced satisfies Eq. 3.8B.

Under such a condition, the kinetic energy of the body is $KE = ½\ v^2$ and the potential energy is $PE = -\mu/d$. Putting $d = a$ and replacing the value of v in the expression for KE and adding, we get the total energy TE as

$$\begin{aligned} TE &= -\mu/a + \frac{1}{2}v^2 \\ &= -\mu/a + \frac{1}{2}\mu/a \\ &= -\frac{1}{2}\mu/a \\ &= -\frac{1}{2}\mu^2/L^2 \end{aligned} \tag{3.9}$$

Here, we have used the fact that under balanced conditions, $a = L^2/\mu$. This equation states that the total energy of the body is negative and determined by the value of L or the radius "a." It increases toward zero as "a" increases, and ultimately, on reaching zero, it sets itself free from the control of the force.

Because the effective total energy remains negative, the Earth–satellite system remains coupled under the influence of the Earth's gravitational field. Only when some excess positive energy is acquired by the satellite, the total energy becomes zero again. Energy can be added by adding motion to the satellite, and only then will it be free from the influence of the Earth, even at finite range r. For this, the requirement is that the energy of a satellite in circular motion at a radius "a" must be increased by an additional amount of ½ μ/a, to make the total energy zero. Thus, if the incremental energy for making the satellite free from the field is expressed as ΔE,

$$\Delta E \geq \frac{1}{2}\mu/a \tag{3.10}$$

If excess energy is provided to this satellite in circular orbit with radius "a" through the additional cross-radial velocity, so that its final value is v, the excess energy added is given by

$$\begin{gathered} \Delta E = \text{Finalenergy} - \text{Initialengery} \\ \left(\tfrac{1}{2}v^2 - \mu/a\right) - \left(-\tfrac{1}{2}\mu/a\right) \\ \left(\tfrac{1}{2}v^2 - \tfrac{1}{2}\mu/a\right) \end{gathered} \tag{3.11A}$$

This excess energy allows the satellite to deviate from its original orbit. To break free from the Earth's influence, this should be more than the amount ½ μ/a. Thus, the

excess energy above the balanced condition that is required to achieve the condition of no gravitational influence is given by

$$\frac{1}{2}v^2 - \frac{1}{2}\mu/a > \frac{1}{2}\mu/a \tag{3.11B}$$

Conversely, for the satellite to remain under the influence of the Earth and move in a closed orbit (Maral & Bousquet, 2006).

$$\begin{aligned} &\frac{1}{2}v^2 - \frac{1}{2}\mu/a < \frac{1}{2}\mu/a \\ &\text{or}, v^2 < 2\mu/a \\ &\text{or}, L^2/\mu < 2a \end{aligned} \tag{3.11C}$$

Eq. 3.11C could also be reached by considering the final energy to be less than zero. The detailed derivation is just for the purposes of understanding. Therefore, consolidating the facts we have discussed so far, the value of the angular momentum per unit mass of a satellite, L, at distance "a" from the Earth's center must be such that $L^2/\mu a = 1$ to maintain a circular orbit of radius "a." Furthermore, at this same location, if the L value is increased, it remains bound under the Earth's influence unless $L^2/\mu a \geq 2$ when it breaks free. But what happens to the orbit shape when the value of this term is between 2 and 1, or even less than 1? That is what we are going to learn next.

A variation of the circular orbit results is an elliptical orbit. To the right of Fig. 3.3, if the orbiting satellite at A_1 at a distance d_1 from the Earth has a velocity v_1 that is essentially cross-radial and is more than that required for a circular orbit,

$$\begin{aligned} &v_1 > \sqrt{\frac{\mu}{d_1}} \text{ or, } L^2/\mu > d_1 \\ \text{or,} \quad &L^2/(\mu d_1) > 1 \end{aligned} \tag{3.12A}$$

At the same time, the value of L is well within the limit to keep the satellite bound. Hence,

$$L^2/(\mu d_1) < 2 \tag{3.12B}$$

We call the factor L^2/μ, as the radius "h" of the equivalent circular orbit or the equivalent circular radius for a given L; then, Eq. 3.12A and B, respectively, turn into

$$\begin{aligned} &h/d_1 > 1 \text{ and} \\ &h/d_1 < 2 \end{aligned} \tag{3.12C}$$

To represent the amount by which the expression on the left-hand side is greater than 1, we add a small term to 1 to create the equality. Let this term be called ε' for now, to distinguish it from the conventional expression of ε representing the eccentricity of the ellipse. Thus, we say that

$$\begin{aligned} L^2/(\mu d_1) &= 1 + \varepsilon' \\ \text{or,} \quad h/d_1 &= 1 + \varepsilon' \end{aligned} \tag{3.13}$$

As $v_1 > \sqrt{\mu/d_1}$, there will be an excess centrifugal force over the gravitational pull, and consequently, some excess KE of the satellite over that required for a circular orbit at radius "d_1." Because of this excess centrifugal force, the satellite will initially gain radial acceleration and will move away from the circular path, gaining outward radial velocity, v_r. The radial distance r will gradually increase, and this will consequently decrease the cross-radial velocity, v_θ, to conserve L. However, the gravitational pull on the satellite will also lessen. The effective radial acceleration of the satellite at any distance r thus, will be

$$f_r = v_\theta^2/r - \mu/r^2 \tag{3.14A}$$

Replacing the term v_θ by an equivalent expression with constant L

$$f_r = L^2/r^3 - \mu/r^2 \tag{3.14B}$$

Because L and μ are finite constants and the first term falls off faster than the second with r, there must be a finite r at which this force becomes zero. Beyond this point, the net force changes direction and remains attractive toward the Earth. Therefore, the condition at the radius "r_0" where the forces balanced becomes

$$\frac{L^2}{\mu r_0} = 1$$

or,

$$r_0 = h \tag{3.14C}$$

Using this equation, we see that the balance of centrifugal force and gravitational force occurs when the radius is equal to the equivalent circular radius h for the imparted value of L. Replacing the L^2/μ term from Eq. 3.13A, we find that the forces balance under the condition

$$r_0/d_1 = 1 + \varepsilon' \tag{3.15}$$

The force reverses when "r" exceeds beyond that. Using Eqs. 3.12C and D, we can say that this reversal must occur between $d_1 < r_0 < 2d_1$ for the satellite to remain bound. It can easily be shown that for these two threshold cases, the corresponding ε' needs to be 0 and 1, respectively.

The orbital conditions are illustrated in Fig. 3.4. With excess initial centrifugal force, as the satellite moves radially outward, it gains radial velocity up to a point at which there is a force balance with no excess centrifugal force. Because of positive radial acceleration up to this point, there will be a finite radial velocity that will keep the satellite moving in a radial direction even at and beyond the point where the forces balance. Thus, even at this point of force balance, the satellite does not execute circular motion, as it does not stop its radial excursion owing to the continuing nonzero radial velocity. The radial velocity it has gained lets it continue to move radially outward. However, as it does so, exceeding the radius beyond this point, the gravitational pull starts to override the centrifugal force, and it experiences an effective inward force and becomes decelerated. As a result, its residual radial velocity gradually reduces to zero. Therefore, the total velocity becomes effectively cross-radial again.

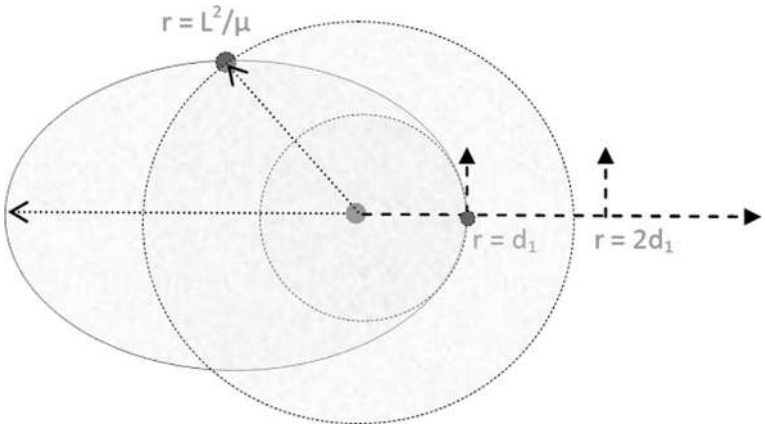

FIGURE 3.4

Orbits determined by L^2/m.

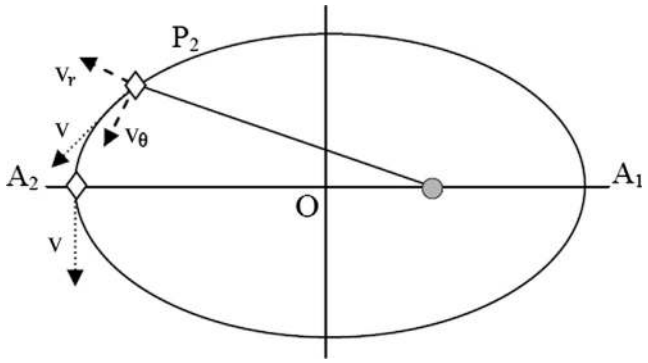

FIGURE 3.5

Velocity components of a satellite in an elliptical orbit.

The satellite has now reached its furthest point A_2 at a distance d_2. This point will be formed directly opposite A_1 is evident from the geometry of the ellipse, because at any other point except this, there is a radial component of the velocity, as shown in Fig. 3.5. From point A_2, with the effective inward force acting, it starts receding toward A_1 with gradually increasing radial velocity. The cross-radial velocity keeps the angular excursion increasing with the continued motion. As the radial distance again falls below r_0, the effective force again reverses direction. The satellite returns to the same condition at A_1, once again following an elliptical shape of orbit. This process continues.

The radial velocity at any intermediate points between A_1 and A_2 may be obtained by using Newtonian dynamics. The radial velocity v_r (r), when the satellite is at a radial distance r can be derived from the effective radial acceleration as (Strelkov, 1975).

$$f_r = v_\theta^2/r - \mu/r^2$$

$$\frac{dv_r}{dr}\frac{dr}{dt} = v_\theta^2/r - \mu/r^2$$

$$v_r dv_r = \left(v_\theta^2/r - \mu/r^2\right)dr$$

$$v_r^2/2 = \int \left(v_\theta^2/r - \mu/r^2\right)dr \tag{3.16}$$

where, we have taken the position of the satellite perigee as the initial condition when the radial velocity was zero. Replacing the expression for v_θ by L/r and integrating between $r = d_1$ to $r = r$, we get

$$v_r^2 = -L^2\left(1/r^2 - 1/d_1^2\right) + 2\mu\left(1/r - 1/d_1\right) \tag{3.17}$$

Using the force balancing condition, $r = L^2/\mu$, we can see that at the point of force balance, the radial velocity does not become zero. Rather, it becomes

$$v_r^2 = \mu^2/L^2 + L^2/d_1^2 - 2\mu/d_1 \tag{3.18}$$

For the satellite to remain held by the Earth's gravity, the gravitational force must supersede on the outward centrifugal force and consequently turn the radial velocity back toward the Earth. For that, the velocity must come down to zero at a finite value of $r \geq d_1$. To achieve the condition of $v_r = 0$, the criterion that must be fulfilled is

$$L^2\left(1/r^2 - 1/d_1^2\right) = 2\mu\left(1/r - 1/d_1\right) \tag{3.19A}$$

This relates radius "r" to known parameters L, μ, and d_1 when $v_r = 0$. One obvious solution to this equation for zero radial velocity is $r = d_1$, which is the condition with which we started. The other solution is $r = d_2$ such that

$$\begin{gathered} L^2/\mu = 2/\left(1/d_2 + 1/d_1\right) \\ \text{or, } 2/h = \left(1/d_1 + 1/d_2\right) \end{gathered} \tag{3.19B}$$

Points d_1 and d_2 in an ellipse with zero radial velocity are its apogee and perigee. We know that the sum of these two lengths is equal to twice the semimajor axis, a. Similar to that, the sum of the inverses of these two lengths is twice the inverse of length h, which is the equivalent circular radius. Using Eq. 3.19B, we get

$$2d_1/h = \left(1 + d_1/d_2\right) \tag{3.19C}$$

Using our definition of ε' and replacing its value from Eq. 3.13A, we get

$$\begin{gathered} 2/\left(1+\varepsilon'\right) = 1 + \left(d_1/d_2\right) \\ \text{or, } d_1/d_2 = 2/\left(1+\varepsilon'\right) - 1 \ = \left(1-\varepsilon'\right)/\left(1+\varepsilon'\right) \end{gathered} \tag{3.19D}$$

Now look at the ratio! This ratio of d_2/d_1 is the ratio of the apogee to the perigee of an ellipse, where the radial velocities are zero. As per the ellipse geometry, this is equal to $(1+\varepsilon)/(1-\varepsilon)$, where ε is the eccentricity of the ellipse, as in Eq. 3.3C. Thus, comparing the two, we can say that what we were calling ε' is nothing but the eccentricity ε of the elliptical orbit the satellite makes. Therefore, ε' and ε are identical (i.e., $\varepsilon' = \varepsilon$). So, using the expressions of Eq. 3.13, we get

$$d_1 = h/(1+\varepsilon) \text{ or, } h/d_1 = (1+\varepsilon) \tag{3.20A}$$

Again from Eq. 3.3A, $d_1 = (1-\varepsilon)a$. Thus, comparing the two, the semimajor axis of the elliptical orbit may be related to the equivalent circular orbit h for the given L by the relation

$$\begin{aligned} &h/(1+\varepsilon) = (1-\varepsilon)a \\ &\text{or, } h/a = \left(1-\varepsilon^2\right) < 1 \end{aligned} \tag{3.20B}$$

Hence, from Eq. 3.20A and 3.20B, we find that, although h is greater than perigee length d_1, it is always less than a. It is also evident that eccentricity ε of the elliptical shape of the orbit is determined by the equivalent circular radius h and, hence, in turn, by the value of L and the distance d_1 at which the velocity is fully cross-radial.

Therefore, let a satellite be moving in a circular orbit with radius d_1 and having angular momentum L_1 such that ${L_1}^2/\mu = d_1$. Then, if its angular momentum is increased to $L = L_2$, such that ${L_2}^2/\mu = h_1$, then the satellite starts traversing an elliptical orbit with eccentricity ε, such that $(1+\varepsilon) = h/d_1$ and with semimajor axis $a = d_1/(1-\varepsilon)$.

Once the shape of the elliptical orbit is defined by "a" and "ε," we may be interested in defining the position of the satellite in this orbit. This may be done by using the angle obtained at the focus or center of the ellipse by the satellite. To do so, we define three angular positions, as discussed subsequently (Maral & Bousquet, 2006; Pratt et al., 1986).

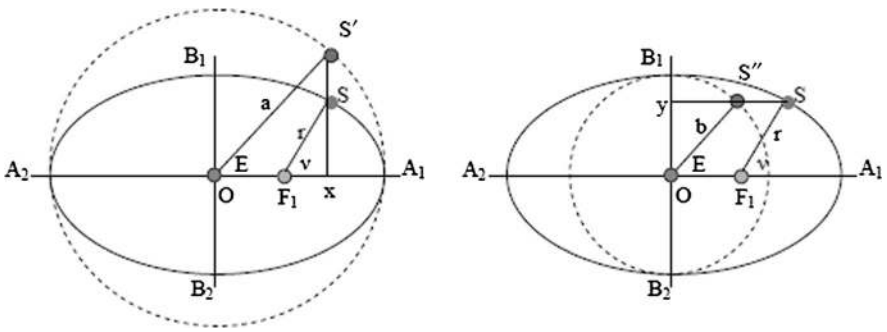

FIGURE 3.6

True anomaly and eccentric anomaly.

3.1.2.1 True anomaly (ν)

True anomaly of a satellite is the angle subtended by the satellite at the focus of its elliptical orbit at any instance between the direction of the perigee and the direction of the satellite, counted positively in the direction of the movement of the satellite (Fig. 3.6).

If ν is the angle of true anomaly, the expression for range "r" of any point on the ellipse as a function of ν becomes

$$r = a\left(1 - \varepsilon^2\right)/(1 + \varepsilon \cos \nu) \tag{3.21}$$

You can validate this by comparing the ranges for $\nu = 0°$ and $\nu = 180°$, and also by putting $\varepsilon = 0$ for a circular orbit. The variations of the orbital shapes and corresponding parameters of the satellite with true anomaly of the orbit has been elaborated in the MATLAB exercise given in Box 3.1.

3.1.2.2 Eccentric anomaly (E)

Now, let us consider a Cartesian coordinate with an origin O at the center of the ellipse with eccentricity ε and semimajor axis 'a'. The positive x-axis is along the direction of perigee on the semimajor axis, and the y-axis is along the semiminor axis, as in Fig. 3.6.

To understand the eccentric anomaly, let us consider a circle, concentric with the ellipse and with radius "a," equal to the semimajor axis of the ellipse. The circle is called the principal circle for the given ellipse. Now, we assume an image of satellite S at S′ located on the principal circle and with the same x coordinate value as the actual satellite S located on the ellipse, that is, the projection of S' on the x-axis is the same as the projection of S on the same axis.

BOX 3.1 MATLAB EXERCISE

The MATLAB program orbit.m was run to generate the following variations of the radial range, radial and cross-radial velocity; angular momentum; and kinetic and potential energy with true anomaly. For a given initial perigee length of 7000 km, if the value of L exceeds that required for circular orbit by a factor of 1.25, the following shown in Fig. M3.1 plots are generated.

Run the program for different ranges and factors. See what happens when the factor is more than 1.3. You can approximately find the ratio of the ranges at the perigee and apogee from the results you obtain upon running the program. Find "a" and compare the expression for ε using it.

(*continued*)

BOX 3.1 MATLAB EXERCISE — *cont'd*

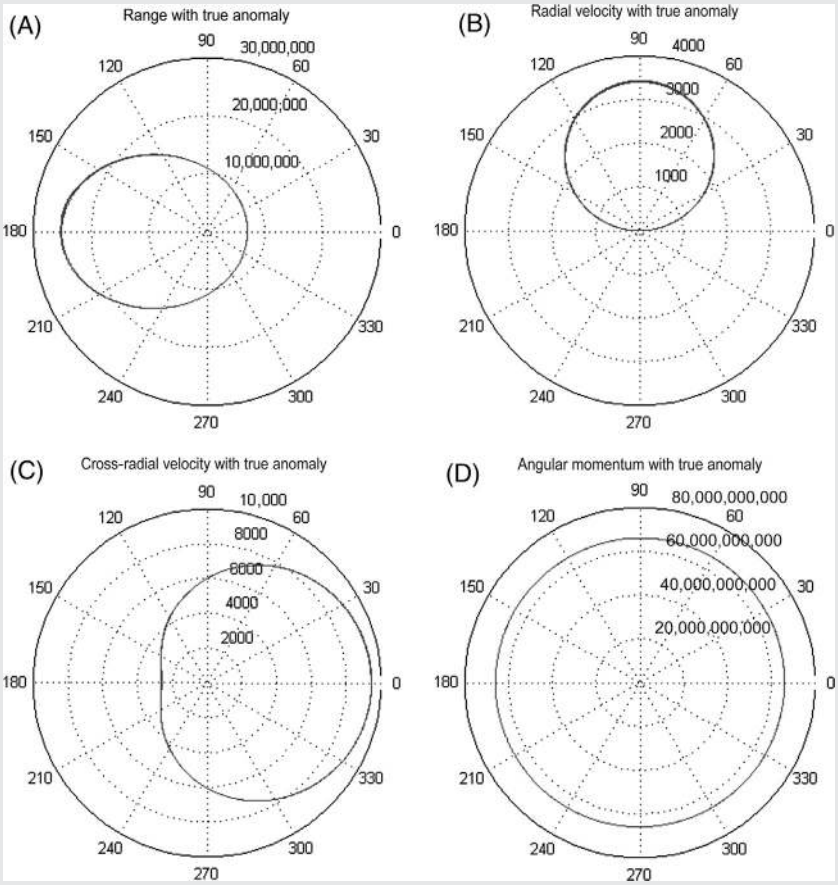

FIGURE M-3.1

Plots of orbital variables.

The angular argument of S′ at the center with the positive x-axis, which is also the direction of the perigee, is called the eccentric anomaly, E. It is also measured positively in the direction of the movement of the satellite. Similarly, if we consider a similar concentric circle with radius b and consider the image of S on this circle at S″ such that they have the same y coordinate, that is, S and S" have the same projections on the y axis, then S″ will also subtend the same angle at the center.

So, x and y may also be represented as

$$\begin{aligned} x &= a\cos E \\ y &= b\sin E \\ &= a\sqrt{1-\varepsilon^2}\sin E \end{aligned} \tag{3.22}$$

Fig. 3.6 shows the figures for deriving the relationship between true anomaly ν and eccentric anomaly E. Because the x projection remains the same for both cases, the relation can be expressed as

$$a\cos E = ae + r\cos n \tag{3.23A}$$

Thus, dividing the whole equation by a and replacing the expression for r, we get

$$\cos E = \varepsilon + \left(1-\varepsilon^2\right)\cos\nu/(1+\varepsilon\cos\nu)$$

or,

$$\cos E = (\varepsilon + \cos\nu)/(1+\varepsilon\cos\nu) \tag{3.23B}$$

Conversely,

$$(\cos E - \varepsilon)/(1-\varepsilon\cos E) = \cos\nu \tag{3.23C}$$

Therefore, one can derive the value of either the ν or E from knowledge of the other. Combining Eq 3.23A and C, the radial range r can be expressed in terms of E as

$$r = a(1-\varepsilon\cos E) \tag{3.24}$$

Another point to note is that because S′ (or S") is the image of S, the time S requires to traverse its complete elliptical orbit is equal to the time required by S′ (or S") to complete its circular orbit.

3.1.2.3 Mean anomaly (M)

From the third law of Kepler, it is evident that the time periods of satellites moving around the Earth depend solely on their semimajor axis, irrespective of their eccentricities. A satellite S_1 with any arbitrary eccentricity "ε" with a semimajor axis "a" will have the same period of revolution about the Earth as that of satellite S_2 in circular orbit with radius "a" and zero eccentricity. Thus, in Fig. 3.7, satellite S_1 and S_2 have the same period because they have the same semimajor axis $OA_1 = a$. If they start at the same time T_0 from point A_1, they will traverse their respective orbits and will complete a full rotation and come back to the same point at the same time instant T_1. It does not matter whether the focus is off-center, as for S_1, or at the center, as for S_2, even though satellite motion is governed by the force at the focus.

This is possible because satellite S_1 moves faster than S_2 when it is around its perigee, and is nearer to the Earth at "F_1" than S_2, which is at a distance a. But the leverage is equally lost, as at other times when S_1 is around its apogee, A_2. The distance being more than a, the satellite then moves slower than S_2. This is also evident

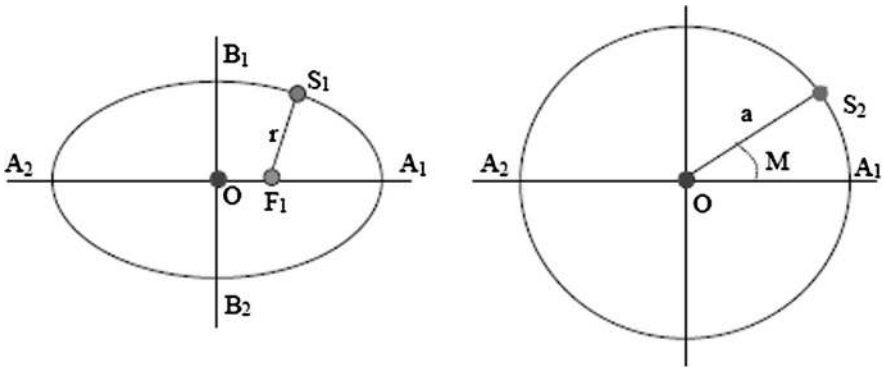

FIGURE 3.7

Mean anomaly and true anomaly.

from the fact that $v \times r$ of the satellite is constant, as mentioned in the explanation of Kepler's law.

Because both satellites will traverse 2π angular distance in equal time T, the mean angular velocity of the satellite S_1 in elliptical orbit is equal to the constant angular velocity of the satellite S_2 in circular orbit, and this is equal to $2\pi/T$. Thus, satellite S_2 in circular orbit may be considered to execute motion equal to the mean motion of any satellite in elliptical orbit with the same semimajor length (equal to the radius for the circular motion), as far as the angular motion is concerned. However, the instantaneous angles that the two will make at any instant t at the focus will be different. It is easier to estimate the angle made by S_2, but it is difficult to do so for S_1. Can we relate these two angles? Let us attempt to do that by relating the areas they sweep; if we succeed, then from the straightforward estimation of the first, we can derive that of the second.

First, let us consider that both S_1 and S_2 start from their perigee A_1 at the same time, $t = 0$, the mean anomaly, M of the satellites after any interval t is equal to the angle that S_2 makes in that time. In the same period of time, let the eccentric anomaly of S_1 be E.

To establish a relation between these angles that these two satellites sweep, let us first consider that in a complete time period of revolution T, the area swept by S_1 and S_2 will be D_1 and D_2, respectively. Then

$$\begin{aligned} D_1 &= \pi ab \text{ and} \\ D_2 &= \pi a^2 \end{aligned} \tag{3.25}$$

Furthermore, from Kepler's second law, individually, they will each sweep equal area in an equal interval of time. Thus, the sweeping rate of S_1 and S_2 will be,

respectively,

$$\dot{\mathrm{D}}_1 = \mathrm{D}_1/\mathrm{T} = \pi \mathrm{ab}/\mathrm{T}$$
$$\mathrm{D}_2 = \mathrm{D}_2/\mathrm{T} = \pi \mathrm{a}^2/\mathrm{T} \tag{3.26}$$

Therefore, the area sweeping rates are obviously constant for each, although they are different for the two satellites, and the area swept is a linear function of time. In any arbitrary time-interval t from t = 0, the area swept by S_1 and S_2 will be, respectively,

$$\Delta_1 = \mathrm{A}_1\mathrm{F}_1\mathrm{S}_1 = (\pi \mathrm{ab}/\mathrm{T})\mathrm{t}$$

$$\Delta_2 = \mathrm{A}_1\mathrm{OS}_2 = (\pi \mathrm{a}^2/\mathrm{T})\mathrm{t}$$

$$\text{So, } \Delta_1/\Delta_2 = \mathrm{b} : \mathrm{a} \tag{3.27}$$

We conclude from this that the ratio of the area swept by S_1 and S_2 on their respective orbits will always be in the ratio b:a.

In the physical world, the satellite S_2 on the equivalent circular orbit of radius "a" will have a constant angular velocity $\mathrm{n} = \sqrt{\mu/\mathrm{a}^3}$ and will make an angle $\mathrm{M} = \mathrm{n} \times \mathrm{t}$, in time t, with the reference axis along the perigee, where "t" is the time elapsed after it crossed the perigee. This angle M is thus the angle subtend at the center by the mean motion and is called the mean anomaly for the satellite in an elliptical orbit.

Now, using the relation established between the corresponding areas swept, it can be easily determined that the area swept by the mean motion at the center is

$$\Delta_2 = {}^1\!/_2\, \mathrm{Ma}^2 \tag{3.28}$$

Again, consider the geometry as in Fig. 3.8 with satellite S on its true elliptical orbit, and also its principle circle carrying its image S′. Let us consider areas $\mathrm{A}_1\mathrm{F}_1\mathrm{S}$ and $\mathrm{A}_1\mathrm{F}_1\mathrm{S}'$, which are the areas swept by satellite S on the true elliptical orbit and its projection S′, on the reference circle, in time t at focus F_1. From geometry, the corresponding areas may be related by

$$\mathrm{A}_1\mathrm{F}_1\mathrm{S} = \mathrm{A}_1\mathrm{XS} - \mathrm{F}_1\mathrm{XS} \text{ and} \tag{3.29A}$$

$$\mathrm{A}_1\mathrm{F}_1\mathrm{S}' = \mathrm{A}_1\mathrm{XS}' - \mathrm{F}_1\mathrm{XS}' \tag{3.29B}$$

$$\text{Now, } \mathrm{A}_1\mathrm{XS}/\mathrm{A}_1\mathrm{XS}' = \int_{\mathrm{x}}^{\mathrm{A}_1} y\,dx \Big/ \int_{\mathrm{x}}^{\mathrm{A}_1} y'\,dx = \int_{\mathrm{x}}^{\mathrm{A}_1} \mathrm{b}\sqrt{1-\frac{\mathrm{x}^2}{\mathrm{a}^2}}\,dx \Big/ \int_{\mathrm{x}}^{\mathrm{A}_1} \mathrm{a}\sqrt{1-\frac{\mathrm{x}^2}{\mathrm{a}^2}}\,dx = \mathrm{b}/\mathrm{a} \tag{3.30A}$$

Here, we have used the equation for the ellipse as $\mathrm{y}^2/\mathrm{b}^2 = 1 - \mathrm{x}^2/\mathrm{a}^2$, and that for the reference circle as $\mathrm{y}^2/\mathrm{a}^2 = 1 - \mathrm{x}^2/\mathrm{a}^2$. Again,

$$\mathrm{F}_1\mathrm{XS}/\mathrm{F}_1\mathrm{XS}' = \mathrm{XS}/\mathrm{XS}' = \mathrm{y}/\mathrm{a}\sin\mathrm{E} = \mathrm{b}\sin\mathrm{E}/\mathrm{a}\sin\mathrm{E} = \mathrm{b}/\mathrm{a} \tag{3.30B}$$

So,

$$\mathrm{A}_1\mathrm{F}_1\mathrm{S}/\mathrm{A}_1\mathrm{F}_1\mathrm{S}' = (\mathrm{A}_1\mathrm{XS} - \mathrm{F}_1\mathrm{XS})/(\mathrm{A}_1\mathrm{XS}' - \mathrm{F}_1\mathrm{XS}') = \mathrm{b}/\mathrm{a} \tag{3.31A}$$

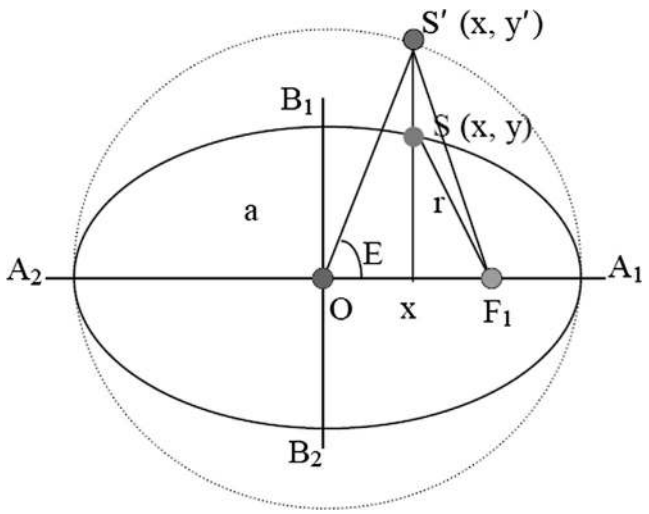

FIGURE 3.8

Relation between eccentric and mean anomaly.

Therefore, these two areas, A_1F_1S and A_1F_1S', are also in the ratio b:a. However, A_1F_1S is the true area swept by the satellite at the focus (i.e., $A_1F_1S = \Delta_1$). So,

$$\begin{matrix} \Delta_1/A_1F_1S' = b/a \\ \Delta_1/\Delta_2 \end{matrix} \tag{3.31B}$$

From the above equation, we can thus say that $A_1F_1S' = \Delta_2$, the area swept by the satellite with mean motion at the center in the same time. Again, from Eq. 3.28, we know that $\Delta_2 = ½\ Ma^2$. Therefore,

$$A_1F_1S' = \frac{1}{2}Ma^2 \tag{3.31C}$$

Using the equivalence in the geometry we have derived in the previous equation, we get

$$\begin{matrix} A_1F_1S' = AOS' - OF_1S' \\ \frac{1}{2}Ea^2 - \frac{1}{2}\ ae\ a\ \textit{sin}\ E \end{matrix}$$

So,

$$\frac{1}{2}Ma^2 = \frac{1}{2}Ea^2 - \frac{1}{2}a\varepsilon a\sin E$$

$$M = E - \varepsilon \sin E \tag{3.32}$$

This is also known as Kepler's equation, from which we can observe that at $E = 0$ and $E = \pi$, the eccentric anomaly and the mean anomaly become the same. Otherwise, M trails the E in the first two quadrants, whereas it leads the E in the next two. In general, we derive the value of E from M using iterative techniques.

So, we have established a relation between M and E, while the relation between E and n have already been obtained in Eq. 3.23. These three parameters, viz. ν, E, and M, can be transformed from one to the other. So, knowing the semimajor axis, we will know the angular sweep rate n of the mean motion of the satellite. Using time elapsed from the instant of crossing the perigee we can derive the mean anomaly, M. From M, we can obtain the eccentric anomaly, E, using Eq. 3.32 with the known value of eccentricity. Again, from the relation as in Eq. 3.23, between the eccentric anomaly and true anomaly, the latter may be derived conveniently. Therefore, knowing the semimajor axis, the eccentricity, and the time from crossing the perigee, we can derive the true anomaly, and hence the position of the satellite in the orbit. These three parameters are required to explicitly define the position of the satellite in its orbit.

3.2 Orbital orientation relative to earth

The discussion up to this point has defined only the shape of the orbit and the position of the satellite with respect to the direction of the perigee. Once the position of the satellite in orbit is known, it is necessary to find the orientation of the orbit with respect to the Earth. This is because, ultimately, we need the satellite position in Earth's reference. This may be done by fixing the orbit orientation in the Earth-centered inertial (ECI) frame. Therefore, we consider the ECI axes on the erect earth with the origin coinciding with the Earth's center. As per the definition of the ECI, the origin moves with the Earth's revolutionary motion, but the orientation of the axes remains fixed in space and does not change with the Earth's rotation or its movement in space.

3.2.1 Orientation parameters

We shall define the parameters that fix the orbit in space and the location of the satellite in the orbit with respect to the ECI (Maral & Bousquet, 2006; Pratt et al., 1986). These orbital orientation parameters are depicted in Fig. 3.9. To understand the definitions of these parameters, it is first necessary to appreciate that because the earth's center is at the focus of the orbit, it remains simultaneously on the orbital and equatorial (XY) planes. The orbital plane is the infinite plane passing through the geocenter and containing the orbit of the satellite. To define the orientation of the plane with respect to the equatorial plane, we need to define two parameters: inclination, *I,* and right ascension of the ascending node (RAAN), denoted by Ω.

3.2.1.1 Inclination (i)

The plane of the satellite orbit may make some definite angle with the equatorial plane of the Earth (i.e., the XY plane of the coordinate system). This angle is called

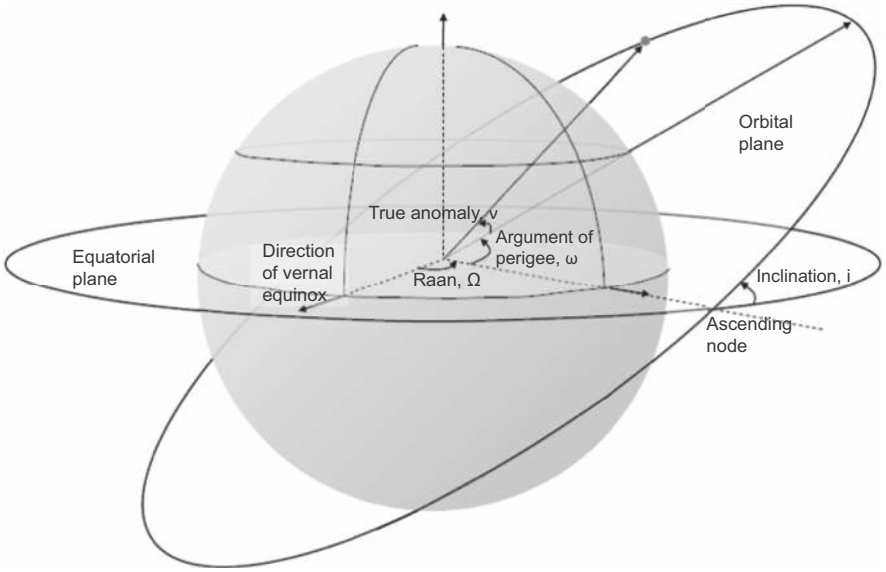

FIGURE 3.9

Orbital orientation parameters.

the inclination. We know that the focus of the orbit coincides with the center of the Earth on the equatorial plane. So, if we draw a vector perpendicular to the orbital plane (orbital plane vector) at the focus, the acute angle it makes with the positive z-axis, which is perpendicular to the equatorial plane, is also equal to the inclination.

3.2.1.2 Right ascension of the ascending node (Ω)

For the same inclination, there may be different azimuthal orientations of the orbit. This is also evident from the fact that the normal on the orbital plane at the focus can make the same angle with the z-axis (i.e., have the same inclination) for many different directions. Thus, the true orientation of the orbital plane is specified once the other parameter, Right ascension of the ascending node (RAAN) is defined.

The intersection of the orbit and the equatorial plane is a straight line passing through the Earth's center (i.e., the origin of the considered ECI coordinate system). This is called the Nodal line. This line simultaneously remains on the orbital and equatorial plane and cuts the true orbit at two points: one where the satellite moves from the southern hemisphere to the northern hemisphere, and the other where it moves from the north to the south. The first point is called the ascending node, and the second is called the descending node. The RAAN is the angle subtend at the center of the Earth between the direction of the ascending node and the positive x-axis of the ECI coordinate, measured positively. Defining otherwise, RAAN is the ECI longitude of the satellite's ascending node. This fixes the azimuthal orientation of the orbit.

These two parameters fix the orbital plane with respect to the equatorial plane. However, the orientation of the actual orbit on this plane has yet to be fixed. This is done by defining the parameter argument of perigee.

3.2.1.3 Argument of perigee (ω)

For a definite inclination and the RAAN, the plane of the orbit with respect to the Earth is fixed, but not the exact orbit itself on the orbital plane. On this defined orbital plane, different orientations of the major axis lead to distinctly separate orbits. For an orbital plane with a given "i" and "Ω," one orbit may have a semimajor axis perpendicular to the nodal line, whereas another may have the axis at a different angle made with it.

The argument of perigee is the angle made at the focus, measured positively on the orbital plane between the direction of the ascending node and the direction of the perigee of the orbit.

Now, with the Argument of perigee defined, the orbit is fixed on the orbital plane. It can thus be concluded that with these five parameters (a, ε, i, Ω, and ω) the orbit of the satellite can be completely defined in ECI frame without any ambiguity. Furthermore, the position of the satellite in this orbit, with respect to the perigee, can be defined by ν, which is obtained from M via E. Again, M can be derived from the semimajor axis "a" and time.

The sum of $\omega + \nu$ is the angle made by the satellite on the orbital plane with the direction of the ascending node at the Earth's center, measured positively from the nodal line. This angle is called the nodal angular elongation or argument of latitude, "u" (Maral & Bousquet, 2006). This is useful in the case of a circular orbit where the perigee is undefined.

Once it is defined, the orientation of the orbit about the Earth remains fixed with reference to space, that is, with respect to the ECI frame. But it always changes with respect to the Earth-centered Earth-fixed (ECEF) as the Earth spins. Thus, the coordinates in ECI are mostly converted to those in the ECEF frame for convenience, for which the angular motion of the Earth is required to be considered.

The shape and the orientations of a satellite orbit for different orbital parameters are derived in the MATLAB exercise of Box 3.2. Focus 3.1 describes the procedure for deriving the position coordinates.

BOX 3.2 MATLAB EXERCISE

Refer to Fig. M3.2A and B. The MATLAB program sat_pos.m was run to generate the coordinates in an ECI frame for orbits with two different sets of parameters. The first orbit has eccentricity $\varepsilon = 0$ and inclination $i = 55°$. The second orbit has $\varepsilon = 0.4$ and $i = 35°$, and $\omega = 10°$. The RAAN in both cases was about 32°. These coordinates were then plotted with a globe for referencing. However, the orbital range is scaled for better representation, and the following plots were generated.

(*continued*)

BOX 3.2 MATLAB EXERCISE — *cont'd*

Note how the eccentric anomaly is determined in the program using the nonlinear least-squares method. This can be replaced by the iterative Newton–Raphson method.

Run the program for different eccentricities, RAAN, and ranges and factors. See what happens when the parameters are changed. Because of scaling, sometimes the orbit may not be well represented compared with the globe.

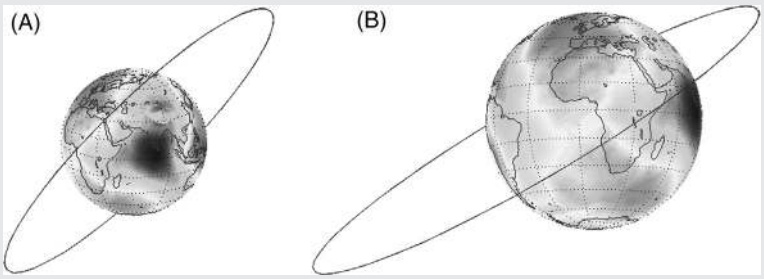

FIGURE M-3.2

Different orbital shapes.

Focus 3.1 Satellite coordinate derivation.

We have already seen how, from the given semimajor axis and time from the crossing of the perigee, we can derive the true anomaly, ν, through an estimation of the mean anomaly, M, and the eccentric anomaly, E. Given ν and five other parameters, we now attempt to find the coordinate of the satellite in ECI. Assume a Cartesian coordinate system with an origin at the focus, x-axis on the orbital plane along the perigee, and y-axis also on an orbital plane. The Cartesian coordinates of the satellite on these axes are:

$$\mathrm{x} = \mathrm{r} * \cos\nu = \mathrm{a}\{1-\varepsilon^2\}/\{1-\varepsilon * \cos\nu\} * \cos\nu$$

$$\mathrm{y} = \mathrm{r} * \sin\nu = \mathrm{a}\{1-\varepsilon^2\}/\{1-\varepsilon * \cos\nu\} * \sin\nu$$

These coordinates are transformed into another reference with the x-axis directed along the ascending node, and the y-axis on the orbital plane and perpendicular to the x-axis. Because ω is the angle between the new x-axis and the former (i.e., the perigial line), in the new frame the coordinates become:

$$\mathrm{x}_1 = \mathrm{x}\cos\omega - \mathrm{y}\sin\omega = \mathrm{r} * \{\cos\nu * \cos\omega - \sin\nu * \sin\omega\} = \mathrm{r} * \cos(\nu+\omega) = \mathrm{r} * \cos(\mathrm{u})$$

$$\mathrm{y}_1 = \mathrm{x}\sin\omega + \mathrm{y}\cos\omega = \mathrm{r} * \{\sin\nu * \cos\omega + \cos\nu * \sin\omega\} = \mathrm{r} * \sin(\nu+\omega) = \mathrm{r} * \sin(\mathrm{u})$$

We must appreciate that the sum $(\nu + \omega)$ is the nodal angular elongation, "u." Effectively, we have just decomposed the range vector components over this angle, as evident from this expression.

Consider another reference frame with an x-axis along the ascending node, a y-axis perpendicular to it but on the equatorial plane, and a z-axis perpendicular to it along the North Pole. This is only a rotation of the reference frame about the x-axis by the amount of inclination angle "i." The coordinates in this frame become:

$$x2 = r * \cos(u)$$

$$y2 = r * \sin(u) * \cos(i)$$

$$z2 = r * \sin(u) * \sin(i)$$

Effectively, we have just decomposed the y1 vector into its component on the equatorial plane and normal to it.

These coordinates convert to coordinates in the ECI frame, which is nothing but a rotation about the z-axis by angle Ω. The vectors become:

$$xi = r\{\cos(u) * \cos\Omega - \sin(u) * \cos(i) * \sin\Omega\}$$

$$yi = r\{\cos(u) * \sin\Omega + \sin(u) * \cos(i) * \cos\Omega\}$$

$$zi = r\{\sin(u) * \sin(i)\}$$

Using the intrinsic relation, the expressions become:

$$x_i = a\{(1-\varepsilon^2)/(1-\varepsilon * \cos\nu)\}\{\cos(\nu+\omega) * \cos\Omega - \sin(\nu+\omega) * \cos(i) * \sin\Omega\}$$

$$y_i = a\{(1-\varepsilon^2)/(1-\varepsilon * \cos\nu)\}\{\cos(\nu+\omega) * \sin\Omega + \sin(\nu+\omega) * \cos(i) * \cos\Omega\}$$

$$z_i = a\{(1-\varepsilon^2)/(1-\varepsilon * \cos\nu)\}\{\sin(\nu+\omega) * \sin(i)\}$$

For further converting it to ECEF, another rotational transformation of the coordinates about the current z-axis is required by an angle equal to the current ECI longitude of the ECEF X axis.

3.3 Perturbation of satellite orbits

The six parameters are sufficient to define the position of the satellite definitely in ECI. However, this is true only when the intrinsic assumptions taken are valid. The assumptions taken are:

a) The Earth is spherical with homogeneous density.

b) No force is exerted on the system that is external to the Earth and the satellite in question.
c) The mass of the satellite is small compared with the mass of the Earth.

In actuality, these assumptions are not perfectly correct. The deviations lead to the perturbations of the satellite motion. The most important of these factors are listed below.

3.3.1 Perturbation factors

3.3.1.1 Nonhomogeneity of the earth

In all of the previous discussions, it has been assumed that the Earth is perfectly spherical with uniform density. However, its shape is actually more closer to an oblate spheroid shape with varying density. Thus, the center of mass of the Earth is not exactly at the geometric center of its shape. Satellites revolving around the Earth experience different gravitational forces and hence adjust accordingly to different effective distances from the true location of the Earth's center of mass. It consequently changes the range and speed, deviating from the designated orbit. This affects the shape of the orbit and the direction of its axes, although to a small extent.

3.3.1.2 External forces

There are many celestial bodies present near the Earth and around the satellite. Among them, the ones that affect the motion of satellites the most are the moon and the Sun. The Sun, mainly due to its massiveness, and the moon, owing to its proximity, exert significant gravitational pull and perturb satellites from their designated course. Moreover, they result in a change in inclination angles and RAAN of the satellite orbital plane. The perigial direction is also deviated as a result. However, the perturbation is expected to be small and depends on the relative location of the satellite and these perturbing elements.

3.3.1.3 Aerodynamic drag

Satellites experience some opposing forces as they traverse the atmosphere, however thin it is. The drag is significant at low altitudes around 200 to 400 km, and negligibly low at altitudes above 3000 km. The atmosphere is vanishingly small at the orbital heights of the navigation satellites. So, the effect of atmospheric friction causes a negligible loss of energy, to a decrease in the orbital radius of the satellites. Cumulatively, over a larger time scale, the elliptical orbit may lose eccentricity and tend to become circular.

3.3.1.4 Radiation pressure

Solar radiation incident on a satellite exerts pressure on it. Satellite solar panels are kept open perpendicular to the solar flux to obtain maximum power and also receive maximum solar pressure. This pressure forces the satellite against its motion as it

moves toward the Sun during its orbit, while it adds to the movement when it recedes from the Sun. Effectually, it modifies the orbital parameters of the satellite.

Out of all these factors, the nonhomogeneity of the Earth and the external gravitational forces perturb the satellite orbit in such a way that the total energy of the system is conserved, whereas others dissipate energy from it.

3.3.2 Implications for the system

Because of these perturbations, the trajectory of satellites is not a closed ellipse with a fixed orientation in space, but an open curve that continuously evolves in time in both shape and orientation. These perturbations may be modeled to the extent of first-order variation. Because the effectual result of these perturbations is variation in orbital parameters, additional derivatives of the orbital parameters, such as da/dt, dε/dt, di/dt, dΩ/dt, and dω/dt, etc., become necessary to describe the position of the satellites more accurately. Because the final position estimation of the user is sensitive to the satellite's position, it is important to consider these parameters for their precision estimation.

From previous discussions, we know that the purely elliptical Keplerian orbit is precise only for a simple two-body problem under ideal conditions. Perturbations lead to a modified elliptical orbit with correction terms to account for these variations. Hence, the typical parameters transmitted in a satellite navigation system to make satellite positions available to users are more than just the six Keplerian parameters, so that the orbits estimated from these parameters are precise, at least to the first order of the perturbations.

Keplerian orbital parameters, along with the perturbation terms, are predicted for the near future by the ground monitoring facilities. They are derived from the range measurements using least-squares fitting of the orbit using a Kalman filter.

3.4 Different types of orbits

From previous discussions, we know that there are a few parameters that define the shape and orientation of the orbits. For example, the semimajor axis determines the period and the range, the eccentricity defines the shape of the orbit, the inclination and the RAAN, fix the orientation. Satellite orbits may be categorized based on these individual parameters.

The most common categories of satellite orbits are based on their radius, or, more generally, on their semimajor axis when the orbit is not circular. Primarily, there are three such types of orbits: low Earth (LEO), medium Earth (MEO), and geosynchronous (GSO). These orbits are described below.

Satellites in LEOs have heights ranging from 500 to about 1500 km above the Earth's surface. Because of their nearness to the Earth, satellites in these orbits have small periods of about 1.5 to 2.0 h. These orbits are used by satellites mainly for remote sensing purposes, because being nearer to the Earth, they have better

resolution of the images they take. They also receive the maximum reflected power from the Earth owing to their proximity. However, because these satellites need to move through large resistive drag, their average lifetime is much lower than others, typically ranging from 2 to 5 years. It is also evident that because the range is smaller, the orbiting speed is fast, even more than that of the Earth's spin, irrespective of the inclination. So, a satellite executes more than 20 complete revolutions around the earth in a day. Therefore, the visibility time of these satellites from any definite point on the Earth is considerably small, typically about 15 to 20 min per pass.

MEO satellites have a radius from around 8000 km to 25,000 km with associated periods ranging from 2.0 to 12.0 h, with a typical visibility time of a few hours per pass. These satellites are generally used for navigation purposes and mobile satellite services. A portion of these orbital region is not generally used for placing satellites because of an inhospitable environment existing there. This is due to the abundance of high-energy charged plasma particles present here and this region is called the Van Allen belt (Tascione, 1994).

Satellites in GSO are placed at a definite distance from the Earth, in circular inclined orbits, such that the angular velocity of the satellites is equal to the angular velocity of the Earth. Thus, the satellite revolves in space once in about 24 h, like the Earth. Consequently, the satellite maintains almost the same longitude at which it has been placed. GSO satellites may have different inclinations depending on the application requirement. The more the inclination angle is, the more it sweeps across the latitudes on both sides of the equator. If we drop a normal from the satellite, the point where it intersects the Earth's surface will constantly change if there is a relative motion between the Earth and the satellite. The locus of this point will form the ground trace of the satellite. The satellites in the GSO make a figure-of-eight as the ground trace. The gradual widening of the trace toward the two ends of the figure is due to the difference in the east–west linear velocity at the equator and at higher latitudes. The formation of the ground trace of a satellite in GSO orbit is described in Box 3.3. These satellites are at a distance of about 36,000 km from the Earth's surface, and because of the large distance, they require a large power of transmission but have large footprints (i.e., area of coverage).

BOX 3.3 MATLAB EXERCISE

The MATLAB program ground_trace.m was run to generate the coordinates of a circular orbit at a GSO orbit with a definite given inclination of $i = 35°$ and equator crossing node at 74°E. This is shown in Fig. M3.3. Note the formation of the figure-of-eight. The next plot is obtained for $\varepsilon = 0.07$, $\omega = 15°$, $i = 55°$, and node at 274°E.

Observe the variation in the shape and orientation of the trace. This results from the eccentric nature of the orbit; it moves faster at one half and slower at the other half, which gives this particular shape.

Run the program for a different nodal point, eccentricity, and inclination, and observe the variations.

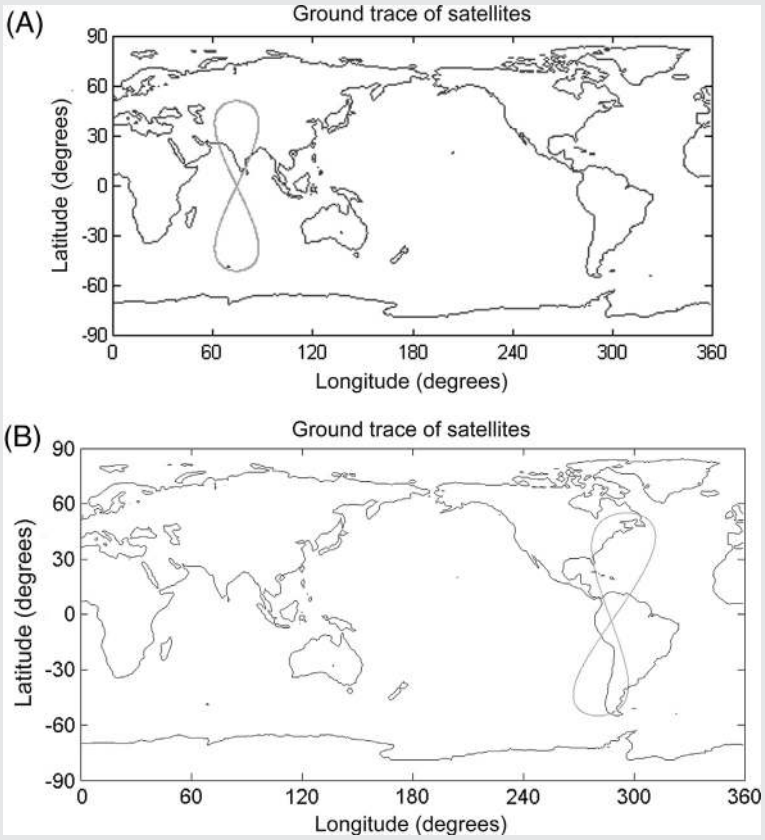

FIGURE M-3.3

Ground trace of satellites.

Geostationary satellites are in a particular type of GSO with zero inclination. Thus, these satellites are fixed on the equatorial plane and ideally remain above the same fixed point over the equator and are therefore mostly used for fixed communication services.

Unlike circular or near-circular orbits, certain orbits are characterized by their eccentricity. The highly elliptical orbit (HEO) is used for satellites meant for communication at higher latitudes. These orbits have a large eccentricity ε approximately 0.8 to 0.9, and hence the ratio of their perigee to the apogee distance is more than 10. Because the satellites sweep equal areas in unit time, as per Kepler's law, they traverse faster when they are nearer the Earth than when they are farther from it. So, when the satellites in these orbits are at the apogee, they move the slowest and thus are visible

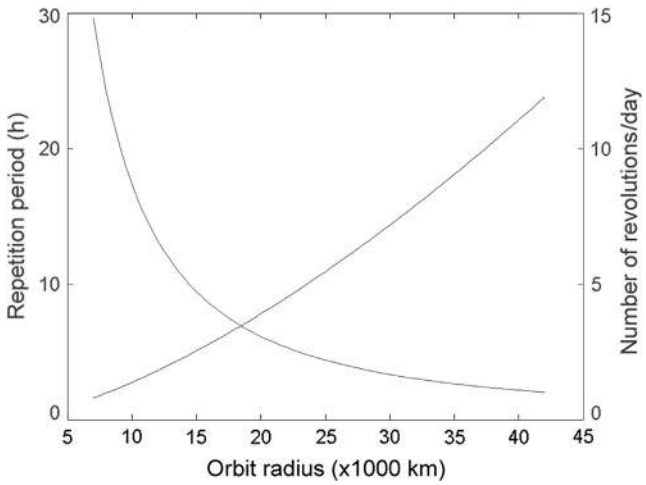

FIGURE 3.10

Variation of repetition period with range and number of revolutions per day.

for a longer time. Such orbits are hence used with a higher inclination, with apogee directed appropriately to get the visibility of satellites over a large interval.

The repetition period of satellites in different orbits depends on their speed and, hence, on the range, and the number of times they reappear at the same location over the Earth changes accordingly. The plot in Fig. 3.10 represents the variation of these two parameters with the range.

3.5 Selection of orbital parameters

In choosing different orbital parameters during the design of the system, different factors come into consideration. Not only does technical feasibility matter in the process, but one also has to be careful about the practicality of implementation. Here, we shall outline only a few theoretical aspects that determine the choice of parameters. However, this provides only a preliminary concept for constellation design. For a detailed design approach, many other factors need to be considered (Spilker, 1996); interested readers may refer to Walker (1984) and Rider (1986).

The Earth rotates with a fixed angular velocity about its axis, whereas satellites also rotate about the center of the Earth. From the discussion in Section 3.1, we know that the velocity of satellites in an ECI frame depends on the distance from the Earth's center (i.e., its range). The nearer the satellite is, the faster it moves. Satellite velocities reduce as they move away from the Earth's surface, and at about 42,000 km from the center, they have an angular velocity equal to the angular velocity of the Earth; thus, satellites in this orbit remain quasi-static over one particular longitude. If the inclination is zero (i.e., for GEO satellites), the satellite remains fixed on the longitude

at the equatorial plane and is always visible on the equator. If it has an inclined orbit (i.e., GSO), it moves along the longitude, making a figure-of-eight.

In satellite navigation, satellite orbits are chosen depending on the visibility criterion of the satellites (Dorsey et al., 2006), which again depends on the service we need. For a regional service, in which the satellites need to serve only a particular section of the Earth, and furthermore, if the region is nearer to the equator with a limited latitudinal extent, it is convenient if the satellites always remain fixed on different longitudes across the service area. Under such conditions, it is likely that all satellites will be visible over the whole service area all of the time.

As we mentioned earlier, and as will be explained later in Chapter 7, the accuracy of estimation of the position depends on the user–satellite geometry, which is determined by the relative position of the satellite with respect to the users. Therefore, satellites need to be dispersed to the maximum extent to obtain the best possible accuracy of positions. To achieve this, all satellites cannot be kept in GEO; some also need to be on the GSO, swinging across the latitudes and giving wide intersatellite separation.

The inclination requirement for the GSO is based on the latitudinal extent that satellites need to serve. For the satellites with inclinations $i°$, the loci of the subsatellite points can move up to a maximum latitude of $i°$ north and south. Users located up to this latitude will see the satellites overhead at certain times of its pass. For those located above $i°$ latitude, satellites will always be seen southward, which obviously will affect the accuracy of the position estimates.

The same design will not be effective for a regional service at higher latitudes. If we use the same GEO–GSO combination even in this case, the satellites will mostly be visible southward for places in the northern hemisphere, and the northern sky will remain devoid of them. The opposite will happen for the southern hemisphere. Moreover, because of the equator-ward excursion of the satellite, it will be out of visibility more often than not. Because visibility remains a major criterion, highly elliptical orbits may be used for such cases. The apogee of different satellites may be configured to remain above the service area by properly choosing the RAAN, inclination, and argument of perigee. The range and visibility may be adjusted by appropriately designing the semimajor axis and the eccentricity. Then, the satellites will move slowly over the region and faster when it goes antipodal, giving a large proportion of the orbital period to the visible time span. However, there can also be other appropriate designs. If we go still higher in latitude, the range of satellite visibility extends across the longitudinal hemispheres. Thus, visibility conditions are not simple, and similar straightforward conclusions cannot be drawn.

When it comes to global services, the whole globe needs to be covered by satellites. At the same time, at least seven to nine satellites must remain visible from any point on the Earth. There are two options. As before, satellites can be put into GEO–GSO orbit. However, at GEO–GSO orbit, the geometry of the satellite constellation relative to a finite location on the Earth's surface only has north–south excursion. Sometimes it creates difficulties in achieving an adequate dispersion of satellites, and thus, to achieve better accuracy of position estimates. Moreover, the power required for transmission from this orbit is relatively large.

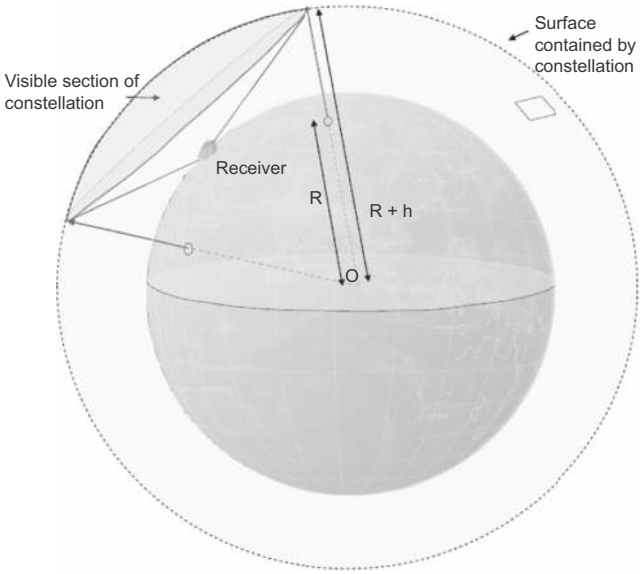

FIGURE 3.11

Estimation of satellites in the space segment.

The second option is to keep satellites at a lower orbit. Here, with a few more satellites in the constellation, one can provide complete coverage with the required number of visible satellites. The number is obtained from the visibility requirement. Let us perform some simple calculations to verify this. Although four satellites are enough for position and time estimations, they do not give enough options to users from which to choose the best four. Because position estimation is sensitive to user–satellite relative geometry, the more satellites the user sees in the sky, the more options he has to choose from for a suitable combination of satellites to obtain better accuracy. Here, we shall do an approximate workout to find the number of satellites required to fulfill these criteria.

For simplicity, let us assume that the Earth is spherical, and a user receiver placed on the Earth surface can see the sky down and up to the horizon (i.e., the lowest look angle has zero elevation). This is shown in Fig. 3.11. It is not a pragmatic assumption, because it is almost impossible to have an unobstructed vision up to this lower elevation. However, this makes our calculations simple by easing the geometry without affecting the result much.

With these considerations, the geometry shown in the figure reduces to a simpler condition in which the angle θ that we get at the center of the Earth, of the maximum extent of visibility of the receiver, is $\cos^{-1}\{R/(R+h)\}$.

So, the part of the sky that lies within the visibility range of the receiver at point P subtends angle θ at the center of the Earth. The area covered at satellite constellation height $R+h$ by this angle at the geocenter may be obtained by integrating the infinitesimal area dS at radius $(R+h)$ over an azimuth of 0 to 2π and over a polar

angle of 0 to θ. The total surface S becomes

$$\begin{aligned} S &= \int_0^{2\pi} \int_0^{\cos^{-1}\left(\frac{R}{R+h}\right)} (R+h)\ d\theta\ (R+h)\ \sin\ \theta\ d\varphi \\ &= \int_0^{2\pi} \int_0^{\cos^{-1}\left(\frac{R}{R+h}\right)} (R+h)^2\ \sin\ \theta\ d\theta\ d\varphi \\ &= -\ 2\pi\ (R+h)^2\ \cos\ \theta\Big|_0^{\cos^{-1}\left(\frac{R}{R+h}\right)} \\ &= 2\pi\ (R+h)\ h \end{aligned} \tag{3.33}$$

So, over the sky of area $S = 2\pi\,(R+h)\,h$, if we need nine satellites over the whole area covered by the constellation surrounding the earth, the total number of satellites that are required will be

$$N = \frac{9}{2\pi\,(R+h)\,h}\,4\pi\,(R+h)^2 = 18\,(R+h)/h = 18\left(1 + R/h\right)$$

This number increases with a decrease in the height h of the constellation.

To verify this, let us use an example. For a GPS system, the height of the constellation is 26,500 km from the center of the Earth on average. Thus, here $(R+h) = 26{,}500$, where $h = 20{,}000$, both in approximate figures. Using the previous numbers, we get

$$N = 18\left(26500/20000\right) = 18\left(265/200\right) = 23.85 \sim 24$$

However, for a GSO height of about 42,500 km radius, this will become

$$N_g = 18\left(42500/36000\right) = 18\left(425/360\right) = 21.25 \sim 22$$

Thus, with a 26,000 km radius, it is sufficient to have 24 satellites to provide about 9 satellites visible between horizons. All the calculations assume that the satellites are uniformly distributed in space. For, a practical value of the cutoff of the elevation angle, generally eight satellites are seen, with the same number of satellites in the constellation. The number would be 22 if they had to be in the GSO orbit. The reason behind the reduction in the requirement with increasing height of the satellites is that the part of the total constellation coming within the visibility span from a point on the Earth's surface for the higher range of the satellites is more.

At orbits lower than the GSO, the velocity of the satellites will be more relative to that of the Earth, and they will appear to be moving with respect to a point on the Earth. However, because all of the satellites will be moving in the same fashion, when one satellite moves out of the visibility range of any point, another will appear by moving in from outside. Thus, statistically, the total number of visible satellites remains the same. Moreover, because it is nearer to Earth, it will need less transmission power to produce the same power flux at the receiver compared with that of a satellite on GSO. But, again, because they experience feeble but finite air drag, the life of satellites on this orbit is less than that in GSO.

Then, why do we not go to LEO? In addition to the larger numbers of satellite requirements, the intrinsic problem with the LEO system is that as it passes through a denser atmosphere, it experiences a large drag, and hence its lifetime is very much

limited. Moreover, the velocity of the LEO satellites is large; it rises and sets at smaller intervals, resulting in a rapid switchover requirement of satellites by the navigation receiver. Therefore, MEO satellites are chosen in general for this purpose.

Conceptual questions

1. Can a satellite move in a stable orbit contained on a plane that does not pass through the center of the earth?
2. Using Eq. 3.11A, derive the escape velocity (i.e., the velocity that must be given to the satellite to escape from the influence of the Earth). Is it necessary to provide this velocity to the rocket right from the takeoff condition?
3. Show that when the limit $L^2/(\mu a) = 2$ is crossed, the ε gets the generic requirement of hyperbola.
4. A satellite in a highly elliptical orbit moves partly through a dense atmosphere and loses part of its energy. What will happen to its semimajor axis, "a," and argument of perigee, ω?
5. A satellite in a circular orbit at a radius "a" is imparted with an excess energy of E. Find the position in the orbit after a time t. If the other orbital parameters are W, i, and ω, find the position of the satellite in ECEF coordinates.
6. From the navigation standpoint, is it better to have a fast-moving satellite nearer to the Earth or a slow-moving one farther from it?
7. Derive Eq. 3.24 from Eq. 3.13A using the definition of L and the relation between h and a.

References

Dorsey, A. J., Marquis, W. A., Fyfe, P. M., & Weiderholt, L. F. (2006). GPS system segments. In C. Hegarty, & E. Kaplan (Eds.), *Understanding GPS - Principles and Applications* (2nd Ed). Boston, MA, USA: Artech House.

Feynman, R. P., Leighton, R. B., & Sands, M. (1992). *Feynman lectures on physics*: Vol-1. India: Narosa Publishing House.

Maral, G., & Bousquet, M. (2006). *Satellite communications systems*. John Wiley & Sons Ltd.

Pratt, T., Bostian, C. W., & Allnutt, J. E. (1986). *Satellite communications*. John Wiley & Sons Inc.

Rider, L. (1986). Analytic design of satellite constellations for zonal Earth coverage using inclines circular orbits. *Journal of the Astronautical Sciences, 34*(1), 31–64.

Roychoudhury, D. (1971). *Padarther Dharmo. Ed. 2*. Poschimbongo Rajyo Pushtak Parshad, Calcutta, India.

Spilker, J.J. Jr. (1996). GPS navigation data. In: B.W. Parkinson, & J.J. Spilker Jr. (Eds). *Global positioning systems, Theory and Applications*, vol, I, AIAA, Washington DC, USA.

Strelkov, S. P., Volosov, V. M., & Volosova, I. G. (1975). *Mechanics*. Mir Publishers.

Tascione, T. F. (1994). *Introduction to the space environment*. Krieger Publishing Co.

Walker, J. G. (1984). Satellite constellations. *Journal of the British Interplanetary Society, 37*(12), 559–572.

CHAPTER

Navigation signals 4

4.1 Navigation signal

One of the most important elements of the whole satellite navigation system is its signal. It is the means through which all information that the system wants to convey to the user is disseminated. This information includes the elements for satellite positioning, time and clock-related updates, corrections, and notifications regarding the current state of the whole constellation. However, the utility of the signal is manifold and is not limited to just giving out this information. Here, we shall attempt to understand the multiple facets of the navigation signal. To appreciate its different aspects, we need to recall some fundamental concepts of communication. These will be discussed briefly for continuity and a better understanding.

4.1.1 Generic structure

The basic purpose of the navigation signal is to notify the user about some primary information and enable him to derive other necessary parameters required to fix his position. This information should reach the user in a convenient, reliable, and secure form. In recent times, there can be no method more convenient than the digital communication system to transmit information through a satellite channel, fulfilling all of these criteria. Thus, the navigation signal is actually a sophisticated form of digital communication signal. Typically, it has a tiered form in which the tiers are constituted by the navigation data, the ranging code, and the modulated carrier. These constituents are multiplied together to form the final signal structure. Each component of this product (i.e., the binary data, binary ranging code, and a sinusoidal carrier) has predefined characteristics designed to meet the service objectives.

The navigation data provides the necessary information of the system, particularly of the space segment and timing, to the user in a binary format. These binary bits are multiplied with much faster binary ranging codes to enable receivers to carry out one-way range measurement. In addition, the orthogonal nature of the different codes used here is exploited in implementing code division multiple access (CDMA). The relatively faster codes, thus multiplied by the data, also spread the spectrum of the navigation data. It also helps in better reception performance and security of the service. Furthermore, for data security and authentication purposes, encryptions in certain forms are also done on this part of the signal. This product of data and code then modulates an even faster sinusoidal carrier. Thus, it rides on the carrier to propagate

Understanding Satellite Navigation, Second Edition. DOI: https://doi.org/10.1016/B978-0-443-36432-7.00015-8

through the intermediate space from the satellite to the receiver. The most popular type of modulation for navigation is binary phase shift keying (BPSK). In certain cases, an intermediate binary subcarrier is also used. This type of modulation, called binary offset carrier (BOC) modulation, which is used to avail certain advantages.

Navigation satellites transmit these modulated navigation signals in allotted bands with a predefined transmission power and defined polarizations, typically circular. Sometimes, an additional pilot channel is also sent with the signal. This does not carry data but is the product of the code and the carrier only. The pilot signal helps the receiver in acquiring and tracking the signal, mainly under poor signal conditions. The signals are transmitted by the satellites synchronously (i.e., when one satellite starts sending a data bit, so do the others). Furthermore, the code and the data, and also the code and the carrier phases are synchronized (Parkinson and Spilker Jr., 1996).

The modulated carrier in this form experiences certain impairments while propagating through the medium from the satellite to the receiver, including power loss, excess delay, loss of coherency, multipath, and so forth. These impairments need to be properly handled. They may be minimized through appropriate designs of the signal parameters or through the proper correction of any error that gets added to the signal at the receiver. A very low signal level is expected at the receiver over the targeted region with even lower power density owing to the spreading of the navigation signal spectrum. Navigation signals also experience interference from other navigation signals in these bands. This interference level needs to be minimized using certain techniques.

Now, we shall discuss in detail each of the individual components of the signal with its related aspects.

4.2 Navigation data

The navigation data, D(t), is the component of the signal that carries all predefined information describing details about the current condition of the system that need to be broadcast to users. This information is transmitted as binary data arranged in a structured form. Here, we shall concentrate on the data for primary systems only. Besides that, our discussion will remain generalized and consolidated and will describe only the key aspects of the navigation data (Navstar GPS Space Segment/Navigation User Interfaces: IS-GPS-200G, 2012).

4.2.1 Data content

At this point, it is necessary to understand the mandatory parameters that should be present in the data. The nominal set of navigation data is determined by the requirements of the receiver. We recall from Chapter 1 that in a primary system, the positions are determined from knowledge of the reference positions (i.e., the positions of the satellites and the measured range of the satellites from the user).

Therefore, the user should be able to obtain satellite positions every time they want to fix their own position. One simple option is to send the position of the satellites as part of the navigation signal. However, that is not a pragmatic choice. The positions of the satellites vary significantly with time. The linear velocity of a satellite at a height of 20,000 km from the Earth's surface is about 4 km/s, which is considerably high. Therefore, its position is expected to drift by a large amount within a specific update interval of the data, however small it is. In addition, estimations of the satellite's position are to be done onboard, since very frequent uploading of the satellite's positions by the ground control system is not possible. Consequently, it adds to the computational load of the onboard process. Within the finite update time of the satellite position in the signal, the satellite will move a distance large enough to add an appreciable error in the user's position estimate. Thus, a more practical option is to send the satellite ephemeris. Ephemerides are the Keplerian parameters of each satellite, using which, along with the appropriate values of the current time, satellite positions can be estimated by the receiver. We have seen previously that there are six such basic parameters to derive the satellite position at any time. Thus, these six parameters need to be transmitted as part of the data for partial fulfillment of the basic receiver needs. In addition, the perturbation parameters are also required for precision.

Apart from satellite positions, satellite ranges are the next important parameter required for position and time fixing. The ranges are derived at the receiver and are derived by multiplying the signal velocity by its propagation time. The propagation time, which is the difference between the reception and transmission time of a particular phase of the signal, in turn, is derived from the relative phase difference between a local synchronous code and the received signal code, using correlation. The absolute time and the total time of travel can be obtained using the time stamp indicated on the signal. This time stamp, signifying the transmission time of a predefined phase of the signal, is thus another parameter that needs to be transmitted with the signal.

These parameters give the receiver all of the information needed to derive the necessary parameters for reference positioning, ranging, and time keeping. However, to increase the accuracy and reliability of the estimations done at the receiver, more data needs to be transmitted through the message, which delivers the necessary precision.

These additional data include variables, which are included mainly for reasons such as the correction of satellite positions, prediction of the state of the constellation, correction of time, etc. In subsequent chapters, we will read about the details of the correction procedure. Here we shall only identify and mention their occurrences in the message structure.

The satellite position derived at the receiver is a sensitive parameter for the estimation of the user's position. Thus, the accuracy of reference positioning determines the accuracy of the user's position fix. The satellites, as mentioned previously, experience perturbations in their orbital motions because of the nonuniformity of many physical factors. Consequently, knowledge of these perturbation factors leads to better positioning. This is the reason why the perturbation parameters of the satellites are also accommodated in the signal.

The time stamps available in navigation messages are marked using satellite clocks. These clocks are derived from atomic standards and are stable in nature. Nevertheless, there is some minor drift in these clocks with respect to the system time, which may lead to affecting the positioning. Hence, to correct the effect of this drift, the total satellite clock deviation may be estimated by the ground system and transmitted through these messages for necessary corrections at the receiver. For the same reason that the ephemerides are transmitted instead of satellite positions, it is convenient to transmit the clock bias, clock drift and drift rate at a definite reference instant instead of the total shift. The total clock shift, Δt_{sat}, may therefore be obtained from these parameters as

$$\Delta t_{sat} = a_0 + a_1(t - t_0) + a_2(t - t_0)^2 \tag{4.1}$$

where a_0, a_1, and a_2 are the clock bias, drift, and drift rate, respectively. t_0 is any arbitrary reference instant for calculating these values, and t is the time of estimation.

There are also propagation impairments that alter the range measurements by modifying the time of transit of the signal. In addition to the clock and orbital correction terms, the correction factors corresponding to these propagation impairments may be disseminated to the user if the exact correction values are already known to the control system. Many of these errors depend on the location of the individual user, and hence cannot be explicitly known by the system. However, there are some parametric models of these impairments from which the receiver can estimate the required correction for himself. The parameters of these models are provided with the message to deal with this problem.

In a frequency division multiple access (FDMA) system, the composite signal received by the receiver can be resolved into its constituent components using the Fourier transform and segregated by passing through different filters. However, for a CDMA system, when a number of signals from different satellites are simultaneously received, each of which occupies the whole bandwidth. In such a system, the individual signals need to be identified and separated from the others by recognizing the corresponding constituent codes. Here, each satellite has its own definite code. So, process is aided if the possible set of satellites currently visible or those expected to rise or set over the horizon soon can be known by the receiver from some data. Then, whenever the receiver is put on, the quick prior prediction makes it easier to specifically identify each individual satellite and hence the possible codes which can be present in the received composite signal.

To support this process, the system may include the signal with a reduced set of ephemeris parameters for all satellites. This list of selected ephemeris data is called an almanac. The approximate positions of the satellites in the constellation can be derived from the almanac. Hence, it keeps the receiver prepared for the acquisition of new data or the switchover of satellites.

Apart from the information required at the user's receiver, certain telemetry data generated at the satellite are needed by the control segment for analysis. These data sets, which may include the integrity assurance, certain specific alerts, flags, and status

data, may be combined in the form of telemetry data and transmitted by the satellite. However, this is done through a different channel.

Many other data may be included in the signal, depending on the design parameters and receiver requirements; these may be added to the navigation data structure. This data is said to be updated when the older parameters values are replaced by the newest ones. The updating rates of the parameters are different and are generally based on consideration of the rapidity with which the true physical parameter changes its values. Fast-varying parameters need to be updated frequently, whereas slow-varying ones are updated at larger intervals. In addition, because all data have an expiration term, the time of applicability may be associated with each type of data.

4.2.2 Data structure

Communication of navigation data occurs just as the way it is done with any other digital communication system. The basic objective here is to deliver the user the information required to fix their position. This information, as we have just learned, is a set of updated values of different parameters constituting the navigation data. These values should reach the user in a convenient, reliable, and secure manner without error. For this, digital binary communication is an excellent candidate.

The navigation data values need to be source coded and converted into binary bit sequences for this purpose. The number of bits used to represent a particular parameter is chosen so that the quantization error is less than the resolution of its values. For example, if the value of a parameter ranges from 0 to 1000, with a resolution of 0.01, there can be $(1000 - 0)/0.01 + 1 = 10^5 + 1$ different values that can be generated. For this, it requires at least 17 binary bits for representation.

These binary bits can take either of two logical values, 0 or 1, typically represented by levels $+1$ and -1, respectively. After being mapped from parameter values to binary bits, the set of this coded data need to be added with appropriate channel coding to defend against channel noise. Channel coding adds redundant bits to the data, making the latter robust against any error occurring during transmission of the signal through the channel.

These navigation data bits are organized in a structured manner in some suitable predefined arrangements for the efficient transmission of information and convenient extraction at the receiver. A fixed number of bits are grouped to form a frame. Then the information is sent frame by frame. There are two alternative approaches for the transmission of the frames. In one, the different parameters are sent in a fixed frame format, and all parameters have definite positions in the frame. Here, the whole framed structure with subframes of the data repeats in a fixed pattern. Each time the frame is repeated, the data is retransmitted with it. Thus, the repetition rate of the parameter is equal to the frame repetition rate. However, the same values of the parameters are retained until their expiry. The update interval of any parameter in the dataset can only be a certain integral multiple of the frame repeat time. The other option is to transmit each parameter or a group of similar parameters in the form of an individual

message. Proper indices may be used to identify of the message type. Each message type, containing the associated parameters, may be broadcast in a flexible order with a variable repeat cycle. The message repetition rate is primarily determined by its priority. Therefore, the message may be repeated at intervals, not necessarily equal for all parameters. Their values are updated at a fixed repetition rate sufficient to achieve and maintain the required accuracy. The latter option, which has more flexibility and options to send more accurate and resolved data, leads to better performance (Navstar GPS Space Segment/Navigation User Interfaces: IS-GPS-200G, 2012). In this option, there is scope to add integrity parameters. The flexible data message format leads to optimization of the transmission of the satellite-specific data, resulting in minimized time for the position to be fixed for the first time, and thus increasing the speed of operation (Kovach et al., 2013). However, the flexible message structure requires higher storage capacity at the satellite compared with that required by the fixed frame format, and also an appropriate priority estimation algorithm.

Irrespective of the data messaging approach, the individual units of the messages, whether subframes or indexed messages, need to carry the preamble bits to facilitate the subframe identification and synchronization.

4.2.3 Data spectrum

The navigation data is composed of some selected parameters, the values of which are encoded in binary. They thus form a random sequence of bipolar nonreturn-to-zero binary bits whose temporal variation may be represented by a series of positive and negative square pulses of amplitude "a" and constant width T_d. Thus, the navigation data s(t) at time t may be expressed as

$$s(t) = a\, p\left(t - kT_d\right) \tag{4.2}$$

Here, $a_k = \pm a$ is the amplitude of the kth bit of the sequence reckoned from an arbitrary instant taken as $t = 0$. k is a monotonically increasing integer that represents the floor value of the argument t/T_d, that is, the integral part of the ratio. It starts from $k = 0$ and increases by one integral step after every T_d interval of time t. T_d is the bit duration in the signal and depends on the rate, R_d, at which the bits are transmitted. p(t) defines the shape of the bit. Here, it is a unit positive pulse defined within the time argument ranging from 0 to T_d. The time variation is shown in Fig. 4.1A. Here, the bits are of finite constant width and constant amplitude. Pulse shaping is not popular in navigation.

The frequency spectrum of this form of signal and the bandwidth occupied by it depend on the bit rate of the data. We know from communication theory that such a signal constituted by pulses of finite width T_d and amplitude "a" has as its spectrum, given by

$$S(f) = a\, T_d \frac{\sin\left(\pi f T_d\right)}{\pi f T_d} = a\, T_d\, \mathrm{sinc}\left(\pi f T_d\right) \tag{4.3A}$$

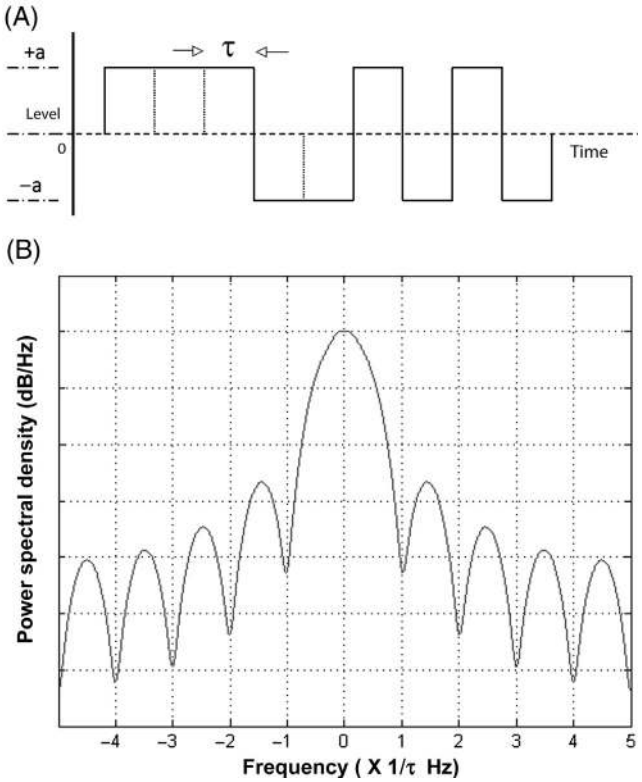

FIGURE 4.1

(A) Time variation and, (B) relative amplitude and power spectrum for a random bipolar NRZ binary signal.

where S(f) is the spectral amplitude function in terms of the signal frequency f.

The spectrum of such a signal is shown in Fig. 4.1B for a binary sequence in terms of its bit rate of $R_d = 1/T_d$. Since sin (x) / x = 1 at x = 0, the spectral peak appears at f = 0. It is also clear from the figure that the primary band of this spectrum, defined as the frequency difference between the first nulls of the main lobe about the primary peak. The first null occurs when $pfT_d = p$, or, $f = 1/T_d$. So, W is given by

$$W = 2/T_d = 2R_d \tag{4.3B}$$

Thus, this bandwidth is directly proportional to the bit rate. The faster the bit rate, the smaller the bit duration T_d, and hence the wider the bandwidth.

Using Parseval's theorem for the Fourier Transform, we get that the sum (or integral) of the square of a function in the time domain is equal to the sum (or integral) of the square of its transform in the frequency domain. The theorem may be stated

mathematically as (Lathi, 1984).

$$\int s^2(t)\,dt = \int S^2(f)\,df \tag{4.4}$$

You can also understand this intuitively simply by considering the total signal as the sum of independent oscillations at all possible components of sinusoidal frequencies. Then, using Eq. 4.4, the total power of the signal, calculated in time domain, is

$$p(t) = \frac{1}{T}\int s^2(t)\,dt = \frac{1}{T}\int S^2(f)\,df \tag{4.5A}$$

So, the power spectral density is given by

$$P(f) = dp/df = \frac{1}{T}S^2(f) \tag{4.5B}$$

The total power of the signal is the sum of the power carried by the individual orthogonal independent frequency components of this signal, and the power spectral density at any frequency f is nothing but the power carried by the spectral component per unit frequency centered at this frequency, f. It follows from this statement that the power spectral density function, P(f) is given by

$$P(f) = \frac{1}{T_d}a^2{T_d}^2\frac{\sin^2(\pi f T_d)}{(\pi f T_d)^2} = a^2 T_d\,\mathrm{sinc}^2(\pi f T_d) \tag{4.5C}$$

Because this is the square of the amplitude spectrum, it is always positive. Obviously, the positions of the nulls remain the same as they were in the amplitude spectrum. Also, note that due to the square term, the power spectrum falls off rapidly about the center frequency. The power content at frequencies away from the DC is small. More than 90% of the power remains within the first null about the center of the spectrum (i.e., within the primary bandwidth). We shall find in Box 4.1 how much of the total power of the signal remains within the first null of the spectrum. This will help us in explaining other features of the signal at a later stage of this chapter.

BOX 4.1 Data Spectrum

The MATLAB program data_psd.m was run to generate the power spectral density plot of a random binary sequence with a data rate of 1 kbps. The plot obtained as a function of the frequency is illustrated in Fig. M4.1, which shows that the normalized power has low absolute values to make the total power, obtained by integrating this density across the frequency, unity. Observe how the side lobes vary across frequency with respect to the central lobe. It exhibits a $\mathrm{sinc}^2(x)$ variation, whose logarithmic values can be seen in Fig. M4.1(A). The power density values are logarithmic (in dB). The values drop to zero at the nulls, as which is also observed in Fig. M4.1(A). The nulls occur at 1-kHz intervals and are in accordance with the fact that the bandwidth is proportional to the bit rate. Furthermore, the total power content in the side lobes is significantly lower than that in the main lobe.

Go through the program. Use the program to obtain the spectra for different data rates.

The spectral data and their corresponding frequencies are in the structure HPSD. Type HPSD in the MATLAB workspace after running the program to see its structure. Type "HPSD.data" and "HPSD.frequencies" to obtain the spectrum and corresponding frequency values. The values are in linear scale and can be plotted using the script [plot (HPSD.frequencies, HPSD.data)]. You can verify that the total power integrates to unity by using the command:

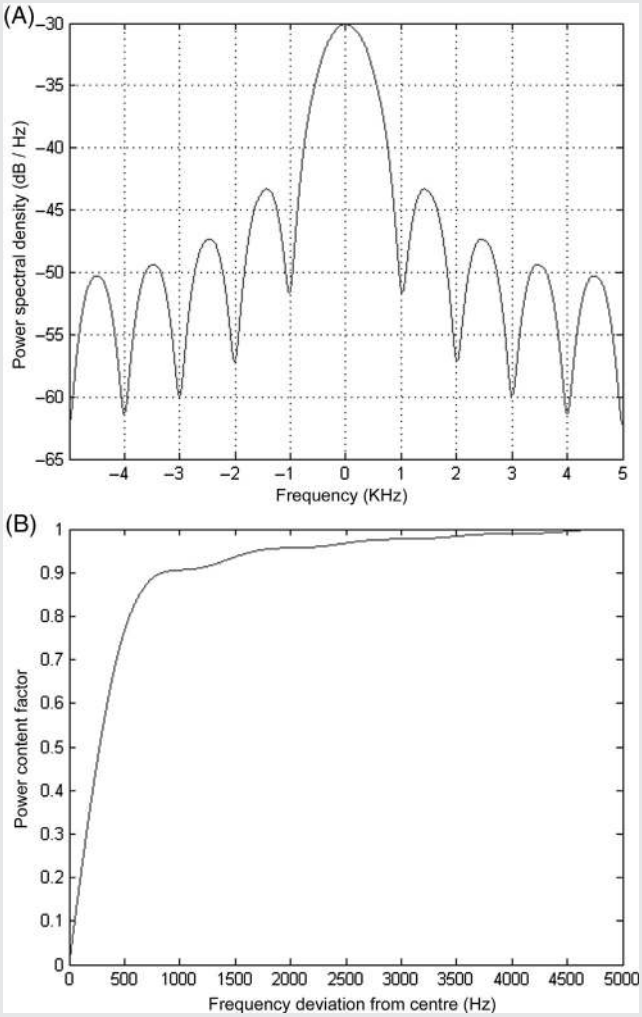

FIGURE M4.1

(A) Power spectral density, (B) Power content plot of a random binary sequence.

(*continued*)

BOX 4.1 Data Spectrum — *cont'd*

[sum (HPSD.data(2:end).∗(HPSD.frequencies(2:end)-HPSD.frequencies(1:end-1)))]

The total power content within different frequency ranges is generated by the same program and is shown Fig. M4.1B. The power within the first lobe of 1000 Hz is more than 90%. Use the program to obtain the power content in different ranges of frequency.

4.3 Ranging codes

It is a requirement for navigation systems that the receiver estimate the distance to the transmitting satellite. This measured distance is used for position fixing. Plus, in certain systems, signals from multiple satellites need to be received by the receiver simultaneously in the same carrier frequency without interference between them. These requirements must be fulfilled in addition to the basic criterion of secured transmission of the data.

Both these requirements can be easily catered to by using a simple technique, CDMA. It is achieved by multiplying the data bits with a pseudo-random binary sequence or pseudo random noise (PRN). This is a term we are using for the first time. We will learn it in the next section in more detail.

Broadly, the pseudo-random binary sequence consists of a fixed and finite length of random binary bits called chips. The same chip sequence repeats after this length. One such complete sequence of chip constitutes a code. So, if the chips repeat themselves after a fixed length of N chips that constitute the sequence, then N is called the code length. These chips are generated at a very fast rate, called the Chip rate. The chip rate is, in general, many integral multiples of the data rate. Thus, within a data period, not only many chips, but also many code sequences are produced. If the data rate is R, the code repetition rate will be $p \times R$, allowing p complete codes to be accommodated within a data bit period. So, N being the code length, the chipping rate will be $N \times p \times R$.

These chips are generated synchronously with the data and multiplied by them. This means the leading edge of a data bit exactly matches the leading edge of a chip. Again, with the chip rate mentioned previously, being exact multiple of data rate, the trailing edge of the same data aligns with the trailing edge of the $(N \times p)$th chip, counted from the beginning of the data. The resultant product after multiplying the data with the code chips also becomes a binary sequence with a bit rate equal to the rate of this sequence of chips. As the binary sequences of the data bits are represented by levels $+1$ and -1, the sequence multiplied product chips remains same as the original pseudo-random (PR) sequence over the length where the data bit is $+1$ and gets inverted where the data bit is -1 (Fig. 4.1). The bandwidth of the signal increases accordingly, compared to that of the data and becomes equal to the bandwidth of the code.

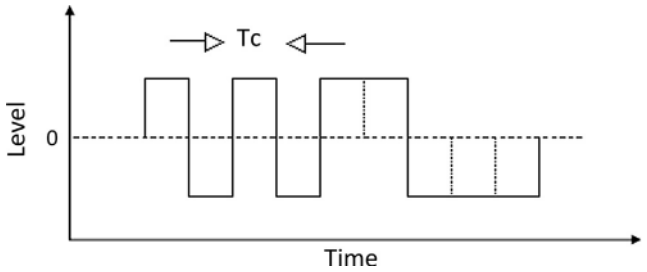

FIGURE 4.2

A random binary sequence.

4.3.1 Pseudo-random noise sequence

When binary bits represented by logical 0s and 1s or their algebraic form, given by +1 or −1, appear in a random fashion to form a sequence, it is called a random binary sequence. The individual bits of this sequence are called "chips" to distinguish them from the information-carrying bits of the data. Fig. 4.2 illustrates a section of such code with chip period Tc.

Before we start describing a pseudo-random sequence, it is important to understand the difference between logical and algebraic variables and operations. The notion of binary numbering is to logically represent two contrasting states by two well-distinguished terms. Typically, they are represented by logical 1 and 0. These could be represented as well by any other form, such as "good" and "bad" or "yes" and "no," or "true" and "false." The representation with numerical 0 and 1 is for convenience.

No algebraic operations, such as multiplication, integration, or addition, are valid in the logical states, considering that these logical variables are different from algebraic ones. However, our conventional processing needs algebraic operations to be done to obtain useful product. So, to carry out algebraic operations, such as correlation on the sequence, it is necessary to represent logical data in some algebraic form so that the algebraic operations can be performed with them. Simultaneously, it is also necessary that, in these algebraic forms, the logical operations can be carried out by some equivalent algebraic operations.

The Exclusive OR (XOR) is a logical operation upon the logical variables A and B in which the result of the operation is also a logical variable represented by $A \oplus B$. The results attain one state when the inputs are different while it attains the other when they are the same. It is the operation for measuring the similarity of the sequence of logical states that these two variables acquire. Notice in the truth table for the XOR operation in Table 4.1 that for 1 and 0 as input, a similarity of two variables results in logical 0, but a dissimilarity, in logical 1. Thus, for any two sequences of bits, their strength of similitude can be represented as the total count of excess 0s over the count of 1s upon carrying out the XOR operations across the sequence length.

Table 4.1 Logical and algebraic form of XOR operation.

Logical Values			Algebraic Values		
A	**B**	**A ⊕ B**	**A**	**B**	**A∗B**
0	0	0	+1	+1	+1
0	1	1	+1	−1	−1
1	0	1	−1	+1	−1
1	1	0	−1	−1	+1

If the logical values are to be substituted by some algebraic representations, the logical operations on these values must also have matching results when the logical operation is substituted by an algebraic equivalence. This is the case when we replace a logical 1 by algebraic −1 and a logical 0 by algebraic +1. The operation of XOR is substituted by algebraic multiplication. The logical truth table and the algebraic product table for these operations are given below in Table 4.1 to establish the fact.

Comparing the two operations, we see that the result of the logical operation of XOR on the logical representations of the binary states of two variables is the same as that obtained for the algebraic operation of multiplication on the algebraic representation of these states. So, we can conclude that when logical 0 and 1 are represented by algebraic +1 and −1, respectively, and the XOR operation can be replaced by multiplication on these data.

The effective similarity between two sequences of logical variables is measured by the sum total of the number of 0s over 1s after XOR-ing the two sequences. Similarly, in the algebraic domain, it is done by summing the counts of +1s over −1s after multiplication. This excess is obtained just by summing up the algebraic product. When averaged, this total process effectively represents the '*Correlation*' between the two sequences. One important aspect of a random sequence is its correlation property. Correlation of any two time signals S_1 and S_2 for a finite delay τ between the signals is defined by the equation.

$$R_{XY}(\tau) = \frac{1}{T}\int_0^T S_1(t)\, S_2\,(t+\tau)\, dt \tag{4.17A}$$

When correlation is obtained between the same sequence, it is called "Autocorrelation". To understand this for a binary random sequence, let us take an infinitely long sequence of binary chips that takes values +1 or −1. Each of these chips is of width T_c extended over time. The sequence is then multiplied by itself. Now, we define a variable that represents the product of the chips of a sequence with itself with a relative delay of n chip length, averaged over the sequence length. We call it the normalized autocorrelation of the sequences, with delay $t = nT_c$. It is given by

$$R_{XX}(\tau) = \frac{1}{NT_c}\int_0^{NT_C} S_1(t)\, S_2\,(t+\tau)\, dt \tag{4.17B}$$

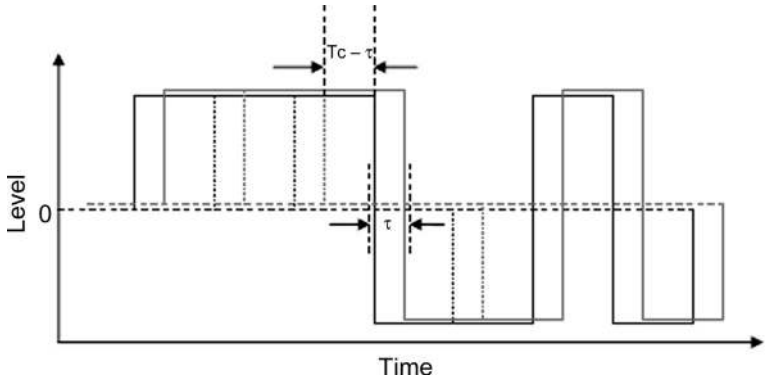

FIGURE 4.3

Signal condition for autocorrelation with finite delay of 't'.

If we keep no relative delay between the two sequences, that is, n = 0 and hence t = 0. Then, the same chips get placed exactly on itself. Because of this exact superimposition of the two sequences, where there is +1 for one sequence, there will also be +1 for the other, and where there is a −1 for one, there will be a −1 for the other. Consequently, when we multiply the corresponding chips now, it always yields +1 at every position. When we sum up the product over the length of N chips of the sequence, the sum becomes NT_c, where T_c has already been defined as the width of each chip on the time scale. The time interval of N chips is also NT_c. This is true for any such binary sequence. So, from the definition, the correlation of such a sequence S_1 with itself with zero delay becomes

$$R_{XX}(0) = \frac{1}{NT_c}\int_0^{NT_c} S_1(t)\, S_1(t)\, dt = \frac{1}{NT_c}\int_0^{NT_c} a_k a_k\, dt = \frac{1}{NT_c} NT_c = 1 \tag{4.18}$$

Let us consider a situation in which the chips of such a sequence are placed on themselves with some finite delay τ. This situation is shown in Fig. 4.3.

Here, the delay $\tau = nT_c$. If N is the total number of chips over which the integration is made, then for integral values of n, Eq. (4.17A) for a discrete autocorrelation function becomes

$$R_{XX}(nT_c) = \frac{1}{NT_c}\int_0^{NT_c} S_1(t) S_1(t + nT_c)\, dt = \frac{1}{NT_c}\int_0^{nT_c} a_j a_k\, dt = \frac{1}{NT_c} T_c \sum a_j a_k = \frac{1}{N}\sum a_j a_k \tag{4.19}$$

where $k = j + n$, that is, the chip represented by a_k comes n bits later than the a_j in the sequence, and the chip width is T_c.

For relative delay of the sequence of 1 bit, that is, n = 1, the bits in a sequence get multiplied by the bit just adjacent to it, which holds true whichever way we move one

with respect to the other. Then, the autocorrelation value becomes

$$R_{XX}(T_c) = \frac{1}{N}\sum_{k} a_k a_{k+1} \tag{4.20A}$$

Because the sequence of bits is random, the adjacent two chips may be the same or different. If they are the same, that is, [+1 & +1] or [−1 & −1], the product becomes +1; when they are different, that is, [+1 & −1] or [−1 & +1], the product becomes −1. For a random sequence, there is an equal chance that these two cases will happen. Therefore, when they are added up, it makes the net sum zero in the summation. It makes the autocorrelation

BOX 4.2 MATLAB Autocorrelation

The MATLAB program autocorr_rand was run to generate the autocorrelation function of a random binary signal. The following figure was obtained using the MATLAB internal function xcorr(), and a random binary sequence of 1000 bits is sampled at a rate of 10 samples per bit (Fig. M4.2).

The function is symmetric on both sides of 0. Run the program for different lengths of the sequence by changing the argument of S_1, but not too high to limit the computational load. Also, see the effect of different sampling rates by changing the upper limit of t. The plot shown will be asymmetric in general, owing to the default nature of the 'xcorr' function.

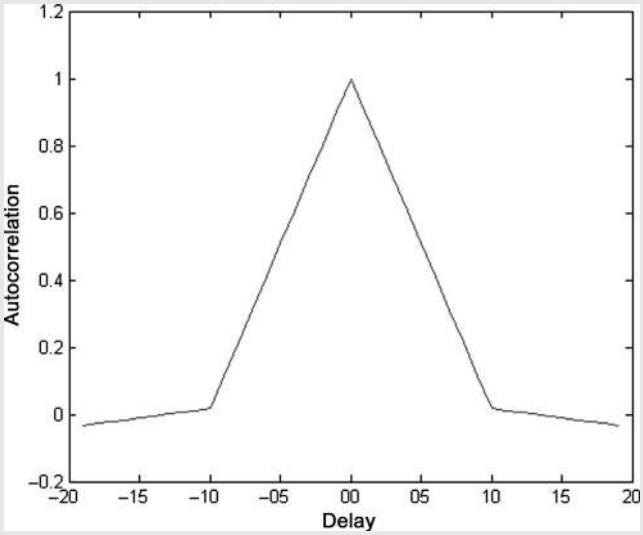

FIGURE M4.2

Autocorrelation function of a random sequence.

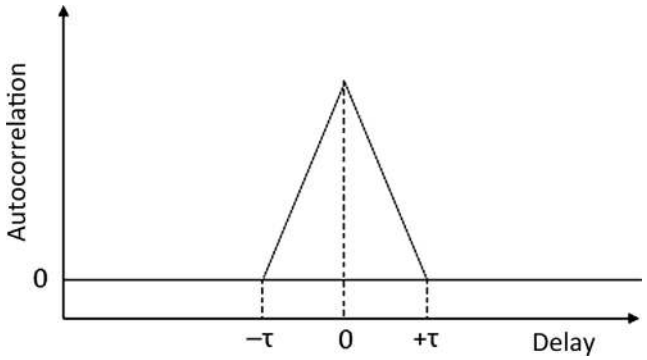

FIGURE 4.4

Autocorrelation function of a random sequence for different delays.

$$R_{XX}(T_c) = \frac{1}{NT_c}\sum_{i=1}^{N}[0.5 \text{ x } (+1) + 0.5 \text{ x } (-1)] \text{ x } T_c = 0 \tag{4.20B}$$

The same argument may be extended when the delay is more than that of 1 bit length.

When the delay is a fraction of a chip length, that is, $0 < \tau < T_c$, for the relative displacement of τ in time, the argument n becomes a fraction (τ/T_c). Here, only a length $(Tc\text{-}\tau)$ of the chip gets positioned on the same chip, and the rest of the length τ is placed over its adjacent chip. This is shown in Fig. 4.3, and it is true whichever way you move the sequence. So, the matched portion of $(T_c - \tau)/T_c$ of each chip will contribute to the sum an amount equal to $(1 - \tau/T_c)$ in Eq. 4.19, whereas the bits laid on their adjacent ones will add up to zero due to the same reason that we described in relation to Eq. 4.20. The autocorrelation will thus become

$$R_{XX}(\tau) = \frac{1}{NT_c}\sum_{1}^{N}\left[\left(1 - \frac{\tau}{T_c}\right)\text{x1} + \left(1 + \frac{\tau}{T_c}\right)\text{x0}\right] \text{x } T_c = \left(1 - \frac{\tau}{T_c}\right) \tag{4.21A}$$

Because this is true for both positive and negative delays, that is, for both right and left excursions of one code with respect to the other, the expression for autocorrelation for a relative delay "τ" will be modified to

$$R_{XX}(\tau) = \left(1 - \frac{|\tau|}{T_c}\right) \tag{4.21B}$$

The value of the autocorrelation is reduced at the rate 1/Tc from one by an amount proportional to the delay between the two signals. Verify the expression in Eq. (4.21B) with our previous arguments by putting $\tau = 0$ and $\tau = T_c$, that is, when they are exactly superimposed and when shifted by T_c, respectively. Fig. 4.4 shows the autocorrelation function of a random sequence, and Box 4.2 illustrates it.

When similar averaged sums of the product of the bits are taken with two different sequences, it is called the cross-correlation of the sequences. The normalized

cross-correlation for two sequences, S_1 and S_2, with amplitudes a and b, respectively, for a delay τ, which is an integral multiple of the chip width T_c, is given by

$$R_{XY} = \frac{1}{NT_c}\sum_{i=1}^{N} S_1(t)S_2(t+\tau)T_c = \frac{1}{N}\sum_{i=1}^{N} a(t)\, b(t+\tau) \tag{4.22}$$

The value of the correlation depends on the bits of the individual sequences, S_1 and S_2.

We have considered fully random sequences until now while defining the concepts of correlation. The integration carried out there or the number of bits N over which the summation has been taken for deriving these parameters were assumed to be very large. Because they are random, there were no restrictions in choosing this length, and the parameter values were defined within this range only.

A pseudorandom sequence, also called a pseudo-random noise (PRN) code, is like a random sequence with a little difference. Instead of the random bits continuing up to infinity, these sequences run randomly for a finite length, and then the same sequence is repeated again, and the process continues recurrently. The random occurrence of the bits over a finite length constitutes a definite sequence pattern and is called a *code*. This has been defined before and mentioned here for convenience. Every bit of code is called a *chip* to distinguish it from the information-carrying data bits. The length of the sequence expressed in the number of chips after which it repeats itself, that is, the number of chips in a code, is called the *code length* and is typically denoted by N. The time interval of repetition of the entire code is called the *code period*. This is equal to NT_c, in which T_c is the *chip width*. The chip width Tc depends on and is actually the inverse of the *chip rate*, R_c, at which the chips are generated. Given a definite chip rate, the code period depends on the number of chips, N, in the code. The code repetition period can also be expressed as $NT_c = N/R_c$ (Cooper & McGillem, 1987; Proakis & Salehi, 2008s).

As a result of this definite repetition, once a single run of the code is identified in terms of its chip sequence and chip rate, the rest of the sequence becomes predictive. Fig. 4.5 shows a typical pseudorandom sequence of code length 7.

Besides the structure, the repeating character of the sequence and its predictive nature cause differences in their autocorrelation properties and their frequency spectrum as well, from those of purely random sequences.

4.3.1.1 Maximal length pseudo-random noise sequence

A useful form of orthogonal pseudorandom sequence code is the *maximal length PRN sequence*. It is also called the *shift register code*, because these codes may be generated with shift registers with proper feedback. It produces a code of length $2^m - 1$, with "m" shift registers. The term "maximal length" (ML) indicates that the sequence repeats only after a length that is the maximum sequence length that can be produced using m shift registers. Because only $2^m - 1$ discrete states are possible for m bits, excluding all zeros, the sequence generates $2^m - 1$ chips before repetition.

Two important properties of an ML sequence are:

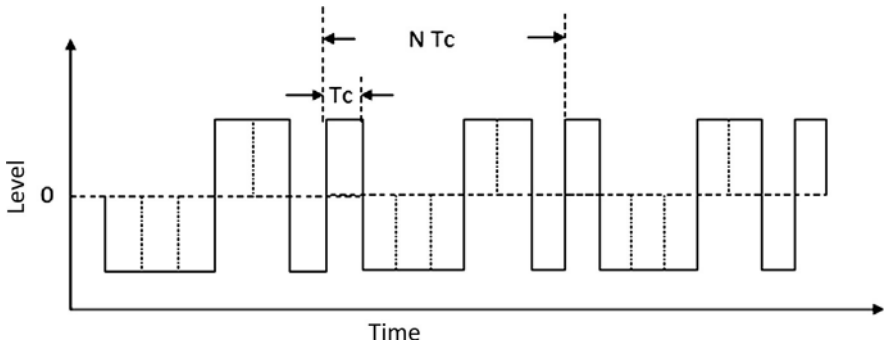

FIGURE 4.5

Pseudo-random sequence.

- Balance nature of the sequence, that is, of its 2^m-1 chips, which is essentially an odd count, the number of -1s (logical 1) in the sequence is one greater than the number of $+1$s (logical 0). So, in the sequence, there are 2^{m-1} numbers of -1, whereas the count of $+1$s is $2^{m-1} - 1$.
- The XOR of the sequence with any shifted version of the same sequence generates the same sequence with a different shift.

Using these two characteristics, let us resume our discussion on the autocorrelation process. The autocorrelation for a PRN sequence is defined as the integral of the products of the same sequence with some definite shift (τ), averaged over a code length. So, if S(t) represents the sequence, the autocorrelation may be expanded as

$$R_{XX}(t) = \frac{1}{NT_c} \int_0^{NT_c} S(t)\, S(t+\tau)\, dt \tag{4.23}$$

It can be easily understood that even here, the autocorrelation with zero delay remains equal to 1 owing to the exact superimposition of the chips. However, because the sequence repeats after a finite length of N chips, the sequence is indistinguishable from the sequence delayed by that length. Thus, the superimposition condition gets repeated in the whole sequence after every N chip shift, that is, after every code period of NTc. Therefore, the autocorrelation values have a repetition period equal to the code period.

Now, let us consider the case of the delay of the integral chip width. When the chips are shifted by a 1-bit delay, each bit of the code aligns with the next bit in the code within the code length, with only the last chip lying on the first of the next recurrence of the code. For a relative shift of 2 bits, two trailing bits of one code get placed on two leading the next. It goes on in this manner. Because the sequence is not infinitely random, the total probability of like chips pairing is not equal in count to the number of unlike chips pairing. Hence, the sum of their product is not zero. It gives a nonzero value to the autocorrelation for such a delay of integral numbers of bits, nT_c, where n is not equal to N. The nature of the sequence, that is, the arrangement of $+1$ and -1s

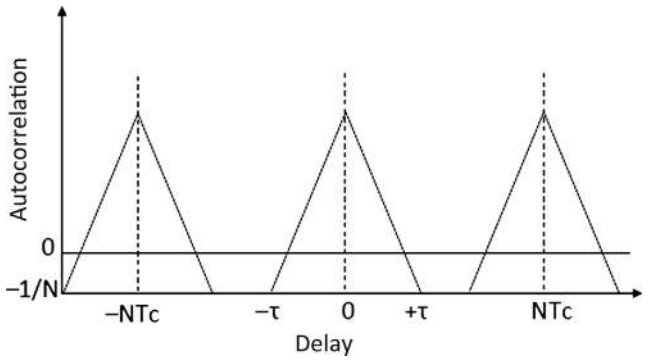

FIGURE 4.6

Autocorrelation function of a PN sequence.

in the finite sequence length, determines what the exact value of this autocorrelation will be.

For any shift of integral numbers of chip length, it becomes the inner product, that is, the bit-by-bit algebraic product, of the sequence. In logical terms, this is nothing but the XOR operation on the shifted version of the same sequence in logical terms. The XOR operation of such sequences results in the generation of the same sequence with a different shift, which is evident from the second property. So, the algebraic inner product of the sequence formed during autocorrelation thus produces the sequence itself with a delay. From the first property, the product sequence has one -1 excess over the number of $+1$s. Upon integrating this product over a time of the complete code duration of N bits, and averaging, the autocorrelation value it yields is

$$R_{XX}(nT_c) = \frac{1}{NT_c}\sum_{i=1}^{N}(a_j a_k)T_c = \frac{1}{NT_c}\sum_{i=1}^{N}(a_m)T_c = -\frac{1}{N} \tag{4.24}$$

The same nature of the correlation function will be repeated over the whole sequence, with the exact superimposition condition returning after N chips. With increasing N, as the sequence approaches a purely random nature, the autocorrelation for delays of integral multiples of chip period tends toward triviality, which is evident from Eq. (4.23). Obviously, the repeating period of the function also increases accordingly. From this, we understand that as the length of the code N increases, the sequence behaves more like a purely random one. Fig. 4.6 shows the autocorrelation of a pseudo-random function.

Readers may find the concepts of autocorrelation illustrated in Box 4.3.

4.3.1.1.1 Spectrum of the codes

This section discusses in detail the spectral characteristics of a PRN sequence. The spectral characteristics will be used in subsequent discussion, and hence, this topic may be viewed as a precursor for the conceptualization of those ideas.

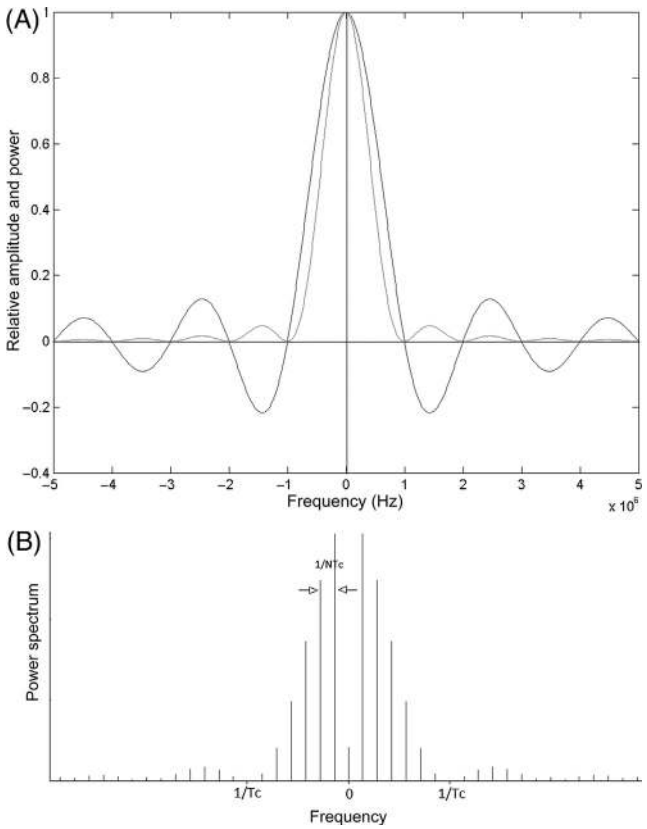

FIGURE 4.7

Spectrum of a pseudo-random code sequence.

The amplitude spectrum of a PRN code is slightly different from that of a fully random one. To understand it, let us consider a code of length N chips with chip width T_c. The code period is consequently NT_c.

Let us consider one complete code of N chips, each of width T_c, recurring over an interval of NT Let$_c$ across the timeline. This sequence with the particular occurrence has an amplitude spectrum whose shape can be represented by a sinc function of nature.

$$S(f) = a\,T_c \frac{\sin(\pi f T_c)}{\pi f T_c} = a\,T_c\,\mathrm{sinc}(\pi f T_c) \tag{4.25A}$$

Thus, this spectrum is a continuous sinc function about f = 0 with nulls at f = 1/Tc and its multiples, the plot for which is shown in Fig. 4.7A. The corresponding power spectrum is also shown.

BOX 4.3 MATLAB Autocorrelation

The MATLAB program autocorr_prn was run to generate the autocorrelation function of a PRN sequence for different positive delays between the two sequences. The following one-sided autocorrelation function is obtained using the definition of the autocorrelation. The samples per chip and the number of recurrences are made configurable. The same variation is obtained for the negative delays between the two (Fig. M4.3).

Note the differences in Fig. M4.2 for a complete random sequence. Also, notice how the circular autocorrelation has been achieved.

Run the program for other sequences and for other values of the configurable parameters.

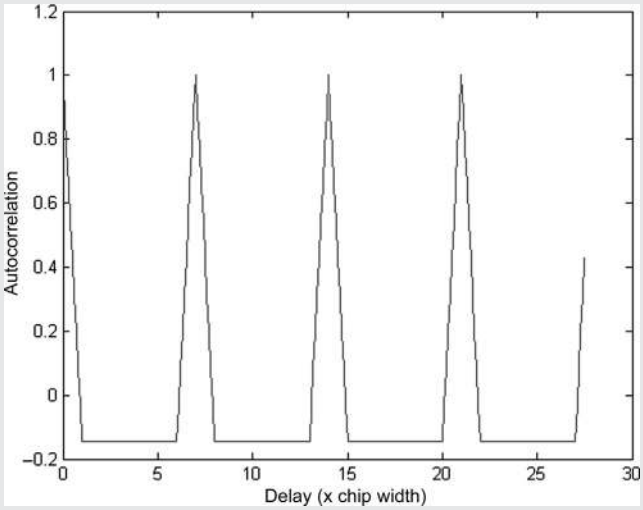

FIGURE M4.3

Autocorrelation function of a PRN sequence.

To explain the nature of the spectrum of the repeating PRN code, we need first to appreciate that the repeating form of this signal in the time domain may be obtained by convolving a single code of N chips with an infinite train of unit impulses, the impulses being separated by the distance of the code width, that iss, NT_c. The expression for this train of impulses is:

$$\tau(t) = \sum_{k=-\infty}^{+\infty} d(t - kNT_c) \tag{4.25B}$$

where $\delta(.)$ is the Kronecker delta such that $\delta(x = 0) = 1$ and $\delta(x \neq 0) = 0$. The convolution of two signals, s_1 and $s_{2,}$ is defined by the expression

$$h(t) = s_1(t) \otimes s_2(t) = \int s_1(\tau) s_2(t - \tau)\, d\tau \tag{4.26}$$

This spectrum of a train of unit impulses in the time domain transforms to a similar unit impulse train in the frequency domain, separated by $1/NT_c$. The corresponding nature of this impulse train may be represented by

$$T(f) \sim \sum_{k=-\infty}^{\infty} \delta\left(f - \frac{k}{NT_c}\right) \tag{4.27}$$

Because the actual signal is formed by the convolution of the two component signals in the time domain, its frequency domain spectrum is formed by the product of the two. Thus, the resultant spectrum is the product of a unit pulse train as in Eq. (4.27) with the continuous sinc function, as in Eq. (4.25A). It turns the product spectrum into discrete lines at an interval of 1/NTc and with an envelope of the sinc function of the first null width of $1/T_c$. The characteristic expression is

$$S(f) \sim \frac{\sin(\pi f T_c)}{\pi f T_c}\, \delta\left(f - \frac{k}{NT_c}\right) \tag{4.28}$$

Then, the corresponding power spectral density becomes

$$P(f) \sim \mathrm{sinc}^2\left(\pi f T_c\right) \delta\left(f - \frac{k}{NT_c}\right) \tag{4.29}$$

The resultant spectrum is shown in Fig. 4.7B. Box 4.4 illustrates the spectral nature of the signal.

However, all previous discussions used relative representation to show the discrete impulsive nature of the spectrum. The exact expression is required to be adjusted so that it represents the correct power density at zero frequency, as well as at other. This exact expression can be shown to be (Cooper & McGillem, 1987).

$$P(f) = \left(\frac{N+1}{N^2}\right)\left[\frac{\sin(\pi f Tc)}{\pi f Tc}\right]^2 \delta\left(f - \frac{k}{NT_c}\right) - \frac{1}{N}\delta(f) \tag{4.30}$$

4.3.1.1.2 Generation of PR codes

The generation of the PRN sequences is based on the background theory of the finite Galois fields and that of the cyclic codes. We start our discussion by briefly introducing the elements of a Galois field.

For any prime number p, there exists a finite field denoted by GF(p) containing p elements. For example, the binary field is a Galois field GF(2). Now, the elements of a binary field with only two elements {0, 1} cannot satisfy equations such as $X^3 + X + 1 = 0$, because these equations have three roots and the field has only two distinct elements.

The GF(2) may be extended to a higher dimension of m to form an extension field $GF(2^m)$. This is the same way in which a one-dimensional number line of real numbers $\{R^1\}$ extends into a three-dimensional vector space of $\{R^3\}$ representing vectors. However, in $GF(2^m)$ space, each dimension can assume either of the two values, 0 or 1.

BOX 4.4 MATLAB Power Spectral Density of Pseudo-random Noise Code

The MATLAB program prn_psd was run to generate the power spectral density (PSD) function of a PRN sequence. The sequence is repeated a large number of times in the code to replicate infinite recurrence. The following one-sided PSD function is obtained using the definition of the PSD employing the square of the distribution of spectral amplitudes obtained through the FFT function. The samples per chip and the number of recurrences are made configurable.

Note the differences between Fig. M4.4A and B. The first is the PSD for random pulses, whereas the second is for the PR sequence. The repeating nature makes the spectrum discrete. Run the program for other sequences and for other values of the configurable parameters.

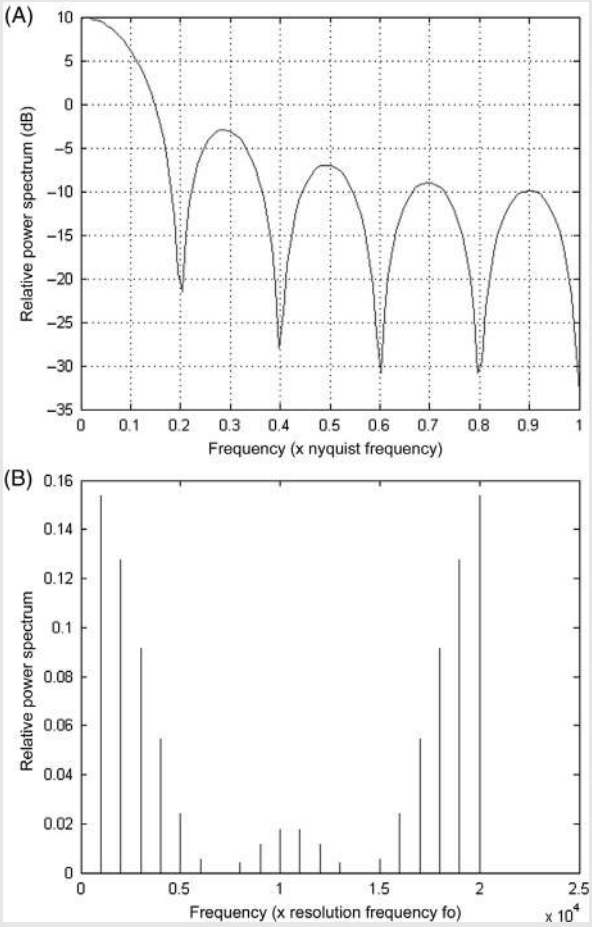

FIGURE M4.4

PSD of a (A) random pulse, (B) PRN sequence.

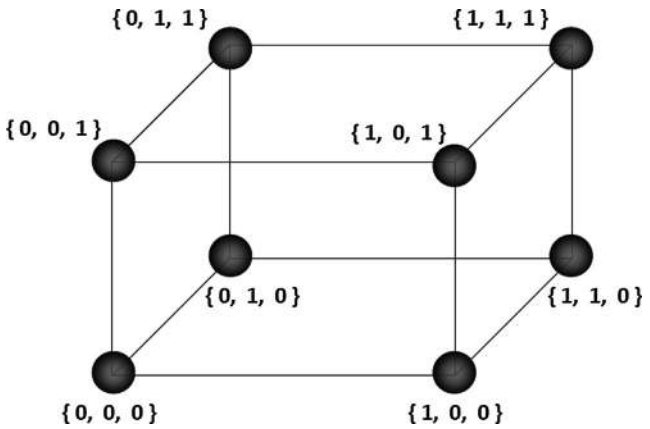

FIGURE 4.8

Elements of a finite field, GF(2^3).

It follows from this that a GF (2^3) field has only $2^3 = 8$ distinct elements. These elements can be represented by s_k, where k runs from 0 to 7. It forms a finite field in which the eight elements can be represented with basis $\{1, X, X^2\}$; for example, $s_j = \{1X^2 + 0X + 1\} \equiv 1\ 0\ 1$, as shown in Fig. 4.8.

This finite field is said to be closed under the operation of multiplication of any two elements of this field, say s_k and s_j, if the product $(s_k s_j)$ folds back to one of the elements in this field. There must be some mapping function f(X) that defines how this folding is to happen.

It is apparent from the previous discussion that the elements of the GF(2^m), save {0, 0, 0}, may be used as representations of the seven possible states during the generation of a 7-bit PRN code. We can arrange these seven states as some ordered set as $F = \{a_0, a_1, a_2, a_3, a_4, a_5, a_6\}$, where the total numbers of states are $n = 2^3 - 1 = 7$ and where each state is represented exclusively by an element of the GF(2^m), that is, $\alpha^k \equiv s_k$. Therefore, the generalized PRN generator should:

- Assume the value of one definite element, sn of the field, for one exclusive state, a_n.
- Arrive once at every possible state in ordered succession upon transition.
- Ensure that the same order of states is reiterated in a cyclic fashion.

Consequently, it is necessary to address the following for the purpose:

- What is the transition process?
- How may these criteria be fulfilled?
- How may the whole thing be implemented?

We attempt to answer them in sequence. Suppose one element of the GF(2^m) is taken as a state in the process of generating the PRN. There must be some mathematical operation done on this that will ensure the change of the current state to the next. That mathematical operation is the transition process and is much more obvious when implemented in real hardware.

It is evident that, if during the process of generation, it is always the next higher ordered state that is assumed upon transition, and in the process, the first state is cyclically reached back after attaining the highest available state, then the states always trace the same path in every recurrence. This can be represented in mathematical form as:

$$1.\ \alpha_j \overset{\text{transition}}{\rightarrow} \alpha_{j+1}$$
$$2.\ \alpha_n = \alpha_0 \qquad \text{where} \quad n = 2^m - 1$$

The ordered set of the states assumed in a cyclic manner are somehow mapped to the successive codes of a 2^{m-1} bit cyclic code. Then the transition reduces to successive changes in the states and that results in the cyclic rotation of the codes in the mapped field. There must be some functional relation that determines this action. To obtain that relation, we now use our knowledge of cyclic codes, in which a cyclic shift of a valid code generates another valid code.

For convenience of understanding, if we take $m = 3$ for the generation of a $2^3 - 1 = 7$-bit PRN code, the extension field will have seven elements. The corresponding cyclic code onto which these elements will be mapped should also be a 7-bit code. So, for a 7-bit code, the same initial code reappears after seven cyclic shifts. Hence, the same state with which the code is mapped is also arrived at after seven transitions. Let g(x) be a valid generator polynomial, which on multiplication with the state a_i, generates the i^{th} code, $c_i(x)$. Representing α_i in polynomial form, in terms of its coordinates, we get

$$\alpha_i = \alpha(X) = a_2X^2 + a_1X + a_0 \tag{4.31}$$

Again, the generator, which should be a 4th-order polynomial, may also be expressed as

$$g = g(X) = g_4X^4 + g_3X^3 + g_2X^2 + g_1X + g_0 \tag{4.32}$$

So, the code word is given by

$$c_i = g(X)\alpha_i(X) \tag{4.33}$$

From the characteristics of the cyclic codes, a cyclic rotation will generate a new valid code. Thus, seven cyclic transition shifts will make the same code reappear. One such shift is executed by multiplying by x and modulo dividing by x^7+1. If Rem[a/b] denotes the remainder of the division a/b, then

$$c_{i+1} = \text{mod}\left\{(x\ c_i), \left(x^7 + 1\right)\right\} = \text{Rem}\left\{x\ g(x)\alpha_i(x)/\left(x^7 + 1\right)\right\} \tag{4.34}$$

Again, from the theory of cyclic codes, the generator polynomial is a factor of $x^7 + 1$, So, we can write

$$x^7 + 1 = g(x)h(x) \tag{4.35}$$

Eq. 4.35 demands both g0 in g(x) and h0 in h(x) to be 1. So, using Eq. 4.33, it can be said that, the codes are systematic.

Because g(x) is a polynomial of order 4, h(x) is of order 3. Generalizing this observation, we find that h(x) is one order higher than that of α(x). It can be shown that h(x) is also a generator polynomial for a cyclic 7-bit code (Proakis and Salehi, 2008). Therefore, Eq. 4.34 can be written as

$$c_{i+1} = \text{Rem}\left[\{g(x)\, x\, \alpha_i(x)\}/\{g(x)h(x)\}\right] = g(x)\text{Rem}\left[x\, \alpha_i(x)\}/h(x)\right] \tag{4.36A}$$

For the orderly sequence of the states to be followed, this code c_{i+1} must be generated by α_{i+1}. It requires

$$c_{i+1} = g(x)\alpha_{i+1} \tag{4.36B}$$

Thus, comparing Eq. (4.45A and B), we get,

$$\alpha_{i+1} = \text{Rem}\left\{ x\, \alpha_i/h(x)\right\} \tag{4.37}$$

This equation answers two of our questions. First, it states that during the generation of the sequence of the code, the next state is achieved by multiplying it by x and modulo dividing it by h(x). So, shifting the elements of α_1 of the GF(2^m) to one order higher place and modulo dividing by h(x) generates α_2, and so on. Thus, this operation comprises the transition process.

Second, because the cyclic codes resulted from the states, sequentially assume the seven possible values and return to the first, and the states are mapped exclusively to the codes by Eq. 4.33, the states also follow cyclic rotations. For implementing the codes that assume the states in a cyclic fashion, we need the feedback of the bit at position x^7 to the position $x^0 = 1$. This can be represented as $x^7 + 1 = 0$.

We have mentioned that h(x) is a generator polynomial of a $n = 2^m - 1$ bit cyclic code and of the same order as the extension field GF(2^m). Thus, for convenient implementation, this function h(x) should be chosen. h(x) is an irreducible, primitive factor of $x^n + 1$, i.e., there is no other value $n' < n$ such that h(x) can exactly divide $x^{n'}+1$. For a 7-bit PRN code, we need states of GF(2^3), and hence we choose a generator of order 3. Now, $x^7 + 1$, which may be factored as

$$x^7 + 1 = (x + 1)\left(x^3 + x^2 + 1\right)\left(x^3 + x + 1\right) = g(x)\, h(x) \tag{4.38}$$

Factors $(x^3 + x^2 + 1)$ and $(x^3 + x + 1)$ are irreducible as well as primitive and can be used here. Taking one of these two primitive polynomials, say $h(x) = x^3 + x^2 + 1$, as our generator polynomial, it becomes clear that equating this to zero implies $x^7 + 1 = 0$, which is equivalent in the binary system to $x^7 = 1$. This ensures the

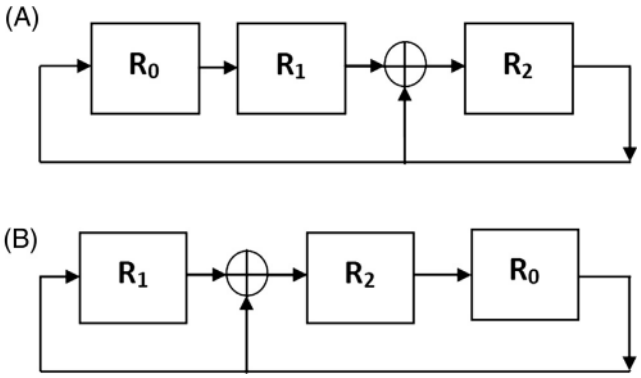

FIGURE 4.9

Implementation of a pseudo-random sequence generation.

cyclic rotation of the codes. For implementation, any initial state, ai may be used. Then, using Eq. 4.37, a higher order shift in the bits of the state with feedback will get the sequence of the states. For implementing $x^3 + x^2 + 1 = 0$, which is equivalent in binary to $x^3 = x^2 + 1$, the bit that attains the position of x^3 on the code upon the upshift, folds back to the position of x^2 and x^0 (LSB) and gets XOR-ed to the bit that is supposed to attain the position owing to the up shift.

The codes will start generating from any initial state, called "seed," selected from the elements of GF(2^3), and they will go on assuming the values cyclically. If we arrange the corresponding states in an ordered manner expressed in accordance with the bases $\{ 1\ X\ X^2 \}$, where moving the bits right is upshift, this will follow as:

$$S = [\{1\,1\,1\},\ \{1\,1\,0\},\ \{0\,1\,1\},\ \{1\,0\,0\},\ \{0\,1\,0\},\ \{0\,0\,1\},\ \{1\,0\,1\}]$$

These codes being systematic, the states are only definite portions of the code. Moreover, the codes being cyclic, taking any one particular bit of the state over the sequence of codes will lead to the generation of the PRN. For example, using the MSB will lead to the PRN sequence of {1 1 0 1 0 0 1}. Because this is cyclic, the same sequence will be obtained if we take any other bit, but with a delay.

To implement this, we first note that the state, α_i, an element of GF(2^3), is a 3-bit word. It can be contained in a 3-bit shift register. To attain the next state, the sequence first must be multiplied by x. This is achieved by upshifting the contents 1 bit toward the MSB. This needs to be divided by $x^3 + x^2 + 1$, and the remainder forms the next state. This modulo division is realized by providing feedback from the output of the MSB register and adding it to the content of x^2 and x^0, modulo 2. The implementation is shown in Fig. 4.9A. The output of any register will provide the code in sequence.

Similarly, the other primitive polynomial, $x^3 + x + 1$, which is also a factor of $x^7 + 1$, may be used to generate another sequence. Here, the modulo divisor is $x^3 + x + 1$. So, the value of the MSB output on upshifting a sequence, must be fed

Table 4.2 Valid states.

Order	x^2	x	1	$x \oplus x^2$
α	0	0	1	0
α^2	0	1	0	1
α^3	1	0	0	1
α^4	1	0	1	1
α^4	1	1	1	0
α^6	0	1	1	1
α^7	1	1	0	0
α^8	0	0	1	0

back to the contents of x^1 and x° for modulo two addition. This implementation is shown in Fig. 4.8B (Box 4.5).

If we represent a definite valid state of the generator by αj, αj is defined by the contents of the three placeholders. For a primitive polynomial, equation, $h = x^3 + x^2 + 1$, if we consider the state [0 0 1] to be α_j, the higher orders of α go as shown in the following table (Table 4.2).

In these three place holders, x^2, x, and x^0, all seven possible different combinations of bits have occurred. If we consider the sequence of the bit appearing at one place as the code, for each such combination, there is a code bit generated, justifying the name maximal sequence, or *m*-sequence.

BOX 4.5 MATLAB: Generation of Maximal Length Pseudo-random Noise Codes

The MATLAB program m_sequence.m is run to generate an *m*-sequence of 7 bits with the primitive polynomial $h = x^3 + x + 1$. It was started with the state S = [1 1 1], and the final repeating sequence generated was:

P1 = [1 1 0 0 1 0 1]

The variable S represents the state variable that is a three-tuple word and carried by the three elements of S. The arrangement and the variation of the elements S(1), S(2), and S(3) of the state variable S following the given relation are shown in Fig. M4.5A.

We need to see whether, if we start with another definite state for this arrangement, the same set of states will be repeated every seven steps. Run the program by changing the initial value of S from [1 1 1] to [1 0 0] and check the final sequence. It is apparent from Fig. M4.5B, that for this case, the criterion is fulfilled starting from the initial state of [0 0 1]. In this figure, the feedback to the position of X^1 is modulo-2 added to the other input coming through the up shift from X^0. The other feedback is directly placed in X^0 because there is no other input.

(*continued*)

BOX 4.5 MATLAB: Generation of Maximal Length Pseudo-random Noise Codes — *cont'd*

Thus, we see that both arrangements lead to the same sequence that recurs every seven steps. The phase of the sequence may differ depending on which point is considered for getting the output.

Also, change the polynomial used by changing the connections in the code, and check the sequence it generates.

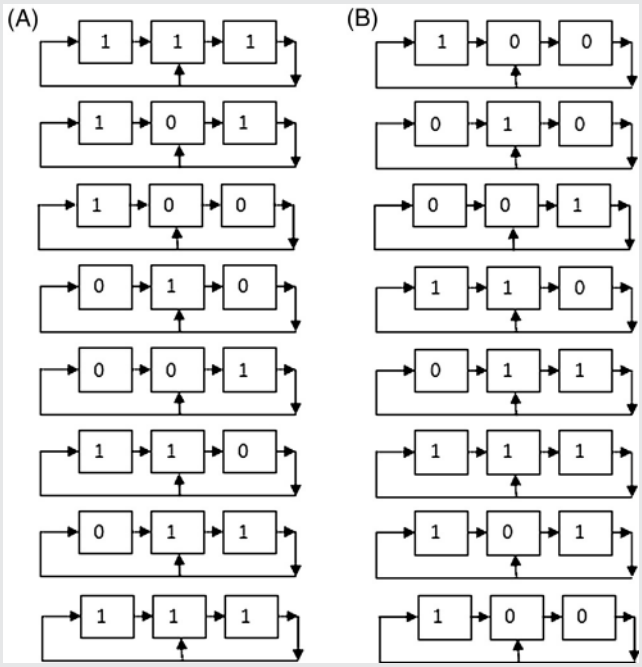

FIGURE M4.5

States of 7-bit m-sequence for primitive polynomial $h = x3 + x + 1$.

Furthermore, we can see that the last column, which represents the XOR value of the first two columns, is only a shifted version of the others. This proves that the modulo-2 sum, which is also the XOR operation of two time-offset versions of the same *m*-sequence, is another offset version of the sequence itself. This is an important property that we shall be using in our explanations later in this chapter and the next.

One question we still need to answer is, because one code set will be produced from one irreducible primitive factor, how many such irreducible polynomials are possible for a code length of $2^n - 1$? It can be easily calculated from the value n. For the purpose, we use Euler's totient function φ. The function, $\varphi(x)$, represents the

count of numbers that are less than x and relatively prime to x. It can be shown that the number of codes, N that are possible is

$$N = \frac{1}{n}\varphi(2^n - 1) \tag{4.39}$$

For $n = 3$, $2^n - 1 = 7$, and so $\varphi(7) = 6$. Thus, $N = 6/3 = 2$, which we have already seen in our discussion. Similarly, for $n = 4$, $\varphi(15) = 8$ and hence $N = 8/4 = 2$, whereas for $n = 5$, $N = 6$. Comparing the numbers, you can derive the fact that the numbers are more when the argument of Euler's function is itself prime. This is obvious because it gives a large number of mutually prime numbers less than itself.

4.3.1.2 Gold codes

Of all orthogonal binary random sequences, the Gold code, owing to its important and exclusive features of bounded small cross-correlations and ease of generation, is extensively used in telecommunications and navigation systems. In the next subsection, we will find how this helps in CDMA systems to keep interference noise to a minimum.

It is known from Euler's function that the number of m sequences increases rapidly with the increase in the code length. Although these m-sequences have suitable autocorrelation properties, most sequences do not have the desired cross-correlation appropriate for navigational purposes, that is, low enough cross-correlation between different codes.

Gold (1967) showed that there are certain m-sequences with better periodic cross-correlation properties than other m-sequences of the same length. Some pairs of m-sequences yield three-valued cross-correlation over the code period given by

$$\begin{aligned} R_{XY} &= \frac{1}{N}[-1, -2^{(n+1)/2} - 1, +2^{(n+1)/2} - 1] \text{ when n is odd} \\ &= \frac{1}{N}[-1, -2^{(n+2)/2} - 1, +2^{(n+2)/2} - 1] \text{ when n is even} \end{aligned} \tag{4.40}$$

Such m-sequences are designated "*preferred sequences.*" When these preferred m sequences of the same code length are taken in a pair and are XOR-ed, a definite new sequence is obtained, known as a Gold and Kasami sequence, or more popularly, "Gold codes".

Changing the phase differences between the same two participating m-sequences gives a different Gold code of the same family. Stated differently, Gold codes generated from the same parent set of m-sequence are said to constitute a family of codes. They have the same three-value cross-correlation between them. Thus, from a single pair of m-sequence of length n with preferred cross-correlation, we can generate n numbers of Gold codes with similar cross-correlation properties between them.

To understand the features of the Gold codes, we recall that XORing the same m-sequence with two different phase offsets generates the same m-sequence again, but with a new phase offset. Because two Gold codes of the same family are produced by XORing the same two definite m-sequences of a preferred pair, the same components reside in these two Gold codes, but with different relative phase offsets. Thus, the two

Gold codes may be represented as

$$G_{1k} = M_1(t) \oplus M_2(t + k_1)$$
$$G_{2k} = M_1(t) \oplus M_2(t + k_2) \tag{4.41}$$

The constituent m-sequences are one of those selected pairs that generate a three-valued cross-correlation defined in Eq. (4.40).

Here, M_1 and M_2 are the logical bit sequences of the constituent m-sequences. Because the logical values can be replaced by the algebraic surrogates m_1 and m_2, respectively, and the operation of XOR by multiplication, we can say

$$g_1(t) = m_1(t)m_2(t + \delta_1)$$
$$g_2(t) = m_1(t)m_2(t + \delta_2) \tag{4.42}$$

where $\delta j = k_j T_c$ and k_j is an integer. So, when the cross-correlation is obtained between these two Gold codes, the same pair of constituents present in the two Gold codes gets multiplied with different phase offsets. When the above two Gold codes are cross-correlated, we get

$$R_{XY}(g_1, g_2, d) = \frac{1}{T}\int g_1(t)g_2(t + d)dt = \frac{1}{T}\int m_1(t)m_2(t + \delta_1)m_1(t + d)m_2(t + d + \delta_2)dt \tag{4.43}$$

The product may also be seen as the multiplication of two self-products of the constituent m-sequences. So,

$$R_{XY}(g_1, g_2, d) = \frac{1}{T}\int \left[(m_1(t)m_1(t + d)\right]\left[m_2(t + \delta_1)m_2(t + d + \delta_2)\right] dt$$
$$= \frac{1}{T}\int [m_1(t + \Delta_1)m_2(t + \Delta_2)] dt \tag{4.44}$$

This is nothing but the cross-correlation of the same constituent m-sequences with some new phase difference $\Delta_2 - \Delta_1$. Hence, this cross-correlation is also a three-valued function. However, for different values of d, different phase differences are produced.

Furthermore, because the phase offset product of m_1 and m_2 is a new Gold code of the same family, that is,

$$R_{XY}(g_1, g_2, d) = \frac{1}{T}\int m_1(t + \Delta_1)m_2(t + \Delta_2)dt = \frac{1}{T}\int g(\tau)\, dt \tag{4.45}$$

It is thus apparent that through the cross-correlation of two Gold codes from the same family, we actually integrate a new Gold code over its code bits and divide by the code period NT_c. Thus, the cross-correlation is nothing but the averaged time integral value of the resultant generated Gold code over the code period.

When the new Gold code thus generated is balanced, the cross-correlation is $-1/N$. However, among all the resultant Gold codes generated, not every one is balanced. When unbalanced codes are generated, the cross-correlation assumes one of the other two possible values among $[\pm 2^{(n+1)/2} - 1]/N$ for odd n and $[\pm 2^{(n+2)/2} - 1]/N$ for even values of n (Box 4.6).

BOX 4.6 MATLAB: Pseudo-random Noise Code

The MATLAB program "autocorr_gold" was run to generate the Gold codes from two 7-bit m-sequences and then estimate their autocorrelation.

The two m-sequences selected are [1 1 1 0 0 1 0] and [1 1 1 0 1 0 0]. These codes are converted to their equivalent algebraic forms and produce a three-valued cross-correlation, as given in Fig. M4.6.

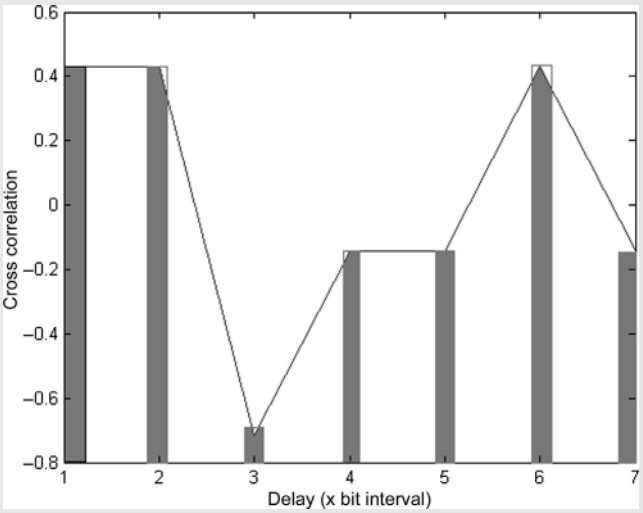

FIGURE M4.6

Cross-correlation of two Gold sequences.

Check that the levels of the cross-correlation are −0.7143, 0.4286, and −0.1429. These values exactly match our expression of $(2^{(n+1)/2} - 1)/N$ and $-1/N$ for $n = 3$, that is, $N = 7$.

All possible XOR results of the selected sequences are:

$$G = \begin{bmatrix} +1 & +1 & +1 & +1 & -1 & -1 & +1 \\ -1 & +1 & +1 & -1 & +1 & +1 & +1 \\ -1 & -1 & +1 & -1 & -1 & -1 & -1 \\ +1 & -1 & -1 & -1 & -1 & +1 & +1 \\ -1 & +1 & -1 & +1 & -1 & +1 & -1 \\ +1 & -1 & +1 & +1 & +1 & +1 & -1 \\ +1 & +1 & -1 & -1 & +1 & -1 & -1 \end{bmatrix}$$

These seven codes form the Gold codes of the same family. Of all the codes generated, two were arbitrarily selected, and cross-correlations were found for different delays. The cross-correlation obtained for different delays is shown in Fig. M4.6. This cross-correlation is also three-valued following the given expression for $n = 3$.

(*continued*)

BOX 4.6 MATLAB: Pseudo-random Noise Code — *cont'd*

The code arrays produced on XORing two selected Gold codes for different relative delays are shown below. The last two codes in the previous section were selected for the purpose. It follows that the codes thus produced are only the shifted versions of the codes of the family or the constituent m-sequences.

$$GX = \begin{bmatrix} +1 & -1 & -1 & -1 & +1 & -1 & +1 \\ +1 & +1 & -1 & -1 & +1 & +1 & +1 \\ +1 & +1 & +1 & -1 & +1 & +1 & -1 \\ -1 & +1 & +1 & +1 & +1 & +1 & -1 \\ -1 & -1 & +1 & +1 & -1 & +1 & -1 \\ -1 & -1 & -1 & +1 & -1 & -1 & -1 \\ -1 & -1 & -1 & -1 & -1 & -1 & +1 \end{bmatrix}$$

Run the program by selecting other Gold sequences.

4.3.2 Effect of multiplying ranging code on signal

In the navigation signal, the data that repeats at the rate $R_d = 1/T_d$ is multiplied synchronously to the individual chips of the code that repeats at a rate of 1/Tc, which is much faster compared with that of the data. Consequently, the product sequence has the bit repetition rate equal to the chip rate of the code. We shall henceforth call these products of the information carrying data with the code chips "encoded data chips" to distinguish them from the normal data bits as well as from the code chips.

The benefit of the PRN resides not only in the sequence of the chips in the code, but also in the relative rate at which the data and the code bits vary in the signal. Typically, the code chips have a rate that is about a few thousand times greater than the data rates. Multiplication of the codes with the data has two effects: the effect on the frequency domain is the *spreading* of the signal, whereas the effect on the time domain is that it provides the signal with a suitable *correlation* property. These two notions form the basis of the important activities carried out with the signal, including ranging and multiple access (MA), in addition to their effect on data security. We will discuss each of these effects in detail.

4.3.2.1 Spreading

We have learned about the spectrum of the PRN sequence in Section 4.3.1. We know that when the code is multiplied with the data sequence, in the time domain, their spectrum gets convolved in the frequency domain. The code sequence of length N, which is repetitive in time after a period of NTc, has a spectrum that is a sequence of discrete lines at interval 1/NTc, the full spectrum given by Eq. 4.30. The data spectrum is a continuous sinc function of the form

$$S_d(f) = AT_d \left[\{\sin(\pi f T_d)\}/(\pi f T_d) \} \right] \tag{4.46}$$

Because of the data bit width of T_d, this spectrum has nulls at $1/T_d$. So, in the frequency domain, on convolving these two spectra, each discrete frequency line of the code spreads out into a replica of the message spectrum.

In general, $T_d > NT_c$, and so, $1/(NT_c) > 1/T_d$. Therefore, the first nulls are very close to zero and hence the width of the main lobe of this data spectrum are much smaller than the separation of the discrete lines of the code spectrum and are fairly accommodated in this interval without aliasing.

If the repetition interval of the code is large owing to large code length, its spectral lines are placed so close to each other that they appear like a continuum, and the total spectrum appears like a continuous sinc function with first nulls at $1/T_c$. This is expected because a high repetition interval tends toward a random sequence whose spectrum is a continuous sinc function. For such a case, the effective spectrum is the convolution of these two sinc functions, one from the code sequence with width $1/T_c$ and the other from the data sequence with width $1/T_d$. But as $T_c << T_d$, it follows that the latter spectrum appears to be almost a line compared with the former, and hence the effective spectrum is almost identical to that of the code.

Finally, the data, which are themselves of spectral width $1/T_d$, after code multiplication, effectively spread out to 1/Tc. The ratio of the width of the spread spectrum to that of the original spectrum of the data is called the bandwidth expansion factor, Be (Proakis & Salehi, 2008). It is equal to the ratio of the chip rate Rc to the data bit rate R_d, as

$$B_e = (1/T_c)/(1/T_d) = T_d/T_c = R_c/R_d \tag{4.47}$$

Multiplication of the data with the code effectively spreads the signal in the frequency domain, as we have just seen, and hence is also known as the *spread spectrum system*. The spectrum thus produced is also called a *direct sequence spread spectrum*. Such systems are generally designed to permit communication of messages under the condition of a very low signal-to-noise ratio or to combat interfering transmissions or for secured communication and for multiple access.

4.3.2.2 Orthogonality and autocorrelation

The code plays an important role in this spreading and de-spreading process. The choice of proper code is important in any such system and is primarily determined by the code characteristics. We already learned in a previous section that the correlation of a signal is related to the inner product, that is, the chip-to-chip multiplication of two signals and averaging the product over the entire code length. This correlation signifies how much one code is structurally similar to another. When the segment of one code is the same as that of the other, maximum correlation is achieved. For almost similar codes, this value is large. For middling similarity, this is moderate, and for almost no similarity, the value approaches zero. So, when the inner product of two codes is zero or near zero, the codes are said to be orthogonal to each other.

In statistical terms, orthogonal means completely uncorrelated. It is also evident from the previous definition that correlation is nothing but the inner product averaged

over the code length. Therefore, drawing the analogy of vector inner (dot) products, if two codes have zero or very low correlation values, they are said to be orthogonal. The orthogonal properties of this sort are among the most desirable attributes of a signal in a wide variety of situations. We already know that two signals, one modulated by a sine wave and the other by a cosine wave carrier of the same frequency, are mutually orthogonal and do not interfere. Here two signals with two different data when multiplied with orthogonal codes cause no interference, even though they are on the same carrier. So, orthogonal codes are vital in satellite navigation and permit a number of signals to be transmitted on the same carrier frequency and occupy the same radiofrequency bandwidth, without interference, resulting in what is called code division multiplexing. Therefore, the cross-correlation values of the codes to be used for navigation signal should be low, whatever the phase differences. Hence, orthogonal codes are very carefully selected for the purpose.

4.3.3 Navigational use of the effects

4.3.3.1 Ranging

Multiplication of the pseudo-random code with the data enables us to measure accurate distances from the satellite to the receiver. This is used not only in navigation, but also in other applications of one-way satellite ranging and in radar systems. Hence, these codes are also known as the ranging codes.

The geometric distance between a transmitter and a receiver may be obtained by measuring the propagation delay of a radio signal and then multiplying it by the velocity of light. We will learn the details of ranging in Chapter 5. Here, we will only have an overview of it.

The codes are used in ranging utilizing their autocorrelation properties. We know that the correlation of the code depends on the delay. If the receiver can synchronously generate the same code as the transmitter, both the satellite and the receiver can generate the same '*code phase*' at a definite instant simultaneously. The phase of a repeating ranging code may be defined by the current state of the code, that is, which chip of the code and what fraction of it is currently being generated.

The code phase generated at the satellite is transmitted through the signal and takes some finite time to traverse the path between and reach the receiver. This delay occurring between the transmission and the reception is the traverse time of the code phase. So, when the signal is received by the receiver, which is synchronously generating the same code as the transmitting satellite, it generates a later phase of the code when it receives a certain code phase of the received signal. The difference in code phases is proportional to the travel time. The relative code phase is due to the incoming signal being estimated through autocorrelation of the signal with time-shifted versions of the locally generated code. The time shift in the local code that results in the highest autocorrelation, affirming the exact match of the two codes, is equal to the relative delay between the local and incoming code. This is equal to the time of propagation. The faster the chip rate of the code is, the steeper the variation of the autocorrelation function profile with delay. This makes the delay estimates more

precise. The estimated delay, when multiplied by the propagation velocity, which is the velocity with which electromagnetic waves traverse through a medium, gives the range of the transmitter from the receiver. However, to know more about this, we will have to wait until we reach the appropriate section in the next chapter.

4.3.3.2 Multiple access

In certain satellite navigation systems, all satellites transmit their signals on the same carrier frequency. This enables the user receiver to operate with a smaller bandwidth at the front end. The signals being multiplied by the different orthogonal codes remain mutually separated and avoid interference. When the composite signal is again multiplied by the required code at the receiver, all other components of the total signal are rejected, and the one associated with that code remains in the receiver with the code removed. This is possible by virtue of the good correlation properties of the codes selected for the purpose.

Because multiple access forms a separate aspect of the signal transmission, which includes other types of multiple access such as FDMA, we will consider this topic separately after the current section.

4.3.3.3 Processing (spreading) gain

The spread of the signal bandwidth at the transmitter and the subsequent dispreading at the receiver of the desired signal lead to a system processing gain (PG). It is also known as the Spreading Gain. In navigation and any other spread spectrum system as well, the term '*Processing Gain*' is important. It is defined as the signal-to-noise ratio (SNR) improvement at the output with respect to that at the input of the processing unit at the receiver. In terms of signal spread, the PG is the improvement in the SNR after dispreading the signal (i.e., in unspread condition) with respect to the SNR when it was spread. It is expressed through the equation

$$\mathrm{PG} = 10 \log \frac{(\mathrm{SNR})|_{\mathrm{unspread}}}{(\mathrm{SNR})|_{\mathrm{spread}}} \tag{4.48}$$

For a navigation receiver, the total received power remains the same; only the spectral range changes from the spread bandwidth to the unspread bandwidth. If P is the total signal power and N_0 is the noise power density, the SNR of the signal before dispreading is

$$\mathrm{SNR}^{-} = \frac{\mathrm{P}}{2\mathrm{R_c}\mathrm{N_0}} \tag{4.49}$$

Here, we used our previous observation that the bandwidth after spreading is equal to Rc, the bandwidth of the code chips.

This signal is multiplied by the identical code at the receiver to recover the data. This removes the code variation of the signal, leaving only the data components. The associated power of the signal is brought back unabated by collating it into the reduced bandwidth of the original data. So, the signal power after dispreading remains P. The random white noise component in the signal, which is also multiplied by the

code at the receiver, retains its random nature. Its amplitude of variation remains the same while its phase may only get inverted when the local code is −1. Therefore, it remains unaltered in terms of its spectral nature, and its power spectral density remains unaltered. Because the effective bandwidth of the signal has now been reduced to that of the data, the total contribution to the noise attached to the signal is reduced by the same factor as the bandwidth, the reduced bandwidth being R_d. The total noise power after dispreading is $N = 2R_dN_0$.

Whereas the total signal power remains the same at the input and output, the noise power is reduced by a factor equal to the factor of reduction in the effective bandwidth. The SNR now becomes

$$SNR^+ = \frac{P}{2R_dN_0} = \frac{P}{2R_cN_0} \times \frac{R_c}{R_d} = SNR^- \times \frac{R_c}{R_d} \tag{4.50A}$$

So,

$$\frac{SNR^+}{SNR^-} = \frac{R_c}{R_d} = B_e \tag{4.50B}$$

where Be is the bandwidth expansion factor and is equal to the ratio of the code rate to the data rate. Thus, the PG is achieved, which by definition can be expressed as

$$PG = 10\log\left(\frac{SNR^+}{SNR^-}\right) = 10\log\left(\frac{R_c}{R_d}\right) = 10\log\left(B_e\right) \tag{4.51}$$

PG is nothing but the bandwidth expansion factor expressed in dB. Because typical R_c is a few tens of thousands ($\sim 10^4$) times R_d, we get for such a case, PG = 10 log ($\sim 10^4$) ~ 40 dB. This enables the system to keep a low signal-to-power ratio of the signal during transmission, yet with an improved value of the same when received at the receiver. This is the basis of the data security availed in the navigation process.

The spreading and dispreading of the signal achieved through multiplying the code with the data also provides data security and signal robustness. However, we shall discuss this aspect in a separate place in Chapter 10.

4.4 Multiple access

Navigation satellites transmit signals that are received by receivers on the Earth. Many satellites transmit the signal simultaneously, which are spatially separated in their orbit. Multiple access in GNSS is the ability to share the same resource of the carrier signal by multiple satellites, enabling the receivers to connect many satellites simultaneously and receive data from each without any interference.

Mainly two types of multiple access are used for satellite navigation purposes: CDMA and FDMA. These are described below.

4.4.1 Code division multiple access

In previous sections, we already learned that by multiplying different signals by distinct orthogonal PRN codes during transmission, it is possible to separately select them at the receiver. The receiver can segregate and accept the desired signal out of the composite and reject the unwanted components present in it.

This is achieved at the receiver by multiplying the composite signal by the corresponding orthogonal code of the desired one. The desired signal is selected by virtue of the large autocorrelation values with the required code. Other undesired signals, forming cross-correlation with the multiplied code, result in low values and are rejected. This is the basic principle behind CDMA.

Considering the scenario for a navigation system, each satellite transmits its unique navigation data by multiplying it with its particular unique code. All such signals transmitted by the different satellites, multiplied by different orthogonal codes, are received as a composite signal by the receiver. All data are transmitted at the same data rate of R_d and the code rate of R_c. The composite signal consisting of all spread signals can be represented in the form

$$S(t) = D_1(t)g_1(t) + D_2(t)g_2(t) + D_3(t)g_3(t) + .. = \sum_i D_i(t)g_i(t) \tag{4.56}$$

where S(t) is the composite signal, Di(t) and gi(t) are the data and code components of the signal from the ith satellite, at time t. When this composite signal is multiplied by a valid code $g_k(t)$ that corresponds to the kth signal in a synchronous manner, the product becomes

$$\begin{aligned} P(t) = \ S(t)g_k(t) &= \sum_i D_i(t)g_i(t)g_k(t) = D_1(t)g_1(t)g_k(t) \\ &+D_2(t)g_2(t)g_k(t) + \ldots\ldots + D_k(t)g_k(t)g_k(t) + \ldots . \end{aligned} \tag{4.57}$$

Upon integration of the product over a data bit period and dividing by the integral value integration period, we get

$$\begin{aligned} p(k) = \left(\frac{1}{T_d}\right) \int P(t)\, dt \ &= \left(\frac{1}{T_d}\right)\left[\int D_1(t)g_1(t)g_k(t)\, dt \ + \int D_2(t)g_2(t)g_k(t)\, dt \right. \\ &\left. + \ldots + \int D_k(t)g_k(t)g_k(t)\, dt \ + \ldots .\right] \end{aligned} \tag{4.58}$$

But because the integration is done over a data period, the data bit remains constant. So, the integration turns into

$$p(k) = \sum \left(\frac{1}{T_d}\right)\left[D_i(t) \int g_i(t)g_k(t)\, dt \ \right] = \sum D_i(t)\left[\left(\frac{1}{T_d}\right) \int g_i(t)g_k(t)\, dt \ \right] \tag{4.59}$$

Each of the components on the right-hand side of the equation becomes the correlation of the individual component codes of the signal and the code used in the receiver.

For all components of this product except the kth one, the codes are different. Because the codes are orthogonal, they produce very low correlation values and vanish

owing to their triviality. These components of the signal are rejected and are only treated as noise. However, only for the kth component, the two codes are identical, and they produce the unit autocorrelation value. Hence, the data bit D_k is retrieved. This may be mathematically expressed for a composite signal with N components as

$$\begin{aligned} p(k) &= \sum \left(\frac{1}{T_d}\right)\left[D_i(t) \int g_i(t) g_k(t)\, dt\right] = \sum D_i(t)\left[\left(\frac{1}{T_d}\right) \int g_i(t) g_k(t)\, dt\right] \\ &= D_1(t) R_{xy}(g_1, g_k) + D_2(t) R_{xy}(g_2, g_k) + . + D_k(t) R_{xx}(g_k, g_k) + . + D_n(t)\, Rxy(g_n, g_k) \\ &= D_k(t) R_{xx}(0) + n = D_k(t) + n \end{aligned} \tag{4.60}$$

Therefore, after this process, the SNR ratio, including the cross-correlation noise, is given by

$$SNR_k = \frac{Pk}{\left[N_0 R_d + \sum_{i=1,\ i\neq k}^{n} R_{XY}(\tau)\right]} \tag{4.61}$$

where R_d is the data rate. Considering equal power P of the transmitted signals with PG received at the receiver from n satellites, SNR_k can be more conveniently written as

$$SNR_k = \frac{P_k}{\left[N_0 R_d + (n-1)\, P/PG\right]} \tag{4.62}$$

4.4.2 Frequency division multiple access

The medium between the transmitting satellites and the receiver can efficiently carry radio waves only within a certain limited bandwidth, limited by the physical characteristics of the medium. Within this bandwidth, a part is assigned for the purpose of navigation. Again, each individual system is allotted a definite portion of this band. In an frequency division multiple access (FDMA) system, each satellite in the navigation system transmits its signal in a discrete channel defined by a specific centre carrier frequency and associated bandwidth. The frequency of each channel is different but contained within the total band allocated to its system. The sinusoidal waves at carrier frequencies are made to carry the encoded data chips through a process called modulation. The concept of FDMA is shown in Fig. 4.10.

Satellites share the total bandwidth allocated to the system. There are however, separation between the bands of adjacent channels used by two different satellites to avoid possible interference; this is called the guard band.

The receiver receives these bands of signals. With adequate bandwidth at the common front end, they can accommodate all available channels. The received signal is then distributed to individual receiving chains. Each of these chains has center frequency aligned with the carrier frequency of the individual satellites and bandwidth just adequate for an individual signal. It thus filters out one individual channel out from the combined received signal obtained from all the visible satellites.

Because each satellite needs to be given a separate width of the band, for large numbers of satellites in the constellation, the total band required for the system and

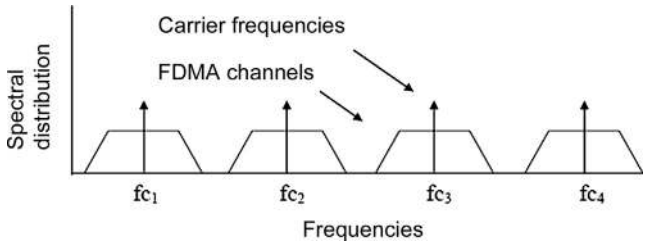

FIGURE 4.10

Signal spectral distribution for FDMA.

hence the front-end bandwidth of the receiver need to be very wide. This constraint is somewhat alleviated by opting for frequency reuse among the satellites. Satellites that are located in antipodal locations in the constellation are never seen from the same point on the earth simultaneously. Therefore, they can be reallocated the same frequency. This reduces the band requirement by almost half. Nevertheless, the number of receiving chains required in an FDMA receiver still depends on the number of satellites to which it wants to have access simultaneously.

4.5 Digital modulation

The signal, consisting of the product of the data and the code, is to be transmitted from the satellite to the user. However, it cannot be sent in this binary baseband form for two key reasons. First, the transmitting antenna needs to be of the order of the wavelength of the signal being transmitted for efficient transmission. The encoded data, which are mostly concentrated within the low frequency ranges and hence have very long wavelengths, would require a very large transmitting antenna for the purpose. Second, the channel through which the signal passes cannot efficiently propagate the DC components and acts as a bandpass filter. Therefore, this signal is ridden on a carrier wave of a suitable high frequency. The technique of the baseband data being put on a high-frequency radio wave to be carried with it, so that it efficiently traverses from the transmitter to the receiver through the path in between, is called "*modulation*". The high frequency of the carrier reduces the antenna size accordingly and carries the signal through the channel unattenuated, as well. Furthermore, modulation over a higher frequency makes it possible to use multiple access techniques such as FDMA and CDMA, besides giving the signal better noise immunity from low-frequency noise sources.

For navigation, encoded navigation data from the baseband is modulated on a carrier with a frequency much higher than the chip rate.

4.5.1 Carrier wave

The carrier is the sinusoidal radio wave of high frequency that is modulated by the encoded data of the signal. The carrier carries the latter through the medium. The choice of carrier signal is basically choosing its frequency. For navigation, it depends on the overall system design. However, the broad frequency band from which the carrier frequency is to be chosen for navigation is specified by the International Telecommunication Union through its recommendations.

For navigation systems using CDMA for multiple access, the carrier frequencies used by different satellites remain the same. For those using the FDMA, the carrier frequencies are different but close to each other. The difference between the centre frequencies used by different satellites is determined by the bandwidth of the signal it carries. In CDMA, because different data are already separated by orthogonal codes, the same carrier can carry different signals at the same time without mutual interference. The sine and cosine signals of the same carrier frequency are also orthogonal, and hence can carry different signals, too.

The unmodulated carrier wave is generated at the satellite using the onboard atomic clock. For satellite navigation, relativistic corrections are done on the transmitting carrier signal. This is because the transmitting satellite and the receiver move relative with respect to the reference frame, and the satellite experiences variation in gravitational potential. To mitigate the relativistic effects of all of these factors that affect the satellite clock, the latter is adjusted to run at a frequency relatively lower than that of the design frequency on the Earth's surface. This frequency, upon reaching the earth and being affected by the relativistic effect, gets transformed into the designed carrier frequency.

4.5.2 Modulation techniques

The common question to be addressed at this point is, "In what form should the carrier carry the information?" The main characteristics of the carrier waveform by which it is defined are its amplitude, frequency, and phase. As a result of modulation of the sinusoidal carrier, one of these features is varied in accordance with variation in the information-carrying encoded and spreaded navigation data acting as the baseband. Thus, through the variation of this particular feature of the carrier, the information is carried through space.

For a digital signal, the information is represented by discrete levels. Not only do the levels vary between discrete values, but the variations take place at discrete intervals, as well. For binary data, only two possible levels can be assumed by the baseband signal. So, upon modulation, any one amongst the initial phase, frequency, or the amplitude of the carrier changes between two fixed values. These two values represent the two binary levels of the baseband signal. Further, these changes occur at discrete but defined intervals. Depending upon the parameter of the carrier that changes, the modulation may be termed as "Phase Shift Keying", "Frequency Shift Keying", or "Amplitude Shift Keying", respectively. There can be multilevel modulations, too, but we shall restrict our discussion to only the binary levels that are

used for the communication of navigation data. Binary keying gives a better error performance, but it has a lower data transfer rate in general. It suffices the purpose because the navigation data is small but needs to be corrected to be transferred to the receiver.

At the receiver's end, the original binary information is recovered by the reverse process known as demodulation. However, depending on the modulation type, demodulation can be complex because it has to recover signals accurately from the weak received signal corrupted by random noise.

When a carrier is modulated by a signal, the modulation process splits in equal two parts the original frequency spectrum of the modulated signal and shifts their centre frequency by an amount equal to the carrier frequency in both the positive and negative directions on the frequency axis. The shape of the original signal spectrum remains unaltered in general. However, under some particular modulations, these shifted signals overlap with each other partially so that the ensuing shape is somewhat different from that of the original signal.

Although the most popular type of modulation for navigation is the BPSK, other types of modulation, including BOC modulation, which gives some additional benefits for the purpose, are also used.

4.5.2.1 Binary phase shift keying

One of the most popular modulation schemes used in the navigation system is the binary phase shift keying (BPSK). This is because such modulation bears constant amplitude and maintains fixed frequency over each symbol interval. However, its phase changes discretely at every change in data symbol. So, the current phase of the modulated signal is determined by the current data value. This technique is easy to implement.

4.5.2.1.1 Time domain representation of binary phase shift keying

The time domain representation of the BPSK modulated signal characterizes how the carrier signal varies with time and how its phase is altered with the variation of the modulating signal. The modulating signal, in our case, is the encoded navigation data.

Because the phase of the signal can vary from 0 to 2π, the maximum separation in phase of two signals at the same frequency can be π. Thus, in BPSK modulation, the carrier phase changes between two different values separated by a phase π to represent the two possible states of the binary data, while its amplitude and frequency are not affected by the data. For a carrier represented by the signal $S = \cos \omega t$, after modulation, the time domain representation of the BPSK signal becomes

$$s(t) = \cos(f(t)) = \cos(wt + f_0) \tag{4.63}$$

where ω is the angular frequency of the carrier and $\varphi(t)$ is the phase at time t and f_0 is the arbitrary initial phase at $t = 0$. This $\varphi(t)$ is the variable that actually carries the information and varies according to the baseband data. The baseband signal is binary and varies between representative levels $a_k = +1$ and $a_k = -1$. Accordingly, f(t) can take discrete values of $f(t) = wt + f_0 + 0$ and $f(t) = wt + f_0 + p$, respectively, to represent the two binary states of the data, a_k, where φ_0 is the arbitrary initial phase. So, the

modulated signal becomes

$$\begin{aligned} s(t) = +\cos\left(\omega t + \varphi_0 + 0\right) \text{ when } a_k &= +1 \\ &= +1\cos\left(\omega t + \varphi_0\right) \\ &= a_k \cos\left(\omega t + \varphi_0\right) \end{aligned} \tag{4.64}$$

and

$$\begin{aligned} s(t) = +\cos\left(\omega t + \varphi_0 + \pi\right) \text{ when } a_k &= -1 \\ &= -1\cos\left(\omega t + \varphi_0\right) \\ &= a_k \cos\left(\omega t + \varphi_0\right) \end{aligned} \tag{4.65}$$

The BPSK modulated signal may thus be represented as

$$s(t) = a_k \cos\left(\omega t + \varphi_0\right) \tag{4.66A}$$

a_k is the kth encoded data chip prevailing at the time t ($k = \text{int}(t/T)$).

From these equations, we can see that the BPSK modulation may also be represented as the product of the data bit with the carrier. This is because changing the phase by $\pi/2$ is just reversing the polarity of the signal, which is equivalent to multiplying the original signal by the complementary unitary data bit. In any case, the amplitude of the modulated signal will remain constant (Fig. 4.11).

Similarly, if the phase values are shifted between $\varphi = \text{wt} + \varphi_0 + \pi/2$ and $\varphi = \text{wt} + \varphi_0 - \pi/2$, for $a_k = -1$ and $a_k = +1$, respectively, it is phase orthogonal with the first case. So, the modulated signal for the two cases of the data bits becomes

$$\begin{aligned} s(t) = \cos\left(\omega t + \varphi_0 + \pi/2\right) \text{ when } a_k &= -1 \\ &= -\sin\left(\omega t + \varphi_0\right) \\ &= a_k \sin\left(\omega t + \varphi_0\right) \\ s(t) = \cos\left(\omega t + \varphi_0 - \pi/2\right) \text{ when } a_k &= +1 \\ &= +\sin\left(\omega t + \varphi_0\right) \\ &= a_k \sin\left(\omega t + \varphi_0\right) \end{aligned} \tag{4.66B}$$

So, the effective carrier may be assumed to be a sine signal instead, with initial phase φ_0.

4.5.2.1.2 Spectrum and Bandwidth

Expanding Eq. (4.66A), we get (Chakrabarty & Datta, 2007)

$$\begin{aligned} s(t) &= a_k[\cos(\omega t)\cos(\varphi_0) - \sin(\omega t)\sin(\varphi_0)] \\ &= [a_k \cos(\varphi_0)]\cos(\omega t) + [-a_k \sin(\varphi_0)]\sin(\omega t) \end{aligned} \tag{4.67A}$$

This means that the signal is equivalent to the combination of a sine and a cosine wave at frequency ω with the effective amplitude a_k projected onto the sine and cosine components of the carrier as $a_k \cos(\varphi_0)$ and $a_k \sin(\varphi_0)$, respectively, on I and Q planes, defined by the orthogonal functional axes of cos ωt and sin ωt. The spectrum of this signal is the same as the spectrum of a_k, shifted by the carrier frequency $f = \omega/2\pi$.

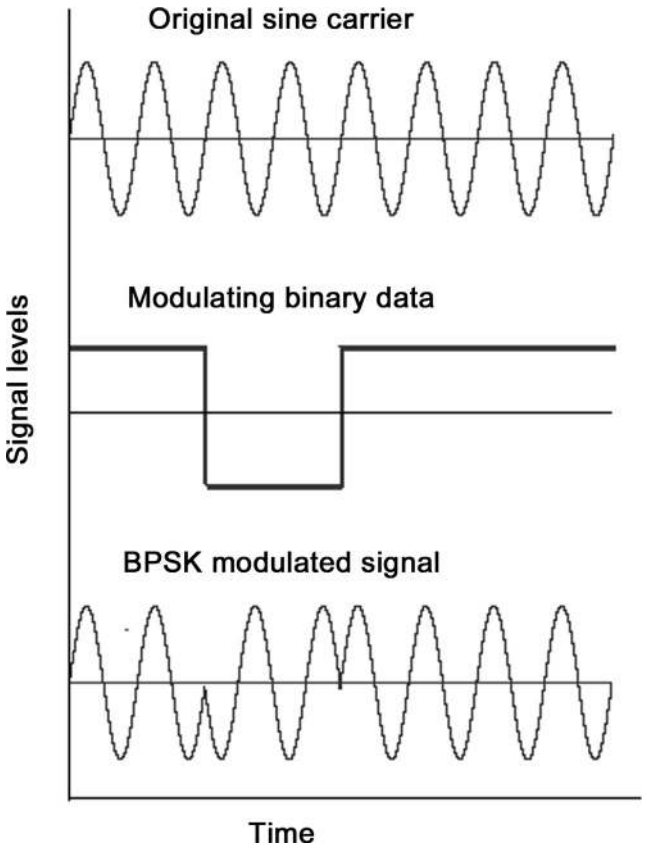

FIGURE 4.11

BPSK modulation.

It is known that the encoded data chips, representing the binary baseband for the final carrier modulation, has a definite frequency spectrum. When this modulates a carrier, the resultant spectrum is the same as that of the data, but only gets shifted by an amount equal to the carrier frequency, and is given by

$$S(f) = aT_c \operatorname{sinc}\{\pi (f - f_c)/R_c\} \tag{4.67B}$$

As the signal is an encoded data, having a chip rate of $Rc = 1/T_c$, the spectrum has a null in its envelope at $f = fc \pm Rc$ and then successively at intervals of Rc on both sides of fc. So, the first lobe has a total width of 2Rc, followed by side lobes of width Rc each. We have already seen that most of the energy remains contained within the first lobe of the envelope, and it is sufficient to take the first null to null width as the bandwidth of the signal. This makes the total bandwidth of the modulated signal 2Rc. Box 4.7 explains the BPSK modulation in both the time and frequency domains.

BOX 4.7 MATLAB Binary Phase Shift Keying Modulation

The MATLAB program bpsk_mod was run to generate the time variation of the BPSK modulated signal. In this program, the sine wave is modulated by a square wave representing the carrier and the modulating EDC, respectively. Fig. M4.7 shows the temporal variation of the modulating and the modulated signal.

In the program, the carrier frequency is taken as four times the chip rate. Run the program with a higher frequency compared with the chip rate. Also, use different modulating chip values. Replace the sine carrier with a cosine carrier. The initial phase fi_0 is taken as zero. Change this value and run the program.

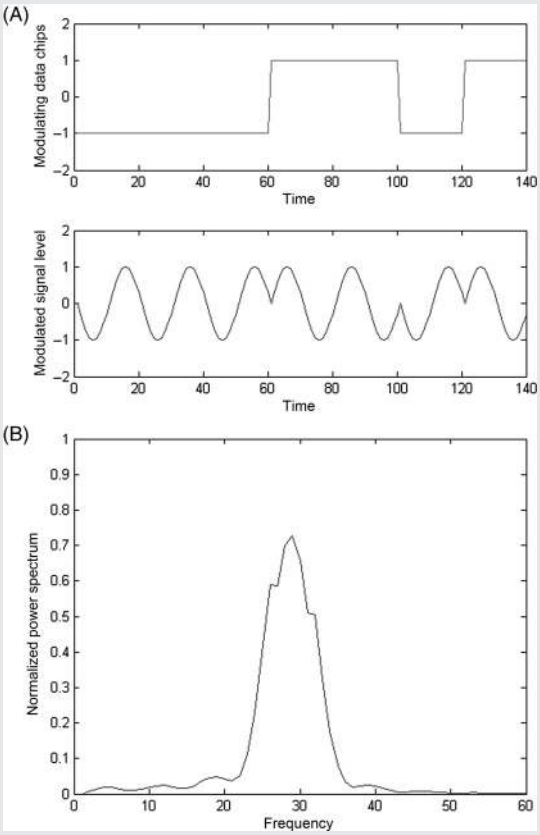

FIGURE M4.7

(A) Modulating encoded data chips and the BPSK modulated signal, (B) power spectral density of the modulated signal.

4.5.2.2 Binary offset carrier modulation

The binary offset carrier (BOC) modulation is actually an extension of the BPSK modulation. It is generated when a BPSK signal is multiplied by a square wave subcarrier (Betz, 2001). The square wave may be sine-phased or cosine-phased. The more conventional sine-phased BOC signal can be mathematically represented as BOC (2011).

$$s(t) = \left[c(t)\ \text{sign}\left\{\sin\left(2\pi f_s\, t\right)\right\}\right] \cos\left(2pf_c t + f_0\right) \tag{4.68}$$

Where s(t) is the signal at time t, c(t) is the encoded data, and fs is the frequency of the subcarrier. Thus, the term sign [sin(2πfst)] represents the value +1 for the phase $0 - \pi$ of the subcarrier, whereas it carries the value −1 for the phase excursion from π to 2π. fc represents the carrier frequency. Similarly, the cosine-phased BOC may be defined. The subcarrier frequency fs is much less than the carrier frequency fc but a few times the chip rate Rc.

Thus, a BOC-modulated navigation signal consists of a sinusoidal carrier, a square wave subcarrier, a PRN spreading or ranging code, and a data sequence. The final signal is produced as the time domain product of these components. The product of the data, PRN code, and carrier essentially makes it a BPSK signal, which has its spectrum about the carrier frequency. This product is then multiplied by a binary-valued subcarrier, which is nothing but a square wave. Multiplying with a square wave of frequency f_s is equivalent to multiplying with each of its spectral components. The spectral components consist of sinusoids with fundamental frequency at f_s and harmonics at its integral multiples like $2f_s$, $3f_s$, etc. As a result, its spectrum again splits and shifts once again by frequency f_s about the carrier frequency f_c. As the center of its spectrum shifts away from the carrier frequency, that is, gets offset, and this shift is realized with a binary subcarrier, this is called offset modulation.

For any practical BOC signal, the carrier frequency, subcarrier frequency f_s, and code rate Rc are chosen as multiples of the reference frequency f_0. So

$$\frac{1}{T_s} = fs = m.f_0$$
$$\frac{1}{T_c} = Rc = n.f_0 \tag{4.69}$$

This refers to the BOC(m, n) modulation. The reference frequency f_0 is generally taken as 1.023 MHz. Furthermore, if we take k to be the total number of subcarrier periods present in one complete code chip period. Then,

$$k = T_c/T_s = f_s/r_c = m/n \tag{4.70}$$

Depending on the relative values of Tc and Ts, the value of k is determined. This value is not always an integer, but it may take semi-integral values, too, as in BOC(5,2). Because a complete period of a square wave has two square pulse elements,

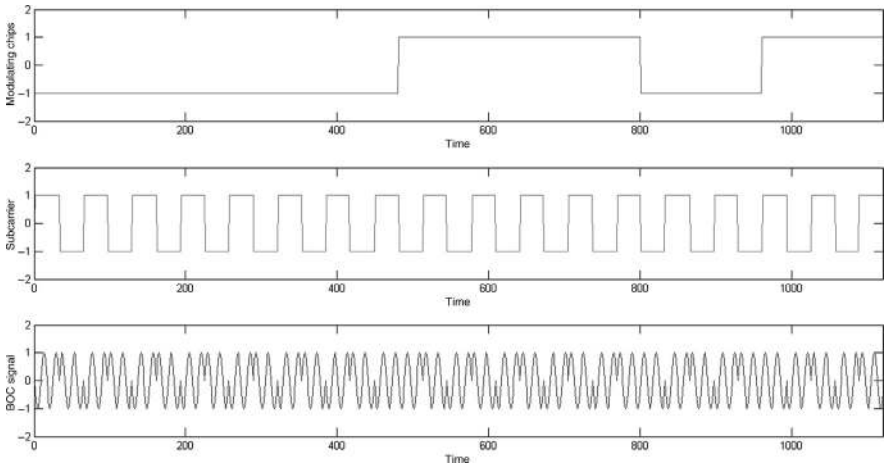

FIGURE 4.12

Time variation of a BOC(5,2)-modulated signal.

one positive and one negative, the double of the k value, that is, $2k = 2m/n$, represents the total number of such square pulses present within a chip. This is denoted by N_{BOC} (Binary Offset Carrier Modulation, 2009) and is used to represent many characteristics of the BOC signal.

Let us try to understand modulation by first taking a simple case in the time domain. In a BOC(1,1) modulation, there is one complete oscillation of the square wave within the period of one chip. So, a "+1" chip now becomes a "+1 −1" sequence, and a "−1" chip gets converted into a "−1 +1" sequence upon multiplication by the square wave. We will call these finer chips formed on BOC multiplication "BOC chips" to distinguish them from the original subcarrier or encoded data chips. For an arbitrary modulation order, in the BOC (m, n) case, a "1" or +1 value of encoded chips becomes an alternating sequence of "+1 −1 + 1 −1 + 1…" with 2(m/n) elements. Similarly, a "−1" becomes an alternating "−1 + 1 −1 + 1…" sequence, also with 2(m/n) elements. So, when BOC modulation is applied to PRN-coded navigation binary signals, each original encoded data chip is split into N_{BOC} numbers of finer widths of Ts/2. The case for BOC(5,2) is illustrated in Fig. 4.12.

There are N_{BOC} subdivisions within a chip period, with each subdivision carrying either a +1 or a −1 square pulse alternately. For integral values of m/n, the number of BOC modulated chips is even, with equal numbers of +1 and −1s within every chip width. This makes the mean signal level and hence the DC power of the data perfectly zero. When this ratio is a subinteger, the number of symbols within a chip period is odd. Consequently, they do not average out to zero in a chip period, and hence manifest some finite DC power.

Let us consider the spectrum of the signal. We know that the effect of multiplying a signal in the time domain with a new tone carrier of frequency f results in a shift of the signal in the frequency domain by an amount f. What is a square wave made of? A square wave signal of repeating frequency fs is the combination of several independent sine and cosine waves, that is, tone frequencies with ±fs as the fundamental and its integral multiples, i.e., f_s, $2f_s$, $3f_s$, etc. extending to infinity but with diminishing level.

When this offset carrier is multiplied by the original signal, it is equivalent to multiplying the latter by each of these component tone frequencies of the square wave. It shifts the spread spectrum of the encoded signal by ±nfs, where n is an integer. The resultant spectrum is an offset form of the original signal shifted by an amount ±fs and its multiples from the carrier frequency fc and on both sides of it. Each of them is a replica of the original in shape. The one that is shifted by the fundamental frequency fs has the maximum power and is typically filtered out and used for demodulation.

The nulls of a sinc function representing the spectrum of the encoded data chips, that is, the baseband nulls, occur at integral multiples of Rc. When, m/n is an integer, that is, fs an integral multiple of Rc, a shift of fs in the original spectrum as a result of the subcarrier modulation, will accommodate f_c/R_c complete spectral humps within the spectral range between fc and f_c+f_s and hence will place a null at the position of the carrier frequency, f_c. This is true for both positive and negative shifts of the spectrum. When the signal is carrier demodulated, it makes the DC component of the resultant spectrum, signifying the average power, perfectly zero.

However, if this ratio is a semi-integral number such as 3/2 or 5/2, the splitting and offset movement of the spectrum will accommodate sub integral numbers of spectral humps in the range from fc to $f_c + f_s$ and will place one of the side lobe peaks at the carrier frequency, f_c. Therefore, it cannot eliminate DC power. This corroborates our observation we had regarding the average power from the time signal. The offset spectrum of the BOC for the two cases is shown in Fig. 4.13. Here, the frequency axis is shown relative to the carrier frequency and scaled by the reference frequency f_0.

For a BOC(5, 2) signal, the spread of the original encoded data chips has a spectral spread of 2 MHz on both sides about the carrier. Again, the BOC subcarrier was of 5 MHz. Thus, the spectrum of the original signal, after multiplying by the subcarrier, will appear about the frequency line at ±5 MHz from fc. The separation between the first main peak on the positive and negative side of the carrier will thus be $5 \times 2 = 10$ MHz. Furthermore, each original spectrum had a ±2 MHz bandwidth of the main lobe, that is, separation of the first nulls from its main peak. The ratio 5/2 being a subinteger, there will be a peak at the center frequency, which is precisely the second data lobe peak. Considering the width of these two separated peaks on either side, the total bandwidth becomes $2 + 10 + 2 = 14$ MHz. With the BOC modulation, we can shift the spectrum away from the carrier frequency by an amount of our choice by suitably choosing the subcarrier frequency. However, we have to increase the bandwidth of the receiver accordingly to properly receive them.

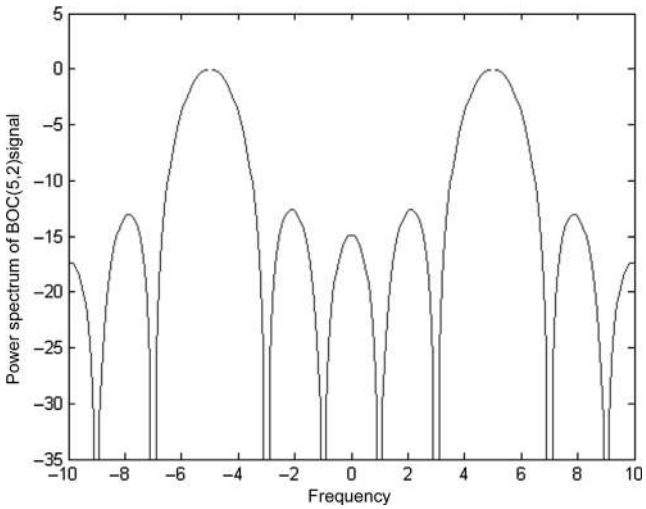

FIGURE 4.13

Spectrum of a BOC(5,2) signal.

An obvious question one may ask at this point is, "What advantages do we really get in doing this?" The main idea behind BOC modulation is that the total spectrum shifts by an amount fs, about the original carrier frequency fc, upon such modulation. Now, suppose we want two BPSK signals to operate at the same carrier frequency. It is a likely phenomenon for satellite navigation, in which the preferred carrier frequencies are limited. Using another set of BPSK signals with the same carrier frequency will cause interference at the receiver. However, BPSK-modulated signals will have most of their spectral power concentrated around the main lobe that exists about fc. Multiplying one of these signals by a square wave subcarrier to form a BOC will split the spectrum of this signal and will place the two resultant shifted spectral lobes at equal distances of fs on two sides of the center frequency f_c, preferably at the null location of the other signal. It will also keep the power low around the center. Consequently, it reduces the interference between the BOC-modulated signal and that of the original BPSK, and yet both can use the same primary carrier frequency and the same primary modulation.

Autocorrelation of BOC(m, n) can be obtained from its time domain features. As a result of this multiplication of the code chips with the subcarrier, the time domain signal is further subdivided into thinner BOC chips. The width of these finer BOC chips is Ts/2, which is N_{BOC} times finer than the original chip width. Thus, if the same BOC signal is multiplied with exact superimposition, that is, with zero delay, it generates an autocorrelation value of 1. Whenever a relative shift is applied between them, variation of the product of the chips occurs, but the variation of the subcarrier

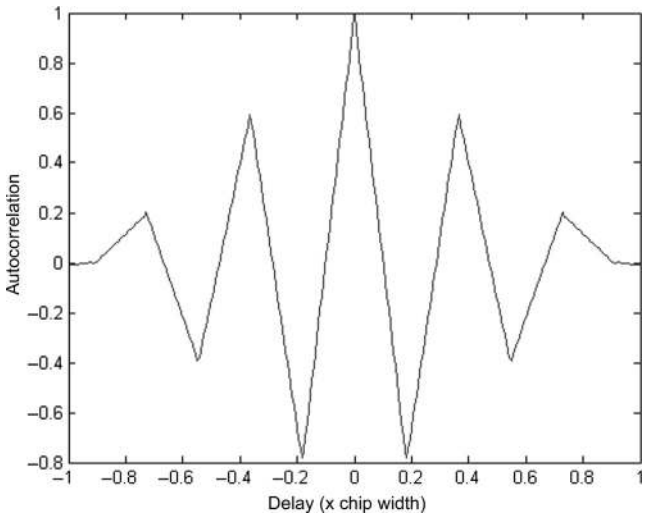

FIGURE 4.14

Autocorrelation of a BOC(5,2) modulated signal.

occurs with N_{BOC} times more rapidly than normal coded signal. The product of the chips varies over time between $+1$ and -1.

The correlation function is given by

$$R_{BOC}(\tau) = \frac{1}{T} \int c(t)\, c(t-\tau)\, s(t)\, s(t-\tau)\, dt = \frac{1}{T} \int A(t)\, B(t)\, dt \tag{4.72}$$

where $A = c(t)\ c(t-\tau)$ and $B = s(t)\ s(t-\tau)$. $c(t)$ and $s(t)$ being the code and the subcarrier bits at time t, respectively. Concentrating on the second part of the integral, we see that B is the product of two subcarriers shifted by a delay τ. This term generates a product, which is also alternating positive and negative square pulses, but not necessarily of equal width. Therefore, the value of the term B is a recurrent function for the shift τ and changes between $+1$ and -1. Because the width of the subcarrier square wave is smaller, the product $B(\tau)$ has a faster rate of variation. Therefore, this correlation R_{BOC} also varies at an equally fast rate. This rate is also k times faster than that of the only code correlation. This improves the estimation accuracy of correlation during ranging, and therefore, BOC modulation helps in more precise ranging compared with normal BPSK modulation. The autocorrelation of a BOC(5, 2) signal is shown in Fig. 4.14 (Box 4.8).

Although BOC modulation typically means BOC (m,n), the BOC modulation can have several variants. A popular type is alternative BOC (Alt-BOC), which we shall discuss next (Shivaramaiah & Dempster, 2009). The other types of BOC, like Multiplexed BOC will be discussed in Sec. 4.7 due to their relevance to the topic.

BOX 4.8 MATLAB Binary Offset Carrier Modulation

The MATLAB program boc_mod was run to generate the time variation of the BOC-modulated signal. In this program, a preselected PRN is multiplied by a sine-phased binary subcarrier with a frequency ratio of 1:1 with the chip rate. The different components of the BOC signal and the autocorrelation of the product signal are shown in Fig. M4.8A and B, respectively.

Change the frequency to the chip rate ratio by altering the values of m and n in the program. Observe how the number of carrier phase variations changes in the signal. Also, notice the variation in the autocorrelation within the envelope.

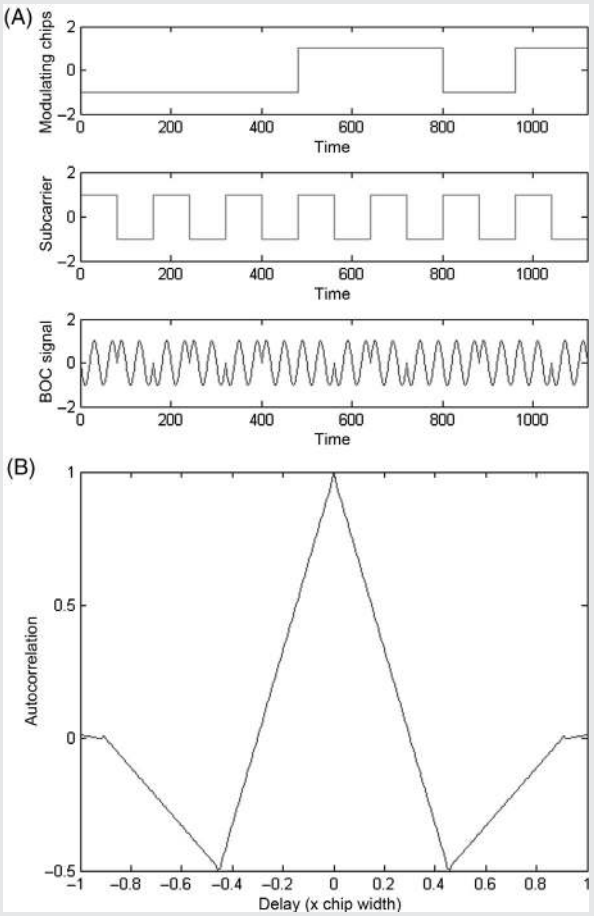

FIGURE M4.8

(A) Different components of a BOC(1,1) signal, (B) autocorrelation of a BOC(1,1) signal.

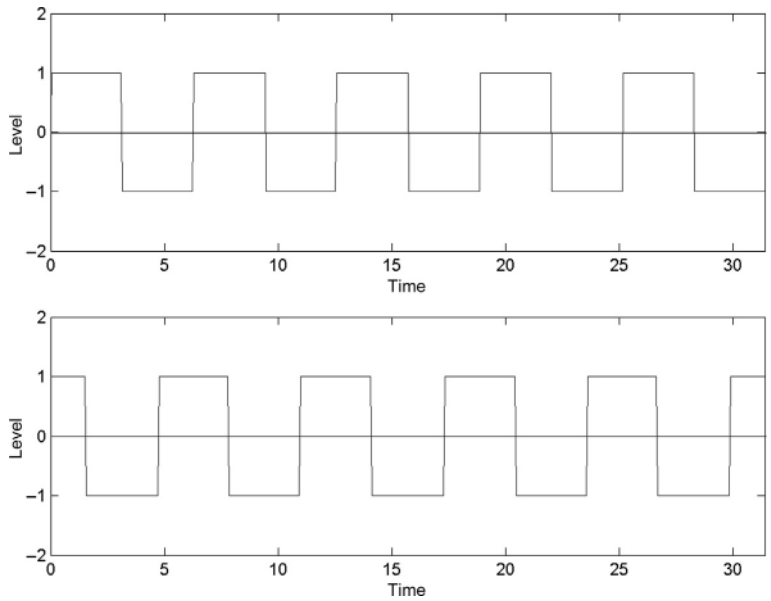

FIGURE 4.15

Sine-phased and cosine-phased binary offset carriers.

4.5.3 Alt-BOC modulation

The BOC modulation, as we have seen in Eq. (4.68), is a multiplication of the data, the code, the carrier, and the subcarrier. Among these elements, the carrier and the subcarrier can have orthogonal counterparts. That is, the carrier may be either a sine or a cosine wave, and similarly, the subcarrier may be a sine-phased or a cosine-phased square wave. The inner products of these orthogonal pairs become zero over a complete period. Their temporal variations are shown in Fig. 4.15.

From this figure, we can make out that their inner product, over a time that is an integral multiple of their period, is zero. Thus, representing a complete square wave subcarrier with four ranges of phases, 0 to $\pi/2$, $\pi/2$ to π, π to $3\pi/2$, and $3\pi/2$ to 2π, with each range separated by time Ts/4, one may represent the sine- and cosine-phased square wave vectors as $S_s = [1\ 1\ -1\ -1]$ and $S_c = [1\ -1\ -1\ 1]$, respectively. The inner product of these two carriers is zero, and hence they are orthogonal. This can also be shown mathematically as

$$\begin{aligned} P &= \int_0^T s_1(t)s_2(t)\,dt = \int_0^{T/4} s1(t)s2(t)\,dt + \int_{T/4}^{T/2} s1(t)s2(t)dt + \int_{T/2}^{3T/4} s1(t)s2(t)\,dt + \int_{3T/4}^{T} s1(t)s2(t)\,dt \\ &= (T/4)(+1)(+1) + (T/4)(+1)(-1) + (T/4)(-1)(-1) + (T/4)(-1)(+1) \\ &= +T/4 - T/4 + T/4 - T/4 = 0 \end{aligned} \tag{4.73}$$

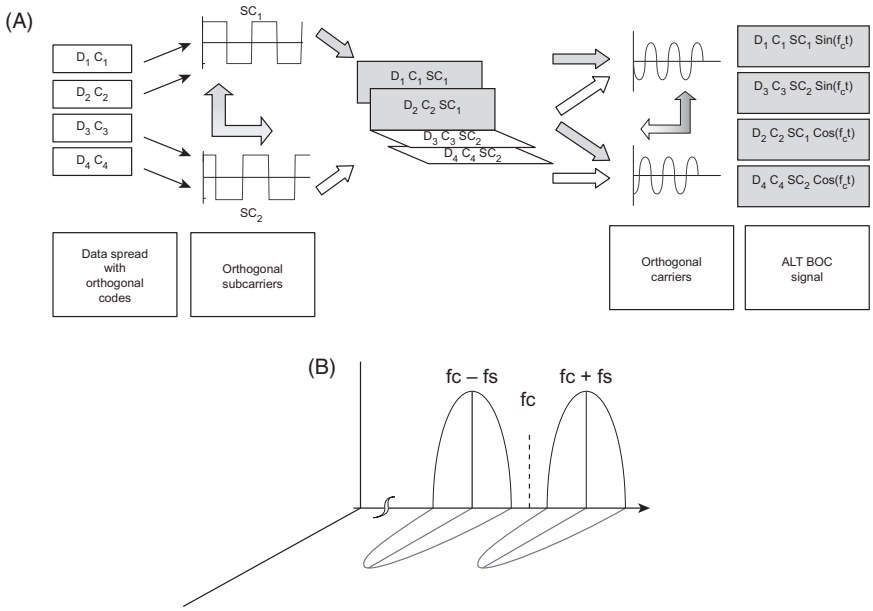

FIGURE 4.16

(A) Alt-BOC modulation scheme, (B) Alt-BOC spectrum.

This property enables two such BOCs to carry different sets of signals independently, still being orthogonal and not affecting one another.

In alt-BOC, the sine-phased binary subcarrier multiplied by the sine and the cosine carriers, respectively, forms a set of two orthogonal composite carrier components. Similarly, the cosine-phased binary subcarrier on the same sine and cosine carriers forms another set of two separate orthogonal carriers. These two components are also orthogonal to the former two by virtue of the subcarrier orthogonality. Thus, four mutually orthogonal composite carrier–subcarrier components are formed, each carrying a separate set of encoded baseband data exclusively without interference (Betz, 2001; Margaria et al., 2007). Thus, the Alt-BOC signal may be represented as

$$S(t) = D_1(t)c_1(t)\,\text{sign}[\sin(2\pi f_s t)]\cos(2\pi f_c t) + D_2(t)c_2(t)\,\text{sign}[\sin(2\pi f_s t)]\sin(2\pi f_c t) + D_3(t)c_3(t)\,\text{sign}[\cos(2\pi f_s t)]\cos(2\pi f_c t) + D_4(t)c_4(t)\,\text{sign}[\cos(2\pi f_s t)]\sin(2\pi f_c t) \quad (4.74)$$

where D_i and c_i are the data and code bit sequences, respectively, f_s is the subcarrier frequency, and f_c is the carrier frequency. The four different orthogonal codes for the four channels provide additional isolation over their spectral distinctions. However, the orthogonal channels may use the same data or code as appropriate or necessary. Even some channels may have no data at all, and are called pilot channels. The codes

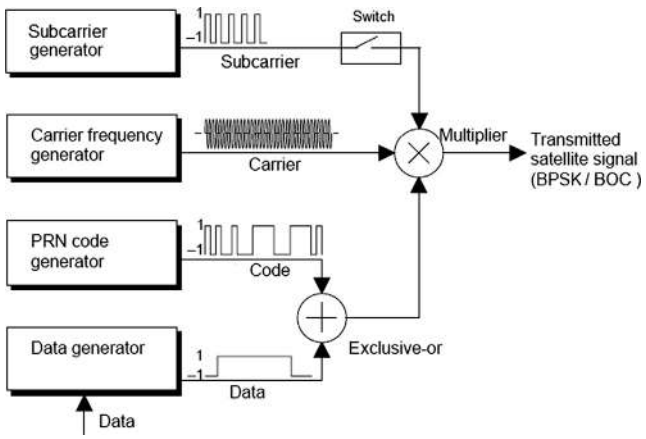

FIGURE 4.17

Schematic arrangements for BPSK and BOC modulation.

and the subcarriers may be intelligently selected so that, unlike simple BOC, the signal spectrum shifts only to any one of the upper or lower subcarrier frequencies about the carrier (Navipaedia, 2013). The Alt-BOC modulation scheme is illustrated in Fig. 4.16A; its spectrum is shown in Fig. 4.16B.

Each of these resultant signals will separately have constant amplitude. This is because the operation of subcarrier multiplication to BPSK to form BOC keeps the amplitude invariant. However, when these individual signals are combined to form the composite Alt-BOC signal, this constancy is lost in the resultant phased sum of these components. Hence, the amplitude of an Alt-BOC modulated signal is not constant. Such a nonconstant envelope of Alt-BOC modulation has certain negative implications at the receiver, and hence, nonconstant envelope Alt-BOC is generally not used in practice.

To solve this problem, a constant envelope modified version of Alt-BOC modulation was introduced. (Betz, 2001). This was achieved by introducing a new signal called an intermodulation product as one of the orthogonal components. This is made up of a definite combination of individual components but does not contain usable information (Soellner & Erhard, 2003; Ward & Betz, 2006).

A schematic arrangement for the BPSK- or BOC-modulated signal generation is shown in Fig. 4.17. The generated signal may be made of either of the two by choosing the switch position appropriately. Keeping the switch open makes the output a BPSK-modulated signal, whereas closing the switch makes it a BOC-modulated signal.

4.6 Typical link calculations

Very low navigation signal levels around −133 dBm are expected over the targeted region. In addition to the nominal channel noise, these signals may also experience

interference from other GNSS signals in these bands. This interference level may be minimized with the help of BOC modulation and a CDMA access scheme. The receiver will also receive propagation impairments such as channel attenuation, scintillation, multipath, etc., and these effects should be considered to obtain the effective signal condition at the receiver. A typical link calculation in the allocated navigation frequency is shown in the table below.

Types of signal	Units	Values
Frequency	GHz	1.57542
Wavelength	m	0.1904
EIRP	dBw	23.00
Range	km	20,000.00
Path loss	dB	182.00
Atm. Atn.	dB	1.00
Total attenuation	dB	183.00
Received power	dBw	−160.00
Sky temperature	K	250.00
LNA noise temperature	K	80.00
Equivalent system noise temp	K	330.00
Equivalent system noise temp	dBK	25.20
Boltzmann constant	dB	−228.60
Rcd. noise power density at LNA I/P	dBw/Hz	−203.40
Noise bandwidth of spread signal	dB	63.00
Total Noise	dBw	−140.40

From this table, we can see that the signal power is 20 dB below the noise power when the signal remains spread in 2 MHz bandwidth. The signal is received by the receiver in this form. When the codes are known to the receivers, they can perform the correlation and consequently despreads the signal to concentrate the total signal power to a narrower bandwidth. Then, there is a gain of around 40 dB in the SNR and the signal power rises 20 dB above the noise power.

4.7 Compatibility and interoperability

The NavStar Global Positioning System (GPS) of the USA was the first global positioning service that has been in operation since 1978. It was the sole service of its kind for many years. However, today, the scenario has completely changed. During the last decade, the replenishment and modernization of existing global satellite

navigation systems have been witnessed, while the development and deployment of other new global navigation systems have also been observed. Vis-à-vis, the regional satellite navigation systems are emerging fast along with their global peers. Now there are more than hundreds of satellites available and dedicated to providing the navigation service from space.

However, the signals used for the transmission of these systems are mostly in the same frequency band. Almost the same center frequencies are used as carriers, and with similar bandwidth. Now, this leads to a technical problem. As various systems transmit signals over the same geographic region at the same time using signals in close-by frequencies. It leads to interference amongst the different signals, causing degradation of system performance. Moreover, with the passage of time, as more and more accuracy and availability are in demand for the satellite navigation-based positions, such enhanced performance can be achieved by utilizing more than one system with a single receiver. This, in another way, demands the existence of more than one signal at one place at a time. The notion of compatibility and interoperability deals with these two apparently contradicting requirements of the coexistence of signals from multiple GNSS systems.

4.7.1 Compatibility

When two or more signals exist over the same space and time and in the same frequency band, and yet they are designed in a way that they do not interfere with each other, so that standalone positioning can be done successfully with any one of the signals, then the signals are said to be compatible.

In other words, while compatibility deals with the noninterference of a signal on any receiver while it is simultaneously receiving any other system's signal.

For the compliance of the compatibility requirements, it is necessary that the two signals remaining in the same band and with the same center frequency avoid interference. Moreover, the two systems may need to serve the same area of service. Thus, physical separation is not warranted. With no spectral, physical or temporal separation of the signals, this is achieved by utilizing the variation in the shape of the modulation of different signals in the same band. In a modulated navigation signal, the power spectrum appears in the form of crests and troughs. To achieve the necessary isolation, the modulation is required to be made in such a way that the peak (crest) of one coincides with the null (trough) of the other and vice versa. It can be achieved by splitting and shifting the original spectrum accordingly or by maintaining orthogonality.

Take the example of BPSK modulation on a PRN code. The spectral peak occurs just at the carrier frequency. In other words, the energy of the signal is localized at the center frequency. Now, if another signal uses the same carrier frequency with the energy concentrated at the center frequency, then there would be an overlap of the spectrum and hence interference. Therefore, for the second signal, the spectrum needs to be shifted from the center. For this, the BOC modulation is utilized.

We have already seen earlier in this chapter how the BOC modulation is done by multiplying the signals with a square subcarrier to achieve spectral separation. BOC splits the spectrum and effectively shifts the spectral peak away from the central frequency, so that the resultant spectrum is at an offset from another signal with the original central spectrum, both using the same carrier. Thus, the compatibility requirement is fulfilled.

The amount of separation is determined by the specification index of the BOC modulation. BOC(m,n) represents that the carrier is modulated by a code of code rate f1 and then multiplied with a subcarrier of rate f2, where f1 and f2 are in the ratio m:n. A typical signal spectrum after BOC(5,2) modulation is shown in Fig. 4.13. Recall from the earlier section once more that, when m is an exact multiple of n, there is a null at the center while when it is not, a peak with reduced power is obtained. Further, for the same indices of BOC, the sineBOC and the cosBOC, where the square subcarriers are odd and even functions of time, respectively, have a phase difference of $\pi/2$. Therefore, they offer an additional degree of freedom to separate the signals from one another.

4.7.2 Interoperability

When the signals from two or more different navigation systems can be combinedly used at the navigation receiver to obtain position with better performance, than those obtained from a single system, then the signals are said to be interoperable. It involves using signals from different GNSS systems to provide better capabilities at the user level than relying solely on one system's open signals.

In practical terms, interoperability means that user equipment can exploit all available navigation signals from various navigation systems and produce a combined solution with performance benefits (e.g., improved accuracy and availability). Toward this, different systems transmit signals in such a way that they allow normal receivers to combine them to produce an improved navigation solution. Interoperability also ensures that one system continues to operate if the station of the other fails. Thus, reducing the vulnerability of single-mode failures.

It is important to understand here that Interoperability demands compatibility of the two signals; however, compatibility does not necessarily ensure interoperability. For achieving the latter, certain more criteria are to be fulfilled (Hein, 2006).

Factors affecting signal interoperability include:

- *Reference frames:* Reference Frame is the realization of the reference system, through observations of a set of station coordinates and deriving reference parameters, and thus providing the basis for positioning.
  Each GNSS has its own reference frame (e.g., WGS84 for GPS, GTRF for Galileo, PZ90 for Glonass). Since all coordinates used by a system is with respect to its respective frame and such frames have natural differences, just using another system's signal won't suffice producing correct position values. Interoperability is

only guaranteed if the difference between the frames is below the target accuracy or if the differences are precomputed and compensated.

- *Time references:* Time reference frames are different real-time realizations of UTC/ TAI (Atomic Time), which are international civilian time standards. Like the reference for position coordinates, two navigation systems also use different time frames. Each implements their respective time frame using their own time reference derived from their own set of atomic clocks. In a similar manner, to bring uniformity between the time references, the differences between the time frames are also required to be compensated. Therefore, a relationship between the two references must exist and be known to the receivers.
- *Signal design:* Signal structures, messages, carrier frequencies, codes, and modulations impact interoperability. Signal interoperability occurs when signals provided by different GNSS systems are similar enough for a GNSS receiver to use them with very minor modifications, that, the signals must be scalable.

The essence is the fact that interoperability does not mean that all signals should be the same. Neither does it mean that both systems need to use the same reference frames or time frames. Interoperability can be achieved by making the factors that affect interoperability, to be scalable between themselves so that they can be used by the same receiver.

For the signals to be scalable, it is required that the signals have a Common center frequency. That is, to implement interoperability, two or more signals from different systems must coexist, and hence, the compatibility between the signals must be warranted first. We have already seen in the previous section, how to design a signal with the same center frequency for different systems without interfering with each other and also without increasing the complexity of the receiver and its processing algorithms at the same time. To implement compatibility between two signals, BOC modulation is carried out. Further, for interoperability, signal structure of the additional signals has to be uniform across the systems with the same power spectral density. For this, Multiplexed BOC (MBOC) modulation is a viable solution. MBOC is a variant of BOC and an important modulation scheme in modernization and optimization of the navigation signal. It aims at optimizing the spreading modulation by combining two different BOC modulated signals so that a desired resultant PSD is obtained.

For practical implementation, the navigation signals have been modernized by different systems, in such a way that the new signals are compatible and also interoperable. For example, two systems, say GPS and Galileo, are compatible but not interoperable. However, when modernization of the system is done, it is made to make the systems interoperable, as well. For practical implementation, it is agreed upon that, for the interoperable navigation signals, the MBOC that combines two BOC signals, viz. BOC(1,1) and BOC(6,1) in the power ratio X:Y will be used. That is over a definite period of time, $X/(X+Y)$ portion of the power will be of BOC(1,1), and $Y/(X+Y)$ portion of the power will be of modulation BOC(6,1). Now, this ratio may be maintained in the signal in different ways.

- *Composite BOC (CBOS):* In this approach, the abovementioned proportion may be achieved through using a weighted sum of the two signals, in the power ratio of X and Y. Here, both the BOC modulations are simultaneously present, and only the amplitudes of two different BOC signals are different.
- *Time multiplexed BOC (TMBOC):* In Time Multiplexed BOC, only one signal is present at a time while their power ratio is maintained by apportioning their present time in the signal in a definite ratio, so that over the composite time, the X:Y power ratio is maintained.
- *Quadrature multiplexed BOC (QMBOC):* In the QMBOC implementation method, the BOC(1,1) and BOC(6,1) components are combined in a quadrature multiplexing manner, say as sinBOC(1,1) and cosBOC(6,1), with desired amplitude factors.

The CBOC, TMBOC, and QMBOC vary in their baseband waveforms. But the aim of combining them in such a way, is that the PSD of the proposed solution should be identical for all the interoperable systems.

When the MBOC modulation contains BOC (1,1) and BOC(6,1) components with 10/11 and 1/11 power sharing, the combined signal is represented as MBOC(6, 1, 1/11). The PSD of the combined signal, MBOC(6, 1, 1/11) modulation signal is defined as follows:

$$S_{MBOC(6,1,1/11)} = \frac{10}{11} S_{BOC(1,1)}(f) + \frac{1}{11} S_{BOC(6,1)}(f) = \frac{10}{11} T_c \left(\frac{\sin^2(\pi f T_c)}{(\pi f T_c)^2} \right) \tan^2\left(\frac{\pi f T_c}{2} \right) + \frac{1}{11} T_c \left(\frac{\sin^2(\pi f T_c)}{(\pi f T_c)^2} \right) \tan^2\left(\frac{\pi f T_c}{12} \right) \quad (4.75)$$

where S is the spectral power, f is the frequency, and Tc is the code chip duration. This MBOC modulation contains BOC (1,1) and BOC(6,1) components with 10/11 and 1/11 power sharing, respectively, and thus ensures the interoperability between the different signals.

GNSS service providers have proposed adopting different methods for implementing MBOC modulation. The GPS System uses the TMBOC implementation method, which combines the BOC(1,1) and BOC(6,1) components in a time-multiplexing manner (Betz, 2001). Galileo uses the CBOC implementation method, which combines the BOC (1,1) and BOC(6,1) components in a baseband level with desired amplitude factors (Avila-Rodriguez et al., 2008). BeiDou uses the QMBOC implementation method, which combines BOC (1,1) and BOC(6,1) components in a quadrature multiplexing manner with desired amplitude factors (Yao et al., 2010).

Conceptual questions

1. Is it possible to raise the signal power from a single satellite above the noise floor at the receiver without performing autocorrelation with the local code using a high-gain antenna only?

2. What problems may occur if the data and the ranging codes are not synchronous at the transmitter?
3. What are the different ways that Eq. 4.75 may be implemented?
4. How does the length of a PRN code affect the performance of a satellite navigation system?
5. Upon multiplying the spreading code with the incoming signal at the receiver, what changes happen to the noise contained in it?
6. With 2 orthogonal codes and a square wave of given frequency and with a carrier wave, how many different data sets can be independently transmitted without interference?

References

AltBOC Modulation (2013). Navipedia. Available at: https://gssc.esa.int/navipedia/index.php/AltBOC_Modulation. Retrieved on: 13.09.2024.

Avila-Rodriguez, J. A., Hein, G. W., Wallner, S., Issler, J. L., Ries, L., Lestarquit, L., De Latour, A., Godet, J., Bastide, F., Pratt, T., & Owen, J. (2008). The MBOC modulation: The final touch to the Glileo frequency and signal plan. *Journal of the Institute of Navigation, 55*(1), 15–28. doi:10.1002/j.2161-4296.2008.tb00415.x.

Betz, J. W. (2001). Binary offset carrier modulations for radionavigation. *Journal of the Institute of Navigation, 48*(4), 227–246. https://doi.org/10.1002/j.2161-4296.2001.tb00247.x.

Binary Offset Carrier Modulation (2009). Wikipedia. Available at: https://en.wikipedia.org/wiki/Binary_offset_carrier_modulation, Retrieved on: 13.09.2024.

Chakrabarty, N. B., & Datta, A. K. (2007). *An Introduction to the Principles of Digital Communications*. New Age International Publishers, New Age International Publishers.

Cooper, G. R., & McGillem, C. D. (1987). *Modern communications and spread spectrum*. McGraw-Hill.

Global Positioning System Directorate, Navstar, GPS Space Segment/Navigation User Interfaces: 2012 IS-GPS-200G, Available at https://navcen.uscg.gov/gps-constellation, Retrieved on 16.09.2024.

Gold, R. (1967). Optimal binary sequences for spread spectrum multiplexing. *IEEE Transactions on Information Theory, 13*(4), 619–621. https://doi.org/10.1109/TIT.1967.1054048.

Hein, G. (2006). GNSS interoperability: Achieving a global system of systms or "does everything have to be the same? *Inside GNSS*, Vol-Jan/Feb,2006. 57–60, Available at: https://insidegnss.com/auto/0106_Working_Papers_IGM.pdf, Retrieved on 16 July, 2024.

Kovach, K., Haddad, R., Chaudhri, G. (2013) LNAV Vs. CNAV: More than Just NICE Improvements, ION-GNSS+, 2013, Nashville Convention Centre, Nashville, USA.

Lathi, B. P. (1984). *Communication Systems*. Wiley Eastern Limited, Wiley Eastern Limited.

Margaria, D., Dovis, F., & Mulassano, P. (2007). PC104 based low-cost inertial/GPS integrated navigation platform: Design and experiments. *Journal of Global Positioning Systems, 6*(1), 89–96. doi:10.5081/jgps.6.1.89.

Parkinson, B. W., Spilker Jr., J.J. (1996). Global Positioning Systems, Theory and Applications, Vol-II, AIAA, Washington DC, USA.

Proakis, J. G., Salehi, M. (2007). Digital Communications, 5th Edition, Mc. Graw Hills, USA.

Shivaramaiah, N. C., Dempster, A. G. (2009). The Galileo E5 AltBOC: Understanding the signal structure. IGNSS Symposium, Australia, 2009, International Global Navigation Satellite Systems Society.

Soellner, M., Erhard, P. (2003). Comparison of AWGN code tracking accuracy for alternative-BOC, Complex-LOC and complex-BOC modulation options in Galileo E5-band, Proceedings of the European Navigation Conference, Graz, Austria, April, 2003.

Ward, P. W., Betz, J. W., Heegarty, C. W. (2006). GPS Satellite Signal Characteristics, In: Kaplan, E. D. and Hegarty, C. J. (Eds.), Understanding GPS Principles and Applications, Artech House, MA, USA.

Yao, Z., Lu, M., & Feng, Z. M. (2010). Quadrature multiplexed BOC modulation for interoperable GNSS signals. *Electronics Letters, 46*(17), 1234–1236. doi:10.1049/el.2010.1693.

CHAPTER

Navigation receivers 5

Preamble

In Chapter 2, we learnt that the navigation receivers accept the navigation signals and derive the position from them. In this chapter, we will provide technical details about the receiver. We will start with the generic receiver structure and its different classifications. Then, we will continue with details of the different functional units of the receiver and describe the functionalities of each.

5.1 Navigation receiver

Satellites in the space segment accomplish their objectives by transmitting the necessary signals. It is the task of the user receiver to receive these signals and eventually estimate its own position. It uses the information, either readily available or derived from the signals. For this, the signals transmitted from different satellites need to be simultaneously received and processed efficiently. This is done by a *navigation receiver*. It is the instrument the user uses to fix his or her position.

5.1.1 Generic receiver

From the system point of view, a navigation receiver is not very different from any digital communication receiver. It has to do the same job as any communication receiver: that is, receive a signal and derive data from it, and use it for the applications. Thus, communications elements are predominant here. However, in terms of processing capability, navigation receivers need to have some added features over a typical communication receiver. This is because of the nature of the signal and the associated criticalities, and also due to the techniques through which the necessary information is derived. It is also obvious that related applications that the receiver supports, are different in accordance with the end objective of the receiver.

In this chapter, we will look in detail at how navigation receivers work. We shall stick to the most common implementations of the architectural design of the receiver and will analyze its theoretical aspects with a focus on its working principles.

To understand the way a receiver works, we have to start from the signals with which the receiver interacts. We first need to understand the condition of the signal

Understanding Satellite Navigation, Second Edition. DOI: https://doi.org/10.1016/B978-0-443-36432-7.00006-7

the receiver receives. The major receiver characteristics are defined in terms of the features of this signal. In the last chapter, we learned about signal characteristics and how signals are generated and transmitted. Here, we will start by reiterating what we have learnt there.

The signal consists of basic navigation information that remains embedded within it in a tiered structure. The job of the receiver is to isolate the individual signal and extract the information from it.

From the previous chapter, we also know that the signal is transmitted in either code division multiplexing access (CDMA) or frequency division multiplexing access (FDMA) mode by different satellites. Multiple access is necessary, so that the receiver can receive signals from different satellites simultaneously without interference. Moreover, irrespective of the technique used for access, there is typically a pseudo-random code multiplied with the message for ranging purposes. This encoded data chips modulate the carrier.

In this chapter, we will see how the receiver acquires the signal and then uses it for further processing. Signals from different satellites are received by a common interface and subsequently pass through a common front end. After this, the individual signals are separated, acquired, and processed in separate channels of the receiver. These discrete channels thus obtain the signals either in the same frequency and with different codes for CDMA or in different frequencies but with the same ranging code for FDMA.

The signals are carried by a predesignated carrier frequency with circular polarization. The sinusoidal carriers are modulated by the encoded navigation data, which is already spread by the ranging code. Although the most popular type of modulation for navigation is the Bipolar Phase Shift Keying (BPSK), other types of modulation, including binary offset carrier (BOC) etc, are alternative options. Obviously, the modulation type needs to be known to the receiver so that the correct demodulation processes can take place.

Subsequent to carrier demodulation, the processing consists of using the ranging code to find the range from the satellites. These codes are known to the receiver a priori, in terms of the code parameters such as the code sequence, code length, code rate, and so forth. In addition, if any encryption is made to the code, the encryption details, including the algorithms and the key, plus other resources to decrypt it, need to be available to the receiver. The range of the satellite is then derived using this code. This is done by correlating a local code with the received one. The code is then removed by multiplying the encoded data chips with synchronous local code. The carrier and the code now being removed, the remaining navigation data is specifically identified from the predefined data structure. These parameters are used in turn to find the satellite position, other corrections and finally the user position. To carry out the whole process a minimum power of the signal over the noise power, i.e., the Signal to Noise Ratio (SNR) is necessary.

Navigation satellites transmit navigation signals in allotted bands with a given equivalent isotropic radiated power (EIRP). Yet, a low signal level is expected over the targeted region after it traverses through the intermediate path. In addition, every

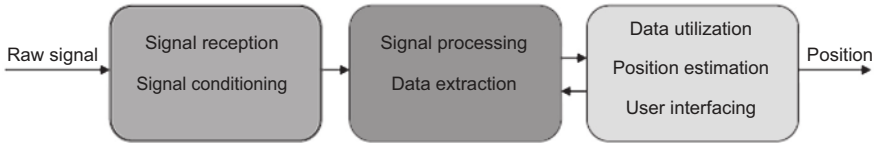

FIGURE 5.1

Functional segments of a generic receiver.

navigation signal experiences interference from signals in the same bands from other satellites or from the delayed multipath signal from the same satellite. Both effects make the received signal-to-noise ratio (SNR) poor. These interference levels need to be minimized with appropriate modulation and through proper design (Navstar, 2012).

Thus, the basic architecture of the receiver has three main sections composed of

- Signal reception and conditioning.
- Signal processing and data extraction.
- Data utilization and position estimation.

The schematic of a generic receiver is shown in Fig. 5.1.

5.1.2 Types of user receiver

We start our discussion on navigation receivers by classifying different receivers. However, it is not possible to categorically segregate the receivers in a strict sense because the same receiver may fall into different categories according to different bases of categorization. For instance, a "carrier phase-based ranging receiver" can also be seen as a "precise receiver." These classifications, although not standard, provide an understanding of the divergent features of receivers. The basic categories are described in the following subsection as per the mentioned basis.

5.1.2.1 Ranging technique

One important task to be accomplished at the receiver is the measurement of the satellite's range. Previously, we mentioned that range is calculated from the difference between transmission and reception time. On the basis of which of the signal parameters, code phase or carrier phase is used for ranging, the receivers may be of the following types.

5.1.2.1.1 Code phase-based ranging receivers

When the range is measured in a receiver on the basis of the propagation time of a particular code phase from the satellite to the receiver, it is designated a code phase-based ranging receiver. The propagation time is the difference between the receiving time and the transmission time of any definite code phase of the signal. The ranges measured through this process are noisy and lead to errors in position estimates.

5.1.2.1.2 Carrier phase-based ranging receivers

The range can also be measured by deriving the propagation time of a particular phase of the carrier wave. Receivers primarily using this mode of measurement for ranging are referred to as carrier phase-based ranging receivers. Here, the receiver needs measurements of the phase of the carrier signal received with respect to a locally generated synchronized sinusoid. Moreover, it also requires estimating the integer ambiguity. The latter can be aided by measurements of the ranging code. This is typically used by receivers needed for precise applications. The requirement of the integer ambiguity estimation adds to the complexity of the receiver and increases computational load, making the receiver costly.

5.1.2.2 Access technique

Different navigation systems are designated for different access techniques. So, from the system's point of view, receivers can be divided on this basis into the following.

5.1.2.2.1 Code division multiplexing access receivers

CDMA receivers operate in conjunction with a CDMA system in which the satellites transmit the same carrier frequency but with different ranging codes. Here, the combined signal channel is simple, and the front-end bandwidth of the receivers is comparatively small. However, this is at the cost of identifying the exact code present in the signal, which thus results in extra processing load and time.

5.1.2.2.2 Frequency division multiplexing access receivers

FDMA receivers operate with an FDMA system in which different satellites transmit at different carrier frequencies but with the same ranging codes. Here, the combined signal channel has a comparatively wider bandwidth. This wide bandwidth accommodates frequencies of all available signals. Consequently, the receiver is required to have a wider band of operation at its input, but, unlike CDMA receivers, less overhead time needs to be spent to identify the separate carriers. However, the system front-end bandwidth may be reduced by properly using the frequency reuse plan, as we saw in the previous chapter.

5.1.2.3 Precision

Receivers can also be classified on the basis of the precision they offer. It determines the applications for which they can be used. The precision requirement of a receiver is primarily determined by the kind of service for which it is meant. There are certain factors in receiver construction that help to achieve the required precision. These factors may imply improvements in terms of both computation and hardware used. On this basis, the receivers can be of the categories mentioned below.

5.1.2.3.1 General purpose (standard) receivers

These are receivers that give standard precision in determining the position of the user. They are meant for standard services and are relatively smaller in size and cheaper in cost. This makes these receivers popular for general purpose navigational use.

5.1.2.3.2 Special purpose (precise) receivers

These receivers are used for precision applications such as surveying and other geodetic purposes. For achieving precision, receivers depend on relative positioning, processing of the carrier phase of the signal, and many other similar features to improve performance. Variants of such receivers can even use precision service with decryption capability in order to achieve the goal. Such precise receivers also differ by the type of hardware units they use, such as an oven-controlled crystal oscillator (OCXO) or atomic clock, along with qualified components, as demanded by the applications for which they are used.

The primary and differential receivers may also fall under this category. But we deliberately avoid discussion of this here until we describe the differential positioning in Chapter 8.

5.1.3 Measurements, processing, and estimations

The final objective of the receiver is to fix its position. Position (x,y,z), which is obtained by solving the quadratic observation equation $R = \sqrt{(x - x_s)^2 + (y - y_s)^2 + (z - z_s)^2}$. Here, x_s, y_s, and z_s are the known satellite position coordinates, and R is the measured range. Hence, the known parameters are required to be derived from the signal by the receiver itself for solving the equation. These are done through two major activities in the receiver, viz., *reference positioning* and *ranging*. The following subsections will describe these activities, including all of the related processing necessary to achieve them.

5.1.3.1 Reference positioning

Reference positioning is the process of locating the exact position of navigation satellites, which are used in the observation equation. For this, the satellites transmit ephemerides repeatedly in the signal. Ephemeris consists of a set of Keplerian parameters required for satellite position estimation. We already learned in Chapter 2 that these Keplerian parameters are estimated at the ground segment and are uploaded to satellites. The satellites, in turn transmit them to users through the signal. It was also clear from Chapter 3 that a minimum of six parameters are required for estimation of the satellite position. There are additional parameters in the signal that can take care of small deviations in position resulting from the perturbations.

The true satellite orbit is different from its designated orbit, and it changes with time, resulting in an effective change in these parameters. The most recent ephemeris information, along with the pertinent perturbation parameters, is updated by the satellite in its message available in the navigation signal. Using these, the receiver

can calculate the satellite position at any instant, following the equations and methods described in Chapter 3.

5.1.3.2 Ranging

Ranging is the activity to measure the distance of the user from each reference satellite. It is one of the important parameter necessary to estimate user's position. The distance, that is, the range, is obtained from the total time taken by the signal to travel from the satellite to the user. Thus, the expression for the measured range is

$$R = c\,(t_2 - t_1) \tag{5.1}$$

Here, t_1 is the time of transmission of a definite phase of the signal, t_2 is the time of reception of the same phase at the receiver, and R is the measured range. "c" is the velocity of light in vacuum. The assumption underlying this method of calculating range is that, electromagnetic waves travel at a constant velocity, which is the velocity of light. However, certain errors creep in when assuming this, which we will address in the next chapter. The range is thus derived from the difference between the current time t_2 and the transmission time t_1 of the current received phase. This is obtained from the delay in the received signal code observed at the receiver with respect to a synchronized version of the same code generated locally. The time stamps available in the received data are used as references. The delay in terms of the integral and partial code periods are measured. We shall read about these methods in detail later in this chapter. There we shall learn how time t_2 and t_1 are identified in a receiver in connection with the appropriate module carrying out the process.

5.1.3.3 Signal processing

It is clear that both prerequisite estimations we have just discussed need to be derived from the information-laden signal. Thus, the first basic requirement for this is the signal acquisition.

To acquire the signal and for subsequent information derivation, some preliminary signal processing needs to be done. We now discuss the theoretical essentials of such signal processing.

The combined modulated signal is presented at the input of the receiver antenna as a variation of the phase of an electric field. As the signal passes through the antenna, this is converted to an equivalent analog variation in electrical signal in the receiver. Finally, it is converted into binary numbers representing the values of the parameters. For a normal navigation signal, all the information is used to modulate the carrier in terms of the phase variation of the signal. Therefore, first, the receiver must follow the phase variation of the incoming signal and wipe off the carrier to obtain the data.

This is done by comparing the carrier phase variation of the incoming signal with a local version of the carrier. This local carrier is generated as a reference in the receiver at the same frequency. Then, comparing the phase of the input signal with this reference, the phase difference is determined. This difference is used for correcting the phase of the locally generated signal and aligning it with the input phase. This way, any further phase variation in the incoming signal is determined from the derived

differences generated. For BPSK signals, these phase variations are used to obtain the variations in the binary encoded data phase.

To estimate the relative phase difference and its variation, the frequency of the local reference signal needs to be the same as the incoming one. The frequency of the incoming signal, however, does not strictly remain the same as the transmission frequency owing to the Doppler effect. This occurs when there is relative velocity between the receiver and the satellite. So, in addition to the signal phase, the rate of change in the phase and its variations, i.e., frequency deviation resulting from the Doppler, is also needs to be estimated and followed. For this, once the phase difference between the two is identified, it will be corrected and any subsequent variations in the signal phase or frequency are readily followed by the local reference signal by following its instantaneous phase. The width of the encoded data chip also varies proportionately with Doppler. So, Doppler values obtained by the receiver at the carrier level are also equally useful for proper data demodulation and decoding.

Many associated signal processing activities must be done on the signal before ranging and reference positioning. These include analog-to-digital conversion of the received signal; signal acquisition and tracking; and signal demodulation. However, we shall discuss them at appropriate points when describing the different modules of the receiver.

Before we go into more detail, we will discuss some very basic mathematical concepts. Here, we shall treat the signals as vectors and analyze them. This will help us understand the total process.

Let us suppose two orthogonal reference axes are X and Y. Two mutually orthogonal vectors A and B are present here, where A makes a relative angle θ with X, and hence the same angle is made by B with -Y. This is shown in Fig. 5.2.

So, the component projection of A and B on X, that is, the dot product of A + B with X, is

$$C_x = A\cos\theta + B\sin\theta \tag{5.2A}$$

and the component projection of A and B on Y, that is, the dot product of A + B with Y, is,

$$C_y = A\sin q - B\cos q \tag{5.2B}$$

Note that the resultant vector of the original and that of the component vector remain invariant as $C_x{}^2 + C_y{}^2 = A^2 + B^2$.

Now, consider two sinusoidal waves, $S_c = a\cos(\omega t + \phi)$ and $S_s = b\sin(\omega t + \phi) = b\cos\{(\omega t + \phi) - \pi/2\}$. These two waves are mutually orthogonal because they differ by a phase of $\pi/2$. This is ensured by the fact that their inner product is zero. The dot product of two functions is their inner product and is given by

$$\langle S_c,\ S_s\rangle = \frac{1}{T}\int_0^{2\pi} S_c(t)\,S_s(t)\,dt = \frac{ab}{2T}\int_0^{2\pi} \sin(2\omega t + 2\varphi)\,dt = 0 \tag{5.3}$$

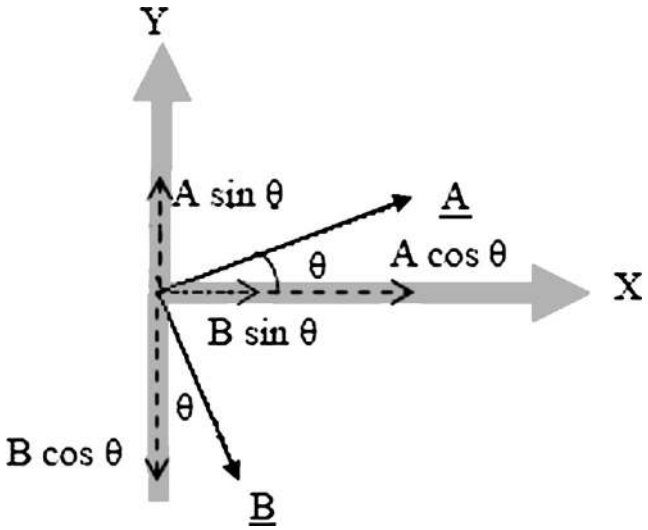

FIGURE 5.2

Vectorial representation of signals.

These sinusoidal waves, Sc and Ss may also be considered two vectors, such as A and B. So,when the phase difference between Sc(t) and Ss(t) is maintained at $\pi/2$, they behave like two orthogonal vectors and similarly have zero as their dot products.

Unitary signal $\cos(\omega t)$ and $-\sin(\omega t) = \cos(\omega t + \pi/2)$ constitute the references. These references are similar to X and Y axes, respectively, and can be combined and represented as $X + jY$, where 'j' represents orthogonal phase. When these signals are multiplied with orthogonal references $X = \cos(\omega t)$ and $Y = -\sin(\omega t)$, the product thus formed is

$$\begin{aligned}(S_c + S_s)\cdot(X + jY) &= \left[a\cos(\omega t + \varphi) + b\sin(\omega t + \varphi)\right]\left[\cos(\omega t) - j\sin(\omega t)\right] \\ &= \frac{a}{2}\left[\cos(2\omega t + \varphi) + \cos(\varphi)\right] - j\frac{a}{2}\left[\sin(2\omega t + \varphi) - \sin(\varphi)\right] \\ &\quad + \frac{b}{2}\left[\sin(2\omega t + \varphi) + \sin(\varphi)\right] + j\frac{b}{2}\left[\cos(2\omega t + \varphi) - \cos(\varphi)\right]\end{aligned} \tag{5.4}$$

So, upon low-pass filtering, the components that survive are

$$C = C_i + j\,C_q = \left[\frac{a}{2}\cos(\varphi) + \frac{b}{2}\sin(\varphi)\right] + j\left[\frac{a}{2}\sin(\varphi) - \frac{b}{2}\cos(\varphi)\right] \tag{5.5}$$

This equation resembles Eq. (5.2A, B). The relative phase angle φ between the considered signals and the references carries the same significance for the signals as θ carries for the vectors in Eq. (5.2A, B).

So, comparing the equivalent equations, the operations of multiplication of orthogonal reference unit sinusoids with the signals and subsequent low-pass filtering are equivalent to the vector operation of resolving the vectors onto the reference axes, i.e., dot multiplication of the vector with unit vectors.

Now, let us derive some special cases out of the general equation we had in Eq. (5.5). Notice that if only the in-phase component S_c exists in the signal, that is, $b = 0$, then the products on the cosine component and sine component would respectively be

$$C_i = \frac{a}{2}\cos(\varphi) \tag{5.6A}$$

$$C_q = \frac{a}{2}\sin(\varphi) \tag{5.6B}$$

It follows from this that the ratio of these components becomes

$$C_q/C_i = \tan(\varphi) \tag{5.6C}$$

So, the ratio would give us the phase difference between the reference and the signal. Again, if these components are squared and added, then

$$R = \sqrt{\left(C_i^2 + C_q^2\right)} = \frac{a}{2} \tag{5.6D}$$

So, this will give us the modulus of the amplitude of the signal. The same arguments are valid if there is only the S_s component of the signal. The process of multiplying the signal by a reference and subsequently low-pass filtering it is called mixing. This operation will be used many times in receiver signal processing.

5.1.4 Noise in a receiver

At this point, it is important to introduce the concept of noise. The signal inside the receiver remains in the form of electrical variables. When the signal passes through different units of the receiver, some unwanted and uncorrelated random electrical variations of spurious nature are added to it. These are referred to as *noise*. When the noise is large, this results in an error in identifying the correct signal and deriving the correct value of parameters from it as well. Eventually, it affects the measurements done in the receiver. This is analogous to the condition in which we want to hear someone delivering a speech in a crowded room with lots of people talking among themselves. We concentrate on the speaker while the crosstalk creates noise in the background. This makes it difficult to realize what the speaker is actually saying. The more people talk, the more noise there is, making understanding the speaker more difficult. At some point, it becomes unintelligible.

The signal propagates through the medium in the form of electromagnetic waves. Other random electromagnetic emissions by natural or manmade sources are also present within the band of the signal. These get added to the actual signal and are picked up as noise when received. Similarly, after the signal is received at the

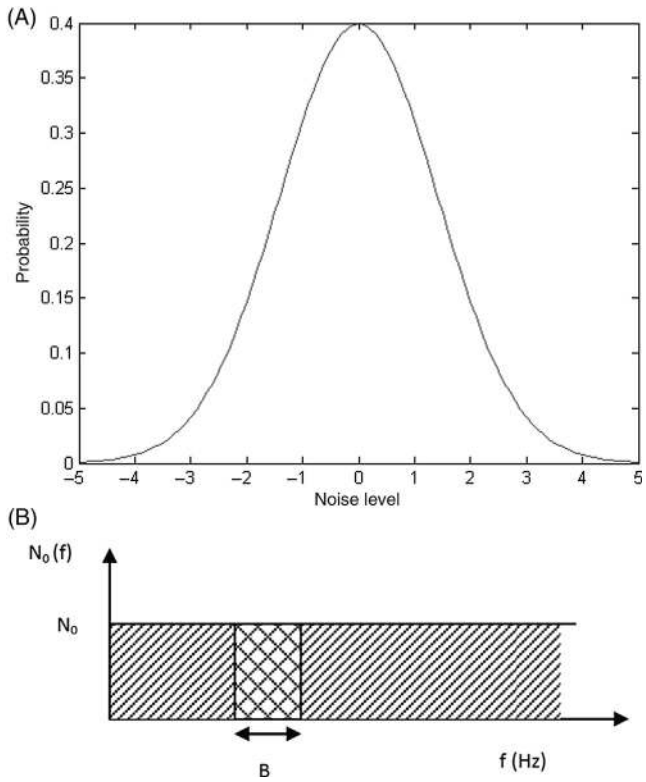

FIGURE 5.3

(A) Noise probability density, and (B) noise power spectral density.

receiver and is transformed into electric parameters of voltage and current therein, the concerned hardware, which is at definite temperatures, also generates similar electrical random variations. These components adhere to and distorts available voltage signals adding to the noise.

All of these unwanted components are additive and random in nature. So, their value at any instant has no relation to the values at any other instant. When these noise values are added up over a considerable time, the sum becomes zero. This means that the noise has a zero mean value. However, the square of these values, when averaged over time, gives the variance σ^2 of the noise and is the index of noise intensity. Furthermore, they generally follow a definite statistics. Then amplitude probability distribution is Gaussian about this zero mean, as shown in Fig. 5.3A.

These kinds of noise are spread across all space and at all times. But how much of it gets added to our signal? This cannot be done from the time domain analyses of the noise, and we need to see its spectral distribution; that is, we need to see how the same noise is distributed across all frequencies.

If we see the frequency spectrum of this noise, we find that within the band of interest, it has components of equal strengths across frequency. Therefore, it is called white noise. Consequently, a simple model for the thermal noise assumes that its power spectral density Gn(f) is flat for all frequencies, as shown in Fig. 5.3B, and is denoted by a one-sided spectrum as (Maral & Bosquet, 2006)

$$G_n(f) = N_0 \tag{5.7}$$

So, this thermal noise is additive white, zero-mean, and Gaussian noise.

We have seen that noise is present at all frequencies, and being white, the spectral amplitude in all frequencies is the same within the band of interest. Since the baseband spectrum of any signal is distributed about the zero frequency, the baseband noise is useful for its analysis. But noise addition takes place mainly when the signal is in a modulated form, and hence bandpass in nature. Thus, under such conditions, the bandpass form of the noise is convenient to deal with. The random noise can be expressed in a bandpass form (Lathi, 1984). The noise at frequency f_c is represented as

$$n(t) = n_c \cos(2\pi f_c t) + n_s \sin(2\pi f_c t) \tag{5.8A}$$

where n_s and n_c are the amplitudes of low-frequency noise components about the DC and bandlimited to f_m where 2fm is the modulated signal bandwidth and f_c is the carrier frequency of the radio frequency (RF) signal. Therefore, this expression states that the noise in the bandwidth of the signal is equal to the noise in low-pass components of the noise of equal width, shifted to the mentioned band. This is the bandpass representation of the noise, where n_c and n_s are the cosine and sine components of the noise amplitude. The noise power in each component is the same, that is, $n_c^2 = n_s^2 = n^2$. This noise can also be represented by the vectorial sum and the corresponding phase as

$$n(t) = n_r \cos(2\pi f_c + \varphi) \tag{5.8B}$$

where $nr = (n_c^2 + n_s^2)^{1/2}$ and $\tan\varphi = (n_s/n_c)$. Because both n_c and n_s are slowly varying random components, both $|n_r|$ and φ vary slowly but in a random fashion.

From Parseval's theorem, we know that for power signals, the spectral power density at any frequency is proportional to the square of the spectral amplitude. It is the same across all frequencies for noise. So, the noise power spectral density may be represented by a constant, which we have already seen in Eq. (5.7). It is important to see how we are actually representing the signal. If the signal is represented in a two-sided spectrum, where both positive and negative frequencies are considered, the noise should also be represented likewise with two-sided density $N_0/2$. This is done mainly for radiofrequency (RF) when the signal remains modulated. Once the signals are filtered in a receiver and heterodyned down to baseband, they are conveniently represented in a single-sided spectrum, and hence the noise there should also be represented as a single-sided density of N_0. So, the signal received by a receiver with a bandwidth B has the noise power given by N_0B.

Finally, because the noise is generated from the thermal condition of a body, it can be represented by a linear function of its temperature T, as

$$N_0 = kT \tag{5.9}$$

where k is the proportionality constant called the Boltzmann constant, and T is called the noise temperature, which may not be the actual physical temperature of the body. With this introductory note on noise, we return to our main topic and describe the building elements of the receiver.

5.2 Functional units of user receivers

5.2.1 Typical architectures

The architecture of a navigation receiver is typically made up of three distinct functional modules which are (a) signal reception and conditioning, (b) signal processing and data extraction and (c) position determination. To achieve these mentioned objectives, each module is again made up of different functional components, which remain more or less the same for every typical receiver. These functionalities are:

- Receive RF signal from different satellites and conditioning.
- Digitization of the signal.
- Acquisition of the desired signal phase and keep tracking of its variation.
- Removal of the Doppler, carrier demodulation, and code removal.
- Perform measurements of signal transit time (ranging).
- Decode the navigation message to determine satellite position, etc.
- Derive other relevant information.
- Estimate the position, velocity, and time (PVT).
- Display PVT and provide a suitable interface.

The first functional component in a receiver is the analog RF section. This is responsible for picking up the raw electromagnetic signal from the medium through a passive or active antenna and converting it to electrical form. It is followed by subsequent analog signal conditioning on the resultant electrical parameter. Signal conditioning includes amplification, filtering, frequency translation, and finally sampling of the signal and analog-to-digital conversion. The output is a stream of digital binary samples of the signal at an intermediate frequency (IF).

The next functional section is responsible for high-speed digital signal processing of the data. The discrete digital samples are worked on to demodulate the signal from IF to baseband, find the relative code delay of the signal to find the range, and also wipe the code off to output the stream of navigation data bits.

The last component is a processor-based computational unit responsible for deriving the required navigation parameters and finally fixing position. It also feeds the

necessary parameters back to its previous units. This section also looks after the proper display of the data and the overall management of the receiver.

In this section, we will describe in detail the different functional units of the receiver, with their working principles. The condition of the signal and its related alterations upon passing through them is also discussed. These functional modules are the building blocks of the receiver to accomplish its final objectives. At every stage, we will also describe how the noise varies and affects the signal at each of these generic modules of the receiver.

5.2.2 Radio frequency interface

5.2.2.1 Antenna

The signals transmitted by the satellites are a continuous flow of electromagnetic energy. The first task of the receiver is to receive this energy and convert it into electrical parameters of current and voltage that can be used to derive information. This is done by the antenna. Thus, the antennas are the transducers converting the electromagnetic energy propagating through space to the electrical energy in the receiver and vice versa in the opposite direction.

As the GNSS receivers operate in receive-only mode, the GNSS antennas work essentially in one direction and pass these received signals along to the GNSS receiver. The antenna design is such that it is able to receive the signal over the entire signal bandwidth. It should also have the necessary sensitivity and gain at the required center frequencies of the signal carrier. It should also have the required polarization appropriate for the signal. Such an antenna, designed in accordance with the preassigned frequency and polarization and with the requisite gain pattern, prevents unwanted components from entering it. For accommodating signals in multiple frequencies, it may use a single antenna with a large bandwidth or may resort to multiple antennas at different bands when the difference between the frequencies is too large to accommodate in one antenna.

Any antenna has a definite beamwidth, meaning that it can receive signals coming onto it within a definite spatial angular range. The GNSS antenna needs to pick up a signal from any part of the sky and for any orientation of the receiver. Therefore, it has to retain the same gain over a large angular range about its boresight. Consequently, it has a low absolute gain across its large beamwidth owing to the low directivity of the antenna.

The atmosphere prevailing in the path of the propagation of the signal also emits energy in an electromagnetic form, creating noise. The noise thus created, unlike the signal, consists of radiation that is incoherent and random in nature. Noise is radiated at all frequencies, and those in the passband of the receiver are picked up and collected incoherently by the antenna of the receiver. This is called atmospheric noise or sky noise. The signal, whose power already remains embedded below that of the noise, due to spreading of the spectrum, gets immersed in noise deeper as a result.

Different types of antennas are used based on the type of receiver. The common types of GNSS antennas are:

- *Patch antennas:* These are common and compact antennas. They have a flat, square, or rectangular shape and are often used in consumer devices.
- *Helical antennas:* These antennas have a helix-shaped radiating element. They are suitable for applications where size constraints are less critical.
- *Choke-ring antennas:* Circular in shape, choke-ring antennas are often used in automotive applications to reduce multipath. They can be mounted on vehicle roofs.
- *Rugged antennas:* Designed for harsh environments (e.g., industrial or military), rugged antennas offer superior performance but are larger and heavier.

Structurally, the antennas used in GNSS receivers are formed by a radiating element, mounted on a ground plane, followed by an amplifier. Large antennas are sometimes protected by a radome. The *Radiating element* is responsible for the antenna bandwidth and radiating characteristics. The *Ground plane* conditions the radiation pattern shape, particularly at low elevation angles. The *Amplifier chain* sets the receiver noise figure.

The antennas in a navigation receiver are typically passive. Major elements of a Passive Antennas are the radiating element and feed. They are best suited for applications in low-power environments, as in a handled satellite navigation receivers. Such antennas are placed close to the following amplifier to minimize internal path losses. For critical applications and large receivers, on the other hand, an active antenna may prove to be more useful. They have an active filter and a low noise amplifier (LNA) housed in the antenna itself.

All antennas need to have feeds for circular polarization to receive the circularly polarized signals, with the phase centre either made exactly zero or precisely known. In addition, a good quality antenna would also carry out the multipath suppression and interference handling capabilities, without any implication to receiver sensitivity.

5.2.2.2 Low noise amplifier

As we have mentioned in terms of its reception mode, the navigation receiver is no different from any digital receiver. Its front end is also identical to any typical receiver. This RF section treats the navigation signal the same way a communication signal is treated at any communication receiver. The received power of the navigation signals is so low, it remains embedded within the noise. Moreover, the antenna cannot provide additional gain to the signal level. Hence, it is necessary to see that the signal does not get degraded further.

The signal always gets added with the noise as it proceeds through the hardware of different sections of the receiver. The noise added to it also gets amplified by the same factor as that of the signal when it passes through any amplifier. So, if the received signal is amplified at the beginning to a large extent without the further addition of noise, the effect of any addition of noise by a subsequent section remains proportionately small and hence does not affect the signal much. Thus, the

SNR obtained at the input of the first amplifier is approximately maintained at all subsequent stages. It is important to see that the first amplifier itself does not add too much noise. Otherwise, it will defeat the objective of the amplification. Therefore, a low noise amplifier (LNA) is used.

The purpose of the LNA is to amplify the RF input signal, adding the minimum possible noise. It has a filter preceding it that rejects the out-of-band frequency to reduce the incorporation of unwanted noise. This filter needs to have a large bandwidth because the signal here remains spread in spectrum owing to its multiplication with the ranging code. The filter followed by the LNA, in combination, called a preamplifier, is typically placed near the antenna to reduce the effects of noise introduced by the connector and filter present between.

Let S be the signal power at the input of the LNA and N_0 be the associated noise power spectral density, making the ratio of signal to noise power density as S/N_0. Now, any pragmatic amplifier will add some noise itself in addition to amplifying the noise already present at its input. This noisy amplifier may be equivalently regarded as a noise-free amplifier with a compensatory additional noise at its input. This additional noise is such that the total output noise after amplification is equal to the combined contribution of the two noise components, one which was already there, mixed with the signal at the input and the other actually added by the amplifier. The noise contribution of the amplifier is quantitatively represented by its noise figure F. F is the ratio of the total noise power at the output of the amplifier due to the combined contribution of the input and the amplifier, to the amount of noise present at the output explicitly due to the input noise only. So, if the input noise is N_0 and the noise added by the amplifier with gain A is N_A, the noise figure of the amplifier is given by (Maral & Bousquet, 2006)

$$F = \frac{(N_0 A + N_A)}{N_0 A} \tag{5.10A}$$

The noise contribution of the amplifier N_A may be equivalently regarded as an equivalent input noise N_a amplified by the amplifier, such that $N_A = A\,N_a$. So,

$$F = \frac{(N_0 + N_a)A}{N_0 A} = \frac{kT_0 + kT_a}{kT_0} = 1 + \frac{T_a}{T_0} \tag{5.10B}$$

where we have used the relation $N = kT$. To set a common reference for all amplifiers, the noise figure F is defined when the amplifier input noise temperature is at the predefined standard value of 290 K. So, T_0 is set as 290 K. It follows from this that the noise contribution of an amplifier, equivalently converted to its noise temperature is

$$T_a = (F - 1)T_0 \tag{5.10C}$$

So, the total effective noise temperature at the input of the amplifier due to its own noise is $(F - 1)T_0$, making the corresponding noise density equal to $k(F - 1)T_0$. This

makes the total effective S/N_0 at the amplifier input as

$$S/N_0 = \frac{S}{kT_i + (F-1)kT_0} \tag{5.11}$$

where $T_i = N_i/k$ is the noise temperature at the input of the amplifier because of the noise already present in the input signal.

Extending this idea to all subsequent amplifiers in the chain, the effect of the noise added by the next amplifier at its own input is $k(F_1 - 1)T_0$. But to bring all noise contributions to the same reference, we calculate their equivalent noise at the input of the LNA. The equivalent noise owing to the first amplifier following the LNA with noise figure F1 and amplification A_1 at the input of this LNA is $(F_1 - 1)kT_0/A$. So, we see that the effect of the noise added by the next amplifier is drastically reduced by the factor of the LNA gain. Similarly, that of the next amplifier with F_2 and A_2 as the respective noise figure and gain will be $(F_2 - 1)kT_0/(A_1A)$. The effect thus becomes less conspicuous for amplifiers at later stages. Considering all such contributions, when the noise component in the signal at the input of the LNA is N_i, the effective noise becomes

$$N_{eff} = N_i + (F-1)kT_0 + (F_1 - 1)kT_0/A + (F_2 - 1)kT_0/AA_1 \ldots\ldots \tag{5.12}$$

5.2.3 Front end

The RF component of the received signal, received by the antenna system and passing through the preamplifier, proceeds further through the receiver. In this part, the signal is modified and made ready for processing. The activities are commonly known as signal conditioning and are done at the front end of the receiver. It consists of downconverting the signal to IF, filtering, sampling, and converting into discrete digital data. All of these steps in this section will be discussed in sequence. However, for all such purposes, we need a timing reference, and hence, a timing device is required. It is important to have a precise timing source in navigation, and therefore, we will start our discussion with it. The architecture of a typical navigation receiver front end is shown in Fig. 5.4.

5.2.3.1 Timing devices

The source of all timing devices inside the receiver is the reference oscillator. It provides a time and frequency reference for the whole receiver. All local signals generated at the receiver are derived from either the local oscillator (LO) or from a clock. Both the LO and the clock are driven by this reference oscillator.

Because this reference oscillator serves all timing requirements of the receiver, the performance of the receiver depends on its precision. In addition to the short-term and long-term stability, the phase noise, power, and size of the reference oscillator are also important aspects determining the receiver characteristics. The stability of this reference affects all the time and the frequency units derived from it.

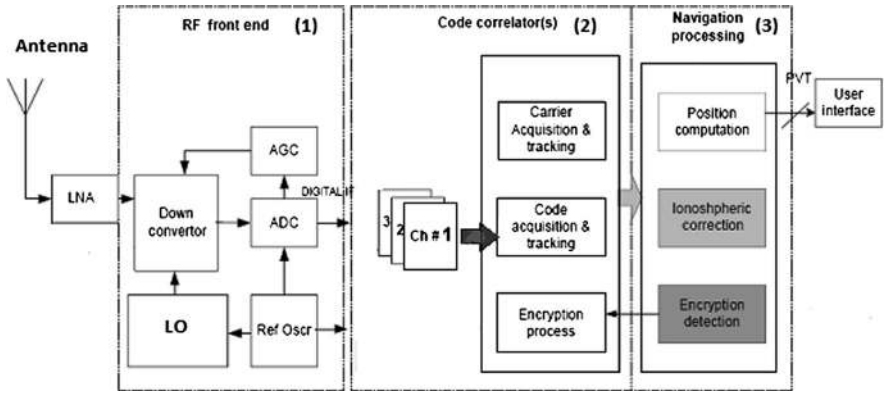

FIGURE 5.4

Architecture of a typical receiver.

A standard receiver may use a quartz crystal oscillator as the frequency standard. These oscillators are sensitive to the temperature and their stability may vary between 10^{-5} to 10^{-6} over a typical operating temperature range. Therefore, the frequency excursion must be confined, mainly through temperature control. A temperature-controlled crystal oscillator (TCXO) is typically used for this purpose. A more effective means is to use an oven controlled crystyal oscillator (OCXO). However, it is commonly used in more precise and larger receivers owing to the cost and size.

Where size and cost are not constraints, precise atomic clocks can be used. This is common for the receivers meant to monitor the space segment or for precise applications such as surveying. In addition, chip-scale atomic clocks are being used for this purpose. These have weights of a few tenths of grams and perform much better than crystal oscillators, and with much less power consumption.

5.2.3.2 Intermediate frequency downconversion

The signal received from the antenna is first filtered and amplified at the preamplifier. Then, it is converted to a convenient lower frequency for further filtering and amplification before digitization. This is a heterodyning approach. Lowering the frequency allows the receiver to use a lower sampling rate for further processing, which eases the hardware requirement and reduces the processing load. This lowered frequency of suitable value, which is a few orders below the carrier frequency, is called the intermediate frequency (IF). The process of reducing the frequency is referred to as downconversion. The IF frequency, however, remains a few multiples of the code rate.

Conventional downconversion of the carrier frequency f_c of the signal to the IF at f_{IF} is conveniently achieved by heterodyning. Heterodyning is done by mixing two separate signals of different frequencies and selecting the lower frequency component of the resultant product. Here, the output of a local oscillator, whose frequency is

f_{IF} away from the carrier frequency fc, i.e., f_c - f_{IF}., is mixed with the incoming signal. Mixing, that is, the multiplication of two signals, is implemented by passing their sum through a nonlinear device. The product yields two components. One of them has frequency which is the sum of the two frequencies and the other has the difference frequency. The LPF carried out subsequently removes the sum frequency component, allowing the signal with the difference frequency, equal to f_{IF} to pass on. Let us consider the input signal to be represented in the phase quadrature form as

$$S(t) = a_r \cos\left(2\pi f_c t - \varphi\right) = a_i \cos(2\pi f_c t) + a_q \sin(2\pi f_c t) \tag{5.13}$$

where $a_r = (a_i^2 + a_q^2)^{1/2}$, is the resultant amplitude, and φ is the phase with respect to the cosine reference, given by $\tan\varphi = a_q/a_i$.

In a receiver, downconversion is carried out by first mixing the RF signal with the frequency of the local oscillator, $f_{LO.}$ This frequency is kept as the difference between the carrier and the required IF frequency, that is, $f_{LO} = fc - f_{IF}$. So, when the input is multiplied by this signal, we obtain the product as

$$\begin{aligned} S(t)\cos(2\pi f_{LO}t) &= a_i\cos\left(2\pi f_c t\right)\cos(2\pi f_{LO}t) + a_q\sin(2\pi f_c t)\cos(2\pi f_{LO}t) \\ &= \frac{a_i}{2}\left[\cos\left\{2\pi(f_c - f_{LO})t\right\} + \cos\left\{2\pi(f_c + f_{LO})t\right\}\right] \\ &\quad + \frac{a_q}{2}\left[\sin\left\{2\pi(f_c - f_{LO})t\right\} + \sin\left\{2\pi(f_c + f_{LO})t\right\}\right] \end{aligned} \tag{5.14A}$$

Thus, upon multiplying, the resultant beat frequencies produced are at $f_c - f_{LO}$ and $f_c + f_{LO}$, respectively. This signal is then passed through a bandpass filter. The lower frequency of the two, i.e. $f_c - f_{LO}$, is selected and passed by the filter, whereas the higher frequency component, $f_c + f_{LO}$ is rejected and eliminated. Thus, at the output of the filter, we get

$$S_{IF}(t) = \frac{a_i}{2}\cos\left\{2\pi(f_c - f_{LO})t\right\} + \frac{a_q}{2}\sin\left\{2\pi(f_c - f_{LO})t\right\} = \frac{a_i}{2}\cos\left(2\pi f_{IF}t\right) + \frac{a_q}{2}\sin\left(2\pi f_{IF}t\right) \tag{5.15}$$

The above Eq. (5.15) when compared with Eq. (5.13) that the downconversion only reduces the frequency from the RF to the IF, keeping the other features of the signal unaltered. Furthermore, this bandpass filtering limits the out-of-band noise from entering the receiver. In the IF, besides the convenience of signal processing, it is possible to filter out-of-band noise with a sufficient roll-off. The schematic for the IF downconversion is shown in Fig. 5.5.

If any stray components present at the frequency $f_{LO} - f_{IF} = f_c - 2f_{IF}$ also generate a component at the frequency $f_c - f_{LO}$, if it is multiplied by the LO output. This signal is called the image because this frequency is located at an equal distance from the f_{LO} frequency as the actual signal, but on the opposite side. However, the signal at the image frequency is not our desired signal and should be restricted to contributing to the IF. Thus, care must be taken to remove the image frequency that adds to the noise. This is done at the level of the preamplifier, even before mixing, through proper filtering. Since the frequency separation between the true signal and its image is $2f_{IF}$, a higher value of IF separates them more widely and improves the rejection of the image.

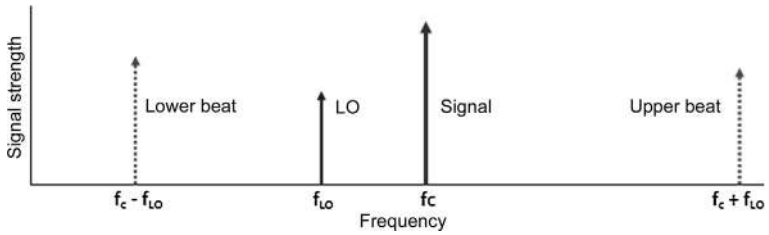

FIGURE 5.5

Signal, LO, upper beat, and lower beat frequencies.

Conversion to the IF is sometimes done in two successive stages for better image rejection. This is called the double heterodyne technique. Another important point is that if any Doppler frequency is present in the RF signal, the same shift is retained in the IF as well. Fig. 5.5 shows the position of the signal carrier, LO frequency, image, and beat frequencies along the spectral line in relation to the downconversion.

Considering the noise components, when the signal from the LO is mixed with the signal, the product with the accompanying noise generates the following:

$$n_{LO} = \frac{n_c}{2}\cos(2\pi f_{IF}t)\cdot\cos(2\pi f_{LO}t) + \frac{n_s}{2}\sin(2\pi f_{IF}t)\cdot\cos(2\pi f_{LO}t) \tag{5.16}$$

Upon low-pass filtering, the components thus generated are

$$n_{IF} = \frac{n_c}{2}\cos(2\pi f_{IF}t) + \frac{n_s}{2}\sin(2\pi f_{IF}t) \tag{5.17}$$

So, the effect of the IF downconversion on the noise is that it produces similar bandpass noise at the IF.

Another technique of downconversion is to achieve it during the sampling. This is called the bandpass sampling (BPS). Here, the sample rate is chosen in a manner that the sampled signal has the signal spectrum in the predefined frequency range. We will discuss this method of BPS when we describe the sampling process of the signal.

5.2.3.3 Analog to digital converter

The signal obtained until now is in analog form with continuous variation over time. It has a bandwidth spread by the codes and referred to as the *precorrelation* bandwidth. The analog values of the signal are available at the input of the *analog-to-digital converter* (ADC), which converts this continuous signal into a discrete form. The analog values at definite discrete and equidistant instances are selected. The values at all intermediate times are discarded. This process is called sampling; the selected values form the samples of the analog signal. These discrete sample values are converted to corresponding digital levels and converted to bits using binary coding. The process of sampling and quantization is illustrated in Fig. 5.6.

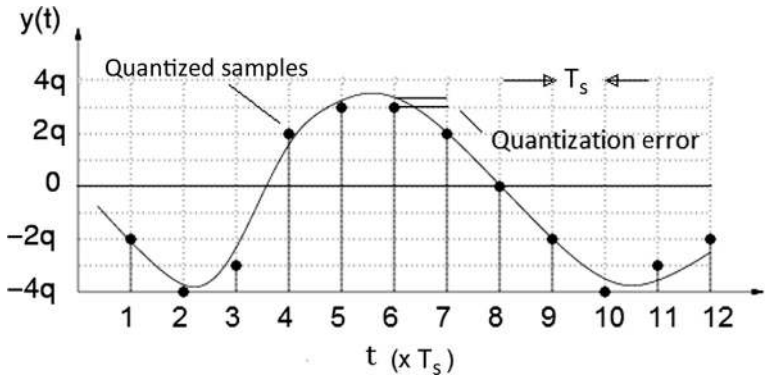

FIGURE 5.6

Sampling and quantization.

5.2.3.3.1 Sampling

Today's receivers are digital in nature and can work only on discrete digital values. To enable processing in the digital domain, the continuous signals are sampled generally in the IF before they are converted to baseband.

The sampling procedure measures the instantaneous amplitude of the continuous signal at discrete regular intervals. It keeps the signal level values only at these discrete instances and ignores the rest. However, from sampling theory, it is known that the whole signal may be recovered from the sampled data if the sampling is done at a sufficiently fast rate.

The important question is, at what rate should the signals be sampled to preserve all the necessary information so that the signal can be faithfully reconstructed? This is governed by the criterion set by the Nyquist sampling theorem.

The *Nyquist sampling theorem* states that a band-limited analog signal can be perfectly reconstructed from the complete sequence of its samples if the sampling rate exceeds twice the highest frequency contained in the original signal.

The encoded data is evenly spread on two sides about the IF frequency, f_{IF}. Therefore, from the theorem, the ADC sampling rate must exceed twice the sum of the IF frequency and the signal's single-sided bandwidth. This satisfies the requirement for perfect reconstruction of the original signal. The chip period of the encoded data being Tc, the maximum frequency contained in the signal is $f_{IF} + 1/T_c$. This makes the sampling rate $2f_{IF} + 2B$, where $B = 1/Tc$. At the same time, to prevent the spectral fold over, which distorts the signal, the minimum value of the f_{IF} that may be chosen must exceed the single-sided precorrelation bandwidth, that is, $f_{IF} \geqq B$. Thus, combining the two, we see that the minimum sampling rate can be determined from the relation $f_s \geq 2(2B)$. This makes the minimum sampling rate twice the null-to-null signal precorrelation bandwidth.

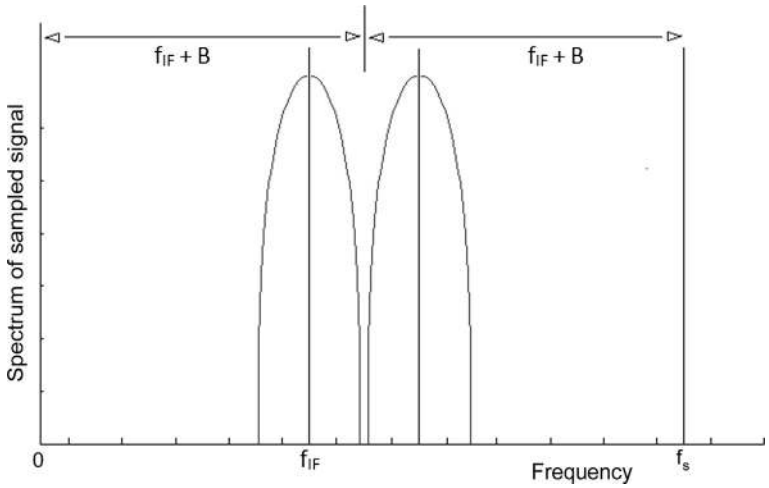

FIGURE 5.7

Spectrum of sampled signal.

This can also be easily understood from a spectral view of the process. Sampling is multiplying the time variation of the signal by unit impulses located at regular time intervals of sampling, T_s. This train of unit impulses, when transformed to the spectral domain, becomes a train of impulses at an interval of $1/T_s = f_s$. So, the spectrum of the sampling impulses is lines at DC and at distances that are integral multiples of f_s (Lathi, 1984). The process of multiplication of the two signals the time domain results in convolution of the individual spectrum of the signals in the spectral domain. Convolving the signal spectrum with this impulse train results in an array of replicas of the same signal spectrum, with the origin shifted to each of the impulse locations at nf_s but reduced in level. This is shown in Fig. 5.7.

This array is passed through a bandpass filter to recover the signal. For the condition in which no two adjacent replicas overlap, that is, no aliasing occurs, the separation between the two adjacent impulses of the train must accommodate two single-sided bandwidths of the IF downconverted signal. So, the sampling frequency can be written as

$$f_s \geq 2(f_{IF} + B) \geq 4B \quad [\because f_{IF} \geq B] \tag{5.18}$$

For most compact forms of downconversion and sampling, avoiding aliasing or spectral fold over, the optimal sampling rate is four times the one-sided bandwidth of the signal. However, this is only a special case with the lowest IF frequency, that is, $f_{IF} = B$. For all other f_{IF} values, the required sampling rate is higher.

In a real navigation scenario, the signals are modulated by pseudo-random noise encoded data bits. Here, the sampling rate should preferably not be an exact multiple of both the IF and chip rate. This ensures that the samples are not sampled at the

same carrier and code phase in every cycle but collectively encompass the shape of the signal waveform (Groves, 2013). Considering this, the exact sampling frequency of the ADC is then determined.

5.2.3.3.2 Quantization

The samples of the signal are discrete in time, but still have continuous values of their levels. Quantization is the approximation of the sampled signals in some discrete levels, and then the representation of these levels with some known digital codes. The whole range of possible sampled values of the signal is divided into a number of smaller range of values. A discrete level within each range, called the quantization level, is identified to represent all sample values lying within the corresponding range. Each of these levels is digitally represented by one of the digital codes. These digital codes are basically made up of some finite binary bits. The number of bits in the code depends on the number of quantized levels. Hence, it can take only some finite sets of values.

In the quantization process, because we represent a range of sample levels by a single quantized value, it results in an effective error in the representation of the true value. This error is known as a quantization error. This error, which is basically an error resulting from limited levels for the representation of the codes. So, very obviously it decreases with an increase in the number of quantization levels for the same range of sampled values. This can be done by increasing the number of binary bits by which the codes are represented.

The errors resulting from quantization may also be treated as equivalent noise. The difference between the true value of the sample and the value of the quantum level by which it is represented is treated as noise called quantization noise. It can be shown that for linear quantization and evenly distributed signal, the ratio of the signal power, S quantization noise power, Nq, can be expressed as (Mutagi, 2013)

$$S/N_q = 1.8 + 6n \text{ in dB} \tag{5.19}$$

where n is the number of bits used to represent the levels, so that $2^n = N$, the number of levels. It follows that a difference of 1 bit will result in a difference of 6 dB in the SNR.

However, the signals in the conventional satellite navigation system are already embedded in noise. That means the amplitude of noise at any instant is much higher than the amplitude of the signal. So, any increase in the quantization levels will mostly be used to represent noise. Therefore, only a few bits may be used for quantization instead. This will sufficiently indicate the levels of polarity of the sampled noisy signal at the instant of sampling.

Increasing the sampling rate or adding quantization bits has implications for processing as well as the cost of the receivers. This is because the increased numbers of these parameters demand increased processing capacity in terms of bits handled per second for subsequent signal processing. So, the low-cost receivers may use single-bit quantization of sampling. This will trade-off the receiver complexity with adding

quantization noise. Therefore, in the process, it reduces the effective SNR referred to as the implementation loss. Better performance is obtained when a quantization level of two or more bits is used for the purpose. Although it does not look like a huge improvement at the RF level, it affects precision at final position fixing by improving the SNR.

The quantization process is generally improved with automatic gain control (AGC). In a navigation system, the signal is of constant amplitude. Because no information is carried by the amplitude, its variations in the signal, caused by various effects, may be compensated without distorting or compromising any information present in it.

Owing to the amplitude variation, the signal may vary between large extremes such that the range crosses the nominal dynamic range of the quantization process. To handle this, amplifiers with a large dynamic range are required, which is difficult to implement. In such situations, alternatively, the AGC can have an effective role. It can vary the amplification of the input to the ADC to keep it matched to the dynamic range. However, it only ensures that the composite signal mixed in noise maintains the range. The SNR remains unaltered while the actual signal level embedded in it may vary.

Focus 5.2 Quantization error

The effective SNR can be represented in terms of signal SNR (SNR_n) and the SNR resulting from the quantization noise (SNR_q) as

$$SNR_{eff} = \left(SNR_n{}^{-1} + SNR_q{}^{-1}\right)$$

With 2-bit quantization, SNR_q becomes $12 + 1.8 = 13.8$ dB $= 10^{1.38} = 24$. whereas $SNR_n = -20$ dB $= 1/100$.

So, the effective SNR, considering the quantization noise over and above the signal noise becomes

$$SNR_{eff} = \left(100 + \frac{1}{24}\right)^{-1} = \frac{1}{100.04}$$

In logarithmic terms, the effective SNR becomes

$$SNR_{eff} = -10\log(100.04) = -20.01 \text{ dB}$$

So, the degradation owing to the use of fewer quantization bits is negligible.

5.2.4 Baseband signal processor

The signal forwarded by the front end of the receiver is a combination of all the signals received from every satellite visible to the receiver. In addition, each signal is composed of all of the signal components: the data, the code, and the carrier in the IF. This composite signal enters the region where it is treated explicitly for the

purpose of identifying individual signals, separating them, and subsequently wiping off the code and the carrier to obtain the navigation data. For this purpose, this sampled and digitized form of the signal, still modulated with IF and added with Doppler, is then processed in the baseband signal processor. The details of this processing will be described in this section.

The baseband signal processor demodulates the sampled signals and recovers the navigation data, removing the carrier and the code added to it. It does so by correlating the signal with the internally generated replicas of the code and the carrier. This section of the receiver is hence called the correlator and data demodulator. Along with the process of code and carrier removal from the signal, it simultaneously performs the process of code or/and carrier-based ranging.

The architecture of the correlator that receives data from its previous section can be divided into different parallel processing arms. Each arm processes separate signals simultaneously and independently. For CDMA, the same composite signal enters as the input to each channel arm, where the required component is segregated from the rest. For FDMA receivers, these signals are first separated by filtering, and each separated channel is loaded into an arm. Each of these arms, therefore, processes a separate signal channel.

To understand clearly what goes inside this module, let us start with a simple situation. The carrier frequency of the signal is now downconverted to f_{IF}, and the frequency is known. Besides, assume that the carrier phase is known at any arbitrary instant of time. Also, assume that the code phase at that particular instant is also approximately known. This is a hypothetical situation because it will never exactly happen in an actual scenario. However, this is the condition the receiver attempts to attain. So, starting with this assumption gives us an understanding of what the receiver is trying to achieve in the whole process.

With the knowledge of the f_{IF} and carrier phase, the signal can be demodulated if the resultant component is multiplied with a synchronized carrier and then filtered. By multiplying with the synchronized code, the code in the signal is also removed, so that only the data bit remains. This is done in the section specifically designed for the carrier and code wipe-off. The schematic of such a section of the receiver is shown in Fig. 5.8.

Two distinct sections are present here: one consisting of the carrier wipe-off segment, and the other with the code wipe-off segment. The arrangement in each of these sections, as it appears here, is of the open-loop type.

The initial job the receiver needs to do is mix a synchronous sinusoid with the known frequency and the phase of the carrier, to wipe out the carrier. For this, a local carrier is generated with the estimated frequency and phase. This local carrier is mixed with the incoming signal. This yield the output after low pass filtering as

$$s(t) = A_k\, c(t) \cos\left\{2\pi\left(f_{IF} - f_{LO}\right) + \delta\varphi\right\} \tag{5.20A}$$

where A_k is the data bit value, c(t) is the code chip at time t, f_{IF} is the known IF frequency, f_{LO} is the local oscillator frequency and $\delta\varphi$ is the difference in the initial

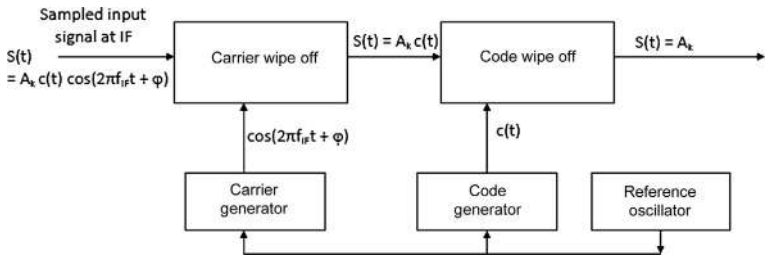

FIGURE 5.8

Schematic of the code and carrier wipe-off section.

phase of the two signals. Because the frequency set at the local oscillator is the exact carrier frequency in the signal (as per our assumption), then $f_{IF} = f_{LO}$. Now, if the phase of the local carrier be matched with that of the signal, then we can put $\delta\varphi = 0$ into this equation. Then, the carrier of the incoming signal is eliminated to produce

$$s(t) = A_k\, c(t) \tag{5.20B}$$

A small offset δf in the local frequency from the IF will lead to a slowly oscillating signal, while a little offset in the phase, $\delta\varphi$ will cause the amplitude to get reduced by a factor $\cos(\delta\varphi)$. The resultant signal will then be

$$s(t) = A_k\, c(t) \cos\left(2\pi\delta f + \delta\varphi\right) \tag{5.20C}$$

Then, the local carrier is generated and set to the particular IF frequency and the phase is continuously attempted to stay synchronized with the received signal across time. This synchronized local carrier, when mixed with the received signal and low-pass filtered, the signal gets carrier demodulated, leaving only the levels, $A_k c(t)$, of the encoded data chips.

The code wipe off works in a similar fashion. This can be understood by remembering two things: first, what a complete oscillation for a sinusoidal carrier is a complete code excursion for a code; and second, the low pass filtering, which is a frequency domain concept, is equivalent to integration in the time domain. Thus, the code can be similarly removed by a coherent code generated locally to recover the navigation data.

Recall that during carrier wipe off, we multiplied the local carrier with the incoming signal and then did a low-pass filtering of the product. Similarly, here we generate a local replica of the code and multiply it with the code in the incoming signal. The product is then integrated over a few integral multiples of the code length. The result thus obtained is given in Eq. (5.21) below, where the local and the signal code phases are separated by delay, τ.

$$P = \int c(t)\, c(t+\tau)\, dt \tag{5.21}$$

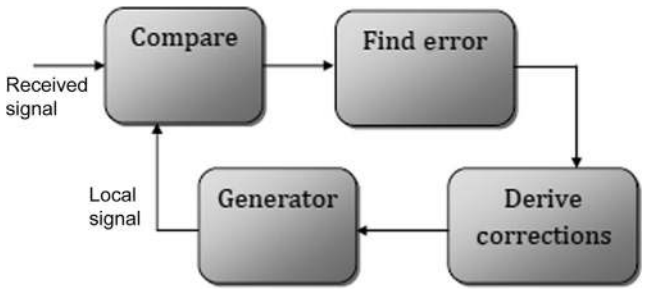

FIGURE 5.9

Schematic for a closed-loop arrangement of a signal follower.

Here, for convenience, we are not showing the presence of the data bits because these operations are all carried out within a single data bit interval, and we assume bit reversal does not occur here. This is equivalent to Eq. (5.20A, B) for carrier tracking. The time over which the integration is to be done must be an integral multiple of the code repetition period. When P is normalized by dividing this integral by the integration time, we get the autocorrelation of the code with delay τ. That is,

$$\frac{P}{T} = \frac{1}{T}\int_0^T c(t)c(t+\tau)\,dt = R_{xx}(\tau) \tag{5.22A}$$

We have seen in Chapter 4, in Eq. 4.21, that this value becomes $R_{xx}(\tau) = (1 - |\tau|/T_c)$, where τ is the delay between the two codes and T_c is the code period. So, when the receiver exactly identifies the code phase of the incoming signal and generates the local code synchronously with it, the above value reduces to

$$\frac{P}{T} = R_{xx}(0) = 1 \tag{5.22B}$$

However, the assumptions that the exact Doppler and the code frequency and phase is known at the beginning of the process is hypothetical. The local oscillator or the code generator cannot be made synchronous with the input at the beginning or in a single shot. In any pragmatic case, only the designated value of the carrier frequency is known and not its current phase. This frequency changes owing to the Doppler present in the signal, which remains unknown a priori. Moreover, there may be a drift in the satellite oscillator that will result in a fixed shift of the signal carrier frequency.

The unique ranging code of an FDMA system is known, but the current code phase is still unknown to the receiver. In a CDMA system, the individual code present in the particular signal is also not known. These different issues need to be taken care of.

To know these signal parameters exactly and follow them over time, open-loop estimates are not sufficient. These activities are carried out in a closed decision-making loop whose generic structure is shown in Fig. 5.9.

When the receiver is switched on for the first time or a new satellite comes into view, the condition of the code and the carrier is completely unknown to the receiver. Starting blindly from a completely unknown state of the carrier as well as of the code, the receiver needs to chase these parameters, lock on to the frequency of the incoming signal, and then follow its phase closely.

Identifying a signal and leaving a coarse estimate of its code and carrier phase including the Doppler is done by a process called signal acquisition.

5.2.4.1 Signal acquisition

Whatever be the technique utilized to remove the code and carrier at the receiver, the signal first undergoes a separate procedure in which the receiver approximately adjusts its local carrier and code generators and sets them within close proximity of the signal frequency and phase. This is called signal acquisition.

The receiver may have the oscillator tuned at the designated IF frequency f_{IF}, using which, the IF frequency is removed from it at the carrier wipe-off portion. However, the phase mismatch will affect the resultant signal amplitude. Also the signal can still have a small residual Doppler frequency, making the resultant signal oscillating very slowly. It may arrive at the code wipe-off section in this form.

To avoid this, the acquisition process searches for the approximate residual Doppler frequency. Moreover, identification of the exact unique code present in the signal and the approximate code phase of a particular individual signal also needs to be done.

Doppler shifts depend on the relative dynamics of the user and the receiver, and hence vary for different signals. Besides, the ranging codes of the signals, although transmitted synchronously from the different satellites, differ in their phase when received, owing to differences in the ranges of the satellites. So, the questions we need to answer through this activity are:

- What is the residual Doppler frequency of this signal?
- What is the ranging code of this signal across all the possibilities?
- What is the code phase of the signal in terms of the chip number and fraction of it?

It requires searching in time and frequency space for the appropriate phase and frequency of the signal carrier and code.

The signal itself remains embedded within the noise, and so the receiver may need to acquire the signal under difficult conditions. On the other hand, it needs to be done within a short period of time to reduce the overall time taken for position fixing. Thus, it is necessary to make the acquisition process simultaneously fast and sensitive. The conventional method of search is through hardware and in the time domain. The codes can be searched serially or in parallel. The most popular methods of code acquisition are

- Serial search acquisition.
- Parallel code and frequency space search acquisition.

5.2.4.1.1 Serial search method

In a serial search, different values of the code phase and Doppler frequencies within the feasible range of these parameters are searched. This is done in a sequential fashion. Different discrete values of the Doppler frequencies are generated by the receiver in a sequential order and mixed with the incoming signal. For each such frequency mixed with the signal, the receiver checks for the all the possible codes. For any code chosen, every individual code phase with a predefined phase interval is generated and mixed to the incoming signal, in sequence. Normally, the search is done every half chip spacing for the code. Each code phase and Doppler shift searched is called a "bin," whereas each combination of the two is called a "cell." The filtered product is then integrated over a finite time to obtain the autocorrelation. The autocorrelation value is estimated by integrating over an integral multiple of the code length. The time spent correlating a signal in each cell is called the "dwelling time"(Groves, 2013). The cell values that truly matches those of signals will yield maximum correlation value. So, practically, the integral exceeds a certain threshold, it indicates a match, and then the selected frequency and the code with its corresponding code phase used for the cell are designated as the acquired value. If the integral does not cross the threshold, new combinations are tried. In this way, the receiver checks for locking with all possible code phases in a single code and also over all possible codes in sequence in a CDMA system for a definite Doppler.

It is the simplest of all the well-known algorithms. However, in this algorithm, since each possible combination of Doppler frequency and code phase is tried in sequence until the threshold is exceeded, it requires a large locking time. For FDMA, however, because only a single ranging code is used, it needs to identify only the code phase, which makes the process much faster. Nonetheless, the method works better in noisy conditions.

To see how the signal varies at different parts of the process in quantitative terms, the samples at any instant t will be represented by

$$S(t) = A_k c(t) \cos\{2\pi(f_{IF} + f_d)t + j_0\} \tag{5.23A}$$

where A_k is the level of the k^{th} data, c(t) is the current code chip, f_d is the deviation in the frequency owing to the Doppler and other reasons and j_0 is the arbitrary constant initial phase of the signal. The acquisition value for the Doppler is f'_d with phase j'_0, and the code phase selected corresponds to delay τ with respect to that in the sampled signal. So, the frequency $f_{IF} + f'_d$ is loaded onto the oscillator for the carrier wipe off. The output from the carrier wipe-off section is thus

$$S(t) = \frac{A_k}{2} c(t) \cos(2p\Delta f\, t + \Delta\varphi) \tag{5.23B}$$

$\Delta f = (f_d - f'_d)$ is the residual Doppler, that is, the difference between the true offset and the selected offset of the carrier frequency from the IF, and $\Delta\varphi = (j_0 - j'_0)$ is the constant phase offset. Similarly, because τ is the selected code delay, the code value

generated is $c(t+\tau)$. The signal after the code multiplication becomes

$$S_{acq}(t) = \frac{A_k}{2} c(t)c(t+\tau)\cos\left(2p\Delta f\, t + \Delta\varphi\right) \tag{5.23C}$$

These samples are accumulated over a time interval that is an integral multiple of the code length, typically about half of the data bit duration. These product samples are summed over time T, in which the samples are close enough to consider it as integration, yielding (Van Dierdonck, 1996).

$$S_{int}(t) = A_k R_{xx}(\tau)\,\mathrm{sinc}(\pi\Delta f T)\cos\left(\Delta\varphi\right) \tag{5.23D}$$

The value of the expression S_{int} increases as Δf, $\Delta\varphi$, and τ tend to zero. This value should exceed a predetermined threshold before the signal is said to be acquired. This expression is essentially a sine cardinal (sinc) function for the frequency offset, a cosine function of the phase offset, and a linear function of code delay, τ. Since, sinc function is involved, it is evident that the minor peaks appear for certain offset frequencies, as well. Similarly, for CDMA, even for different codes, minor peaks may appear owing to the limitations in the code cross-correlation function. Such secondary offset peaks have much lower power and should be intelligently discarded.

Because the functional nature of the correlation is known, so is the distribution of its peaks for offset t. Therefore, the threshold may be set accordingly, so that the minor peaks remain below it and are not detected even in the presence of expected noise.

The associated uncertainty in frequency that may result from the Doppler or other reasons is used to set the precorrelation filter bandwidth. This limits the search range. If the receiver has no a priori knowledge, the initial uncertainty is larger, requiring substantial time to acquire the signal as more frequency bins are required to be searched. Searching for codes starts from the early side to avoid false locking with the multipath component, which always trails the direct signal.

The noise present in the signal deteriorates the autocorrelation results. However, the effect of the noise can be reduced by taking the integral over a longer time interval, that is, over a large integral multiple of the code length. But this is limited by the length of the data bit. Any data bit inversion during the correlation integration deviates from the result. This is the reason why, in some cases, where low SNR is expected, a pilot channel containing only the product of the code and the carrier but no data bits is sent synchronously but separately from the data channel. The absence of any data bit removes the limitation of integration time while acquiring the signal. So, the signal may be acquired even from a weak SNR condition through a longer integration period. Once the pilot channel is acquired, the synchronicity allows the receiver to switch over to the data channel without further acquisition.

If the process is actually executing the reacquisition of a signal it had acquired before but has lost the lock thereafter, it may draw information regarding the time, carrier, and code offsets from what was obtained before and stored in the last operating session. This is known as “warm start,” and it helps in the acquisition process by

drastically reducing the acquisition time. However, the last saved information should be checked for validity across the session before use. The search efficiency may also be enhanced with exclusive searching of individual channels so that no two channels search for the same satellite signals over the entire course of acquisition.

When a complete match is established between participating signal components, the autocorrelation is naturally high. For a CDMA system, the presence of different codes in the composite signal results in the formation of cross-correlation noise during the process. This reestablishes the requirement of proper choice of codes with suitable correlation properties so that the cross-correlation noises do not cumulatively add up to such a considerable amount that it appears like an autocorrelation peak, resulting in a false locking condition. Noise will effectually determine the performance of the acquisition process, leading to finite probabilities of a missed detection of the signal and false locking, as well.

5.2.4.1.2 Parallel search method

The parallel search method is the one in which the sequential search of the Doppler and code, and carrier phase, done in the previous case, is replaced by an equivalent parallel process. This immensely increases the searching speed (Scott et al., 2001), which was a serious limitation in the serial search process. Therefore, it accounts as a time-economical alternative to the serial search method. This method is based on the Wiener–Khinchin theorem.

The Wiener–Khinchin theorem (Proakis & Salehi, 2007) states that for a wide-sense stationary process, x(t), the power spectral density $P_{xx}(f)$ is the Fourier transform of its autocorrelation function $R_{xx}(\tau)$. Similarly, the cross-spectral density $P_{xy}(f)$ of two such wide-sense stationary processes, viz. x(t) and y(t), is the Fourier transform of their cross-correlation function, R_{xy}. So, if F[•] represents a Fourier transform operation,

$$F\left[R_{xx}(\tau)\right] = P_{xx}(f) = X(f) \cdot X(f) \tag{5.24A}$$

$$F\left[R_{xy}(\tau)\right] = P_{xy}(f) = X(f) \cdot Y(f) \tag{5.24B}$$

The signal samples of x(t) may be transformed using fast Fourier transform (FFT) to form its amplitude spectrum X(f). Similarly, the FFT of the reference signal y(t) may be obtained to get Y(t). Now, if these two spectra obtained by transforming time signals are multiplied in the frequency domain, the inner product we get either represents the power spectral density when the codes are the same or the cross-spectral density when the codes are different (Proakis & Salehi, 2008). On doing the inverse FFT (IFFT) on this spectral product, we get the correlation values of the input and the reference signal for different values of the delays τ simultaneously. Thus, the total process of the sequential search for different possible relative code phase delay values is replaced by a single step. The used code is selected if the IFFT shows a peak exceeding a threshold, and the phase delay is estimated from the relative position of the peak.

However, the cost one has to pay for this is the increased complexity of the computation process at the correlator. The process may be executed only for the code search after complete carrier detection. Alternatively, the process may be carried out in 2 dimensions, with one dimension representing the carrier Doppler and the other the code phase. So, from the peak obtained in this, both the phase offset and the residual Doppler may be identified. Thus, the parallel frequency space search method provides the correlation values for all possible code shifts in a single go, and hence drastically reduces the search time of the acquisition process. But it is more complex than a serial search and also works poorly in noisy conditions (Scott et al., 2001).

Irrespective of which method is used to carry out the process of acquisition, for their implementation, it is necessary that the receiver knows in advance what the possible set of codes is and the expected range of Doppler frequencies of the signal that it is searching for. This knowledge limits the uncertainty bound during correlation for identification and thus determines the precorrelation filter bandwidth. In the same manner, the residual acquisition accuracy determines the width of the postcorrelation uncertainty.

5.2.4.2 Signal tracking

Acquisition provides only approximate estimates of the frequency and code phase parameters. With these values, the code and carrier demodulation start working just after the acquisition process. Although it approximately wipes off both, it is not exact, and hence some residuals remain in the signal. The output can then be represented in the form of Eq. 5.23C. Besides, it is incorrect to believe that once estimated, the signal frequency and relative carrier and code phase will remain the same forever. This is for the obvious reason that the dynamics of the satellite and the receiver will continue to change, thus changing the Doppler. Moreover, the presence of any frequency drift in the signal will add to the deviation. So, there will be a residual frequency and phase present in the signal even after acquisition of the signal, which can grow with time if left uncompensated.

To handle these effects, the local oscillator used for the carrier wipe off and the clock used for the generation of the code must also have the ability to change the frequency and consequently the phase with finer resolution so that it is able to trace the exact carrier frequency and phase of the input signal and then follow it.

To facilitate this, a numerically controlled oscillator (NCO) replaces the fixed oscillator for signal generation. An NCO is a digital signal generator that generates the discrete values of a complete sinusoidal wave with fixed resolution. These values are systematically generated at regular intervals and at discrete time instants synchronously with clock inputs. With every clock tick, its phase accumulator, which is basically an N-bit counter, increases its count by 1. Each count represents the least count of phase, which is $2\pi/2^N$ and which defines the resolution of the oscillator. The phase of the accumulator thus increases by this amount at every tick of the clock. As the counter counts modulo 2^N, the phase accumulates from 0 to 2π and resets again. There is a corresponding sinusoidal value stored for every phase. The phase-to-amplitude converter sends the amplitude corresponding to its accumulated phase,

at any instant, to discretely generate the wave. The frequency of the generated wave depends on N and the clock rate. If the clocking rate is R_{clk}, the frequency it generates is $f_N = R_{clk}/2^N$.

Such an NCO is used to drive both the carrier and the code generator. Using these, the input signal is followed exactly in terms of its carrier and code phase through a process known as tracking, which we will now discuss in detail.

5.2.4.2.1 Carrier tracking

At the outset of the carrier tracking, the carrier offset value obtained in the acquisition, including the fixed f_{IF} is fed to the carrier NCO to generate the corresponding frequency. Consequently, the signal after acquisition has its nominal carrier wiped off and most of its Doppler removed. To remove the rest and any further variation of it, carrier tracking is done. The main purpose of tracking is to minimize the residual carrier frequency and phase values in the signal and follow its variations with time. This is done by changing the locally generated carrier accordingly so that it chases and follows the temporal phase variation of the input carrier faithfully.

Either the phase or the frequency of the local carrier may be allowed to be attuned to track the corresponding parameter of the incoming signal. Phase tracking may be achieved through a *phase-locked loop* (PLL), which is a closed-loop arrangement to follow the carrier phase. However, for large deviations in frequency, chasing the signal with a PLL is time-consuming. In addition, it requires a large operational range of PLL. Compared to it, the carrier frequency tracking is more robust. It performs well in poor signal-to-noise and high dynamics environments because the tracking lock may be maintained here even with larger errors. This is why frequency tracking is preferred in many receivers. Such receivers may use a frequency locked loop (FLL) instead for the purpose. However, it does not provide the integrated Doppler values, which are provided directly by the phase tracking arrangement. In some receivers, FLL is used during the initial part of the tracking as an intermediate process between acquisition and phase tracking. When the signal remains in a well-acquired state, it switches over to PLL.

The PLL works by discrete differential adjustment of the phase of the local reference carrier. It is implemented in a closed loop consisting of the carrier wipe-off arrangement, whose local oscillator is controlled by feedback from the output signal of the wipe-off. This feedback, proportional to the differential phase values, drives the oscillator in a way to minimize the difference. The total control loop is shown in Fig. 5.10 and performs the following activities:

- Generate a reference signal of a certain frequency and phase.
- Compare it with the input and find the error in frequency and phase.
- Derive a correction term from the error.
- Generate the corrected reference signal by adjusting its frequency and phase at the oscillator using the correction term.

After the generation at the NCO, the reference carrier is mixed with the incoming signal. It removes most of the carrier oscillation frequencies. The code is also removed

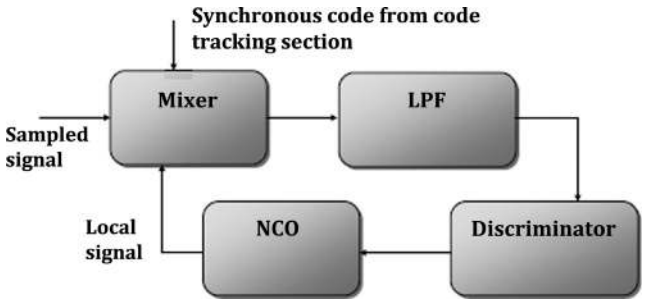

FIGURE 5.10

Schematic of a PLL.

from this signal by multiplying it with the synchronized local code obtained as the output from the code tracking section. A very narrow band low-pass loop filter separates out the sinusoid with only the error components. Correction terms are derived from this signal inside the processor and fed back to the oscillator, completing the loop. These activities continue in a cyclic fashion over time so that at every instant, the locally generated carrier is exactly in phase with the incoming one. So, it has the following generic blocks arranged in the manner, as shown in Fig. 5.9. The exact implementation of the PLL is shown in Fig. 5.10.

Whenever the sampled signal arrives riding on the IF carrier, its exact phase is not known. So it is multiplied by two orthogonal local reference signals. This reference is initially set to IF but can be tuned to frequencies in the neighborhood. This multiplied product is passed through a low-pass loop filter. This is equivalent to the incoming signal getting projected onto the references accordingly. We have seen this in mathematical detail in Section 5.1.2 of this chapter. We call these projections of the incoming signal on the cosine and the sine components of the reference signals, respectively, the in-phase component, I, and the quadrature phase component, Q. From these components, we can derive the relative phase angle between the incoming signal and the local reference.

Let the incoming signal samples at IF be given by the following equation, where A_k is the data level.

$$S(t) = A_k \cos\{2\pi(f_{IF} + f_d)\, t + j_0\} \tag{5.25}$$

The local reference carrier in two orthogonal phases may be represented by

$$S_c(t) = \cos(2\pi f_{acq}\, t) \tag{5.26A}$$

$$S_s(t) = \sin(2\pi f_{acq}\, t) \tag{5.26B}$$

f_{acq} is the nominal frequency set to the oscillator after acquisition, and is the sum of the f_{IF} and the estimated Doppler shift $f_{d'}$, obtained through the acquisition process, that is, $f_{acq} = f_{IF} + f_{d'}$. The incoming signal is first mixed with the orthogonal components

of S_c and S_s. Passing the product through the loop filter yields respectively

$$I(t) = \frac{A_k}{2}\cos(2\pi\delta f\, t + j_0) \tag{5.27A}$$

$$Q(t) = \frac{A_k}{2}\sin(2\pi\delta f\, t + j_0) \tag{5.27B}$$

These signals, thus obtained at the loop filter output, have frequency $\delta f = f_d - f_{d'}$. Thus, these two components provide signals with phase and frequency equal to the offset in the phase and frequency, respectively, of the reference with the incoming signal.

The mixed signal after filtering should ideally be a DC if the two signals are perfectly frequency matched. Practically, it is of very low frequency, representing the error frequency only. So, the LPF used here can have a narrow bandwidth. However, a very narrow band will not work in case of any large frequency residual during the operation. Such situations may arise owing to unaccounted Doppler shifts. Therefore, the PLL may lose the lock under such condition. At the same time, wider bandwidth allows larger noise to enter the loop, thus deteriorating the system's precision.

This signal is then used for generating the correction terms. It is done at the discriminator in this case. The discriminator converts this error signal into a correction term that drives the NCO to generate the correct phase. It is basically a phase-to-amplitude converter. Thus, depending upon whether the error term is positive or negative, the clock rate driving the NCO is accordingly stepped up or down, respectively, so that the local reference is synchronized with the input. This process continues over time to keep track of the variations in the signal phase. However, questions that arise here are:

- How to convert sinusoidal I and Q signals into a correction signal for driving the NCO? The answer to this defines the discriminator characteristics.
- How does the NCO respond to this correction signal to remove the error?

In such a technique for carrier tracking, the problem with using an ordinary PLL is that it is sensitive to the phase reversals, that is, π phase shifts in the signals. In a navigation receiver, the input signal at this point is multiplied by the encoded navigation data bits. Even if the codes are removed, the data bits, A_k, will stay and will shift the phase of the signal by phase π at the instant of transitions. Consequently, the phase difference with the reference changes abruptly.

This problem can be eliminated if either there is no such transition in the binary data chips or if the PLL discriminator is insensitive to such π phase shifts. Here, we will only discuss discriminator algorithms that are insensitive to the data bit variations and intrinsically handle the phase reversal occurring as a result.

This algorithm, which generates a correction value for driving the oscillators by deriving the error terms from I and Q signals, constitutes the discriminator and resides in the processor. They work on the fact that the data bit reversal identically affects both the I and Q components of the signal. The Costas generic discriminator with a differential coder uses the product of I and Q as the discriminator input. This product

of two components gives

$$\begin{aligned} I(t)Q(t) &= \frac{A_k^{\,2}}{4}\cos(2\pi\delta f\, t + \varphi)\, x \sin(2\pi\delta f\, t + \varphi) \\ &= \frac{A_k^{\,2}}{8}\sin\{2(2\pi\delta f\, t + \varphi)\} = \frac{A_k^{\,2}}{8}\sin 2\Theta \end{aligned} \tag{5.28}$$

As A_k gets squared, there is no effect of the bit reversal. From this, it derives the error function sin 2Θ at time t as,

$$D_{QxI}(t) = \frac{I(t)\,Q(t)}{A_k^{\,2}/8} = \sin 2\Theta \tag{5.29}$$

So, when there is a total phase error of Θ, the discriminator finds a sin 2Θ value as the error parameter. It offers double the nominal sensitivity. Moreover, the sine function repeats in every π radians. So, it cannot discriminate between φ and $\pi + \varphi$. This discriminator, therefore, has the limitation that it works perfectly for $-\pi/2 < \varphi < \pi/2$ but shows a sign error beyond this limit.

A slightly modified version of the algorithm is to get the discriminator function by taking the ratio of the components on the I and Q axes. From the ratio of the two components, we can derive the phase difference and can accordingly generate the correction term. From Eq. (5.26A, B), the two components can be written as,

$$\begin{aligned} I(t) &= \frac{A_k}{2}\cos(2\pi\delta f t + \varphi) \\ Q(t) &= \frac{A_k}{2}\sin(2\pi\delta f t + \varphi) \end{aligned} \tag{5.30}$$

So, the ratio is expressed by the value of Q over I as

$$D_{Q/I}(t) = Q/I = \tan\Theta \tag{5.31}$$

This term is also independent of the data bits. So, when the error is Θ, the error parameter derived is tan Θ. However, this equation too, relates the error and the control term in a nonlinear fashion. Therefore, instead of deriving the correction term in this trigonometric form, it can be linearized by taking the inverse tangent function of the ratio. So,

$$D_{atan}(t) = \tan^{-1} Q/I = \Theta \tag{5.32}$$

This is the total phase difference between the incoming and the local carrier at time instant t. Thus, the inverse tangent of the ratio of the signal components available at any instant in the I and Q arms, respectively, represents the total phase error.

The discriminator output variation as a function of the total phase error is called the discriminator characteristic. The characteristics of these three methods are shown in Fig. 5.11. Note from the figures that for all small phase errors, the discriminator characteristics for both of the nonlinear cases can be approximated to linearity.

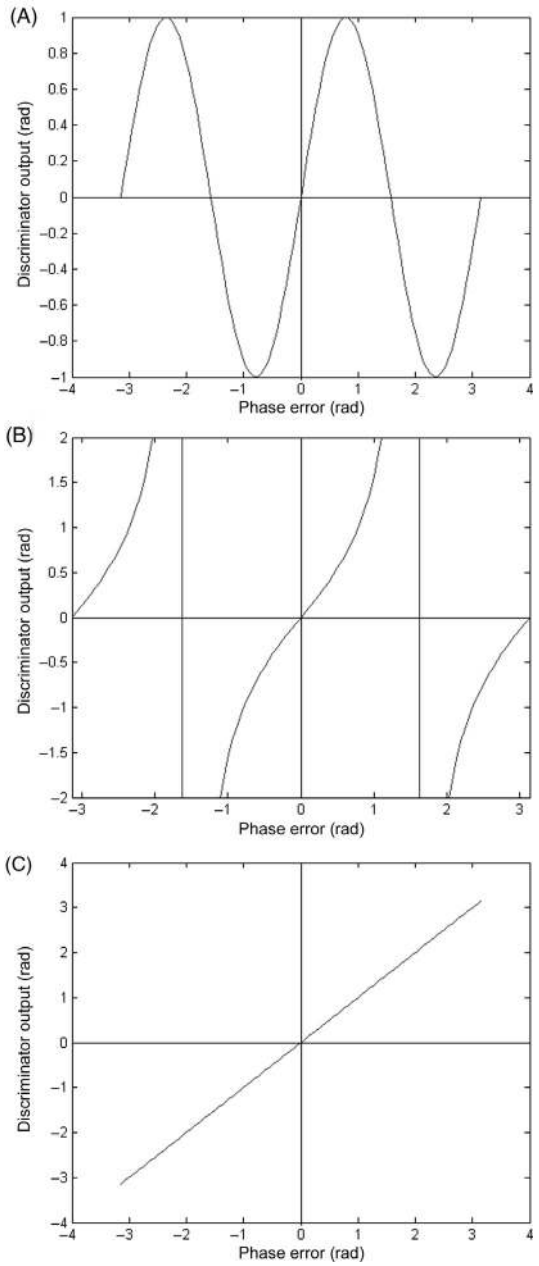

FIGURE 5.11

Discriminator characteristics for (A) D_{QXI}, (B) $D_{Q/I}$, (C) D_{atan}.

Thus, the resultant error signals are converted by the discriminator into error terms which is used for driving the NCO. The NCO accepts this value for the correction and adjusts the signal generated accordingly to follow the input.

Because the bit reversal does not affect the operation of carrier tracking, it can be operated without considering the bit transition. When full carrier synchronization is achieved, the sinusoidal variation is completely removed from the signal.

The noise incorporated in the PLL is a function of the loop bandwidth. This noise may deteriorate the tracking performance. So, to keep the noise to a minimum, the designed loop bandwidth is kept to a minimum requisite value.

5.2.4.2.3 Code tracking

The acquisition process estimates the approximate carrier as well as the code phase. From this situation, the receiver starts tracking the code. The code phase and frequency vary for the same reasons that vary the carrier and calls for tracking the same.

From the sampled data, the exact code phase of the received signal is identified, which is required for two different purposes. The first and the most obvious is that it is used to wipe off the code to extract the navigation data bits. The second and equally important use of this estimation of the code shift is that the satellite range is estimated from this value.

To exactly follow the chipping code, it is required to vary the chipping rate of the local code accordingly. Therefore, the code needs to be driven by a code NCO. The code clock is generated in the same way in the code NCO as the reference offset carrier is generated in the carrier NCO. Therefore, it is required that some code rate correction parameter be generated that will determine how much faster or slower the NCO must run to catch up and get aligned the input. This, in turn, demands a closed-loop arrangement. Here, too, we will carry out the procedure similar to carrier tracking, and the basic idea of the tracking system will remain the same as what we discussed referring to the schematic in Fig. 5.9.

Code tracking is the process by which the receiver follows the variation in the propagation delay and thus the variation in the received code phase by estimating the differential shifts in the incoming signal code phase with respect to a reference code generated at the receiver. This is done using a delay locked loop (DLL). Like PLL, DLL is a closed-loop arrangement used to detect differential change in the phase of a code. It is implemented with the code removal section, with its output going to the integration and dump circuit that we described during the acquisition process. The integration results drive the discriminator to generate the correction signal for controlling the code NCO, which in turn modulates the clock speed accordingly to get aligned with the code phase of the input signal.

The carrier recovered during carrier tracking is generally used to remove the modulation before code tracking. However, in some situations, the carrier is not removed and the code is still tracked, and is referred to as the noncoherent mode of tracking.

Coherent code tracking are said to be done for cases in which the carrier has been exactly identified and wiped off from the signal. In coherent tracking, the effects of the

Doppler on the code width are also removed using aids from the section that tracks the carrier. This presents unmodulated binary-encoded chips to the code tracking system. However, it is difficult to achieve coherence at the beginning, and hence it always starts with the noncoherent mode initially for all practical cases. In the noncoherent mode, the samples integrated at the code wipe-off section have a factor of cos(df) for frequency offset δf. However, that does not affect the code correction parameters, unless the δf term varies. The number of samples accumulated is $Me = T/T_s$, where T is the time of integration and T_s is the sampling interval. This number may vary a little because of the Doppler code during the noncoherent operation. But this variation has negligible effect (Dierendonck, 1996).

Because the acquisition process has already found the coarse phase, the task of the tracking system is only to do its fine-tuning and follow any subsequent variation in the code phase with time. To track variations in the code phase, it should first generate an error signal from the integrated samples, where the error proportionately indicates the current code delay. The error term should be proportional to the shift required in the NCO to drive the signal generator, so that it moves faster or slower accordingly to catch up with the incoming signal.

Recall that during carrier tracking, we multiplied the local carrier by the incoming signal. Then, the product was passed through a low-pass filter to get the error in terms of the phase difference. Using this error term the corrections were done. Compared with the carrier tracking loop, as shown in Fig. 5.10, only two things are required to be remembered: A complete oscillation for a sinusoidal carrier is a complete code excursion for a code. Second, the mixing and subsequent low-pass filtering operation of the carrier is equivalent to autocorrelation of the code. We similarly generate a local replica of the code and multiply it with the encoded signal in both I and Q components of the signal. Now, integrating the product in both components over a few integral multiples of the code length, we get the result

$$P_I = A_k \int c(t)\, c(t+\delta) \cos\left(2\pi\delta f t + \delta\varphi\right) dt \tag{5.33A}$$

$$P_Q = A_k \int c(t)\, c(t+\delta) \sin\left(2\pi\delta f t + \delta\varphi\right) dt \tag{5.33B}$$

where τ is the offset of the local code with respect to the code of the incoming signal. Here, we are not considering the variation of the data bits A_k for convenience because these operations are all carried out within a data bit interval, and we assume bit reversal does not occur here.

When these integrals are normalized by dividing this integral by the time length over which the integral has been taken, we get the expression as shown below

$$\frac{P_I}{T} = \frac{1}{T} A_k \int c(t)\, c(t+\delta) \cos\left(2\pi\delta f t + \delta\varphi\right) dt = A_K\, R_{xx}(\tau)\, \mathrm{sinc}(\pi\delta f t) \cos\left(\delta\varphi\right) \tag{5.34A}$$

Similarly,

$$\frac{P_Q}{T} = \frac{1}{T} A_k \int c(t)\, c(t+\delta) \sin\left(2\pi\delta f t + \delta\varphi\right) dt = A_K\, R_{xx}(\tau)\, \mathrm{sinc}(\pi\delta f t) \sin\left(\delta\varphi\right) \tag{5.34B}$$

In our previous chapter, describing basic signal characteristics, we found that the correlation of a pseudo-random sequence is highest when there is an exact superposition of the two waves. This value falls off with the relative shift of the two signals and grounds to the value of $-1/N$ at a complete one or more chip offset between the two. This variation is symmetric on both sides. Thus, the correlations between two such sequences are equal if the coder in one of them is equally early or late with respect to the code in the other. Both $+\tau$ and $-\tau$ result in the same autocorrelation values for normal BPSK signals, given by (Cooper & McGillem, 1986)

$$R_{xx}(\tau) = \left(1 - |\tau|/T\right) \tag{5.35}$$

This depreciation in the correlation value from its maximum value of 1 indicates the delay between the two signals. This is also the offset in the incoming code with respect to the local reference code. This offset of the locally generated code with respect to the incoming signal code may be identified and adjusted by using the symmetric nature of the correlation characteristics. The key is to use two additional separate local codes for the purpose, one early and the other equally late from the reference code. We call the reference code, seeking synchronicity, as the prompt code.

This forms the early–late (E–L) gate DLL (Cooper & McGillem, 1986; Dierendonck, 1996; Groves, 2013; Spilker, 1996; Van Dierendonck et al., 1992; Ward et al., 2006). It is widely used in code tracking because it has been an optimum tracking method for fine synchronization of digital signals. As mentioned, this E–L DLL consists of an early and late version of the locally generated code. These codes are equally shifted in phase with the prompt code on two opposite sides. These versions of the codes are used to find the correlation independently, but simultaneously with the incoming signal. By comparing the results of the two autocorrelation values, the required shift may be provided to all the versions of the local code, such that the correlation values with the early and late versions become equal, in both magnitude and sign. Recalling the symmetric nature of the autocorrelation function, it can be understood that, this will align the local prompt code with that of the incoming signal. Most modern receivers use this method for the purpose; its schematic is shown in the Fig. 5.12.

Now, let us see mathematically how we estimate the delay using some simple mathematics and our previous knowledge of the correlation. In an E–L gate DLL, two codes equally offset by a value δ from a prompt code are generated and used for correlation. One of them, which is phase advanced with respect to the prompt code, is called the *early* code. The other, whose phase trails the prompt code, is called the *late* version of the code. So, for a definite delay τ of the prompt code with respect to the input, the offset of the early code with respect to the input is $dE = \delta - \tau$, and that of the late code is $dL = \delta + \tau$. Because the exact delay cannot be identified from the individual correlation values, the delay is obtained using the difference in the correlation process. The corresponding arrangement in the correlator is shown in Fig. 5.12.

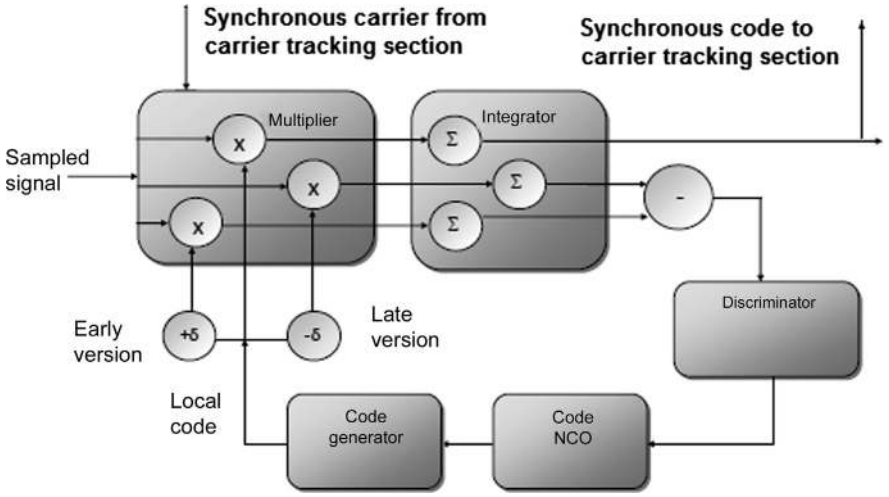

FIGURE 5.12

Schematic for a delay locked loop.

In a manner similar to Eq. (5.23D), the integrated values for the I and Q signals of the early and late versions over an integration time of T can be represented as (Dierendonck, 1996; Groves, 2013; Van Dierendonck et al., 1992)

$$I_E = R_{xx}(\delta - \tau)\,\mathrm{sinc}(\pi\delta fT)\cos(\delta\varphi) \tag{5.36A}$$

$$Q_E = R_{xx}(\delta - \tau)\,\mathrm{sinc}(\pi\delta fT)\sin(\delta\varphi) \tag{5.36B}$$

$$I_L = R_{xx}(\delta + \tau)\,\mathrm{sinc}(\pi\delta fT)\cos(\delta\varphi) \tag{5.37A}$$

$$Q_L = R_{xx}(\delta + \tau)\,\mathrm{sinc}(\pi\delta fT)\sin(\delta\varphi) \tag{5.37B}$$

This equation shows that the integrated sample values depend on the frequency mismatch δf and the phase mismatch $\delta\varphi$.

5.2.4.2.4 Coherent code tracking

For coherence tracking, the carrier is perfectly synchronized, and hence $\delta f = 0$ and also $\delta\varphi = 0$. Under such conditions, only the I components exist while the Q components vanish or carry only the noise. The prompt, early, and late versions of the correlator then give, respectively,

$$P = I_P = R_{xx}(\tau) \tag{5.38A}$$

$$E = I_E = R_{xx}(\delta - \tau) \tag{5.38B}$$

$$L = I_L = R_{xx}(\delta + \tau) \tag{5.38C}$$

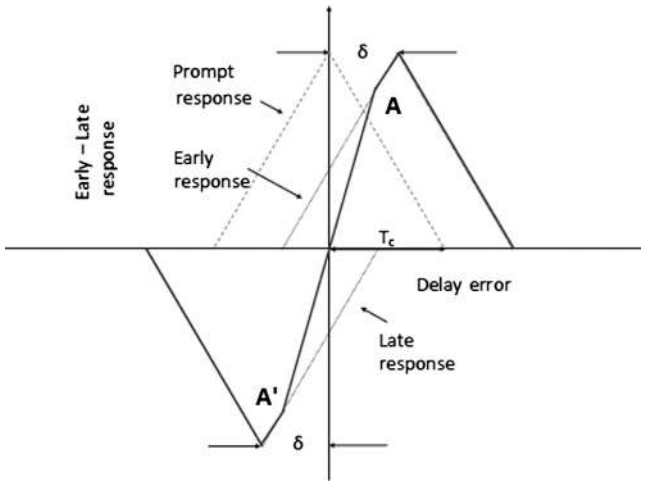

FIGURE 5.13

Discriminator characteristics.

For normal BPSK modulation, the expression we obtain for the correlation is given by Eq. (5.35). So, the expressions for these components we obtained in Eq. (5.38) become

$$R_{xx}(\delta - \tau) = 1 - \frac{(\delta - \tau)}{T} \tag{5.39A}$$

$$R_{xx}(\delta + \tau) = 1 - \frac{(\delta + \tau)}{T} \tag{5.39B}$$

Considering the case, when the delay of the prompt code with respect to the input is within the E–L offset, then in such a discriminator the differences of the early and late correlation becomes,

$$\begin{aligned} D_{E-L} &= \{1 - (\delta - \tau)/T\} - \{1 - (\delta + \tau)/T\} \\ &= \frac{1}{T}\{(\delta + \tau) - (\delta - \tau)\} \\ &= \frac{2}{T}\tau \end{aligned} \tag{5.40}$$

The discriminator function is shown in Fig. 5.13.

In the working region of the discriminator, the characteristics of the differenced autocorrelation are linear, antisymmetric about zero, with slope $2/T_c$. This represents the portion AA′ in Fig. 5.13 of the E–L discriminator characteristics.

If the code in the incoming signal is aligned with the prompt code, it is equally displaced in phase from these two codes and will produce equal correlation values with both versions, and the difference will be zero. If it is skewed toward one of them, the corresponding correlation will be higher than the other. The difference will be

positive if it is skewed toward the early version and negative if it is skewed toward the late version. From the magnitude of the difference, the amount of skewness can be determined, as it is done in Eq. (5.40). Using this equation, the relative delay of the prompt code with respect to the incoming signal can be estimated.

From this, it is clear that both the positive and negative offsets of the prompt code may be identified using the autocorrelation difference. For obvious reasons, the balanced condition occurs when $\tau = 0$, and then the prompt code may be said to be aligned with the incoming code. For any nonzero values, we can shift the prompt code and its early and late versions to attain the triviality. The E–L correlator output that is proportional to the offset τ acts as a correction factor and drives the code NCO. The latter, in turn, adjusts the shifts in the code phase to align the two codes, which serves our objective.

When the condition $|\tau| > |\delta|$ exists, a balance condition can never be achieved, and hence, the DLL is out of its operating range. This is evident from the characteristic curve. Therefore, either the E–L offset needs to be widened, or it calls for better acquisition.

It also follows from this, that the offset of the E–L increases the sensitivity of the system by increasing the offset response gradient to 2/T from the 1/T value of an independent autocorrelation function. But it reduces the linear operating range in the process.

Furthermore, because of its inverse dependence on T, when the bit lengths are small, that is, the code rates are high, this discriminator has a higher sensitivity, and hence its response has a sharp rise as the errors deviate from zero. For a flatter slope, the values of the correlation are not very different if the delay error is small. As a result, a receiver that may not resolve the difference for a slower code rate can distinguish it in the case of a faster code rate. Therefore, a faster code rate yields better performance in terms of finding the exact delay.

5.2.4.2.5 Noncoherent code tracking

The previous section assumes that a coherent condition of the signal exists, in which the carriers are exactly removed by matching the reference signal in phase and frequency. For coherent code tracking to take place, accurate carrier tracking is necessary. In fact, there is a considerable interdependence between carrier and code tracking, which makes each of them fragile. So, for many practical situations, noncoherent tracking take place. In a noncoherent DLL, the signal is treated for code tracking with residual Doppler offset, data modulation, and unknown carrier phase. In such a condition, the incoming signal of the early and late versions of the code after integration becomes as given in Eqs. (5.36A, B) and (5.37A, B).

There can be different noncoherent discriminator algorithms for code tracking. One of the most popular is the E–L power discriminator. Here, instead of directly differencing the two correlation values, we square the two and add I and Q to get the total power in these two orthogonal components. So,

$$\begin{aligned} P_E &= I_E{}^2 + Q_E{}^2 = R_{xx}{}^2(\delta - \tau)\mathrm{sinc}^2(\pi\delta f\tau) \\ P_L &= I_L{}^2 + Q_L{}^2 = R_{xx}{}^2(\delta + \tau)\mathrm{sinc}^2(\pi\delta f\tau) \end{aligned} \tag{5.41}$$

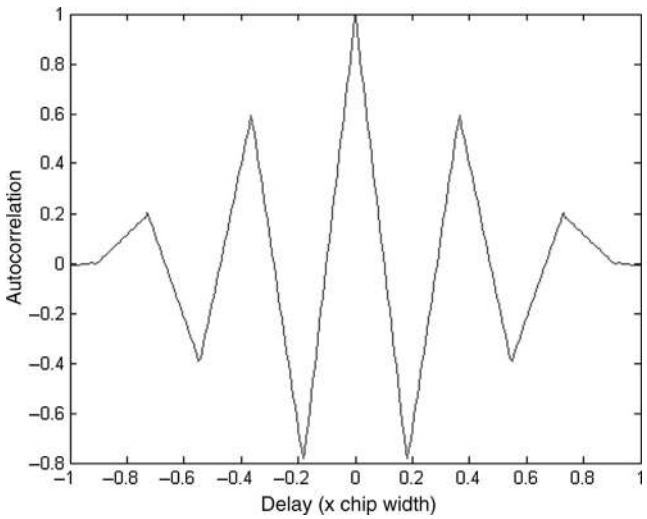

FIGURE 5.14

Autocorrelation of a BOC signal.

Now, once again, differentiating the early power from the late power signals, we get

$$P_E - P_L = \left[\{1-(\delta-\tau)/T\}^2 - \left[\{1-(\delta+\tau)/T\}^2\right]\right]\text{sinc}^2(\pi\delta fT) = \left[\frac{4}{T}(1-\delta/T)\tau\right]\text{sinc}^2(\pi\delta fT) \tag{5.42}$$

Thus, for any fixed phase offset, it can be tracked in the same manner as for coherent mode, since the discriminator output remains proportional to the code offset τ, assuming the frequency offset δf remains unaltered during the process.

5.2.4.3 Tracking binary offset carrier signals

The BOC (m,n) signals may be seen as normal BPSK signals with the encoded data additionally multiplied by a square wave with a rate m/n times faster than the code. So, tracking a BOC-coded data is also done in a fashion almost similar to that of the BPSK. One of the most popular techniques for code tracking is the Very Early-Very Late (VEVL) correlator, which we shall discuss now.

5.2.4.3.1 Very early–very late correlator

We have seen that the ideal autocorrelation characteristic of a BOC signal is a regular bipolar triangular variation of width $1/T_s$, while its amplitude is enveloped within the autocorrelation function profile of a normal spreading code of one sided width $1/T_c$, where T_s and T_c are the subcarrier and code chip widths. This is as shown in Fig. 5.14. The resultant profile has a main peak at the middle for exact superimposition of the signals with diminishing adjacent side peaks at regular delay intervals of T_s. The

peaks correspond to the shifted matching of the subcarriers, while their diminishing amplitude is due to the relative shift of the pseudo-random noise (PRN) codes.

Due to the presence of the close adjacent peaks, the E-L gate can lock to a different peak away from the center. To arrest this, the idea in the VEVL gate approach is that it employs additional correlators, that is, VEVL gates implemented away from the prompt gate in addition to the nominal Early and Late gates. Because of the symmetric nature of the envelope, adjacent peaks at an equal distance from the center on two opposite sides have the same relative peak height. Since the subcarrier period is known, the distances in terms of delays from the center where the adjacent peaks will occur can be predetermined. The VE and VL correlators are placed equally at these delay offsets on two sides of the prompt.

As the side peak heights fall off symmetrically on both sides of the main peak, the VE and VL correlators must get equal values of peak when the prompt is aligned with the incoming code, at the center of the envelope. However, if the prompt version has coincided with a peak based on the E-L gates, but still a comparison indicates a higher amplitude on either VE or VL, it means the prompt has latched to a side peak, and hence the codes need to be shifted for balancing. Because the peaks occur at intervals equal to the period of the subcarrier, T_s, the receiver must make the appropriate jump of either $+T_s$ or $-T_s$, in the direction of the correct peak until the autocorrelation values at VE and VL balance.

5.2.4.4 Tracking imperfections

5.2.4.4.1 Correlation loss

Correlation loss is defined as the difference between the signal power expected at the output of an ideal correlation receiver from the transmitted signal and the signal power actually recovered in such a receiver, over the same bandwidth. The correlation loss in a typical navigation receiver occurs due to the rejection or filtering of certain portions of the signal band, especially the higher frequency ones. Although we have seen earlier that most signal power remains confined within the first null of the signal, excluding the rest of the spectrum has some minor effects on the shape of the data bits. Due to finite filtering, some of the high-frequency components of the complete spectrum get cut off. This removes the sharper edges of the bits in the time domain and gives the rising and falling edges a small but finite curvature. When correlation is done on these bits, the peak that is generated is not sharp but is curved at the top. The reduction in value of the correlation with zero delay from the expected unitary value is the convolution loss (Fig. 5.15).

5.2.4.4.2 Jitter and phase noise

Jitter and phase noise are two different perceptions of the same physical effect. Jitter is described as fluctuations of the exact time variations of a binary bit. It is manifested as small, rapid and random drifts, particularly in its transition instants. The phase noise, on the other hand, is the appearance of spurious frequency components when seen in the frequency domain.

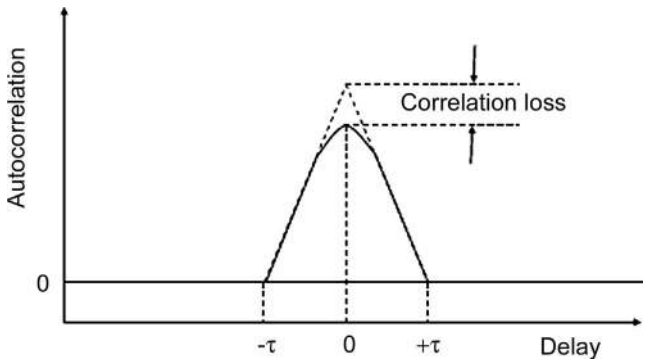

FIGURE 5.15

Correlation loss.

We will attempt to understand it, starting from basic yet simple instances that are relevant to navigation. If we have a pure sinusoidal signal and we count the phase and track it continuously with time, it should give us a linearly increasing value modulo 2π, that is, a saw tooth variation extending from 0 to 2π. However, in a pragmatic case, a signal shows in small and random variations in phase. This leads to a broadening of the spectrum of the signal from being a single line, with additional components appearing at nearby frequencies. This not only results in deviation in the phase of the contaminated time signal but also results in deviation in the time of occurrences of the wave events, say the zero-crossing time, and changes the spectrum of the signal at any instant of time.

The less the amplitude of these unwanted frequency components generated the less the phase variations of the signal. Thus, the potential deviation that may be caused by phase noise is represented by the relative amplitude of these unwanted components appearing at different frequencies over the working range. It is also sometimes represented by the relative power density of the spurious components with respect to that at the signal center frequency, with units dBc/Hz.

For a phase shift keying signal, the receivers are sensitive to these variations. This is obvious because the data is encoded in the phase and its variation. When demodulated with a synchronous carrier generated at the receiver, these unwanted abrupt variations either advance the estimated phase of the signal or lag it with respect to the actual present in the input signal. Consequently, they cause phase reversals in the modulated signal to occur at an instant slightly different from the position of true occurrence. Effectually, the receiver thus identifies a bit transition with some time deviation from where it would ideally be. This is the phase jitter in binary data (Fig. 5.16).

This problem is serious in the case of navigation because a deviation in the signal phase or bit transition time leads to errors in ranging. This is because range is determined from the true delay of a phase of the code or carrier, owing to the

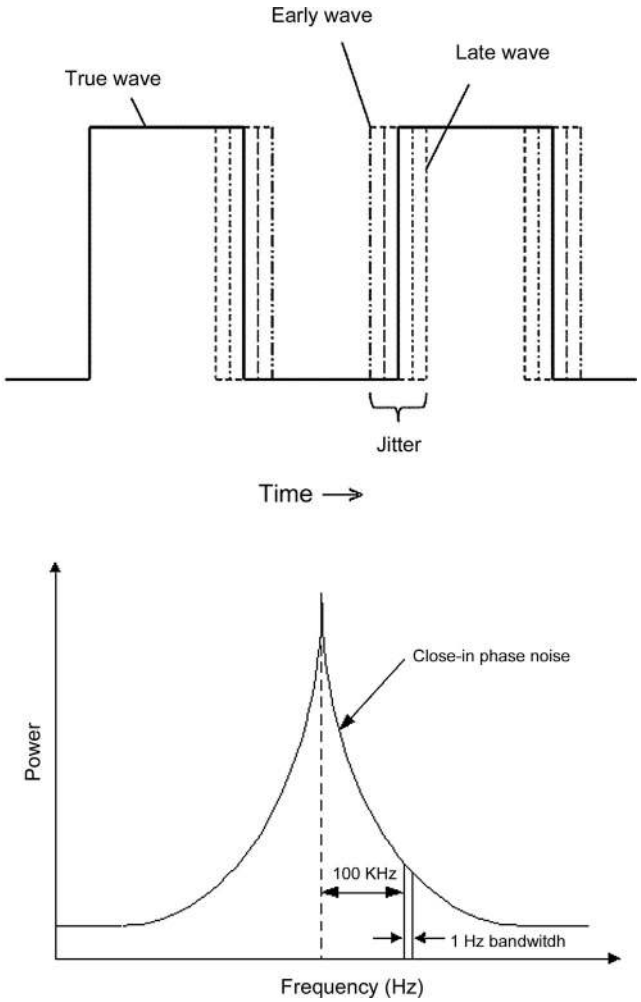

FIGURE 5.16

Phase noise and jitter.

propagation only. Because the received and demodulated code bits are deviated due to jitter, they diverge from representing the true propagation time. Consequently, the position estimation derived from the ranges suffers in terms of accuracy.

5.2.5 Pseudo ranging

We have learned that one of the prime objectives of the receiver is to carry out satellite ranging. The ranges may be obtained from the code phase as well as the carrier phase of the signals transmitted from the satellites. Here, we shall see how they are done.

Pseudo range is obtained from the satellites visible to a receiver. Pseudo range is the approximate range of the satellite from the receiver as measured by the latter. In these measurements, the associated measurement errors remain present, making it different from the true geometric range and hence termed as the "*Pseudorange.*"

To understand ranging, let us start with a simple question: How do we measure the traverse time of anything that is moving between two points A and B in space? The answer is simple: We check the time at which it starts at point A, that is, the start time, and also the time at which it reaches point B, that is, the end time. The traverse time is the difference between these two noted times. Now that we have the traverse time, we can find the distance it has moved if we know its velocity of movement. However, it is assumed that it moves with the same constant velocity throughout.

For ranging, we need to identify "*something*" that moves from the satellite to the receiver and with a constant velocity. We already learned that the only means by which the space segment communicates with the user receiver is through the signal. It is only this signal that moves from the satellite to the receiver. Because it is an electromagnetic wave, it moves with a constant velocity c. Therefore, that *something* must be a specific marker on this signal. A specific marker is required so that we can identify exactly when it started from the satellite and when the same marker reached the receiver.

We have read about the signal structure and understand that the three main elements of the signal are its data, code, and carrier. Of these, the data are random, whereas the code and the carrier are structured and well known. It is convenient to use some features of the latter two to find the traverse time. Of all the characteristics, the code and carrier phases are the only features linearly related to time. Therefore, the differences in their phases are proportional to the differences in their occurrence times. This means that if the frequencies remain the same, both the code and the carrier phase values increase linearly with time. So, the change in phase of the signal being issued over the propagation time can be used for the purpose. Here, we need to remember that the carrier phase repeats after a 2π value and the code phase after the code period.

Therefore, the pseudo range may be measured from the time of a definite phase of the carrier or code of the signal that it takes to travel from the satellite to the receiver. The distance, that is, the range, is derived by multiplying this traveling time by the velocity of travel. The expression for the measured range is

$$R = c(t_2 - t_1) \tag{5.43}$$

Here, t_1 is the time of transmission of a definite phase of the signal, t_2 is the time of reception of the same phase at the receiver, and R is the measured range. "c" is the velocity with which the particular signal phase or code travels through intermediate space. The velocity of light in a vacuum is used here. The assumption underlying this method of calculating range is that waves travel with a constant velocity of "c."

The two main drawbacks in the process are that the phases can be measured only in modulo the total phase of the repetitive code or carrier. Besides, there is no common

clock that can measure both the time of transmission at the satellite and the time of reception at the receiver. Subsequently, in the following two sections, we will see, despite these drawbacks, how the code and the carrier phases are utilized for ranging.

We learned at the beginning of this chapter that receivers can be distinguished on the basis of ranging types, and we mentioned two types of ranging: code-based and carrier-based. Here, we elaborate on them.

5.2.5.1 Code phase-based ranging

The pseudorandom code, which is a component of the signal, is also used for the purpose of range measurements. This is true whether it is a CDMA or an FDMA system. This pseudo-random code remains synchronous with the data as well as the carrier. We already learned this in our previous chapter. In the code-based ranging technique, the basic measurement made by a navigation receiver is the transit time of a particular code phase from a satellite to the receiver, which is then multiplied by c to get the range.

To define the code phase, recall the previous statement that, what is a complete oscillation for a sinusoidal wave is a complete code excursion for a code. Thus, the code phase at any instant of time is defined as the ratio of the number of chips (integral and fractional) of the total code executed by the code at the current time, to the total number of chips constituting the complete code. So, it is the fraction of the total code of the current code state that is currently in.

For proper ranging, all of the timing measurements need to be with respect to a common reference and using a common clock. To fulfill the need of a common clock, we assume that the satellite transmitting clock and the receiver clock are synchronous and generate the same time at any instant. Moreover, the reference must be a common marker for the measurement of both the transmission and receiving time. Now, recalling that the data and the codes are synchronous, we can take advantage of the time stamp present in the data to obtain the transmission time of a certain code phase received at the current instant, whereas the time of the reception of the same code phase can be obtained from the synchronous clock, which is keeping the system time. The difference between these two provides the transit time, which is used to derive the range.

5.2.5.1.1 Ranging algorithm

The basic assumption in this type of ranging is that the satellite and the receiver clock are synchronous. Although two different clocks are used for the purpose, it is assumed that they are completely aligned in time, such that using time from one clock is the same as using it from the other. We will discover in the next chapter how we can make the system unconstrained from this restraining assumption, but for now, we shall assume it to be existing.

If the clocks are assumed to be synchronous, both the satellite transmitter and the receiver will generate the same code phase at the same instant. Thus, the code phase received by the receiver at any instant will be phase lagging from the one currently being generated by the receiver. This is due to the finite time taken by the satellite

signal to reach the receiver. Utilizing this, the phase lag is measured in the following manner.

The messages of the navigation data are transmitted in a definite repetitive structure, say, in frames and subframes. These subframes are made up of integral numbers of data bits accommodating many more complete codes. The starting of a frame and subframes can be explicitly identified using the fixed pattern of the data bits transmitted at the beginning of each subframe. These patterns, therefore, can act as periodic reference points for time. The beginning of these markers is time stamped and the time marks of these points are transmitted in the data. So, the transmission time of the time reference point immediately preceding the current received code is obtained from the time stamp. Now, to know the exact time of transmission of the current code phase received, we need to know the total time elapsed from the last received reference pattern point up to the current received code chip and its fraction within the code.

Therefore, the first job in this regard is to find the time difference of the currently received code phase relative to this time reference point, whose time of transmission is obtained. The receiver counts the total number of complete codes 'n', that have been received from the time of receiving of the time reference point (beginning of the pattern) until the beginning of the current code. It provides the time from the reference till the beginning of the current code. The receiver also estimates the current code phase, i.e., the fractional part of the code that has elapsed. This is equivalent to knowing the total number of complete chips that have elapsed in the current code and the fractional part of the chip that the receiver is currently receiving. It is more convenient to obtain the current code phase by autocorrelating a local replica of the same code with the incoming one. The delay that results in maximum autocorrelation between the two indicates the fractional code elapsed.

Autocorrelation is carried out with a locally generated replica of the code with the code of the current received signal. The phase difference between the local and the received code phase may be estimated from the autocorrelation. This is done by utilizing the relative delay obtained between these two codes, as described in Section 5.2.4.2.4. The delay in the local code that maximises the autocorrelation is the relative delay between the codes. As the phase of the local prompt code is known at any instant, that of the incoming code can be obtained from the shift required to get the maximum correlation. It provides the fractional code difference part, f. So, if T_0 is the time of transmission of the marked time reference point, n is the total number of complete codes elapsed since then, f is the fractional part of it being received and T_c is the code period, then the transmission time t_1 of the currently received phase of the code may be expressed as (Fig. 5.17).

$$t_1 = T_0 + nT_c + f\,T_c \tag{5.44}$$

The receiver keeps a separate counter to keep the count "n" of the complete code elapsed. The estimation of the fractional part 'f' of the code is done through autocorrelation. We have already seen during code tracking how this phase could be

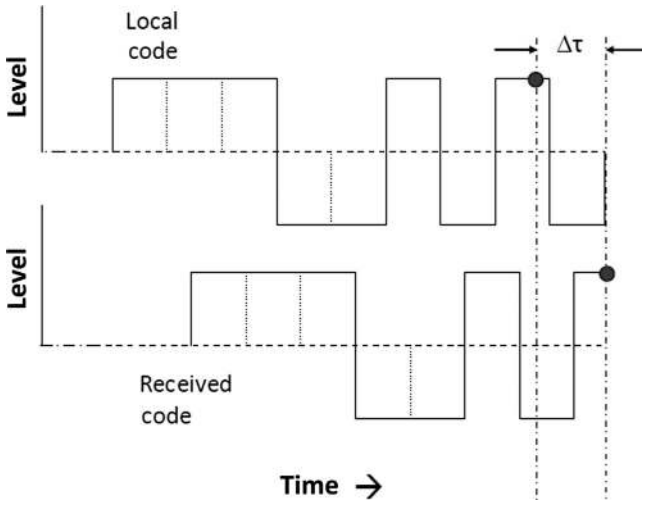

FIGURE 5.17

Estimation of transmission time.

obtained using an EL gate DLL. These estimations are carried out respectively after every small and predefined interval. The receiving time 't_2' is directly obtained from the receiver clock time.

Once both values of t_1 and t_2 are calculated, the time difference (t_2-t_1) is multiplied by the speed of light, c, to get the range. However, this estimation carries with it errors owing to propagation and other assumptions. These biased time delay measurements are referred to as pseudo-ranges.

As this algorithm utilizes the start of the frame as a time reference, its use is only possible once the signal is demodulated and the data bits are retrieved. Code-based ranging can only start after the navigation data frame has been identified to obtain the parameter values.

Furthermore, it is unlikely that the receiver clock will remain synchronous with the transmitting clock at the satellite from the outset. The measurements are contaminated with the clock synchronization error at the beginning. However, once the position is estimated, the clock shift is also determined. This estimation of the clock shift is used to steer the receiver clock to get it aligned with the system time. For subsequent times, the clock is continuously disciplined with this system time.

5.2.5.2 Carrier phase-based ranging

The technique of carrier phase-based ranging is also done on the assumption that the transmitting and receiving clocks are synchronous. Under this condition, the transmitter at the satellite and the receiver will be generating the same phase of the carrier at the same instant. Also, for the same reason described above, the carrier phase being received at any instant by the receiver will lag the carrier phase that

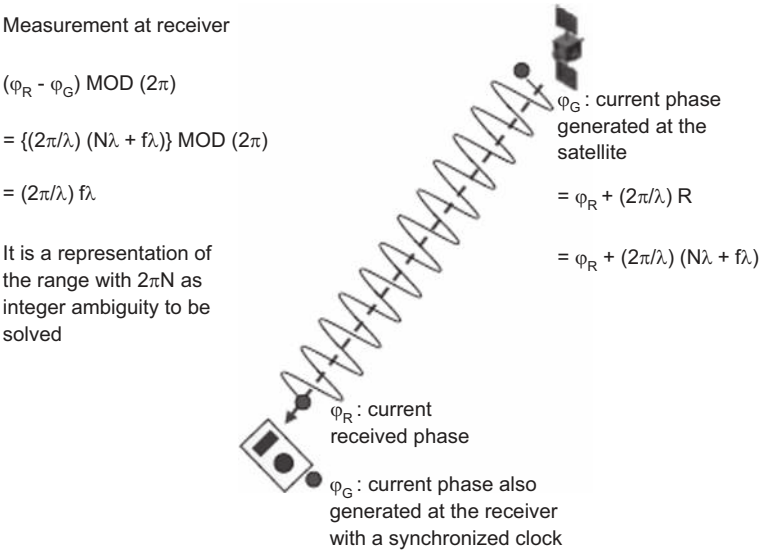

FIGURE 5.18

Carrier phase-based ranging.

the receiver is itself generating at that instant. This phase lag is proportional to the time of propagation of the signal because the carrier phase has a linear variation with time. Let a particular phase received currently at the receiver be representative of its transmission time, t_1. Similarly, the current phase of the carrier being generated at the receiver at the current instant is representative of the current time t_2. So, the phase difference between the two is the parameter from which the propagation time can be obtained. Multiplying, as usual, this propagation time by the velocity of light, we get the pseudo range (Fig. 5.18).

However, there is a difficulty in measuring the transmission time using such carrier phase measurements. As the received phase measurement can only be done modulo 2π, successive carrier phases cannot be distinguished. So, there is no reference with respect to which the absolute value of the above carrier phase difference may be determined. That means, the measured $\delta\varphi$ phase difference between the current locally generated and the received signal carried phase can only remain between 0 to 2p, whereas the true absolute difference in phase corresponding to the propagation time is, $2N\pi+\delta\varphi$, where N is an integer. So, if $\varphi 1$ and $\varphi 2$ are the true phases of the transmitted signal received and the local oscillator at the receiver, then,

$$\begin{aligned} j_2 &= j_1 + 2p/l\, R \\ &= j_1 + 2p/l\, (Nl + fl) \end{aligned} \tag{5.45}$$

where, R is the range between the satellite and the user. Here, R is expressed in terms of the wavelength l as $R = Nl + f_l l$, N being the integer paart and f_l is a fraction.

Rearranging the above equation, we get,

$$\Delta\varphi = \varphi_2 - \varphi_1 = N2\pi + 2pf_l = N2\pi + \delta\varphi \tag{5.46}$$

Here, $\delta\varphi$ is the fractional part of the phase difference, which is actually measurable. N also represents the number of complete 2π radians that the phase of the signal advances while traveling from the satellite to the receiver and is an unknown quantity.

Because the measurements are only possible in modulo 2π, we only get the differential fractional phase $\delta\varphi$ in the measurement. But, the integral part of the difference cannot be measured and is called the "integer ambiguity." This value needs to be solved for proper ranging. This is an involved task and adds complexity to the receiver. Searching for N is called ambiguity resolution, which is necessary to get the absolute values of the phase difference. There are different techniques for resolving ambiguity (Cosentino et al., 2006).

Once the integral value is obtained through the ambiguity resolution process, we get the absolute phase difference $\Delta\varphi = 2N\pi + \delta\varphi$. The corresponding time of traverse is obtained as, $\Delta T = \Delta j / 2pf$, where f is the frequency of the signal. Multiplying ΔT by the velocity of light, c, we get the corresponding carrier phase-based range, R_{car}. The corresponding equation turns into

$$R_{car}(t) = c\Delta T = \frac{c}{2\pi f}\{N2\pi + \delta\varphi\} = \frac{\lambda}{2\pi}\{N2\pi + \delta\varphi\} \tag{5.47}$$

Note that the integer ambiguity is a one-time unknown generated at the beginning of the carrier phase measurement process. As time progresses, the equation still holds the same value of N, but with the updated values of $\delta\varphi$. This is because, the currently received $\delta\varphi$ value changes with time. So, at any later time $t + dt$, the range is

$$R_{car}(t + dt) = \frac{\lambda}{2\pi}\{N2\pi + \delta\varphi(t + dt)\} \tag{5.48}$$

The incremental range from the instant of the start of the measurement can be obtained by differencing the two time-separated equations. With this operation, we get

$$\Delta R_{car} = R_{car}(t + dt) - R_{car}(t) = \frac{\lambda}{2\pi}\{\delta\varphi(t + dt) - \delta\varphi(t)\} \tag{5.49A}$$

Or

$$\Delta R_{car} = \frac{\lambda}{2\pi}\ \Delta\delta\varphi \tag{5.49B}$$

The LHS is the differential range with respect to the beginning of the measurement process, and the right-hand side (RHS) of the equation is same range expressed in terms of the accumulated differential phase from the same instant. The temporal change in range results in the Doppler and is related as $df_d = 2\pi/\lambda\ (dR/dt)$.

So, combining the above equations and representing the Doppler frequency as f_d, we get

$$\frac{\lambda}{2\pi}\Delta\delta\varphi = \Delta R_{car} = \int \frac{dR_{car}}{dt}dt = \frac{\lambda}{2\pi}\int f_d\, dt \tag{5.50}$$

So, $\Delta\delta\varphi = \int f_d\, dt$. Thus, the accumulated phase difference in the LHS can be regarded as the integrated Doppler, that is, again derived from the integrated delta range.

In code-based ranging, the maximum error in phase identification that may occur corresponds to one code chip. The maximum range error that may happen in such a process of matching is given by

$$\delta R_{cod} = cxchipwidth = c/codechiprate = c/R_c \tag{5.51}$$

Assume that if the ranging is done by comparing the carrier phases of the received signal with that generated locally, provided the integer ambiguity is exactly identified, the corresponding range error will correspond to one carrier cycle and is equal to

$$\delta R_c = cxcarrierperiod = c/carrierfrequency = c/f_c \tag{5.52}$$

So, the ratio of the maximum error E is

$$E = \frac{\delta R_{cod}}{\delta R_{car}} = f_c/\ R_c \tag{5.53}$$

Because the carrier frequency is many times greater than the chip rate of the code, the inaccuracy is reduced manifold by the use of the carrier phase. Thus, the carrier phase measurement is much more precise than that of the code phase measurement. The use of a carrier phase, although it improves receiver performance, is computationally more intensive for realization. This includes resolving issues such as cycle slips and other phase errors, in addition to resolving the integer ambiguity.

While continuously measuring the carrier phase of the received signal, the measured phase sometimes shows an abrupt change or a discontinuity in the values. This is called a cycle slip. This causes unwarranted errors in the integrated Doppler term $\Delta\delta\varphi$, appearing in 5.49B or 5.50. This may occur for reasons such as excessively low received signal strength, receiver anomaly, interference, or ionospheric disturbances. The receiver processing algorithm must be robust enough that it can identify any cycle slip occurring during the carrier phase measurement and mend any damaging effects resulting from it. A simple way to handle it is to restart the process of phase-based ranging afresh again, resetting all accumulated values once the cycle slip occurs.

5.2.6 Navigation processor

A navigation processor is one of the important subsystems of the user receiver. It is marked as Section (3) in Fig. 5.4. The navigation signal carries the navigation data with it, the format of which is known a priori to the receiver. The navigation processor receives from its previous modules the decoded data. This data is obtained

in separate channels from all visible satellites simultaneously with the respective estimated range of each. The navigation processor, then processes them to calculate satellite position. Finally, using this information, the navigation processor calculates the user's position. Although the ranging is done in the processor of the receiver, it is categorically separated from the navigation processor because they have distinct differences in functionality.

To achieve this end, the demodulated data stream from all different channels is required to be received by the processor. It checks and stores the data and utilizes the necessary algorithm for position fixing.

The data are used by the algorithm to obtain the navigation solutions for the final position fix. Associated tasks, such as controlling the display and other user interfaces and interfacing with external devices, are executed by this processor. In some receivers, a separate logical module is added to these nominal processing tasks, which observes the activities and perform the management of receiver functionalities. We will now describe the sequence of procedures done on the derived data until the position is estimated and displayed.

5.2.6.1 Handling navigation data

The first job of the navigation processor is to retrieve and store the navigation data. At this stage, the processor is provided with only an uninterrupted stream of data. It needs to identify the frames or the specific message structures and then select the values of the definite parameters from their respective positions in these messages, as per the defined format. For this, it is important that the receiver identifies when the message frame has actually started in the stream of bits. All subsequent data bits can then be relatively located with respect to this initial reference. However, decoding the channel codes is necessary at this point.

Frame identification and synchronization are achieved by using a specific preamble. The preamble consists of a specific pattern of bits at the beginning of the frame transmitted with the signal. When this pattern is located in the bit stream at the receiver, it is identified as the beginning of a frame. The definite pattern is chosen such that there is little chance that the same pattern appears in the data in between. Otherwise, false detection may occur. The probability of false detection decreases with an increase in the preamble code length and increases with the length of the frame. However, the true preamble is repeated after every frame width, but a similar repetitive pattern appearing probabilistically within the message body is highly unlikely.

Like false locking, there can be missed detection. This condition arises when preamble bits are incorrectly received owing to an error in communication. The receiver cannot identify the preamble and goes on searching until it finds the next.

To avoid false detection and counter missed detection, the repeating nature of the preambles is verified during locking, considering that they must reappear after a regular interval of bits. An appropriate algorithm must be defined to ensure that the identification of the proper preamble has been achieved. For example, the frame may

be said to be locked when four successive correct preambles are detected at an interval of the frame length.

Data is now checked for corrections, and identification of the frames has been done. Each of the constituent parameters of the navigation data needs to be extracted, scaled if necessary and stored along with the time of data and its period of validity. This is because the same navigation data will remain valid up to only a finite interval. Whether this validity has expired or the data is still useable needs to be checked with every use. The data are typically updated well within this period, and hence the validity naturally gets extended further. The process of decryption needed to be done on the classified data sent being encrypted, is performed before they are used here. The stored data is then further processed to get the user's position.

5.2.6.2 Ephemeris extraction and reference positioning

The navigation signal contains ephemeris data, which is required for finding the positions of the respective satellites. These ephemerides are identified from the data, separated out, and stored. During use, the necessary and eligible data is selected from the dataset already stored. Because the same ephemeris remains valid over a range of time, this stored data is updated only when a new set of ephemeris data appears in the transmitted signal. In deriving the values of the ephemeris and for any other parameters as well, from this set of navigation data, appropriate scale factors may need to be applied. When the ephemeris is known, current satellite positions are calculated from it using relations as described in Chapter 3.

5.2.6.3 Selection of satellites

We shall learn in Chapter 6 that at least four satellites are required to find the user's position and time in an ordinary receiver, and that the accuracy of position estimation depends on the relative geometry of the user and these four satellites. It is represented by a term called geometric dilution of precision (GDOP). The next job of the navigation processor is to select the best four satellites based on the GDOP. However, an approximate position of the user receiver and the satellites needs to be known a priori to obtain the GDOP. If the approximate user position is not known to the receiver, an alternative approach may be to use any four satellites at first and get the first position estimate, sacrificing the position accuracy. Now, using this approximate position, one may obtain the DOP values and select the most suitable four satellites to further obtain the precise position.

The DOP values must be updated at frequent intervals, if not at every estimate, because, owing to the dynamics of the user and the satellite, this value goes on changing with time.

5.2.6.4 Range corrections

Although the range estimation is done in the processor, it may be considered an activity separate from those activities done by the navigation processor with the objective of position fixing. From the perspective of the navigation processor, the range is obtained from an external ranging processor.

The atmosphere around the Earth affects the traveling speed of RF signals and causes propagation delay errors. The error values may either be derived from the correction parameters sent in the data or may be obtained directly from dual frequency range measurements. The range may be corrected using the derived errors for correction. Similar corrections may be made for the range errors occurring for reasons other than those for propagation, like the clock error, ephemeris error, etc.

5.2.6.5 Calculate user position and time

Using the corrected pseudo range measurements and the calculated satellite positions, the user position coordinates and the time offset of the receiver clock from that of the satellite can be calculated by solving the following range equation:

$$R_i = \sqrt{(x_{si} - x)^2 + (y_{si} - y)^2 + (z_{si} - z)^2} + b \tag{5.54}$$

where (x, y, z) are the user position coordinates; the satellite coordinates (x_{si}, y_{si}, z_{si}) are known from ephemeris data, where i is the satellite number, that is, 1, 2, 3, 4. The pseudo range R_i for four satellites estimated in the receiver by measuring signal propagation delay. We will learn about the necessary algorithms for position estimation in the next chapter. To improve the computed position accuracy, a Kalman filter may be used. Kalman filters are briefly described in Chapter 9.

5.2.6.6 Convert position

The user position calculated from simultaneous equations is in a Cartesian coordinate system. It is usually desirable to convert positions to geodetic coordinates and represent the position in terms of latitude, longitude, and altitude. Assuming the shape parameters of the Earth, which can be obtained from the datum, these conversions may be easily done.

5.2.6.7 User interface

The position and time thus obtained need to be presented to the user through a suitable interface. A convenient display interface is popularly used for this purpose. Typically, other information such as the signal strength, satellite positions, and expected precision is displayed along with the position. Graphical displays such as sky plots showing the satellite positions and geographical grids for user positions are also common.

The user interface is also needed for purposes other than the display of positions, such as configuring the receiver, exchanging data with other devices through suitable interfaces for applications, and storage. The user interface also needs to support encryption key input for certain types of receivers.

Finally, the whole receiver is packed in a form suitable for the user. Receivers developed for any particular application need to have some appropriate casing suitable for that specific application. Fig. 5.19 shows a type of complete navigation receiver in its final shape.

FIGURE 5.19

Complete navigation receiver. *Courtesy: CFRSI.*

5.3 Multifrequency–multiconstellation receivers

The earlier forms of receivers were capable of receiving signals from only one system. Therefore, their design was targeted at a single constellation of satellites. However, in recent times, the scenario has changed drastically. Multiconstellation–multifrequency satellite navigation receivers are now being used across the globe. It provides reliable positioning with accuracy to the centimeter level. A wide spectrum of professional receivers is available today with different numbers of satellite constellations and signals that it can access. The more the numbers, the better the performance in terms of availability, accuracy, and resilience, even in challenging environments.

Navigation receivers in phones, cars, and other consumer devices usually use signals on just one frequency. Dual-frequency receivers can receive two signals from each satellite system. Multifrequency receivers, on the other hand, receive a multitude of signals from any satellite navigation systems. Such multifrequency receivers achieve the most accurate, reliable, and robust positioning possible.

On top of robust performance and easy removal of ionospheric errors, usually done by utilizing dual frequency, there are other advantages of a receiver having access to more frequencies and more constellations.

- *Better error corrections:* Dual-frequency capable devices can estimate and compensate for ionospheric delays leading to better ranging and accurate positioning.
- *Resilience through RAIMS:* Having access to many satellites creates redundancy, which enables a comparative analysis of the satellites and their signals. Having such comparative information allows the receiver to detect and remove accidental faults of ranging signals for improved positioning accuracy.
- *Jamming/Interference robustness:* Interference happens when other signals on the same frequency overpower the legitimate satellite navigation signals. Using signals on multiple frequencies provides the diversity advantage and allows the receiver to switch to another frequency if interference on one frequency is detected.

- *Spoofing detection:* Receivers that make use of multiple frequencies can use these frequencies for additional spoofing checks. By comparing range (distance to satellite) information from various signals, anomalies can be detected and flagged.
- *Compatibility with RTK networks:* RTK or real-time PPP techniques practically require dual-frequency receivers. Nevertheless, the use of triple-frequency receivers will further improve the ambiguity resolution algorithm results.
- *Better multipath rejection:* Multipath is the distortion of direct line-of-sight signals occurring when they are contaminated by identical signals reflected from objects such as buildings, cars, or trees. New signals with new modulations and higher chip rates provide additional resilience against multipath issues.

The emergence of satellite navigation receivers supporting multiconstellations has kept pace with the increasing number of systems and satellites in the sky over the past decades.

Conceptual questions

1. Do you expect the accuracy of the ranging to change if the E–L correlator difference is changed?
2. How can the navigation process handle a situation when it is reading from a stored navigation file, and a new set of data arrives?
3. How does it help to have the code-based ranging simultaneously when carrier phase-based ranging is done?
4. What are the advantages of using E–L power rather than E–L during code tracking?
5. Which of the mentioned PLL discriminators would you prefer to use when there is a finite probability of large deviations?

References

Cooper, G. R., & McGillem, C. D. (1986). *Modern communications and spread spectrum*. McGraw-Hill.

Cosentino, R. J., Diggle, D. W., de Haag, M. U., Hegarty, C. J., Milbert, D., & Nagle, J. (2006). 'Differential GPS', In Kaplan, E. D., & Hegarty, C. J. (Eds.), Understanding GPS Principles and Applications, 2nd Ed., Artech House, Boston, MA, USA.

Groves, P. D. (2013). *Principles of GNSS, inertial and multisensor integrated navigation system*. Artech House.

Lathi, B. P. (1984). *Communication systems*. Wiley Eastern Limited.

Maral, G., & Bosquet, M. (2006). *Satellite communications systems*. John Wiley & Sons Ltd.

Mutagi, R. N. (2013). *Digital communication: Theory, techniques and applications*. Oxford University Press.

Navstar GPS Space segment/navigation user interfaces. IS-GPS-200G. Global positioning system directorate. (2012). Available at: https://www.gps.gov/sites/default/files/2025-07/IS-GPS-200N.pdf. Retrieved on 21.04.2024.

Proakis, J. G., Salehi, M. (2007). Digital Communications, 5th Edition, Mc. Graw Hills, USA.

Scott, L., Jovancevic, A., & Ganguly, S. (2001). Rapid signal acquisition techniques for civilian and military user equipments using DSP based FFT processing. In *2001 Proceedings of 14th international technical meeting of the satellite division of the institute of navigation* Salt Lake City, UT, pp. 2418–2427.

Spilker, Jr., J. J. (1996). 'Fundamentals of Signal Tracking Theory', In Parkinson, B. W. & Spilker, J. J. Jr. (Eds.), *Global Positioning Systems, Theory and Applications*, Vol-I, AIAA, Washington DC, USA.

Van Dierendonck, A. J. (1996) 'GPS Receivers', in Parkinson, B. W., & Spilker, J. J. Jr. (Eds.), *Global Positioning Systems, Theory and Applications*, Vol-I, AIAA, Washington DC, USA.

Van Dierendonck, A. J., Fenton, P., & Ford, T. (1992). Theory and performance of narrow correlator spacing in a GPS receiver. *Navigation, 39*(3), 265–283. https://doi.org/10.1002/j.2161-4296.1992.tb02276.x.

Ward, P. W., Betz, J. W., Hegarty, C. J. (2006). 'Satellite Signal Acquisition, Tracking and Data Demodulation'. In Kaplan, E. D., & Hegarty, C. J. (Eds.), *Understanding GPS Principles and Applications, 2nd Ed.*, Artech House, Boston, MA, USA.

CHAPTER

Navigation solutions 6

Preamble

In this chapter, we shall learn to perform the most important activity in the whole satellite navigation process, "estimating the position." This is important because the whole purpose of the navigation is to achieve this objective. Here, we shall first understand the approach to obtain the solution intuitively. Then, we shall identify the inputs required to form the mathematical equations for finding the position, are obtained. Finally, we shall obtain the solution to the equations mathematically, using the linearization technique, and will discuss a few intricacies of the process. As a continuation, we will also learn other methods to obtain the same solution.

6.1 Fundamental concepts

In a real-life scenario, all distances are required to be measured in a three-dimensional (3D) space. In Chapter 1, we mentioned that to represent the position of a point with respect to a reference, we need to fix the position of the reference origin and get the distance of the point from it along three orthogonal directions. Now, let us see in detail the geometrical aspects of setting distances along three orthogonal directions. We know that a point in a 3D space is the result of the intersection of three nonparallel planes. So, our task to define the point reduces to defining these three planes. Once the reference system is set, the origin defined, and the directions of the three orthogonal axes fixed, the origin takes the coordinate (0, 0, 0). To define the position of point P (x_1, y_1, z_1), we first fix a distance x_1 along axis x. This defines a plane $x = x_1$ that is parallel to the yz plane at this point, at a distance x_1 from the origin along the x axis. This constrains the possible locations of the point anywhere on the two-dimensional (2D) plane. Now, the job is to define the other two planes orthogonal to the one already defined. At this stage, we define another plane, $y = y_1$, which is parallel to the xz plane with the normal distance, y_1, from the origin. The condition of lying simultaneously on both the planes further restricts the locus of our point on a straight line parallel to the z axis formed by the intersection of these two planes already defined. Then, as the final plane $z = z_1$, perpendicular to the z axis, is defined, it intersects the mentioned line of locus at $z = z_1$. We now have the intersection of the three planes at the position (x_1, y_1, z_1). Thus, these three mutually perpendicular planes completely fix our point at point P (x_1, y_1, z_1). This is shown in Fig. 6.1.

Understanding Satellite Navigation, Second Edition. DOI: https://doi.org/10.1016/B978-0-443-36432-7.00012-2

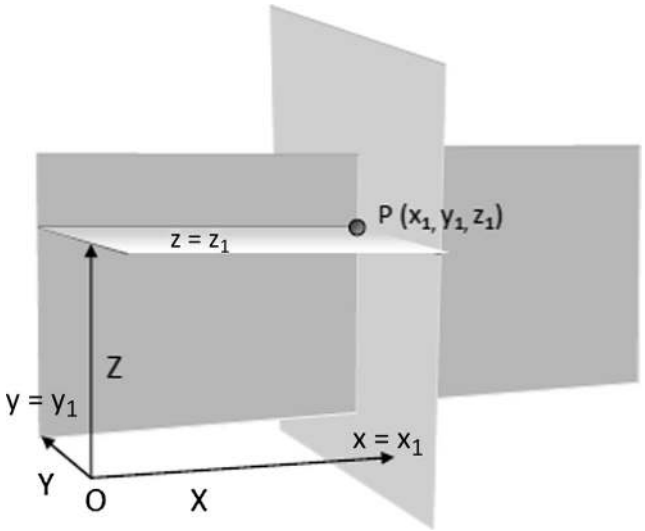

FIGURE 6.1

Defining a position in three dimensions.

Because the task is only to define the planes, it can be done with respect to any arbitrary new reference point in the frame whose coordinates are known. The point P can be fixed even then using its relative distances with respect to that new reference point. However, even then, coordinates of the point P may be obtained with respect to the original reference point, since we know the position of this new secondary reference in the original frame. The planes being defined with respect to the new reference, may be represented in terms of the original frame by vectorially adding the distance of the new origin to it. Remember, we said the vectorial distance and not simple range, because it requires both a sense of direction and magnitude to define the point.

But, what if we know only the radial range from this new reference point to our point of interest instead of the vectorial distance? In a 3D space, any distance vector should have three independent components. In a spherical system, the three coordinates are the radial range and two angular deviations from some fixed plane. So, when we mention only the range, it means we lose two sets of information out of three. Even in such cases, the exact position of the point of interest may still be derived by adding some more independent information, which effectually compensates for the loss. This may be done by adding independent range measurements from other new reference points whose positions are known. The basic idea is to form intersecting surfaces to reduce the common intersection to a point.

This is the basic concept of positioning used in satellite navigation. Here, the new planes are relative to different reference points, which are the point of locations of three satellites whose absolute positions are known in the chosen reference frame. The

ranges from these satellites to the point in question form the independent information from which three independent spherical surfaces may be obtained. Using these, the position of the point P may be derived by locating the point of intersection of these three spherical surfaces in terms of absolute reference. However, because the surfaces thus created are nonlinear, an adequate number of such surfaces are required to explicitly indicate the position.

In a 3D space, two planes intersect to form a straight line that is a linear function of the coordinates. Whereas two spherical surfaces intersect to form a circle, which is a quadratic function. So, unlike the former case, in which an additional plane surface sufficiently and uniquely defines a point, here an additional spherical surface intersects with the circle at two different points and hence is not enough to explicitly fix a point.

How much information, therefore, is sufficient for this? This may be elucidated by considering an example. First, let us understand a scenario where we attempt to represent the position of a point, P, located on the xy plane, that is, in a 2D space.

In 2D space, there are two unknowns for the location of a point, P. In Cartesian coordinates, these are "x" and "y" with respect to the absolute reference point O at the origin of the axes. The point may also be represented in terms of its range from the origin and its direction given by the angle it makes with any one of the axes. The range may be obtained from the individual Cartesian coordinates as $r = \sqrt{x^2 + y^2}$and the angle, $\theta = \tan^{-1}(y/x)$. If we know only the radial range of the point from this reference, we can only represent the distance as

$$r^2 = x^2 + y^2 \tag{6.1A}$$

This is the equation about the origin with radius r. In squaring the values, we actually lose the information about its sign and cannot find θ from it. Thus, we have a deficit of information, its exact direction.

Furthermore, let there be more such information available that states that the radial range of the same point from a new reference point at (x_1, y_1) is r_1. So,

$$(x - x_1)^2 + (y - y_1)^2 = r_1^2 \tag{6.1B}$$

The above equation represents another circle centered at (x_1, y_1) with radius r_1. Replacing Eq. (6.1A) in Eq. (6.1B), we get

$$x_1^2 + y_1^2 - 2xx_1 - 2yy_1 = r_1^2 - r^2 \tag{6.2}$$

This is a linear equation of the form $ax + by = c$, where $a = 2x_1$, $b = 2y_1$, and $c = r^2 - \{r_1{}^2 - (x_1{}^2 + y_1{}^2)\}$. Thus, two quadratic equations formed out of two observations in a 2D space represent two circles that intersect at two different points that lie on a straight line represented by a linear function of x and y. The values of the coordinates are yet to be determined. The solution can be obtained with an additional equation. Stated mathematically, this establishes the fact that the quadratic nature of the range equations result in two possible roots of the unknowns ; and we need an additional equation to get the exact solution.

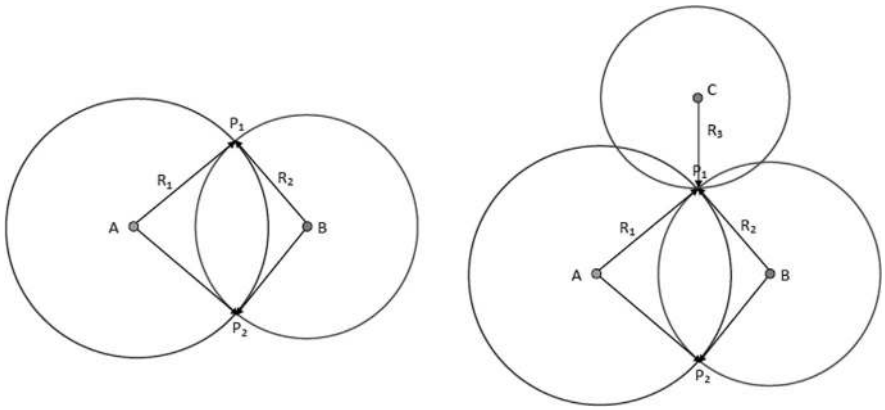

FIGURE 6.2

Two-dimensional case of position fixing.

The same fact is also evident from the corresponding geometry of the equations as shown in Fig. 6.2. In 2D space, using only the range information R_1 and R_2 from two relative reference points, A and B, respectively, leads to solutions with ambiguity with probable positions at P_1 and P_2, where the conditions set by both equations are satisfied. In addition, if point P is known to be positioned at a distance R_3 from another relative reference point C, it must lie on the circumference of the circle around C with radius R_3. This intersects only the point P_1 among the two probable. Only then can we unambiguously find the position of P.

We can generalize this observation for higher-order spaces with more numbers of unknowns. For "k" numbers of unknowns, k nonlinear equations of order two leave us with two equiprobable solutions. Thus, we need one more equation to solve for the unknowns explicitly. Therefore, a total of $[k + 1]$ equations are required. So, in real-life conditions, where the observation equations are quadratic in a 3D space, it requires $3 + 1 = 4$ equations to solve for positions explicitly using them. But this is not the reason why it says that four satellites are needed to get position solution in satellite navigation.

Focus 6.1 Requirement of equations for solution

Here, we explain with simple examples the requirement for the number of equations in the case of spherical nonlinearity. We treat the problem for both cases of solving with a constraint equation and for an additional observation equation of spherical nature.

Suppose we have a second-order equation such as:

$$x^2 + y^2 = 9 \tag{i}$$

To solve for variables x, y, and z, we need more equations like this. Let another equation be

$$x^2 + y^2 - 10x + 9 = 0 \tag{ii}$$

Combining Eqs. (i) and (ii), we get the value of x as

$$\begin{aligned} x &= 18/10 \\ &= 1.8 \end{aligned} \tag{iii}$$

Thus, the point at which these two equations simultaneously satisfy has the value of x as 18/10. However, taking this expression for x derived in Eq. (iii) and putting it in any of the equations of Eqs. (i) or (ii) leaves us with a quadratic in y. Putting it in Eq. (i), we get,

$$\begin{gathered} (18/10)^2 + y^2 = 9 \\ \text{or,} 100y^2 = 576 \\ \text{or,} y = \pm 2.4 \end{gathered}$$

Thus, from these two Eqs. (i) and (ii), we cannot obtain an explicit solution of (x,y) even in a 2D case. Now, we need to add a new equation.

First, let us suppose that we add a constraint equation of the form

$$3x + 4y = 15 \tag{iv}$$

This is a constraint equation that states that the solutions should also simultaneously lie on the line defined by it. Putting the value of $x = 1.8$ into this equation, we get the exact value of y as:

$$\begin{aligned} y &= (15 - 3 \times 1.8)/4 \\ &= 2.4 \end{aligned}$$

Thus, we get the exact solution for x and y.

Second, assume that we have a separate equation of the form

$$5x^2 + 5y^2 - 18x - 44y + 93 = 0 \tag{v}$$

Notice that all of the nonlinear equations that we have used are spherical.

Again, using the derived value of $x = 1.8$ here, we get

$$\begin{gathered} 16.2 + 5y^2 - 32.4 - 44y + 93 = 0 \\ \text{or,} 5y^2 - 44y + 76.8 = 0 \end{gathered} \tag{vi}$$

So, the possible solutions of y are:

$$\begin{gathered} y = 6.4 \\ \text{and } y = 2.4 \end{gathered}$$

Therefore, the actual solution of (x, y) is (1.8, 2.4), which we get from three independent equations.

Let us consolidate what we have learned in this discussion:

- First, the position of any unknown point P may be represented in a reference frame by knowing the position of an arbitrary reference point S in the frame and the vectorial distance from to S the point of interest, P.

- If, instead of the vectorial distance, only the radial distance (range) is known from S, then it lacks adequate information to explicitly define the position of the point, P. This may be compensated by adding enough numbers of a similar range information from other such reference points of known location, S.

6.2 Generation of observation equation

In satellite navigation systems, the preferred absolute reference system is the geocentric earth-centered earth-fixed (ECEF). However, it may be transformed into any other frame according to the requirements. The representation of the position of any arbitrary point in this frame may be done using secondary references. In GNSS, these secondary references are the navigation satellites in the sky. For this, we need the absolute positions of the satellites and the vectorial distances of the point from the satellites. However, because it is not feasible to obtain vectorial distances, positioning of the point can still be done, as we have just seen, if we know the ranges from more numbers of satellites placed at known locations. This is known as trilateration- the estimation of the position of a point unambiguously based on the measurements of its radial distances from three or more known reference locations.

Therefore, to estimate the position of a point using a satellite navigation system, it is necessary to have two things ready: the position of the satellites and the distance of the point in question from these satellites. Range observation equations are generated from this information, and the position is estimated in 3D space by solving these equations. Therefore, two aspects are important at this point:

1 To obtain the required range information
2 To solve the equations

We have discussed the first aspect in the previous chapter, where we have discussed how ranging is done in a navigation receiver. Therefore, we shall concentrate only on the second here.

Ranges of satellites are measured at the receiver. If these ranges measured from three satellites, S1, S2, and S3, are R_1, R_2, and R_3, respectively, we get three quadratic equations, formed using three reference positions and the corresponding ranges. These equations are

$$R_1 = \sqrt{(x_{S1} - x)^2 + (y_{S1} - y)^2 + (z_{S1} - z)^2} \tag{6.3A}$$

$$R_2 = \sqrt{(x_{S2} - x)^2 + (y_{S2} - y)^2 + (z_{S2} - z)^2} \tag{6.3B}$$

$$R_3 = \sqrt{(x_{S3} - x)^2 + (y_{S3} - y)^2 + (z_{S3} - z)^2} \tag{6.3C}$$

where x_{si}, y_{si}, and z_{si} are the position coordinates of the ith satellite ($i = 1, 2, 3$), and x, y, and z are the coordinates of the unknown user position. This constitutes

the set of three observation equations, which are nonlinear and quadratic. We have previously seen its geometrical interpretation, where the three equations form three intersecting spheres with two common points in 3 dimensional space, which can be equally probable solutions. Therefore, either an additional measurement from a fourth satellite is required, or there must be some separate, independent relationship existing between the user's coordinates. The latter is called the constraint equation. This additional information, augmenting the three observation equations, suffices to obtain the particular solution for the position.

Thus, the nonlinearity of range equations demands four navigational satellites to solve the unknown position coordinates. However, this issue of solving the nonlinearity problem can be resolved in a different manner. Nevertheless, we shall see that even without nonlinearity, we still require four satellites to solve the position; the reason for this is different and will be clear in the next section. First, let us see how this nonlinearity problem is resolved.

6.3 Linearization

From our discussion in the last section, the problem of position fixing is reduced to solving the problem of simultaneous quadratic equations. At the same time, we know that the three simultaneous quadratic equations in Eq. (6.3) cannot be solved to get the unknowns, x, y, and z, unambiguously. The quadratic equations give two possible solutions for their unknown variables. We therefore need more information to solve the unknowns.

There are three different methods to attack this problem. One is to take an additional independent observation equation and solve four simultaneous quadratic equations. The second option is to use a constraint equation instead, to resolve the ambiguities that arise on solving three quadratics. A constraint equation is a definite relation that the unknown variables always maintain between them. The final possibility, as chosen in most cases of navigational receivers, is that these quadratic equations are linearized to form three linear differential equations. We will now see how it is done.

Linearization, defined in this context, is the technique of converting quadratic observation equations into linear differential equations about suitable fixed point. This point may be an initial guess of the solution (Kaplan et al. 2006). These linear equations are then solved by standard methods to get the differential values of the true position coordinates with respect to those of the initial guess. Once these differential values are estimated, they can be added to the initial guess to obtain the absolute position solution.

To elaborate on this, we first start from Taylor's theorem, which says that if the value of a multivariate function f(X) is known at a point X_0, its value at a nearby point X is

$$f(X) = f(X_0) + f'(X_0)dX + \frac{1}{2}f''(X_0)dX^2 + . \tag{6.4}$$

where f′ and f″ are the first- and second-order derivatives of function f, respectively, with respect to X and obtained at the known position X_0. dX is the difference between X and X_0.

In our case, the function is the range, R, of the satellite from the user position, P, which is a function of both, the position of the user, P = (x, y, z), and that of the satellite, $P_s = (x_s, y_s, z_s)$. Thus, we can write function $R = R(x_s, y_s, z_s\ x, y, z)$ as

$$R = \sqrt{(x_s - x)^2 + (y_s - y)^2 + (z_s - z)^2} \tag{6.5}$$

For any instant (supposing we have frozen the time at that instant), the known satellite positions are fixed. Effectively, the range remains a function of unknown user position variables (x, y, z). At this instant, let us consider an approximate (practically close enough) user position, $P_0 = (x_0, y_0, z_0)$. Now, expressing the range at true position P by expanding the range function about the assumed position P_0 according to Taylor's theorem, and considering only up to the first-order derivatives, it follows from Eq. (6.4),

$$\begin{aligned} R(x, y, z) &= R(x_0, y_0, z_0) + \partial R/\partial x|_{P0}\Delta x \quad + \partial R/\partial y|_{P0}\Delta y + \partial R/\partial z|_{P0}\Delta z \\ \text{or, } R(x, y, z) - R(x_0, y_0, z_0) &= \partial R/\partial x|_{P0}\Delta x + \partial R/\partial y|_{P0}\Delta y + \partial R/\partial z|_{P0}\Delta z \end{aligned} \tag{6.6}$$

The higher-order derivatives can be neglected owing to our assumption of the close proximity of our approximated position to the true values. Here, the finite differences along the coordinates between the two points are represented as

$$\begin{aligned} \Delta x &= x - x_0 \\ \Delta y &= y - y_0 \\ \Delta z &= z - z_0 \end{aligned} \tag{6.7}$$

The geometrically calculated range from the P_0 to the known satellite location (x_s, y_s, z_s) is R_0, that is, $R_0 = R(x_0, y_0, z_0)$. So,

$$R_0 = \sqrt{(x_s - x_0)^2 + (y_s - y_0)^2 + (z_s - z_0)^2} \tag{6.8}$$

Eq. (6.6) can be rewritten as

$$\begin{aligned} R - R_0 &= (\partial R/\partial x\Delta x + \partial R/\partial y\Delta y + \partial R/\partial z\Delta z)|_{P_0} \\ \text{or,} \Delta R &= (\partial R/\partial x\Delta x + \partial R/\partial y\Delta y + \partial R/\partial z\Delta z)|_{P_0} \end{aligned} \tag{6.9}$$

where $\Delta R = R - R_0$, is the finite differential range between the true and the approximated position. This is illustrated in Fig. 6.3.

Partially differentiating the expression of the range equation (Eq. 6.5) with respect to x, y, and z at the approximated position of $P_0(x_0, y_0, z_0)$, and putting the values into Eq. (6.9), we get

$$\begin{aligned} \Delta R &= -(x_s - x_0)/R_0\Delta x - (y_s - y_0)/R_0\Delta y - (z_s - z_0)/R_0\Delta z \\ &= (-G_\alpha)\Delta x + (-G_\beta)\Delta y + (-G_\gamma)\Delta z \end{aligned} \tag{6.10}$$

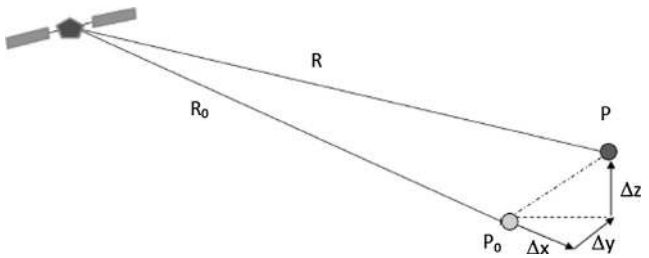

FIGURE 6.3

Elements of the linearization process.

$-G_\alpha$, $-G_\beta$ and $-G_\gamma$ are the partial derivatives of the range at the approximated point with respect to x, y, and z, respectively. Because the position coordinates of this approximate point (x_0, y_0, z_0) are known, the values of $-G_\alpha$, $-G_\beta$ and $-G_\gamma$ can easily be determined.

The nonlinear range equations with unknown coordinates have now turned into a linear differential equation about the nominal position, assumed a priori, with relative errors in position as unknowns. Thus, three linearized observation equations can be obtained and solved to derive these position errors for each coordinate. Because the approximate position is known, the true position can be determined from it by adding the estimated relative errors to it.

However, we still need four independent observation equations from four satellites, even after linearization, to find the position and time. To understand that, let us recall how the user receiver measures the ranges of each reference satellite. It measures the range from the time delay with which a definite phase of the signal, transmitted from the satellite, is received at the receiver. The fundamental question here is, how does the receiver know when any signal is being transmitted by the satellite? Here comes the utility of the ranging codes. We learned in Chapter 4 that in a satellite navigation system, the ranging codes and carrier phase of the signal are transmitted synchronously with the navigation data frame. The time of transmission of the beginning of each data frame being known from the time stamp present in the signal, the transmission instant of each code bit can be exactly derived from it using the code chip rate. The received time is derived from the clock present in the receiver itself. Thus, the propagation time is measured from the difference between the time at which a message was transmitted and the time when the message was received at the receiver. This time interval is multiplied by the velocity of light, c, to obtain the range.

The transmission and the received times are obtained from two different clocks: the former from the satellite clock and the latter from the receiver. But the issue here is that the receiver clock does not have as much accuracy and precision as the satellite clock. The satellite clock is an atomic clock of very high stability, about $\sim 10^{-13}$, and thus keeps time very accurately. The receiver clock, on the other hand, is cheap

and its stability is low, of the order of about $\sim 10^{-6}$ to 10^{-9}. Thus, the clock at the receiver is not synchronous with the satellite atomic clock and drifts with respect to the latter, leading to a relative clock offset. There remains an intrinsic time delay (or advancement) between the satellite and the receiver time. This affects the ranging process and hence the measured range. The error in ranging is equal to the product of the offset between the two clocks and the velocity of light.

Let a definite phase of the signal be transmitted at true time T_t, which is also the satellite clock time. Also, let this phase be received at true time T_r after a traverse time of $\Delta t = T_r - T_t$. At the instant of receiving, if the receiver clock is shifted by an amount, $+\delta t_u$, with respect to the satellite time, the time that the receiver registers on receiving the phase is $T_r + \delta t_u$. Thus, to the receiver, the apparent time of propagation is

$$\begin{aligned} \Delta t_u &= (T_r + \delta t_u) - T_t \\ &= (T_r - T_t) + \delta t_u \\ &= \Delta t + \delta t_u \end{aligned} \tag{6.11A}$$

The range thus obtained at the receiver is

$$\begin{aligned} R &= c\Delta t_u \\ &= c\Delta t + c\delta t_u \\ &= \rho + c\delta t_u \end{aligned} \tag{6.11B}$$

An error of $c\delta t_u$ occurs in the range of the process owing to its clock shift. It must be appreciated that an error of 1μs leads to an error of 300 m. This resultant offset in range remains added to the measured range and causes error in positioning, if not corrected. Thus, the unknown receiver clock offset also needs to be determined from the measured range.

This receiver clock offset is taken as an unknown variable and solved for, while solving for the position. So, even for the linear equations, one more unknown is added in addition to the three unknown differential coordinate variables. Thus, to get the solution for these four unknown variables, four linearized observation equations are required. This results in the requirement of four satellites and their corresponding range measurements for position and time estimation.

6.4 Solving for position

With the introduction of a new unknown (i.e., the receiver clock shift to the satellite clock), the basic observation equation changes as given in Eq. (6.11B) and below as:

$$R_i = \rho_i + c\delta t_u$$

where R_i is the pseudorange measurement to the ith satellite, ρ_i is the corresponding true geomentric range, and δt_u is the receiver clock offset with respect to the satellite

time. Because all satellite clocks are synchronous, this shift is the same for all observations to different satellites. The effective additional length that gets erroneously added to the range as a result of this clock bias is $c\delta t_{u,}$ where c is the velocity of light in vacuum.

Four observation equations for four satellites can be written as follows by expanding the geometric range as a function of coordinates and adding it to the effective path due to the clock bias.

$$\begin{aligned} R_1 &= \sqrt{(x_{S1}-x)^2+(y_{S1}-y)^2+(z_{S1}-z)^2}+c\delta t_u \\ R_2 &= \sqrt{(x_{S2}-x)^2+(y_{S2}-y)^2+(z_{S2}-z)^2}+c\delta t_u \\ R_3 &= \sqrt{(x_{S3}-x)^2+(y_{S3}-y)^2+(z_{S3}-z)^2}+c\delta t_u \\ R_4 &= \sqrt{(x_{S4}-x)^2+(y_{S4}-y)^2+(z_{S4}-z)^2}+c\delta t_u \end{aligned} \tag{6.12}$$

These simultaneous observation equations are linearized about the approximate solution of $X_a = (x_0, y_0, z_{0,} c\delta t_{u0})$, and the resultant linearized equations become

$$\begin{aligned} \Delta R_1 &= -G_{\alpha 1}\cdot\Delta x - G_{\beta 1}\cdot\Delta y - G_{\gamma 1}\cdot\Delta z + \Delta b \\ \Delta R_2 &= -G_{\alpha 2}\cdot\Delta x - G_{\beta 2}\cdot\Delta y - G_{\gamma 2}\cdot\Delta z + \Delta b \\ \Delta R_3 &= -G_{\alpha 3}\cdot\Delta x - G_{\beta 3}\cdot\Delta y - G_{\gamma 3}\cdot\Delta z + \Delta b \\ \Delta R_4 &= -G_{\alpha 4}\cdot\Delta x - G_{\beta 4}\cdot\Delta y - G_{\gamma 4}\cdot\Delta z + \Delta b \end{aligned} \tag{6.13A}$$

where all terms are under the terms defined in Eqs. (6.6–6.10) and have the ordered index for the four different satellites. Δb is the new term added and represents the finite difference of the effective range error owing to the receiver clock bias from the same error assumed in the initial guess of it (i.e., $\Delta b = c[\delta t_u - \delta t_{u0}]$). The set of equations in Eq. (6.13A) may be written in matrix form as

$$\Delta R = G_a * \Delta X_a \tag{6.13B}$$

where

$$G_a = \begin{pmatrix} -G_{\alpha 1} & -G_{\beta 1} & -G_{\gamma 1} & 1 \\ -G_{\alpha 2} & -G_{\beta 2} & -G_{\gamma 2} & 1 \\ -G_{\alpha 3} & -G_{\beta 3} & -G_{\gamma 3} & 1 \\ -G_{\alpha 4} & -G_{\beta 4} & -G_{\gamma 4} & 1 \end{pmatrix}$$

$$\Delta R = \begin{bmatrix} \Delta R_1 & \Delta R_2 & \Delta R_3 & \Delta R_4 \end{bmatrix}^T \text{and}$$

$$\Delta X_a = \begin{bmatrix} \Delta x & \Delta y & \Delta z & \Delta b \end{bmatrix}^T.$$

Now, ΔX_a may be obtained by standard techniques such as iteration, simple least-squares solution, weighted least-squares solutions, and so forth (Axelrad & Brown, 1996; Strang, 2003). The least-squares solution becomes

$$\Delta X_a = \left(G_a^T G_a\right)^{-1} G_a^T \Delta R \tag{6.14}$$

When this derived ΔX_a is added to the initially assumed approximate position, X_a, about which the equations have been linearized, the true position solution is obtained as $X = X_a + \Delta X_a$.

Recall that we assumed at the beginning that the approximated point X_a is near the true position such that the linearity condition in the error holds good and higher-order differentials of Taylor's theorem may be omitted. However, it is not always possible to approximate such a position because the receiver may have no idea about the location. In such cases (which are more likely), the estimation may start with any arbitrary approximate position where the above conditions of close proximity is not fulfilled, and hence higher order terms in Taylor's series exist. As a result of neglecting these higher-order terms in the estimation process, the solution arrived at will carry some error. Nevertheless, it will bring us closer to the real position. So, this solved position of the first estimation may now be taken as the initial guess, and another iteration of solving for the position may be carried out with the same set of data to reach a further nearer position. This way, after a few iterations for a single definite point, the solution will converge to the true position when no more significant change in the solution is obtained upon further iteration. These situations may thus be handled through the iteration process, in which the previous steps are required to be repeated until a converged solution is obtained. Box 6.1

Box 6.1 MATLAB for Position Fixing

The MATLAB code position_main.m was run to obtain the position solution from known values of satellite positions and corresponding ranges. The input to the program is the navigation and observation information preloaded in text files. From the navigation data present in the former file, the positions of the visible satellites at any instant are obtained, whereas the corresponding range information was obtained from the latter. On running the program, the following information is provided in sequence:

The position and range of satellites.

x = 22657881.0793	in m
y = 13092933.5636	in m
z = 5887881.983	in m
R = 22889484.2157	in m

The program then assumes an approximate position and displays it as:

Approximate position assumed:

x_apx = 302536.5663 in m
y_apx = 5772741.575 in m
z_apx = 2695567.787 in m
b_apx = 10 in m

From these data, the best set of four satellites is selected by obtaining the minimum dilution of precision (DOP), which the program flashes as output as:

The minimum DOP obtained is 0.094484.

The program starts the iterative calculation of the position following the user input for the number of iterations required.

The program then displays the results it derives sequentially, as in the following.

Iteration # n
Approximate ranges to the selected four satellites are:

$$1.0e+007^{*}\begin{bmatrix} 2.2673 & 2.3734 & 2.1757 & 2.0181 \end{bmatrix} \text{in meters}$$

Differences in ranges are: dR

$$1.0e+004\begin{bmatrix} -3.9911 & -4.5629 & -4.5205 & -4.5642 \end{bmatrix} \text{in meters}$$

The linearized observation equation is: dR = G * dX.

$$-39910.5553 = 0.4043 * dx + -0.74338 * dy + 0.53285 * dz + 1 * db$$
$$-45{,}629.4328 = -0.5439 * dx + -0.04069 * dy + -0.83816 * dz + 1 * db$$
$$-45{,}204.8555 = 0.0474 * dx + -0.58482 * dy + -0.80978 * dz + 1 * db$$
$$-45{,}641.5591 = -0.2551 * dx + -0.95848 * dy + -0.12731 * dz + 1 * db$$

Solution for dX is: GT * inv(GT*G):

$$10^{4*}\begin{bmatrix} 0.4120; & 0.3869; & 0.3305; & -4.0461 \end{bmatrix} \text{in meters}$$

Solution after n iterations is:

$$10^{6*}\begin{bmatrix} 1.1965 & 6.2759 & 1.5954 & 0.1143 \end{bmatrix} \text{in meters}$$

Finally, after the requisite number of iterations is over, it displays the final solution as:
The final solution of the coordinates of the user is:

explains the estimation process, where the solution is obtained after a few iterations.

Focus 6.2 Solving for position

We assume the following constant values for the radius of Earth, Re, and the radial distance of satellites, Rs, from the Earth's center expressed in km is as below:

$Re = 6.3781 \times 10^3$
$Rs = 2.6056 \times 10^4$

Let the true position of the user be:

Latitude = 22° N
Longitude = 88° E

The coordinates in the ECEF frame are:

$x_t = 206.3853$ in km
$y_t = 5.9101 \times 10^3$ in km
$z_t = 2.3893 \times 10^3$ in km

Let the clock offset of the user receiver be such that $c*\Delta t = b = 15$ in km. These are unknown values initially. Only the satellite positions and measured ranges are known. The solution of the position estimation, obtained from measured ranges and the approximate position, must converge to these values.

Let the Cartesian coordinates of satellites S1, S2, S3, and S4 in the ECEF frame in km, as obtained from the satellite ephemeris transmitted by the satellites in their message, be:

Sat: S1	**Sat: S2**	**Sat: S3**	**Sat: S4**
$x_{S1} = 2.1339 \times 10^3$	$x_{S2} = 0.0$	$x_{S3} = 4.1006 \times 10^3$	$x_{S4} = 2.0581 \times 10^3$
$y_{S1} = 2.4391 \times 10^4$	$y_{S2} = 2.4484 \times 10^4$	$y_{S3} = 2.3256 \times 10^4$	$y_{S4} = 2.3525 \times 10^4$
$z_{S1} = 8.9115 \times 10^3$	$z_{S2} = 8.9115 \times 10^3$	$z_{S3} = 1.1012 \times 10^4$	$Z_{S4} = 1.1012 \times 10^4$

The measured range for satellite S1 to S4, expressed in km, are:

$R_{t1} = 1.9708 \times 10^4$
$R_{t2} = 1.9702 \times 10^4$
$R_{t3} = 1.9773 \times 10^4$
$R_{t4} = 1.9714 \times 10^4$

Initially, the true position of the user is not known. Thus, let us take an initial approximate position in Cartesian coordinates in the ECEF frame as:

$\mathbf{x_{a0} = 458.9177}$ **km**
$y_{a0} = 5.8311 \times 10^3$ km
$z_{a0} = 2.5433 \times 10^3$ km
$b_{a0} = 10$ in km

And the ranges calculated in km from the initial approximate position to four satellites are:

$R_{a01} = 1.9703 \times 10^4$
$R_{a02} = 1.9726 \times 10^4$
$R_{a03} = 1.9723 \times 10^4$
$R_{a04} = 1.9691 \times 10^4$
$dR_{a0} = [4.2000; -23.5262; 50.2975; 23.1277]$

The directional cosines with respect to the approximate position of satellite S1 are:

$\mathbf{G\alpha_1 = 0.0851}$	$\mathbf{G\alpha_2 = -0.0233}$	$\mathbf{G\alpha_3 = 0.1847}$	$\mathbf{G\alpha_4 = 0.0813}$
$G\beta_1 = 0.9424$	$G\beta_2 = 0.9461$	$G\beta_3 = 0.8839$	$G\beta_4 = 0.8990$
$G\gamma_1 = 0.3234$	$G\gamma_2 = 0.3230$	$G\gamma_3 = 0.4296$	$G\gamma_4 = 0.4303$

The observation equations after linearization turn into:

$04.2 = -\ 0.0851\ dx - 0.9424\ dy - 0.3234\ dz + db$
$-23.5262 = +\ 0.0233\ dx - 0.9461\ dy - 0.3230\ dz + db$
$50.2975 = -\ 0.1847\ dx - 0.8839\ dy - 0.4296\ dz + db$
$23.1277 = -\ 0.0813\ dx - 0.8990\ dy - 0.4303\ dz + db$

This can be expressed in the form: $dR = G_a * dX_a$

$$\begin{pmatrix} 04.20 \\ -23.5262 \\ 50.2975 \\ 23.1277 \end{pmatrix} = \begin{pmatrix} 0.085055 & 0.94244 & 0.32337 & 1 \\ -0.023277 & 0.94611 & 0.32301 & 1 \\ 0.184740 & 0.88393 & 0.42959 & 1 \\ 0.081258 & 0.89903 & 0.43029 & 1 \end{pmatrix} \begin{pmatrix} dx \\ dy \\ dz \\ b \end{pmatrix}$$

The dX_a can be simply solved as: $dX_a = G_a^{-1} * dR$

$$dX_a = \begin{pmatrix} -252.9364 \\ 73.1880 \\ -156.2947 \\ 1.1212 \end{pmatrix}$$

Hence, the new positions after the first iteration become $X_{a1} = X_{a0} + dX_a$:

$x_{a1} = 458.9177 - 252.9364 = 205.9813$ km

$y_{a1} = 5.8311 \times 10^3 + 073.1880 = 5.9043 \times 10^3$ km

$z_{a1} = 2.5433 \times 10^3 - 156.2947 = 2.3870 \times 10^3$ km

$b_{a1} = 10 + 001.1212 = 11.1212$ km

After the first iteration, we come closer to the actual solution of the position than the first approximation.

Now, with the new values of x, y, z, and b, we repeat the steps. From the position obtained after the first iteration, the ranges calculated from the initial approximate position to the four satellites and expressed in km are:

$R_{a11} = 1.9710 \times 10^4$

$R_{a12} = 1.9704 \times 10^4$

$R_{a13} = 1.9775 \times 10^4$

$R_{a14} = 1.9716 \times 10^4$

$dR_{10} = [-2.3798, -2.3653, -2.3110, -2.3670]$

Note that the absolute values of differential ranges have reduced compared with the first iteration. The directional cosines with respect to the approximate position of satellite S1 are:

$G\alpha_1 = 0.0979$	$G\alpha_2 = -0.0105$	$G\alpha_3 = 0.1971$	$G\alpha_4 = 0.0940$
$G\beta_1 = 0.9385$	$G\beta_2 = 0.9435$	$G\beta_3 = 0.8779$	$G\beta_4 = 0.8942$
$G\gamma_1 = 0.3312$	$G\gamma_2 = 0.3313$	$G\gamma_3 = 0.4364$	$G\gamma_4 = 0.4377$

The observation equations turn into the form: $dR = G_a * dX_a$

$$\begin{pmatrix} -2.3798 \\ -2.3653 \\ -2.3110 \\ -2.3670 \end{pmatrix} = \begin{pmatrix} -0.0979 & -0.9385 & -0.3312 & 1 \\ 0.0105 & -0.9435 & -0.3313 & 1 \\ -0.1971 & 0.8779 & -0.4364 & 1 \\ -0.0940 & -0.8942 & -0.4377 & 1 \end{pmatrix} \begin{pmatrix} dx \\ dy \\ dz \\ b \end{pmatrix}$$

The dX_a can be simply solved as: $dX_a = G_a^{-1} * dR$

$$dX_a = \begin{pmatrix} 0.4042 \\ 5.8132 \\ 2.3114 \\ 3.8808 \end{pmatrix}$$

Thus, the updated positions after the second iteration become $X_{a2} = X_{a1} + dX_a$:

$x_{a2} = 205.9813 + 000.4042 = 206.3855$ km
$y_{a2} = 5.9043 \times 10^3 + 005.8132 = 5.9101 \times 10^3$ km
$z_{a2} = 2.3870 \times 10^3 + 002.3114 = 2.3893 \times 10^3$ km
$b_{a2} = 11.1212 + 3.8808 = 15.0020$ km

After the second iteration, the solution converges to the true position.

6.5 Other methods for position fixing

6.5.1 Solving range equations without linearization

Here, we discuss how to fix the positions of the user by using the same range measurements, but with different methods to get the solution. A number of methods have been put forward by researchers in this field that employ analytical method to find the solution. However, we will describe only two methods that use the original quadratic observation equation, but will handle it with two different approaches. The first will be done by using an additional linear equation called a constraint equation; the other will logically select the true position from two alternatives.

6.5.1.1 Using a constraint equation

As stated before, it is possible to solve for four unknowns from quadratic equations without linearization. For this, we need a constraint equation defining the fixed relationship that the coordinates follow, in addition to the four quadratic equations. This makes a total of five equations, and is in accordance with our previous observation for the requirement of the equations: four unknowns and one more constraint equation to remove the quadratic ambiguity.

One such constraint may be the assumption that the radial range of the unknown point is equal to the radius of the Earth, Re, that is, the point is on the Earth's surface, and b is an unknown constant, $b = b_c$. So, the difference between the square of the radius of the user position and the square of the error resulting from clock shift is also a constant (Grewal et al., 2002). This constraint may be mathematically represented as

$$\left(x^2 + y^2 + z^2\right) - b^2 = {R_e}^2 - {b_c}^2 = k^2 \tag{6.15}$$

We have chosen this constraint to make our computations simple when we describe the process. However, other constraints relating to the position coordinates and bias will do, as well, provided the constraint equation is independent.

The first observation equation was

$$R_1 = \sqrt{\left(x_{S1} - x\right)^2 + \left(y_{S1} - y\right)^2 + \left(z_{S1} - z\right)^2} + c\delta t_u \tag{6.16}$$

Expanding the square terms and denoting $c\delta t_u$ as b, we get the equation

$$R_1 = \sqrt{x_{S1}^2 + x^2 + y_{S1}^2 + y^2 + z_{S1}^2 + z^2 - 2x_{S1}x - 2y_{S1}y - 2z_{S1}z} + b \tag{6.17A}$$

With a few manipulations, it follows from the above equation

$$R_1^2 = x_{S1}^2 + x^2 + y_{S1}^2 + y^2 + z_{S1}^2 + z^2 - 2x_{S1}x - 2y_{S1}y - 2z_{S1}z + 2R_1b - b^2 \tag{6.17B}$$

Replacing the constraint Eq. (6.15) in Eq. (6.17B), we get

$$R_1^2 - k^2 - R_s^2 = -2xx_{S1} - 2yy_{S1} - 2zz_{S1} + 2R_1b \tag{6.18A}$$

$$\text{or,} \quad A_1x + B_1y + C_1z + D_1b = k_1 \tag{6.18B}$$

where $A_1 = 2x_{S1}$, $B_1 = 2y_{S1}$, $C_1 = 2z_{S1}$, $D_1 = -2R_1$, and $K_1 = {R_s}^2 + k^2 - {R_1}^2$. We can construct four such linear equations with each observation equation and the constraint, and solve for the four unknowns. The simultaneous equations thus formed are

$$\begin{aligned} A_1x + B_1y + C_1z + D_1b &= k_1 \\ A_2x + B_2y + C_2z + D_2b &= k_2 \\ A_3x + B_3y + C_3z + D_3b &= k_3 \\ A_4x + B_4y + C_4z + D_4b &= k_4 \end{aligned} \tag{6.19A}$$

This can be written in matrix form as

$$GX = K \tag{6.19B}$$

$$\text{where } G = \begin{pmatrix} A_1 & B_1 & C_1 & D_1 \\ A_2 & B_2 & C_2 & D_2 \\ A_3 & B_3 & C_3 & D_3 \\ A_4 & B_4 & C_4 & D_4 \end{pmatrix}$$

$$X = \begin{bmatrix} x & y & z & b \end{bmatrix}^T$$

$$\text{and } k = \begin{bmatrix} k_1 & k_2 & k_3 & k_4 \end{bmatrix}^T$$

Using the standard least-squares method, the solution for X becomes

$$X = \left(G^TG\right)^{-1}G^TK \tag{6.20}$$

6.5.1.2 Bancroft's method

In our general discussion about finding the solution, we said that it becomes convenient to find a solution if the original quadratic observation equation is turned into a linear one. The equation was then linearized to serve the purpose. In the last subsection, we put an additional constraint on the positional coordinates to get the solution. In Bancroft's method, the equation is kept quadratic, and some algebraic manipulations are carried out using the given relation to reduce the equations to a least-squares problem. Then, from the two possible solutions of this quadratic

equation, the required solution is logically chosen. This method of solution is algebraic and noniterative, computationally efficient, and numerically stable, and admits extended batch processing (Bancroft, 1985). It is a classic example of efficiently handling quadratic conditions and was further analyzed by Abel and Chaffee (1991), Chaffee and Abel (1994).

The observation equation is first written in terms of satellite position, user positions, and receiver bias as

$$R = \sqrt{(x_s - x)^2 + (y_s - y)^2 + (z_s - z)^2} + b \tag{6.21A}$$

Expanding the terms in the observation equation as functions of the unknown terms of the user and the satellite, we get

$$x_s^2 - 2x_s x + x^2 + y_s^2 - 2y_s y + y^2 + z_s^2 - 2z_s z + z^2 = R^2 - 2Rb + b^2 \tag{6.21B}$$

Rearranging the terms, we get

$$(x^2 + y^2 + z^2 - b^2) - 2(x_s x + y_s y + z_s z - Rb) + (x_s^2 + y_s^2 + z_s^2 - R^2) = 0 \tag{6.21C}$$

However, the intelligent part comes at this point. Instead of solving directly for X, notice that the quadratic unknown terms, that is $(x^2 + y^2 + z^2 - b^2)$, remain in the form of a scalar. Those who are aware of the special theory of relativity (STR) can identify that this form is similar to that of the Lorentz equation in STR. Thus, this composite term is called the Lorentz inner product of X, defined as $[a\ b\ c\ d]^*[a\ b\ c\ d]^T = a^2 + b^2 + c^2 - d^2$. Then Eq (621C) may be expressed as a common quadratic equation of form $<X^*X^T> + b<X> + a = 0$, where $X = [x\ y\ z\ b]$ is a multivariate vector of dimension 4. This function may be defined as

$$\begin{aligned} l &= < X^* X^T > \\ &= x^2 + y^2 + z^2 - b^2 \end{aligned} \tag{6.22}$$

Remember that this term λ is a scalar function of the unknown variables in X. Similarly, defining the vector $S = [x_s\ y_s\ z_s\ R]^T$, consisting of all known variables, we get

$$\begin{aligned} < S^* S^T > &= (x_s^2 + y_s^2 + z_s^2 - R^2) \\ &= \alpha \end{aligned} \tag{6.23}$$

Thus, α is a known scalar. Using these definitions, Eq (6.21C) becomes

$$\lambda - 2\beta X^T + \alpha = 0 \tag{6.24A}$$

where $\beta = [x_s\ y_s\ z_s - R]$. Here, α and β are known and λ and X are unknown quantities. So, Eq. (24a) can equivalently be written as

$$\beta X = \frac{1}{2}\lambda + \frac{1}{2}\alpha \tag{6.24B}$$

Because this equation holds well for each of the satellites, a similar equation may be formed from "n" different satellites to form the matrix equation

$$BX = \frac{1}{2}\Lambda + \frac{1}{2}A \tag{6.24C}$$

λ, which is a scalar function of the user position and clock bias, remains the same for all satellites. Hence, $\Lambda = \lambda\, U$ and $U = [1\ 1\ 1\ 1\ \ldots.]^T$. Each α, being a function of the respective satellite coordinates and corresponding ranges, A has different elements in it. So, $A = [\alpha_1\ \alpha_2\ \alpha_3\ \ldots.\ \alpha_n]^T$. Similarly, B has different values of β in its different rows corresponding to different satellites, as

$$B = \begin{pmatrix} x_{S1} & y_{S1} & z_{S1} & -\rho_{S1} \\ x_{S2} & y_{S2} & z_{S2} & -\rho_{S2} \\ x_{S3} & y_{S3} & z_{S3} & -\rho_{S3} \\ & & \vdots & \\ x_{Sn} & y_{Sn} & z_{Sn} & -\rho_{Sn} \end{pmatrix}$$

Since we have n satellites, B is an $[n \times 4]$ matrix, U is $[n \times 1]$, and A is an $[n \times 1]$ vector. The dimension of X is [4 x 1]. If we have at least 4 satellites, a least-squares solution solves the normal equation. From Eq. (6.24C), we can derive the least-squares solution X^* of X as

$$\begin{aligned} X^* &= \left(B^T B\right)^{-1} B^T \left(\tfrac{1}{2}\Lambda + \tfrac{1}{2}A\right) \\ &= K\left(\tfrac{1}{2}\Lambda + \tfrac{1}{2}A\right) \end{aligned} \tag{6.25}$$

where $K = (B^T B)^{-1}\, B^T$ is a $[4 \times n]$ matrix. However, our solution X^* involves λ, which again is a function of X. Substituting $X*$ into the definition of the scalar λ, we get

$$\begin{aligned} 1 &= < \tfrac{1}{2}K(L + A)^* \tfrac{1}{2}K(L + A) > \\ &= \tfrac{1}{4}\lambda^2 < KU^*KU > + \tfrac{1}{2}\lambda < KU^*KA > + \tfrac{1}{4} < KA^*KA > \end{aligned} \tag{6.26A}$$

$$\text{or,} \quad \lambda^2 < KU^*KU > + 2\lambda\left(\langle KU^*KA\rangle - 1\right) + < KA^*KA \geq 0 \tag{6.26B}$$

$$\text{or,} \quad \lambda^2 C_1 + 2\lambda C_2 + C_3 = 0 \tag{6.26C}$$

where $C_1 = < KU^*KU >$, $C_2 = < KU^*KA >$ and $C_3 = < KA^*KA >$.

This is a scalar quadratic equation in λ. You may verify by comparing the dimensions of each constituent matrix of the given operations that the equation contains all scalar coefficients. All three of these coefficient values can be computed because all components in them are known. Hence, the two possible solutions for λ (λ_1 and λ_2) can be obtained. Each of these two solutions is valid, but these are scalar functions of X and not X itself. Thus, each value of λ can be put into Eq. (6.25) to obtain the final closed value of X, as

$$\begin{aligned} X_1 &= K\left(\tfrac{1}{2}\lambda_1 U + \tfrac{1}{2}A\right) \\ X_2 &= K\left(\tfrac{1}{2}\lambda_2 U + \tfrac{1}{2}A\right) \end{aligned} \tag{6.27}$$

One solution for this will only give a logical result that makes sense. For example, for ground-based users, one solution for X will be on the surface of the Earth with a radius of R, and one will not. Thus, one of the two is selected through rational reasoning, and the other is rejected. The mathematical equivalence of this, however, is the use of a constraint equation (or inequation) only a constraint equation. Box 6.2 describes the method for solving for position using Bancroft's method.

Box 6.2 MATLAB for Bancroft's Method

The MATLAB program Bancroft.m was run to obtain the solution, as shown above. Information regarding the satellite position and the measured ranges was obtained from an external file. This file, "sat_pos.txt," was read by the program through in-line commands.

Run the program and use different sets of data to check for the following:

- How does the condition of matrix B change as the satellite passes close by
- What happens when the measured range is exact (i.e., $x_s^2 + y_s^2 + z_s^2 - R^2 = 0$) so that $A = 0$

Focus 6.3 Solving with bancroft's method

We illustrate here an example of solving the position of a point using the measured ranges and the satellite positions as input. For the Cartesian coordinates of satellites S1, S2, S3, and S4 in an ECEF frame in km, as obtained from the satellite ephemeris, transmitted by the satellites in their message:

Sat: S1	Sat: S2	Sat: S3	Sat: S4
$x_{S1} = 2.1339 \times 10^3$	$x_{S2} = 0.0$	$x_{S3} = 4.1006 \times 10^3$	$x_{S4} = 2.0581 \times 10^3$
$y_{S1} = 2.4391 \times 10^4$	$y_{S2} = 2.4484 \times 10^4$	$y_{S3} = 2.3256 \times 10^4$	$y_{S4} = 2.3525 \times 10^4$
$z_{S1} = 8.9115 \times 10^3$	$z_{S2} = 8.9115 \times 10^3$	$z_{S3} = 1.1012 \times 10^4$	$z_{S4} = 1.1012 \times 10^4$

And the measured range from a definite position P on the Earth, after all corrections are made on that for satellites, is

$$R_{t1} = 1.9708 \times 10^4$$
$$R_{t2} = 1.9702 \times 10^4$$
$$R_{t3} = 1.9773 \times 10^4$$
$$R_{t4} = 1.9714 \times 10^4$$

We need to find the position of P. The first job is to use the position and range information to generate the B matrix. For our case, the B matrix becomes

$$B = \begin{bmatrix} 0.2134 & 2.4391 & 0.8912 & -1.9708 \\ 0 & 2.4484 & 0.8912 & -1.9702 \\ 0.4101 & 2.3256 & 1.1012 & -1.9773 \\ 0.2058 & 2.3525 & 1.1012 & -1.9714 \end{bmatrix} \times 10^{04}$$

From this value of B, the K matrix is derived as:

$$K = \begin{bmatrix} 0.06 & -0.06 & -0.02 & 0.02 \\ 0.38 & -0.37 & -0.39 & 0.39 \\ 0.11 & -0.16 & -0.16 & 0.21 \\ 0.52 & -0.54 & -0.56 & 0.57 \end{bmatrix} \times 10^{-2}$$

Now, because both KU and KA values are known and formed using known parameters, these can be used to generate Eq. (6.26B) with coefficients c1, c2, and c3, respectively, where

$c1 = -1.1445 \times 10^{-09}$, $c2 = -0.810$, $c3 = 1.4786 \times 10^{08}$

The solutions for the equation thus formed in Eq. (6.26c) can be obtained using standard methods of solving quadratic equations, and are:

$\lambda 1 = -8.5821 \times 10^{08}$ and $\lambda 2 = 1.5053 \times 10^{08}$

Putting these values into Eq. (6.27), we get vectors X1 and X2 as:

$$X1 = [\ 0.041;\quad 1.137;\quad 0.468;\quad 16.026\ ] \times 10^{03}$$

$$X2 = [\ 0.223;\quad 6.464;\quad 2.619;\quad -1.979\ ] \times 10^{03}$$

To validate the feasibility of the two results thus obtained, the radius of the two solution points is determined. These radii turn out to be R1 and R2 for solutions X1 and X2, respectively, where

$R1 = 1.2299 \times 10^{3}$ km
$R2 = 6.9787 \times 10^{3}$ km

Considering that the point of interest was on the Earth's surface, the first solution does not satisfy the case because its radius is too short, whereas the second solution does, and looks more probable. So, X2 is our solution.

6.5.2 Doppler based positioning

Among different other methods, the Doppler-based position fixing is important. It was the technique first used by many initial satellite navigation systems. This technique was used for the first time with satellite Sputnik when the position of the satellite was determined using the Doppler frequency from known receiver positions. Here, we describe the fundamentals of position estimation using Doppler (Axelrad & Brown, 1996).

We first define Doppler frequency as a shift in the frequency of the received signal from what is transmitted. This shift occurs due to the relative radial motion between the transmitter and the receiver. Thus, if v_{rs} is the radial velocity of the receiver relative to the transmitter and away from it, the shift in the received frequency of the signal of wavelength λ owing to the Doppler is given by

$$\Delta f = -v_{rs}/\lambda \tag{6.28}$$

We have used the convention that when the relative distance between the transmitter and the receiver increases, the velocity is taken as positive. Therefore, when the

radial distance with the transmitter decreases and the receiver approaching each other, the frequency increases. So, negative velocity leads to a positive Doppler frequency; whereas for positive relative frequency, the received frequency decreases, causing a negative Doppler frequency. Furthermore, because λ is fixed for a signal, the relative velocity v_{rs} at any instant can readily surrogate the Doppler shift. In this section, we will use the terms "Doppler shift" and "relative radial velocity" synonymously.

Doppler and integrated Doppler can be used to determine the position of the receiver when the position and the velocity of the transmitter are precisely known. We have seen that the range measured by the receiver can be expressed as

$$R_1 = \sqrt{(x_{S1} - x)^2 + (y_{S1} - y)^2 + (z_{S1} - z)^2} + b \tag{6.29}$$

where the notations carry their usual meanings as used before in this chapter. Because the relative velocity is the rate of change in the range, we get

$$\begin{aligned} v_{rs} &= dR/dt \\ &= (\alpha_s v_{sx} - \alpha_r v_{rx}) + (\beta_s v_{sy} - \beta_r v_{ry}) + (\gamma_s v_{sz} - \gamma_r v_{rz}) + db/dt \end{aligned} \tag{6.30}$$

where $\alpha_s = \partial R/\partial x_s$, $\beta_s = \partial R/\partial y_s$, and $\gamma_s = \partial R/\partial z_s$. Similarly, $\alpha_r = -\partial R/\partial x$, $\beta_r = -\partial R/\partial y$, and $\gamma_r = -\partial R/\partial z$. Here, v_{sx}, v_{sy}, and v_{sz} are components of the satellite velocities, and v_{rx}, v_{ry}, and v_{rz} are the components of the receiver velocities along the X, Y, and Z axes, respectively. $db/dt = d(\delta t_u)/dt$ is the drift in the range due to the error drift of the receiver clock. These velocity components of the satellite and user, multiplied by their respective projection factors α, β, and γ, along the radial line joining them, contribute to the total relative radial velocity.

Now, to calculate position conveniently, the receiver must remove the effect of their velocity. Thus, an effective choice is that the receiver remain stationary during the estimation; then, under the condition of static receiver location, v_{rx}, v_{ry}, and v_{rz} become zero. The previous equation reduces to

$$v_{rs} = (\alpha_s v_{sx}) + (\beta_s v_{sy}) + (\gamma_s v_{sz}) + db/dt \tag{6.31}$$

We have already seen that derivatives α_s, β_s, and γ_s are the direction cosines of the vector joining the satellite and the receiver. These are nonlinear functions of the current satellite and receiver positions. The unknown position coordinates in these terms can be obtained using various methods. Extended Kalman filtering is one of the most popular among them.

Conceptual questions

1. Is it possible to find the position of a flying aircraft by measuring its range from a known position on the Earth? If yes, how many such receivers will be required to find it?
2. Instead of using the measured range, if we take the range difference values, the common term of clock bias cancels out, and the equations are left with three

unknowns. Is it possible to use only three satellites and the corresponding three difference equations to derive the position coordinates?

3. What advantages do we obtain by using an atomic clock while determining the position and velocity?
4. Do you expect the accuracy of the navigation solution to improve if more than four satellites are used for the purpose?

References

Abel, J. S., & Chaffee, J. W. (1991). Existence and uniqueness of GPS solutions. *IEEE Transactions on Aerospace and Electronic Systems, 27*(6), 952–956. https://doi.org/10.1109/7.104271.

Axelrad, P., & Brown, R. G. (1996). GPS navigation algorithms. *Global positioning systems: Theory and applications. AIAA, 1*, 409–433. https://doi.org/10.2514/4.472497.

Bancroft, S. (1985). An algebraic solution of the GPS equations. *IEEE Transactions on Aerospace and Electronic Systems, 21*(1), 56–59. https://doi.org/10.1109/TAES.1985.310538.

Chaffee, J., & Abel, J. (1994). On the exact solutions of pseudorange equations. *IEEE Transactions on Aerospace and Electronic Systems, 30*(4), 1021–1030. https://doi.org/10.1109/7.328767.

Grewal, M. S., Weill, L. R., & Andrews, A. P. (2002). *Global positioning systems, inertial navigation, and integration*. Wiley https://doi.org/10.1002/0471200719.

Strang, G. (2003). *Introduction to linear algebra*. Wellesley-Cambridge Press.

CHAPTER

Errors, impairments, and mitigations

7

Preamble

In our previous chapters, we have talked about the theoretical ways of fixing positions. But the conditions under which we derived these parameters were very hypothetical, since we assumed that all the measurements that we are doing at the receiver during ranging are perfect and the positions of satellites were determined without any error. However, in all practical scenarios, we cannot do the position fixing without making errors. These errors creep into our measurements from almost every segment of the system, corrupt them, and make our position estimates wrong. We cannot completely get rid of this menace, but we can substantially reduce it. For that, we categorically need to know how the errors are actually occurring. In this chapter, first, we identify these errors coming from different sources and quantify their relative effects on position estimations. Finally, we shall also briefly discuss how to negotiate with these errors.

7.1 Scope of errors

The only means through which the system information reaches the user receiver is the navigation signal. This information is derived at the ground stations using the measurements done at the monitoring stations. It is practical to realize that some errors are always getting added in this whole process. Errors also occur while the receiver derives the information from the signal.

It is important to note here that we are not much concerned about the communication errors. Communication errors result in incorrect identification of the navigation data bits. However, these data bits are either coded with forward error correction or have provisions for a cyclic redundancy check to identify and restore their correctness. Therefore, whenever any error in the received bit occurs, they are either corrected or discarded. These errors that may lead to erroneous information in the receiver are not used in the process. So, we concentrate here on the errors in measurements and estimates.

We now know that the only relationship that is used between the measurements and estimates of our required parameter is the observation equation of the form:

$$R = \sqrt{(x_s - x_u)^2 + (y_s - y_u)^2 + (z_s - z_u)^2} \tag{7.1A}$$

Understanding Satellite Navigation, Second Edition. DOI: https://doi.org/10.1016/B978-0-443-36432-7.00020-1

To this equation, we assumed that the receiver clock bias is offset by an amount δt_u with respect to the system reference time. This adds a compensation term to our expression of the measured range and we get the modified the observation equation to

$$\begin{aligned} R &= \sqrt{(x_s - x_u)^2 + (y_s - y_u)^2 + (z_s - z_u)^2} + c\delta t_u \\ &= \sqrt{(x_s - x_u)^2 + (y_s - y_u)^2 + (z_s - z_u)^2} + b \end{aligned} \tag{7.1B}$$

where b is the effective error in measured range due to the receiver clock bias. Both the reference positioning parameters (x_s, y_s, z_s), i.e., the satellite location, and the ranging parameter R have their respective positions in this equation. These known values are used in the equation, and the equation is typically linearized to obtain the definite relationship of the unknowns $X = (x_u, y_u, z_u, b)$ with these known values. Use of linearization method is nothing but differentiating this relation into a linear form and solving of simultaneous linear equations of the form

$$\begin{aligned} \underline{G}\Delta\underline{X} &= \Delta\underline{R} \\ \Delta\underline{X} &= \underline{G}^{-1}\Delta\underline{R} \end{aligned} \tag{7.2A}$$

where $G = \partial R/\partial X$, ΔX is the difference of the true receiver position X with respect to a known assumed initial reference position X_0, and ΔR is the difference in measured range of the receiver R with respect to the range R_0, geometrically calculated from the point X_0. So, replacing $\Delta\underline{X} = (\underline{X} - \underline{X}_0)$ and $\Delta\underline{R} = (\underline{R} - \underline{R}_0)$, we get

$$\underline{X} = X_0 + \underline{G}^{-1}\left(\underline{R} - \underline{R}_0\right) \tag{7.2B}$$

Now, if the measurements are erroneous so that R turns to R + dR due to error, the solution also becomes $\underline{X} + d\underline{X}$, where

$$\begin{aligned} \underline{X} + \underline{dX} &= X_0 + \underline{G}^{-1}(R + dR) - \underline{G}^{-1}R_0 \\ \text{or,} \quad \underline{dX} &= \underline{G}^{-1}dR \end{aligned} \tag{7.2C}$$

So, the error in solution dX is directly related to the measurement error dR through the inverse of the matrix G. So any error in the measured range values will ultimately lead to an error in position estimates. The magnitude of the position errors will be dependent upon both the range measurement error dR and the relative geometry represented by G. Therefore, to reduce the error in the position estimation solution, on one hand, the error in measurements, that is, dR, has to be small. On the other hand, G^{-1} should be such that it does not inflate the errors in dR. Now, as for any arbitrary matrix A, the inverse of the matrix $A^{-1} = C_A{}^T/|A|$, where C_A is the cofactor matrix of A and |A| is its determinant. For the above requirement of G^{-1} to be fulfilled, |G| should not be very small, i.e., G should not be singular or near singular. In other words, the matrix G has to be well-conditioned. To achieve this, the rows of G must be linearly independent and well separated.

Thus, we have seen that the requirements to make the estimation error dX small are to minimize dR and to make G well-conditioned. But before going into any further

detail, we shall see in Box 7.1 how the estimated position, fixed using observation equations, assuming no clock bias, will vary with the error in the range.

BOX 7.1 MATLAB

The MATLAB program posi_err.m was run to find the positional error for a definite set of satellites with their respective positions as given below.

Satellite positions:

[32.2°N; 67.0°E]; [0.5°N; 73.8°E]; [−15.3°N; 91.4°E]; [5.6°N; 117.2°E].

The corresponding ranging errors were

[5.2; 4.1; 3.7; 9.2] in meters.

The error in Cartesian coordinates, thus obtained, was

dx = −6.832 m; dy = 16.259 m; dz = 7.887 m

This makes the effective radial error 19.749 m. The corresponding condition number of the G matrix was 57.382, which is quite high compared to the desirable value of nearly one.

Change the satellite positions, keeping the range errors the same, and see the variation in position errors. Check the condition number of the matrix G every time. Arrange the errors in order by this parameter of G.

Similarly, keep the satellite positions fixed and change the range errors, and see the result.

7.1.1 Sources of errors

You must be willing to know about the factors responsible for introducing errors in the measurements. That is what we are going to address in this section. First, we shall discuss here the formal classification of these errors. Then we shall elaborate on each of these kinds. Errors in the known parameters of the observation equation come from various sources, and all three architectural segments of a typical navigation system contribute to these errors. So, we generally categorize the errors on the basis of the segment from which the errors are coming. Under each segment, there are different reasons for the errors to be generated.

The primary sources of error at the various segments are (Parkinson, 1996):

- *Control segment errors:* Ephemeris error.
- *Space segment errors*: Satellite clock bias, satellite code bias.
- *Propagation errors*: Ionospheric delay, tropospheric delay, multipath.
- *User segment errors*: Receiver noise, receiver bias.

Sometimes it is convenient to classify errors by their characteristics. On this basis of how they spatially vary, the errors can be divided into

- *Constant errors:* These are the errors that are constant over the geographic location of the users and remain the same for all users irrespective of the receiver's position.

These errors are already present in the signal before they start traversing toward the users and hence are not influenced by the position of the receiver. In other words, they are global in nature. This category includes errors like the satellite clock bias, satellite hardware delay, etc.

- *Correlated errors*: These are the errors that are dependent upon the location of the users and are geographically correlated at the same time. The errors dependent upon the receiver-satellite geometry or those itroduced by the medium as the signal propagated through it, are of this type. Errors like the ephemeris errors, ionospheric, and tropospheric errors fall under this category. The amount of these errors varies from place to place as the receiver relocates. However, there remains a large correlation between the values at one place and those in its vicinity. This makes it possible to derive the approximate error value at one place if the same value at any adjacent place is known.
- *Uncorrelated errors*: These are the errors that are also dependent upon the location of the users but are not geographically correlated. These errors are independent and mutually exclusive, such that one cannot estimate the error magnitude at one place from any other related information of the same at another place. Errors due to multipath and noise fall under this category.

We shall once again review these error categories in our next chapter, for a different purpose; however, while the individual errors will be described here.

7.2 Control segment errors

In our previous discussion, we have seen that the ephemeris and clock correction parameters are computed at the ground control segment. These values are updated at regular intervals and transmitted to the users through the navigation message. During this process of computing some errors are generated, which are discussed below.

7.2.1 Ephemeris errors

While estimating the ephemeris of the satellite, the control segment uses different models that predict its future orbital locus. In this process, there remain some modeling errors that lead to errors in the ephemeris issued by the control segment. This is called an ephemeris error.

How does the ephemeris error affect the range? The ephemerides are the parameters from which the satellite positions are derived. These satellite positions in turn are the parts of the observation equation, as given in Eq. (7.1B), which is again given below

$$R = \sqrt{(x_s - x_u)^2 + (y_s - y_u)^2 + (z_s - z_u)^2} + c\delta t_u$$

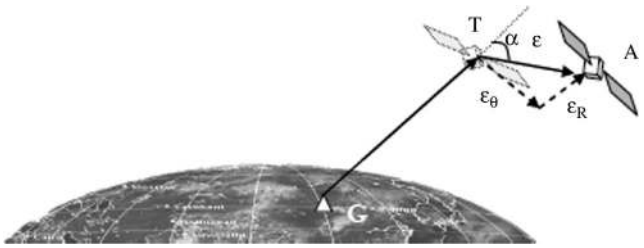

FIGURE 7.1

Ephemeris error.

Notice that here we equate the measured range on the left-hand side to the theoretical Euclidean range obtained from the satellite and user positional coordinates on the right-hand side plus the error due to the clock. The measurement of the theoretical range is done from the true position of the satellite. However, the use of wrong satellite position coordinates due to the ephemeris error will result in the calculation of a theoretical range of the satellite with respect to a position where the satellite is not actually located. So, this can no longer be equated with the measured range R. While an equation is formed, as in Eq. (7.1), it will result in an unbalanced equation of range. This will eventually lead to errors in the user position solution.

Despite this fact, we really have no means to correct the values of these satellite coordinates in the expression. So, instead, we keep the satellite coordinates as derived from the transmitted ephemeris and then add a compensatory term in the theoretical expression of the equation. This extra term compensates for the range error that occurs due to putting of the incorrect satellite coordinates and balances the equation. The two sides are now ready to be equated through the expression

$$R = \sqrt{(x_s - x_u)^2 + (y_s - y_u)^2 + (z_s - z_u)^2} + c\delta t_u + \delta r_{eph} \tag{7.3}$$

In this expression, the values of the satellite coordinates x_s, y_s, and z_s, are actually those derived from the ephemeris and thus contain error, and δr_{eph} is the compensatory term that balances the resultant range error.

Fig. 7.1 describes the deviation of the estimated position of the satellite from its true position. Here, the apparent position of the satellite is at A, whereas its true position is at T. The deviation $S = \varepsilon$ can be resolved into ε_θ and ε_R. ε_θ is normal to the radial distance GT and does not affect the range when measured from the ground receiver, G. The radial error ε_R is along the radial distance and adds an extra magnitude to the actual range of the satellite. Thus, it is this effective range error component that affects ranging and is of concern here. It is this term ε_R that is used in Eq. (7.3) as δr_{eph}, considering the sign accordingly.

It is obvious that, for a particular observation, the compensatory term δr_{eph} is dependent upon the position of the receiver. When we separate the total ε into its components, the radial component of the error that actually affects the range is ε_R.

Now $\varepsilon_R = \varepsilon \cos \alpha$, where α is the angle made between the range and the error vector. The error vector being fixed for a particular satellite with its respective ephemeris error, the angle α is dependent upon the relative position of the satellite and the receiver. So, for a different location G of the receiver, α will be different, and so will the value of ε_R for the same value of ε. Consequently, different amounts of errors will be added to the actual radial range due to the same ephemeris error.

To understand this effect a little more mathematically, we shall first see how a very small error in x_s, y_s, and z_s due to ephemeris error will effectually change the range.

Let the errors in the satellite coordinates, i.e., the difference in the true and transmitted value of the satellite position coordinates, due to the ephemeris error, be $dS = [dx_s\ dy_s\ dz_s]$. Since we know the expression of the absolute radial range R in terms of the satellite coordinates, we can derive the resultant radial error dR due to this error in the satellite coordinates as

$$dR = (\partial R/\partial x_s)|_{xs}dx_s + (\partial R/\partial y_s)|_{ys}dy_s + (\partial R/\partial z_s)|_{zs}dz_s \tag{7.4A}$$

Note that here the derivatives are measured at those satellite coordinates $[x_s\ y_s\ z_s]$, derived from the transmitted ephemeris. From Eq. (7.1), the expression for the derivatives can be obtained as

$$\begin{aligned}
\partial R/\partial x_s|_{xs,ys,zs} &= (x_s - x_u)/\sqrt{(x_s - x_u)^2 + (y_s - y_u)^2 + (z_s - z_u)^2} \\
\partial R/\partial y_s|_{xs,ys,zs} &= (y_s - y_u)/\sqrt{(x_s - x_u)^2 + (y_s - y_u)^2 + (z_s - z_u)^2} \\
\partial R/\partial z_s|_{xs,ys,zs} &= (z_s - z_u)/\sqrt{(x_s - x_u)^2 + (y_s - y_u)^2 + (z_s - z_u)^2}
\end{aligned} \tag{7.4B}$$

Note that the derivatives are the cosines of the angles between the range vector and the axes of the coordinates. Therefore, Eq. (7.4) can be written as

$$\begin{aligned}
dR &= (\partial R/\partial x_s)dx_s + (\partial R/\partial y_s)dy_s + (\partial R/\partial z_s)dz_s|_{xs,ys,zs} \\
&= \cos\alpha dx_s + \cos\beta dy_s + \cos\gamma dz_s \\
&= e_x dx_s + e_y dy_s + e_z dz_s \\
&= \underline{e} \cdot d\underline{S}
\end{aligned} \tag{7.4C}$$

where $\underline{e}$ is the unit vector along the range and e_x, e_y, and e_z are its components along the three coordinate axes. This shows that the effective radial error in range is equal to the sum of the projection of the total satellite position error, dS along the radial direction between the user and the satellite. It is also evident from the expressions of each component that they are dependent upon the receiver position coordinates, which are implicitly present in the cosines of the angles, and hence on receiver–satellite geometry. Referring to Fig. 7.2, if T and A are the true and apparent positions of the satellite due to the ephemeris error, there is a substantial change in range for the receiver Rx_1, while for Rx_2, the difference is trivial.

Though the ephemeris error values change with the position of the users, there exists a definite function that the variation follows. So, these errors are correlated over space. However, this function changes slowly across the space so that for nearby distances the variation is so small that it may be considered to be constant. To establish this, we shall start by referring to Fig. 7.2.

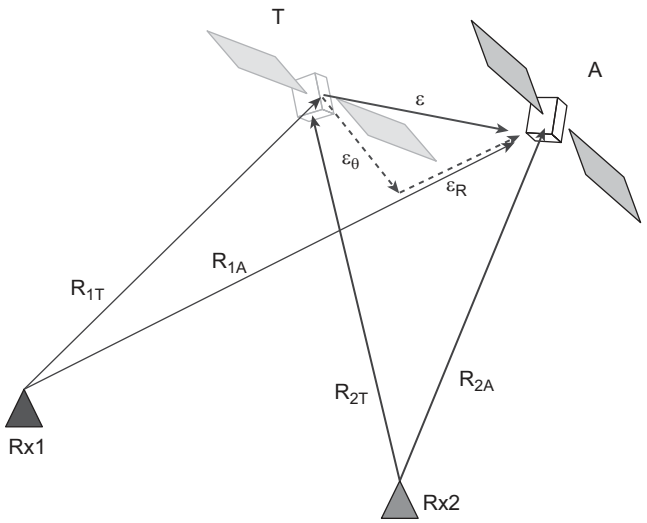

FIGURE 7.2

Geometric variation of ephemeris error.

Using Eq. (7.4C) we can say that the difference in the ephemeris error at the two locations is

$$\Delta dR = (e_1 - e_2) \cdot dS \tag{7.5}$$

Here, e_1 and e_2 are the unit radial vectors from the two receivers, Rx_1 and Rx_2, respectively, located at nearby positions $[x_{u1}\ y_{u1}\ z_{u1}]$ and $[x_{u2}\ y_{u2}\ z_{u2}]$. This can be written by expanding the terms e_1 and e_2 in terms of the position coordinates as

$$\Delta dR = \left[\frac{(x_s - x_{u1})}{\rho_1} - \frac{(x_s - x_{u2})}{\rho_2}\right] dx_s + \left[\frac{(y_s - y_{u1})}{\rho_1} - \frac{(y_s - y_{u2})}{\rho_2}\right] dy_s + \left[\frac{(z_s - z_{u1})}{\rho_1} - \frac{(z_s - z_{u2})}{\rho_2}\right] dz_s \tag{7.6A}$$

where r_1 and r_2 are the ranges measured from the ground receivers R_{x1} and R_{x2} respectively to the apparent satellite positions at (x_s, y_s, z_s).

For nearby stations, we can always put the condition that the range remains almost equal. This makes $\rho_1 \approx \rho_2 = \rho$. This modifies the above equation to

$$\Delta dR = (x_{u2} - x_{u1})/\rho dx_s + (y_{u2} - y_{u1})/\rho dy_s + (z_{u2} - z_{u1})/\rho dz_s \tag{7.6B}$$

Again, each of the coefficients in the above equation is the ratio of the coordinate differences between the receivers to the range to the satellite. So, for small differences in receiver positions, each of these ratios is negligibly small, making the total equation approach zero.

So, the triviality of this equation indicates that for two closely placed receivers, the ephemeris errors are almost the same. In Box 7.2, we shall see how this ephemeris error affects the range for different positions of the receiver and for a given deviation of the satellite.

BOX 7.2 MATLAB

The MATLAB program eph_err.m was run to obtain the ephemeris errors for a given variation of the receiver position and for a given position of the satellite. Plots are obtained for a specific deviation of the satellite. It is shown in Fig. M7.2.

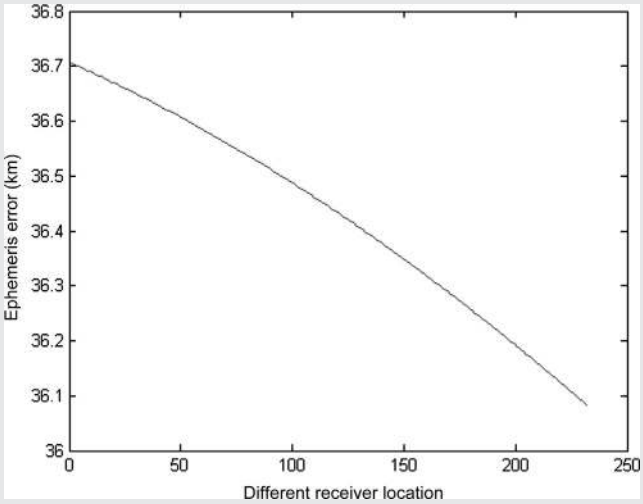

FIGURE M7.2

Variation of ephemeris errors for different receiver locations.

Note that even for large deviations of the satellite from the true satellite position, the corresponding error observed over a large departure of the receiver is quite small, since the error vector gets more orthogonal to the range vector.

Run the program again with different departures of the receiver and also for larger deviations of the satellite, and observe the major differences in this result.

7.3 Space segment errors

The space segment errors include all those errors in ranging that occur due to the elements in the satellites and signals issued by it. These include primarily the satellite clock error and the satellite code bias.

7.3.1 Satellite clock error

The satellites carry atomic clocks, which provide the reference time and frequency for all the activities done in the satellite, including the time stamping of the signal. The satellite clocks, despite being atomic clocks, have their respective biases and drifts. These drifts generally come from the associated electronics of the clock that determine the transition resonance condition of the atoms in such a clock. This error is very small, as the precision remains $\sim 10^{-13}$ or better. But, since this error grows cumulatively and we measure the range by multiplying the time by the velocity of light c (3×10^8 m/sec), small variations also result in considerable range errors. The effective range deviation due to the clock error is given by

$$b_s = -c\delta t_s \tag{7.7}$$

where c is the velocity of light and δt_s is the satellite clock error. The negative sign is due to the fact that if δt_s is positive, making the satellite clock advance with the system time, the signal transmission time from the satellite will be marked later than what it actually is. So it would appear that the traveling time is less by δt_s, leading to a reduction in the effective calculated range.

However, as we have read in the previous section, the satellite clock errors are estimated by the control segment, and the corrections are transmitted along with the signal. Using them, the users can correct the corresponding effects in their measured range during position fixing. Still, there remain some residual errors that occur due to the estimation of these clock biases and drifts at the control segment. These residual errors cannot be corrected; hence, an equivalent compensatory range error has to be added in the range measurement due to this fact. So, effectively, what remains in the range is the residual error due to inaccuracy in the ground segment estimation of the satellite clock bias. As a result, the observation equation in Eq. (7.3) changes to

$$R = \sqrt{(x_s - x_u)^2 + (y_s - y_u)^2 + (z_s - z_u)^2} + c\delta t_u - c\delta t_s + \delta r_{eph} \tag{7.8}$$

7.3.2 Code bias

The ranging is done by estimating the delay incurred by the signal in propagating through the intermediate path from the satellite to reach the receiver. It is assumed that the ranging codes are transmitted by all the satellites synchronously, that is, the start of the transmission of a code or any specific code bit within it occurs at the same instant in all satellites. Moreover, where the same encoded data bits are transmitted using multiple frequencies, precisely the same code phase is assumed to exist for the two different frequencies at any instant. But pragmatically, this is not the case. Some small time differences always remain between them. A part of this is contributed by the hardware delay in transmitting the signals from the marked time in the time stamp to the actual instant it is transmitted from the antenna phase center of the satellite. These differences are of the order of nanoseconds, which are of the order of typical hardware delays of the devices. But, even this delay amounts to about a meter of

difference in the range. Moreover, this delay is different for different satellites. Also, the differential value of this hardware bias adds to the differential code bias between two same codes transmitted by the same satellite but on different carrier frequencies. These errors are effective when calculations are done by comparing two different signals.

7.4 Propagation and user segment errors

7.4.1 Propagation errors

The propagation errors in a navigation signal are those that occur when the signal propagates through various atmospheric layers. Each of these layers contributes in a different way to the error in the received signal. The signals pass through the ionosphere and then through the troposphere. In both these layers, the signals experience some impairment, causing possible errors in the measured range.

7.4.1.1 Ionospheric effects

The radio waves of the navigation signal experience an additional delay as the signal traverses through the ionosphere, a part of the atmosphere of the Earth. This additional delay gets converted into equivalent excess range as an error in the measured range at the receiver, since the receiver derives the range from the traverse time. This delay contributes the most to the total range error, and so it is important that we understand this in greater detail. But the ionosphere is a vast subject and excessively interesting. So, we should be cautious not to lose track of our main discussion while exploring this wonderful part of nature – the ionosphere.

The ionosphere is the part of the atmosphere that extends from 50 km to above 1000 km above the Earth's surface. This layer of the atmosphere has large numbers of free electrons and ions that are generated from the abundant ozone and oxygen molecules present there by absorption of solar radiation. These free electrons again get recombined with the ions present there, diminishing the free electron density. These two processes, viz., generation and recombination, occur simultaneously and with equal rates at equilibrium to produce and sustain a definite density of free electrons. However, this density, being a function of the solar flux, varies with time of day, season, solar activity periods, and various other factors. The path integral of the ionospheric electron density is known as the total electron content (TEC). So

$$\mathrm{TEC} = \int \mathrm{N_e}(s)\mathrm{d}s \tag{7.9}$$

If we consider a straight line along the signal path, which is passing through the ionosphere and connecting the satellite to the receiver, with unit cross-section area, then it forms a cylinder of volume V where $V = 1 \times s$; s is the length that this line crosses through the ionosphere. Since the cross section is unity, i.e., $A = 1$, the number of electrons present in this cylinder equals $\int$Ne(s) dl x $A = TEC$. So, we may also define TEC as the total number of ionospheric free electrons present in this cylindrical

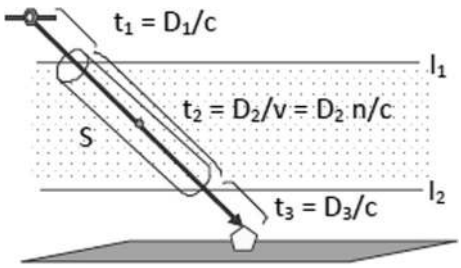

FIGURE 7.3

Ionospheric total electron content and traverse time.

volume of unit cross-section along this signal path. For obvious reasons, the length of the line varies depending on the elevation of the look angle. So, the part of the ionosphere that the path covers through the ionosphere will be different. Therefore, paths with different elevation angles will contain different total electron contents. So, the TEC for slant and vertical look angles will be different. It will also be different for different times of day and for different seasons, as the density of the ionospheric electrons changes with these factors. In Fig. 7.3, the total number of electrons present in the cylinder S is the total electron content for the shown path. The unit for TEC is electrons/m^2. However, the pragmatic values of the parameter when expressed in this unit are very large. Hence, a more convenient unit for the same is TECU, where 1 TECU $= 10^{16}$ electrons/m^2.

The ionosphere has a different refractive index than free space, which is denoted by n. Thus, the velocity with which the codes in the signal move through this region is c/n, where c is the velocity of light in free space. Therefore, in the figure, if D_1 and D_3 are the length traversed above and below this region, respectively, and D_2 is within it and if t1, t2 and t3 be the respective time the signal takes to traverse through D_1, D_2 and D_3, then, $t_1 = D_1/c$, $t_2 = D_2 n/c$ and $t_3 = D_3/c$. It makes the excess time taken in traversing the ionospheric section to

$$\Delta t = (D_1 + D_2 n + D_3)/c - (D_1 + D_2 + D_3)/c \; = \; = (n-1)D_2/c \tag{7.10A}$$

This causes an additional error in the range of equivalent path length given by

$$c\Delta t = (n-1)D_2 \tag{7.10B}$$

The deviation of the refractive index $(n-1)$ is a function of TEC, which we shall derive in the next subsection. Fig. 7.4 shows the typical temporal variation of the vertical TEC at a station near the magnetic equator.

7.4.1.1.1 Ionospheric delay

As the radio waves traverse through the ionosphere, there is an interaction between the wave and the electrons. The electric field of the wave given by $\mathbf{E} = E_0 \exp(j\omega t)$, which is oscillatory in nature, forces the free electrons in the medium to oscillate with

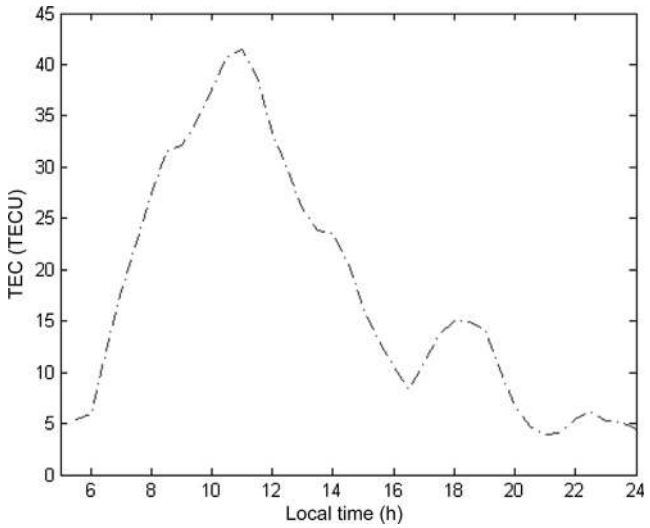

FIGURE 7.4

Typical variation of ionospheric total electron content with local time.

it. Since the electrons are free, there is no other force acting on them. So, the force equation on these electrons can be written as:

$$ma = e\mathbf{E} = eE_0\exp(j\omega t) \tag{7.11}$$

where m is the mass of the electron, e is the charge, and a is the acceleration produced. **E** is the incident electric field with amplitude E_0 and angular frequency ω. So, deriving the electron velocity, v, and its displacement, x, by integrating the above equation once and twice, respectively, with respect to time, and accordingly considering the boundary conditions, we get

$$v = eE_0\exp(j\omega t)/mj\omega = \frac{e}{j\omega m}\mathbf{E} \tag{7.12A}$$

$$x = -eE_0\exp(j\omega t)/m\omega^2 = -\frac{e}{m\omega^2}\mathbf{E} \tag{7.12B}$$

So, both the velocity and the amplitude of the motion of the electrons decrease as the frequency ω of the forcing signal increases. The velocity containing the imaginary term 'j' indicates that the velocity is in quadrature phase with the forcing field. Further, the negative sign in x implies that the displacements of the electrons are just opposite to the implied field.

Now, using the above expression of v, the resultant current density J, generated due to the motion of the electrons originating as a result of the imposed electric field, is given by:

$$\begin{aligned} J &= N\,e\,v \\ &= -j(Ne^2/m\omega)\cdot E \end{aligned} \tag{7.13A}$$

where N is the electron density in the region. So, the resultant conductivity σ can be expressed as

$$\sigma = J/E = -j\left(Ne^2/m\omega\right) \tag{7.13B}$$

Due to this finite conductivity produced, a conduction current flows as these electrons move through the medium. This current, in turn, influences the effective relative permittivity of the medium and the refractive index. So, the corresponding Maxwell equation can be written as

$$\begin{aligned} \nabla \times B &= \mu_0 J + \mu_0 \varepsilon dE/dt \\ &= \mu_0 \sigma E + \mu_0 \varepsilon_0 dE/dt \end{aligned} \tag{7.14}$$

Here, σ is the conductivity of the ionosphere. μ_0 and ε_0 are the permeability and permittivity, respectively, in this region, which can otherwise be treated almost as free space in the absence of conducting electrons. For the medium with propagating field strength given by E, the current density J is expressed as $J = \sigma^* E$, and B is the resultant magnetic field. Again, considering the field generated by the propagating signal to be sinusoidal with angular frequency ω,

$$\begin{aligned} E(t) &= E_0 \exp(j\omega t) \\ \text{or,} \quad dE/dt &= j\omega E(t) \\ \text{So,} \quad E(t) &= -(j/\omega) dE/dt \end{aligned} \tag{7.15}$$

Replacing this expression in Eq. (7.14), we get

$$\nabla \times B = \mu\varepsilon_0 (1 - j\sigma/\omega\varepsilon_0) dE/dt \tag{7.16}$$

Thus, due to the partial conductance of the medium, an imaginary term appears in the expression, and the effective relative permittivity gets transformed into a complex parameter

$$\varepsilon' = \varepsilon_0 (1 - j\sigma/\omega\varepsilon_0) \tag{7.17}$$

The complex refractive index "n" of the medium is thus obtained utilizing the standard relation as:

$$n^2 = \left(\frac{\varepsilon'}{\varepsilon_0}\right) = \left(1 - \frac{j\sigma}{\omega\varepsilon_0}\right) \tag{7.18A}$$

Replacing the value of σ from Eq. 7.13(B), we get,

$$= \left(1 - \frac{Ne^2}{m\varepsilon_0\omega^2}\right) \tag{7.18B}$$

$$= \left(1 - \frac{\omega_p^2}{\omega^2}\right) \tag{7.18C}$$

The ω_p is called the plasma frequency. The final expression for the ionospheric refractive index "n" is hence obtained by putting values of the constants e, m, and ε_0,

and we get

$$n = \sqrt{1 - \frac{80.6N_e}{f^2}} \tag{7.19A}$$

where N_e is the density of free electrons responsible for conductivity σ and $f = \omega/2\pi$ is the frequency of the wave in Hertz. For satellite signals, the frequency being very high, Eq. (7.19) can be approximated to

$$n = 1 - \frac{40.3N_e}{f^2} \tag{7.19B}$$

Consequently, the dispersive velocity with which the phase of the wave travels becomes

$$v_p = \frac{c}{\left(1 - 40.3Ne/f^2\right)} > c \tag{7.20A}$$

So whenever electromagnetic waves pass through this region, their phase moves faster compared to the velocity of the wave in vacuum, resulting in an effective phase advancement at the receiver. This is called the Phase velocity, v_p. The velocity with which the energy contained in the wave flows is called the Group velocity, v_g. For the ionosphere, the product of the phase velocity v_p and the group velocity v_g is constant, i.e., $v_p \times v_g = c^2$. Consequently, the group velocity with which the codes move becomes

$$\begin{aligned} v_g &= \frac{c^2}{c/\left(1-40.3N_e/f^2\right)} \\ &= c\left(1 - 40.3N_e/f^2\right) < c \end{aligned} \tag{7.20B}$$

Therefore, the energy contained in the signal and carried by the constituent codes and data traverses more slowly than in a vacuum, causing an additional code delay.

Now, let the path that the signal passes through the ionosphere be *l*. Following Eq. (7.8), the excess time taken by the codes to traverse a path length of *dl* is equal to

$$\begin{aligned} \Delta t(dl) = \frac{dl}{v_g} - \frac{dl}{c} &= \left(dl/c\right)\left(1 + 40.3N_e/f^2 - 1\right) \\ &= \frac{40.3}{cf^2}N_e dl \end{aligned} \tag{7.21A}$$

So, integrating it over the length of S that the signal traverses through the ionosphere, we get the total excess time of traverse as

$$\Delta t(s) = \left(1/c\right)\left(\frac{40.3}{f^2}\right)\int_S N_e dl \tag{7.21B}$$

This additional delay is thus proportional to the integral path of the electron density along the path of the wave. The integral quantity $\int$Ne dl is the TEC of the ionospheric path through which the wave passes. Consequently, the excess path that gets added up with the measured range due to the assumption of uniform velocity is thus

$$\begin{aligned}\delta l &= c\,Dt(l) = \left(\frac{40.3}{f^2}\right)\int_S N_e\,dl \\ &= (40.3/f^2)\,TEC\end{aligned} \tag{7.21C}$$

This delay is corrected to obtain improved performance. Focus 7.1 and the following Box 7.3 demonstrate how the TEC is derived from the measured ranges. The correction methods are discussed in a later section.

BOX 7.3 MATLAB

The MATLAB program TEC_est.m was run with a given file containing measured range values in frequencies 1575.42 and 1227.6 MHz for a definite day. The variation observed in TEC for a station located near the geomagnetic equator is as shown in the following figure. Observe the high TEC value manifested (Fig. M7.3).

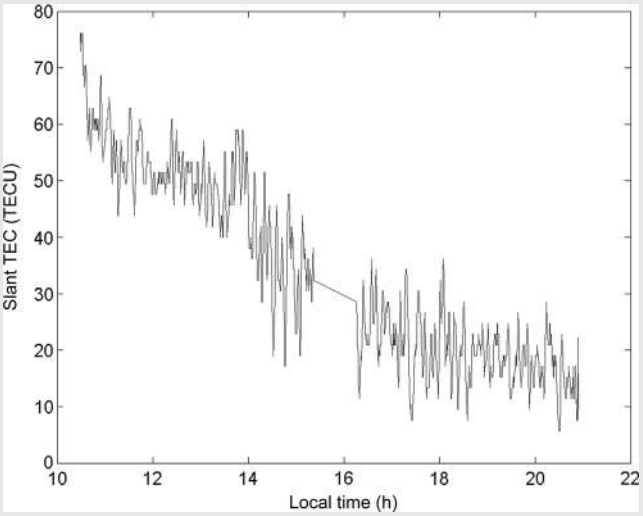

FIGURE M7.3

Variation of TEC.

Go through the program and identify how the TEC is derived from the measured ranges. Use the program to find the equivalent excess path and add necessary scripts to correct the range. Plot the variation of the measured and the corrected ranges. Verify that corrected ranges are equal for both frequencies.

Focus 7.1 Ionospheric TEC measurements

The ranges measured at two frequencies, 1575.42 and 1227.6 MHz, of a specific navigation satellite are 20,217,324.41 m and 20,217,331.67 m, respectively. To find the true range, assuming that the difference is due to the ionospheric delay only, we write

$$D1 = D + \delta_1 = D + \left(40.3/f_1^2\right)\text{TEC}$$

and

$$D2 = D + \delta_2 = D + \left(40.3/f_1^2\right)\text{TEC}$$

So,

$$D1 - D2 = \delta_1 - \delta_2 = 40.3\left(1/f_1^2 - 1/f_2^2\right)\text{TEC}$$

or,

$$\text{TEC} = (D1 - D2)/40.3 \times \left(1/f_1^2 - 1/f_2^2\right)^{-1}$$

Putting in the values, we get

$$\text{TEC} = 7.26/40.3 \times \{1/(1227.60)^2 - 1/(1575.42)^2\}^{-1} \times 10^{12} = 691126.10 \times 10^{12}$$
$$= 6.9 \times 10^{17} = 69\text{TECU}$$

Hence the correction for D1 is $\delta 1 = 40.3 \times 6.91126 \times 10^{17}/(1575.42 \times 10^6)^2 = 11.22$. So, the corrected range is 20,217,324.41−11.22 m = 20,217,313.19 m.

7.4.1.1.2 Faraday rotation

Another effect that takes place on the propagating navigation signals as they pass through the ionosphere is the Faraday rotation. As the electric fields of the radio waves with a definite polarization move across the magnetic fields of the Earth, the field direction undergoes a rotation that is proportional to the TEC and also to the total path, in addition to the magnetic field strength.

7.4.1.1.3 Ionospheric Doppler

The Doppler effect is the change in frequency of the received signal due to the relative velocity between the transmitter and receiver. When the transmitter and the receiver approach each other, the phases of the transmitted signal, thus received at the receiver, will change relatively faster due to this relative velocity compared to the phase change observed when the distance between them is constant. This consequently results in an effective increase or decrease in the frequency of the signal as experienced by the receiver. This phenomenon occurs whenever the effective optical path between the transmitter and the receiver changes with time. So, if we represent the received signal phase φ_r as

$$\varphi_r = \varphi_t - \frac{2\pi}{\lambda}\text{R} \tag{7.22}$$

where φ_t is the current phase at the transmitter, R is the range between the transmitter and the receiver, and λ is the wavelength, then the corresponding change in the received phase due to the change in R with time will be

$$\frac{d\varphi_r}{dt} = -\frac{2\pi}{\lambda}\frac{dR}{dt} \tag{7.23A}$$

This change in phase is solely due to the change in the intermediate path of the signal and is in addition to the true change in the signal phase by the signal generator at the transmitter. So, it causes an additional frequency deviation δf and is equal to

$$\begin{aligned}\delta f &= \frac{1}{2\pi}\frac{d\varphi}{dt}\\ &= -\frac{1}{\lambda}\frac{dR}{dt}\\ &= -\frac{v}{\lambda}\end{aligned} \tag{7.23B}$$

In the ionosphere, the increase in the effective path length due to the ionospheric TEC is given in Eq. (7.21). So, as the TEC varies with time, so does the effective additional path. This, in turn, results in additional phase variation, causing a change in the received frequency even if the satellite-receiver distance remains constant. So, the total effective path variation is the sum of the geometric path variation and the variation due to the change in TEC along the path. The effective rate of phase variation at the receiver resulting in a change in received frequency due to the change in TEC along the path is the ionospheric Doppler.

Using Eq. (7.21C), we found that the excess pth due to TEC is $dl = 40.3\ TEC/f^2$. Hence, the rate of change in this path is d(dl)/dt. The corresponding ionospheric Doppler will therefore be

$$df = \frac{1}{\lambda}\left(\frac{40.3}{f^2}\right)\frac{d(TEC)}{dt} \tag{7.24}$$

There are techniques to estimate the ionospheric path delay utilizing this ionospheric Doppler after segregating it from the Doppler due to geometric path variation (Acharya, 2013).

7.4.1.1.4 Ionospheric scintillation

Ionospheric scintillations are the rapid fluctuations in the phase and amplitude of the received signal as it passes through the ionosphere. Scintillations are caused by local rapid variations in the ionospheric refractive index due to the local irregularities in the electron density along the path through which the wave is traversing. In equatorial regions of the ionosphere irregularities are generated after the local evening. It also caused abrupt small regions of very low electron density surrounded by higher density regions. These are called ionospheric bubbles, which move from near the equator toward the higher latitudes, approximately along the geomagnetic lines of force. These are prominent sites of ionospheric scintillation (DasGupta et al., 1982). Their details will also be discussed in Chapter 9. Both amplitude and phase scintillations are formed

by destructive and constructive combinations of the signals occurring in a random manner.

It is very important to understand here that the ionospheric scintillations do not *directly* affect the code-based range measurements of the navigation signals like the ionospheric delays, since it does not affect the propagation time. However, heavy scintillation may lead to a sudden lowering of the received power, such that it results in inaccurate identification of the correlation peak at the receiver correlator, thus deteriorating the accuracy of the range estimates. Rapid phase variations combined with lower signal power may cause the phase-locked loop to lose its lock to the respective signal. This, in turn, may degrade the dilution of precision (DOP) and thus affect accuracy. The scintillation effects, like the delay, are more severe in the equatorial regions and during the high solar activity time (Bandyopadhayay et al., 1997). Typically, the lower L band frequencies are more affected than the higher frequencies.

7.4.1.2 Tropospheric effects

The troposphere is the part of the atmosphere that lies nearest to the Earth's surface. It extends up to about 12 km from the Earth's surface and comprises the gaseous components most important for living beings. It is mainly made up of nitrogen and oxygen, while other gases like CO_2, water vapor, and traces of a few other gases are also present. There is also liquid water and other precipitable elements present in the troposphere at definite heights. These constituents remain mixed in almost fixed proportions. However, over time and space, they vary, though not significantly. As navigation signals pass through these dry and wet components of the troposphere, they incur some related impairments that affect the ranging.

7.4.1.2.1 Tropospheric delay

As the navigation signal travels through the different parts of the atmosphere, it experiences varying refractive indices, which are different from those of the vacuum. Therefore, these electromagnetic waves passing through the troposphere experience a velocity different from the velocity in the vacuum, c. So, according to the Fermat principle, the ray bends to minimize the total optical path (Ghatak, 2005). Consequently, the satellite signals transmitted by the satellites experience an additional delay in reaching the receiver on the ground. The excess refractive index of the medium over the vacuum is $\Delta n = n - 1$. The additional delay accounted for by the signal as it passes through a length *dl* of this layer of the atmosphere is given by

$$\begin{aligned} dt &= dl/v - dl/c \\ &= dl(n/c - 1/c) \\ &= (dl/c)(n - 1) \end{aligned} \tag{7.25A}$$

So, the effective excess path Δr added by the troposphere during ranging is

$$\Delta r = \int_L c\,dt = \int_L (n - 1)\,dl \tag{7.25B}$$

where L is the total length of the path through the troposphere. It is interesting to note that the tropospheric refractive index n exceeds that of the vacuum by a very trivial amount. So, $n - 1$ is a very small number. To make it convenient for use, this term is scaled up by 10^6 to generate the tropospheric refractivity N, that is, $N = (n - 1) \times 10^6$. This term N may now be directly used for calculating the delay with appropriate scaling.

The parameter N can be divided into dry and wet components, N_d and N_w, respectively. The dry component is contributed by the gases, while the wet components are from the water vapors and liquid water present in this region. Although the absolute values of the delay are comparatively small, the relative contribution of the dry component is much greater than the wet component. However, the variability of the wet component is many times greater than the dry component. Both of these components result in a delay in the signal and hence introduce errors in navigation receivers during ranging. But, unlike the ionosphere, here the delays are not dispersive, that is, they do not depend upon the frequency of the wave traveling through it. So, as $dn/d\omega = 0$, the same delay is experienced by all the frequencies.

This erroneous excess range needs to be eliminated from the measurements, and for that, we need to know the delay exactly. There are models to find out the delays offered by the dry and wet components of the troposphere.

7.4.1.2.2 Attenuation

The tropospheric components, like rain, fog, clouds, vapor, etc., are all responsible for the attenuation of the waves traveling through the troposphere. In this part of the atmosphere, the main causes of attenuation are absorption and scattering. These phenomena occur when the wave interacts with the tropospheric elements mentioned above.

Absorption involves dissipation of the energy of the wave as it passes through the tropospheric elements. In conductors or imperfect dielectrics having finite conductivity, this occurs in the form of the movement of the electrons, that is, conduction current due to the incident field, causing dissipation. Each water droplet present in the rain, cloud, fog, etc. may be treated as an imperfect dielectric, and the traversing wave loses a part of its energy as it is incident on them during propagation.

Scattering involves the diversion of the directed energy of the wave to different directions. Under the influence of the electric field of the propagating signal, the water molecules exhibit electronic polarization using a part of the incident energy. It occurs during part of the complete phase cycle of the incident field. Consequently, the energy of the wave is transferred to the molecule as potential energy. This energy is released and transferred back by the medium in the other part of the phase cycle of the wave when these molecules in the medium act as secondary sources of radiation. However, the released energy is not only radiated in the direction of the actual wave but also gets scattered in all other directions in a noncoherent manner. Hence, there is an effective cause for the loss of the wave energy.

The more the wave interacts with the scattering particles, the more the attenuation, and hence the effect increases with heavier rain rates, denser medium, and longer effective paths through the medium. It is also to be noted that there are associated scintillations experienced by the wave on passing through the troposphere. However, the attenuation and the tropospheric scintillations are low at frequencies typically used for navigation and also do not affect the ranging process.

7.4.1.3 Multipath

Multipath is the phenomenon of fluctuations in signal strength formed by the incoherent combination of the direct signals with the same signal coming from different directions through reflection, scattering, etc. Due to the extra path traveled by the multipath components of the signal and also due to the reflection or scattering, these indirect components of the signals have different amplitudes and phases compared to the one received directly. Therefore, upon combination, there occurs an abrupt phase change of the wave and consequent reduction in the amplitude of the signal. The strength of the variation depends on the site and the distance from which the reflection takes place.

In Chapter 5, we found that the received direct signal enters the correlator, where it is correlated with the local code and the delay in the prompt version of this local code required to achieve the peak is identified as the propagation time and it is then utilized to find the range. You may recall that this identification of the peak was done by comparing the correlation values with early and late versions of the local code with the incoming signal. In the discriminator, the early and late correlation values exactly balance and reduce to zero when the prompt version of the code at the receiver is exactly aligned with the incoming one.

In the case of multipath, the incoming signal is a compound signal containing the direct and a reduced portion of the reflected signal, which is also different in phase and amplitude.

Such a compound signal affects the ranging by shifting the balanced condition due to the presence of the additional delayed signal. Let N be the total number of bits in the sequence of interval T. Δ is the offset of the prompt code from the true incoming code, and τ is the early and late offsets. We shall consider only small values of the offset Δ such that $|\tau| > |\Delta|$. The offset of the incoming code with the late code is $(\tau - \Delta)$, and that with the late code is $(\tau + \Delta)$. With this offset, the correlation Rc of the early code with the incoming signal will be

$$\begin{aligned} R_c(\Delta + \tau) &= \frac{1}{N} \int c(t + \Delta + \tau)c(t)dt \\ &= \frac{1}{N}\left[1 - \frac{|+\tau + \Delta|}{T}\right] \\ &= \frac{1}{N}\left[1 - \frac{(\tau + \Delta)}{T}\right] \end{aligned} \tag{7.26A}$$

Similarly, the correlation value with the late code is

$$\begin{aligned} R_c(\Delta - \tau) &= \frac{1}{N} \int c(t + \Delta - \tau)c(t)dt \\ &= \frac{1}{N}\left[\left(1 - \frac{|-\tau + \Delta|}{T}\right)\right] \\ &= \frac{1}{N}\left[1 - \frac{(\tau - \Delta)}{T}\right] \end{aligned} \tag{7.26B}$$

So, from the above, we find that the balanced conditions can only occur when $|\Delta| < |\tau|$, and the condition required to be satisfied for it may be given as:

$$\begin{aligned} R_c(\Delta + \tau) &= R_c(\Delta - \tau) \\ \text{or, } \Delta + \tau &= \tau - \Delta \\ \text{or, } \Delta &= 0 \end{aligned} \tag{7.27}$$

Now, if, in addition, another delayed version of the signal is received due to multipath, the total autocorrelation function becomes different. We shall estimate the error thus occurring for the simplest case when the delay δ due to the multipath is small, such that $|\tau| > |\delta + \Delta|$. We have a correlation with the delayed signal for the early code as

$$\begin{aligned} R_c(\Delta + \tau) &= \frac{1}{N} \int c(t + \Delta + \tau)c(t - \delta)dt \\ &= \frac{1}{N}\left[1 - \frac{|\tau + \Delta + \delta|}{T}\right] \\ &= \frac{1}{N}\left[1 - \frac{(\tau + \Delta + \delta)}{T}\right] \end{aligned} \tag{7.28A}$$

For the late section of the correlator, the correlation value becomes

$$\begin{aligned} R_c(\Delta - \tau) &= \frac{1}{N} \int c(t + \Delta - \tau)c(t - \delta)dt \\ &= \frac{1}{N}\left(1 - \frac{|-\tau + \Delta + \delta|}{T}\right) \\ &= \frac{1}{N}\left[1 - \frac{(\tau - \Delta - \delta)}{T}\right] \end{aligned} \tag{7.28B}$$

Now, if we assume that both the direct and the multipath signals reach the receiver with the same strength, then the altered condition for the balance is

$$\begin{aligned} (\tau + \Delta) + (\tau + \Delta + \delta) &= (\tau - \Delta) + (\tau - \Delta - \delta) \\ \text{or, } \tau + \Delta + \tau + \Delta + \delta &= \tau - \Delta + \tau - \Delta + \delta \\ \text{or, } 4\Delta &= -2\delta \\ \text{or, } \Delta &= -\delta/2 \end{aligned} \tag{7.29}$$

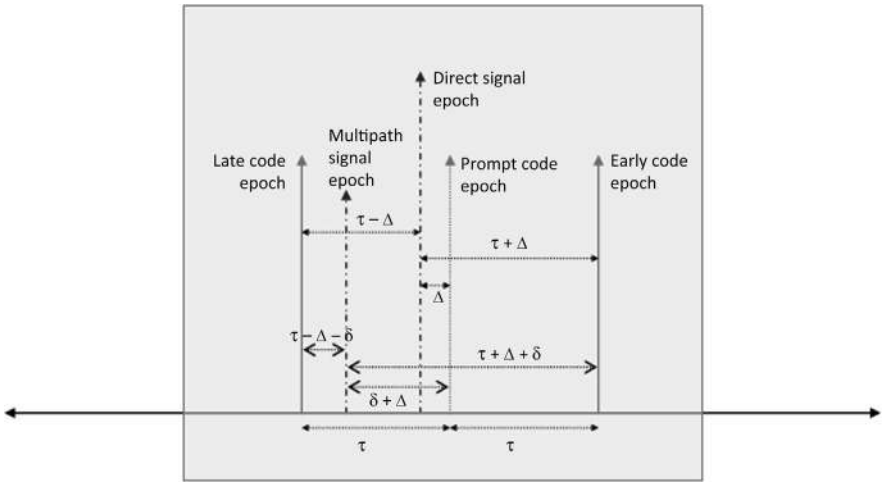

FIGURE 7.5

Relative code phase conditions for multipath scenario.

So, instead of $\Delta = 0$, the balance condition is achieved when the offset of the local code with the true signal is $\Delta = -\delta/2$. Therefore, there is an error in the estimate of travelling time by $\delta/2$.

Fig. 7.5 illustrates the relative code phase conditions for both scenarios in which the delay due to multipath is δ.

It follows from the above that in such a case, the discriminator does not go to zero exactly when the two codes are aligned, but at some skewed value. This is because, even when the early and late components of the autocorrelation balance for the direct component, the multipath component adds a nonzero component to it and hence biases the zero crossing condition. So, this causes the range error to occur.

In the above example, we have implicitly considered that the received power of the direct and the multipath signals is exactly the same at the point of correlation.

7.4.2 User segment error

7.4.2.1 Receiver noise

Receiver hardware always has some noise associated with it. It also picks up noise from the external environment in the receiver band while receiving the signal. This noise adds up with the signal and corrupts the measurement process, and hence the measurements and the estimates, in turn, deviate from their true values. The effect of the receiver thermal noise and the phase noise on the measurement process has already been discussed in Chapter 5. Recall that we estimated the error that occurred during the code tracking as a result of noise in the discriminator of the loop. Although the long-term average of this noise is zero, the individual discrete measurements have random errors, which cause the receiver to assume the peak of the correlation at a point slightly deviated from the true peak. This, in turn, causes an error in the estimation

of the propagation time, eventually resulting in a ranging error leading to the wrong estimation of the user position.

7.4.2.2 Receiver clock bias

Receiver clocks, being typically inexpensive quartz clocks, are relatively less precise than the atomic clocks of the satellites and drift over time. Hence, at any instant, the clock shows a relative bias and drift compared to the satellite or system time. This has already been discussed in Chapter 6, and its effect is included in the nominal observation equations for estimation during position fixing.

7.4.2.3 Receiver hardware bias

As the signal passes through the hardware of the receiver, due to the finite hardware delay time, it experiences some lag between the instant of being received at its antenna phase center and being identified at the correlator. This adds up as an additional propagation delay and hence results in some very small but finite ranging error. These delays are generally dependent upon the signal frequency. So, in a receiver, especially with multiple frequencies, this dispersive delay may have a significant effect and should be taken care of very well.

7.4.3 Overall effect

Consider an observation equation in the form given in Eq. (7.6), rewritten here for convenience,

$$R = \sqrt{(x_s - x_u)^2 + (y_s - y_u)^2 + (z_s - z_u)^2} + c\delta t_u - c\delta t_s + \delta r_{eph}$$

We have already mentioned that in such an equation, we always equate the measured value of the range R, that is, the left-hand side of the equation, to the theoretical expression of the same, giving the geometric range on the right-hand side. Since the measured range has different errors that add up with it the corresponding equivalent range errors are required to be added to the geometric range to equate this as the true model of the range. The added terms account for the errors, like the receiver clock error, satellite clock error, and ephemeris error effects, as they have been added to the equation. In cases where any of these impairment parameters go unaccounted for or the necessary parameters are not used, it leads to an error.

More precisely, adding the errors mentioned above, the updated range equation turns into

$$R = \sqrt{(x_s - x_u)^2 + (y_s - y_u)^2 + (z_s - z_u)^2} + c\delta t_u - c\delta t_s + \delta r_{eph} + \delta r_{ion} + \delta r_{trp} + \text{other errors} + \varepsilon \tag{7.30}$$

where $\delta r_{eph,}$ $\delta r_{ion,}$ and δr_{trp} represent the effective range error due to the ephemeris error, ionospheric, and tropospheric delay of the signal, respectively. The other errors include the ranging errors due to multipath, etc., and ε represents the error due to noise.

Due to the total effect of all the errors, the true range is not known exactly. The measured range from satellite to receiver is an estimated range with errors and is called pseudorange. The following Box 7.4 demonstrates the effect of random errors and bias type errors in ranges.

BOX 7.4 MATLAB

The MATLAB program estimation_error.m was run with 10 m (1σ) of random error in the ranges, which has a normal distribution. The plot of the errors obtained for random bias for different ranges is shown below (Fig. M7.4A).

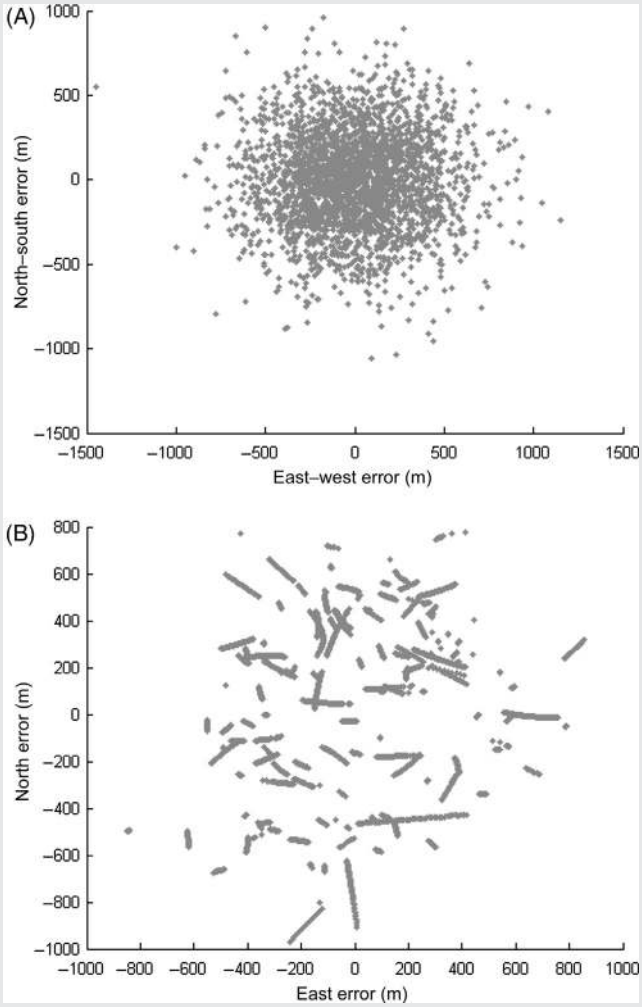

FIGURE M7.4

(A) Error plots for continuously distributed random error, (B) Error plots for discretely distributed random error.

Observe how the estimated position spreads about the true position. The spread similarly shows a normal distribution in its radius. Also note that the position estimation errors are larger in magnitude than the random error introduced.

The same program was run with random but discretely different biases, with biases −5, 0, +5, and +10 for the four ranges used, and the above plot was obtained. Observe in Fig. M7.4B that the errors are now collated into groups. However, they show abrupt change with time to form another collation. The changeover occurs when the satellites used for estimation are changed to different sets.

Run the MATLAB program estimation_error.m with different values of 1σ error with the random error option and observe how the estimated positions spread about zero values. Run the same with the random bias option. See the errors. Compare them.

7.5 Techniques of error mitigation

You must agree by now that the range values thus obtained through measurement cannot be directly used at the receiver for position fixing. This is because a wrong solution of the user position will be obtained unless all the error terms are removed. This readily follows from Eq. (7.2). So, our next objective will be to remove the excess errors in the measured pseudorange to get the accurate solution. The need for correcting errors in the pseudorange equation can also be understood from the above exercise in Box 7.2. So, the extra terms in addition to the geometric range and receiver clock bias are required to be eliminated from the equation. Correction of error terms is generally made in two ways, as discussed in the following subsections.

7.5.1 Reference-based correction

In reference-based correction, there exists a reference station whose position is exactly known. The true position of this reference can be obtained by using some different independent means, like ground-based surveying. The reference station can derive the values of the range correction by comparing the measured and the expected range and update this information as frequently as required, and also can disseminate it to the users around it.

As we have seen, the error in the solution for position X is given by Eq. (7.2) as $dX = G^{-1}\ dR$. Here, dX is the error in position solution, G is the observation matrix depending upon the satellite–receiver geometry, and dR is the ranging error.

The ranging errors dR of the users may be assumed to be equal to the dR of the reference station. Furthermore, if the users are adequately near to the reference, even the G may be assumed to be almost the same. In such a case, the dX will also be the same between the user and the reference. Then, corrections are generally carried out in which the reference station informs the user only about the position errors dX. The reference station obtains this error by comparing its true position with that estimated using the satellites. This difference is transmitted to the users located near

the reference. The users utilize the same errors in their estimated position to correct them. The users derive their position X, obtained by using their own measured range R and their own value of G, and then using the correction dX transmitted by the reference station, correct their position estimates to precise values. However, this method of correction is only valid for limited conditions and is not typically used.

For most practical cases, G cannot be the same for the users and the reference receivers. In such cases, the individual range error for different satellites, dR, is derived by the reference station, which is transmitted to the users. These ranging errors are used by the users as appropriate in generating their own observation equations. So, they correct their measured range R using this. The users also generate their own G to find their position estimate, X. However, here only the constant and the correlated errors can be corrected with a certain accuracy. There are still uncorrelated errors, which differ drastically between positions of reference and those of the users, and these errors cannot be corrected in this way. All these and other methods of differential corrections will be discussed later in Chapter 8 in an elaborate manner.

We have already learned about the satellite clock shift in Section 7.3.1. What is important here is that these clocks are continuously tracked by the ground system, and the corrections for the clock drifts are generated. The clock biases and drift parameters, estimated at the master control station (MCS) are then transmitted to the user through navigation parameters at appropriate intervals. Here, the MCS derived values act as the reference for all users. The MCS estimates and disseminates the corrections in real time. The MCS utilizes sophisticated methods and tools to generate accurate deviations in the satellite clocks. Although these methods are very accurate, there still remains some error in estimating the clock drift and bias by the ground segment. So, some amount of residual error, however trivial, remains uncorrected while range measurements are done at the receiver. Since clock errors are constant errors and the same for all users, both the reference station and the users may correct these errors in their respective ranges.

7.5.2 Direct estimation of errors

Save the clock error, which is estimated and transmitted typically by the system itself, the reference-based correction of errors over a large geographical area demands augmented facilities to cater to the error information for the users. However, this causes the limitations of the usage, puts additional compulsion on the receiver to receive reference station data, and obviously increases the cost of usage and operation as well.

Direct estimations are made using models and real-time measurements and need no additional reference for correction. The various error terms that are directly estimated are described in the following sections.

7.5.2.1 Ionospheric error

In the navigation services, generally two or more frequencies are used for the transmission of the data. However, depending upon the requirements, the receivers

can be of single frequency type, or dual or multiple frequency type. The former can receive signals only in one of the available frequencies, while the latter can receive and process signals in two or more frequencies. The ionospheric delay being dispersive provides great leverage to the dual- or multiple-frequency users. It enables them to estimate the ionospheric delay on itself. Here is how it is done.

We know that the ionospheric delay adds an equivalent extra range δr_{ion} to the true geometric range ρ during the range measurements, which is a function of frequency f and TEC, as given in Eq. (7.21C) as

$$\delta r_{ion} = \left(\frac{40.3}{f^2}\right)TEC$$

So if the range R_1 measured by a receiver in one of the frequencies f_1, is added with ionospheric delay δr_{1ion}, then

$$\begin{aligned} R_1 &= \rho + \delta r_{1ion} \\ &= \rho + \left(\frac{40.3}{f_1^2}\right)TEC \end{aligned} \tag{7.31A}$$

where ρ is the true geometric range and TEC is the total electron content along the signal path. However, there is no way that this excess path δr_{1ion} can be segregated and derived from this single measurement. So, the TEC values along the path through which the signal passes cannot be known anyway from this.

In dual-frequency receivers, a separate and independent measurement is available in the other frequency f_2. Let the range measured there be R_2; then

$$\begin{aligned} R_2 &= \rho + \delta r_{2ion} \\ &= \rho + \left(\frac{40.3}{f_2^2}\right)TEC \end{aligned} \tag{7.31B}$$

Now, if these two measured ranges R_1 and R_2 are differenced, the result is the difference in the excess path incurred in the two frequencies as the common true geometric range present in both the measurements gets canceled. The difference thus yields

$$R_1 - R_2 = 40.3(TEC)\left(\frac{1}{f_1^2} - \frac{1}{f_1^2}\right) \tag{7.31C}$$

In this expression, since all the other parameters save the TEC are known, we can derive the TEC values from it. The exact relation turns into

$$TEC = \frac{(R_1 - R_2)}{40.3\left(\frac{1}{f_1^2} - \frac{1}{f_2^2}\right)} \tag{7.32}$$

So, once the TEC value at any instant along any definite path is derived and thus known, the true range R can be derived from any of the measured ranges as

$$\rho = R_1 - \frac{40.3}{f_1^2}(TEC)$$

Using the expression for TEC from Eq. 7.32, we get

$$\rho = R_1 - (R_2 - R_1)/\left(f_1^2/f_2^2 - 1\right) \tag{7.33A}$$

Calling $(f_1^2/f_2^2) = m$, we get

$$\rho = R_1 - (R_2 - R_1)/(\mu - 1) \tag{7.33B}$$

On the other hand, single-frequency receivers can correct ionospheric errors using the models of the ionosphere. In these receivers, the corrections are obtained by using parametric models, which provide either the ionospheric delay or the TEC for any location and time, using predetermined coefficients. The two important such models are the Klobuchar model and the NeQuick model. In the Klobuchar model (Klobuchar, 1987), the vertical ionospheric delay is obtained as a function of the local time and geographic location of the receiver. It is a semiempirical model expressed as a half cosine function, given as

$$D(\lambda, \varphi, \tau) = a + b\cos\left\{\frac{(\tau - c)}{d}\right\} \tag{7.34}$$

where D is the vertical delay at local time τ, and the parameters a and c are constants. Parameters b and d represent the amplitude and width of the cosine function. Both b and d are dependent upon the latitude λ and longitude φ of the receiver location and can be derived in the form of their third-order polynomials. The corresponding coefficients are known as Klobuchar coefficients and given for a specific day. The parameter b becomes zero for a certain period of the day when $|(\tau - c)/d| \geq \pi/2$, and then the delay remains constant and equal to 'a'.

However, it is understandable and does not need any special mention that the dual-frequency receivers do better ionospheric corrections than the single-frequency receivers.

7.5.2.2 Tropospheric error

Tropospheric errors are corrected for both wet and dry tropospheric delays using models. Some well-known models are the Hopfield model (Hopfield, 1969) and the Saastamoinen model (Spilker, 1996).

This model presents the height profile of tropospheric refractivity N ($N = 10^6 \times (n - 1)$, where n is the index of refraction). This profile may be used to derive the excess path traversed by the navigation signal, where the excess path is given by $Dl = (n - 1)l$, where l is the true geometric path length. The model is theoretically based on an atmosphere with a constant lapse rate of temperature. It treats "dry" and "wet" components of N separately, giving their profiles with the height of the surface above sea level relative to the heights h_d and h_w, respectively, where the indices have been actually measured. The expression for the total zenith delay is given by

$$\delta r_{trp} = 10^{-6}\left[\int_0^h N_d(h_d)(1 - h/h_d)^4 dh + \int_0^h N_w(h_w)(1 - h/h_w)^4 dh\right] \tag{7.35A}$$

To estimate the zenith delay up to the satellite height, the wet component may be integrated to the tropospheric height of about 12 km, while the dry component needs to be integrated up to the stratosphere due to the presence of considerable amount of refracting gases at these heights, however much less than that in the troposphere. Typically, each model has its own defined height limits, up to which it remains valid.

7.5.2.3 Receiver hardware delay

The receiver hardware delay changes slowly. These delay values may be estimated offline and in advance using different available techniques, and the estimation may be updated at intervals.

7.5.2.4 Other errors

Other errors, such as multipath, can be neither modeled explicitly nor measured, and hence cannot be corrected in this manner. Removal of multipath can be done by using some intelligent design of the receiver, as in a rake receiver. Other methods include using a choke ring for large receivers, or using a properly modeled Kalman filter. Receiver noise can be reduced by using qualified components, reducing the tracking loop bandwidth, or by using a Kalman filter.

Upon correcting these errors on the measured range, more accurate values of the ranges are derived. Then the position is estimated using these corrected ranges.

7.6 Effect of errors on positioning

In the previous chapter, we found that the position estimated is nothing but the common intersecting point of the four spheres defined with their centers at the locations of each reference satellite and having a radius equal to their respective ranges. This narrows it down to a single point when the ranges are exact. In cases where we have a certain ambiguity in the range, the derived positions are also ambiguous by a certain width. It follows readily that due to the range ambiguity, the intersection sprawls from a point to a finite volume, and the required true position should lie somewhere in this common volume defined by the ambiguous range. The extent of this ambiguous volume will define the accuracy of estimation. So, the intention would be to reduce this uncertainty space to get better accuracy. This is depicted in Fig. 7.6.

In the following section, we shall study, both qualitatively and quantitatively, how this volume, defining the extent of error in position fix, is dependent upon the relative orientation or geometry of the respective four satellites participating in the position fixing. So, the effect of errors on position measurements is defined in terms of dilusion of precision (DOP), which relates the range errors to the position coordinate error. It is a function of geometry that the satellites bear with the receiver and that we shall derive here in mathematical terms.

Let us start with a very simple analogy. Suppose A and B are asked to get the position of a particular place on a map. It was found that A is fairly confident that the longitudinal location of the place is between φ and $\varphi + d\varphi$, but has large ambiguity

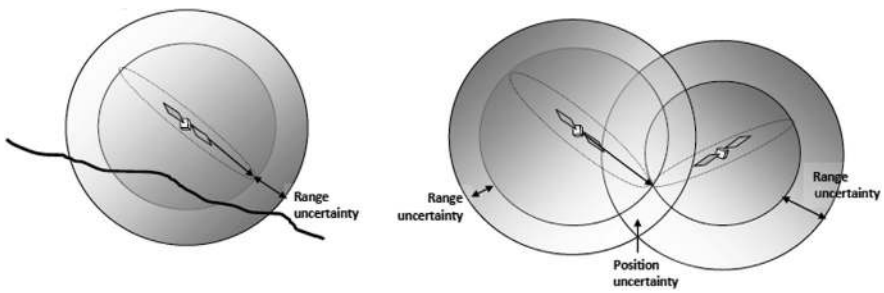

FIGURE 7.6

Orientation of error volume.

over its latitude. On the other hand, B knows almost exactly that the latitude of the place they are looking for is between λ and $\lambda + d\lambda$, but has no knowledge of its longitude. So, combining these facts, the location of the place boils down to a location between longitude φ and $\varphi + d\varphi$ and latitude λ and $\lambda + d\lambda$. Thus, the total uncertainty reduces to an area of $d\varphi d\lambda$, and hence the location can be very easily identified. Now, think what would happen if both of them were uncertain about the latitudinal position of the place. Then, even after combining the information that both of them have, there would have remained a large uncertainty about the latitude of the place. This indicates that better positioning can be done if the ambiguities of the information, by combining which we derive the position, are independent and differently directed, preferably orthogonal.

In the real scenario of position fixing in a 3D environment, after correcting the range error to the maximum possible extent, there still remain some residual range errors, which cause ambiguities while deriving the positions. This indicates that the true position should lie within an annular spherical cavity where the width of the annularity is the range ambiguity, σ_r. Now, notice that after correction, the residual error can only be specified by the statistical parameters of standard deviation σ_r or variance, σ_r^2, assuming zero mean error over a large ensemble.

Now, the range ambiguity from another satellite will also produce a similar annular ambiguity space. If the satellites are so placed that these ambiguity spaces have much overlap, it will result in large effective uncertainty in position fixing. But, had the other satellite been positioned such that the ambiguity spaces intersect each other orthogonally or nearly so, it would consequently reduce the common uncertainty region, thus improving the precision of the position estimate. It is achievable when the contributing satellites remain well separated from each other. So, with reference to the user point, if we consider a tetrahedron, formed by the user as its apex and four satellites as the four base corners, the above argument indicates that the maximum volume of the tetrahedron will result in the highest precision of the position estimates. This is shown in Fig. 7.7.

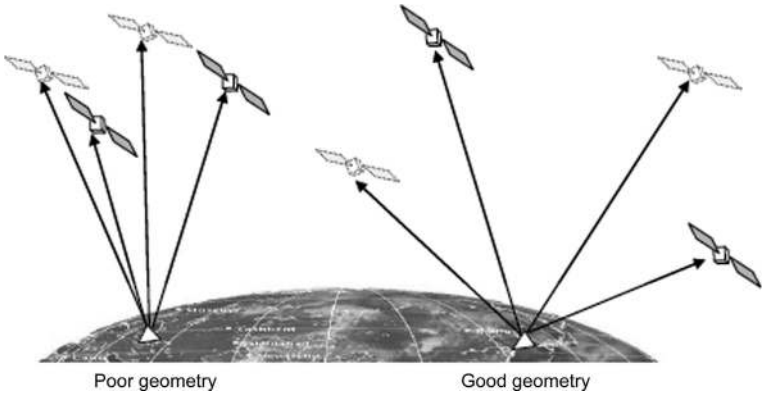

FIGURE 7.7

Desirable positions of satellites for better accuracy.

7.6.1 Dilution of precision

Let us now deduce the fact mathematically that we have stated in the previous subsection. Assuming that the range errors are independent and identical, the solution for position may be obtained as discussed in Chapter 6. However, now, due to the presence of the residual error in the range, there will be some consequent errors in the position estimate. Here, we derive how much these errors will be present in the solution.

For this, let the measured pseudorange R be corrected for its errors, and the residual error that remains after correction be dR. Note that this error is not definite but a stochastic value (otherwise it could have been corrected). So, the pseudorange error is given by

$$\mathrm{dR} = \left[\begin{array}{cccc} \frac{\partial \mathrm{R}}{\partial \mathrm{x}} & \frac{\partial \mathrm{R}}{\partial \mathrm{y}} & \frac{\partial \mathrm{R}}{\partial \mathrm{z}} & \frac{\partial \mathrm{R}}{\partial \mathrm{b}} \end{array}\right] \cdot \left[\mathrm{dx} \quad \mathrm{dy} \quad \mathrm{dz} \quad \mathrm{db}\right]^{\mathrm{T}} = \mathrm{G} \cdot \mathrm{dX} \tag{7.36}$$

where G is the observation matrix depending upon the user–satellite geometry and dX is the geometric error vector including the position errors [dx dy dz] and the clock bias error, db.

This equation relates the position estimation error dX that occurs as a result of the ranging error dR through G. Furthermore, this may be used to obtain the relationship between the covariance of these two sets of errors (Axelrad & Brown, 1996; Conley et al., 2006). Using the above equation,

$$\mathrm{dX} = \mathrm{G}^{-1}\mathrm{dR} \tag{7.37}$$

Multiplying the above equation by its transpose,

$$\begin{aligned} \mathrm{dX}\mathrm{dX}^{\mathrm{T}} &= \mathrm{G}^{-1}\mathrm{dR}\mathrm{dR}^{\mathrm{T}}\mathrm{G}^{-\mathrm{T}} \\ &= \left[\mathrm{G}^{-1}\mathrm{G}^{-\mathrm{T}}\right]\mathrm{dR}\mathrm{dR}^{\mathrm{T}} \\ &= \left[\mathrm{G}\mathrm{G}^{\mathrm{T}}\right]^{-1}\mathrm{dR}\mathrm{dR}^{\mathrm{T}} \end{aligned} \tag{7.38}$$

Now, we take the expectation value on both sides. Considering that the elements of G are definite and fixed, G matrices should remain out of the expectation operation. Hence,

$$\begin{aligned} \mathrm{E}\left[\mathrm{dX}\mathrm{dX}^{\mathrm{T}}\right] &= \left[\mathrm{G}\mathrm{G}^{\mathrm{T}}\right]^{-1}\mathrm{E}\left[\mathrm{dR}\mathrm{dR}^{\mathrm{T}}\right] \\ &= \left[\mathrm{G}\mathrm{G}^{\mathrm{T}}\right]^{-1}\sigma_{\mathrm{R}}^{2} \\ \text{or,} \quad \sigma_{G}^{2} &= \mathrm{H}\sigma_{\mathrm{R}}^{2} \end{aligned} \tag{7.39}$$

where $\mathrm{H} = \left(\mathrm{G}_{1}^{\mathrm{T}}\mathrm{G}_{1}\right)^{-1}$ and $\sigma_{\mathrm{R}}^{2} = \mathrm{E}\left[\mathrm{dR}\mathrm{dR}^{\mathrm{T}}\right]$, and we have assumed that dR is the same for all satellites.

Notice that the diagonal elements of the expectation values of the matrix E[dX dX^{T}] are nothing but the covariance of the individual errors along different axes. So, equating them to the diagonal elements of H matrix, we get

$$\begin{aligned} \mathrm{E}\left[\mathrm{dx} \quad \mathrm{dx}^{\mathrm{T}}\right] &= \sigma_{\mathrm{x}}^{2} = \mathrm{H}_{11}\sigma_{\mathrm{R}}^{2} \\ \mathrm{E}\left[\mathrm{dy} \quad \mathrm{dy}^{\mathrm{T}}\right] &= \sigma_{\mathrm{y}}^{2} = \mathrm{H}_{22}\sigma_{\mathrm{R}}^{2} \\ \mathrm{E}\left[\mathrm{dz} \quad \mathrm{dz}^{\mathrm{T}}\right] &= \sigma_{\mathrm{z}}^{2} = \mathrm{H}_{33}\sigma_{\mathrm{R}}^{2} \\ \mathrm{E}\left[\mathrm{db} \quad \mathrm{db}^{\mathrm{T}}\right] &= \sigma_{\mathrm{b}}^{2} = \mathrm{H}_{44}\sigma_{\mathrm{R}}^{2} \end{aligned} \tag{7.40}$$

These equations show that the variances in position estimates depend upon two factors:

1. The variance of user range error $\left(\sigma_{\mathrm{R}}^{2}\right)$.
2. The elements of matrix H that depend upon G and in turn on the user–satellite geometry.

From the above derivations, we can express the standard deviation of errors along any coordinate axes in terms of the standard deviation of the error in range measurement. So,

$$\begin{aligned} \sigma_{\mathrm{x}} &= \sqrt{\mathrm{H}_{11}}\sigma, \\ \sigma_{\mathrm{y}} &= \sqrt{\mathrm{H}_{22}}\sigma_{\mathrm{r}}, \\ \sigma_{\mathrm{z}} &= \sqrt{\mathrm{H}_{33}}\sigma_{\mathrm{r}}, \\ \sigma_{\mathrm{b}} &= \sqrt{\mathrm{H}_{44}}\sigma_{\mathrm{r}} \end{aligned} \tag{7.41A}$$

The standard deviation in total position estimation is:

$$\begin{aligned} \sigma_{\mathrm{p}} &= \sqrt{\sigma_{\mathrm{x}}^{2} + \sigma_{\mathrm{y}}^{2} + \sigma_{\mathrm{z}}^{2}} \\ &= \sigma_{\mathrm{R}}\sqrt{\mathrm{H}_{11} + \mathrm{H}_{22} + \mathrm{H}_{33}} \\ &= \mathrm{PDOP} \cdot \sigma_{\mathrm{R}} \end{aligned} \tag{7.41B}$$

where the position dilution of precision (PDOP). $\mathrm{PDOP} = \sqrt{\mathrm{H}_{11} + \mathrm{H}_{22} + \mathrm{H}_{33}}$

Similarly, the standard deviation in time estimation is:

$$\begin{aligned} \sigma_{\mathrm{b}} &= \sigma_{\mathrm{R}}\sqrt{\mathrm{H}_{44}} \\ &\mathrm{TDOP} \cdot \sigma_{\mathrm{R}} \end{aligned} \tag{7.41C}$$

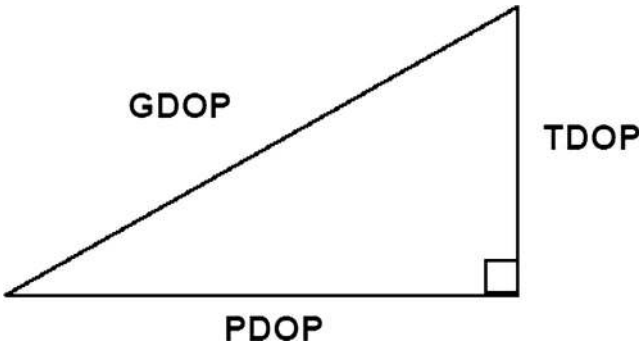

FIGURE 7.8

Relationship between the DOPs.

where the time dilution of precision (TDOP), $\text{TDOP} = \sqrt{H_{44}}$

So, the standard deviation of total error is

$$@rcl@\sigma_G = \sqrt{\sigma_x^2 + \sigma_y^2 + \sigma_z^2 + \sigma_b^2} = \sigma_R\sqrt{H_{11} + H_{22} + H_{33} + H_{44}} = \text{GDOP} \cdot \sigma_R \tag{7.42}$$

where the geometric dilution of precision, $\text{GDOP} = \sqrt{H_{11} + H_{22} + H_{33} + H_{44}}$

Thus, the various "DOPs" parameters are defined as above on the basis of the stochastic error equations. They provide a quantitative contribution of the user–satellite geometry to the error. Comparing, we can see that

$$\text{PDOP}^2 + \text{TDOP}^2 = \text{GDOP}^2 \tag{7.43}$$

Recalling the Pythagoras theorem, the relationship between GDOP, PDOP, and TDOP may be looked upon as the three sides of a right-angled triangle, where PDOP and TDOP form the two perpendicular sides of the triangle and GDOP is the hypotenuse (Fig. 7.8).

The DOP depends upon the geometry of the participating satellites (Spilker, 1996). We have seen intuitively that the wider the satellites are separated, the better the accuracy. Now, let us see the same from the mathematical perspective using the expressions that we have developed. In terms of GDOP, for better accuracy of position, for any definite range error, the elements of the H matrix should be small. Now, $H = (GG^T)^{-1}$, and hence, as H is generated by the inverse of the G and G^T matrices. So, for the above condition to be satisfied, the G matrix should be well conditioned, that is, G should not be singular or near singular, or in other words, the value of the determinant of G should be far away from zero, as already mentioned in Section 7.1. This is possible when the two rows in the G matrix are not similar or close to each other and preferably orthogonal. Now, when can the two rows of the G matrix be

similar? The G elements are constituted by the directional cosines of the satellites at the receiver point. The two rows of G can come closer if all these direction cosines are almost the same, that is, two satellites are closer by. To satisfy the above criterion of well-conditioned G, the directional cosines of two satellites, constituting two rows of the matrix, should not be equal or near to each other. Therefore, it implies that positions of the different satellites must be very different from each other; that is, the satellites should have the widest separation, as seen from the receiver.

The standard deviation of the range error, incurred by the user referred to as "σ_r" above, is also called the σ_{UERE}, where UERE stands for user equivalent range error.

7.6.2 Horizontal and vertical dilution of precision

The geometric DOP or its positional component, that is, PDOP, can be resolved into components about the conventional axes of coordinates, viz. X, Y, and Z, as given in Eq. (7.41A).

$$\begin{aligned}\sigma_x^2 &= H_{11}{s_R}^2\\ \sigma_y^2 &= H_{22}{s_R}^2\\ \sigma_z^2 &= H_{33}{s_R}^2\\ \sigma_b^2 &= H_{44}{s_R}^2\end{aligned}$$

But these components, although easy to derive, are not in a convenient form of representation. Expected errors or their precisions about the Earth-centered X, Y, or Z direction do not give a feel of the error magnitude and sense to one who is measuring the position at a local point on the ground. So, these DOP parameters are converted to a more convenient form in local coordinates, and they are along the local horizontal and vertical directions. They are accordingly referred to as horizontal DOP (HDOP) and vertical DOP (VDOP), and obtained by decomposing the PDOP along horizontal and vertical directions, respectively.

7.6.3 Weighted least squares solution

The position solution obtained in Chapter 6 through linearization was based upon a fundamental assumption that the ranges have no error in them. However, the same approach is valid when the range errors for all the satellites are statistically independent and identical. It is on this assumption that the DOP values have been developed in the last subsection. However, this is not true in pragmatic cases. Often, this error, also represented by the σ_{UERE}, is neither independent nor identical. So, under such conditions, the least squares position estimate does not hold good as an optimal estimate.

If the pseudorange errors are Gaussian and the covariance of ranging errors ε for the visible satellites is given by the matrix M, then the optimal solution for user position relative to the approximated point Xa, as described in Section 6.4, is given by the weighted least squares estimate (Strang, 1988).

$$dX = \left(G^T M^{-1} G\right)^{-1}\left(G^T M^{-1}\right)dR \tag{7.44}$$

Check that this expression converts to the conventional form when the errors are identical when the error covariance matrix M becomes unity.

7.7 Error budget and performance

It is during the design phase that the maximum permissible range errors allowable in the system are fixed and apportioned to different sources. The upper bound is a hard limit determined by the system's capabilities and defines the system's performance. This is called error budgeting. Any excess error that is introduced into the system during operation is correctable and may be eliminated through appropriate methods. The errors are removed through different processes, as we have discussed in this chapter. Focus 7.2 explains an error budget for a typical satellite navigation system.

Focus 7.2 Error budget

Assuming that the average error over the ensemble is zero, the typical values of the standard deviations of the residual error may be expressed as:

Notice that the errors are individually independent of each other, and the root sum squared values of the errors are taken as the effectual error.

Ephemeris Error	2 m
Clock error	2 m
Ionospheric error	5 m
Tropospheric error	1 m
Receiver noise	1 m
Multipath, etc.	1 m
Total	**6 m**

So, if we take the HDOP and VDOP as 3 and 4, respectively, for a system at a place, the horizontal and vertical precision of the position estimation at that place becomes $6\text{ m} \times 3 = 18$ m and $6\text{ m} \times 4 = 24$ m, respectively.

Conceptual questions

1. Show that the GDOPs derived from the local DOPs are equal to the sum of the GDOPs derived in the Earth-centered Earth-fixed system.
2. Derive the expressions for DOP along north, east, and up directions in an east-north-up system in terms of elevation and azimuth.
3. Pragmatically, the multipath signal comes with reduced power compared to the direct one. Find the condition of correlation balance when the multipath signal power is k times ($k < 1$) the direct signal, and compare with Eq. (7.29).

4. If frequencies f1 and f2 are used in a dual frequency receiver for estimation of the ionospheric TEC, comment on the choice of f1 and f2 values toward more accurate estimates.

References

Acharya, R. (2013). Doppler utilised Kalman estimation (DUKE) of ionospheric delay for satellite navigation. *Advances in Space Research, 51*(11), 2171–2180. https://doi.org/10.1016/j.asr.2012.12.022.

Axelrad, P., & Brown, R.G. (1996). GPS navigation algorithms. In: Parkinson, B.W., Spilker Jr., J.J. (Eds), Global Positioning Systems, Theory and Applications, Vol-I, AIAA, Washington DC, USA.

Bandyopadhayay, T., Guha, A., DasGupta, A., Banerjee, P., & Bose, A. (1997). Degradation of navigational accuracy with global positioning system during periods of scintillation at equatorial latitudes. *Electronics Letters, 33*(12), 1010–1011. https://doi.org/10.1049/el:19970692.

Conley, R., Cosentino, R., Leva, J.L., de Haag, M.U., & Van Dyke, K. (2006). Performance of standalone GPS. In: Kaplan, E.D., Hegarty, C.J. (Eds.), Understanding GPS principles and applications. Second ed. Artech House, MA, USA.

DasGupta, A., Aarons, J., Klobuchar, A., Basu, S., & Bushby, A. (1982). Ionospheric electron content depletions associated with amplitude scintillations in the equatorial region. *Geophysical Research Letters, 9*(2), 147–150. https://doi.org/10.1029/gl009i002p00147.

Ghatak, A. (2005). *Optics*. Tata Mc Graw Hill Publishing Limited.

Hopfield, H. S. (1969). Two-quartic tropospheric refractivity profile for correcting satellite data. *Journal of Geophysical Research, 74*(18), 4487–4499. https://doi.org/10.1029/jc074i018p04487.

Klobuchar, J. A. (1987). Ionospheric time-delay algorithm for single-frequency GPS users. *IEEE Transactions on Aerospace and Electronic Systems, 23*(3), 325–331. https://doi.org/10.1109/TAES.1987.310829.

Parkinson, B. W. (1996). GPS error analysis II. *Global positioning systems*. AIAA.

Reitz, J., Milford, F. J., & Christy, R. W. (1990). *Foundations of electromagnetic theory*. Narosa Publishing House..

Spilker, J. J., Jr. (1996). Tropospheric effects on GPS. In: Parkinson, B.W., Spilker Jr., J.J. (Eds), Global Positioning Systems, Theory and Applications, Vol-I, AIAA, Washington DC, USA.

Strang, G. (1988). *Linear algebra and its applications*. Jovanovich, Publishers.

CHAPTER

Differential positioning and augmentation

8

Preamble

In Chapter 6, we learned how a standalone receiver estimates its absolute position from range measurements. Chapter 7 described the effects of having errors in the measurements from which these positions are derived. In this chapter, we shall find how to reduce the impact of these errors on positioning using *Differential Positioning* techniques. As the name itself suggests, in contrast to absolute positioning, here the positioning is obtained by differencing the measurements of the receiver with respect to some reference measurements or its derivatives. Therefore, it demands the presence of one or more additional receivers as a reference. Here, we shall first elucidate the basic idea of differential positioning and briefly mention the options for correcting ranges using it. Then we shall readily move to a brief review of the types of error. The theoretical aspects of the variation of these errors are essential for understanding the correction techniques and form the basis of different possible variants of the correction approaches. The different techniques of differential positioning and their related intricacies will be discussed subsequently in detail, including both the code-based and carrier-based procedures. After generalizing the differential positioning under different theoretical perspectives, we shall finally have some details of two specific implementations, the real-time kinematics (RTK) and the satellite-based augmentation systems (SBAS).

8.1 Differential positioning

To estimate the position of a user, we need mainly two things: the position of the satellite and the range between the user and the satellite. This is evident from the observation equation from which the positions are derived. We have also seen that the range measurement at the receiver is impaired by different factors that introduce additional errors to these measurements. Although these errors are either estimated through measurements or by using models for correcting the ranges, the obvious uncertainty involved with these correction processes results in retaining some residuals of these errors. These residual errors effectively deteriorate the final position estimation.

Differential system is the method of eliminating or alleviating these errors with the help of additional reference measurements and their derivatives determined at a

Understanding Satellite Navigation, Second Edition. DOI: https://doi.org/10.1016/B978-0-443-36432-7.00014-6

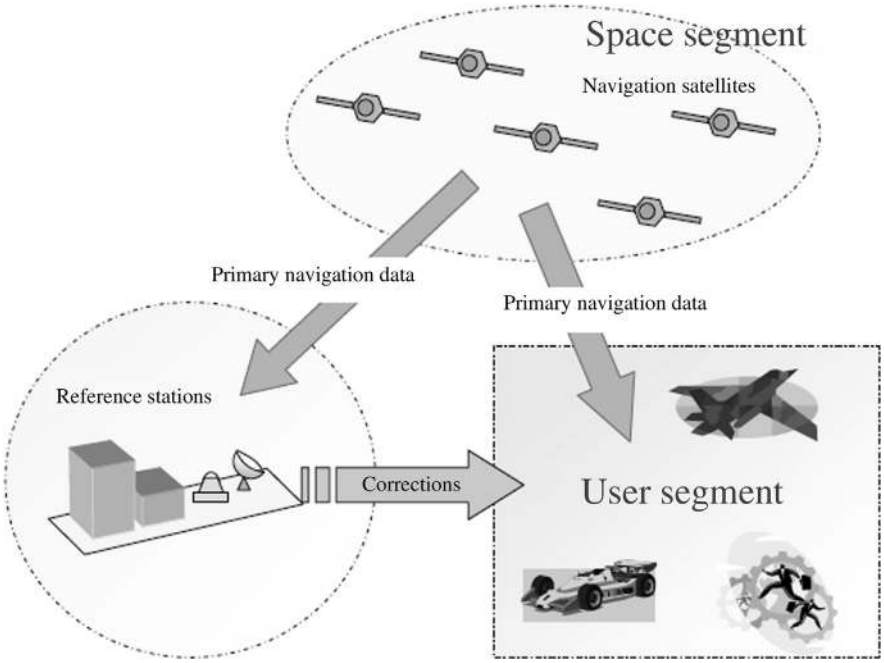

FIGURE 8.1

Schematic for differential system.

reference point whose position is known a priori and very accurately. So, the differential positioning in satellite navigation may be defined as a technique to estimate precise positions using additional information derived from the measurements at the reference receiver situated at a known position.

In such reference-based correction, these reference stations should be able to derive the correct values of the parameters needed for user range error correction and can disseminate this information to the users and update them at the required rate. These parameters may either be probable position errors at the user location or the consolidated range errors, or even be the individual components of the error in ranging. Depending upon the technique used for correction, the disseminated information may also be just the ranges measured at the reference station.

It may be required to transmit the parameters to the users around the reference station in real time or it can be stored for posterior use through post processing. The schematic for a differential positioning system is shown in Fig. 8.1.

8.1.1 Overview of differential corrections

In Chapter 7 we have already learnt about the different sources and types of errors that affect the position estimation at the user receiver. We have also learnt that if these errors can be corrected, the accuracy of the position estimation improves. One of the

techniques of correction is by using the measurements of a reference station whose position is known very precisely. Here, we shall detail the kind of corrections that can be obtained from these reference receivers to correct the parameters for the users.

We have already mentioned that corrections can be done at different levels of the data. It can be done on the final position estimates as well as at the level of measured ranges, as well. To understand the rationale for using the corrections at different levels, we need to recall how we estimated the position from the knowledge of the range of the satellite from the user. We know that the range equation is given by

$$R = h(X) \tag{8.1}$$

Here, R is the range, h is the nonlinear function for the range in terms of the satellite position, $X_{s,}$ and user position, X. We want to know how any change in the user position coordinates is related to the change in the range. Differentiating the above equation with respect to the true position, $X = X_t$, we get

$$\begin{aligned} dR &= (\partial h/\partial X)|_{X_t} dX \\ &= G|_{X_t} dX \end{aligned} \tag{8.2A}$$

Where G is the Jacobian of the range function 'h', denoted by $G = [\partial h/\partial x\ \partial h/\partial y\ \partial h/\partial z]$. This states that any change in the true position by dX of the receiver will lead to the actual change in range by dR, related by Eq. (8.2A). Conversely, a change in the range, due to measurement error, etc., by an amount dR will lead to the position estimation error of dX, where dR and dX are related by

$$\delta X = G^{-1}|_{X_t} \delta R \tag{8.2B}$$

Let the range measurement have a finite error of δR, which results in a position error of δX. Then, the error δR in range measurement is related to δX by the relation 8.2B. With the known position of the reference receiver, G can be easily derived. Knowing G, the above differential relations may be readily obtained. Now, let us see if the position error at the user location may be obtained from the same at the reference station. To get that, let us find how this positioning error δX varies spatially. Differentiating Eq. (8.2B) with respect to X, we get,

$$\begin{aligned} \frac{d}{dX}(\delta X)dX &= \frac{d}{dX}(G^{-1}\delta R)dX \\ &= \delta R \frac{d}{dX}(G^{-1})dX + G^{-1}\frac{d}{dX}(\delta R)dX \end{aligned} \tag{8.3}$$

So, in order that this position error remains invariant between two locations, d/dx (δX) should be zero, which requires the following conditions to be satisfied

$$\frac{d}{dX}(G^{-1}) = 0 \tag{8.4A}$$

and

$$\frac{d}{dX}(\delta R) = 0 \tag{8.4B}$$

It shows that, for the positional error at two places to be equal, it is not sufficient only for the range error δR to be the same. Also, the matrix G, which is determined by the user satellite geometry, needs to be equal at these two places. So, only if both the above criteria are fulfilled, the estimated positional error at the reference remains spatially invariant and hence may be used to correct the estimated positional error at the user. However, this technique has certain major limitations.

First of all, the assumption that G remains identical is unrealistic. Equality of G implies two things. First, it should consist of the same satellites at the user and the reference location. So, the best set of satellites seen by the user should also have to be the best set of satellites amongst those seen by the reference. Under a typical distance between the reference and the user receivers, it is very unlikely that these two sets stay the same. To cater to such a condition, the reference station has to derive its position and the corresponding error values for all possible sets of four satellites amongst the visible ones, so that the user can select one particular set that corresponds to the set he is using. So, the reference station has to derive the solution is ${}^{n}C_4$ number of combinations, where n is the number of visible satellites. Typically, 'n' remains around 7, and hence the total number of solutions set is 35. This is tedious and impractical. Second, recall that the elements of G are constituted by the directional cosine terms cos α, cos β, and cos γ. These terms are functions of position. So, even if the satellite set remains the same, the geometry does not remain the same at the user and the reference locations, thus changing the values of the elements of the G matrix. Therefore, this equality of G demands the user and the reference to always be in very close vicinity. This can only be an approximation, and for most pragmatic cases, they remain different.

The second requirement is the equality of δR, which is nothing but the equality of the ranging errors. As we know from previous descriptions, many of the errors determined by the reference station vary with space and time in a correlated manner. Even the correlated errors retain their correlation within a certain range, and it worsens as the distance between the user and the reference increases. Besides space decorrelation, the time latency between the estimation instant and the instant of applying it for correction makes δR different. So, the ranging error δR, which may be equal between the two locations at a certain instant, may not remain the same after a time interval. So, while the reference and the user have different ranging errors δR or different values of matrix G, the corrections derived in terms of position errors will also not be the same. It implies that, in general, the position corrections are the reference station cannot be directly used at the user receivers.

Next, we once more focus on Eq. (8.2B), which is $G^{-1}\delta R = \delta X$. It follows from the equation that the position estimation errors dX may be reduced by reducing the range errors δR. Again, the range error at the user location, δR_u, may be expressed using Taylor's series in terms of the range error δR_r at the reference receiver as

$$\delta R_u = \delta R_r + \frac{d}{dX}(\delta R_r)|_{Xr} dX + \frac{1}{2}\frac{d^2}{dX^2}(\delta R_r)|_{Xr} dX^2 + \ldots \tag{8.5}$$

where dX is the differential position between the reference and the user. The higher-order terms are practically too small for consideration. So, we can derive the range errors at the user position using those at the reference receiver and its first-order derivatives. This enables the user to correct the measured range, using only the range error information of the reference and the geometry-dependent derivatives evaluated there. Once δR_u is obtained, the matrix G is generated with its own values derived by the user. Using the derived G and the obtained $\delta R_{u,}$ the needed corrections in positions δX are found using Eq. (8.2B). Upon correcting, the precise X values are obtained.

If the measured ranges at the reference receiver and at the user receiver are $R_r^m = R_r + \delta R_r$ and $R_u^m = R_u + \delta R_u$respectively, where R_r and R_u are the true ranges there, then differencing the two measured ranges, we get,

$$R_u^m - R_r^m = (R_u - R_r) + (\delta R_u - \delta R_r) \tag{8.6A}$$

Using Eq. 8.5 in Eq. 8.6A and considering only first-order variations in δR_u, Eq. (8.6A) turns to

$$R_u^m - R_r^m = (R_u - R_r) + \frac{d(\delta R_r)}{dX}|_{Xr}\, dX \tag{8.6B}$$

This removes the spatially invariant and comparatively larger zeroth-order errors of the user receiver from its measurements. Thus, the true range difference between the user and the reference, $\Delta R = R_u - R_{r,}$ may be obtained. When the distance between the reference and the user is comparatively small, the assumption $d(\delta R_r)/dX|_{Xr} = 0$ holds good. Otherwise, the derivatives are required to be derived and used to get the true range difference, ΔR. Then, using the relation again as in Eq. (8.2A), we can write

$$\Delta R = G\Delta X \text{ or, } \Delta X = G^{-1}\Delta R \tag{8.7}$$

So, knowing differential range ΔR, we can find he relative position, ΔX. For this, we only need enough information to construct G defined at the reference point. Thus, relative position may be accurately obtained by differencing the whole range measured by the reference station from the range measured by the user. Once DX is estimated, it may be added to the exact position of the reference station to get the user position. The inaccuracy in reference position, however, affects the whole estimate.

Overall, we found that the spatial variation of the ranging errors plays an important role in all occasions. In the following subsection, we shall learn about the different classes of errors and the methods of eliminating them.

8.1.2 Error review

Before describing the theoretical aspects of corrections that we need to do in a differential system, it is first required to know the characteristics of the errors. Understanding of these characteristics are important for the correction of the range at the user location. So, in this section, we shall briefly review the different types of errors that we learnt in Chapter 7, specifically concentrating upon their spatial and temporal behavior, which forms the basis of their differentiation (Enge, 1996). More

precisely, we need to know the spatiotemporal characteristics of the errors with respect to the reference and the user.

8.1.2.1 Common Errors (ε_0)

Common Errors are those which are common to both reference and user. These are the errors that remain spatially unaltered irrespective of the relative user and reference position. They are also independent of the relative geometry of the satellite and the user. Hence these errors cannot be related to the positions of the satellite or that of the user or even the propagation path between them. In other words, it is global in nature. However, they can vary with time. So, the common error $\varepsilon_0(x, t)$, experienced by a user at a location x at any instant t, can be expressed as

$$\varepsilon_0(x, t) = \varepsilon_0(t) \tag{8.8}$$

For example, the satellite clock error is a common error. These errors, once estimated at any point, can be used at any other point for correction at the same instant. Such errors can be completely removed in differential mode.

8.1.2.2 Correlated Errors (ε_c)

Correlated errors are those for which a definite correlation exists between the value at the reference and at the user receiver location, respectively. These errors are not constant over space but have definite functional forms of variation within this range. Thus, the error at any distance from the reference point may be derived from the error at the reference point, provided this spatial function and the distance between them are known. Therefore, the correlated error ε_c at any point x at any time t may be expressed as

$$\varepsilon_c(x, t) = \varepsilon_c(x_0, t) + \partial\varepsilon_c/\partial x|_{x0,t}dx + \frac{1}{2}\partial^2\varepsilon_c/\partial x^2|_{x0,t}dx^2 + \ldots \tag{8.9}$$

Here, dx is the spatial difference between the reference point x_0 and the user point x. The first and higher-order differentials are derived at x_0 and may vary with time. So once ε_c (x_0, t) is known, $\varepsilon_c(x, t)$ may be estimated by knowing $\partial\varepsilon_c/\partial x$ at the point (x_0, t). Thus, these errors are partially removed after differencing the ranges and more after deriving the spatial derivatives at the reference point and using them for further corrections at the user location. The finite residual that still exists is due to the higher-order components. The effect of neglecting the higher-order derivatives gets worse with increasing distance from the reference point. Hence, the correction degrades with distance.

Propagation errors are correlated errors such that the shorter the distance between the two receivers, the more similar the errors are. Ephemeris errors are also correlated errors, as their values change with the position of the users. However, this change is so small over short distances that the ephemeris errors may be considered to be constant between the reference and user positions when their relative distance is small. Referring to Eq. (8.9), it means the first-order derivatives are negligibly small. We have already derived this quantitatively in Chapter 7.

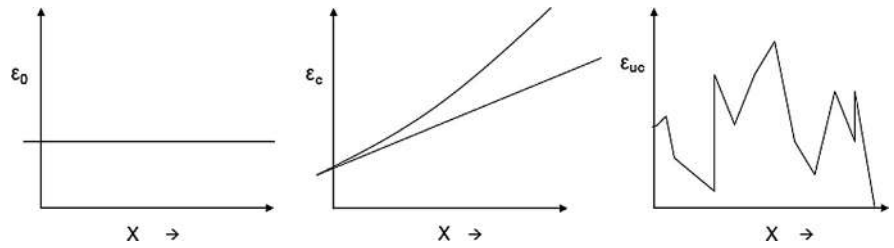

FIGURE 8.2

Variation of different types of errors.

8.1.2.3 Uncorrelated errors (ε_{uc})

There are some errors that are not constant, and neither are they correlated between the reference and the user receivers. These errors are independent between reference and user and spatially vary in a completely arbitrary manner. They are unpredictable and cannot be related by any definite function. Such errors are called uncorrelated errors. Due to the nature of the errors, they can never be estimated for a point from the knowledge of others. Hence, these errors at the user location cannot be derived from those at the reference station, and hence, they cannot be removed at all. Errors due to the multipath and receiver internal thermal noise are a type of error.

All these divisions are based upon the nature of the errors and the manner in which they vary over space. In other words, the basis of this classification is whether the variations in these errors between the reference and the user can be expressed as a function of their separation or not. Fig. 8.2 shows the spatial variations of different types of errors.

In a similar fashion, the errors vary with time. Time correlation of the errors is also important, as the latency between the time of estimation of the error at the reference station and the time of application of the same error at the user receiver determines the accuracy of the corrections. Some of the errors, such as the clock errors, vary quickly, and the corresponding corrections are required to be updated at frequent intervals and used immediately. The other errors, such as the ephemeris errors, vary rather slowly, such that even with considerably large latency between the correction generation and its application, accuracy is not affected much. These errors may be updated at a slower rate.

8.1.3 Classifications of differential positioning

In the differential positioning, the errors of the individual users are eliminated or their impact is significantly reduced by utilizing additional information from the reference station, thus improving the position estimation accuracy. However, the differential positioning can be made using different techniques, which can form the basis of its classification.

In this section, we provide a brief overview of the different basis upon which the differential techniques of positioning can be categorized. Although these are not standard classifications, such systematic distinction helps in the theoretical understanding of the system. We shall discuss these important classes in finer detail in our next section.

8.1.3.1 Position/range-corrected differential positioning

This category is based on the parameter used for which the differential corrections are made. The corrections to be applied at the user receiver can be done at different levels of data. The correction can be done on the final position estimates made in a user receiver, making it a "position differential correction." It may also be applied at the level of measured ranges, which may be referred to as the "range differential correction."

Position corrections are only possible for receivers located at a close proximity to the reference. It reduces the computational load at the receiver and is very simple to apply. However, the range-based correction is a better option than doing corrective operations in the estimated positions, the reasons for which we have already discussed in Section 8.1.1. The range errors may be provided to the user as a whole by the reference receiver in a consolidated manner, or they may be resolved into individual components from various sources, and these components may be supplied to the users for corrections.

The correction parameters are derived by the reference station and are obtained from its own measured ranges. Sometimes, ancillary equipment to measure the atmospheric parameters is also collocated at the reference station from which the corresponding atmospheric delays may be derived. For the most effective applications of these correction parameters, the measurement methods need to be the same in the reference and at the user receiver. Therefore, for position corrections, the method of derivation must be identical, while for range corrections, both the reference and the user must either use code-based ranging or both should employ the carrier phase based ranging method.

8.1.3.2 Absolute/relative differential positioning

For the type of differential positioning in which the measured range is corrected and not the derived positions, there may be two different approaches for correction. In one of them, the correction is done at the user receiver, in which the absolute error parameters are disseminated by the reference. On correcting the measured ranges with these error values, the receiver obtains the ranges which are absolute in terms of the system reference frame, say Earth Centred - Earth Fixed (ECEF), for instance. Consequently, the positions thus derived from it are also absolute with respect to this frame.

Alternatively, the reference may convey its total measured range. So, on differencing this at the user, from its corresponding measurement of range, the resultant becomes a differential range of the user relative to the reference station. This relative range is a function of the relative separation as per Eq. (8.3); all observations are

transformed relative to the reference station, that is, with respect to a new frame centered at the reference position. Consequently, the positions of the user thus derived are also relative, with respect to this reference station only.

Accordingly, the differential positioning may be termed as "Absolute differential positioning," or it can be "Relative differential positioning," respectively. For relative positioning, the vectorial difference between the user receiver and the reference position is determined. It is called the baseline. Baseline determination in relative positioning is possible with both code and carrier-based measurements. It is also possible when either the user receiver is static and does not change its position with time, or when it is dynamic and roving around the reference. Once the relative position is determined, the absolute position of the user may be derived by adding the absolute position of the reference station to it.

8.1.3.3 Code-based/carrier phase-based differential positioning

Depending upon the types of measurements that are used for the corrections at the user and the reference receiver, the differential positioning may be classified into code-based and carrier phase-based differential positioning.

In code-based differential positioning, the code-based measured ranges, which are absolute but noisy measurements, are exchanged or used for corrections. On the other hand, the carrier phase-based differential positions employ the measured phase delay at each receiver for this purpose. Since the measured carrier phase has an integer ambiguity, the differential ranging also needs resolving for this ambiguity. However, the carrier phase-based differential positioning is more precise than the code-based method, since the period of the carrier is much shorter than that of the code.

8.1.3.4 Real-time/postprocessed differential positioning

Depending upon the application for which the differential system is being used, the corrections may be applied in real time for instantaneously obtaining the precise position, or it may be done through postprocessing where the precise results are obtained postfacto. Real-time differential positioning requires a radio communication link to communicate, and the results are obtained almost instantaneously. It is hence important in applications like real-time surveying, although the final accuracy available in such a process is less than that obtained through postprocessing.

Post processing is generally done in the case of carrier phase-based ranging, in which both the reference and the user receiver collect the data, store it, and later share the same for generating the precise corrective values to get accurate positions of the user. Postprocessing results are more accurate (El-Rabbani, 2006) and need no link between the reference and user while giving more options for data corrections and editing.

8.1.3.5 Static/kinematic differential positioning

For a given fixed position of the reference receiver, when the differential positioning is done for the user receiver, which is also stationary in nature, then Static Differential

positioning is said to be done. On the other hand, if the user receiver is moving, or dynamic in nature, then it is called Kinematic differential positioning.

Static differential positioning generates more redundant position solutions and is capable of eliminating zero-mean noise errors upon statistically combining them. Hence, they are more accurate than their kinematic counterparts. Kinematic differential positioning, though it has comparatively lower accuracy, is advantageous for real-time positioning like for auto-navigation applications.

8.1.3.6 Single/multiple-reference differential positioning

Reference receivers are responsible for providing the corrective data to the individual receivers attached to it. Differential positioning may be distinguished by the number of reference receivers it uses. Some may have a single reference to serve a local area, while others may be served by multiple reference stations. It is obvious that the latter option is used to overcome the constraint of the limited spatial boundary that the system can serve. Multiple references are required for a larger area of service, in which additional reference stations are effective to combat the spatial and temporal decorrelations of the error.

Although, in most of cases, the reference stations are used as generating and disseminating correction parameters only, there are systems that use this reference station as an additional source of ranging data, improving the Geometric Dilution of Precision (GDOP). This, in turn, improves the accuracy of the estimation as well as its availability. It also aids in estimation for carrier phase-based ranging, too.

8.2 Differential correction techniques

In this section, we shall explore the different methods employed for differential corrections. We shall start by defining the term baseline, which is the vector joining the user receiver and the reference station. Throughout the discussion, we shall consider that this baseline, indicating the position difference between the reference and the user, is small. This is referred to as a short baseline. This warrants that the satellite range difference between the two stations may be expressed as a linear function of their positional difference, that is, the baseline length. Further, for short baselines, the radio waves incident on the two receivers from the satellite may be assumed to be parallel, and so the angles that the vectors pointing toward the satellite from the reference and the user receivers make with the baseline are the same. It also implies that the ephemeris error is almost constant between the two receivers. The assumed short baseline also keeps the other correlated errors, like the ionospheric and tropospheric errors limited, within the first order of variation. In this discussion, we neglect the effects of the uncorrelated errors, like the multipath.

8.2.1 Code-based methods

8.2.1.1 Absolute differential methods

While estimating positions with code-based range measurement, we have already seen that the results are corrupted with ranging errors. Further, in Chapter 5, we have learnt

that these types of range measurements are noisy leading to poor precision. But, unlike carrier phase-based measurements, these range values are unambiguous. The noise terms include mainly the receiver's self-noise. In addition, the ranges are biased by propagation errors like the ionospheric and tropospheric errors and clock bias. So, the measured range R_r at the reference receiver may be represented as

$$R_r = \rho_r + c\delta t_r - c\delta t_s + \delta r_{ion,r} + \delta r_{trp,r} + n_r \tag{8.10A}$$

where R_r is the measured range at the reference location compared to ρ_r, which is the true range to the satellite from the reference station. $c\delta t_s$ and $c\delta t_r$ are the range equivalent of the satellite and reference receiver clock bias values, respectively with respect to the system time. Similarly, $\delta r_{ion,r}$ and $\delta r_{trp,r}$ are the excess path equivalents for ionospheric and tropospheric delays, respectively, at the reference receiver. n_r is the reference receiver noise.

Similarly, for the user receiver, the measured range R_u is obtained as

$$R_u = \rho_u + c\delta t_u - c\delta t_s + \delta r_{ion,u} + \delta r_{trp,u} + n_u \tag{8.10B}$$

where the variables are the same as those for the reference receiver, with the subscript "u" referring to the user location.

But the reference station knows its precise position. So, it can find out its own geometric range ρ_r from the satellite by finding the Euclidian distance between its own known position and the satellite position derived from the transmitted ephemeris. Hence, it contains the true range r plus the ephemeris error $dr_{eph.r}$. Then, replacing ρ_r in the Eq. 8.10A, it turns into

$$R_r = \rho_r' + c\delta t_r - c\delta t_s + \delta r_{eph,r} + \delta r_{ion,r} + \delta r_{trp,r} + n_r \tag{8.10C}$$

Also, the user can only use the transmitted ephemeris to find the satellite position. Let the range of the user receiver to the ephemeris-derived satellite location, expressed in terms of its (unknown) coordinates be ρ_u'. Therefore, the corresponding range Eq 8.10B becomes

$$R_u = \rho_u' + c\delta t_u - c\delta t_s + \delta r_{eph,u} + \delta r_{ion,u} + \delta r_{trp,u} + n_u \tag{8.10D}$$

So, differencing the measured geometric range, of the reference station from its corresponding Euclidian distance, we get

$$\begin{aligned} \varepsilon_r &= R_r - \rho_r' \\ &= c\delta t_r - c\delta t_s + \delta r_{eph,r} + \delta r_{ion,r} + \delta r_{trp,r} + n_r \end{aligned} \tag{8.11}$$

Now, this collective range errors at the reference receiver location, ε_r can be used by the users to correct their own range errors. On applying this correction, the corrected pseudo-range of the user R_{cu} becomes

$$\begin{aligned} R_{cu} &= \rho_u' + c(\delta t_u - \delta t_r) + (\delta r_{eph,u} - \delta r_{eph,r}) + (\delta r_{ion,u} - \delta r_{ion,r}) \\ &\quad + (\delta r_{trp,u} - \delta r_{trp,r}) + (n_u - n_r) \\ &= \rho_u' + c\delta t_{ur} + \delta r_{eph,ur} + \delta r_{ion,ur} + \delta r_{trp,ur} + n_{ur} \end{aligned} \tag{8.12}$$

where, $R_{cu} = R_u - R_r + r'_r$, $\delta t_{ur} = (\delta t_u - \delta t_r)$, $\delta r_{eph,ur} = (\delta r_{eph,u} - \delta r_{eph,r})$, $\delta r_{ion,ur} = (\delta r_{ion,u} - \delta r_{ion,r})$, $\delta r_{trp,ur} = (\delta r_{trp,u} - \delta r_{trp,r})$, and $n_{ur} = (n_u - n_r)$. Since the reference and the user differ in their error amounts due to their location difference, there remain the error residuals, however small. Here, δt_{ur} is the differential clock bias between the reference and the user. The satellite clock bias term δt_s, being common to both, has been eliminated, and the user clock bias has become relative to the clock bias of the reference station.

Typically, the reference station clock is corrected and disciplined with the satellite clock, and hence, this part contains the error due to the receiver clock error only. The ephemeris error changes very slowly with separation, and hence the relative ephemeris error $\delta r_{eph,u,}$ may be assumed to be insignificant. The ionosphere has a large correlation over space and time. Hence, over smaller distances, the relative ionospheric delay $\delta r_{ion,ur}$, which is nothing but the difference in ionospheric errors at the two stations, is small. Besides, for dual-frequency receivers, the user and the reference station correct their own ionospheric errors. So, for most of the practical scenarios, $\delta r_{ion,ur}$ thus can be taken as zero. The same argument holds for $\delta r_{trp,ur}$ also for short baselines. In such cases, the equation turns into

$$R_{cu} = \rho'_u + c\delta t_{ur} + n_{ur} \tag{8.13}$$

But, this assumption of insignificant residuals of path errors due to the cancellation of the ionospheric and tropospheric delays may not be true for certain geographic regions where the ionosphere gradient is large and for certain periods of time. These delays may substantially change within a limited spatial or temporal extent. For such cases of rapid spatiotemporal variations, the delay at the user position is not the same as that of the reference site, and hence the errors do not exactly cancel out. Then, the ionospheric errors at the user location may be derived in terms of those at the reference station using Taylor's series to represent the spatial variation as

$$\delta r_{ion,u} = \delta r_{ion,r} + \partial(\delta r_{ion,r})/\partial X|_{Xr} dX + \frac{1}{2}\partial^2(\delta r_{ion,r})/\partial X^2|_{Xr} dX^2 + \ldots \tag{8.14A}$$

This makes the difference $\delta r_{ion,\,ur}$ be equal to

$$\delta r_{ion,u} - \delta r_{ion,r} = \partial(\delta r_{ion,r})/\partial X|_{Xr} dX + 1/2\partial^2(\delta r_{ion,r})/\partial X^2|_{Xr} dX^2 + \ldots \tag{8.14B}$$

For short baselines, the higher-order differentials generally do not contribute significantly and hence can be neglected. So, the delay difference may be expressed in terms of the first-order differentials with respect to baseline length only. This derivative is thus required to be derived along with the errors and transmitted to the users for appropriate error cancellations.

Similarly, for the temporal variations, the difference in ionospheric excess path due to the propagation delay between the time of estimation t_1 and the time of application t_2 may be obtained as

$$\delta r_{ion}(t_2 - t_1) = \partial r/\partial t|_{t=t_1} \Delta t \tag{8.15}$$

where, $\Delta t = (t_2 - t_1)$. This temporal derivative may be derived at the reference time. The same argument holds true for the tropospheric errors. These terms help to remove the unbalanced errors between the reference and the user receivers from Eq. (8.12). The changes can be seen in Eq. (8.13).

In cases where these distances are large or the derivatives are large enough, the higher-order terms are so conspicuous that they cannot be neglected. In such cases, the best result is achieved when the user receiver itself is able to estimate its own ionospheric delay. There, the dual-frequency receivers are necessary for correcting their own ionospheric delays. Alternatively, many reference stations may be used such that wherever the user receiver is, it remains within the region of first-order variation of the ionospheric delay for any one of the reference receivers.

It is important to note here that the corrections at the user receiver are done for all errors obtained in a consolidated manner from the reference receiver. These corrections are only restricted to the same specific satellites for which the errors have been derived at the reference. Nevertheless, the composite errors for a specific satellite can be segregated using certain techniques into their individual components. The ionospheric delays may be obtained by using dual-frequency receivers. The tropospheric delays may similarly be obtained from the empirical models using parameters obtained from the meteorological instruments installed at the reference station. Further, systems with a number of reference stations set up over extensive regions can also track the locus of individual satellites and estimate their true current position and thus derive the ephemeris error, $\delta r_{eph,}$ along with the clock errors.

Similarly, as in Eq. (8.13), considering the residues are negligible, the Eq. (8.10D), after corrections of each individual error, turns into

$$R_{cu} = \rho'_u + c\delta t_{ur} + n_{ur} \tag{8.19}$$

So, irrespective of the way the errors are corrected, now we have an equation with three unknowns in ρ_u and an unknown δt_{ur} plus some noise. The corrected ranges, thus contains the geometrically derived ranges to the ephemeris-derived positions of the satellites and the clock bias. This can then be used for generating the observation equation and finding the position of the user. n_{ur} represents the differences in the self-noise between the user and the reference receivers. These noises are random and uncorrelated and hence do not cancel out by any means. So, upon differencing the reference correction, the effective noise thus produced is the difference between the individual noises at the user receiver and the reference station. Since the two noises are independent the effective noise σ after differencing at the user receiver will be

$$\sigma_{eff} = \sqrt{\sigma_u^2 + \sigma_r^2} \tag{8.20A}$$

where σ_u and σ_r are the standard deviations of the individual measurements at the user and of that derived for correction at the reference, respectively. If the two σ values are the same, $\sigma_u = \sigma_r = \sigma$, then this becomes

$$\sigma_{eff} = \sqrt{2}\sigma \tag{8.20B}$$

Focus 8.1 Added noise

To understand the effect of differencing the error values at the user, let us consider that the noise at the reference and the noise at the receiver are both Gaussian with equal standard deviation, σ. In this composite noise, the effectual noise of value n will be produced when one of the noise components assumes value n_1 and the other assumes a value $(n - n_1)$. So, the total probability of occurrence of noise value n is equal to the sum of all possibilities of one acquiring value n_1 and the other value $n - n_1$. So, the effectual probability is:

$$\begin{aligned} p(n) &= \int p(n_1 = n_1)p(n_2 = (n - n_1))dn_1 \\ &= n_1 * n_2 \end{aligned}$$

The integration runs from $-\infty$ to $+\infty$. Thus, the effective probability distribution is the convolution of the individual distribution.

So, writing the probabilities in terms of the Gaussian distribution, we get:

$$\begin{aligned} p(n) &= \int \left[A\exp(-x^2/2\sigma^2) \times A\exp\left\{-(n-x)^2/2\sigma^2\right\}\right]dx \\ &= A^2 \int \exp -(n^2 - 2nx + 2x^2)/2\sigma^2 dx \\ &= A^2 \int \exp -(n^2/2 - 2nx + 2x^2 + n^2/2)/2\sigma^2 dx \\ &= A^2\left[\int \exp -(n^2/2 - 2nx + 2x^2)/2\sigma^2 dx\right]\exp(-n^2/4\sigma^2) \\ &= A^2\left[\int \exp -(x - n/2)^2 / \left\{2\left(\frac{\sigma}{\sqrt{2}}\right)^2\right\} dx\right]\exp(-n^2/4\sigma^2) \end{aligned}$$

The integral in the above equation is definite. It is similar to the integral of a Gaussian distribution of a variable x about the mean n/2 and standard deviation $\sigma/\sqrt{2}$. We know that the integral of a Gaussian function is independent of the mean value, and hence this definite integral becomes independent of n and equal to $\left(\frac{\sigma}{\sqrt{2}}\right)\sqrt{2\pi} = \sqrt{\pi\sigma^2}$ (Papoulis, 1991). Calling this constant value K, this probability p(n) becomes:

$$\begin{aligned} p(n) &= K\exp(-n^2/4\sigma^2) \\ &= K\exp\{-n^2/2\left(\sqrt{2}\sigma\right)^2) \\ &= K\exp\{-n^2/2\sigma_{eff}^2) \end{aligned}$$

where K is a constant. This is nothing but a scaled Gaussian distribution with effective σ given by:

$$\sigma_{eff} = \sqrt{2\sigma}$$

This effect is illustrated in Box 8.1.

Box 8.1 MATLAB Exercise

The MATLAB program noise_addition.m was run to observe the effect of adding two signals carrying noise of unity standard deviation value, that is, $\sigma = 1$. The effective noise thus produced gets enlarged compared to the original noise. This is shown in Fig. M8.1(A) and M8.1(B) below. Fig. M8.1(A) shows how the time variation gets effectively amplified, while Fig. M8.1(B) shows the increment in the effective standard deviation value, σ.

Understand the program and identify the different parameters used. Run the program with different original σ and for different sample numbers, and observe the effect.

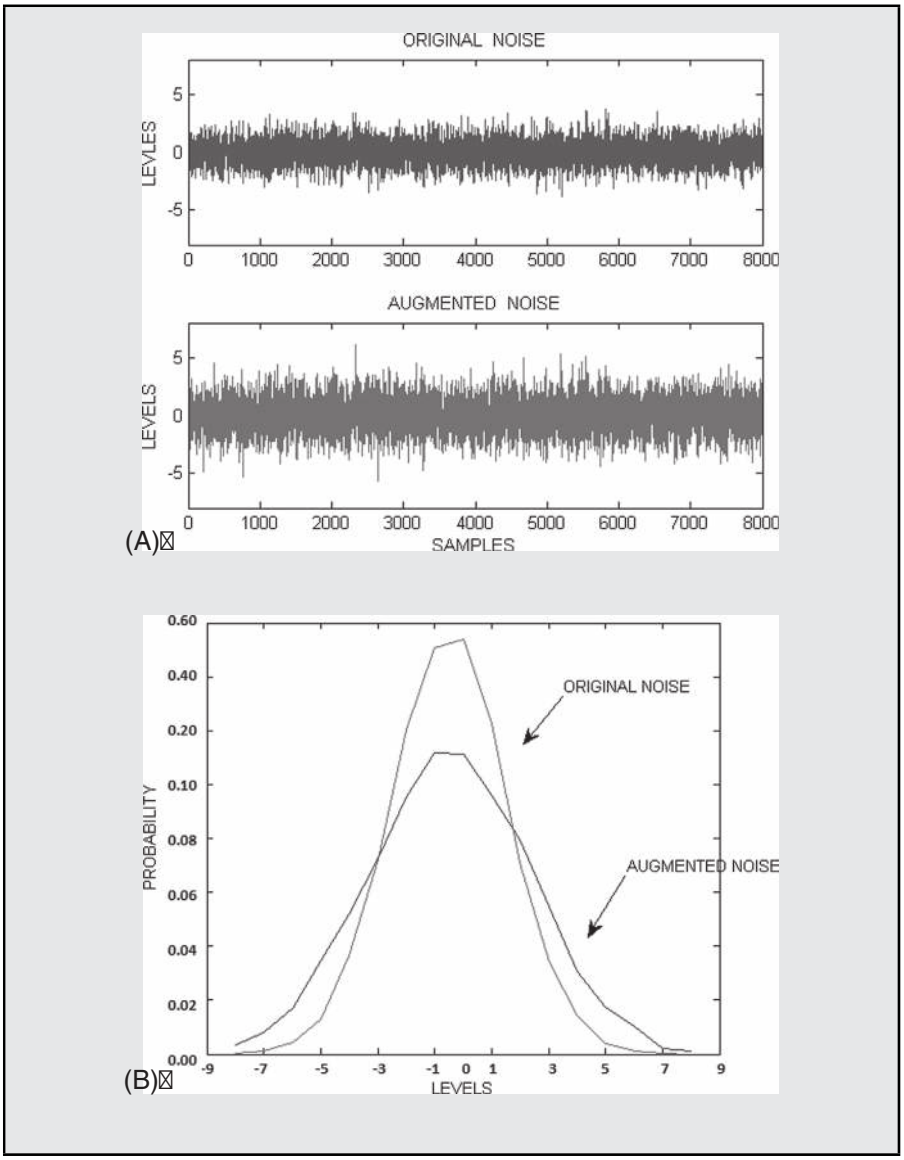

8.2.1.2 Relative differential methods

Next, consider the case of relative differential positioning using the code-based measurements. Here, instead of disseminating the range errors only, the reference station provides the total measured satellite ranges to the users. So, on differencing this satellite range measured at the reference station from that measured at the user

receiver, differential range is obtained. This differential range is the function of the relative distance between the reference and the user. That is, this differential range is a function of the baseline, and of the satellite-receiver geometry. So, this method is used for the cases where the user is interested in knowing his location with respect to the position of the reference station. So, the differential positions in terms of the baseline vector between the user and the reference are estimated here. When the absolute reference station position is also known to the user, the user can always obtain their position with respect to absolute references using this derived differential position.

This relative differential positioning can be done with code-based ranging. Rewriting the uncorrected measured range again for both the reference and the user location, we get

$$R_r = \rho'_r + c\delta t_s - c\delta t_r + \delta r_{eph} + \delta r_{ion,r} + \delta r_{trp,r} + n_r \tag{8.21A}$$

$$R_u = \rho'_u + c\delta t_s - c\delta t_u + \delta r_{eph} + \delta r_{ion,u} + \delta r_{trp,u} + n_u \tag{8.21B}$$

The meanings of the terms are the same as those defined for Eq. (8.10C) and (8.10 D). Unlike the previous case, where only the consolidated range error was transmitted by the reference, here the whole range R_r measured at the reference is made available to the user. The user utilizes this total range measured by the reference to estimate the relative position through different differencing techniques that we discuss below.

The carrier-phase based relative differential method is generally used in conjunction with the code based measurements to resolve the integer ambiguity, a related issue that we shall come across while learning the carrier phase-based methods. However, code based methods can also be used as an independent method for relative positioning, but with lower accuracy compared to the phase-based methods.

8.2.1.2.1 Single differencing technique

A single difference equation is formed when the range measurements obtained at the user receiver is differenced once from the measurements equation obtained at the reference receiver for the same satellite and at the same instant. Now, differentiating the Eq. (8.21A) from (8.21B), which represent the above two measurements respectively, get

$$\begin{aligned} \Delta R_{ur} &= R_u - R_r \\ &= \Delta\rho'_{ur} + c\Delta\delta t_{ur} + \Delta\delta r_{eph,ur} + \Delta\delta r_{ion,ur} + \Delta\delta r_{trp,ur} + n_{ur} \end{aligned} \tag{8.22}$$

Notice that, the common satellite clock error has got eliminated here. Now, concentrating on the errors due to the ionospheric delay and the tropospheric delay, these errors are supposed to be different at the users and reference locations for long baselines, leaving the corresponding differential terms nontrivial. The general approach that may be used to mitigate the effect here is also to provide the delay rate information, as we have discussed above. The second and higher-order terms can be neglected. Otherwise, the dual-frequency receivers have to be used.

Considering the case of short baseline, the ephemeris error too cancels out. Further, the ionospheric and tropospheric delays cancel almost completely due to their correlation such that the differential terms turn zero, the ΔR_{ur} term difference becomes,

$$\Delta R_{ur} = \Delta\rho'_{ur} + c\Delta\delta t_{ur} + n_{ur} \tag{8.23}$$

Now, let us see how we can replace Euclidian expression for the range difference $\Delta\rho'$ as a function of the baseline. The variation in range may be expressed in terms of the positional difference vector ΔX as

$$\rho'_u = \rho'_r + \partial\rho'/\partial X|_{Xr}\Delta X + \frac{1}{2}\partial\rho'/\partial X^2|_{Xr}\Delta X^2 + \text{higher} - \text{order terms} \tag{8.24A}$$

Therefore, the range difference may be written as

$$\Delta\rho' = \partial\rho'/\partial X|_{Xr}\Delta X + \frac{1}{2}\partial\rho'/\partial X^2|_{Xr}\Delta X^2 + \text{higher} - \text{order terms} \tag{8.24B}$$

For short baselines, only the first-order derivative is significant, while the higher-order derivatives are vanishingly small. So, the difference for short baselines becomes

$$\Delta\rho' = \partial\rho'/\partial X|_{Xr}\Delta X \tag{8.24C}$$

This can be expanded in terms of individual coordinates as

$$\Delta\rho' = \partial\rho'/\partial x|_{Xr}\Delta x + \partial\rho'/\partial y|_{Xr}\Delta y + \partial\rho'/\partial z|_{Xr}\Delta z \tag{8.24D}$$

Where Δx, Δy, and Δz are the components of the baseline vector, ΔX. But these differentials of the range with respect to the coordinates at the reference position Xr are nothing but the direction cosines of the range vector with respect to the coordinate axes. This becomes obvious on writing the derivatives in terms of the functional expression. So, writing the geometric Euclidian range R in terms of the coordinates and then differentiating at the reference point, we get

$$\begin{gathered}\rho' = \sqrt{(x_s - x_r)^2 + (y_s - y_r)^2 + (z_s - z_r)^2} \\ \partial\rho'/\partial x_r|_{xr} = -(x_s - x_r)/\rho = -cos\alpha \\ \partial\rho'/\partial y_r|_{xr} = -(y_s - y_r)/\rho = -cos\beta \\ \partial\rho'/\partial z_r|_{xr} = -(z_s - z_r)/\rho = -cos\gamma\end{gathered} \tag{8.25}$$

where α, β, and γ are the angles that the range vector or the corresponding unit vector makes at the reference position X_r with the coordinate axes. So, if **e** be that unit vector and e_x, e_y, and e_z are its components along the x, y, and z axes, respectively, then $e_x = \cos\alpha$, $e_y = \cos\beta$, and $e_z = \cos\gamma$. So, the differential range becomes

$$\Delta\rho' = -e_x\Delta x - e_y\Delta y - e_z\Delta z \tag{8.26}$$

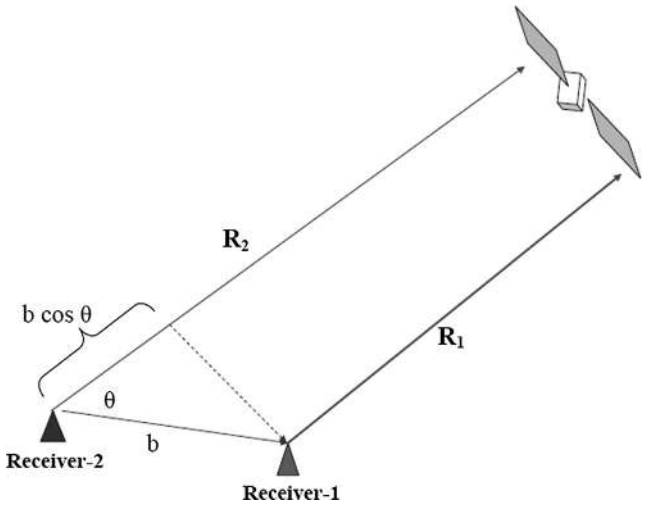

FIGURE 8.3

Geometric relation of range difference with baseline for single differencing.

Recalling that the baseline b is nothing but the vectorial difference between the two stations, it can be expressed as a variation of their position coordinates. Thus,

$$\begin{aligned} b &= X_r - X_u \\ &= -(\Delta x x + \Delta y y + \Delta z z) \end{aligned} \tag{8.27}$$

In other words, Δx, Δy, and Δz are the components of the baseline b along the respective reference axes. So,

$$\begin{aligned} \Delta\rho' &= -\mathbf{e} \cdot \mathbf{b} \\ &= b cos\theta \end{aligned} \tag{8.28A}$$

This is evident from Fig. 8.3, where $\Delta\rho$ can be expressed as b cos θ, where b is the baseline length and θ is the angle between the direction of the satellite from the receivers and the baseline.

For short baselines, the incident rays from the satellite are parallel, and this angle θ is equal at both the receivers. Then

$$\Delta\rho' = b cos\theta \tag{8.28B}$$

So, using Eq. (8.28B) in Eq. (8.23), we get

$$\begin{aligned} \Delta R_{ur} &= b cos\theta + c\Delta\delta t_{ur} + n_{ur} \\ &= \left[-e_x \; -e_y \; -e_z c\right]\left[\Delta x \; \Delta y \; \Delta z \; \delta t_{ur}\right] + n_{ur} \\ &= G_1\left[\Delta x \; \Delta y \; \Delta z \; \Delta\delta t_{ur}\right] + n_{ur} \end{aligned} \tag{8.29}$$

where $G_1 = [-e_x\ -e_y\ -e_z\ c]$ is defined at the reference position. Since the reference position is known, the unit vector components in G_1 can be generated from its coordinates. Hence, G_1 becomes a well-known parameter.

The solution for the differential coordinates Δx, Δy, Δz, and $\Delta\delta t_{ur}$, thus, may be obtained using the standard least squares method. This method has the advantage that transmission of the measured range suffices the need of the algorithm, and the individual errors are not required to be estimated at the reference station. This eliminates much of the computational load at the reference station and reduces the latency in turn. For users explicitly requiring relative distance, the reference location even need not be surveyed and may also be relocating with time. However, this method has more use in carrier-based techniques, which we shall learn in a later subsection.

8.2.1.2.2 Double differencing technique

A double difference equation is formed when the single differenced range measurements obtained for two different sets of satellites but for the same pair of receivers, are differenced.

For n numbers of visible satellites which are common to the reference and the user, n-1 such independent single difference equations can be formed for a definite pair of reference and user receiver. If θ_1 and θ_2 are the corresponding angles that the baseline makes with the direction of the two satellites S_1 and S_2 respectively, at the reference receiver location, then using Eq. (8.28A), the corresponding equation can be written as

$$\begin{aligned} \Delta R^1_{ur} - \Delta R^2_{ur} &= b\cos\theta_1 - b\cos\theta_2 + n^1_{ur} - n^2_{ur} \\ \text{or,}\quad \nabla\Delta R^{12}_{ur} &= b(\cos\theta_1 - \cos\theta_2) + n^{12}_{ur} \end{aligned} \tag{8.30A}$$

where ΔR^1_{ur} and ΔR^2_{ur} are the single differenced measured ranges for satellite S1 and S2, respectively, between the user and the reference. $G_1 = [-e_{1x}\ -e_{1y}\ -e_{1z}]$ and $G_2 = [-e_{1x}\ -e_{1y}\ -e_{1z}]$ are both known. Notice that the common term of relative receiver clock bias has been eliminated. The geometry is evident from Fig. 8.4.

Similarly, as in the case of single difference, this equation may be written in the matrix form as

$$\nabla\Delta R^{mn}_{ur} = b.(G_1 - G_2) + n^{mn}_{ur} = G_{12}[\Delta x \Delta y \Delta z] + n^{mn}_{ur} \tag{8.30B}$$

where $G_{12} = [e_{x2}{-}e_{x1}\ e_{y2}{-}e_{y1}\ e_{z2}{-}e_{z1}]$, is the difference of the corresponding elements in G_1 and G_2 for single differencing for satellite S_1 and S_2. Notice that the relative receiver clock bias, which was present in the single difference equation, has been eliminated by further differencing. This reduces the load of estimating one unknown variable and hence requires only three sets of observations for finding the differential solution. The aspects and approach for single and double differencing are illustrated in Focus 8.2.

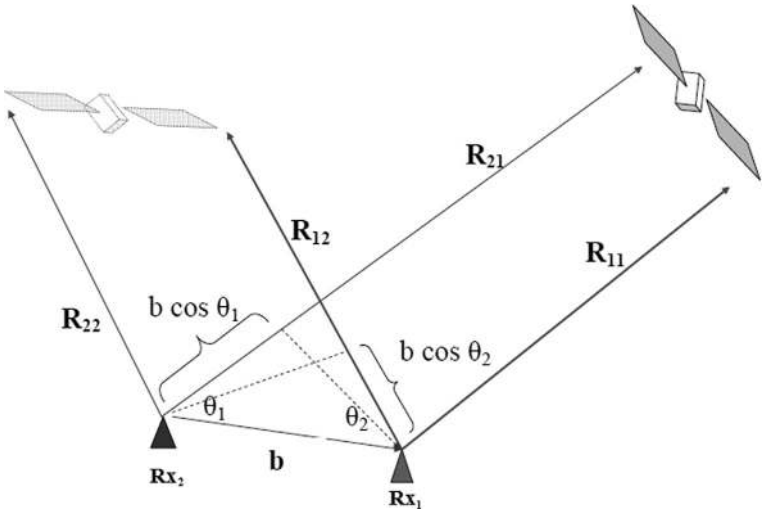

FIGURE 8.4

Double difference in range and relation to baseline.

Focus 8.2 Aspects of differencing

The range of a definite satellite S1 measured using code phase in two different frequencies of 1575.42 MHz (L1) and 1227.6 MHz (L2) for station A situated at a known location is, respectively:

22646708.32 m
and 22646719.32 m

The same parameters, when measured at another station B located at an unknown location, are:

22658409.71 m
and 22658419.71 m

From the above, the ionosphere-free measured range from station A and station B becomes, respectively:

22646690.99 m
and 22658393.54 m

The ionospheric delay causes more than 15 m of excess range in L1 and more than 25 m in L2. Differencing the ionosphere-free ranges at the two stations, we get:

$$dR_1 = 22658393.54 - 22646690.99 \text{ m}$$
$$= 11702.55 \text{ m}$$
$$= 11702.5 \text{ m}$$

Instead, differencing the total measured range would have given us:

$$dR'_1 = 22658409.71 - 22646708.32$$
$$= 11701.39 \text{ m}$$

The difference between dR_1 and dR'_1 is small indeed. So, even if we directly differ the ranges, the ionospheric delay for small baselines being almost the same, irrespective of its magnitude (15 and 25 here), gets almost eliminated.

So, if b is the baseline, then:

$$b\cos\theta 1 + \delta t_{ur} = 11,702$$
$$\text{or}, -(e_{x1} \cdot b_x + e_{y1} \cdot b_y + e_{z1} \cdot b_z) + \delta t_{ur} = 11,702$$

The ranges measured at the same time toward a different satellite S2 for stations A and B, respectively, in frequency L1 are 22,713,461.72, and 22,711,149.54 m.

The corresponding difference in range dR2 becomes:

$$dR_2 = 22713461.72 - 22711149.54 \text{ m}$$
$$= 2312.18 \text{ m}$$

So,

$$b\cos\theta 2 + \delta t_{ur} = 2312$$
$$-(e_{x2} \cdot b_x + e_{y2} \cdot b_y + e_{z2} \cdot b_z) + \delta t_{ur} = 2312$$

Differencing the two single differences, we get:

$$b(\cos\theta_1 - cos\theta_2)$$
$$= [(e_{x2} - e_{x1}) \cdot b_x + (e_{y2} - e_{y1}) \cdot b_y + (e_{z2} - e_{z1}) \cdot b_z]$$
$$= 11,702 - 2312$$
$$= 9390$$

Now, the surveyed position of the reference station is:

$$x_r = 2067.9947 \text{ m}$$
$$y_r = 5921962.0445 \text{ m}$$
$$z_r = 377.8407 \text{ m}$$

Then the corresponding calculated ranges with the two satellites from the reference station become:

$$R_1 = 21182426.32 \text{ m}$$
$$R_2 = 22712324.35 \text{ m}$$

Note that the measured ranges are different from these calculated ranges. This is due to the presence of errors in the measurements and the effect of ephemeris errors in the calculations. However, here the errors are exaggerated compared to the pragmatic values for convenience and highlighting.

Then, using x_r, y_r, z_r, and the ephemeris-derived satellite position, we get:

$$e_{1x} = 0.03036, e_{1y} = 0.86960, e_{1z} = 0.49281$$
$$\text{and } e_{2x} = -0.45908, e_{2y} = 0.57847, e_{2z} = -0.67424$$

So,

$$e_{2x} - e_{1x} = -0.48945$$
$$e_{2y} - e_{1y} = -0.29112$$
$$e_{2z} - e_{1z} = -1.16706$$

However, these three equations are not linearly independent. Hence, solutions for three unknowns cannot be obtained from these equations only. More similar measurements are required for solving.

8.2.2 Carrier phase-based methods

Carrier phase-based differential methods are those in which both the reference station and the user receiver use their carrier phase measurements for estimation of the range of the receivers at their respective positions, as described below (El-Rabbani, 2006).

We have already read in Chapter 5 that the phase measurements of the received signal give ranges that are many times more precise than those obtained using the code phases. However, the cost one has to pay for it, is the added computational complexity. We can recall that the carrier phase-based ranging is precise but has the limitation of integer ambiguity. It is the integral number N of the wavelengths present in the range, at the instant when the receiver starts measuring the phase difference of the incoming signal with respect to the locally generated carrier, the latter being synchronized with the satellite. This implies that at any instant the satellite and the receiver generates the same phase of the carrier. Different techniques are used to resolve this problem of ambiguity. Here, the same techniques can also be used for differential estimations. The carrier phase-based differential estimation of position is significantly useful when precise positioning is done with respect to the reference station, that is, for relative differential positioning. Here too, like the code-based technique, single differencing and double differencing, and even triple differencing are done. The basic idea is to reduce the number of unknowns to be solved for utilizing the commonalities between the user and the reference.

The measured parameter in the carrier phase technique is the phase of the carrier. If φ is the measured fractional phase at the receivers, obtained by comparing the received phase with that of the local carrier, ρ is the true range and N is the integer ambiguity, then the measurements done by the reference and user receivers, respectively, from the same satellite S may be written as

$$(\lambda/2\pi)\varphi_r = \rho_r - N_r\lambda + c\delta t_r - c\delta t_s - \delta r_{ion,r} + \delta r_{trp,r} + n_r \tag{8.31A}$$

$$(\lambda/2\pi)\varphi_u = \rho_u - N_u\lambda + c\delta t_u - c\delta t_s - \delta r_{ion,u} + \delta r_{trp,u} + n_u \tag{8.31B}$$

The subscripts u and r represent the above parameters for the user and the reference, respectively. λ is the wavelength of the signal. The rest of the notations in the above equations signify usual parameters as described in previous sections. Notice here that the ionospheric error has the opposite sign compared to that obtained for the range measurements. It is because, unlike the code, which gets delayed as it passes through the ionosphere, the carrier phase experiences equal phase "advancement".

8.2.2.1 Single differencing technique

We have already seen in connection with the code-based relative methods how the relative range equations are formed by differencing the respective individual measured

ranges. Similar difference equations may be formed by using the respective phase measurements, too. The measured phase at the reference receiver with signals from satellite s may be expressed as in Eq. (8.31A), and that measured phase at the user receiver is expressed as Eq. (8.31B). On differencing these two, we get

$$(\lambda/2\pi)(\varphi_r - \varphi_u) = (\rho_r - \rho_u) - (N_r - N_u) + c\Delta\delta t_{ru} - \Delta\delta r_{ion,ru} + \Delta\delta r_{trp,ru} + n_{ru} \tag{8.32}$$

Thus, the common satellite clock bias gets removed. Now, considering a short baseline, the differences in the excess paths between the receivers due to the ionospheric and tropospheric and tropospheric delays also reduce to vanishingly small values. Also, for short baselines, the true range differences can be expressed with only first-order derivatives in the form

$$\begin{aligned} \rho_u &= \rho_r + \partial\rho/\partial x\, dx + \partial\rho/\partial y\, dy + \partial\rho/\partial z\, dz|_{X_r} \\ \text{or, } \rho_u - \rho_r &= \partial\rho/\partial x\, dx + \partial\rho/\partial y\, dy + \partial\rho/\partial z\, dz|_{X_r} \end{aligned} \tag{8.33}$$

So, as seen for the code phase case, here too, the above single difference equation in Eq. (8.32) turns into

$$\begin{aligned} &(\lambda/2\pi)\Delta\varphi_{ru} = (\lambda/2\pi)(\varphi_r - \varphi_u) \\ &= (\partial\rho/\partial x\, dx + \partial\rho/\partial y\, dy + \partial\rho/\partial z\, dz - N_{ru}\lambda + c\Delta\delta t_{ru} - \Delta\delta r_{ion,ru} + \Delta\delta r_{trp,ru} + n_{ru}) \end{aligned} \tag{8.34}$$

Similarly, as in Eq. (8.25) and Eq. (8.26), the derivatives can be expressed in terms of unit vectors as $\partial\rho/\partial x_r = -e_x$, $\partial\rho/\partial y_r = -e_y$, and $\partial\rho/\partial z_r = -e_z$, where dx, dy, and dz are the differential elements of the baseline b. N_{ru} is the difference of the integer ambiguity for the two stations, i.e. (N_r - N_u). Both N_r and N_u being integers, N_{ru} is also an integer. So, assuming the ionospheric and tropospheric errors nearly vanish on differencing, the equation can be written as

$$(\lambda/2\pi)\Delta\varphi_{ru} = (-\overline{e_r} \cdot b) - N_{ru}\lambda + c\Delta\delta t_{ru} + \varepsilon_{ru} \tag{8.35}$$

where $\overline{e_r}$ is the unit vector from the reference station to the satellite s. ε_{ru} is the error considering the difference between the individual receiver noises, viz. n_r _ n_u, and added to it all other differential residual uncorrelated errors between the two receivers.

For n number of visible satellites, which are common to the reference and the user, n such single difference equations can be formed for a definite pair of reference and user. The matrix form of the equation becomes

$$(\lambda/2\pi)\begin{bmatrix} \Delta\varphi_{ur}^{s1} \\ \Delta\varphi_{ur}^{s2} \\ \vdots \\ \Delta\varphi_{ur}^{sn} \end{bmatrix} = \begin{bmatrix} -e_x^1 & -e_y^1 & -e_z^1 & c \\ -e_x^2 & -e_y^2 & -e_z^1 & c \\ \vdots & \vdots & \vdots & \vdots \\ -e_x^n & -e_y^3 & -e_z^1 & c \end{bmatrix} \begin{bmatrix} dx \\ dy \\ dz \\ \delta t_{ur} \end{bmatrix} + \begin{bmatrix} N_{ur}^1 \\ N_{ur}^2 \\ \vdots \\ N_{ur}^n \end{bmatrix} | + \begin{bmatrix} \varepsilon_{ur}^1 \\ \varepsilon_{ur}^2 \\ \vdots \\ \varepsilon_{ur}^n \end{bmatrix} \tag{8.36A}$$

or

$$(\lambda/2\pi)\Delta\boldsymbol{\varphi}^s{}_{ur} = \mathbf{G}_1 \cdot dX + \mathbf{N}\lambda + \boldsymbol{\varepsilon} \tag{8.36B}$$

In this single difference equation, **G** is a n×4 matrix, d**X** has three relative positional and a relative time offset element. There are n integer ambiguity values

as unknowns in the nx1 matrix **N**. $\boldsymbol{\varepsilon}$ contains the nx1 noise elements whose individual values are not known, but the variance of which may be used for solving for d**X**. This cannot be readily solved using the least squares method due to the presence of the Nλ terms. However, techniques like the carrier smoothed code-based range measurements may be used for estimating N, following which dX may be solved.

The estimation of N, that is, finding the integer ambiguity value, can be done, one at a time, using the code-based measurements. For that, each of the rows in Eq. (8.36B), the rows in G_1.dX can be replaced with the corresponding elements in single differenced code-based range measurement, that is, ΔR_{ur} in Eq. (8.29), for a short baseline. Then, the corresponding integer ambiguity N can be obtained as

$$N = \{(\lambda/2\pi)\Delta\Phi^{s}{}_{ur} - \Delta R_{ur}\}/\lambda \tag{8.37}$$

There are other methods of solving for the integer ambiguity, like the popular Least-square Ambiguity Decorrelation Adjustment (LAMBDA) method, using measurements in more than one frequency. Alternatively, it can be solved for dX by tactfully eliminating the N. If we take similar measurements at two different instants over a gap of period in the interval of which the measurement of the phase remains continuous, then the initial integer ambiguity, which remains common for both, vanishes on differencing. Therefore, writing any row of Eq. (8.36B) for these two time instants, k_1 and k_2, we get

$$(\lambda/2\pi)\Delta\Phi^{s}_{ur}(k_1) = G_1(k_1)\cdot dX + N\lambda + \varepsilon(k_1) \tag{8.38A}$$

$$(\lambda/2\pi)\Delta\Phi^{s}_{ur}(k_2) = G_1(k_2)\cdot dX + N\lambda + \varepsilon(k_2) \tag{8.38B}$$

Subsequently, differencing the two, we get

$$\begin{aligned}(\lambda/2\pi)\delta\Delta\Phi^{s}_{ur}(\Delta k) &= (\lambda/2\pi)\left[\Delta\Phi^{s}_{ur}(k_1) - \Delta\Phi^{s}_{ur}(k_2)\right]\\ &= \left[G_1(k_1) - G_1(k_2)\right]\cdot dX + \delta\varepsilon(k)\\ &= G_{1\Delta k}\cdot dX + \delta\varepsilon(k)\end{aligned} \tag{8.39}$$

where $\delta\Delta\Phi^{s}_{ur}$ is the differenced value of the single differenced phase across the separated time. $G_{1\Delta k} = [G_1(k_1) - G_1(k_2)]$. The integer ambiguity N, which remains the same over the whole session, thus gets eliminated from the equation on differencing.

Now the general least squares solution for dX may be derived from it as

$$dX = (\lambda/2\pi)\left[G^{T}_{1\Delta k}G_{1\Delta k}\right]^{-1}(G_{1\Delta k})^{T}\delta\Delta\Phi(k) \tag{8.40A}$$

Further, if the variance of the error $\delta\varepsilon$ is known for each satellite and if they form a matrix M, the weighted least squares solution may be obtained as

$$dX = (\lambda/2\pi)\left[G^{T}_{1\Delta k}M^{-1}G_{1\Delta k}\right]^{-1}(G^{T}_{1\Delta k}M^{-1})\delta\Delta\Phi(k) \tag{8.40B}$$

Here, $G_1(k_2)$ and $G_1(k_1)$ need to be widely separated to provide a well-conditioned value of $G_{1\Delta k}$ that determines the precision of the estimation of dX. This means that the time interval needed between two sets of measurements should be sufficiently

large. So, this technique can be applied only for static applications where the solution may be obtained over a considerable period of time.

It is important to appreciate and remember that the convenience of linearity is obtained by considering a short baseline. Due to this assumption, it becomes possible to express $r_t - r_u$ as a linear function of dx, dy, and dz to form G_1 in Eq. (8.33), which eases the problem to a great extent.

8.2.2.2 Double differencing technique

The differential method has the intrinsic advantage of cancellation of the common errors. We have seen this in the code range method as well as in the single difference phase method. However, even after the single differencing, the relative clock bias parameter still remains in the equation as an additional unknown term for solving for dX. Many of the applications that use this relative positioning technique are interested in obtaining precise positions. Hence, the relative clock offset parameter $\Delta\delta t_{ru}$ is not necessary to estimate and may be removed during the estimation process. This may be done by generating the double differenced (DD) phase equations. As for the case of range equations, the DD is obtained by generating another single difference equations. So, for n + 1 visible satellites, n such independent DD can be formed. with a separate satellite and then differencing the two single difference equations. So, for $n+1$ visible satellites, n such independent DD can be formed.

Using Eq. (8.35), the two single difference equations between the user and the reference receiver for satellites m and n may be respectively expressed as

$$\begin{aligned}(\lambda/2\pi)\Delta\varphi_{ur}^{m} &= (-e_r^m \cdot b) + N_{ur}^m\lambda + c\Delta\delta t_{ru} + \varepsilon_{ur}^m \\ (\lambda/2\pi)\Delta\varphi_{ur}^{n} &= (-e_r^n \cdot b) + N_{ur}^n\lambda + c\Delta\delta t_{ru} + \varepsilon_{ur}^n\end{aligned} \tag{8.41}$$

Differencing the two equations, we get the DD equation as

$$(\lambda/2\pi)\nabla\Delta\varphi_{ur}^{mn} = (-e_r^{mn} \cdot b) + N_{ur}^{mn}\lambda + \varepsilon_{ur}^{mn} \tag{8.42}$$

where $\varepsilon_r{}^{mn} = \varepsilon_r{}^m - \varepsilon_r{}^n$.This forms the conventional double difference equation, where we have assumed that the ephemeris, ionospheric, and tropospheric error residuals have already been removed on single differencing. Any residual thereof is insignificant and random in nature, to be treated as noise and included in ε_{ur}^{mn}. Notice that here the relative clock bias of the $\Delta\delta t_{ur}$, being the same between the same user receiver and reference, gets completely canceled out.

Considering the discussion we had in reference to the linearity of the geometric range variation for short baselines and the derivation of the range difference in Eq. (8.28), this equation can also be expressed in terms of the angle θ that the baseline b makes with the unit vector e. Thus, the expression becomes

$$(-e_r^{mn} \cdot b) = b(\cos\theta_m - \cos\theta_n) \tag{8.43}$$

Here, θ_m and θ_n are the respective angles with satellites m and n, respectively. So, putting this relation from Eq. (8.43) in the above Eq. (8.42), we get

$$(\lambda/2\pi)\nabla\Delta\varphi_{ur}^{mn} = b(\cos\theta_m - \cos\theta_n) + N_{ur}^{mn}\lambda + \varepsilon_{ur}^{mn} \tag{8.44}$$

Eq. (8.42) can also be written as

$$\begin{aligned}(\lambda/2\pi)\nabla\Delta\varphi_{ur}^{mn} &= (G_{ur}^{m} - G_{ur}^{n})\cdot dX + N_{ur}^{mn}\lambda + \varepsilon_{ur}^{mn}\\ &= G_{ur}^{mn}\cdot dX + N_{ur}^{mn}\lambda + \varepsilon_{ur}^{mn}\end{aligned} \tag{8.45}$$

where $G_{ur}^{mn} = \left(G_{ur}^{m} - G_{ur}^{n}\right)$, the geometric observation matrix for double difference. But, apart from eliminating the relative receiver clock bias, we have not gained much in this differencing until now, since the problem term N still remains in the equation.

Similar to the single difference approach, the integer ambiguity can be resolved using the corresponding code-based DD ranges for short baselines. Further, when measurements at more than one frequency are available, then the integer ambiguity can be resolved using a wide-laning technique with the Melbourne–Wubbena combination. Instead of resolving ambiguities one at a time, it can be done as a set, using the least squares ambiguity search technique or utilizing the LAMBDA method.

Once the integer ambiguities are known, the carrier phase measurements and their differentials become unambiguous as their equivalent code-based counterparts. Thence, the estimation of the relative position vector is straightforward.

This linear equation may also be solved in the same manner as we have done for the single difference case by using equations separated by time. This strategically avoids the problem of finding the integer number N. Differencing two double difference equations separated by time gives a Triple difference equation.

8.2.2.3 Triple difference method

For the same pair of satellites, DD can be estimated at a large time difference. Then these obtained two double differences may again be mutually differenced to get the triple difference of the range observation equation. Thus, for triple difference, it becomes

$$\begin{aligned}\Delta^3\varphi_{ur}^{mn}(\Delta k) &= \nabla\Delta\varphi_{ur}^{mn}(k_2) - \nabla\Delta\varphi_{ur}^{mn}(k_1)\\ &= \left[G_{ur}^{mn}(k_2) - G_{ur}^{mn}(k_1)\right]\cdot dX + \left[\varepsilon_{ur}^{mn}(k_2) - \varepsilon_{ur}^{mn}(k_1)\right]\\ &= G_{ur}^{mn}(\Delta k)\cdot dX + \varepsilon_{ur}^{mn}(\Delta k)\end{aligned} \tag{8.46}$$

So, for each pair of satellites, similar differences may be made at considerably large intervals. By this time, both the satellites, their positions having changed, will give a new set of independent equations. The scenario is described in the schematic in Fig. 8.5.

So, to solve for the three unknowns, three such triple differences are required to be established, and hence three independent pairs of visible satellites need to be measured for range over a large interval of time that needs at least 4 visible satellites. As mentioned earlier, this method demands a large time latency for providing the first solution. In cases where such large latency is inappropriate, it is required to

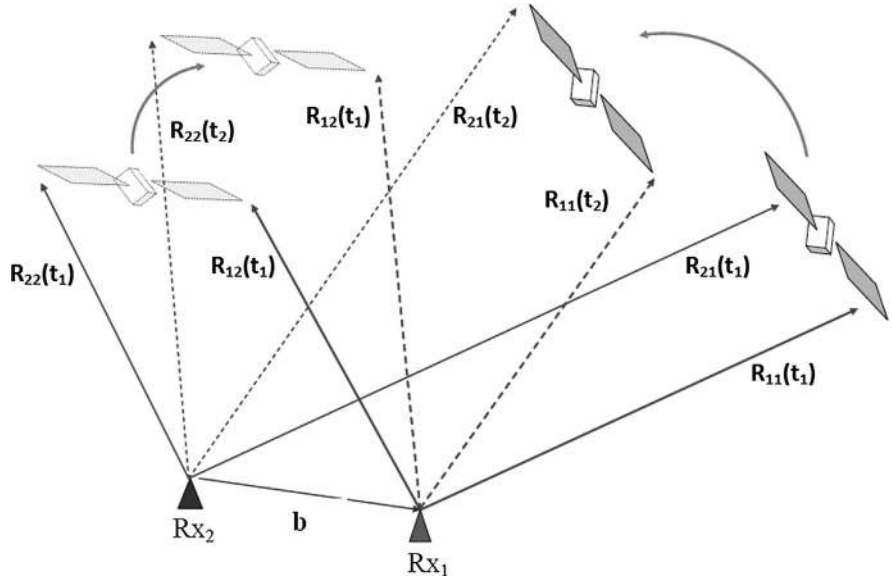

FIGURE 8.5

Schematic of the scenario to generate triple difference equations.

resort to the DD method, where some ambiguity-resolving technique is required to be employed to estimate N. Then, the value of dX may be solved for.

Resolving ambiguity is nothing but solving for integer values of N. It is one of the key issues in relative positioning, mainly due to the constraint that N has to be an integer. Two approaches are mainly followed for the purpose (Cosentino et al., 2006). In one approach, it is done by finding the optimum value of N, disregarding the integer constraint for N. This involves solving for the float value of N. The smoothed code-based measurements are used in this process, typically aided by a Kalman filter. When the carrier phase measurements are double differenced, with the result left with functions of the baseline vector and the DD integer ambiguity. The ambiguities are then fixed to float numbers using standard least-squares techniques. This simply estimates the ambiguities as floating point numbers. Finally, the integer ambiguities are derived by setting the ambiguity to that integer value which optimizes the residuals in the float solution. For this, the float solution is adjusted to the nearest integers, which offers minimum error to the equations formed. Thus, the true value of N is obtained.

Otherwise, it is done by first limiting the estimate region for N to a set of possible integer values of N and then searching for the best value.

Once the estimate of integers is given, it is straightforward to solve for dX. Table 8.1 lists the different popular methods of differential positioning. However, this list is not exhaustive.

Table 8.1 Some popular methods for differential positioning.

Methods	At reference station (RS)	At user end
Absolute methods		
Method 1	1. Calculate position X, Y, Z for all possible sets of 4 satellites visible. 2. Compute position error (ΔX, ΔY, ΔZ) with respect to the known location for each set separately. 3. Broadcast position correction data to the respective users for each set.	1. Select an optimum set of 4 satellites and measure pseudo-ranges. 2. Compute the uncorrected position. 3. Receive and apply the RS position correction (ΔX, ΔY, ΔZ) for the corresponding set of the satellite actually used by it. 4. Obtain corrected position solution.
Method 2	1. Measure pseudo-ranges (PR) for all visible satellites. 2. Calculate PR correction with respect to the known location. 3. Broadcast range corrections for all satellites to all users.	1. Select an optimum set of 4 satellites and measure pseudo-ranges. 2. Receive pseudo-range corrections from RS. 3. Apply appropriate pseudo-range correction to pseudo-range data. 4. Obtain corrected position solution.
Relative methods		
Method 3	1. Measure all satellite pseudo-ranges 2. Broadcast pseudo-range to all users	1. Select an optimum set of 4 satellites and measure pseudo-ranges 2. Receive pseudo-ranges from RS 3. Differentiate the respective pseudo-ranges to get corrected relative range data 4. Solve for the corrected relative position solution

(*continued on next page*)

Table 8.1 Some popular methods for differential positioning—cont'd

Methods	At reference station (RS)	At user end
Method 4	1. Carry out carrier phase measurements of all visible satellites 2. Disseminate the carrier phase measurements to users along with PR measurements	1. Carry out carrier phase measurements for an optimum set of 4 satellites 2. Use double difference techniques 3. Resolve ambiguity using PR data 4. Estimate relative position from the reference station

8.3 Implementation of differential systems

Until now we were discussing the different techniques of applying the correction to the errors at the user receivers. In this, we have learnt about using both the code-based ranges and the carrier phase-based measurements for differential corrections. Here we shall talk more on the implementation part of it. We shall see that depending upon the applications, areas of coverage etc. for the differential corrections, the types as well as the architecture needed for implementation become different. Implementation of the differential positioning methods mainly depends upon a few aspects, viz. the accuracy required, real time or post processed solution required, static or kinematic user and area to be covered.

Typical navigation receivers measure the pseudo ranges using the code-based techniques. It is because code-based measurements of pseudo-range is easy to implement in a receiver than measuring carrier phase. So, it is also more convenient to obtain the differential corrections using range-based techniques. The major requirement here is the measurement of range at a (El-Rabbani, 2006; Langley, 1998, 1993) reference and the user receiver. The subsequent processing part is rather simple. However, the accuracy of the solution is not as good as the carrier phase-based techniques due to the relative period of the code and the carrier, and also due to the presence of the intrinsic noise in the measurements.

In contrast, solving positions with carrier phase-based measurements is much more complex and computationally intensive. In such cases, ambiguity resolution is unavoidable. It adds intricacies to the process and typically works out well for relative positioning. The carrier phase-based measurements are used in systems like the RTK and precise point positioning (PPP), which we shall discuss later in detail.

Provisions of quick solutions, frequent updates, simple computational algorithms with precision enough for general applications, make this range-based differential methods very popular. On the other hand, applications,such as surveying, precision

construction, machine automation, precise agriculture, geodesy, etc., demanding high precision of obtained position (Leick, 1995) must go for carrier phase methods.

For the carrier phase techniques, the static and post processing methods may have better precisions, compared to that for kinematic user and real-time processing. Applications like precise time determination etc., that do not require position solutions in real time and hence can avail the advantage of postprocessing using single difference technique. They can also use data separated by large spatial differences. This gives improved accuracy and reduces computational complexity as well. Applications employing phase-based corrections like RTK may also have multiple reference stations for the same reason of extending the area of application.

A single reference station is sufficient for the purpose where the total area to be served is small. The limit of the spatial extent that a single reference station can serve is based on the factor of the distance the error correlation exists. Similarly, the temporal correlation of these errors determines the maximum allowable latency of using the corrections and hence determines how frequently and up to what distance the correction can be provided. Thus, the number of references required is based upon both the extent of the area of service as well as the accuracy needed.

We know that many of the errors are spatially and temporally correlated and remain almost constant for small distances between the reference and the users. At most, the spatial variation of the errors may be of first order. Such cases may be handled using the local area differential systems, where the user receiver can safely use real-time correction information, when the user remains within the line of sight of the reference station. This is easiest to establish, and corrections are valid only within a limited distance defined by the correlation of the propagation conditions.

For a larger extent of the service area, the above methods start showing up large errors (Kee, 1996). The estimates get worse with increasing distance between the reference station and the user. The behaviour of the errors become different and there remains considerable nonlinearity in its spatial variation. Consequently, the errors cannot be corrected by a single reference station. Additionally, another constraint pertaining to large areas of service is the limited transmission range of a single reference station. Moreover, due to the limited visibility of the single station, the user and the reference receivers can see different sets of satellites when they are separated by large distances, restricting direct use of the corrections.

To alleviate the problems faced in the local area differential systems, the simplest method is to establish several such discrete local area differential systems that contain a network of reference stations distributed over the total area under service. Then, the user receiver obtains the corrections from its nearest reference transmitters and corrects its errors. The underlying assumption is that at least one of the reference stations remains located so close to the user, irrespective of the location of the latter, that the corrections can be applied without much residual error. But, fulfillment of this condition demands the establishment of a large number of reference stations to cover a large area. This approach is used in the networked RTK, which serves larger areas.

The concept of a coalition of many local area differential systems to serve even large areas like that of a country needs to be graduated to a modified approach of

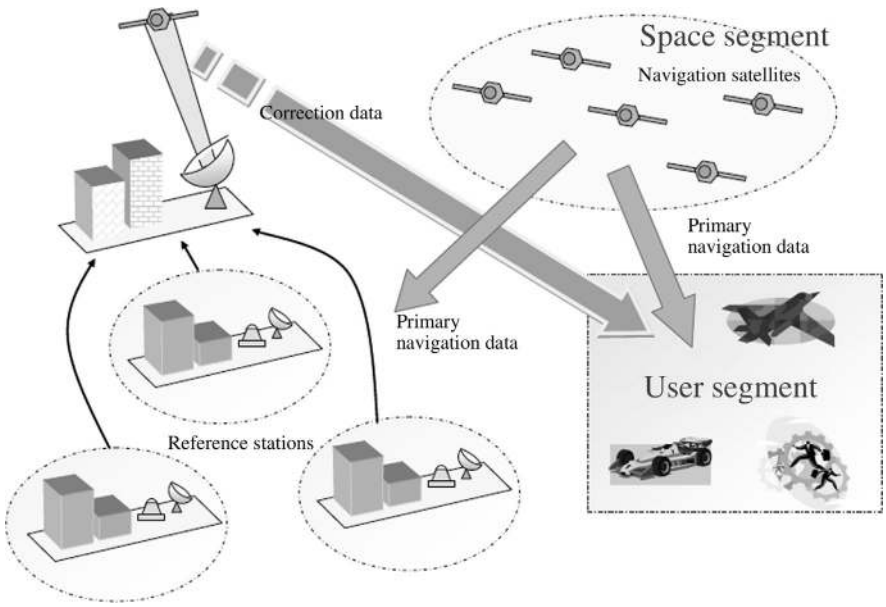

FIGURE 8.6

Architectural segments of a SBAS system.

wide area augmentation. The problems of establishing a large number of reference stations may be alleviated with the approach that, instead of transmitting the total range or the consolidated range error, the components of the errors are separated, and individual errors for each satellite are transmitted to the user. Thus, in this case, the range error or correction information does not remain limited to a definite satellite with a particular line of sight. For geographically correlated errors, the question of higher-order nonlinearities does not arise either, as the errors are derived from the predefined grid points nearest to the user position. This idea is implemented with code-based reference positioning in SBAS, while the same implementation with carrier phase-based measurements is utilized in PPP.

Dissemination of correction information can take place using terrestrial RF networks, or using the internet or preferably using a satellite for larger areas of service. The schematic of such a system is shown in reference to the SBAS in Fig. 8.6.

8.4 Real-time kinematics (RTK)

The primary navigation system has limitations in providing high accuracy. This is because of the errors in the measured ranges. These errors occur due to errors in the estimated satellite positions, that is, the ephemeris error, satellite clock error, signal propagation error, etc. We have already classified the errors earlier in this chapter.

The errors can be constant errors, like the satellite clock errors, which are global in nature. There are also correlated errors, like ephemeris errors and propagation errors, which vary with the receiver locations. The correlated errors, being satellite-receiver location-specific, remain the same for all receivers in the same vicinity. Therefore, one way of getting rid of these errors is by differencing the measured ranges, adopting the differential positioning technique. We have learnt about different differential methods utilized to reduce these errors using a reference receiver and thus achieving improved positioning accuracy.

RTK is an implementation of such a differential positioning technique with satellite navigation systems, which uses carrier phase-based differential corrections to provide precise position to the user in real time. In the following few subsections, we are going to discuss a few important aspects of RTK (Morton et al., 2020; Real-time Kinematics, 2024; RTK-Fundamentals, 2018).

8.4.1 RTK architecture

The basic architecture of the RTK consists of two receivers. One of them, called the *Base Station,* is located at a well-surveyed point. This base station can be a reference receiver with precise measurement capabilities. The base station receives the signal from the visible satellites and measures the pseudo-ranges. In RTK, the ranges are measured using the Carrier phase technique. Since the position of the base station is known and the positions of the satellites are available from the navigation signal, the geometrical ranges can be derived, and then the consolidated ranging errors can be estimated by simply differencing them.

The other receiver is called the Rover, and it is this receiver whose position is required to be estimated with accuracy. This receiver is also capable of using the Carrier phase range. The Rover also measures its ranges from the visible satellites using the carrier phase measurements. It remains within a limited vicinity of the Base station.

The linear distance between the base station and the rover receiver is called the baseline. For RTK, the rover is supposed to remain typically within around 15 km of the base station to get the best results with centimetric accuracy. The reason for this will be discussed shortly.

8.4.2 RTK measurements and processing

8.4.2.1 Real-time positioning

To facilitate differential corrections between the base station and the rover exchange of data in real time is necessary. Therefore, typically, a dedicated communication channel needs to exist between the rover and the base for this information exchange, either through a direct link or through a network via an RTK server. On receiving the correction data, the rover processes the same and finds its precise position. So, the rover receiver needs to be equipped with the RTK processing capability.

In real-time operation, the data collected at the reference station reaches the rover after some small but finite delay. The data at the base station is formatted, packetized, and transmitted over the link (Langley, 1993). The same is received at the rover and passed on to the roving receiver's software. This cannot all occur simultaneously, and so there is a latency, which, depending on the link data rate, might be around seconds. This delay might be acceptable for some static-point surveying applications, and the rover to processes the data at any instant may need to wait to receive the corresponding time-stamped data from the base station.

8.4.2.2 Postprocessing

The processing of the measurements made by the roving receiver and those received from the base station through the link is carried out in a receiver. It can also be carried out in an external computer in postprocessing mode by recording the time-stamped data. When carrying out a double-difference solution, the processing software must match the time tags of the data from the reference station and the roving station (Langley, 1998).

8.4.2.3 Correction approach

In the previous section, we learnt about different approaches to differential corrections. In modern RTK, the measured carrier phases are transferred from the base station to the rover. Then, using the differential of the measured carrier phases, the relative distance between the base and the rover is precisely estimated.

In this approach, the base station rebroadcasts its measured carrier phase based range. Typically, a radio modem, in the terrestrial UHF or VHF bands, is used for the purpose of data transfer between the base station and the rover. This communication mode is usually restricted by the limitations of the line of sight and radio communications over long distances. The Radio Technical Commission for Maritime Services (RTCM) standard is used for transferring data. Another method is to send the data over the Internet. The NTRIP protocol (Networked Transport of RTCM via Internet Protocol) enables the mobile RTK receiver (rover) to access data from the RTK base station over the Internet.

The rover unit receives the data transmitted over the suitable channel and selects the necessary data from it. It then compares its own based range measurements with those received from the base station. In the process, the common errors are eliminated, and the precise relative range is obtained from which the rover accurately estimates its relative position with respect to the base. The position of the base station being accurately known, the rover position is also estimated with an accuracy of the same order.

A few important aspects are important to mention here. Since the method utilizes the carrier phase measurements, resolving the ambiguity remains one of the major tasks in the process. The key feature enabling the high accuracies afforded by RTK operation is the ability to correctly determine the carrier-phase integer ambiguities, even while the rover is in motion. The ambiguity resolution approach is mentioned at the end of Section 8.2.2. While the float solutions can be of accuracy from meter to

decimeter level, the accuracies of the final integer ambiguity resolved solutions are in the centimetric and subcentimetric range.

Next, it is important to note here that, in the classical RTK method using a single reference station, the rover needs to work within a short range from the reference station to keep the accuracy within the allowable limit. As a rule of thumb, the error increases approximately at the rate of 1 ppm (parts per million). So, over a range of 1 km, the error increases by 1mm. The operating range of RTK positioning is thus usually limited to a distance of up to 15 km, and is not effective for a very long baseline. Although RTK provides accuracy to calculate the relative position of the user to around millimeters, their absolute position is accurate only to the same accuracy as the computed position of the base station.

Due to the motion of the satellites and changes in their clocks, the correction values change rapidly with time. Therefore, the base station needs to compute the errors with good rapidity to suit the purpose. For the typical modern receiver, this is not a very demanding requirement, unless there is a cycle slip in the phase measurements and the ambiguity has to be resolved afresh. Further, since the system works with a single base station, no redundancy of the reference measurements is usually available if the base station experiences any malfunction.

8.4.3 Networked real-time kinematics

It is now known that the accuracy of the RTK system deteriorates with the distance of the rover from the base station. This restricts the area over which the rover can move with a single base station. To alleviate the problem, instead of one base station, a network of base stations is used in many cases. Such a network can serve over a large area of interest. This method of executing RTK by using a network of reference stations is known as network RTK (NRTK). Here, a network of continuously operating reference stations (CORS) is established, 60 to 70 km apart from each other.

RTK network approach consists of four basic activities, viz.

1. Data collection at the reference stations.
2. Processing of the data and generation of correction values as necessary.
3. Broadcasting the appropriate data for correction.
4. Executing the positioning algorithm at the rover utilizing information from the NRTK.

All the computations of the network are done at the dedicated control center where the processing algorithm is housed. It controls the entire activities of the network. It also performs several tasks, including the quality check of data, applying antenna phase center corrections, ambiguity fixing, in addition to the modelling and estimation of necessary systematic errors with their derivatives, and interpolation of errors.

8.4.3.1 RTK formats

Two of the most popular NRTK correction formats are:

1. *Master-Auxiliary concept (MAC):* In the Master-auxiliary approach, the rover receiver estimates the error at its position, using the correction data with respect to the closest CORS. At least five CORS are selected by the rover, which creates a cell around its position. The selection of the CORSs that compose the cell is made by the control center, considering the CORS availability and the number of satellites.
2. *Virtual reference station (VRS):* In the VRS approach, pseudo-range and carrier phase observations, which come from at least three stations, are continuously collected and processed by a control center. The error values and their spatial gradients are derived. The control center then interpolates these values to a location near the position of the rover, as if they were acquired by a hypothetical receiver station in place in that position. This is the "virtual station." The correction data are then transmitted to the rover, as if they were being sent by the virtual station. Finally, the position is derived at the rover, with the effective baseline between itself and the virtual station.

Despite having various advantages, there are obvious downsides of the real-time methods of differential positioning. First, the precision obtained is not as high as of static techniques. This is because in dynamic techniques, the thermal noise and other random errors are not eliminated. Moreover, real-time estimations need the addition of a suitable communications link between the reference station and the measuring receiver.

8.4.4 RTK applications

The major applications of RTK are:

- Survey and Precise mapping.
- Precise infrastructure developments like laying out pipes, road alignment, etc.
- Machine Control, Construction, and setting out of utilities.
- Intelligent transportation system.
- Navigating UAV for precise delineation, UAV-based delivery, mapping, etc.
- Precise Farming.

8.5 Augmentation system

In literary terms, "Augmentation" means expansion or extension to an existing system. In satellite navigation, the term is used to mean adding to the receiver's abilities and performance over its normal capabilities with a standalone primary system by providing additional information to the user and installing additional infrastructure.

The primary navigation systems, like the GPS, Galileo, or GLONASS, etc., have certain limitations which hinder their use in standalone mode for critical applications. For example, civil aviation requires very stringent precision in the derived positions of their aircraft, during approaches and while landing. In addition to high accuracy, this particular application also demands high availability, continuity, and, most importantly, the integrity of the system. The necessary requirements in performance cannot be fulfilled by the standalone primary navigation services. We have discussed the terms, viz., the accuracy, availability, continuity, and integrity, before in Section 2.1.3. However, before moving any further, we restate them with reference to the current topic, for completeness and also for understanding the basic requirements.

- *Accuracy*: Accuracy refers to the degree of closeness of the derived position to its true position. This demands that the position estimated by using the satellite navigation system should be very close to the actual position.
- *Integrity*: Integrity of the system refers to the quantitative metric for representing the reliability of the system-derived positions, including the ability to provide a timely warning when the derived positions errors are out-of-range and deemed unreliable. Therefore, the user can be sure of his position being within the limiting error if no warning is issued. This adds a sense of reliability to the user of the system.
- *Availability*: Whenever the navigation system complies with the accuracy offered by the system and with the integrity requirements (if added in the offer), it is said to be "Available" to the user. For any service offered, it is also expected that the GNSS system should always be available to the user on demand at any time and at any location within the area of service. Critical applications like Civil aviation have very stringent requirements for availability.
- *Continuity*: Once the service has started, it should be continuously available till the length of time required by the user. Continuity is denoted by the probability that a service will continue to be available for a specified period of time.

8.5.1 Concept of augmentation

To achieve the stringent performance conditions that standalone primary systems cannot provide, some additional independent system (consisting of infrastructure, signals, processing, etc.) must be added over the existing system, so that combinedly, they can cater to these requirements. Such additional infrastructure and resources, along with associated data and processing, added to an existing primary navigation system for providing added information to the user, constitute *the Augmentation system*.

The above requirements can be catered to in general by considering the following facts:

- *Receiver positioning is done by utilizing the estimated satellite coordinates from the transmitted ephemeris and the measured ranges. For enhancing the accuracy*

of the system, the resultant errors incurred by using the primary system only must be corrected. The corrections must be made with such precision that the residual errors are much less than the targeted accuracy.

- *There must be a process of communication between the user and the augmentation system. The precise correction parameters should be made available to the users uninterruptedly.*
- *To serve the required integrity, there should be means to identify if, there is a certain probability that a largely wrong estimation of position is made even after using the correction parameters. If such a situation is identified, there should be a way to inform the user about the same.*

Implementation of the above can be achieved by augmenting the primary navigation systems with additional ground infrastructure and with necessary processing resources. In accordance with the definition, differential systems (like DGNSS, RTK, PPP, etc.), are also different variants of the Augmentation system. However, these systems are generally without the provision for integrity. In this section, out of the different available variants, we shall discuss specifically the Satellite Based Augmentation System (SBAS). Nevertheless, we have already discussed the RTK in the previous chapter and shall elaborate on PPP in Chapter 11.

8.5.2 Satellite-based augmentation system (SBAS)

A Satellite based augmentation system is an augmentation system over a primary navigation system, which separately estimates the individual errors of the primary system utilizing its measured data from different ground stations and uses a satellite for disseminating the estimated errors to the users for achieving the augmentation goals.

8.5.2.1 SBAS architecture

Architecturally, an augmentation system over a primary navigation system consists of the following ground elements:

Reference stations: The SBAS ground infrastructure consists of a network of reference stations. These reference stations, installed at well-surveyed locations across the whole area of service and sometimes beyond, are typically in duplicate or even in triplicate. Each station measures and records all observations from the respective visible satellites of the system. The measured pseudo ranges and carrier phases at each of these reference receivers, along with other auxiliary measurements, are sent to the master control center (MCC).

Master control center (MCC): The Master control center is the site where all the processing of the data is done from the measurements obtained and collated from the reference stations. MCC is established at a suitable location, typically within the area of service, to which all the data collected by the reference stations can be sent conveniently. All required processing for estimating the correction values

and generating the integrity information is done at the MCC. It houses all the necessary processing resources for this purpose. Finally, it arranges the data in a definite frame structure and sends it for transmission to the users. Since MCC serves information for critical services, a hot redundancy is always ready to take over in case of exigency.

Data dissemination unit: Transmission of the processed corrections and integrity data in an SBAS system is done using a geostationary satellite. For this reason, it obtained the name of satellite-based augmentation system. For this purpose, the SBAS system has a ground-based uplink station to transmit data to the GEO satellites.

In addition, there are communication links to transfer the data from the reference stations to the MCC and to transfer the processed corrections and integrity data from the uplink stations. The schematic of the SBAS architecture is shown in the following Fig. 8.6.

8.5.2.2 SBAS data processing

While the reference stations collect the raw data from the satellites, all the processing of this data is done at the MCC. The measured raw data is collated, and the bias values are removed after appropriate preprocessing. Finally, the different error values and the integrity parameters are derived.

8.5.2.2.1 Correction components

One of the most important activities to be accomplished at the MCC is to obtain the individual errors and generate the correction parameters.

- *Ephemeris error:* The positions of the navigation satellites are estimated by the primary system in advance and transmitted to the users in the form of ephemeris parameters through the navigation data. Naturally, the a priori estimates contain errors, using which, the receiver incurs errors in user positioning. Toward achieving improved accuracy, the current satellite positions are precisely obtained at MCC. These precise satellite positions are used for deriving the correction values for the errors incurred in using the ephemeris parameters of the navigation data.
- *Satellite clock error:* The time of transmission of the signal is utilized in the user receiver for estimating the range of the satellite. This time is marked in the navigation signal, and the satellite clock is used for the purpose. These satellite clocks are atomic clocks with very high stability. Yet they experience certain finite bias and drift over time and deviate from the system master clock. The necessary corrections of these clocks are estimated at the MCC.
- *Ionospheric errors:* The ionosphere adds excess path delay to the signals of the primary system travelling through it. This excess delay adds equivalent excess path in the ranges, when measured at the user receiver, and in turn, causes errors in user positions. Only the dual-frequency receivers can intrinsically estimate these errors and correct them. For SBAS, which serves critical applications with single-frequency receivers, the augmentation system estimates the delay and

communicates it to the users. Since the ionospheric errors are location-dependent, the total service area is divided into a number of grids with orthogonal grid lines intersecting perpendicularly at the grid points. The augmentation system estimates the vertical ionospheric errors at these predefined grid points, separated typically by $5° \times 5°$ along latitude and longitude, and transmits the same to the users through SBAS correction messages. This separation is determined from the assumption that the ionospheric variations between these points are small enough, such that linear extrapolation holds good. These values are called grid ionospheric vertical delay (GIVD) and are represented in equivalent excess path in L1 (1575.42 MHz) frequency. Along with the GIVD, an index of possible error in GIVD called the grid ionospheric vertical error index (GIVEI) is also sent, which represents a statistical confidence parameter for the GIVD. These values are updated every 300 s.

The error processing is done with such precision that the residual error remaining after all corrections are applied is extremely small and meets the requirements intended for the applications.

8.5.2.2.2 Integrity components

To understand the integrity components, we need to first understand the definition of certain important terms (RTCA, 1999). These are given below.

Protection levels: It is expected that the position estimated by the navigation receiver, even after applying all corrections provided by the SBAS system, will have certain small but finite errors. This can be due to the residual errors existing in the corrections derived. The protection levels are values of the distances surrounding the true position of the user, within which the estimated position is required to remain with a certain percentage of confidence. The protection limits surround the true position on all sides, constituting a protection volume around it. In a 3-D space, this can be resolved into two protection limits, viz. the horizontal protection limit (HPL) and the vertical protection limit (VPL). It is estimated and updated over time.

Alert limits: Independent of what the protection level at any instant is, there is a predefined distance defined about the true position, such that for SBAS (or any given application), it is mandatory for the estimated position to remain within the volume created by it. This distance is called the Alert limit. The alert limit also has two components, the horizontal alert limit (HAL) and the vertical alert limit (VAL). For the system to be available for the given application, the protection limits must be contained within the predefined alert limits, that is, $\text{HPL} \leq \text{HAL}$ and $\text{VPL} \leq \text{VAL}$. If the protection volume expands out of the alert volume, the system is required to raise an alert to the user.

Alert condition: An Alert Condition is generated when the user-calculated HPL and VPL does not fit within the bounds of the actual Horizontal and Vertical Alert Limits respectively.

Table 8.2 Important SBAS message types and their contents.

Type	Contents	Remarks
01	PRN mask assignments	Identification of the satellites for which the corrections are being sent.
02–05	Fast corrections	Fast pseudo-range corrections and their statistical error parameter.
06	Integrity information	Statistical Error parameter.
18	Ionospheric grid point masks	Identification of grid points for which corrections are being transmitted.
24	Mixed fast and long-term corrections	Mixed contents of error 02 and error 25 types.
25	Long-term satellite error corrections	Slow-varying satellite ephemeris and clock errors.
26	Ionospheric delay corrections	Grid ionospheric delay and its error index.

Time-to-alert (TTA): The alarm message is a message that warns the user not to use the information transmitted through the primary navigation system or through the SBAS. TTA is the time period starting from the time the alarm condition was actually generated to the time the receiver equipment receives and enunciates the alert.

8.5.2.3 SBAS data and signal structure

The correction parameters are transmitted in the form of slow and fast correction data messages in the SBAS signal. The data is structured into different message frames comprising of fast and long-term corrections. Some of the important standard SBAS messages are given in Table 8.2 ("Minimum Operational Performance Standards for WAAS," 1999).

The signal structure of the SBAS is similar to that of the primary services. It also has a tiered structure comprising data, code, and carrier. The data rate of the existing SBAS systems, such as WAAS, the European Global Navigation Overlay System (EGNOS), GAGAN, etc., is 250 bits/s. The transmitted data stream attains the rate of 500 symbols per second with ½ rate Forward Error Correction (FEC) encoding. These data are arranged in a frame structure. Each frame duration is 1 s and has its own

frame number, using which the kind of correction or integrity data it is carrying can be identified. Certain frames are transmitted at a higher repetition rate while others have a relatively lower probability of repetition, depending upon the type of information carried by them and their corresponding update priority.

The user, upon receiving the augmentation data, uses this in conjunction with the data from the primary signal. He extracts the required correction values pertinent to him to correct his range measurements from the respective data frames. He also reads all the grid-based ionospheric delay correction terms transmitted by the system and finds out those meant for the grids around the position where he is located. The vertical delays are first interpolated to the approximate receiver position and then converted to slant delays along the signal path. With these, he corrects his ionospheric errors in the range. Finally, the corrected ranges are used for precise positioning. The user also utilizes the integrity values to determine if using the corrections is safe or not. For this, the user SBAS-enabled instrument also calculates error bounds on position errors, that is, the vertical protection limit (VPL) and horizontal protection limit (HPL), to see if these bounds are within the alert limit or not. It raises an alert flag if such a condition is generated.

8.5.2.4 Existing satellite-based augmentation systems

SBAS was particularly aimed at civil aviation. The primary focus of the application, however, was to enable the aircraft to access the runways even in poor weather, even in the absence of the expensive ILS. It was also intended to make landing approaches safer. Further, it was meant for more time and fuel efficient use of airspace, by enabling the aircraft to fly along the shortest possible route even through regions not covered by Radars. The first operational SBAS system was the Wide Area Augmentation System (WAAS), developed by the Federal Aviation Administration of the USA (WAAS, 2014). Thereafter, various countries developed and established their own SBAS system. European Geostationary Navigation Overlay System (EGNOS) is another SBAS system operating over the European region and being managed by the European Commission. Over the Indian region, the GPS Aided Geo Augmented Navigation (GAGAN) is an operational SBAS system, which was developed and implemented jointly by the Indian Space Research Organization and the Airport Authority of India (*GAGAN - Indias SBAS*, 2016; *GAGAN*, 2016). The Multifunctional Satellite Augmentation System (MSAS), operative over Japan, is also amongst those systems set to operate for a long. Currently, many more countries have come up with their own SBAS. Amongst them, the Russians have developed the system for differential correction and monitoring (SDCM) for correction and integrity monitoring of both GPS and GLONASS satellites. The Southern Position Augmentation Network System (South PAN) has been developed and implemented in Australia and New Zealand (*SouthPAN*, 2024). The Korean Augmentation Satellite System (KASS) is also being implemented (*KASS*, 2023). The Chinese BeiDou SBAS (BDSBAS) augments both the GPS and the BeiDou system. A number of SBAS initiatives are being developed in Africa with the ultimate goal of having a single African SBAS in the future. The

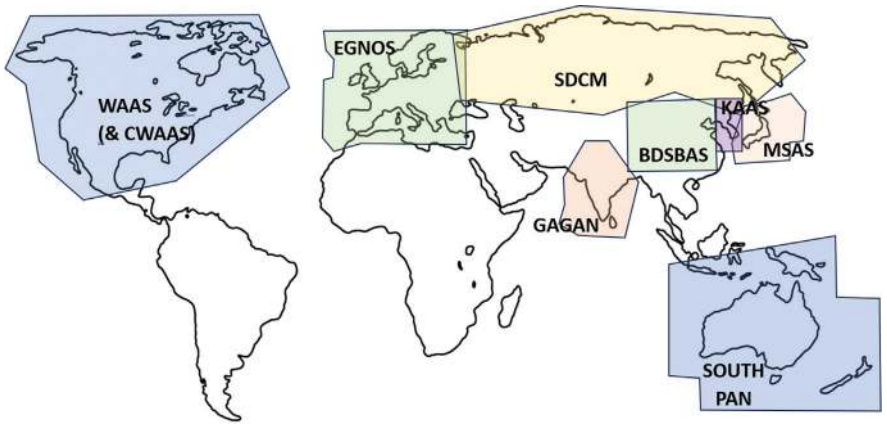

FIGURE 8.7

SBAS systems across the globe.

approximate regions of the existing SBAS systems across the globe are shown in Fig. 8.7. This figure is, however, representative and does not provide the actual coverage or scale.

Conceptual questions

1. Is the carrier phase-based ranging only useful for differential positioning and not for the standalone case?
2. Is it necessary to derive the IPP points while converting given vertical ionospheric delays to slant delays along the satellite path? If yes, why?
3. What are the factors that determine the accuracy in an RTK system where both the user and the reference are moving with time?
4. What similarities do you find in the ground resources required for establishing a differential positioning system over a wide area with code-based ranging with the general control segment architecture that we read about in Chapter 2?

References

Cosentino, R.J., Diggle, D.W., de Haag, M.U., Hegarty, C.J., Milbert, D., Nagle, J. (2006). 'Differential GPS', in Kaplan, ED & Hegarty, CJ (Eds.), *Understanding GPS Principles and Applications, 2nd Ed.*, Artech House, Boston, MA, USA.

El-Rabbani (2006). *Introduction to GPS* (*second edition*). Artech House.

Enge, P.K. 1996. Global positioning systems AIAA Differential GPS II.

GAGAN-GPS Aided GEO Augmented Navigation (2016). URSC, ISRO. Available at https://www.ursc.gov.in/navigation/gagan.jsp, Retrieved on 17 May, 2025.

GAGAN - Indias SBAS (2016). Inside GNSS, January, 2016. Available at: https://insidegnss.com/gagan-indias-sbas/, Retrieved on 22 May, 2024.

KASS- The future of SBAS in Korea (2023). Inside GNSS, February, 2023. Available at: https://insidegnss.com/kass-the-future-of-sbas-in-korea/, Retrieved on 1 June, 2024.

Kee, C. (1996), Wide Area Differential GPS, in Parkinson, BW & Spilker, JJ Jr. (eds), *Global Positioning Systems, Theory and Applications*, Vol-II, AIAA, Washington DC, USA.

Langley, R. B. (1993). Communication links for DGPS. *GPS World, 4*(5), 47–51.

Langley, R. B. (1998). RTK GPS. *GPS World, 9*, 70–76.

Leick, A. (1995), GPS satellite surveying, 2nd Ed, John Wiley and Sons, New York, USA.

Minimum operational performance standards for WAAS (1999). RTCA.

Morton, Y. T. J., Diggelen, F., Spilker, J. J., Parkinson, B. W., Lo, S., & Gao, G. (2020). *Relative positioning and real-time kinematic (RTK) position, navigation, and timing technologies in the 21stcentury: Integrated satellite navigation, sensor systems, and civil applications* (pp. 481–502). Wiley. https://doi.org/10.1002/9781119458449.ch19.

Papoulis, A. (1991). *Probability, random variables and stochastic processes*. McGraw Hill, Inc.

Real-time Kinematic Positioning (2024). Wikipedia, Available at: https://en.wikipedia.org/wiki/Real-time_kinematic_positioning, Retrieved on: 14 May, 2024.

RTK-Fundamentals. (2018). Navipedia, European Space Agency. Available at: https://gssc.esa.int/navipedia/index.php/RTK_Fundamentals, Retrieved on: 12 May, 2024.

Southern Positioning Augmentation Network-SouthPAN. (2024). Geoscience Australia, Available at: https://www.ga.gov.au/scientific-topics/positioning-navigation/positioning-australia/about-the-program/southpan, Retrieved on: 4 June, 2024.

Satellite Navigation—Wide Area Augmentation System (WAAS) (2024). Federal Aviation Administration. Available at: https://www.faa.gov/about/office_org/headquarters_offices/ato/service_units/techops/navservices/gnss/waas Retrieved on: 3 May, 2024.

CHAPTER

Special topics

9

Preamble

This chapter consists of special topics. Experienced readers know that it is customary to keep a separate chapter for those items that do not fit into any other chapter in a book. The topics to be discussed in this chapter are somewhat like that. But they do not fit else where does not mean that they are irrelevant. Rather, their relevance can be seen in many topics throughout this book. So, it would not be just to put them along with any one of them, and that is why they are "Spacial." These topics are of special interest as far as satellite navigation is concerned. Our discussion in this chapter will be on the following two topics: the Kalman filter, the ionosphere, and the space weather. But what is so special about them? Though they are categorically different in nature in terms of their influence, they have a large bearing upon satellite navigation in their own ways. So it is their immense significance that makes them special here. In the opening section of this chapter, we will discuss the theory and working of the Kalman filter in a nutshell. Then we will briefly talk about some of its applications relevant to satellite navigation that improve system performance. In contrast, in the next section, we will cover a subject that deteriorates navigation performances—the ionosphere. The main focus of this topic will be its equatorial aspects, where its high dynamics has a major influence on the satellite navigation system. Finally, we shall learn about the space weather, which under different solar events causes large variations in the geomagnetic conditions and thus influence both the global and regional navigation satellite system performance. In addressing these topics, we shall deliberately avoid difficult mathematical expressions and complex technical jargon, since our main aim is to understand the potential each of them has to improve or deteriorate navigation system performance. It is important to repeat here that readers may happily skip this chapter without any loss of continuity of the topics laid out in this book, but of course at the price of losing many interesting portions of it.

9.1 Kalman filter

9.1.1 Introduction to the Kalman filter

The Kalman filter is a mathematical tool for *estimating* the *dynamic states* of a system from the *noisy measurements* having known relations to these states and aided by

Understanding Satellite Navigation, Second Edition. DOI: https://doi.org/10.1016/B978-0-443-36432-7.00016-X

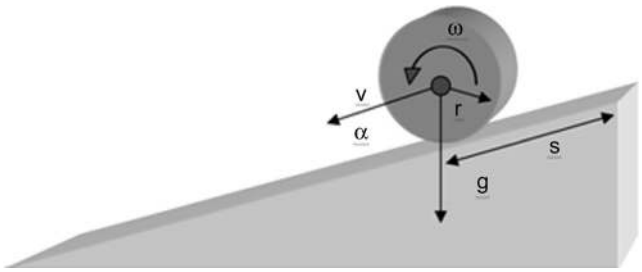

FIGURE 9.1

Description of states.

some prior knowledge about the progression of the states over time. It also provides the confidence value associated with every estimate.

It is a state-space approach in the sense that it assumes that the dynamic behavior of a system can be described by some finite states that completely define the condition of the system. The filter can estimate the values of these states at any instant and also their temporal variations, provided it has some essential information about how these system states evolve over time and some related measurements are available along with it.

It is necessary at this point to define the terms mentioned so that we can conveniently use them later while describing the working of the filter. The *state* of a system is defined by the set of variables which can fully describe the condition of a system. It can be represented quantitatively by distinct values of these variables which may change with time under the effect of factors that influence them. These states may either be independent of each other, so that the change in one does not affect the change in the other; or they can even be dependent, with the variation of one state related to the change in the other. The dependent state variables may be connected through a linear or nonlinear relation.

For example, let us take a solid metallic disc of iron. The physical condition of the disc may be described by a few properties like its physical state (solid), color (red), mass (1000 g), and radius (15 cm). These features describe the state of the disc, and the entries in the parenthesis represent the values of the variables representing the state that the disc is currently in. Notice that the first three variables are independent of each other while the last two are related nonlinearly through the constant density terms.

Now, we leave the disc to roll on its edge down a slope without slipping. In this condition, the dynamic state of a body is defined by the motion it executes under the action of a constant gravitational force, as shown in Fig. 9.1. Its state dynamics are our interest now, and hence accordingly a different set of variables now forms the system states.

The condition of the motion of this body may be represented by three variables: position s, velocity v, and acceleration a along the slope. Among these terms, the acceleration term is constant and independent of the other two variables.

Velocity is represented as the time integral of the constant acceleration, and hence it is linearly dependent upon acceleration, a. When there is no slippage, the angular velocity ω and the angular acceleration α are related to linear velocity v and linear acceleration a through the constant radius term, "r," respectively. So they are alternative representations of the same dynamic states and hence are not distinctly separate state variables. Similarly, the position s is the linear time integral of instantaneous velocity and acceleration a, and hence has a linear dependency with both of these variables. So, the temporal evolution of the states from any arbitrary discrete instant k to $k+1$ separated by time Δt may be represented using Newton's equation of motion as:

$$a_{k+1} = a_k \tag{9.1A}$$

$$v_{k+1} = v_k + a_k \Delta t \tag{9.1B}$$

$$s_{k+1} = s_k + v_k \Delta t + \frac{1}{2} a_k \Delta t^2 \tag{9.1C}$$

where s_j, v_j, and a_j are the position, velocity, and acceleration, respectively, of the disc at instant j.

The state variables may or may not be measurable themselves. However, they must manifest themselves through some measurable variables of the system. In other words, these measured variables of the system must be a function of the identified state variables from which the estimates of the state may be obtained. The functions relating the measurements to the states may also be linear or nonlinear.

In the above example, we can directly have the measurements of position, velocity, and acceleration of the particle as measurements. Alternatively, we can also measure the kinetic energy, K, and potential energy, P, of the disc (by some means). The former is a nonlinear function of its velocity while the latter is a linear function of its position. So, this can be expressed as $K = f_1(v)$ and $P = f_2(s)$. The above-mentioned variables of the dynamic states may be derived from these measurements using a Kalman filter.

With this understanding of the states and measurements, we can start to describe the Kalman filter. Further explanations of other terms will be made as we come across each of them.

9.1.2 Kalman filter basics

9.1.2.1 Initial concepts

The Kalman filter, as we have defined it, is basically a tool that estimates the state variables of a system in an optimal manner along with the confidence in the estimation using the dynamic behavior of these variables and some relevant measurements as input, even in the presence of noise.

Let the system S be defined by a set of state variables X. Thus, X is a collection of variables defined by $X = (x_1, x_2, x_3, \ldots x_n)$. X defines completely the state of the system that we are interested in and varies distinctly over the time of our interest, such that at any instant k, it takes values X_k. The set Z consists of the measurable variables $Z = (z_1, z_2, z_3, \ldots, z_m)$, available from the system, that are related to the state X. The measured values of the set of variables at time instant k are denoted by Z_k.

The values of the variables in X change with time, and the Kalman filter, to estimate the values, needs to know how. For this purpose, it requires an equation that approximately models how the values of the state variables evolve in time from one instant to the next. Accordingly, this equation should be able to define the state variables X_k of any instant as a function of the state variables of just its previous instant, X_{k-1}. In our example of states in Section 9.1.1, Eqs. (9.1A)–(9.1C) are the equations that serve this purpose.

Pragmatically, these relationships are approximate. There are always some unmodeled elements that play a role in varying the exact state values from those determined by the relations while propagating from one instant to the next. Consider, in our example, that there are random frictional forces due to the uneven nature of the path that act upon the disc oppositely to its movement, whose effects are not included in the effective acceleration, a. Moreover, there are also some untraceable forces that are not quite consistent in a practical sense. In all pragmatic cases, these random forces remain acting upon the body yet unaccounted for, causing random variation of the dynamic states by a minute amount. As these variations cannot be represented by any definite model, in a Kalman filter, these are taken as noise and are called the "system process noise."

Therefore, considering the known relation for the system state transition and allowing for the process noise, the true transition may be expressed as the combination of these two. This complete relation is called the system dynamic process model, and is given by:

$$X_k = \Phi(X_{k-1}) + w_k \tag{9.2A}$$

Here Φ is the definite function called the "state transition function," which relates the current states to the preceding ones. It can be linear and nonlinear as well. "w" is the process noise. For a linear case, the new state becomes:

$$X_k = \varphi_k X_{k-1} + w_k \tag{9.2B}$$

Here, φ_k is a discrete matrix called the state transition matrix, and w_k denotes the process noise at instant k. The latter includes all of the errors that may have occurred in using this definite model, which is a mathematical approximation of the true variation. Whatever the nature of the effect of w is, its individual values cannot be known separately. But we need to know the statistical nature of w. For a Kalman filter, w is assumed to be a zero mean white Gaussian noise with Q as the variance. We will henceforth assume this in all our subsequent derivations. Thus, the variables in X

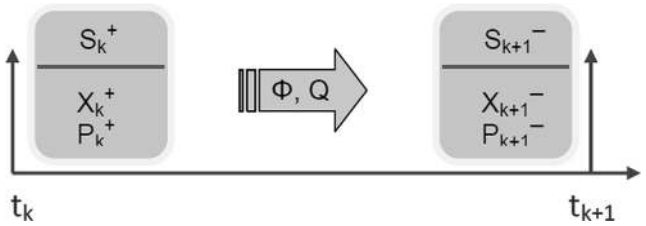

FIGURE 9.2

Time propagation of states.

propagate across time from one instant to the next following Eqs. 9.2(A) or 9.2(B) for the linear case and as shown in Fig. 9.2.

The system S has some measurable variables. Among these, some are functions of the system states of our interest. Measurements of such variables are necessary for our purpose, as it is from these measurements that the states are to be derived by the filter. However, such measurements are added with noise which cannot be segregated by any common means. So, our measurement Z_k at any instant k can be represented through a measurement equation in terms of X_k as:

$$Z_k = h(X_k) + r_k \tag{9.3A}$$

This is the generalized measurement equation, where r is the measurement noise and h is the function that relates the current state with the measurements. "h" is called the observation function. For a linear system, it can be represented as:

$$Z_k = HX_k + r_k \tag{9.3B}$$

where H is called the "observation matrix" or the "measurement sensitivity matrix" and defines the linear relationship.

The system noise at instant k that includes all the errors present in the measurements is r_k. However, we cannot separately identify what the values of r are at any instant. Had this been possible, we could have corrected the errors. For the Kalman filter to operate, we need to know at least the statistical nature of this noise. So, we assume r is a zero mean Gaussian noise with R as the measurement error variance.

For multivariate state X, φ and H are matrices. X becomes a $[n \times 1]$ vector, where the number of state variables is n, and φ is a $[n \times n]$ matrix relating each of the values of n states of one instant with the n state variables of the previous instant. The element φ_{ij} of the matrix relates the ith component of X_k with the jth component of X_{k-1}. This takes zero value if these two elements of the states are mutually independent. H is a $[m \times n]$ matrix where m is the numbers of measurements. Similarly, H_{ij} represent how the ith measurement is related to the jth state variable in X. H becomes identity when the measurements are the direct gauge of the variable themselves and zero if they are not related. Accordingly, w becomes $[n \times 1]$ and r becomes $[m \times 1]$ matrix representing the noise in each individual element in the dynamic equation

and each measurement in the measurement equation, respectively. The corresponding covariance matrices Q and R thus become [n × n] and [m × m] matrices, respectively.

Fortunately, the filter can estimate the states and can update them over time, even in the presence of noise when it knows the form of φ and H explicitly and simultaneously knows the values of only the statistical variances Q and R of the noise terms. Although a conventional Kalman filter demands these noises to be white Gaussian, there are techniques by which even non-Gaussian noises may be incorporated into the filter through noise shaping (Grewal & Andrews, 2002; Maybeck, 1982).

9.1.2.2 Estimation process

The Kalman filter starts with initialization of the state variables in X and with an appropriate error covariance associated with the same. Subsequent to this, the state values are calculated and propagated over time by updating the variables successively through two recurring processes, viz., the measurement update and the temporal update. Consequently, the error covariances also get modified and converge to an optimal limiting value.

9.1.2.2.1 Temporal update

Temporal updating is the process in which the state derived or assumed by the filter at any instant is propagated through time according to the system dynamic process model as given in Eq. (9.2). The state transition matrix is used to obtain the best possible values of the new state variables at the immediate next instant from the current ones. These time-propagated state variables now form the a priori estimate of the state for the next instant.

9.1.2.2.2 Measurement update

Measurements done at any instant are assimilated with the a priori estimate of the state variables already available to the filter from the last temporal update. This further updates the state, and the result thus formed constitutes the posterior estimate of the states. Addition of independent information, resulting from this measurement update, leads to further improvement of the estimation accuracy compared to the a priori estimate. The measurement equation is utilized during this update to relate the measurement to the state variables.

So, if we call the temporal update a prediction process, the measurement update may be referred to as a correction process. It is important to mention here that, along with the state estimates, the Kalman filter also updates the confidence bounds of each of the estimates it generates in both processes. The above-mentioned updates continue iteratively while the Kalman filter offers an optimal solution for the state variables of the dynamic system. The complete iterative process consisting of the temporal update and the measurement update is shown in Fig. 9.3 and is described in Section 9.1.3.

For the purpose of convenience, in the description we demarcate every instant by the point at which the measurements are done. So the times marked by τ_1, τ_2, τ_3, etc., are those specific instants at which the measurements are done. The instant just before any particular measurement instant τ_k is denoted by τ_k^-, and that momentarily after

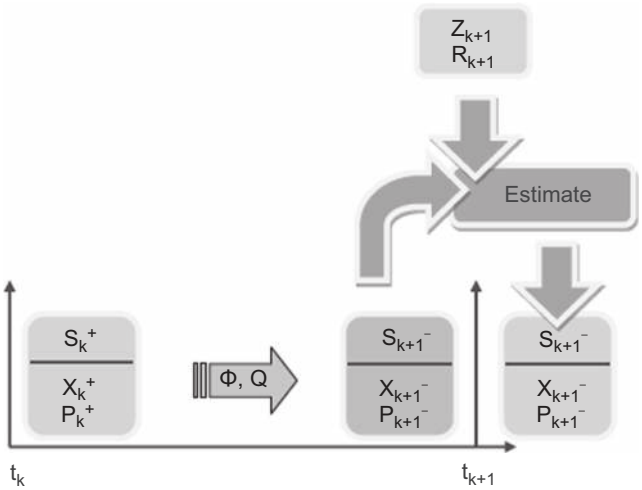

FIGURE 9.3

Complete iterative process for Kalman filtering.

the measurement instant is denoted by τ_k^+. So, the a priori estimate X_k^- of the instant τ_k is available at τ_k^-, while the posterior estimate X_k^+ is available at τ_k^+.

9.1.3 Derivation of the filter equations

With this basic idea of the working of the Kalman filter, let us find out the quantitative expression for the different updates of the state of a system. We assume a linear system and start from an initial guess, X_0^+ of the state variables. The error variance of the estimates is taken as P_0^+ when we are starting the filter process afresh at the instant τ_0. From this initial state X_0 or from any intermediate time τ_k^+, at which the state variables X_k^+ are already determined, the immediate next task is to hop to the next instant and to get the time updated states. The values of the state variables to be arrived at will be X_{k+1}, where k can be zero or any other positive value, as the case may be. Thus, we propagate the state over time using our knowledge of the system dynamics given in the process equation (Eq. 9.2B).

But how do we proceed when we do not have the values of w? With φ as the state transition matrix that carries the system state variables X_k^+ from τ_k^+ to τ_{k+1}^-, the Kalman filter simply updates the states as

$$\hat{X}_{k+1}^- = \varphi X_k^+ \tag{9.4}$$

$\hat{X}_k$ is the ensemble average of all possible values of X_{k+1} each candidate of the ensemble having the noise. It is the best possible estimate that the filter could do with the available information. The noise term w_k, being zero mean vanishes in the process

of finding the expectation value. However, this exclusion of the nondeterministic component in the update must result in some deterioration in the estimate precision. So the error covariance is updated by the filter in such a way that it accommodates and represents this effect. The effective error covariance may be expressed as the sum of two terms; (i) the covariance due to the errors that were already in the state estimate which propagated during this temporal update, and (ii) the covariance of the stochastic resulting as the effect of taking this probabilistic mean as in Eq. (9.4).

From the process equation, it is clear that as $X_k^+$is carried from $\tau_k^+$to τ_{k+1}^-, so are its associated errors. So, if X_k is the true value at instant τ_k^+, let the estimate be $\hat{X}_k^+ = X_k + \varepsilon_k$, where ε is the associated estimation error. This is, however, the best estimated value for the instant. The estimate after the temporal update is $\phi(X_k^+) = \phi(X_k + \varepsilon_k^+)$. For a linear process, the propagated state may be represented as $\varphi X_k + \phi\varepsilon_k^+$. So the error is due to the already existing error $\varepsilon_k^+$is now $\varepsilon_{k+1}^- = \varphi\varepsilon_k^+$after the update at τ_{k+1}^-. Therefore, its covariance is given by

$$\begin{aligned} P(\varepsilon_{k+1}^-) &= E\{[\varphi\varepsilon_k^+] \cdot [\varphi\varepsilon_k^+]^T\} \\ &= E[\varphi\varepsilon_k^+\varepsilon_k^{+T}\varphi^T] \\ &= \varphi P_k^+\varphi^T \end{aligned} \tag{9.5A}$$

Here, $E[\varepsilon_k^+\varepsilon_k^{+T}] = P_k^+$, which is the error covariance of the last state X_k^+. Now the effect of vanishing of "w" will incorporate the value of the covariance of w into this in addition. As Q_k is the variance of w_k, and w_k is uncorrelated to the existing estimate errors ε_k^+, the total error covariance will be just the sum of the two individual covariances. So the effective error covariance after the temporal update is

$$P_{k+1}^- = \varphi P_k^+\varphi^T + Q_k \tag{9.5B}$$

Since P_k^+ has all positive diagonal elements and $\phi P_k^+\phi^T$is quadratic in nature, the above expression reveals that the estimates obtained during the temporal updating process does not improve the confidence level of the solution but rather deteriorates it. So at the instant τ_{k+1} and before the next measurement is done, the a priori estimate of the state at $\tau = \tau_{k+1}^-$is given by

$$S_{k+1}^- = [X_{k+1}^-, P_{k+1}^-] \tag{9.6}$$

This completes the temporal update part of the process.

The measurements are taken at τ_{k+1}. Let Z_{k+1} be the measured value and let r be the error in measurement with variance R. From the measurement equation, we know that:

$$Z_{k+1} = HX_{k+1} + r_{k+1} \tag{9.7A}$$

Now, we already have an estimate of the value of X_{k+1}^-, which was obtained by time propagating the state variables $X_k{}^+$of the previous instant. Additionally, we have its corresponding error variance, P_{k+1}^-, which has also obtained by time propagating P_k^+. This forms the a priori estimate of the state.

So, at this point, we have two sets of data at τ_{k+1}. One of them is from the a priori knowledge of the system state, X^{-}_{k+1} and its covariance P^{-}_{k+1}, while the other is the direct measurement, consisting of Z and R. The measurement and the corresponding X value, viz. ${X_{k+1}}^{m}$ can be expressed as

$$\begin{aligned} Z_{k+1} &= H{X^{m}}_{k+1} + r_{k+1} \\ {X_{k+1}}^{m} &= H^{-1}Z_{k+1} + H^{-1}r_{k+1} \end{aligned} \tag{9.7B}$$

The corresponding error covariance in X is given by

$$P^{m}_{k+1} = E\left\{\left[H^{-1}r_{k+1}\right] \cdot \left[H^{-1}r_{k+1}\right]^{T}\right\} = H^{-1}R_{k+1}H^{-T} \tag{9.7C}$$

These two sets of the estimates of the same state vector X are intelligently combined by the filter such that it gets a new estimate of the updated posterior state at τ^{+}_{k+1} that is better in precision than each individual constituent. In the Kalman filter, this is done by a weighted combination of the two states in accordance to the relative confidence to get the refined state X_{k+1} at $\tau = \tau^{+}_{k+1}$.

Now, leaving the particular case of Kalman filtering for the moment, if we concentrate on any estimation, in general, with a weighted combination of available estimates where the weight values are w_1 and w_2 for the two estimates X_1 and X_2, respectively, the updated estimate will be

$$\hat{X} = w_1X_1 + w_2X_2 \tag{9.8}$$

However, the question is what value of w_1 and w_2 will give us the optimal estimate? A simplified way to derive the weights is to assume that the two states are available with corresponding error variances as σ_1 and σ_2. Since the two states are derived from independent sources, the errors are uncorrelated. Moreover, with w_1 and w_2, as the weights assigned to the two estimates for combination, the normalized weight factor warrants $w_1 + w_2 = 1$. So the weights can be represented as $w_1 = w$ and $w_2 = (1 - w)$.

Since the final estimate is a linear combination of the individual estimates, the resultant error will also be the same linear combination of the errors. Then, if ε_1 and ε_2 are the errors in the individual state estimates, the resultant error will be

$$\varepsilon_{eff} = w_1\varepsilon_1 + w_2\varepsilon_2 \tag{9.9}$$

So the variance of the resultant error will be

$$\begin{aligned} \sigma^{2}_{eff} &= E\left[\varepsilon_{eff} \cdot \varepsilon'_{eff}\right] \\ &= E\left[(w_1\varepsilon_1 + w_2\varepsilon_2) \times (w_1\varepsilon_1 + w_2\varepsilon_2)\right] \\ &= \left[w_1^2\varepsilon_1^2 + w_2^2\varepsilon_2^2\right] \end{aligned} \tag{9.10A}$$

As w_1 and w_2 are definite numbers and the errors in the two estimates are uncorrelated, expectation values of the mutual product of the errors are zero. So it

gives the value of σ_{eff} as

$$\begin{aligned}\sigma_{eff}^2 &= w_1^2\sigma_1^2 + w_2^2\sigma_2^2 \\ &= w^2\sigma_1^2 + (1-w)^2\sigma_2^2\end{aligned} \tag{9.10B}$$

The combination should yield maximum confidence and hence the σ_{eff} should be the minimum. Now, to minimize this quantity, we differentiate the above expression in Eq. (9.9B) with respect to w and equate to zero. So we get

$$2w\sigma_1^2 - 2(1-w)\sigma_2^2 = 0$$

$$\text{or, } w\sigma_1^2 = (1-w)\sigma_2^2$$

$$\text{or, } w = \sigma_2^2/(\sigma_1^2 + \sigma_2^2)$$

$$\text{so, } (1-w) = 1 - \sigma_2^2/(\sigma_1^2 + \sigma_2^2) = \sigma_1^2/(\sigma_1^2 + \sigma_2^2)$$

Thus, we get the two weights as

$$w_1 = \sigma_2^2/(\sigma_1^2 + \sigma_2^2) \tag{9.11A}$$

$$w_2 = \sigma_1^2/(\sigma_1^2 + \sigma_2^2) \tag{9.11B}$$

Using these values of the weights, we get the estimation as

$$\begin{aligned}X &= w_1X_1 + w_2X_2 \\ &= X_1\sigma_2^2/(\sigma_1^2 + \sigma_2^2) + X_2\sigma_1^2/(\sigma^{2_1} + \sigma_2^2)\end{aligned} \tag{9.12}$$

Further, the minimized value of the variance is obtained as

$$\begin{aligned}\sigma_e^2 &= \sigma_2^4\sigma_1^2/(\sigma_1^2 + \sigma_2^2)^2 + \sigma_2^2\sigma_1^4/(\sigma_1^2 + \sigma_2^2)^2 \\ &= \left\{\sigma_2^2\sigma_1^2/(\sigma_1^2 + \sigma_2^2)^2\right\} \times (\sigma_2^2 + \sigma_1^2) \\ &= \sigma_2^2\sigma_1^2/(\sigma_1^2 + \sigma_2^2)\end{aligned} \tag{9.13}$$

Now, coming back to our specific problem, in the case of KF, we have the a priori estimate X_{k+1}^- with proper covariance value P_{k+1}^-, and the other value of X derived from the measurement Z, given by X_{k+1}^m and the corresponding error covariance P_{k+1}^m. Now, we shall combine these two sets in a definite ratio, using the weights, which are derived in accordance with the relation developed in Eq. (9.11).

Therefore, if X_{k+1}^- and X_{k+1}^m are the state values at instant $k+1$ obtained from a priori estimate and derived from measurement, respectively; and if P_{k+1}^- and P_{k+1}^m represent their respective error covariance values; then we can obtain the updated estimate X_{k+1}^+ derived from the two individual estimates using Eq. (9.11) as

$$\begin{aligned}
X^{+}_{k+1} &= (X^{m}_{k+1}P^{-}_{k+1} + X^{-}_{k+1}P^{m}_{k+1})/(P^{-}_{k+1} + P^{m}_{k+1}) \\
&= [X^{m}_{k+1}P^{-}_{k+1} + X^{-}_{k+1}H^{-1}RH^{-T}]/[P^{-}_{k+1} + H^{-1}RH^{-T}] \\
&= [X^{-}_{k+1}P^{-}_{k+1} + X^{-}_{k+1}H^{-1}RH^{-T} - X^{-}_{k+1}P_{k+1-+X^{m}_{k+1}P^{-}_{k+1}}]/[P^{-}_{k+1} + H^{-1}RH^{-T}] \\
&= [X^{-}_{k+1}(P^{-}_{k+1} + H^{-1}RH^{-T}) + (X^{m}_{k+1} - X^{-}_{k+1})P^{-}_{k+1}]/[P^{-}_{k+1} + H^{-1}RH^{-\ T}] \\
&= X^{-}_{k+1} + [(X^{m}_{k+1} - X^{-}_{k+1})P^{-}_{k+1}]/[P^{-}_{k+1} + H^{-1}RH^{-T}]
\end{aligned}$$

After this, we do a few manipulations, first by right-multiplying both the numerator and denominator of the second term in the above expression by H^{T} and then left-multiplying both by H, and this becomes

$$\begin{aligned}
X^{+}_{k+1} &= X^{-}_{k+1} + [H(X^{m}_{k+1} - X^{-}_{k+1})P^{-}_{k+1}H^{T}]/[HP^{-}_{k+1}H^{T}+R] \\
&= X^{-}_{k+1} + [(HX^{m}_{k+1} - HX^{-}_{k+1})P^{-}_{k+1}H^{T}]/[HP^{-}_{k+1}H^{T} + R]
\end{aligned}$$

Again using the measurement equation $Z = HX + r$ and making use of the definite part as the expected value of it, we get

$$X^{+}_{k+1} = X^{-}_{k+1} + (Z_{k+1} - HX^{-}_{k+1})P^{-}_{k+1}H^{T}/\left[HP^{-}_{k+1}H^{T} + R\right] \tag{9.14}$$

$(Z - HX_{k+1})$ is the amount of new information available to the filter for the measurement Z. It is called the *innovation*. The expression $P^{-}_{k+1}H^{T}/\left[HP^{-}_{k+1}H^{T} + R\right]$is called the *Kalman gain*, K. It represents the portion of the innovation that should be added to the a priori estimate to yield the optimal posterior result. The corresponding error variance after update can be written using Eq. (9.12) as

$$P^{+}_{k+1} = \left[P^{-}_{k+1}H^{-1}RH^{-T}\right]/\left[P^{-}_{k+1} + H^{-1}RH^{-T}\right]$$

Doing similar manipulations as above, we get

$$\begin{aligned}
P^{+}_{k+1} &= \left[HP^{-}_{k+1}H^{-1}R\right]/\left[HP^{-}_{k+1}H^{T} + R\right] \\
&= P^{-}_{k+1}R/\left[HP^{-}_{k+1}H^{T} + R\right] \\
&= P^{-}_{k+1}\left(HP^{-}_{k+1}H^{T} + R - HP^{-}_{k+1}H^{T}\right)/\left(HP^{-}_{k+1}H^{T} + R\right) \\
&= P^{-}_{k+1}(1 - HK)
\end{aligned} \tag{9.15}$$

The same expression for X^{+}_{k+1}can be obtained with a different approach. The measured and the estimated states can be written as equations in matrix form, with X^{+}_{k+1}as unknown

$$\begin{aligned}
Z_{k} &= HX^{+}_{k+1} + r_{k+1} \\
X^{-}_{k+1} &= IX^{+}_{k+1} + \varepsilon^{-}{}_{k+1}
\end{aligned} \tag{9.16A}$$

where ε is the error in the a priori estimation with covariance, P^{-}_{k+1}. Then, solving for $X^{+}{}_{k+1}$, we get,

$$\begin{pmatrix} Z_{k+1} \\ X^{-}_{k+1} \end{pmatrix} = \begin{pmatrix} H \\ I \end{pmatrix} X^{+}_{k+1} + \begin{pmatrix} r_{k+1} \\ \varepsilon^{-}{}_{k+1} \end{pmatrix} \tag{9.16B}$$

$$\text{or, } b_{k+1} = AX^{+}_{k+1} + m_{k+1}$$

where $A = [H^T I]^T$, $b = \left[Z_{k+1}^T X_{k+1}^{-T}\right]^T$ is the matrix of the available parameters X and Z at the beginning of the temporal update, and $m = [r_{k+1}\ p_{k+1}]^T$ represents the error portion of the equation. So, considering the covariance of m as $M = E[m \bullet m^T]$, the optimal solution for X (Strang, 1988) is given by

$$X^{+_{k+1}} = \left(A^T M^{-1} A\right)^{-1} A^T M^{-1} b \tag{9.17}$$

Replacing the values of m in M and considering r and p are uncorrelated, we get

$$\begin{aligned} M &= E\{\left[r_{k+1}\varepsilon_{k+1}\right]^T\left[r_{k+1}\varepsilon_{k+1}\right]\} \\ &= E\begin{bmatrix} {r_{k+1}}^2 & r_{k+1}\varepsilon^-_{k+1} \\ r_{k+1}\varepsilon^-_{k+1} & {\varepsilon^-_{k+1}}^2 \end{bmatrix} \\ &= \begin{bmatrix} R_{k+1} & 0 \\ 0 & P^-_{k+1} \end{bmatrix} \\ \text{or, } M^{-1} &= \begin{bmatrix} {R_{k+1}}^{-1} & 0 \\ 0 & {P^-_{k+1}}^{-1} \end{bmatrix} \end{aligned} \tag{9.18}$$

Replacing Eq. (9.18) in Eq. (9.17)

$$\begin{aligned} X^+_{k+1} &= \left(\left[H^T I\right]\begin{bmatrix} R^{-1} & 0 \\ 0 & {P^-_{k+1}}^{-1} \end{bmatrix}\left[H^T I\right]^T\right)^{-1}\left(\left[H^T I\right]\begin{bmatrix} R^{-1} & 0 \\ 0 & {P^-_{k+1}}^{-1} \end{bmatrix}\right)\left[Z_k^T X_{k+1}^{-T}\right]^T \\ &= \left(\left[H^T R^{-1}\ {P^-_{k+1}}^{-1}\right]\left[H^T I\right]^T\right)^{-1}\left(\left[H^T R^{-1}\ {P^-_{k+1}}^{-1}\right]\left[Z_k^T X_{k+1}^{-T}\right]^T\right) \\ &= \left(H^T R^{-1} H + {P^-_{k+1}}^{-1}\right)^{-1}\left(H^T R^{-1} Z_k + {P^-_{k+1}}^{-1} X^-_{k+1}\right) \\ &= \left[H + RH^{-T}\ {P^-_{k+1}}^{-1}\right]^{-1}\left[Z_k + RH^{-T}\ {P^-_{k+1}}^{-1} X^-_{k+1}\right] \\ &= \left[HP^-_{k+1}H^T + R\right]^{-1}\left[Z_k P^-_{k+1} H^T + RX^-_{k+1}\right] \\ &= \left(Z_k - HX^-_{k+1}\right)P^-_{k+1}H^T/\left[HP^-_{k+1}H^T + R\right] + \left(HX^-_{k+1}P^-_{k+1}H^T + RX^-_{k+1}\right)/\left[HP^-_{k+1}H^T + R\right] \\ &= \left[X^-_{k+1}\left(HP^-_{k+1}H^T + R\right) + \left(Z_k - HX^-_{k+1}\right)P^-_{k+1}H\right]/\left[HP^-_{k+1}H^T + R\right] \\ &= X^-_{k+1} + \left(Z_k - HX^-_{k+1}\right)P^-_{k+1}H/\left[HP^-_{k+1}H^T + R\right] \end{aligned} \tag{9.19}$$

Comparing this equation to Eq. (9.14), we can find that it leads to the same expression for X. This matrix solution is nothing but the projection of the true values of X onto a plane spanned by the Z vector, where the final error is orthogonal

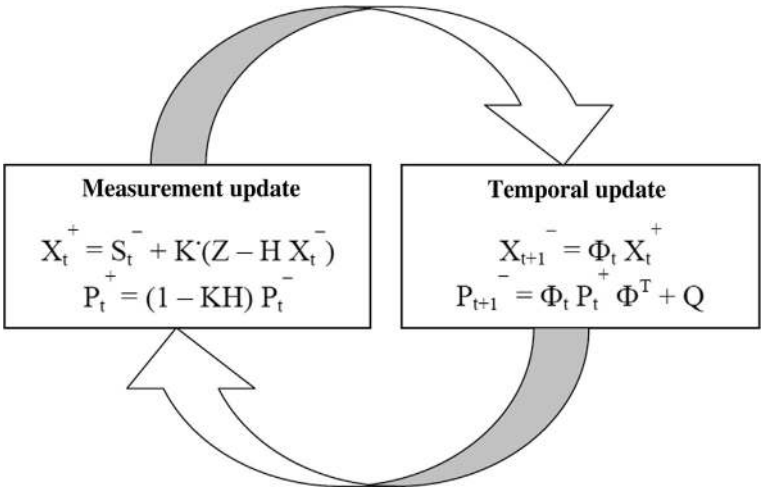

FIGURE 9.4

Iteration cycles of a Kalman filter.

to this plane. So another way to visualize the same is to assume the n-state system as an n-dimensional vector in a vector space and to interpret the same result geometrically.

This ends the measurement update process. At the end of one such iteration of a temporal update and subsequent measurement update, we get the updated state values X_{k+1}^+ at time instant τ_{k+1}^+ and its corresponding error covariance P_{k+1}^+.

In this way, the Kalman Filter function starts from the estimate of the initial values of the state variables and then recurs through the cycles of measurement and temporal updates, as shown in Fig. 9.4, to find the updated estimates of the state in a continuous manner. The process, improves the estimates on successive cycles and ultimately converges to the optimal values of the state variables. The time intervals between successive iterations may be the same or different from cycle to cycle. Accordingly, the state transition matrix φ has to be established and the Q values may have to be changed, if necessary.

One important thing to notice here is the fact that the error covariance improves in a measurement update as it is evident from Eq. 9.15. We have already seen that the variance deteriorates during the temporal update. So for the solution to converge, the improvement in the measurement update must overcompensate the amount of deterioration during the temporal update.

We have only described here the working of the conventional linear Kalman filter. However, the filter may be modified to work even for nonlinear cases and also for conditions when the noises are not Gaussian.

Box 9.1 shows the use of a MATLAB program for Kalman filtering.

BOX 9.1 Kalman Filtering

The MATLAB program Kalman.m was run to obtain the true value of a source voltage when its measurements were corrupted by noise of Gaussian random nature with $\sigma = 1$. The figure below represents the true voltage at 5 V. The measured samples are shown as (X) and the Kalman estimation of the true voltage is shown as diamonds (◊). Note the convergence of the estimates (Fig. M9.1).

Run the program with different values of σ and for different sample lengths and observe the variation. Put in some finite value of Q and also notice the difference.

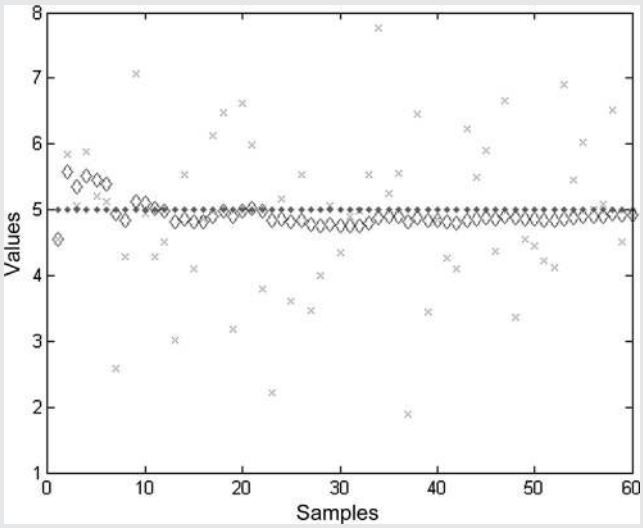

FIGURE M9.1

Estimations in a Kalman filter.

9.1.4 Use of the Kalman filter

9.1.4.1 Precision estimation in a satellite-navigation receiver

The precision of the position estimates in a navigational receiver may be improved by removing the random error components in the estimation by using a Kalman filter. This is a proven technique and needs only proper implementation in the navigation receiver.

A satellite navigation receiver will provide the PVT information to the users. The standard errors expected in such receivers are also present here. The objective of the Kalman filter will be to use the variables available in the receiver, and by means of the filter operations, reduce the associated errors to provide more accurate and precise values of the final PVT output along with a level of confidence on the estimation.

A systematic approach may generate different alternative filter designs for such applications, each based on a particular set of system model. However, it is recommendable to design simplified system models that retain the salient features of the states and its variations yet providing adequate estimation accuracy. In case of a navigation receiver, the system may be described through the observation equation that relates the pseudorange to the position coordinates and time offset. As the measured pseudorange is related nonlinearly to these state variables, an extended Kalman filter (EKF) model is appropriate here. The elements in the measurement matrix in such an EKF are obtained by the partial differentiations of the nonlinear measurement functions. So for an observation $Z = h(X) + r$, the measurement matrix H is given by

$$H_k = \partial h / \partial X|_{X_k} \tag{9.20A}$$

Partial differentiations, with respect to each of the states for a given measurement, that is, the Jacobian will form the elements of a row in this Measurement Sensitivity Matrix, H. A similar row will be generated for different observations at the same instant of measurement update.

9.1.4.1.1 Choice of state variables

The output of the receiver will be the navigation parameters, PVT. So position S_k, velocity V_k, and clock bias B_k are obvious state variables of the filter. To obtain these values, the model also includes variables of one-order-higher derivatives. So the acceleration A_k and the clock drift D_k are also state variables to be considered here. However, this assumes that the derivatives of position from third order onwards and time beyond first order are either zero or negligibly small to impact the values of the parameters over the updating time. But the state can be extended to variables of higher orders, if necessary, for receivers with a higher order of dynamics. So the system state considered consists of the following variables

$$\begin{aligned}
\text{1.Current Position} S_k &= \left[xyz\right]_k \\
\text{2.Current Velocity} V_k &= \left[v_x v_y v_z\right]_k \\
\text{3.Current Accelaration} A_k &= \left[\alpha_x \alpha_y \alpha_z\right]_k \\
\text{4.Clock bias} B_k &= \left[b\right]_k \\
\text{5.Clock drift} D_k &= \left[b'\right]_k
\end{aligned} \tag{9.21}$$

Thus, the complete state vector becomes $X_k = \left[\begin{array}{ccccc} S_k & V_k & A_k & B_k & D_k \end{array}\right]$. It will constitute an $[11 \times 1]$ array to represent the dynamic state in a three-dimensional space.

9.1.4.1.2 Measurement equation

Here, the measurements are the pseudoranges, ρ corrected for the ionospheric, tropospheric, and other available corrections. So

$$Z = \rho \tag{9.22A}$$

Since at any instant the number of measurements depends upon the number of visible satellites, the size of Z is variable. All visible satellites can be used for the purpose with required cutoff in elevation angle.

The measurement done by the receiver, that is the pseudo range, which has a quadratic relationship with the state parameters. The measurement model equation is

$$\begin{aligned} Z_k &= \rho_k \\ &= \sqrt{(x_S - x_k)^2 + (y_s - y_k)^2 + (z_s - z_k)^2} + b_k + r_k \\ &= h(S) + r_k \end{aligned}$$

where h(.) is the nonlinear function for measurement model and r is the residual range error assumed to be normally distributed as N(0,R). Other notations carry their usual meanings.

$$H = dh/dX|_{k(k)} \tag{9.23A}$$

From this equation, using Eq. (9.20), the observation matrix H may be obtained as the partial differentiation of h with respect to the individual state variable

Or:

$$H = \left[\frac{\partial h}{\partial x}\frac{\partial h}{\partial y}\frac{\partial h}{\partial z}\frac{\partial h}{\partial v_x}\frac{\partial h}{\partial v_y}\frac{\partial h}{\partial v_z}\frac{\partial h}{\partial \alpha_x}\frac{\partial h}{\partial \alpha_y}\frac{\partial h}{\partial \alpha_z}\frac{\partial h}{\partial b}\frac{\partial h}{\partial b'}\right]$$

Since the pseudo-range is only a function of position and clock bias and is independent of velocity, acceleration, or clock drift, we get

$$H = \left[-\frac{(x_s - x_r)}{l} - \frac{(y_s - y_r)}{l} - \frac{(z_s - z_r)}{l} \quad 0 \quad 0 \quad 0 \quad 0 \quad 0 \quad 0 \quad 1 \quad 0\right] \tag{9.23B}$$

where $l = \sqrt{(x_s - x_r)^2 + (y_s - y_r)^2 + (z_s - z_r)^2}|_{t_k}$ – l is the true geometric range of the satellite. So we find that for the estimation of H, both the satellite coordinates and the receiver positions must be known for the instant. The satellite coordinates are known to the receiver from the ephemeris. But, what should we use for receiver position coordinates when we are only trying to derive the same? We shall use here the a priori knowledge of the receiver position that it has at the moment of measurement update before the position got refined by the Kalman filtering process.

9.1.4.1.3 Process equation

Although the measurement equation is nonlinear, the process equation may be expressed as a linear relation between the current variables and the same at the next instant. So using Eq. (9.2B), we get

$$X_{k+1} = \varphi \cdot X_k + w_k \tag{9.24A}$$

Where, φk is the linear relation for state dynamics and is taken as

$$\varphi = \begin{bmatrix} I(3) & dt \cdot I(3) & 0.5 \cdot dt^2 \cdot I(3) & 0 & 0 \\ 0 & I(3) & dt \cdot I(3) & 0 & 0 \\ 0 & 0 & I(3) & 0 & 0 \\ 0 & 0 & 0 & I & dt \end{bmatrix}$$

where I(3) is an identity matrix of dimension 3. w is the dynamic model error normally distributed as N(0, Q).

9.1.4.1.4 Kalman filter process

The Kalman filter process starts from the point of initiation with an initial guess of the system state X_0 and its covariance, P_0. Then the standard algorithm is followed to get the evolution of the states through measurement and temporal updates. Following Eqs. (9.4) and (9.5B), the temporal updates become

$$\begin{aligned} \text{State Propagation :} \quad & X_k^- = \varphi_k X_{k-1}^+ \\ \text{Error covariance propagation :} \quad & P_k^- = \varphi_k P_k^+ \varphi_k^T + Q \end{aligned} \tag{9.25A}$$

Then, after the measurements are done, the measurement update is carried out according to the equation of the states and corresponding covariance

$$\begin{aligned} \text{State Update :} \quad & X_k^+ = X_k^- + K_k[Z_k - h(X_k)] \\ \text{Error Covariance update :} \quad & P_k^+ = [I - K_k H_k] P_k^- \end{aligned} \tag{9.25B}$$

Here, K_k is the Kalman Gain at instant k and is given by $K_k = P_k^- H_k^T [H_k P_k^- H_k^T + R_k]^{-1}$. Thereafter, this iterative progress continues updating the values of X and P over time and measurements to obtain continually improving states of the system.

An important thing to observe is that with the EKF, the Kalman gain K, being a function of the observation matrix H, is dependent upon the current state values. This is because H is defined by the derivatives of h derived at the current state values. However, for a linear case, it was a constant independent of the state values. So for nonlinear cases, the covariance update, involving K during the measurement update process, cannot be done without the knowledge of the current state variable values, which is possible in the case of a linear system.

Box 9.2 shows the use of a MATLAB program to improve point estimation using the Kalman filter.

BOX 9.2 Precise Position Estimation

The MATLAB program Kalman_Pos.m was run to understand the working and the improvement obtained by using the Kalman filter. Data were simulated from the visible satellites, using the "true" GPS navigation file from a receiving station named IISC at Bangalore in India. for an

(*continued*)

BOX 9.2 Precise Position Estimation — *cont'd*

arbitrarily selected date. The variation of the satellite positions with time was derived from the files. The true position of the receiver is known a priori. Therefore, the true geometric ranges are calculated from them and added with zero-mean Gaussian measurement noise to create the pragmatic conditions. The standard deviation of the noise added to the ranges is 5 m (1σ).

A single-point positioning (SPP) estimator was also developed to compare the position estimations. Standard SPP-based estimation was done along with Kalman filter-based estimations, and the results were compared. Fig. M9.2 shows the comparison of position estimations using the Kalman filter. The figure clearly indicates the improvement in terms of geographical position when the Kalman filter has been used.

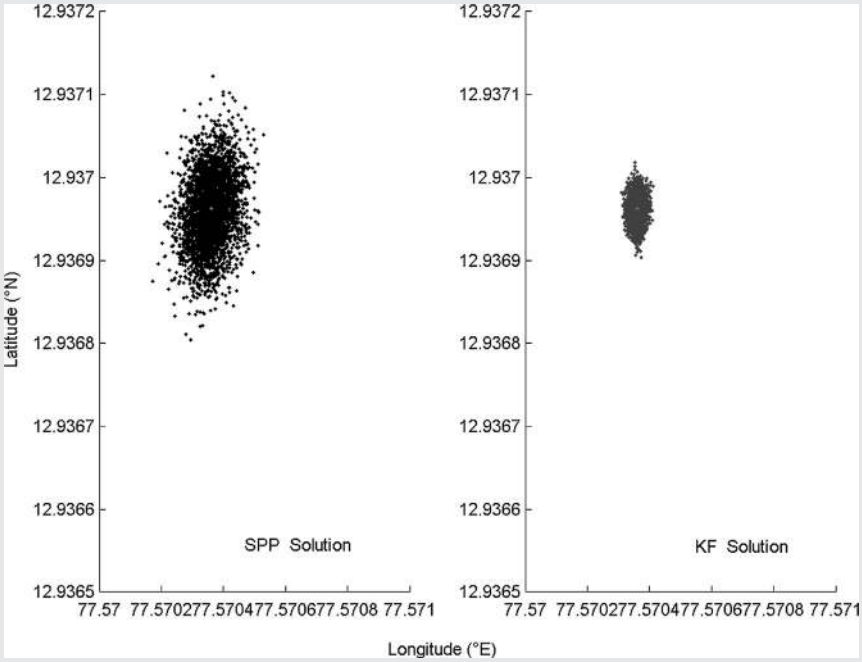

FIGURE M9.2

Improvement in position estimation (geographical).

9.1.4.2 Integration of inertial navigation system and sat-nav

In this section, we will learn a few techniques that intelligently combine the satellite navigation solution with an inertial navigation system (INS) using a Kalman filter. As a result, the individual systems work in a synergistic way in the combined form to yield better performance in terms of accuracy, precision, and availability.

The endeavor to integrate different types of navigation systems with the GNSS was aimed at harnessing the advantages of different systems to effectually obtain a navigation solution with enhanced performance. Here, we take a general view of such integration between the GNSS and INS in a manner that needs no special prerequisites of any definite system.

Here, we will only mention how and where a Kalman filter can be used for this purpose. First, we will point out the complementary nature of the two systems. Then, an overview on the different integration strategies and configurations will be mentioned, with emphasis on the loose and tight architectures.

9.1.4.2.1 Integration goals

The basic motivation behind the integration of any two navigation systems remains the improvement of their combined performance as the two systems can perform in a synergistic manner. The integration of an INS and Sat-Nav has no different intentions as far as the objectives of integration are concerned. This enables the combined system to offer increased accuracy, precision, availability, and continuity (Grewal et al. 2002). In other words, it maintains a specified level of navigation performance, even during the outage of one of the systems.

We have come to understand that the primary satellite navigation systems have some characteristic drawbacks. Position estimates are typically made using the range measured with a code-based ranging technique in a commercial receiver. The code-based ranging is noisy, and hence the positions derived from them have very poor precision, although the accuracy of the estimates may be good enough. Further, it has a stringent requirement of visibility of four good satellites to obtain an accurate solution.

On the other hand, an INS, working on the principles of dead reckoning using the output data from the accelerometer and gyroscope, gives the values of instantaneous position and orientation, that is condition in six degrees of freedom. However, these results are very much prone to the bias of the instruments. Commercial instruments show relatively high bias after a considerable time in operation. Hence, the positions derived from an INS have poor accuracy, although their precision may be much better than the Sat-Nav derived values. So, for the INS, the short-term errors are relatively small, but they degrade rapidly and are unbounded over time; external aid is necessary to maintain their performance (Farrell, 2008). In an integrated system, the accuracy of a Sat-Nav system may be combined with the precision of an INS to offer improved performance.

We have already learned that it requires at least four good satellites to obtain a navigation solution with considerable accuracy in Sat-Nav. However, there are certain scenarios in which this criterion is not fulfilled. For example, in an urban canyon with tall skyscrapers surrounding the users, it is difficult to get four satellites, well dispersed in the sky, to give a good geometric dilution of precision. Again, consider the case of banked turns of aircraft. During such situations, the navigation antenna, which is typically mounted on the back of the aircraft, remains directed toward one corner of the sky, and then it becomes difficult to satisfy this requirement. Further,

in the equatorial region, there is severe scintillation in the signal due to the rapid variations in the ionospheric density in a local scale. This causes rapid fluctuations in the received signals and very frequent loss of lock of the receivers with very low-powered signals, which continues for a few minutes.

INS equipment, being passive and self-contained, is not sensitive to such outages. Therefore, under such conditions, the INS may take over and the integrated system may continue to offer solutions without much degrading its estimation accuracy and also offering enhanced continuity of position solution even in the presence of severe vehicle dynamics.

The typical estimation rate of a Sat-Nav receiver is about 1 s. In addition to that, the initial time to first fix for a typical receiver is quite high. For certain applications, this rate is not sufficient. For such applications, an integrated system may use the combined solution at the estimation rate of the Sat-Nav while continuing to offer solutions using the dead-reckoning feature of the INS for instants in between. Thus, it provides effective position outputs at a rate higher than conventional Sat-Nav. The short-term data of the INS are fairly accurate and available at a very high rate. Therefore, in such a combination, it can effectively interpolate the position locus, derived from Sat-Nav system, between the two successive updates, with the Sat-Nav offering the bias correction aids to the INS at the instants of its updates. The solution accuracy will not significantly degrade for these intermediate instants, while it will draw large leverage in terms of the performance of the service.

Thus, Sat-Nav and INS, having complementary performance characteristics in terms of position estimation, can be integrated to improve the overall navigation performance.

9.1.4.2.2 Integration architecture

The constituent elements of the combined system are the basic navigation receiver, the inertial measurement units like accelerometer and gyroscope providing linear and angular accelerations, respectively, and a processor that performs the integration work. This processor typically contains a Kalman filter, which combines the parameters available from the two units using a preassigned algorithm.

The "depth" of the integration depends upon the integration algorithm. Based on the integration strategy adopted, the individual system units work either independent or in a dependent manner upon coupling. Independent coupling occurs when the integration is done by just combining the information individually derived by the units. Here, the integration occurs at the modular level of the components. Dependent coupling adopts the strategy of sharing the information between the two participating systems. The integration architecture can be described as being made up of different interrelated units. The standard modes of integration with the more common strategies (Greenspan, 1996; Petovello, 2003) are

- Uncoupled integration.
- Loosely coupled integration.
- Tightly coupled integration.

But instead of starting with the different integration modes, we will first review the different elements of integration, including the information generated at different sections and resources available at different units that can be utilized for integration.

In a Sat-Nav receiver the position information is generated at the navigation processor (NP). The resident Kalman filter of the NP uses position, velocity, and acceleration as the state variables along with clock bias and drift. These state variable outputs are available for utilization for integration. This filter typically uses range as its input. However, it can accept individual state variable measurements from other independent sources as additional input for further bettering its estimates.

The tracking loop of the receiver is also a resource element where the information regarding the receiver dynamic can be utilized. The phase-locked loop may be aided with the velocity estimation from other external sources to identify the Doppler and phase shift. Therefore, it can track the signals with better precision as well as accuracy.

In addition, the measurement unit of an INS system is generally equipped with the facility of correcting the estimates, where the INS outputs can be forcefully modified to any definite value by application of correcting bias derived from external independent information. This helps the bias-prone estimates of the INS measurement units to reduce error.

Thus, the elements of integration in an INS and the possible information to exchange are primarily the measurement unit of the INS, consisting of the accelerometer and gyroscope and their output; and also, its bias correction facility for feedback. For a Sat-Nav receiver, the correlator, estimating the Doppler, and the NP, which houses the basic navigation Kalman filter, participate in the integration. With this basic knowledge of the candidate components, we are now in a position to describe the different modes of integration.

a. Uncoupled mode: In this mode of integration, Sat-Nav and INS function independently as stand-alone units. Here the integration processor only combines the individually derived positional data according to the predefined algorithm. The integration is typically an independent Kalman-based assimilation of the two data sources. The position and velocity output of the GNSS receiver and the acceleration of the INS provide the two sets of data. The estimation confidence provided by the intrinsic KF of the receiver, housed at the NP, and the rated measurement accuracy of the INS instruments, constitute the required error covariance for the filter. As per the theory, the resultant error variance of the posterior estimate is better than the individual ones and it reduces until convergence. It is the simplest form of all possible integration modes. Moreover, it is also failure tolerant, in the sense that here each unit functions independently of and transparent to the other. So even if one unit fails, the integration process can continue with only the other. However, in the case of the failure of one of the systems, the integrated system performs equivalent to the surviving system along with its respective individual limitations.

b. Loosely coupled mode: In this mode of integration, the Sat-Nav and the INS unit still estimate position independently. But here the data are integrated in an integration processor, and the information produced therein is fed back to the individual units for corrective actions.

We have already learned that the inertial sensors have high propensity for bias after working for a certain period. Therefore, the units are provided with calibrating facilities for correcting the bias, through which the position and velocity values derived by the dead-reckoning system can be calibrated with respect to any reference value. Using this facility, the solution of the integrated system is used to correct the bias of the INS system. This facilitates the system by providing subsequent solutions of higher accuracy, thus improving the overall performance.

Similar feedback data paths exist to different levels of the Sat-Nav receiver. Recall that the Sat-Nav receiver estimates the Doppler in the signal and removes it in the receiver loops for proper locking. This activity may be aided by the more precise velocity and position information obtained from the integration processor as feedback. Moreover, the Kalman filter within the navigation filter of the Sat-Nav receiver has acceleration as a state, along with position and velocity. The measurement in the receiver, however, is done only on the range from which the states are derived through a nonlinear observation equation. In an integrated system, the position velocity, and acceleration derived by the integrated processor can be used as a separate measurement to do the measurement updating at the Kalman filter through a unitary observation matrix. The improved confidence values of the integrated precise system can also be used in the Kalman filter present in the NP. The navigation solution derived by this Kalman filter in the NP, thus aided by the feedback information from the integrated solution and, produces better results. This, in turn, improves the state estimation in the final integrated system.

It is important to mention once more that here the feedback information flows from the integrated processor to the individual systems and no direct interface between the participating systems exists. Like the uncoupled mode, in loosely coupled mode, the units work independently of one another, and the integration is also a robust approach. Therefore, the INS and Sat-Nav systems operating separately can continue to provide a navigation solution even if one system fails (Godha, 2006).

c. Tightly coupled mode: In tightly coupled mode, the functional elements of the two units, instead of working as separate individual systems, rather act as the components of an integrated estimation system. The measured parameters generated at each of such elements are assimilated in the system integration processor to derive a single navigation solution.

Here the feedback path exists from the INS acceleration sensors to the Sat-Nav receiver's tracking loop. With the excellent short-term performance of the INS, it provides the latter with more precise velocities than the satellite navigation output for better Doppler correction. Further, the receiver estimations are also used to remove the INS bias. Other dependences accommodated in the integration processor result in better accuracy and reduced random noise in solutions even at higher update rates.

Aided with the INS, this mode of integration offers high tolerance to dynamics of the receiver. As the INS velocity solution is fed back to the receiver tracking loop, the variation is well compensated and hence it reduces the requirement of tracking loop bandwidth. This, in turn, reduces the input noise. However, unlike the other two modes, here the two systems working as one unit fail completely when either one of the units fails to perform.

It is relevant to mention here that in both the coupled modes, the tracking loop of the navigation receiver is generally implemented with a Kalman filter. This makes the system work better even in the presence of large tracking noise and thus improves the subsequent range estimates. The feedback acts as an additional input during the measurement updates, expediting convergence and improving performance. Thus, it creates a synergy between the systems.

Fig. 9.5 shows the different configurations of integration between the INS and the satellite navigation system in terms of the individual elements and the feedback paths.

Finally, to conclude this section on Kalman filtering, we can say that due to the generic nature of the filter and adaptive options of its design, the Kalman filter is very popular in satellite navigation systems. Although we have discussed it in relation to the receivers only, it finds its applications in other segments of the system as well.

9.2 The ionosphere

The ionosphere is one of the major issues for satellite navigation systems. This is due to the fact that the measurement principle of the satellite ranges in such systems, from which the positions are derived, is based upon the propagation time of the signals. The ionosphere affects that propagation time in a conspicuous manner. We have already seen in Chapter 7 how the ionosphere adds delay to propagating radio signals used for navigation. Here, we shall learn in more detail about the structure of the ionosphere and its prominent characteristics. As the ionosphere poses a large threat to navigation applications, especially those meant for critical uses, it is important to understand its nature in a comprehensive fashion.

9.2.1 Basic structure of the ionosphere

The neutral molecular density in the atmosphere at heights more than 50 km above the earth surface is very rare, and it further decreases with height. Due to this fact, the sunlight coming from above remains almost unattenuated at these levels, with energy enough to dissociate these molecules into charged ions and free electrons. Moreover, due to the triviality of the existing particle density, the ions thus created spend a considerable lifetime before they recombine to vanish again. Thus, a region is created at these heights between 50 and 1000 km above the earth's surface where the atmosphere contains natural ions and free electrons. This region is known as the ionosphere. The ionization, thus resulting from the photodecomposition of the upper atmospheric gases by the radiation from the sun, produces electron–ion pairs. This ionization process remains in a dynamic equilibrium with the recombination process to offer a definite electron or ion density, creating the ionosphere. The density of neutral atoms decreases exponentially with altitude, whereas the incoming solar radiation intensity decreases exponentially in the opposite direction as it is absorbed by the neutral particles, as it penetrates through them from above. This gives the ionosphere its finite vertical range of extent, where both solar energy and neutral atoms are sufficient to create ions. A definite peak is also formed here as shown in

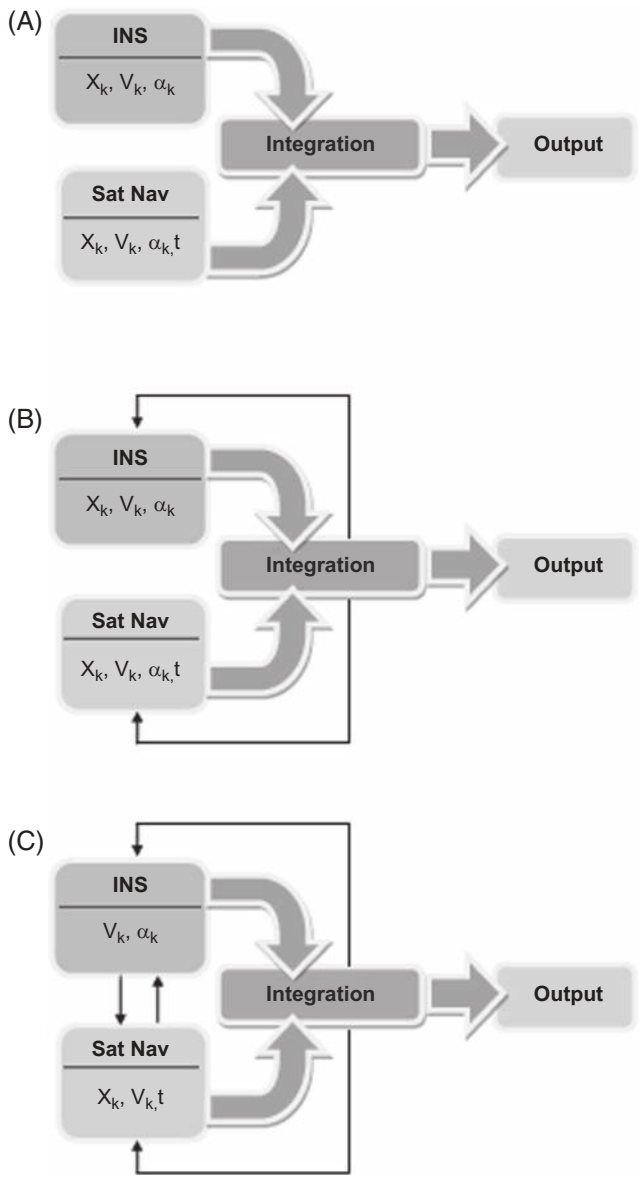

FIGURE 9.5

Configurations of integration in (A) uncoupled, (B) loosely coupled, and (C) tightly coupled modes.

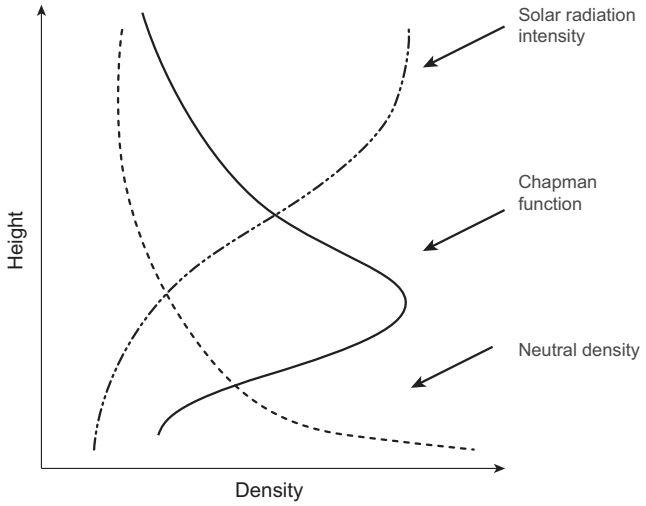

FIGURE 9.6

Vertical profile of the ionosphere.

Fig. 9.6. The lower limit is defined by the penetration capacity of the high-energy solar radiation and the upper limit is restricted by the availability of the neutral atoms for dissociation.

The ionization production function "q" is given by the well-known Chapman function (Chapman, 1931), expressed in terms of the reduced height "z" as

$$q(z) = q_0 \exp\left[1 - z - \exp(-z)\sec\chi\right] \tag{9.26}$$

Here, q(z) is the production rate of the ions at the reduced height z. The reduced height z is the representation of the true height h, relative to the height of the peak density, h_p under the vertical Sun and normalized by the scale height H, that is $z = (h - h_p)/H$. The value q_0 is the production rate at the peak height, while χ is the solar incidence angle at the point in question.

The electron density is determined by its equilibrium value due to this photoionizing production and the loss due to recombination. For lower heights, where the neutral particles are found in abundance, the loss factor is proportional to the square of the electron density, N. Hence, if α is the constant of proportionality at equilibrium when the production and the losses are equal

$$\begin{aligned} q(z) &= \alpha N^2 \\ \text{or, } N(z) &= \sqrt{q(z)/\alpha} \end{aligned} \tag{9.27A}$$

For higher altitudes, the loss due to recombination is linear with the electron density. Hence, with β as the proportionality constant, the condition at equilibrium

is,

$$q(z) = \beta N$$
$$\text{or, } N(z) = q(z)/\beta \tag{9.27B}$$

At all heights in between, the loss varies intermediately between the linear and quadratic function of N, and the equilibrium density is hence accordingly determined (Risbeth & Garriot, 1969). The variation of the ionospheric profile with height is shown in Fig. 9.6. The peak production value is found to lie at an altitude of about 350 km. This height and the peak ionization value varies with solar zenith angle, χ. However, as the solar radiation is not constant, the incident solar flux changes changes with time, and also there is physical transport of the ions, the electron density is variable both spatially and temporally. Thus, the distribution and dynamics of this ionospheric plasma are both dependent upon a complex combination of the neutral atmosphere, solar heating, photoionization, electrical conductivity, neutral winds, etc., all interacting with the magnetic field of the earth.

The structure of the ionosphere is horizontally stratified into layers of various ion composition and structure. Lower layers are ionized by highly penetrating components of the solar radiation, like hard X-rays; while in the upper layers, the soft X-rays or extreme UV component of the sun's rays carry out the ionization (Klobuchar, 1996). These ionospheric layers have been given the designations of D, E, F1, and F2 regions, from the earliest ground-based probing using radio-wave reflections. The peak production of plasma occurs in the F region, from 400 to 600 km. With a typical electron density of $\sim 10^{12}/m^3$ near the peak, this varies with time of day, season, solar activity periods, and for various other reasons. At altitudes above the peak, the ionospheric density decays monotonically with increasing altitude. Below this peak, the density at the lower portion of the ionosphere varies greatly from day to night. The D and E regions of the ionosphere essentially disappear when production stops at sunset whereas the F1 and F2 layer combine to form a common F layer. Total Electron Content (TEC) is an important parameter of the ionosphere. This is defined in Chapter 7.

The ionospheric characteristics vary drastically with time and location. The total global distribution of the ionosphere may be divided into three distinct regions:

1. Equatorial region, extending up to $\pm 25°$ on both sides of the magnetic equator.
2. Mid-latitude region, extending from latitudes $\pm 25°$ up to $\pm 65°$.
3. High-latitude region, extending from above $65°$ up to the poles.

Each of these regions has its own characteristics and has effects on propagating radio signals. However, considering few very important and interesting occurrences pertaining to navigation occurring in the equatorial region, and bearing in mind the brief scope we have to describe the ionosphere, we restrict our current discussion to the equatorial ionosphere and related phenomena.

9.2.2 Equatorial ionosphere

The equatorial region extends from the magnetic equator to about ±25° geomagnetic latitude and is very dynamic in nature. This region has the highest ion production rate, as most of the solar flux is directly incident over this region. Moreover, it is very sensitive to variations in the geomagnetic conditions that control the movements of these charged particles. In addition to large ion generation, the equatorial region is characterized by the occurrence of a prominent phenomenon of equatorial anomaly and formation of severe irregularity. It has associated consequences of offering large and varying delay. Also, the ionospheric irregularities and the consequent equatorial Spread-F phenomenon, leads to severe scintillation to the propagating radio signals. Both of these phenomena affect the navigational signal propagating through this region, which will be discussed next.

9.2.2.1 Equatorial ionospheric anomaly

The ionized particles, that is, electrons and ions, coexist in the ionosphere in the form of plasma. The ionospheric vertical profile of the electron density, being created by the solar influx, is expected to form higher density at locations with vertical solar flux, that is, with zero solar zenith angles. But for the equatorial ionosphere, prominently during the equinoctial period when the sun remains vertically above this region, an anomalous behavior has been observed. It shows a trough of electron density at the equator with a dynamic enhancement in the density at a certain low latitude location. This occurs because the plasma is moved from the region of the magnetic equator to either side in a range of latitudes up to around 20° north and south of it. This is called the equatorial ionization anomaly (EIA). This was first observed by Appleton, who showed the anomalous nature of the equatorial ionospheric electron density distribution at noon. This F region depletion is called the bite-out at the equator. This plasma gets transported and peaks at around ±15° dip latitude (Appleton, 1946). Mitra (1946) was the pioneer to propose an explanation of the phenomenon, attributing the anomaly to the diffusion of the plasma from the equator toward the poles along magnetic lines of forces. Later, Martyn (1947) introduced the idea of equatorial vertical drift, and explained the anomaly in the light of the combined action of the vertical drift and diffusion. The general process by which this plasma movement occurs is now known and proved to be happening by the vertical drift of plasma followed by the diffusive movement toward the higher latitudes. This is known as the Plasma Fountain. Although much has been understood about this variation, definite functionalization of its day-to-day behavior is still lacking.

The development of the EIA depends on a complex interaction of a number of atmospheric processes and shows considerable variability with local time, longitude, and season. It sets off at the equator upon generation of an eastward electric field at the equator due to the dynamo effect aided by the neutral winds. This electric field exerts a Lorentz force on the plasma at the equatorial F layer. The ExB force thus produced causes both ions and electrons move in the upward direction, resulting in no net current. This drift thus lifts the charged plasma from the site of its abundance and puts

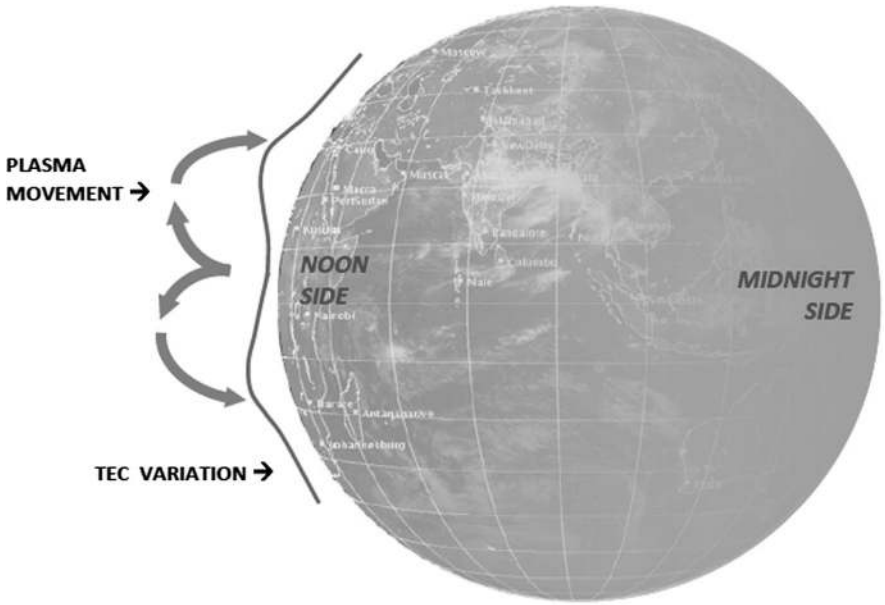

FIGURE 9.7

Plasma fountain effect and equatorial anomaly.

it in a greater altitude. The plasma, thus lifted at the equatorial region, now controlled by gravity-aided diffusion, moves along the magnetic field, sliding toward higher latitudes. The combined mechanism of vertical lift due to the drift and subsequent diffusion gives the plasma a fountain-like pattern and hence is called "fountain effect." It redistributes the electron density by transporting them from the equatorial region, resulting in a trough there, and gradually them toward higher latitude. Finally, they are dumped, forming the crest around 15° to 20° latitude. This results in what is known as the equatorial anomaly (Fig. 9.7).

The EIA exhibits day-to-day variability, and there are variations with seasons and solar activities as well. The daily variability affects both the latitudinal extent of the anomaly, at which the anomaly crest is formed; and the strength of the anomaly, that is the peak density at crest with respect to the trough. The magnitude of this variability depends upon the strength of the electric field produced at the equator and also the controlling geomagnetic and solar parameters and the extent to which they affect the transport process of plasma. The neutral wind also plays a role in the process.

9.2.2.2 Equatorial spread F

Equatorial spread F (ESF) is a geonatural phenomenon in which the vertical profiles of the equatorial ionosphere are reshaped after sunset. A large vertical plasma density

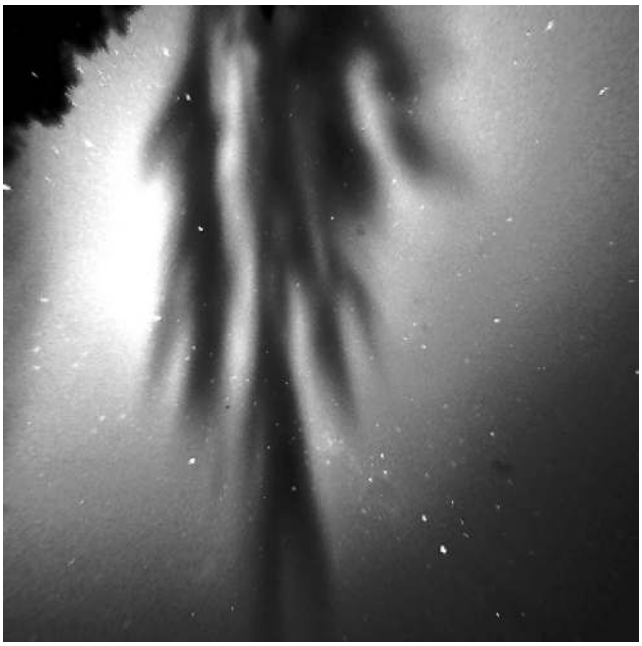

FIGURE 9.8

Equatorial spread F.

gradient developed in this region during the postsunset period initiates the plasma instabilities responsible for ESF. It occurs on time scales ranging up to hours and across a length ranging to tens of kilometers.

With the sunset, the driving mechanism of photogeneration that maintains the vertical equilibrium condition of the ionosphere, holding denser peaks of the ionospheric layers over the relatively rarer ones, ceases to continue. The plasma now starts drooping downward due to the action of the gravity in a magnetic field and in the process creates an instability (Rayleigh-Taylor instability). This further redistributes the plasma in a spatially irregular fashion, with different orders of magnitude and extent. This phenomenon is called the ESF, and causes random and abrupt penetration of high F-region density into lower-density regions adjacently below it as shown in Fig. 9.8. The term "spread-F" was used because the F-region characteristics appeared to be spread over a finite height when probed through ground-based observations.

One of the distinguishing features of this phenomenon is the occurrence of local and small-scale plasma depletions known as ionospheric bubbles. They are small, confined regions with abrupt low electron density surrounded by relatively higher densities.

The plasma irregularities that occur in the F region also influence the performance and reliability of space-borne systems including satellite navigation, causing disruption to the satellite signals. It causes the waves propagating through this irregular ionospheric medium to experience a random local but rapid fluctuation in amplitude and phase. This is called Scintillation.

Thus, scintillations occur generally at night and normally prevail from after sunset up to midnight. The highest levels of scintillation are observed near the locations of the anomaly around the equatorial anomaly peak, where the vertical density gradient is the highest. Although it is not certain to occur every day even in equinoctial months, it is most probable during this time (Acharya et al., 2007).

The redistribution of electron density with occurrences of peaks and crests in an unpredictable manner in terms of locations and time not only causes variations in the delay of the navigation signals but also causes any ionospheric model to fail. So models used for ionospheric delay compensations in satellite navigation perform badly in this region. Moreover, strong scintillation taking place at these locations causes deterioration in positioning accuracy or even loss of lock of the signals in the navigation receivers.

9.2.3 Models of the ionosphere

We need to reiterate at this point that our main purpose here is to understand the effect of the ionosphere on navigation. So, to keep the focus, we will only concentrate on those features of the ionosphere that have a direct bearing on navigation systems. Therefore, here we will only touch upon those aspects of the ionospheric models that have direct consequences to navigation.

In general, the ionospheric models can be divided into two main categories: the theoretical models and the empirical or semi-empirical models. Theoretical models utilize the physics behind the origin and distribution of the electron density to obtain the model output. They are most commonly developed by solving the differential equations considering the physical processes, including photochemical reactions, drifts, diffusion, collisions with neutral particles, winds, etc.

The empirical models, on the other hand, avoid the uncertainties of the theoretical understanding. They depend upon pragmatic data, partially or totally, to obtain the variational form of the electron density of the ionosphere. Due to their empirical nature, they are as good and representative as the data used for developing the models.

In addition, there are certain algorithms for near real-time estimation procedures of the ionospheric TEC, which are loosely termed models. However, they are actually algorithms in a strict sense.

Depending upon the portability of the models, they are either global or local in nature. Local ionospheric models are mainly developed to accommodate localized phenomena and hence are mostly restricted to a definite zone.

Although all types of models have their respective importance with their merits and demerits, all are not relevant for navigational purposes. In addition to the requirement at the control segment, the navigational needs of the models are mainly at the receivers, where the computational resources and capacities are limited. For navigation receivers, we need some models that are described by very few simple inputs, computationally not intensive but still offering adequate accuracy of estimates. Therefore, here we shall only mention the names of a few theoretical models, and then readily move to discuss some of the important global models of navigational interest and their salient features. Very popular theoretical models include the following (AIAA, 1998):

- Time-dependent ionospheric model (TDIM)
- Coupled thermosphere-ionosphere-plasmasphere model (CTIPM)
- Global theoretical ionospheric model (GTIM)
- Sheffield University plasmasphere-ionosphere model (SUPIM)

These models give spatial electron density distribution as a function of location and time. They typically use inputs like neutral density, temperature, and wind. Some models also include drift pattern, electron energy model, neutral wind, and ion temperature as input in addition to other factors like solar activity, solar production rates, etc. Equations are thus formed for continuity, momentum, and energy, considering drift and diffusion to obtain the solution. Some models couple the ionosphere with the plasmasphere to derive the combined density behavior along geomagnetic fluxtubes, solving equations thereof.

9.2.3.1 Parameterized ionospheric model

Among the empirical models, the Parameterized Ionospheric model is a popular global model for ionospheric density. In this model, the output from many theoretical ionospheric models, including TDIM and GTIM, is parameterized in terms of solar activity, geomagnetic activity, and season. The user inputs required by the model are location, time, and solar and geophysical conditions like F10.7 and K_p, etc. The output represents the ion density profiles, which are represented as linear combinations of empirical orthonormal functions with appropriate weights. However, as it uses the theoretical model output as data for modeling, its performance limitations include the inherent inabilities of the parent model including limitations in precisely representing the specific pragmatic situations like the ionospheric disturbances during geomagnetic storms.

9.2.3.2 International reference ionosphere

The International Reference Ionosphere (IRI) is an empirical ionospheric model providing the distribution of the electron density and other parameters in time and space. This model is recommended by the Committee on Space Research and the

International Union of Radio Science, and is based on a compilation of rocket and satellite data. Incoherent scatter data have been used for improved low-latitude performance. The model defines some specific profiles relevant to the real ionosphere and describes the electron density in terms of these functions. It uses global maps as inputs for certain parameters. These parameters can alternatively be provided by the user.

9.2.3.3 NeQuick

NeQuick is another empirical ionospheric model that uses solar parameters for estimation of the ionospheric electron density and therefore estimating delay or the total electron content. It is a four-dimensional ionospheric electron density model, which provides electron density in the ionosphere as a function of the position and time. It allows computation of ionospheric delays, or more precisely the total electron content (TEC) as the integrated electron density along any ray path.

The input parameters of the model are the position (longitude, latitude, and height); the epoch, in month, date, and UT; and the solar activity, either expressed as F10.7 or R12. Alternatively, the NeQuick model may also be driven by the Effective Ionization Level, Az, as a surrogate that replaces the solar flux parameter and is also an empirical function of the location. The version of NeQuick used for GNSS is called the NeQuick-G.

9.2.3.4 Klobuchar model

The Klobuchar (1987) model is the global parametric model for the TEC and is being used in navigational applications. Here, the total TEC is represented as a half cosine function in terms of some prespecified quasistatic parameters. It is a parametric model, giving the vertical ionospheric delay δ in seconds of the day at any local time t given in seconds of day as

$$\begin{aligned}\delta(\mathrm{t}) &= \mathrm{a} + \mathrm{b}cos\left(\frac{t-c}{d}\right)\text{when}\left|\frac{t-c}{d}\right| < \pi/2\\ &= \mathrm{a} \qquad\qquad\qquad\qquad \text{when}\left|\frac{t-c}{d}\right| \geq \pi/2\end{aligned}$$

The coefficients $\mathrm{a} = 5 \times 10^{-9}$ and $\mathrm{c} = 50{,}400$ are constants representing the constant bias and the time of peak, respectively. The parameters "b" and "d" are location-dependent and are derived using the geomagnetic longitude of the location and some specific coefficients that vary from day to day. The function indicates a constant delay during certain portions of local nighttimes. The variation is shown in Fig. 9.9.

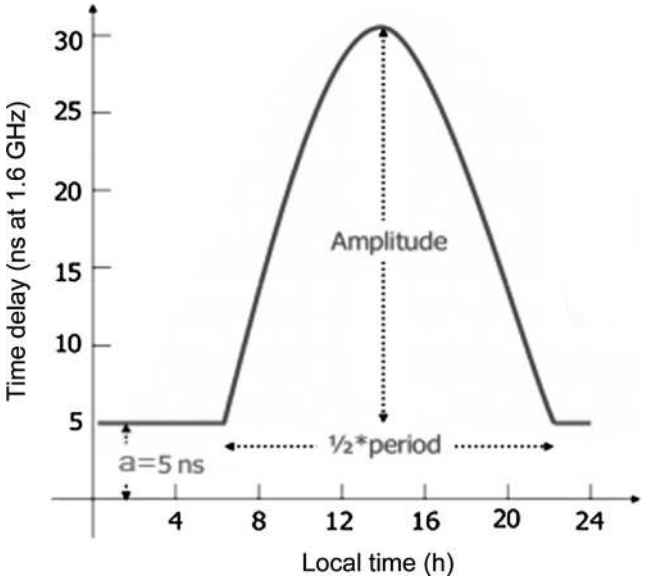

FIGURE 9.9

Variation of ionospheric delay in the Klobuchar model.

Box 9.3 shows the use of a MATLAB program for Klobuchar estimation.

9.2.4 Other methods of estimating the ionosphere

A dual-frequency receiver can directly estimate the delay using relative propagation time of the two frequencies from which the ionospheric TEC can be obtained. The method has been discussed in detail in Chapter 7 in connection to the correction of navigation ranging errors. The other methods of estimating the ionospheric TEC are by using Faraday's rotation of the signal polarization and by using Doppler measurements of signal passing through the ionosphere.

BOX 9.3 Klobuchar Estimation

The MATLAB program klobuchar.m was run to generate the following figure representing the Klobuchar estimation of ionospheric delay for a specific location. Notice the variation of the vertical delay amplitude with time and also the width of the half-period of the variation. The amplitude and the width vary from place to place (Fig. M9.3).

Run the same program with different locations in terms of latitude and longitude and observe the changes.

(*continued*)

BOX 9.3 Klobuchar Estimation — *cont'd*

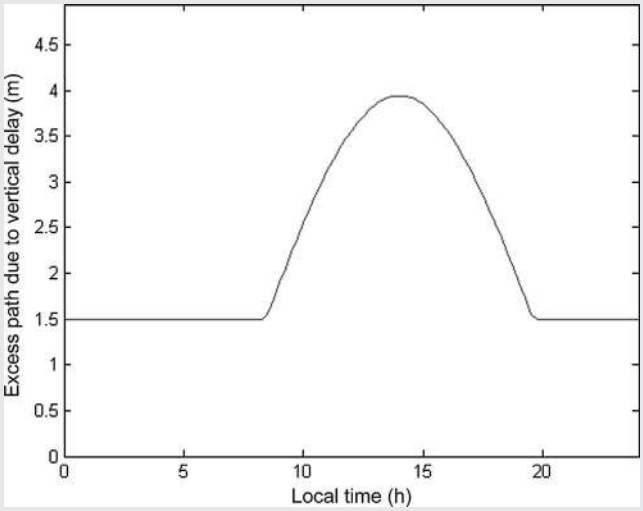

FIGURE M9.3

Vertical ionospheric delay from Klobuchar model.

9.3 Space weather and satellite navigation system

9.3.1 Introduction to space weather

"Space Weather" is the short-term conditions in the interplanetary space and in the outer atmospheric spheres of the planets, essentially caused by solar activities, including the solar wind and its associated electric and magnetic fields.

At the location of the earth, "Space Weather," unlike the weather that we experience terrestrially, has its effects remain mostly contained in the upper atmosphere and ionosphere, thanks to the presence of the geomagnetic field. Most of the times, the effects are not readily perceptible to us on the earth surface.

"Space Weather" events, nevertheless, can cause damages to assets in space and those at higher altitudes. It can also induce electric field and current in the ionosphere, affecting its plasma distributions. Under certain extreme situations, the effects hit the ground infrastructures inducing currents in the pipelines, power grid lines, etc., causing serious damages and affecting lives.

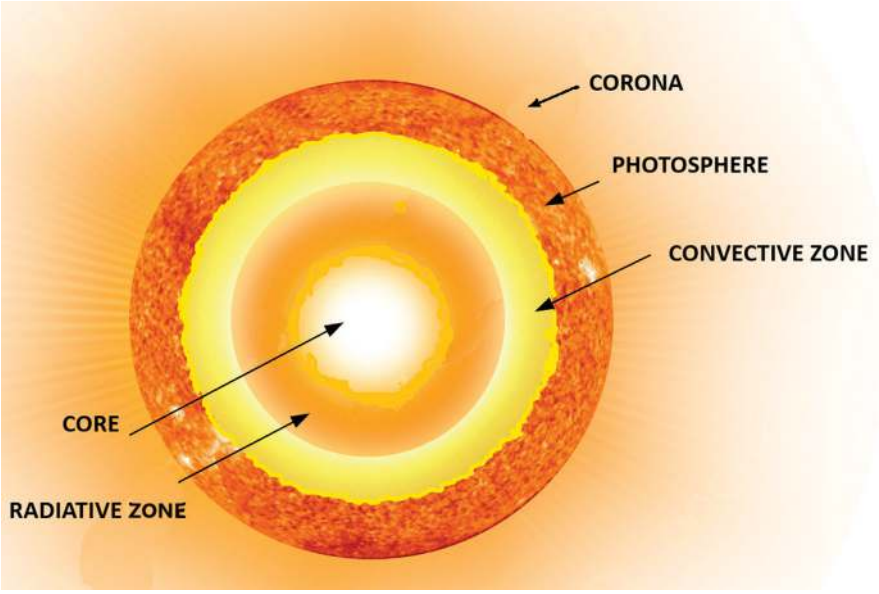

FIGURE 9.10

Layers of the sun.

9.3.2 Drivers of space weather

All the activities that define the space weather has its origin in the Sun. Therefore, it is important to know about the Sun and the solar activities (Karpen & Antiochos, 2016).

9.3.2.1 Structure of the sun

The Sun is an average-sized star located in one of the arms of the Milky Way galaxy and is placed almost midway from the center of the galaxy to its periphery. The Sun is the star that holds and keeps the solar system in existence.

The Sun is a huge ball of burning gas, mostly made up of Hydrogen. It also contains some amount of Helium and other heavier elements. It was born about 4.6 billion years ago and has enough fuel now to burn for about another 5 billion years. Therefore, the Sun is in its middle-age as we are watching it now. The solar radius is approximately 690,000 km. Its radius is 10 times the radius of Jupiter and more than 100 times that of the earth. It means the Sun can accommodate one thousand Jupiter or one million earths in it. It is the largest and the heaviest object in the solar system. Its mass is about 2×10^{30} kg and contains more than 99% of the total mass of this solar system. Structurally, the Sun has five distinct divisions from its center to its outermost layer, as described below (Fig. 9.10) .

- *Core*: The Sun's core extends from its center up to about 20% of the Sun's radius. It has a density of nearly 150 gm/cc. and its temperature is around 15 million degrees, making the solar core the hottest part of the solar system. The constituent Hydrogen in the core undergoes fusion to create Helium ions and releases energy. This energy released is the source of all solar energy including the heat and light radiated by it.
- *Radiative zone*: From the outer edge of the core, up to about 70% of the radius, there is a radiative zone, in which energy transfer occurs by means of radiation, that is, through photons.
- *Convective zone:* Between the outer edge of the radiative zone till the Sun's visible surface photosphere, the transfer of heat takes place through convection, that is, by physical movement of the constituent plasma. This region is called the convective Zone.
- *Photosphere*: This is the visible portion of the Sun. It is the deepest part of the Sun from which the visible light is emitted. The temperature here is more than 5000 K. This is the region which we can see as the surface of the Sun.
- *Corona*: Corona is the outermost layer comprising of very hot but low-density plasma, constituting the atmosphere of the Sun. The temperature of the corona can reach up to 1 million K, which is anomalously higher than that of the Photosphere. Yet, due to the low density the radiation density from the Corona is so low that it remains hidden against the bright background of the photosphere.

9.3.2.2 Rotation of the sun

The Sun rotates about its own axis while also revolving around the galactic center. The Sun being made up of plasma, does not have a rigid structure and hence have different rotational velocities at different regions. Its equatorial region rotates faster and takes about 24.5 earth days to complete one sidereal rotation. The poles rotate slower and takes about 35 earth days for the one sidereal rotation. On average, one rotation of the Sun takes about 27 earth days to complete. However, this latitudinal differential rotational velocity vanishes toward the interior of the sun.

9.3.2.3 Solar radiation

The Sun radiates its energy in a wide spectrum of electromagnetic waves. Radiation from the Sun, is a mixture of EM waves ranging from infrared (IR) on one end to extreme ultraviolet rays (EUV) and X-Rays on the other. However, the intensity is maximum at the visible light, which is more popularly known as sunlight.

- *F10.7: The F10.7 index is a measure of the radiation level generated by the Sun at a wavelength of 10.7 cm. It is the measure of the total emission power at this wavelength from all sources present on the solar disk, per unit spectral width and per unit area at the mentioned frequency. The value is measured in Solar Flux Units (SFU), where 1 sfu* $= 10^{-22}$ *W* m^{-2} *Hz* $^{-1}$.

9.3.2.4 Solar activity and related variables

The hot plasma of the Sun carries out radial convective movements and also cross-radial movement due to the rotation. The relative motion of the participating charged plasma generates magnetic fields of the sun. The magnetic fields remain in form of bundles. Due to the differential rotation of the different latitudinal zones and radial layers of the Sun, these magnetic fields get twisted and tangled and exhibit different levels of activities. These magnetic activities of the Sun forms major driver of the space weather.

The solar magnetic fields form bundles called magnetic flux ropes and have source and sinks in the Sun. These magnetic flux ropes follow different structures due to the rotation of the Sun. Some of these ropes protrude out of the sun's surface, forms arch structures, generate crossovers, and even snap at the cross-over points restructuring the magnetic field. The amount of such magnetic activities occurring in the sun determines its dynamism. The active and the benign period of the solar magnetic activities appear in a cyclic manner, exhibiting peak in every 11 years. This period is called a Solar Activity Cycle. The polarity of the Sun's magnetic field gets inverted in one cycle. The scientific tracking of the solar cycle started in 1756.

9.3.2.4.1 Sunspots

The Sun shows dark areas on its photosphere, called the Sunspots. They are formed by the highly concentrated magnetic fields emerging from the solar surface. These are relatively cooler areas than their surroundings and hence appear black against other bright areas of the photosphere. The size of a sunspot can even be larger than the dimension of the earth.

- *Sunspot Number (SSN): 'Sunspot number' quantifies the abundance of spots which varies with the solar magnetic activities. During lowest solar activity there can be several days with no sunspot, while the sunspot numbers can exceed to more than 200 during the activity crest.*

9.3.2.4.2 Solar flare

A solar flare is a relatively intense, localized emission of electromagnetic radiation in the Sun's atmosphere. The magnetic flux ropes sometimes cross over one another and finally snap at the cross-over point to redistribute the fields and energy. This is called *Magnetic Reconnection* which consequently releases the stored magnetic energy. Reconnection of energetic magnetic lines of forces, located near the sunspots, releases enormous amount of energy. This leads to sudden and extreme acceleration of charged plasma. These accelerated charges, in the process, releases the energy in the form of emissions electromagnetic waves across a broad spectrum. As a result, sudden bright light is seen and high energy X-Rays and EUV are detected simultaneously. Some of these charged particles acquire tremendously high energy of the order of hundreds of MeV, resulting in a high-energy particle emission during the flare. The occurrence of solar flares varies with the 11-year solar cycle and maximizes during the activity peak. The EUV and X-rays from solar flares is absorbed by the daylight

side of earth's upper atmosphere, in particular the ionosphere. This absorption can temporarily increase the ionization of the ionosphere, particularly in the lower layers.

- *Particle Flux Unit (PFU)*: *The Sun emits charged protons, whose flux increases during Proton event, particularly during the solar Flare. The magnitude of the emission is measured in particle flux unit (PFU). 1 pfu is the numbers of protons that hits per unit area per second per steradian. It is measured in pfu, where 1 pfu = 1 particle per square centimeter per second per steradian. For measuring the incoming solar particle flux on the earth, it is typically measured at geosynchronous orbit heights.*
- *Watts/m^2*: *The Sun emits X-ray radiation. X-rays do not come from the Sun's photosphere, but from the solar corona, which is at million degrees temperature, enough to emit X-rays. The Radiation Level is determined by the amount of X-Ray energy passing per unit time per unit area, that is, the power flux, and is measured in Watts/m^2. The X class of flares emits X-ray radiation of power flux more than 10^{-4} watts/m^2.*

9.3.2.4.3 Coronal mass ejection

Solar flares are often, but not always, accompanied by coronal mass ejections (CMEs), which is an eruptive solar phenomenon. At the Sun, magnetic flux ropes sometimes form an arcade consisting of a series of closely occurring loops. The flux lines of force in the loop quickly reconnect into a lower arcade of loops leaving a helix of magnetic field unconnected to the rest of the arcade. This detached closed loop of magnetic flux rope and the material that it contains may violently expand outwards, escape the gravitational pull of the Sun and travel through interplanetary space at a speed of over a million kilometers per hour, forming a CME (Fig. 9.11). It can have more devastating effects on the earth than the flare.

9.3.3 Solar wind

The space that is present outside the outer sphere of the earth and other planets, between the planets, starting from the Sun up to the end of the solar system and much beyond it, in all directions from the Sun, is filled with charged and energetic particles. These particles, ejected from the Sun in form of a continuous flow and dashing through the interplanetary space, constitute what is known as the "Solar Wind" (Goldstein, 2016). The solar wind creates a vast bubble of the charged particles that includes the Solar System and extends beyond it, forming what is known as the Heliosphere. All the planets and other bodies in the Solar system are inside this Heliosphere. The boundary of the heliosphere where the solar wind meets the interstellar medium is called the Heliopause.

The heat generated at the core of the Sun flows right up to the Sun‘s surface and energizes all the constituent atoms of the Sun. Energetic plasma particles, which are constituted mainly by Hydrogen nuclei and electrons move with extraordinary

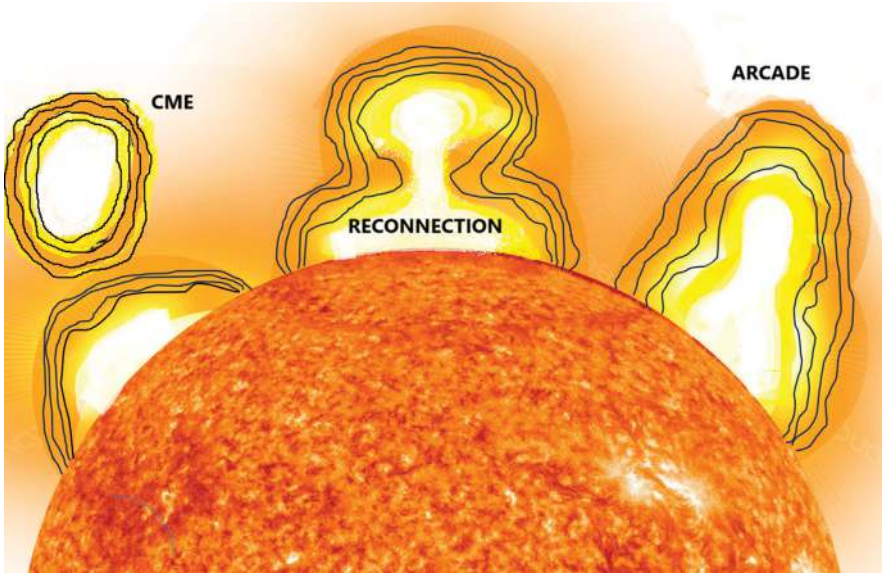

FIGURE 9.11

Coronal mass ejection.

speed. But, these particles are hold within the Sun due to the enormous gravitational attraction of the latter. But, as the particles move radially outward, the attraction of the gravity reduces. At some point, the thermal energy overcomes the gravitational potential energy of the Sun and breaks out of the Sun's attraction into the deep interplanetary space. Nevertheless, the difference between the high thermal pressure in the solar corona and the low pressure in the interplanetary space also aids the generation of this wind. Therefore, the energized protons and electrons, freeing themselves from the attraction of the Sun, constitute the solar wind.

The Solar Wind is primarily characterized by the parameters like the wind speed, its particle density, and the temperature etc. The solar wind speed is the average speed with which the solar wind particles move in space. Based on speed, the solar winds are categorized into "Slow Solar Wind" and "Fast Solar Wind". The slow winds have typical velocities of 350 km/s, when measured at the earth's distance, that is, 1 AU from the Sun, while the fast winds have the velocity of more than 700 km/s. at 1 AU. During the quiet periods of the Sun, when the solar activity is minimum, the slow winds are emitted from a latitudinally narrow region near the equator of the Sun, known as the "Streamer Belt." The fast winds blow from its polar regions, extending deep down toward the equator. They are emitted out to the interplanetary space, from the open field lines of the Sun. These regions are known as the "Coronal Holes.". The scenario changes as the Sun becomes more and more active. Then, the dense coronal

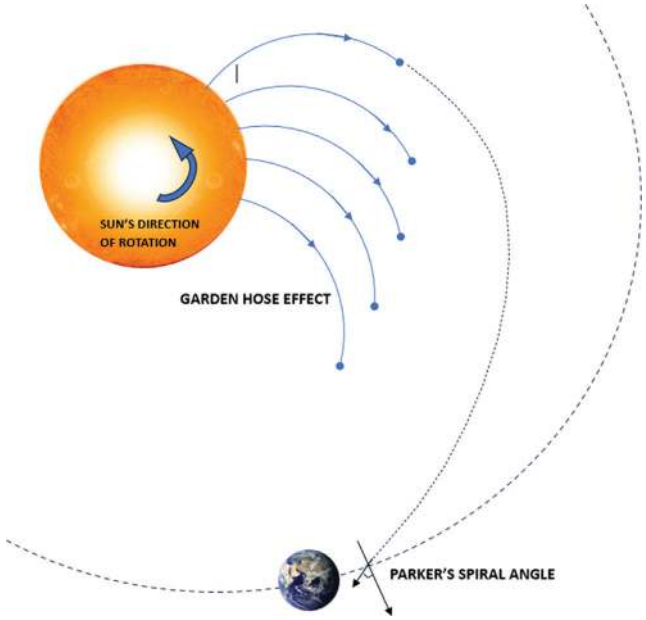

FIGURE 9.12

Garden hose effect and Parker's angle (seen from above the Sun's pole).

region, emitting slow solar winds extends more toward the polar regions and restrict the coronal holes, emitting fast-moving winds to a limited space near the poles. Thus, during the high activity periods, there are more slower winds than fast.

As the emitting particles move away from the Sun, they move into larger space and hence their density falls. The slow solar wind has density is typically around 10 particles/m^3 at 1 AU. This is more than twice the density of the fast solar wind, which remains around 3–4 particles/m^3 at the distance of the earth from the Sun.

This plasma in the solar wind is tightly coupled with the Magnetic field of the Sun. When these plasmas move away from the Sun, they also bring the solar magnetic field lines with them. In fact, the particles are said to remain frozen with the co-travelling solar magnetic fields. These magnetic fields are known as the interplanetary magnetic field (IMF). These magnetic fields are typically represented using a geocentric solar magnetic frame where the magnetic field vectors are represented as Bx, By, and Bz.

This charged plasma and the associated magnetic field fills up the interplanetary space. As the open end of the fields move radially out, the other end of them, having their origin in the Sun rotates with the Sun. So, the field lines spread out in a curved path due to the rotational motion of the Sun. This is known as the "Garden hose effect.". Due to this bending, at 1 AU, the direction of the incoming magnetic fields is not normal to the earth's orbit, but makes a definite angle with it, called the Parker's Spiral Angle or simply the Parker's Angle, which is approximately 45° (Fig. 9.12).

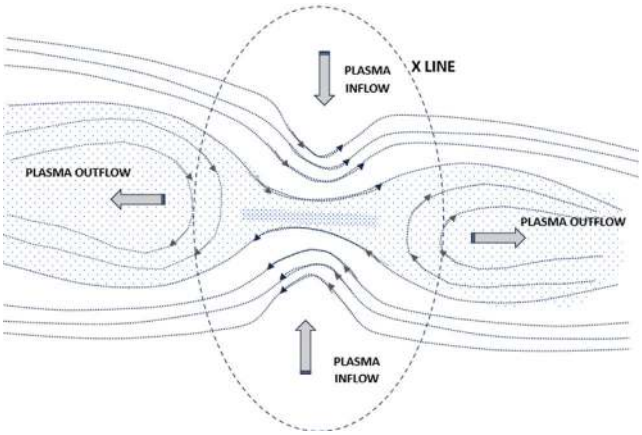

FIGURE 9.13

Magnetic reconnection.

The interaction of the solar wind with the geomagnetic fields results in many currents and electric fields and associated phenomena.

The solar wind flowing through the interplanetary space is supersonic in nature. Their velocity is greater than the velocity with which any mechanical disturbance can flow through the plasma environment. Now, when they come near to the earth, it starts experiencing the effects of the earth's geomagnetic fields. As a result, this supersonic flow of charged plasma experiences an abrupt retarding force and get transformed to subsonic nature, creating a shock at the interface called the Bow Shock.

9.3.4 Solar wind—magnetosphere interaction

9.3.4.1 Magnetic reconnection

Magnetic reconnection is the redistribution of the magnetic field lines which may occur whenever there is a close proximity of two or more antiparallel field lines embedded with plasma. In this process, two stretched antiparallel magnetic fields reorient themselves by getting snapped at the point of proximity and getting connected to the adjacent end of the antiparallel parts. In a 2-dimensional concept, the approaching antiparallel lines of forces come closer by at points forming somewhat a X shape, called the X-line. Due to the increasing magnetic pressure, the cross current that flows between the two antiparallel layers get extremely squeezed. As a result, collisional resistance gets into effect between the constituting charges. This results in instability and ultimately results in the merging of the field lines (Borovsky, 2016; Karimabadi et al., 2016) (Fig. 9.13). The reconnection of the stretched magnetic lines releases large amount of energy in form of kinetic energy and heat. It can accelerate particles up to nearly the speed of light. The formation of the necessary antiparallel configuration for the magnetic reconnection of the IMF with the geomagnetic field lines occurs at

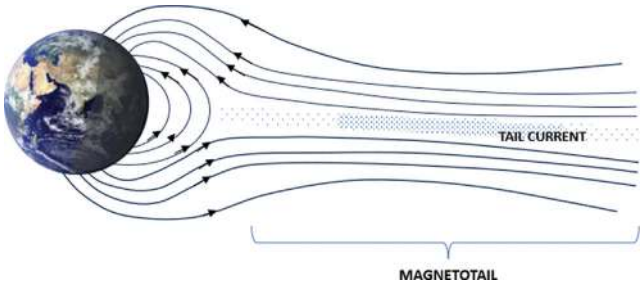

FIGURE 9.14

Magnetotail and tail current.

the dayside when the IMF-Bz is directed Southward, while the geomagnetic field is naturally always Northward with respect to the earth. It also occurs at the nightside magnetotail between the North and the South lobes of the tail.

9.3.4.2 Magnetotail

The solar wind and its associated IMF, flowing radially away from the Sun, upon interaction with the geomagnetic fields undergo magnetic reconnection under suitable conditions, when the IMF Bz is directed southward. The reconnected geomagnetic field lines have one end on the earth and the other connected to the IMF. The hot solar wind plasma, which remains freezed with the IMF carries enormous momentum. This solar wind plasma pulls the reconnected field lines downstream to the night side and to a large distance away from the earth forming a tail-like structure, parallel to the earth–Sun line called the Magnetotail (Fig. 9.14). The field lines reaching there from the north and south of the earth form radial antiparallel lobes near the earth's magnetic equatorial plane. The hot and relatively dense plasma that is found between the two lobes of the magnetotail is called the plasma sheet. The plasma sheet is typically thick, and it carries the cross-tail current.

9.3.5 Currents in magnetosphere

Charges constituting the plasma moves in a magnetic field in response to an electric field, or a pressure difference, or on acquiring kinetic energy through different processes. Whenever, such a movement is initiated in a magnetic field, a drift force is exerted on the plasma. This drift is a function of the velocity of the plasma in the magnetic field and the spatial distribution of the latter. The drift forces on the plasma defines how currents are generated in the magnetic fields. We discuss below a few important currents induced in the magnetosphere due to the space weather system (Ebihara, 2016; Sazykin, 2016).

9.3.5.1 Chapman–Ferraro current

As the plasma particles travelling from the Sun through the interplanetary space in the form of the solar wind, approaches the geomagnetic field, the plasma particles experience a Lorentz force, $F = v \times B$. The direction of motion of the plasma is earthward and that of the geomagnetic fields is from the south to the north of the earth. Therefore, the positively charged particles drift toward the dusk side while negative electrons toward the dawn. This leads to the formation of an effective dusk ward current, called the Chapman and Ferraro current, that flows along the magnetospheric boundary on the dayside.

9.3.5.2 Birkeland / Field aligned currents

During the southward orientation of the IMF Bz, magnetic reconnection occurs between the geomagnetic fields and the IMF. These reconnected geomagnetic field lines, which has one end connected to the earth and the other to the IMF, are pulled by the associated energetic plasma downstream across the polar cap region toward the geomagnetic tail. These reconnected field lines are almost vertical at the polar cap regions. So, as they move relative to the plasma in the ionosphere, it results the generation of an electric field perpendicular to the motion in the reference frame of the earth. This field is across the polar cap and directed from the dawn to the dusk side resulting in a dusk ward current that flows across the polar cap. Thus, this forms a generator region, driving a conventional current along the lines of force into the ionosphere at the dawn region and out of the ionosphere at the dusk region. This is called the Region-1 current.

Similarly, after the reconnection at the night side, the geomagnetic fields return back toward the earth, regaining its dipolar shape. The field lines move toward the earth from the tail region and return to the dayside. The field lines are approximately dipolar now with both the ends connected to the earth at the two hemispheres. The terminal ends, which are immersed in ionosphere, now move toward the sun side and at much lower latitudes. The resultant stress of this movement generates an opposite field as compared to the previous case, that is, toward the dawn side in the polar cap region. This field drives a current along the filed lines in a sense which enters the ionosphere at the dusk side and leaves it at the dawn side at the outer polar cap region. This is known as Region-2 current. While Region-1 current is closed by the magnetopause current, Region-2 current is closed by the partial ring current

9.3.5.3 Cross tail current and sub-storm wedge

It is known from Ampere's law ($\nabla \times B = \mu_0 J$) that for any part across the two lobes of the geomagnetic tail, where the antiparallel field lines result in a nontrivial curl of B, it is necessary to have a current J flowing to hold the reversal of the field. This current is called the Tail Current, which flows from the dawn to the dusk side. This current also holds the magnetic pressure gradient that points toward this region. This current is closed by the magnetospheric boundary currents.

During the southward IMF Bz, large volume of magnetic flux is transferred to the nightside, accumulating at the tail lobes. This, in turn, increases the tail current across the lobes. At a certain point, the magnetic pressure grows to an unsustainable level, producing a current instability which leads to the reconnection of the field lines across the lobes. This gets rid of the excess flux. In certain case this produces the substorm. A current system appears during Substorms and is called the sub storm current wedge. This current is a diversion of a portion of the cross-tail current in the near tail which flows along the field lines and closes in a limited portion of the ionospheric auroral electrojet. The current flowing primarily in the nightside, enters the ionosphere from the dawn side and exits the ionosphere from the dusk side, that is, it has got the polarity of region-1 current.

9.3.5.4 Ring current

The ring current is formed by trapped energetic particles moving in the inner portions of earth's magnetosphere. The charges drift around the earth, extending to higher latitudes, executing gradient, and curvature drifts. The positive charges move from east to west while the negative charges in the reverse direction, forming an effective Westward current. Intense ring current can depress the north-south magnetic field at earth's surface but increase the effective field in the outer magnetosphere.

9.3.6 Events in magnetosphere

9.3.6.1 Substorm

A substorm is a brief disturbance in the earth's magnetosphere during which the energy stored in the magnetospheric tail, mostly contributed by the solar wind, is released and the magnetic field lines get reorganized. Substorms are more frequent and occur for the shorter duration, approximately about 2 to 3 h. However, substorms occurring during the geomagnetic storms, are typically more intense in nature.

Substorm has three distinct phases, viz. the *growth phase*, the *expansion phase,* and the *recovery phase.* The growth phase is the period when the magnetotail lobes accumulate energy. The IMF Bz remains mostly southwards during this period. Consequently, due to the dayside reconnection and subsequent convective motion, more filed lines accumulate at the magnetotail lobes. The magnetotail lobes become obese and stretched with an excessively large amount of energy stored in them. The stretching results in the auroral oval moving equatorward. This phase lasts on average, typically for 30 to 90 min.

The substorm expansion phase occurs during the dipolarization of the magnetotail magnetic field after the nightside reconnection with subsequent injection of energetic particles into the inner magnetosphere. This results in the magnetotail lobes shedding portions of its magnetic flux. In the polar ionosphere, substorm expansion phases are identified by a sudden brightening and poleward expansion of the nightside aurora, as the fields get relaxed and the magnetotail currents are diverted into the ionosphere through field-aligned current systems forming the sub-storm current wedge.

The end of the expansion phase and start of the recovery phase are indicated by a reduction of the auroral intensity. It takes over an hour for the magnetic field and the magnetospheric current systems to get normalized in this phase.

9.3.6.2 Geomagnetic storm

A *geomagnetic storm*, is a temporary disturbance of the earth's magnetosphere caused by any large and abrupt shock produced upon it. The events that may drive a magnetic storm may be a solar CME or a co-rotating interaction region, or a high-speed stream of solar wind originating from a coronal hole, impinging upon the dayside magnetosphere. The plasma and the IMF freezed therein, upon interaction with the earth's magnetic field, transfers energy into the magnetosphere. This results in the temporary deformation in the nominal geomagnetic distribution along with the formation of strong electric fields and currents in the magnetosphere and ionosphere. These currents, in turn, causes further variations in the geomagnetic fields.

The geomagnetic storm has three major phases: *the initial phase, the main phase,* and the *recovery phase*. The initial phase is said to have occurred when the abrupt increase in the solar wind pressure initially compresses the magnetosphere. This is referred to as a storm sudden commencement (SSC). It results in an enhanced Dst index. *Storm-time Disturbance index (Dst)* is the measure of the increment in horizontal magnetic field, measured at the equatorial region over its nominal values. However, not all geomagnetic storms start with SSC.

During the *main phase* of a geomagnetic storm, energetic plasma gets temporarily coupled with the earth's closed magnetic fields and creates a large Ring current, which is a westward current around the equatorial region. This westward current creates a reverse horizontal component magnetic field at the equatorial region on the earth surface, rapidly reducing the Dst to large negative values, which can span from −50 nT during very weak storm up to approximately −600 nT during extreme storm. The negative Dst values are also a proxy of the ring current strength. The duration of the main phase can vary between 2 and 8 h.

During the recovery phase, the coupled energetic charges, contributing to the ring current, get gradually lost due to collision and other processes. This results in the gradual reduction in the ring current till it almost vanishes. The recovery phase may last from as short as few hours to as long as few days.

The largest recorded geomagnetic storm, the Carrington Event in September 1859, took down parts of the then existing telegraph network, starting fires and electrically shocking telegraph operators. The frequency of occurrence of the geomagnetic storms varies with the sunspot cycle. During solar maxima, geomagnetic storms occur more often, with the majority driven by CMEs.

9.3.7 Effects of space weather on satellite navigation

If a geomagnetic storm of the scale of Carrington event occurring today, it would cause trillions of dollars of damage to human assets and services. It would affect the

global economy, in addition to its effects on human lives. Satellites, power grids and radio communications would be devastated, and could cause electrical blackouts on a massive scale. Satellite Navigation system will also be adversely affected by the space weather, both at the system level as well as in the application level. Some of the major effects of space weather on the sat-nav system are listed below.

9.3.7.1 Spacecraft charging

The energetic particle emissions of the Sun during events like solar flare or CME, can cause serious damages to space assets like navigation satellites. It may result in building up of charges on the spacecraft surface, on the dielectric surfaces, etc. and can distort the potential around the satellite. Accumulation of surface charges can also lead to discharges between the surfaces. It can also cause internal electrostatic discharge, which can seriously damage the sensitive electronic and optical systems including the solar arrays.

9.3.7.2 Satellite orbital drag

Deviations in the satellite orbits occur due to the drag of the atmosphere. This is most significant for the LEOs up to around 600 km. During the space weather events, the nominal atmosphere gets heated up and expands increasing the density at higher altitudes. As a result, the satellites at higher altitudes also start facing considerable drag. However, this effect is most prominent for LEO satellites but does not significantly affect the navigation satellites, which are typically in MEO or in some cases in GEO/GSO orbits.

9.3.7.3 Propagation disruptions

Unaccounted Additional delay: The space weather events like solar flare emits large amount of X-rays and increased solar ultraviolet emission, which penetrate deep into the lower atmosphere. The energy is absorbed by the atmosphere and results in sudden excess photogeneration of plasma, particularly in the lower layers of the ionosphere. This causes an extra TEC, which in turn increases the propagation delay of thenavigation signals. The additional delay remains unaccounted in any delay model used for its correction and therefore its positioning accuracy suffers. Similar unaccounted abrupt variations in the ionospheric TEC can also occur at the equatorial region due to the phenomena like the prompt penetration and disturbance dynamo, resulting in serious degradation in the performance of the navigation system.

Ionospheric Plasma Instability and Scintillation: In addition to creating large TEC, the excess zonal fields induced by the space weather events, uplifts large amount of plasma to higher altitudes. After the local sunset, the plasma at lower heights quickly gets recombined and vanish while the upper layers continue to exist. This causes a top-heavy condition in the ionospheric plasma profile. Under certain conditions, Rayleigh–Taylor instability sets in, which creates irregularities in the equatorial ionospheric plasma. These irregularities result in scintillations in the propagating navigation signal in this region. In the polar region, the ionospheric irregularities are formed due to precipitation and gradient drift instabilities, the former

Table 9.1 Solar and space weather monitoring satellites.

Solar observatories and Solar Wind measurements				
Solar and Heliospheric Observatory (SOHO)	ESA and NASA	L1 point	Solar atmosphere remote sensing and Solar Wind	May, 1996
Solar Dynamics Observatory (SDO)	NASA	Inclined geosynchronous orbit	Understanding and addressing the Sun–earth relation	March 30, 2010
Solar Terrestrial Relation Observatory (STEREO)	NASA	Solar orbit with period of 346 and 388 days	Stereoscopic imagery of Sun and solar events	Launched in 2006
Parker Solar Probef	NASA	Eccentric orbit around the Sun	Study of Solar Corona	Launched in 2018
WIND	NASA	L1 point	Data for plasma and energetic particle investigation	launched in 1994
Advanced Compositional Explorer (ACE)	NASA and ESA	L1 point with halo orbital	Solar wind and interplanetary observation	Launched in 1997
Deep Space Climatological Observatory (DSCOVR)	NASA/NOAA	L1 point	Solar CME observation	Launched in 2015
Aditya-L1	ISRO	L1 point	Solar wind measurements and solar observations	Launched in 2024

(*continued on next page*)

Table 9.1 Solar and space weather monitoring satellites—cont'd

Magnetospheric and upper atmospheric measurements				
Geostationary Operational Environmental Satellite (GOES)	NASA/NOAA	Geostationary orbit	Continuous imagery and data on atmospheric and solar conditions	First launch in 1975
Geo Tail	NASA and JAXA	Geocentric orbit in HEO 9×30 Re	Studying the dynamics of the earth's magnetotail	Launched in 1992
Van Allen Probe (Formerly Radiation Belt Storm Probe) (VAP)	NASA	Two satellites in highly elliptical orbit	Study the Val Allen Belt	Launched in 2012
Magnetospheric Multiscale MMS	NASA	Highly elliptical orbit with changing parameters for dayside and nightside probing	Magnetic reconnection on the night side of earth	March 2015

being enhanced during the space weather event. Scintillation causes loss of lock of weaker signals and also deterioration in the accuracy of the positioning (Kelly, 2009).

9.3.8 Space weather observations

Space Weather is being continuously observed from the earth and from the space, as well. Since the starting of the space age, artificial satellites have been used to observe and measure the Solar and interplanetary conditions along with the space weather parameters. Based on their major aims of study, these satellites can be broadly divided into three categories, viz. (1) the solar observatories, (2) the solar wind and inter planetary condition measuring satellites, (3) the satellites measuring the magnetospheric and ionospheric/upper atmospheric conditions. Further, depending upon their orbital location and characteristics, these satellites can be again categorized into (1) Sun orbiting satellites, (2) L1 point satellites, (3) GEO-based satellites, and (4) satellites in HEO and other orbits.

Table 9.1 provides a summary of the major solar and space weather measuring satellites.

Conceptual questions

1. With a noisy a priori estimate of a state available, and with the state itself as the measured parameter with added noise, verify, using vectorial geometry, that the expression for the best estimate tallies with that obtained from measurement update. Assume that the two noises are orthogonal. Also assume that the noise amplitude is the square root of its corresponding variance.
2. What happens when the true noise variance is greater than the assumed one in a Kalman filter?
3. What will be the effect on the estimate x_{k+1} when the measurement z_{k+1} is unavailable? How does the effect propagate in time?
4. State whether the two frequencies used for estimation of ionospheric TEC should be close by or widely separated to have better sensitivity.
5. Express the local production function in terms of normalized height with respect to the local peak (Khazanov, 2016).

References

Acharya, R., Nagori, N., Jain, N., Sunda, S., Regar, S., Sivaraman, M. R., & Bandopadhyay, K. (2007). Ionospheric studies for the implementation of GAGAN. *Indian Journal of Radio and Space Physics, 36*(5), 394–404.

AIAA. (1998). *Guide to reference and standard ionospheric models*. ANSI/AIAA.

Appleton, E. V. (1946). Two anomalies in the ionosphere. *Nature, 157*(3995), 691. https://doi.org/10.1038/157691a0. 691.

Borovsky, J. E. (2016). Solar wind-magnetosphere interaction. *Space Weather Fundamentals* (pp. 47–73). CRC Press. https://doi.org/10.1201/9781315368474.

Chapman, S (1931). The absorption and dissociative or ionizing effect of monochromatic radiation in an atmosphere on a rotating earth. *Proceedings of the Physical Society, 43*(1), 26–45. https://doi.org/10.1088/0959-5309/43/1/305.

Ebihara, Y. (2016). *Ring current space weather fundamentals* (pp. 149–172). CRC Press. https://doi.org/10.1201/9781315368474.

Farrell, J. A. (2008). *Aided navigation: With high rate sensors*. McGraw-Hill Publications.

Godha, S. (2006). Performance evaluation of low cost MEMS-based IMU integrated with GPS for land vehicle navigation application (M.Sc. thesis), UCGE Report No. 20239, Department of Geomatics Engineering, University of Calgary, Canada.

Goldstein, M. L. (2016). *Solar wind space weather fundamentals* (pp. 21–33). CRC Press. https://doi.org/10.1201/9781315368474.

Greenspan, R. L. (1996). GPS and inertial integration. In B. W. Parkinson, & J. J. Spilker Jr (Eds.), *Global positioning systems, Theory and Applications,* vol, II. AIAA, Washington DC, USA.

Grewal, M. S., & Andrews, A. P. (2002). *Kalman Filtering: Theory and practice using MATLAB*. Wiley https://doi.org/10.1002/0471266388.

Grewal, M. S., Weill, L. R., & Andrews, A. P. (2002). *Global positioning systems, inertial navigation, and integration*. Wiley https://doi.org/10.1002/0471200719.

Karimabadi, H., Le, A., Roytershteyn, V., & Daughton, W. (2016). *Magnetic reconnection space weather fundamentals* (pp. 95–113). CRC Press. https://doi.org/10.1201/9781315368474.

Karpen, J., Antiochos, S., Space weather fundamentals the sun. In: G.V. Khazanov. CRC Press.

Kelly, M. C. (2009). *The earth's ionosphere: Plasma physics and electrodynamics*. Academic Press.

Khazanov, G. V. (2016), *Space Weather Fundamentals* (13, pp. 971–978). CRC Press, Boca Raton, FL.

Klobuchar, J. A. (1996). Ionospheric effects on GPS. In B. W. Parkinson, & J. J. Spilker Jr (Eds.). *Global positioning systems, Theory and Applications*: vol. I. AIAA, Washington DC, USA.

Klobuchar, J. A. (1987). Ionospheric time-delay algorithm for single-frequency GPS users. *IEEE Transactions on Aerospace and Electronic Systems, 23*(3), 325–331. https://doi.org/10.1109/TAES.1987.310829.

Martyn, D. F. (1947). Atmospheric tides in the ionosphere - I: Solar tides in the F2 region. In *Proceedings of the Royal Society of London, A189* (pp. 241–260).

Maybeck, P. (1982). *Stochastic models, estimation and control*. Academic Press.

Mitra, S. K. (1946). Geomagnetic control of region F2 of the ionosphere. *Nature, 158*(4019), 668–669. https://doi.org/10.1038/158668a0.

Petovello, M. (2003). Real-time integration of a tactical-grade IMU and GPS for high accuracy positioning and navigation (Ph.D thesis). UCGE Report No. 20173, Department of Geomatics Engineering, University of Calgary, Canada.

Risbeth, H., & Garriot, O. K. (1969). *Introduction to ionospheric physics*. Academic Press.

Sazykin, S. (2016). *Magnetospheric electric fields and current systems space weather fundamentals* (pp. 115–130). CRC Press. https://doi.org/10.1201/9781315368474.

Strang, G. (1988). Linear algebra and its applications. Harcourt, Brace, Jovanovich Publishers, San Diego, USA.

CHAPTER

Security, reliability and integrity of Sat-Nav system 10

10.1 Introduction

Satellite Navigation (Sat-Nav) has become the keystone technology today in human society. A large number of human activities done today are based on it. The reason for such proliferation is the fact that Sat-Nav technology has earned the credibility of a *secure* and *reliable* system. So, before we start the chapter, let us first understand the literary meaning of the terms, viz. Security and Reliability.

Security is defined as the state of being free from danger or threat. Security measures include the procedures followed or actions taken to ensure attaining this state. Reliability means the quality of being trustworthy and performing consistently well, even in disturbed or uncongenial conditions.

For any satellite navigation system, the threats to the nominal performance may arise naturally from the operating conditions. It may also arise from intentional human activities carried out with the aim of disrupting the operation. The natural disruptions or degradation of performance may result from extensive noise sources present in the medium, impairments leading to large attenuation in signal and consequent power loss, etc. However, more threatening are the intentional attempts of disruptions that may include unauthorized access and data breaches to the navigation signals, intentional transmission of noise to screen the signal from being received correctly, and issuance of fake but 'lookalike' signals to mislead the user into using it instead of the actual one. These latter disruptions are not only denting the operational performance of system but also may become critical to life and assets for certain applications.

For satellite navigation, security is said to be attained when the sat-nav system is guarded against all possible threats and impairments that can degrade the performance. Since the navigation signals travel through the open medium, these signals are most exposed and vulnerable to the mentioned impairments and menacing activities. Security is therefore essential for making it robust against such impairments and protecting, it against breaching attempts, and defending it from imitating. This leads to the overall trustworthiness of the system.

Security is a precondition for delivering reliable service. A secured system provides uninterrupted availability of the system, prolonged continuity, in addition to the warranted accuracy. Thus, it wins users' trust and dependability to be called as

Understanding Satellite Navigation, Second Edition. DOI: https://doi.org/10.1016/B978-0-443-36432-7.00005-5

a Reliable system. A secured and reliable sat-nav system offers the following to the users.

- *User trust*: Reliable sat-nav systems build user confidence and trust, which is essential for user satisfaction and continued usage.
- *Safety*: In critical applications like aviation, maritime, strategic usage, etc., system security and reliability are crucial to prevent accidents, errors, financial losses strategic failures, etc.
- *Efficiency*: Secured and reliable systems are less prone to outages and hence reduce downtime and performance degradation, leading to more efficient execution of applications and, in turn, better resource utilization.
- *Compliance*: Many critical applications, like those used in civil aviation, have stringent regulatory requirements. Compliance to such requirements can be met through high levels of system reliability.

Integrity is another aspect of a reliable system. It involves ensuring that the data within the system is accurate, consistent, and unaltered, such that the data or its derivatives can be used for critical applications. Integrity also involves informing upon infringement of such conditions. Data integrity is crucial for the system's functionality and for making informed decisions. Security mechanisms help maintain data integrity by preventing unauthorized modifications. Integrity is also a factor to be ensured for reliability of a system.

Toward achieving reliability, the sat-nav systems have adopted various features as they have evolved over the years. These include the protection of the navigation data against all possible forms of external factors that may lead to errors and failures. It extends from protection against general propagation errors and unintentional interference to protection against intentional jamming and fake signals. Further, to add to the security metric, it also includes methods to ensure secrecy, so that only the valid users can use the system, and also methods for authenticating the transmitted signal so that the valid users are not deceived by counterfeit signals.

The security, and integrity features are so intertwined and interdependent that it will not be appropriate to tag any feature added to the signal to be exclusively serving any one of them. Therefore, in the subsequent sections, we shall discuss different features added to the navigation signals and mention their contributions pertaining to these security and integrity aspects. We shall learn briefly about the few techniques being used in the modern systems that maintain or enhance their performance levels under different conditions. Starting from elementary forward error correction (FEC) techniques that improve the accuracy of the system in the presence of noise, we shall learn about the data and code encryption used to make the service available to only legitimate users. Ways adapted to save the system from intended disruption of service through Jamming and Spoofing will be discussed, and finally, we shall learn about methods of signal authentication to save the users from being spoofed. We shall also learn here the Integrity parameters and their uses in sat-nav systems toward their improved reliability.

10.2 Error detection and correction

The sat-nav signal traverses through the open medium and is most exposed to different types of risks that can deteriorate the system performance and, hence, in turn affect its consistent performance. To safeguard the signal from such possible methods of degradation, the signal needs to be protected. The most common type of impairment that leads to signal deterioration and hence hinders the system performance is the propagation environment and associated noise. The noise added to the signal causes the signal bits to be erroneously detected at the receiver. This can be corrected using two different approaches at the receiver. One such approach is parity checking, while the other approach is the Forward Error Correction (FEC) scheme in signals.

In general, the primary navigation system data rates are slow, and hence there is little chance of a big error occurring at the receiver. However, with the gradual modernization of the systems, more data is deemed to be required to be transmitted over the navigation signal. This demands faster data rates and the presence of noise with the characteristic very low received signal power, which enhances the possibility of transmission error. The nominal FEC techniques work well here toward their mitigation.

FEC is a technique used in communication systems. It involves adding redundant data, known as error-correcting codes, to the original data before transmission. The FEC enables the receiver to identify and correct errors in the received data. The extra code bits are added to the original data at the time of transmission, which helps in detecting and correcting errors at the receiver end. The major advantage of FEC is that, unlike some other error correction methods, FEC does not require the transmitter to re-transmit the data. It reduces latency and improves efficiency of the system, making this approach very much suitable for the satellite navigation systems. So, in addition to various communication systems, like satellite communications, wireless networks, data storage systems, etc., FEC is also widely used in modern Global Navigation Satellite System (GNSS), including SBAS.

10.2.1 Basis of error correction

As the navigation signal propagates through the channel, it picks up noise. Noise is composed of random electrical disturbances that add unwanted variations to the signal. This additive noise may corrupt the signal to the extent that the receiver fails to identify the true bnary level carried by it. To recover the true content of the signal, considerably high signal power needs to be transmitted so that the received signal levels are adequately large for the noise to distort it beyond recognition. In other words, the signal-to-noise ratio needs to be large. Like any practical communication channel, in satellite navigation, too, the signal power is power-limited. This, in turn, makes the signal susceptible to channel noise. Yet, the error due to this noise can be reduced to a minimal level such that the resultant errors can be accepted by the system without sacrificing its necessary performance.

The foundation of channel coding rests on the Shannon–Hartley theorem (Shannon-Hartley theorem, 2024), from which it can be proved that for an information rate R that is less than channel capacity C of a noisy channel, there exists a code that enables information to be transmitted with an arbitrary small probability of error despite the presence of noise in the channel. Capacity C is directly related to the channel bandwidth.

These codes, generally referred to as channel codes, are generated from data bits by adding some redundant bits to them. These extra bits are a linear function of the data and are redundant in the sense that they carry no additional information in themselves. However, their addition makes it possible to detect and even correct a limited number of errors in the message regenerated at the receiver. The code bits use the difference between channel capacity C and information rate R, and can have a maximum rate of C– R. So, for a band-limited channel, a lower bit rate R allows more redundant bits to be accommodated and makes the system more robust to errors owing to noise. For navigation, the data rate is small, so the addition of extra code bits raises no issue. The symbol rate, as the combined rate of data and code, is generally referred to, consequently depends on the number of code bits added. Adding code bits and keeping the data bit rate unchanged, however, results in an increase in signal bandwidth.

The code bits may be used at the receiver end to identify any error occurring during transmission and to recover the true data. The immunity necessary against the noise depends on how correctly the data needs to be retrieved at the receiver, i.e., the required performance demanded by any specific application. The correctness of the received data is quantified by the ratio of erroneous bits to the total number of bits received by the receiver. This is called the bit error rate (BER).

It follows directly that a tradeoff must happen between the transmitted power, the information rate or signal bandwidth, and the performance of the transmission system in terms of BER. For the same transmission power, the BER can be improved either by lowering the information bit rate and using additional code bits or by increasing the channel capacity. Performance may also be improved by maintaining the information rate and bandwidth, while increasing the transmission power. Else, the application needs to be adjusted for working with higher BER.

There can be two options for handling the errors. The errors in every unit of the transmitted messages may be detected at the receiver and if error is identified, it is discarded to get the same data over again. Because the navigation data is transmitted repeatedly in either fixed or varying intervals between updates, the receiver can readily receive the same message over the channel once again if it discards the one received with error. However, rejecting the data and waiting for their scheduled retransmission every time a bit error is encountered will result in a large lag time. Therefore, FEC may instead be done on the data that will correct most of the errors in the received data bits concurrently, and hence reduce the effective errors introduced as a result of channel noise. Consequently, only the data that is not rectified even with FEC will need to wait for retransmission. This reduces the overhead time for waiting.

Different types of error detection and correction methods may be used for navigation signals. Two important variants of channel coding for navigation are systematic cyclic codes and convolutional codes. Because the theory for these codes is involved, here we shall discuss only the basic underlying principle of error detection and correction. The basic components in such an error detection or correction technique consist of three main operations: code generation at the transmitter, code validation, and error identification at the receiver. Next, we explain these major activities (Lin & Costello, 1983; Mutagi, 2013; Proakis & Salehi, 2008).

10.2.2 Code generation

Generation of the code is done at the transmitter using the data bits as input. It results in the formation of a code, typically a linear function of the input bits, which is transmitted to the receiver. The main mathematical element of the generation process is the generator matrix.

10.2.2.1 Generator matrix

The operation of generating codes from data bits may be executed by multiplying the input data bits with a definite matrix of suitable dimension, called the *generator matrix*.

The k bit message may be regarded as a $[1 \times k]$ matrix M, or rather, a k bit row vector that, upon multiplying with a generator matrix G of dimension $[k \times n]$, produces an array of n code bits, that is, a matrix C of dimension $[1 \times n]$. Thus,

$$C = M \cdot G \tag{10.1}$$

Because the message word is k bits long, there are 2^k different combinations of bits of this length, whereas there can be 2^n ($>2^k \mid n>k$) different possible code words out of an n-bit code. The question is, which 2^k words out of these 2^n combinations will form the code? This is determined by the structure of G.

The generator G may be assumed to be formed by the basis set of n linearly independent vectors of dimension k, constituting the column space of G. One code bit is generated by the projection of the message word (which is also one of the vectors in the k-dimensional space) onto one basis. Because in the matrix G, there are n vectors (n columns) in k-dimensional space (k rows), redundant bits are generated as a result of such projection of the message word onto the columns of G. The complete code vector is therefore the total projection of the message on the basis vectors in the generator matrix.

Seen in a different way, a 1 at the jth position of the message selects the jth row vector in the generator, while a 0 unselects the corresponding row, for contribution in the final code. Likewise, any definite combination of 1s and 0s in the message generates a code that is the combination of corresponding row vectors in the generator at which the message bit was 1. Mapping from the possible messages to the legitimate codes is shown in Fig. 10.1.

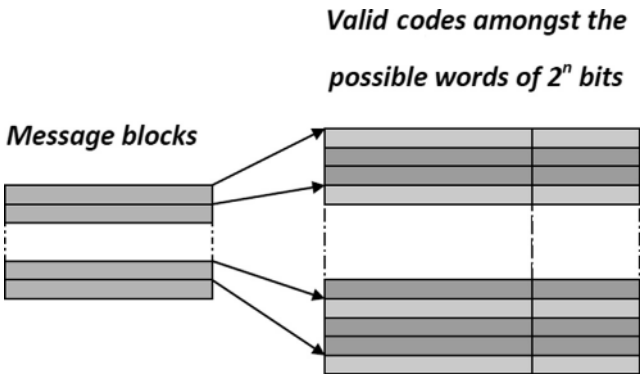

FIGURE 10.1

Messages mapped to valid codes.

In navigation signal, the data containing the values of the required parameters needs to be explicitly present in the navigation message, so the codes necessarily need to be systematic. For systematic codes, the first m elements are the message bits themselves, whereas the rest form the parity bits. Therefore, the code appears as

$$C = m_1\ m_2\ m_3\ \ldots\ \ldots\ \ldots\ m_k\ p_1\ p_2\ \ldots\ \ldots\ p_{n-k} \tag{10.2}$$

For a systematic code, the leading $[k \times k]$ sub-matrix of G constitutes a unitary matrix, which constitutes the systematic part. The subsequent product of the data array from the $(k+1)$th column of G and onward till the nth column creates the trailing $[k \times (n-k)]$ submatrix produces the $(n-k)$ parity bits. Thus, the generator matrix, G, for systematic codes may be represented as

$$G = [I \mid P] \tag{10.3}$$

For example, a [k x (k+3)] generator is like,

$$\begin{bmatrix} 1 & 0 & 0 & \cdots & \cdots & 0 & 1 & 0 & 0 \\ 0 & 1 & 0 & \cdots & \cdots & 0 & 0 & 0 & 1 \\ 0 & 0 & 1 & \ldots & \ldots & 0 & 1 & 1 & 0 \\ \vdots & \vdots & \vdots & \cdots & \cdots & \vdots & \vdots & \vdots & \vdots \\ \vdots & \vdots & \vdots & \cdots & \cdots & \vdots & \vdots & \vdots & \vdots \\ 0 & 0 & 0 & \cdots & \cdots & 1 & 0 & 1 & 1 \end{bmatrix}$$

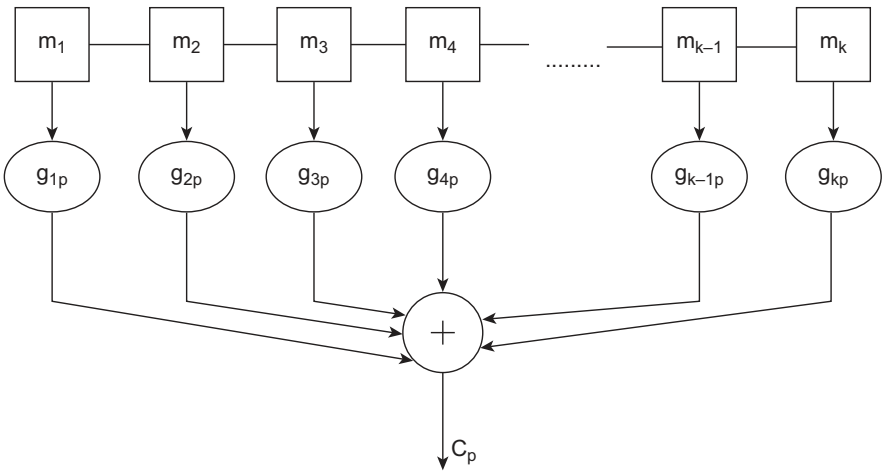

FIGURE 10.2

Implementation of code generator.

For this example, the parity generator is arbitrarily taken as:

$$P = \begin{bmatrix} 1 & 0 & 0 \\ 0 & 0 & 1 \\ 1 & 1 & 0 \\ \vdots & \vdots & \vdots \\ \vdots & \vdots & \vdots \\ 0 & 1 & 1 \end{bmatrix}$$

So,

$$C = [M \mid MP] \tag{10.4}$$

For each systematic part in the code, representing the k-tuple message, there can be 2^{n-k} parity parts possible. Of these, only one will be valid for one definite message, as shown in Fig. 10.1. Here, matrix P maps the message bits into the appropriate $n - k$ parity bits with the leading systematic part to get code C.

Considering the combined systematic and parity part, the j^{th} code bit is formed by the logical addition of the product of the message bits with the corresponding elements of the jth column in G. Therefore, it may also be seen as the binary sum of the message bits, where the elements of the jth column is 1, indicating that the corresponding bit is to be selected. This may be implemented using registers in the following manner, as shown in Fig. 10.2.

It is evident from the figure that the p^{th} code bit can be expressed as $C_p = \sum m_j g_{jp}$, which is nothing but the matrix multiplication of the message bit array with the p^{th} column of the generator matrix.

The code can also be written in a polynomial of order $(n-1)$ as

$$C = c_0 + c_1X + c_2X^2 + c_3X^3 + .. + c_{n-1}X^{n-1} \tag{10.5A}$$

Similarly, the corresponding message may also be written as a polynomial of order $k-1$ as

$$m = m_0 + m_1X + m_2X^2 + m_3X^3 + .. + m_{k-1}X^{k-1} \tag{10.5B}$$

where c_i and m_i are the binary coefficients and X^j represents their position indices.

Therefore, there can always be a polynomial g(X), called the generator polynomial, of order $n-k$, which, when multiplied by the message polynomial, will generate the code.

Once n numbers of code bits are generated from a set of k data bits, it is also important to know how these k bits are updated or renewed. In block codes, after the generation of the code word from the data, all of the k data bits are removed, and the next set of k data bits takes their place. For the convolutional codes, once the k data bits generate a code, it gets shifted by m bits, where $m < k$. The shift is such that the oldest m bits amongst the k bits of the message with the highest significance get out, and new m bits enter the sequence with the least significance. Thus, $k-m$ bits of the previous message remain in the array, acquiring higher significance owing to the shift.

10.2.3 Received code verification

This includes the verification process of the received code at the receiver. It checks whether the code received V is a valid code or whether it has been corrupted over the channel during transmission. The main mathematical element of this activity is another matrix called the parity check matrix.

10.2.3.1 Parity check matrix

For every $[k \times n]$ generator matrix G of the code, there exists a matrix H^T of dimension $[n \times (n-k)]$ such that the row space of G is orthogonal to the column space of H^T. Therefore, for a given matrix G, the matrix H^T is such that the inner product of a vector in the row space of G and the corresponding columns of H^T is zero. Stated in mathematical notations, the matrix product $GH^T = 0$. So,

$$CH^T = MGH^T = M \cdot 0 = 0 \tag{10.6}$$

Thus, we can affirm a received code V to be correct and it is a valid code C of generator G, that is, $V = C$, if and only if $VH^T = 0$. The matrix H is called the parity check matrix of the code. Expressed elementwise, the i^{th} element of this matrix product may also be written as

$$s_i = c_1h_{i1} + c_2h_{i2} + c_3h_{i3} + .. + c_nh_{in} \tag{10.7}$$

In a fashion similar to the generation of the code bit, the parity checking may be implemented by storing code bits in a shift register and adding them selectively in accordance with the elements of H.

For systematic codes, this orthogonality condition, $GH^T = 0$, is fulfilled when the H matrix is such that upon multiplication with the code, it selects the parity bit p_j from the parity part of the code. It then also selects those bits from the systematic part of the received code which constitute p_j and XOR them to reconstruct the same parity bit from its respective constituents in the received message. Finally, the reconstructed parity bit is XORed with the received parity bit. If the code bits remain unaltered on transmission, the systematic part would recreate the p_j exactly and, on XORing with the corresponding parity bit, would result in a zero. So, the general form of the parity check matrix H for a systematic code will be

$$H^T = \begin{bmatrix} P \\ I \end{bmatrix} \tag{10.8}$$

where P is a $[k \times (n-k)]$ matrix and I is an identity matrix of dimension $(n-k)$.

If the received code V is a valid code, it may be represented by M_jG. Multiplying V with the H^T matrix, the result becomes

$$VH^T = M_j\,[I\,|P] \cdot \begin{bmatrix} P \\ I \end{bmatrix} = M_j\,[IP + IP] \tag{10.9}$$

This should yield zero if the parity bit is thus regenerated from the systematic part and the received bits are identical. This condition is only fulfilled if both parts are received correctly. Therefore, for the parity matrix G shown in the example, the H matrix will be:

$$H = \begin{bmatrix} 1 & 0 & 1 & \ldots & 0 & 1 & 0 & 0 \\ 0 & 0 & 1 & \ldots & 1 & 0 & 1 & 0 \\ 0 & 1 & 0 & \ldots & 1 & 0 & 0 & 1 \end{bmatrix}$$

10.2.4 Error identification

The final step of the process is the identification of the error. This is an extension of the code validation using the results obtained during the process. Here, the key mathematical element of the error identification process is the Syndrome.

10.2.4.1 Syndrome

Each bit of an error correction or detection code is a function of a set of data bits. So, when the systematic data bits involved in generating a definite code are combined at the receiver in exactly the same way as to produce the parity bits of the code, the product should ideally be identical to the corresponding parity bit actually received.

However, if these contributing systematic data bits get corrupted during transmission, they cannot produce the same code bit again. So, bit-wise XORing the reconstructed parity with the received parity bit at the receiver results in a nonzero value. The same argument holds if the received systematic bits are not correct.

This nonzero result is called the syndrome. So, the difference between the actually transmitted code bit and the one locally regenerated at the receiver from the received systematic bits is what generates the syndrome. A nonzero syndrome indicates an error in one or more constituent systematic bits received or the received parity bit. For a received code V, which is the true code combined with the error e, the syndrome may be expressed as

$$S = VH^T = (C + e)\,H^T = CH^T + eH^T = M\left[GH^T\right] + eH^T = 0 + eH^T \qquad (10.10)$$

According to the definition of the parity check matrix, $GH^T = 0$. Thus, syndrome S becomes the product of the error sequence in the code with the parity check matrix, H^T. It can also be deduced from this that syndrome S will be 0 if $e = 0$, that is, the received code has no error. Syndrome S helps the receiver to identify errors and correct them.

That we have learned the key elements of error detection and correction codes, we shall now understand how their features are used in navigation. A suitable one amongst the major classes of block codes and convolutional is used for the purpose (Lin & Costello, 1983).

Mere transmission of the error correction codes is not enough for navigational purposes because it requires extended reliability and security of data. The data needs to reach the user not only errorless under all channel conditions, but also with the indemnity assurance of signal security. The signal should be transmitted in such a manner that it cannot be figured out by an unauthorized user, and nobody can hinder real users from getting the actual message. Moreover, impairments such as multipath and interference should also have the least effect on the signal. These issues are handled using the other components of the signal and will be discussed in the following section.

Focus 10.1: Error Correction Coding

We here demonstrate all the above processes using the generator of a 7-bit code word from a 4-bit message. A particular generator matrix was utilized with the following parity:

$$P = \begin{bmatrix} 1 & 0 & 0 \\ 0 & 0 & 1 \\ 1 & 1 & 0 \\ 0 & 1 & 1 \end{bmatrix}$$

The systematic code generator was:

$$G = [I \mid P] = \begin{bmatrix} 1 & 0 & 0 & 0 & 1 & 0 & 0 \\ 0 & 1 & 0 & 0 & 0 & 0 & 1 \\ 0 & 0 & 1 & 0 & 1 & 1 & 0 \\ 0 & 0 & 0 & 1 & 0 & 1 & 1 \end{bmatrix}$$

If two 4-bit message words are chosen as follows:

$$\mathrm{m} = \begin{bmatrix} 0 & 1 & 1 & 0 \\ 1 & 1 & 1 & 0 \end{bmatrix}$$

The two 7-bit code words generated from the two selected messages are:

$$\mathrm{C} = \mathrm{m} \cdot \mathrm{G} = \begin{bmatrix} 0 & 1 & 1 & 0 & 1 & 1 & 1 \\ 1 & 1 & 1 & 0 & 0 & 1 & 1 \end{bmatrix}$$

We take a random sequence of 7 error bits for the two 7-bit code words as follows:

$$\mathrm{e} = \begin{bmatrix} 1 & 0 & 1 & 1 & 1 & 1 & 1 \\ 0 & 1 & 1 & 0 & 1 & 1 & 0 \end{bmatrix}$$

The resultant received words for the two codes after the addition of the errors are as follows:

$$\mathrm{R} = \mathrm{c} \oplus \mathrm{e} = \begin{bmatrix} 1 & 1 & 0 & 1 & 0 & 0 & 0 \\ 1 & 0 & 0 & 0 & 1 & 0 & 1 \end{bmatrix}$$

The resultant matrix is obtained from the generator as:

$$\mathrm{H}^{\mathrm{T}} = \begin{bmatrix} P \\ I \end{bmatrix} = \begin{bmatrix} 1 & 0 & 0 \\ 0 & 0 & 1 \\ 1 & 1 & 0 \\ 0 & 1 & 1 \\ 1 & 0 & 0 \\ 0 & 1 & 0 \\ 0 & 0 & 1 \end{bmatrix}$$

Finally, the syndrome is obtained by multiplying the received code R with HT as:

$$\mathrm{S} = \mathrm{R} \cdot \mathrm{H}^{\mathrm{T}} = \begin{bmatrix} 1 & 1 & 0 \\ 0 & 0 & 1 \end{bmatrix}$$

10.3 Signal spreading and long codes

From the discussion on the spectrum of the signals in Chapter 4, we have learnt that the navigation data of data rate R_d, upon multiplication with the faster codes of rate R_c, gets spread over a relatively larger bandwidth of the latter. The spreading code being normalized in power, its multiplication does not vary the total power of the signal. So, the total power, which was initially contained within the data bandwidth of R_d, now gets spread across the width of the wider code bandwidth of R_c. As a result, the original power density of the navigation signal gets depreciated by a factor of R_d/R_c

Table 10.1 GNSS power spectral densities.

Types of Signal	Units	Values
EIRP	dBw	23.00
Total attenuation	dB	183.00
Data rate	Hz	300
Received power	dBW	−160.00
Equivalent system noise temp	dBK	25.20
Boltzman constant	dB	−228.60
Rcd. noise power density	dBw/Hz	−203.40
Spread signal bandwidth	dB	63
Spread signal power spectral density	dBw/Hz	−223
Data bandwidth	dB	23
Unpread signal power spectral density	dBw/Hz	−183

upon spreading. If P is the total signal power, then the power spectral density before and after multiplication of the spreading codes are P/R_d and $P/R_{c,}$ respectively. The signal power density reduces to even below the typical noise floor at the receiver. This signal spreading and consequent burying of the signal power below the noise is also a tool against unauthorized usage and provides protection to the GNSS signals.

We refer to the table for link calculation used in Chapter 4 and restate it in Table 10.1.

We use the necessary parameters from the above table for understanding the scenario. The received power observed there is around −160 dBw, while the received noise power density is −203 dBw/Hz. As the signal bandwidth after spreading is about 2 MHz, which is 63 dB in log scale, the spectral density of signal power is −223 dBw/Hz. So, over the spectral region where the signal is present, the average signal power per unit spectral width is deeply embedded below the noise power density.

When the signal reaches an authentic receiver, this spread signal is once again multiplied by the exact code. So, for an authentic , the signal after this multiplication is

$$S(k) = a(k)\, C_i(k)\, C_i(k) = a(k) \times 1 \tag{10.11}$$

where i runs for all code chips placed under the period of the k^{th} data bit. Multiplied synchronously by the same code again, the synchronous product of the code chips becomes 1 all along the period of the data bit. Consequently, the encoded data chips turn into plain navigation data bits only. As a result, the signal bandwidth becomes R_d again. As seen previously during spreading, here too, the multiplication of the power-normalized codes does not change the total power of the signal. Only the total signal power now gets concentrated back within the spectral width of R_d.

Consider the data in the above Table 10.1. The signal spectral power density now becomes −183 dB/Hz, and the noise density remains the same as −203 dBw/Hz. So,

the signal power consequently rises by 40 dB and gets above the noise floor. It can now be processed further for position fixing. Thus, the power of the received signal, which was spread over the code bandwidth, on multiplication with the 'exact' code can be brought back within the original data bandwidth to avail the Processing gain, PG (40 dB in this example).

Now, this is only possible when the receiver knows the exact code. Otherwise, any other receiver, without the knowledge of the code, cannot decode it. For such cases, multiplication of any code different from the one in the signal leads to the product given by

$$S(k) = a(k)\, C_i(k)\, C_j(k) = a(k) \times r_i \tag{10.12}$$

where r_i is the random sequence of $+1$ and -1s, each of 1 code chip duration, within the period of the k^{th} data bit. Therefore, the whole sequence turns into a random sequence. When integrated over the data period, it yields a zero, instead of yielding a(k).

Since well-selected codes are used for the purpose of navigation, which have very low values of cross correlation, the product $Ci(k) \times Cj(k)$ is always almost a pure random sequence, integrable to zero. This produces very good rejection of the signal as a result.

So, if the encoded data chips are not multiplied by the exact code sequence, the product remains as noise, and the data cannot be recovered by any means. Therefore, without knowing the actual code, the data cannot be retrieved, nor can the noise-embedded signal be used for ranging. Thus, the code used in the navigation signal also helps in securing the data from unauthenticated users having no knowledge of the actual code (Cooper & McGillem, 1987).

To make predicting the code by any unauthorized user extremely difficult, longer codes are selected for spreading purposes. The code lengths chosen particularly for the purpose of signal protection may run up to several weeks or even up to about a year with chip rates of the order of megahertz. Such long codes are almost impossible to hack with standard processes.

10.4 Encryption

Security of the navigation signals includes the protection of the signal from unauthorized uses. Signal protection pertains to the activities and approaches used to resist such unauthorized use of the signal. Some of the navigation signals are for select users and different from those meant for common use. These signals, designed for purposes like better accuracy, quick position fixing ability, improved navigation data, etc., are intended for targeted users. In order to prevent others from using it, it is customary to protect these signals, and one of the methods for doing the same is signal encryption.

In Chapter 4, we have learnt that multiplication of the data with a very long code protects the signal from unauthorized users. Due to the unpredictability of the code

sequence, it was not possible for such users, who are not aware of the code structure, to predict the code. But that is not enough. Because, with the current availability of supercomputers, the code length of a few weeks to a year may be identified promptly. Some services, on the other hand, are extremely critical and they require the corresponding signals to be fully proof of any possible unauthenticated use. Hence, the data and the code are required to be protected from such users, even if the code is known to them. This is achieved through the Encryption of the code and data.

Encryption is the transformation of a meaningful sequence of bits into a new and apparently random arrangement from which the actual sequence cannot be deciphered without the knowledge of the transformation function. Although Encryption is typically applied to the baseband data bits in communications, in satellite navigation, the encryption is done on the code or the encoded data bits.

In GNSS, the data is not the only item for protection, but also the code is. It is the code that determines and delivers the accuracy. Higher accuracy is obtained with faster code rates while the data remains the same. Now, if we want the accuracy to be delivered selectively, then we must have two codes, one providing normal accuracy and the other a precise one. So, the code that gives precise accuracy should be encrypted to prohibit it from being used by unauthorized users. Unless the user knows how the coding bits are encrypted, they can never regenerate the exact codes. If the codes are not generated, the navigation signal, which remains below the noise floor, cannot be regained above the noise threshold for use.

To understand encryption, within the limited scope of the book, let us start with the definition of cryptography (Katz & Lindell, 2007). Cryptography is the science and study of secret writing. Modern cryptography is generally used to protect data transmitted over any medium against unauthorized use. The original intelligible binary message is converted into an apparently random arrangement of constituent bits and is called a cipher. The process of transforming a plain message into a cipher message is called encryption, the reverse process being called decryption. The main element that controls both encryption and decryption is called a cryptographic key, which can be one or more for the process of this conversion.

The encryption process consists of an algorithm and a key. The key is a sequence of binary bits that is independent of the message and controls the algorithm. The flow of data and parameter selection inside an algorithm is determined by the key, and so the algorithm will produce a different output for the same input, depending on the specific key being used at the time. Changing the key thus changes the output of the algorithm. The cipher message is then transmitted, and upon receiving it can be transformed back to the original message by using a decryption algorithm and the same key that was used for encryption. There can be different keys for encryption and decryption, although.

Various encryption schemes, standards, and algorithms for encryption are readily available and have been extensively reported in the literature over the past few decades. The strength of the standard encryption scheme, its computation requirement, and the predictable time for breaking the ciphering are the determining factors of an encryption process. Typically, a cryptographic system has five components:

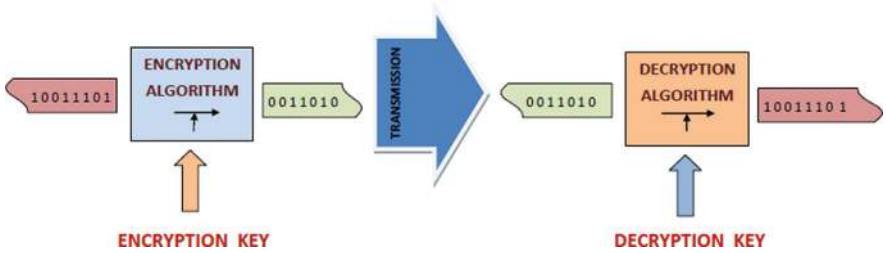

FIGURE 10.3

Encryption and decryption of data.

1. Plain message M = m
2. Cipher message C = c
3. Key K = k
4. Encryption algorithm E_k: E_k (m|K = k) –> c
5. Decryption algorithm D_k: D_k(c|K = k) –> m

For a given key k, D_k is the inverse of E_k, that is, $D_k(E_k(m)) = m$ for every plaintext message m. The Fig. 10.3 below illustrates the encryption and decryption of data.

For efficient encryption to take place, it must satisfy three general requirements:

1. *The key must result in efficient encryption and decryption transforms.*
2. *The system must be easy to use.*
3. *The security of the system should depend only on the secrecy of the keys and not on the secrecy of the algorithms E or D.*

The last requirement implies that the reliability of the encryption process does not change if the encryption and the decryption algorithms are known to all. Therefore, the cipher algorithms should be inherently so strong that it is not possible to create or break a cipher simply by knowing the method of encryption or decryption, respectively, without knowing the key(s). This feature is needed because the algorithms may be in the public domain and known to all. Encryption delivers both secrecy and authenticity, the two indispensable features for security, and hence leads to reliability.

10.4.1 Secrecy requirements

Secrecy ensures that the signal transmitted by the system is used only by the intended users. So, the essential aim is that unauthorized persons cannot generate the plaintext from the cipher message without the decryption key for any message created using the authorized encryption key. This is like protecting your data from a hacker. The requirements for this purpose are the following:

- The exact decryption process being dependent upon the key, it should also be computationally infeasible for any invalid user to systematically determine the

decryption transformation D_k from intercepted cipher message C, even if the corresponding plain message M is known, that is, "D_k" cannot be determined from the knowledge of "m" and "c." Thus, the decryption process is apparently a Black Box to the users.
- It should also be computationally infeasible for anyone knowing E_k to systematically determine the plain message M from the corresponding cipher message C. This requirement ensures that only the decryption key needs to be protected. Even the encryption key can be revealed if it does not give away the decryption key.

10.4.2 Authenticity requirements

Authentication makes certain that the signal used by the rightful users is genuine and not a counterfeit one. The basic objective of providing authenticity is that unauthorized persons cannot create the cipher message without knowing the encryption key, which can be decrypted by the authorized decryption key. This is like protecting the users from the pretender. The requirements for ensuring authenticity are:

- The exact encryption process being dependent upon the key, it should also be computationally infeasible for anyone to systematically determine the encryption transformation "E_k" given C, even if the corresponding plain message m is known. In other words, "E_k" cannot be determined from the knowledge of "m" and "c" by comparing them.
- It should also be computationally infeasible for anyone knowing D_k to systematically find the correct cipher message C such that $D_k(C)$ is the plain message m, even if "m" is known, that is, C cannot be determined from the knowledge of D_k and "m." Authenticity requires only that the encryption key should be protected.

From the above discussion, it is apparent that, to ensure both authenticity and secrecy, both keys are required to be protected. Encryption can be classified into symmetric and asymmetric types, which are defined as follows:

- *Symmetric or single-key encryption:* In symmetric encryption, the encryption and decryption keys are the same or can be determined easily from each other. Hence, in symmetric encryption, secrecy and authenticity cannot be separated.
- *Asymmetric or two-key encryption:* In this type of encryption, the encryption and decryption keys differ, and it is computationally infeasible to determine one from the other. Here, the secrecy and authenticity can be provided separately by protecting D_K with the decryption key K_d for secrecy and E_K with the encryption key K_e for authenticity.

In a satellite navigation system, the data is encrypted by the system while the decryption is done by the users. So, the decryption key, which is consistent with the encryption key, whether symmetric or asymmetric, needs to be disseminated only to the authentic user. This must be some protective means that the unauthentic

users are not able to get it anyhow. Key distribution generally remains an operational management issue.

In satellite navigation, the encryption of the spreading code is a system-level approach for resilience and data security, in which the whole sequence of the PRN code is encrypted using an encryption technique. Once encrypted, the chips are used for modulation of the data and hence spreading the signal. The encryption is done using a secret key by the system before the complete signal is generated.

The same key used for encryption is used for decryption, too. Hence, this type is called the symmetric key approach. Only the authorized users have possession of the key and therefore, can only decrypt the encrypted code and retrieve the data. This symmetric key encryption of the full spreading code is a strong defense against unauthorized use of the signal and also against faking the actual data. It therefore fulfills both the security and authenticity requirements simultaneously upon using the identical key. But the advantages gained in encrypting the navigation signals are not without challenges. One of the critical challenges faced by the system in this process is the distribution of the encryption keys to a large number of authorized users in the field in a safe and reliable manner. To ensure security, the keys are required to be changed periodically, which is also a complex and intricate task in itself by nature.

10.5 Security against threats

With the advancement of GNSS technology, the global satellite navigation system has largely expanded its footprint in the daily activities of human life, and its impact has increased as well. Alongside the increasing application, general technology is becoming accessible to all, with increasing knowledge its technical intricacies. The readily available information about the essentials of the technology, while improves the understanding of the system and usage on one hand, it also enhances the capability and ease of disrupting the services on the other. The increased reported incidences of disruptions in GNSS services quantitatively establish the fact.

The primary objective of all the satellite based navigation services is the continuous and correct generation and updating of the user position. To achieve the end, it requires the signal, being transmitted from the navigation satellites, to be received by the receiver without significant errors or distortions. However, as the signal passes through the open atmospheric interface, the signal becomes vulnerable to intentional alterations or degradations.

Security of navigation signals, as discussed before, includes the state of well-being of information carried by the signals, in which the possibility of successful yet undetected alteration and disruption of information is kept low or tolerable. In this section, we shall discuss two important approaches which are currently used for purposefully altering the GNSS signals, viz. Jamming and Spoofing, done with the intention of disrupting the services. We shall define and explain them, mostly focusing on the ways for their detection and mitigation.

10.5.1 Jamming

Any signal that is not necessary to a navigation receiver for achieving its final aim may be considered as noise to it. Nevertheless, the level of noise should be limited to an acceptable threshold for the receiver to work properly. Noise within the acceptable limit results in bit errors, which can be mitigated using FEC, as discussed in the earlier section. Beyond this acceptable level, the unwanted signal interferes with the normal working of the receiver leading to the loss of relevant information such that the receiver fails to estimate the correct position. When this additional noise reaches the receiver and starts adversely affecting it, it is known as *interference*.

By the time GNSS signals have travelled from the satellites to the receiver, the signals are at a very low power level. This low power level makes the signals susceptible to interference from other signals transmitted in the same frequency range. If the interfering signal is sufficiently powerful, it becomes impossible for the receiver to detect the actual signal. Thus, the noise dominates the signal and either degrades or entirely inhibits the working of the receiver. Interference is unintentional, where the typical sources are faulty, misaligned, or unmanaged radio equipment.

However, the same theoretical facts are used for intentionally causing interference in the navigation receivers. Large noise power is intentionally transmitted in the frequency range used for satellite navigation signals to degrade the receiver performance. It is then called "Jamming." Jamming thus occurs when the inherently low-powered GNSS signals are overpowered by intentionally generated radio signals on the same frequency, leading to reduced positioning accuracy. Further, the intention of jamming is to make the receivers lose their positioning ability altogether.

10.5.1.1 Jamming types

Jamming can be of multiple types depending on its origin and the nature of the jamming signal. The typical classification of jamming is done on the basis of the spectral width of the jamming noise. It can be of two types,

1. *Narrowband jamming:* Narrowband jamming is said to have occurred when only a small portion of the navigation signal spectral bandwidth is affected with large jamming noise, that is, the spectral range of jamming frequency is significantly smaller than the signal spectral bandwidth. It is very easy to create narrowband jamming as it requires neither sophisticated instruments nor large power. With the narrowband jamming approach, the jammer can potentially completely destroy a part of the navigation signal. Without error correction techniques, the whole message might become unusable because of a lost crucial spectral part (Krutitsky, 2022).
2. *Wideband jamming:* Wideband jamming, on the other hand, occurs when the interfering noise signal is transmitted across a broad range of frequencies. In satellite navigation, the wideband jamming covers the whole signal spectrum and even more. However, only the part of that noise spectrum that falls under the signal spectral width affects the received power. Sometimes, the jamming

noise spectrum shape is matched with that of the navigation signal so that the jamming noise power spectrum looks like that of the signal itself and the jamming power is efficiently utilized.

Besides, there are other types like chirp jamming and tone sweeping jamming, in which a noise with a narrow bandwidth quickly sweeps across the signal bandwidth. Therefore, it covers the entire spectral width of the navigation signal with noise of narrow bandwidth.

10.5.1.2 Quantifying jamming

Jamming makes it difficult for the receiver to operate. Large jamming noise may even force the user receiver to lose its positioning capability. But, altogether, it is the relative jamming noise power which is important. Therefore, the metrics for quantifying jamming are all relative. Typically, two different metrics are used for quantifying jamming which are used as per their relevance to the actual services.

1. *Jamming to signal power ratio (J/S):* From the term itself, it is evident that J/S is the ratio of the total jamming interference power to the total signal power in the receiver bandwidth. The ratio indicates how strong the legitimate signal is compared to the jammer signal. This term is more common in communication systems where signal power is much higher than the noise floor, and hence, jamming strength with respect to the signal is of significance.
2. *Jamming to noise power ratio (J/N):* J/N is the ratio of jamming interference power to noise power in the receiver bandwidth. Unlike J/S, this measure is independent of signal power and is purely dependent on receiver operating bandwidth.

10.5.1.3 Jamming effects on receivers

To understand the effects of jamming on a navigation receiver, it is important here to recall the receiver functional elements and how the signal passes through them. A typical GNSS receiver is shown in the schematic diagram in Fig. 10.4.

It is a common requirement for each of the functional blocks that they all demand some minimum power level below which their operation is impeded. The jamming noise power, in addition to degrading the signal-to-noise ratio, adds to the total power received by the receiver, which under nominal conditions remains very low. This signal, being received by the antenna, first reaches the LNA. Too much power at the receiver input causes the front-end LNA to saturate, causing signal distortion with nonlinearities.

The next stage is the mixer in the downconverter unit. The mixer converts the RF to IF by beating the signal with the local difference frequency. When the input is full of additional noise components with large power, the down-conversion process may produce strong unwanted harmonics, which may in turn cause distortions in the receiver operations. With large input power, the IF amplifier can also get saturated, producing harmonics due to nonlinearity.

The jamming noise, riding with the signal, is then digitized along with the signal. Being added with the jamming noise, which can even be non-Gaussian in nature, the

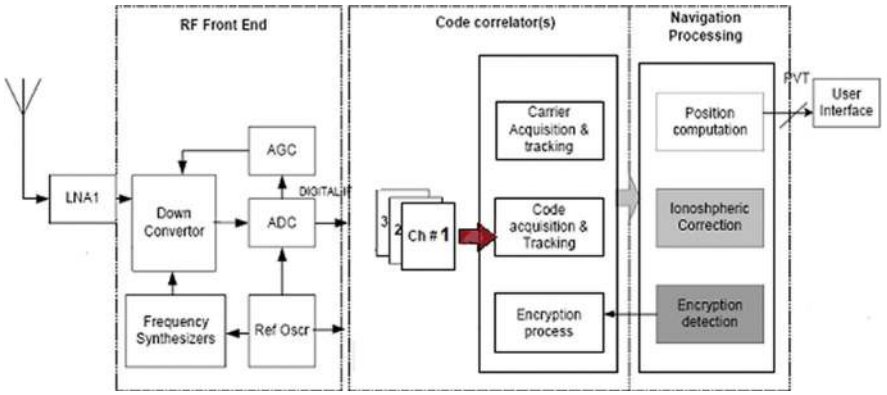

FIGURE 10.4

Schematic of a typical navigation receiver.

distribution of the total signal levels gets changed. As a result, the ADC quantization with the predefined quantization levels may become suboptimal. The large noise power can also drive the ADC beyond its dynamic range, resulting in erroneous digitization of the signal. The digitized jamming signal effectively increases the noise power, that is, lowers the Signal to Noise Ratio (SNR). The effectiveness of the disruption depends upon both the strength and shape of the noise spectrum. The larger the power of jamming, the more the deviation of the effective C/N_0 from its nominal values. As the noise power is increased by the addition of the jamming signal, this C/N_0 is reduced, and the receiver fails to identify the signal from its noise-laden form and therefore loses the lock. An effective rise in the noise floor and consequent fall in the C/N_0 makes it difficult to acquire and track the GNSS signals. It also may lead to erroneous demodulation of the data. Reduced SNR leads to correlation loss and hence results in ranging error.

Depending upon the spectral location and strength of the jamming noise, the relative distance between the jamming source and the receiver, and the receiver's ruggedness to jamming, the effectual result on the receiver may be different. The effective noise entering the receiver may lead to:

- *No effect at all:* The jamming noise power or the disruptions produced due to the jamming signal is insignificant or out of the spectral range. The jamming power is so low that the resultant additional noise is detected and effectively mitigated.
- *Degradation of GNSS signal:* Driving of the receiver front end electronics to nonlinearity and deterioration of C/N_0 of the received signal as discussed above. This may cause the final estimated position accuracy to degrade.
- *Complete loss of tracking of signal:* Saturation of the receiver front end or loss of lock by the tracking loop or the correlator leads to complete loss of a particular satellite or receiver output.

10.5.1.4 Detection and mitigation

10.5.1.4.1 Jamming detection

The first step to counter the jamming is that identify the presence of the jamming noise in the signal. It is only at the postdetection stage that corrective actions can be taken. The detection process of Jamming is straightforward and is done by observing the power level at different stages of the receiver and looking for anomalies. This can be done through the following activities:

- *AGC gain monitoring:* The automatic gain control (AGC) placed at the front end controls the gain to the RF input so that a constant RMS power is maintained. When the jamming noise is present with the signal, the total power of the signal gets abruptly higher than the nominal signal. Accordingly, the AGC gain proportionately gets changed abruptly, indicating the presence of jamming.
- *Postcorrelation C/N_0 monitoring:* C/N_0 of the received signal after the correlation stage in a receiver provides a measure of the signal quality. Continuous observation of this parameter and comparing with a threshold enables to detection of any sudden deterioration in C/N_0 that indicates the presence of jamming.
- *Spectral Profiling:* The spectrum of the nominal GNSS signal remains known to the user. Therefore, the Spectral profiling of the input signal using FFT and/or wavelet transforms can reveal the presence of abrupt large power at frequencies where they are not supposed to be, which is a signature of jamming.

10.5.1.5.2 Jamming mitigation

To maintain the accuracy and continuity of the positioning by the receiver, it is necessary to mitigate the jamming interference at the receiver, in addition to its detection. Like Jamming detection, mitigation of the Jamming can also be done at different stages of the receiver, using different techniques. The approaches to mitigate the jamming interference, once it is identified, is either elimination or abatement of the jamming noise and/or its effects. This can be done in the following ways.

- *Antenna:* An antenna with configurable directive gain may be used to identify the direction from which the jamming radiation is reaching the receiver. Once this is done, the effect may be reduced or nullified by reducing the gain in that particular direction. This can be implemented by using a controlled radiation pattern antenna (CRPA), which can control the reception gain of the antenna from any definite direction. This makes use of the fact that the desired satellite signals and the unwanted jamming signals typically arrive from different directions.
- *RF front end:* The AGC can also be effectively used to reduce the effects of the jamming. AGC adjusts the input power to a fixed constant value. Therefore, when a jamming signal rides on the signal, the total power of the input signal naturally gets enhanced. Upon identifying this, the AGC automatically compresses its amplitude, thus maintaining the constant RMS power that gets into the receiver. This saves the system from driving the components to nonlinearity or outside the dynamic range when jammed. However, this cannot improve the signal $C/N_{0,}$

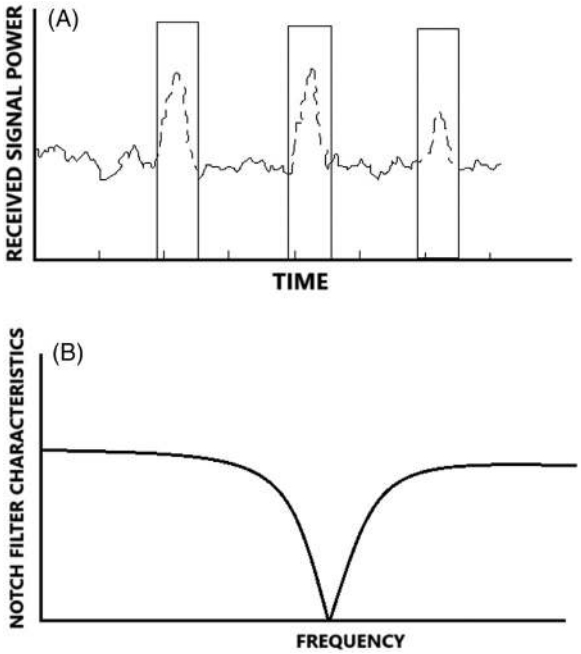

FIGURE 10.5

Signal processing techniques for jamming mitigation.

and neither can it fully arrest the receiver degradation. For improvement in performance, one has to resort to signal processing techniques.

- *Signal processing techniques:* Signal processing techniques used in the receiver can significantly reduce the effects of the jamming. Signal processing can be used in both the time and the frequency domain, depending on the nature of the signal. A few popular signal processing approaches to counter the jamming are the following.

  – *Pulse blanking*: The jamming signal may occur as pulses repeating at particular intervals. Although this feature is more frequently observed in unintentional interference, the use of pulsed noise for jamming is also not uncommon. For such a type, the time domain approach of pulse blanking can be used. In this approach, a particular power threshold is set according to the nominal level of the thermal noise power. When the ADC output samples cross this particular threshold at regular intervals, the input is excluded from passing further down the receiver. Pulse Blanking was implemented before the baseband processing block and is the simplest form of implementation in hardware. Fig. 10.5A *illustrates the technique where the boxed regions are the regions blanked from the input signal.*

- *Notch filtering*: This is a filter-based technique to mitigate the jamming effect of a narrowband static jamming noise. Here, in the total bandwidth of the navigation signal, the region of the affected spectrum is first identified. It is then specified by a center frequency and a narrow bandwidth. This range of frequencies is effectively blanked by the notch filter. A Notch filter is a filter that passes signals at all the frequencies unaltered, except those at and around the notch frequency. These components are blocked by the filter. Spectral components around the notch frequency, at which the jamming is located, being eliminated, the filter output provides signal delivering undistorted performance. It provides the best performance with a single tone CW. If there is more than one CW, then cascaded notch filters can be used. The filter characteristics of such a notch filter are shown in Fig. 10.5B, where the notch is created at the location of the jamming noise frequency.
- *FFT-based / wavelet-based signal processing:* This is a frequency domain signal processing approach. Here, the input signal is transformed to the frequency domain, and the presence of the CW jamming noise is identified as the abrupt increment in the spectral power above a predetermined threshold. An appropriate excision of the spectrum at the identified frequency, followed by an inverse FFT, helps reduce the jamming noise. Frequency excision is a versatile technique that can mitigate pulse, c/w, and narrowband interference. A similar approach with both frequency and time excision is possible with wavelet-based signal processing. The drawback of these techniques is that they need large processing power

The above frequency-based mitigation techniques are more effective for narrowband jamming cases. Wideband jamming, on the other hand, transmits large power for this purpose. Such large power transmission sources can be easily identified, and appropriate administrative actions may be taken to inhibit such transmissions.

The other approach to handle the jamming after identification is to exclude the signal that has been affected by the jamming from being used for positioning. However, this reduces the number of active satellites being used for the positioning and hence deteriorates the DOP. To counter this, the following approaches can be useful:

- *Multiple navigation sensors***:** If the Jamming signal exists over a small period of time, the use of additional navigation sensors, such as inertial measurement units, odometers, or altimeters, can help the receiver fight the jamming effects and maintain the continuity.
- *Multifrequency and multiconstellation Sat-Nav system:* Multiconstellation global navigation receivers can protect their positioning performance from jamming using their ability to track multiple frequencies and multiple constellations. In such a case, if one of the frequencies of an entire system is affected, the receiver can resort to other frequencies to maintain the output availability. Moreover, if one total satellite is affected, switching to other available satellites for positioning also helps in a similar way.

10.5.2 Spoofing

Spoofing is an intentional activity in which one creates a false signal that is similar to the actual navigation signal but containing erroneous data, in order to disrupt the service or deceive the user by forcing the receiver to derive erroneous locations.

Today, all civil navigation signals are transmitted conforming to interface specifications. The receivers will accept any input that conforms to the specifications and treat it as if it came from a actual navigation satellite. These specifications are fully available in the public domain. Combined with the extremely low power levels, the open signal structure of the civilian signals makes it very vulnerable to spoofing. Added to it, the easy availability of hardware makes it trivially simple to spoof a navigation receiver.

Spoofing is a more serious form of interference than jamming. During a spoofing attack, the receiver reports largely inaccurate or entirely wrong positioning. Being spoofed, the receiver receives signals with incorrect information contained within them. Therefore, it is a more critical kind of distortion faced by the receiver, as it forces the user to believe the derived false location as the true location. Spoofing done with malicious intention may drive the user to wrong routes, which can turn out to be severely hazardous and even life-critical.

Since the spoofing approach includes creating a false signal by a signal generator, in most cases, it is necessary to have information regarding the nature of the signal, including its data structure, code features, and modulation techniques, etc., for spoofing it. The generated fake signal is transmitted to the user with a certain power such that, at the location of the target user, the spoofing signal has considerably larger power than the original signal to make the user receiver get locked to it.

10.5.2.1 Spoofing scenario

The spoofing signal should have the same features as those of the actual signal, but, with different data. The carrier frequency, the modulation, the ranging code, and the bandwidth must match the original signal. Only then it will be accepted by the receiver. But, instead of the true data, the fake or expired data is to be transmitted so that the receiver will calculate an incorrect position or time. Once the target signal specifications are known, generating a spoofed signal is not very difficult. Now, all the specifications of the standard GNSS service are available in the public domain. Further, with the increase in GNSS usage, the technical understanding of the system has also increased in general, making it easier for someone to recreate the signal. Nevertheless, the increased availability of programmable radio platforms and open-source simulator software has made creating and transmitting a spoofed signal easy. Positioning and timing applications have a significant impact on everyday life. All these applications have become an attractive target for exploitation for various motives by the spoofers. For example, these spoofing devices can be used to hijack autonomous vehicles or drones and send them on alternate routes.

10.5.2.2 Classes of Spoofing

The spoofed signal mainly takes over the true signal at the RF section. Currently, many types of spoofing have been demonstrated. Spoofing attack can be classified depending on the factors as described below. However, others may have used a different basis for the classification.

10.5.2.2.1 Takeovers

The fist stage of all spoofing is getting the spoofing signal accepted by the receiver rejecting the genuine one. This is called 'Take over'. Takeover mainly takes place at the RF section. It can be of the following categories

Synchronous: Here, the spoofing signal precisely matches the timing of the authentic GNSS signal. It causes minimal disruptions to the signal quality. Hence, it does not allow the tracking loop to identify any spoofing intrusion in the signal. Once the target is identified, a synchronous spoofing first aligns the spoofing signal with the authentic signal, and gradually delays it in time to introduce position errors, and then takes over receiver tracking with slightly larger power than the original.

Asynchronous: Here, the spoofing signal is not time-matched with the true signal. Therefore, these types of signals can be generated easily and independently of the actual signal. However, they can be easily detected by using a simple consistency check at the receiver. Often, asynchronous spoofing is preceded by jamming to first break the "lock" with the real signal.

10.5.2.2.2 Source type

Spoofing may also be classified based on the types of sources used as mentioned below.

Simulator-based: In this type of spoofing, a navigation simulator is used as the source, and it is concatenated with an RF front-end, which is then employed to mimic authentic signals and transmit to the target. Since it does not use the current actual signal, the signals are not synchronized in nature, unless some additional actions to synchronize with the current signal are introduced.

Receiver-based: In this type, a navigation receiver forms the core signal source for spoofing. The receiver receives the actual signal and extracts all available parameters from the true signal. Then this received true signal is tweaked to generate the spoofing signal for transmission to the target. These signals are typically time-synchronized. However, sometimes receivers are used for receiving signals, which are then stored and retransmitted with only a delay, without any further processing.

10.5.2.2.3 Deployment architecture

How the transmitters used for spoofing are deployed may also be a basis for classifying spoofing.

Single transmitter: In this type of spoofing, only a single transmitter is used.
Multiple transmitters: In this type of spoofing, multiple transmitters are used for transmission. Spoofing using multiple transmitters is generally mutually synchronized in nature and, in most cases, also time-synchronized with the GNSS.

10.5.2.3 Different spoofing attacks

Each type of spoofing can be carried out in different ways depending upon the attacker's knowledge, availability of spoofing equipment, target levels and objectives of spoofing, etc. A few of the current common approaches to spoofing are listed below.

Simulated spoofing attack: In a simulated spoofing attack, the whole spoofed signal is simulated. Thus, there is no need for recording or receiving the original signal. The simulated signal is typically asynchronous but made up of the same code and modulation as that of the original signal of the target user. The data bits are carefully selected to deliberately produce the intended false position of the target user when the user receiver employs them. This type of spoofing is also very simple to implement.
Meaconing or relay spoofing attack: Meaconing is the interception and rebroadcast of the GNSS navigation signals. In this spoofing technique, the spoofed signal is only a late version of the original signal. Here, the spoofing activity behaves like a repeater, which receives the actual signal and transmits the same after a delay. Typically, the retransmission is done by passing the received signal through a calibrated delay line and a configurable amplifier. Therefore, the spoofing signals are no longer synchronized with the actual signal. This is one of the simplest types of spoofing. As the true signals are utilized without any alteration, this spoofing type has the potential to spoof any satellite navigation signal.
Forgery spoofing attack: This is a type of spoofing in which the original signal is received live and its components, viz. the carrier, code and data are separated. Then its code and/or the data are manipulated to produce the intended deviations at the user receiver, and this modified signal is retransmitted toward the target to be spoofed. This type of spoofing is not very difficult while being effective, and does not require sophisticated hardware or algorithms. However, this only works on unencrypted open services.
Security code estimation and replay (SCER) attack: To authenticate the actual signal against spoofing, some systems send a set of encrypted security signature code bits as part of the data. Sometimes, a section of the spreading code is also encrypted. An estimation spoofing attack has a complex technique of generating a spoofing signal in which the original signal is recorded, and its encrypted security code is estimated. Once the encryption is cracked, the spoofing signal is then simulated. It consists of the intended fake data and is added with corresponding signatures, encrypted similarly to the original signal using the cracked code. Real-time estimation of the encryption is a very critical preposition, and so this type of spoofing attack is considered an advanced and complex method of spoofing.

Nulling attacks: Here, the spoofing signal consists of two components. One is the spoofed version of the navigation signal that is intended to generate false positioning or timing at the user receiver. The other is the synchronized genuine signal of the system, but with inverted phase. This second component of the spoofing signal, upon combining with the true signal at the receiver, nullifies the latter. So, the actual signal getting eliminated, the receiver is only left with the spoofed version and locks to it. However, nulling is difficult to implement. The exact carrier phase alignment and amplitude matching are very challenging and require calibration of various physical parameters.

10.5.2.4 System level protections

Toward protecting the authentic signal from spoofing, the GNSS service providers resort to various encryption-based and authentication-based approaches at the system level. These methods either encrypt the spreading code and/or the data, or may provide provisions for users to authenticate the signal.

The encryption approach has already been discussed in connection with signal security in an earlier Section 10.3 in this chapter. So, here, we shall discuss only the authentication techniques generally used by the system. Authentication may be achieved by providing authentication signatures for the navigation message or for the spreading code.

10.5.2.4.1 Authentication

The receiver, upon receiving a message, can trust his position (with certain accuracy) if he can ensure that the message that has been received is the same as that has been transmitted by the real navigation system. This can be done by authenticating the received signal. Authentication allows a satellite navigation receiver to verify that the signal used by it is issued by a true and trusted source. The difference between the original and counterfeit signal is the source. While the original signal originates from the true source, i.e., the navigation satellite providing the navigation service, the counterfeit signal has its origin at the spoofing system. The navigation signal authentication establishes the authenticity of the source of the signal and thus assures the user about the genuineness of their derived position.

Authentication does not make any change in data like the encryption system, but inserts some additional information into it. Here, either part of the navigation message or the spreading code may be encrypted and transmitted as part of the navigation message. This information is like some signature or tag generated out of the navigation message or code bits, created using a secret key only known to the service provider. If this signature is processed, it can assure the user that the signal started from the desired source. This makes it difficult for an attacker to manipulate the satellite signal, since the manipulated signal would not create a matched signature.

Navigation message authentication (NMA): This denotes the authentication of the navigation message bits (i.e., the full data frame or a portion of it) by digitally

signing the navigation data, keeping the navigation message unencrypted. The signature is nothing but an encrypted hash function of the message.
Spreading code authentication (SCA): This inserts encrypted chips at some unpredictable portions within the nominal (unencrypted) spreading code, which are later verified through cryptographic functions.

Authentication allows backwards compatibility with older versions of the navigation message. That is, only if one processes this additional information, one gets the benefit of authenticating the signal. Else, for the rest, it remains a normal signal.

Depending upon whether the same or different keys are used, the authentication types can be either symmetric or asymmetric authentication, respectively. Each of these types of authentication has its own pros and cons. For the symmetric authentication case, the challenge is in the secure distribution of the key, without the spoofer having access to it. For the asymmetric case, the public key is transmitted, which can be accessed by anyone. Here, we shall discuss both symmetric and asymmetric authentication with focus on a symmetric algorithm called Timed Efficient Stream Loss-tolerant Authentication (TESLA). While the underlying encryption is symmetric, the authentication here appears asymmetric due to the way keys are revealed over time (Parameter Selection for the TESLA keychain, 2020).

- *Symmetric authentication process:*

To understand how symmetric authentication is done, let us assume the case where the navigation message is authenticated. A part of the navigation message data is encrypted using an *encryption key* to generate the *message authentication code* (MAC). The navigation message and the authentication code are both transmitted to the user through the navigation signal in the form of data bits.

For the user receiver to be able to verify the message with the authentication code, the same key is required to be used. Therefore, the key used for generating the authentication code is also required to be transmitted to the user. Sending the key through a separate secured channel is impractical for GNSS or other satellite navigation users. Sending the key with the code itself defeats the entire purpose of authentication, since the spoofer can then gain access to the navigation data and replicate the entire process with counterfeit data. One way to securely send the keys is to use the keys with limited time validity and keep updating the keys over time. The current key automatically becomes invalid after the stipulated time, and hence, the spoofer cannot use the same key at any future time. Further, the keys are generated in a way that the spoofer can never estimate the future keys from the current keys.

Now, the question arises of how the authentic users get the keys? A delayed symmetric key encryption method can be used here. In such an approach, the message and the Message Authentication Code are both transmitted simultaneously by the transmitter. The receiver, on receiving both, uses the message but buffers the MAC without authenticating it.

After a certain interval of time, the private key is transmitted. Upon receiving the private key, the receiver can verify its previously received MAC, which it kept

buffered. At the receiver end, the authentication code is regenerated using the received message and by using the key. The local code thus generated is compared with the received code. If the received code matches the locally generated code, it establishes the authenticity of the transmitted message and source. The key transmission is delayed to an extent that even if the spoofer gets hold of the key, he cannot use it to modify the corresponding message, since the message has already been used and its validity has expired during the delayed interval.

The next question that comes is, can the spoofer create his own set of MAC using his own private and public key on the spoofing signal? That is, can the spoofer run a parallel authentication process with the counterfeit signal? Then, if the user loses lock to the true signal again and latches on to the spoofing signal, then it starts believing that the parallel counterfeit process is genuine.

This concern can be resolved if the sequence of keys has some onward relationship. For this, the TESLA algorithm uses a very expedient procedure. The key for the authentication is generated here with ingenuity. The keys that are used for encryption have a certain relationship with the other keys received in the sequence. Basically, each key is a part of a series of keys. This chain starts from a secret seed key, K_n. This key is used as input to a hash function "h" to generate the next key, as $h(K_n) = K_{n-1}$. A hash function is a function that takes an input and returns a fixed-size string of bytes, called the hash code. Knowing the function, it is very easy to generate the output for a given input, but it is almost impossible to estimate the input from the output hash code. Therefore, they are called "one-way" functions. This way, each key is sequentially hashed to obtain the root key K_0. Thus, starting from a secret seed key, a chain of keys is constructed by hashing the previous element.

The keys are used and transmitted in the reverse sequence, with K_0 followed by K_1, K_2, …. And so on. Since the key K_n was generated by hashing the key K_{n+1}, so, it is impossible for anyone to predict the future key in the sequence of transmission. So, one can generate past keys from current, but never the future key. The root key is used for key verification, and hence the receiver must possess some information certifying the root key as correct, independently of the information sent through the Signal in Space. Any K_n received following the receiving of the root key can be checked if it follows the same lineage to the root key using the same hash function. Once verified, the key is used to synthesize the digital signature received by using the corresponding message. Keys used by the spoofer will never hash down to the same root key.

This method, however, does not prevent a spoofer from simply generating their own messages, keys, and MACs and broadcasting them in a manner compliant with the specifications. But if the receiver has received the root key or the authentic code of the key chain at least once, then the received key can be used to regenerate the earlier keys through forward hashing and validation.

- *Asymmetric authentication process:*

Asymmetric navigation message authentication is a popular scheme in the GNSS field. Here, the system uses a private encryption key to generate an authentication code word from the original message. The private key is only known to the transmitter.

A public key is also generated at the transmitter. This public key is specific to the particular message and the particular private key. Then the message is transmitted to the user, as usual. Additionally, the authentication code (signature) is also sent with it. When received at the receiver, the latter knows where to expect the signature and the public key in the demodulated data stream. The user then uses the public key to verify that the message and authentication signature correspond.

If the spoofer tweaks any portion of the message without changing the signature, the authentication code does not remain valid anymore for the distorted message, and the spoofing can be easily identified. He cannot create the signature corresponding to the spoofed message either, as the private key is unavailable to him. This defense may, however, require an additional technique in order to deal with a SCER-based attack in which the spoofer rapidly estimates the signature bits of the data stream.

Now, what happens if the spoofer knows the encryption algorithm and uses his own private keys and generates a public key accordingly, and transmits the resultant message? In other words, how does the user know that the "public" key does indeed come from the trusted system operator? In an asymmetric case, the receiver needs some mechanism to ensure that. Therefore, in asymmetric authentication, the whole problem is how to authenticate the key transmission. To resolve this issue, a public key infrastructure is essential for any asymmetric system. The receivers are required to have occasional access, via alternative channels, to infrastructure to provide authenticated GPS system public keys.

Asymmetric encryption has two major drawbacks: first, it is much more computationally intensive than symmetric key encryption; second, much longer keys are required for the same level of security.

10.5.2.5 Spoofing detection and protection

Signal authentication is available to select users who qualify for the service. However, for general users, spoofing can be carried out with far more ease. A powerful spoofing defense is the detection of an attack, followed by the recovery of the actual signals for a true position/timing fix. In this section, we shall first know about the different detection techniques, and following that, we shall discuss the available ways and provisions available for identifying genuine signals.

Spoofing is targeted at specific user receivers. Hence, the detection of spoofing is a receiver-level activity. Various detection techniques employed typically by receivers involve scrutiny of different metrics, any anomaly of which indicates the presence of a spoofed signal. In other words, here too, the consistency check of different parameters with the nominal condition values is key to spoofing detection. The following are the common methods for identifying the presence of spoofing in the signal:

- *C/N_0 monitoring:* The spoofing signal is typically maintained at a power higher than the actual signal so that the receiver easily gets locked to it. Therefore, spoofing may lead to an abrupt rise in C/N_0 in one or more signals beyond a threshold value. This condition is traced for and, when identified, is flagged as a

probable occurrence of spoofing. A similar identification approach can be devised using absolute signal power monitoring.

- *Receiver movement vs power variation:* For genuine navigation signals originating from the navigation satellites, the variation in power with the movement of the user receiver will be small compared to the variations expected when the source is located on the ground. Therefore, if the received power varies rapidly and immensely as the receiver moves on the ground, it indicates a probable spoofing.
- *Dual frequency power and delay comparison:* The same path is traversed by the signals in two different frequencies transmitted from the satellite. Therefore, in dual frequency receivers the received signal power obtained in one frequency can be scaled to the other, provided their respective EIRPs are known. If the signal in one of the frequencies is spoofed, then this relationship ceases to hold good. Thus, by comparing the power in two different frequencies, the presence of spoofing may be identified.
- *Direction of arrival:* The direction of arrival is a very crucial parameter to identify the spoofing. From the ephemeris, the approximate position of the satellites can be obtained. It can even be obtained from the almanac, even if the signal of any specific satellite is not locked to the receiver. The receiver checks if the signal marked from a definite satellite is coming approximately from its respective estimated look angle. A signal being received constantly from a low elevation is also an indication of the spoofing. A receiver can either use interferometry to measure the direction of arrival using 3 or more antennas with different phase offsets, or use a CRPA antenna for the purpose.
- *Code and carrier phase consistency:* The authentic signal has its code and the carrier phase exactly synchronized to each other. Except for a very small difference at the transmitter and due to ionospheric propagation, the two phases run synchronously. The user receiver may take warning from an unusual code-carrier divergence when the spoofing signal is not synchronized.
- *Solution consistency check:* The complexity of the spoofing increases many times if more numbers of satellite navigation signals are targeted. Therefore, typically only one or two signals are affected, while the receiver receives many more signals from other satellites. Then the solutions derived with the unaffected signals will be largely different from the solution when any of the affected signals are included. This approach, also used as a RAIM algorithm, may provide an indication of spoofing. A similar inconsistency will also be observed in the derived clock parameters. A spoofing signal, unless controlled very precisely, can cause the receiver clock error to change too rapidly.
- *Consistency checks with other solutions:* The GNSS-based solutions may be checked with other solutions derived from sources like INS, etc. If there is a large inconsistency observed between the two, then there is a probability that spoofing has happened.
- *Cryptographic authentication:* If the signal code/data is added with encrypted signature bits, then it provides an additional option to the user to verify if the

signal it is receiving is obtained from the desired source or not. However, the authentication option is available to the receiver only when provided by the system.

Once the existence of a spoofing signal is identified and confirmed, it can be discarded by the user receiver utilizing various techniques, and then the authentic signal may be logged. It is however, understandable that it is almost impossible to recover the authentic GNSS navigation signal in two scenarios. One is an attack that involves nulling of the true signals. Here, the cancellation of the genuine signals precludes their use. However, this type of attack is still experimental and has not yet been implemented in real scenarios. The other is an attack where the spoofer is very high powered and effectively masks the true signals or saturates the front end of the user receiver, to the point where they are unrecoverable.

Modern GNSS receivers have several approaches to combat spoofing. Algorithm-based spoofing protection schemes look for signal anomalies. These sophisticated integrity algorithms are derived and fine-tuned on a vast amount of real-world data.

10.6 System integrity

System integrity in GNSS refers to the ability of the GNSS system to carry out its intended functions in an unimpaired manner within the prescribed limits of its performance, even in uncongenial conditions, including the ability to inform the user in a timely manner about the occurrence of any deviation from the intended performance.

In simple terms, Integrity is the measure of the trust that can be placed in the correctness of the information supplied by a navigation system. It includes the ability of the system to provide timely warnings to users when the system should not be used for navigation. In safety-critical applications such as aviation or marine navigation, the correctness and precision of derived receiver locations are crucial. GNSS signals can sometimes be incorrect due to various intrinsic, as well as extrinsic factors. But the user needs to detect such issues to prevent the safety-critical applications from failing, which may lead to catastrophic consequences.

System anomalies in a satellite navigation system can be a consequence of system malfunctions in the space or control segment, or due to signal in space aberrations. The most common anomaly source reported during operations was clock anomalies in the space segment. However, other issues have also been observed.

We know that the information from the system reaches the users through the signal. Therefore, implementation and maintenance of integrity can be achieved by (1) ensuring the security of the signals (2) covering the integrity watch on it (3) disseminating integrity parameters through the signal. The parameters, like the alert limit, integrity risk, protection level, and time to alert are used as the observation indices. These terms have been discussed in Chapter 8. We shall not reiterate the same here anymore. However, we may recall that it needs the involvement of the system service provider or the control segment to estimate these statistical numbers

from which the integrity parameters are estimated. Therefore, these integrity estimates need the support of the service provider.

However, for nominal navigation services, the provider does not support any integrity information, and hence the user receiver can derive no additional information from the signal in this regard. In such a case, the receiver needs to derive the integrity estimates from the nominal signal by itself. Here, in the following section, we discuss the way the receiver does so in an autonomous way.

10.6.1 Receiver autonomous integrity monitoring (RAIM) system

It is basically the responsibility of the system to estimate the system integrity parameters and disseminate them to the users. However, the primary navigation systems do not provide integrity information. Then, if under any circumstance, any primary navigation satellite starts to broadcast incorrect information in its navigation signal, the resultant position estimation will be incorrect. But graver is the fact that in no simple way the receiver can detect this. In such cases, the receiver has to assess the integrity condition itself.

Receiver autonomous integrity monitoring (RAIM) (What is System Integrity? - Building Strong System Defenses, 2024; System integrity, 2024) is a technology used in sat-nav receivers to assess the integrity of the signals that are being received at any given time without the need of any integrity information contained in the signal. It is particularly applicable to receivers intended for critical applications.

It is done by utilizing a resident algorithm at the user receiver, typically by comparing the consistency of the derived position solutions, and without any extra information required be sent to the user through the signal.

RAIM is essential because it can detect and, in certain cases, can inhibit the occurrences of position errors arising from the error sources without any human intervention. Therefore, it saves the critical applications from offering erroneous output, which may sometimes lead to hazardous consequences. Any additional information, toward the signal integrity, provided by the system or by any augmentation over the system (e.g., WAAS), complements basic RAIM and improves RAIM quality.

We recall the definition of Integrity of a GNSS receiver as the ability to continue its positioning function even in the presence of uncongenial conditions. It is interesting to understand how, without any additional information, the receiver detects any flawed signal and continues operating. Popular RAIM algorithms follow these steps:

Step 1: Fault detection (FD) in the signals.
Step 2: Isolation of satellites issuing faulty signals.
Step 3: Protection levels computation (although this step may be optional).

In fault detection, the typical approach taken is the consistency check. For this, the receiver needs to have at least one more satellite visible than the minimum required to find the position. For example, it requires 4 satellites to find the 3D position in GNSS. Then, for implementing the RAIMS, it requires at least 5 satellites in view.

This allows the receiver to have ${}^5C_4 = 5$ different solutions for the same position. Each position solution, derived from four satellites, has one of the visible satellites that does not contribute to the solution. If all the signals are good, all solutions will be approximately the same. Otherwise, if the n^{th} satellite is faulty, then the one solution that deters the nth satellite will have a different (correct) solution than all others. The other four, where the nth satellite is involved in determining the solution, will have significantly different solutions. Thus, this nonconsistency of all the available solutions will allow the receiver to identify that there is a faulty satellite present. RAIM also compares the difference between each expected and observed pseudo-range. Under a no-fault condition, all the extra pseudo ranges should be consistent with the computed position, but not when there is a faulty signal. Thus, the detection of the fault is carried out.

If more than one redundant signal is present, then even identification of the faulty signal can also be done. In general, for fault detection and exclusion (FDE), the following steps may be taken:

(1) RAIM uses redundant signals from multiple satellites to produce several GPS position fixes.
(2) It then compares these position solutions and checks for consistency.
(3) If any signal is faulty, RAIM detects the corresponding solutions as outliers and accordingly identifies them. The faulty signal is then excluded to continue the receiver operation.

In many cases, RAIM is implemented in a reference receiver whose position is predefined. In such cases, the mere comparison of expected and measured pseudo ranges can detect and identify faulty signals. Traditional RAIM uses FD only; however, newer receivers incorporate fault detection and exclusion, which enables them to continue to operate in the presence of a failure.

An efficient RAIM algorithm will offer consistent availability and continuity of the system to the receiver. Augmented systems, like SBAS, also provide integrity signals separate from its primary service. Therefore, SBAS-enabled receivers can use this separate signal broadcast in conjunction with the RAIMS to indicate these problems directly.

A key assumption usually made in RAIM algorithms discussed here is that only one satellite may be faulty; that is, the probability of multiple satellite failures is negligible.

Since the FD and FDE features of RAIM are dependent upon the number of visible satellites, RAIM efficiency may be slightly lower for mid-latitude operations and slightly higher for equatorial regions due to the nature of the orbits. The use of satellites from multiple GNSS constellations or the use of SBAS satellites as additional ranging sources can improve the availability.

In brief, RAIM is a statistical consistency test of multiple pseudo-range measurements. Thresholds set too tightly result in excessive false detections and exclusions,

yielding poor usability. Too loose, and RAIM only detects and excludes large faults, resulting in poor availability.

Advanced RAIM, employs redundant, dual-frequency measurements from multiple GNSS constellations and hence provides better levels of performance than RAIM with a single constellation. However, it has cost concerns on its flipside.

References

Cooper, G. R., & McGillem, C. D. (1987). *Modern communications and spread spectrum*. McGraw-Hill, Inc.

Katz, J., & Lindell, Y. (2007). *Introduction to modern cryptography introduction to modern cryptography* (pp. 1–527). CRC Press.

Krutitsky, E. (2022). Introduction to jamming. *Cybersecurity*. https://doi.org/10.13140/RG.2.2.32263.47522.

Lin, S., & Costello, D. J. (1983). Error control coding: Fundamentals and applications. *Computer applications in electrical engineering*. Prentice Hall.

Mutagi, R. N. (2013). *Digital communication: Theory, techniques and applications*. Oxford University Press.

Neish, A., Walter, T., Enge, P. (2018). Parameter Selection for the TESLA keychain. Stanford University, Available at https://web.stanford.edu/group/scpnt/gpslab/pubs/papers/NeishIONGNSS2018ParameterSelectionTESLAKeychain. Retrieved on: 24 December, 2024.

Proakis, J. G., & Salehi, M. (2008). *Digital communications* (5th ed.). Mc Graw Hill.

Shannon-Hartley theorem. (2024). Wikipedia. Available at: https://en.wikipedia.org/wiki/Shannon%E2%80%93Hartley_theorem. Retrieved on: 16 December 2024.

System integrity. (2024). Wikipedia. Available at: https://en.wikipedia.org/wiki/System_integrity. Retrieved on 02 January, 2025.

What is System Integrity? —Building Strong System Defenses. (2023). Reason Cybersecurity Ltd. Available at https://cyberpedia.reasonlabs.com/EN/system%20integrity.html. Retrieved on 02 January, 2025.

CHAPTER

Applications and services 11

11.1 Introduction

Navigation services primarily offer position and time to their users. But how do the users utilize this information so that it effectively works to serve purposes? No service is worthwhile if it is not used for any applications. Rather, it is the applications that decide the performance targets for any offered service. It is no different for Satellite Navigation. Radio signal-based navigation started in the last decade of the nineteenth century, when the radio signals from the coast were used ingeniously for the navigation of the ships adjacent to the shore. However, it is during the last few decades, with the advent of the satellite based navigation that it has taken on a global shape and proliferated deep into society and into human lives.

The main aim of this chapter is to make the reader aware of the extensive range of applications that are possible with satellite navigation and also to mention the huge volume of work that has been done in this regard. So, we shall in this chapter, instead of concentrating on some specific applications only, first discuss the current scenario of global navigation satellite system (GNSS) based applications as a roundup of the entire efforts gone into this over the time frame. Our aim will be to bring forth the prevailing applications in different fields, showing how each of them benefits personal, societal, or scientific needs. However, we shall finish the chapter by describing a few selected applications with more technical details.

11.1.1 Advantages over other navigation systems

Position, velocity, and time estimates obtained from the satellite navigation systems can be efficiently used in a variety of applications. Similar navigation parameters can be derived from other systems. But, in certain terms, the GNSS-based applications have features more advantageous than the other forms of navigation. Here we list out these features that are exploited to utilize the system, making it more suitable than others.

- *Message-based signal structure:* The navigation receiver interacts with the GNSS signal to derive all the possible information it needs to estimate its position. The messages incorporated into the signal not only provide the data for reference positioning but also aid the receiver in self-correcting actions, inform status, or to actuate other related applications. For example, geo-tagged disaster warning

Understanding Satellite Navigation, Second Edition. DOI: https://doi.org/10.1016/B978-0-443-36432-7.00004-3

information may be disseminated through the system message. This feature is unique for GNSS.

- *Multiscale Accuracy:* GNSS offers multiscale accuracy from a few meters (normal standalone GNSS) up to a few centimeters (RTK or PPP), depending upon the receiver and the technique used. Unlike other systems, which have only some definite accuracy options, here the user has the option to select the accuracy as per the requirement of their application, enhancing the scope of the uses.
- *Dissemination of Time:* This is a unique feature of GNSS-based navigation that provides precise time along with precise position. Certain applications like computer networks need precise time rather than position while some require both time and position. In such cases, the GNSS stands to be the best option available for the users.
- *Satellite Integrity Information:* In Chapter 2, we have learnt that the ground system of the satellite navigation system, in addition to keeping track of the dynamics of the satellites, also continuously observes the signals that the satellites transmit to the users. This enables the systems to readily transmit any anomaly in the signal or constellation observed, through proper messaging or other means. This simultaneous availability of integrity information is an added advantage to the users of the GNSS to continue or adjourn certain applications based upon it.
- *Propagation signatures on the signal:* Besides all the above, the satellite signals in radio frequency, while propagating through the medium between the satellites to the earth, experience the effects that the medium impresses upon them. From these signatures in both the realm of time and amplitude, certain characteristics of the medium can be efficiently derived. Thus, satellite navigation provides a scope for observing the propagating medium through the appropriate derivation of its received signal using the right applications.

11.2 Applications overview

Considering the global scenario, Satellite navigation has become a keystone technology in the daily life of man. It is not only being used for personal navigation purposes in cars and mobile telephones, giving positions, but also serving a great deal in industrial and commercial sectors like energy distribution networks or banking systems, or in business transactions, or in time and frequency synchronizations. Applications also span from transport and communication to land survey, agriculture, scientific research, tourism, and whatnot.

The feat of demonstrating the benefits of satellite navigation technology and proliferating them to the depths of society should be accredited to the Global Positioning System (GPS) of the United States, christened as 'NavStar'. The the use of navigational products for societal and strategic applications started with its predecessors of GPS like the Transit and the Timation system. However GPS, providing freely accessible global navigation services alone for the last few decades, have seen its applications growing continuously. Its applications are still being developed, covering

all walks of life and sectors of the world. So, while discussing the applications, although all the current systems, including GLONASS, Galileo, BeiDou, etc., have their contributions and associated involvements, the authority and influence of the GPS have to be acknowledged. In the last decade, with the inclusion of various new systems, the associated applications have been enormously boosted.

In this section, we first briefly review the current applications of the navigational system in a holistic manner. It will provide an understanding of the different perspectives of utilizing the system, along with their importance and usefulness.

11.2.1 Application architecture

Before entering further into the main description of the applications, we shall discuss the most general forms of the architecture exploited for the implementation of these applications. This will have reference while explaining the application details and will provide a view of how the information from different ancillary sources is assimilated with position data to achieve the application goal. This will also give an idea of the resources and infrastructure that each of these applications demands. There are broadly two types of architecture used in these applications. These are viz. Standalone and Extended architecture, which we shall now describe.

- *Standalone Architecture:* There are some typical navigational applications that, in general, require only an ordinary navigation receiver with appropriate intelligent utility algorithms already embedded within it. Additional information, e.g., maps, traffic conditions etc., if needed by the utility, may be made available either through preloading or by augmenting it with a collocated device. The baseline is, all the resources used for such applications are local and do not require any communication of data to external remote entities.

The position solution obtained by the navigational receiver is intelligently used by the associated utility software with any necessary auxiliary data to produce intelligible and useful information. This value-added information, thus created, is finally interfaced through a proper graphical user interface (GUI) for convenient and effectual use by the user. Fig. 11.1 shows the schematic for such applications.

- *Extended Architecture:* There are satellite navigation applications in which the navigation solutions are supported by auxiliary data, are not local but fetched through a communication link. Also, there are applications in which the navigation solution estimates at one location are transferred to another to serve the application objectives. Typically, these applications obtain the solution from the receivers and then connect with a centralized information base, typically a server, which may have additional access to the auxiliary data. Data exchange and processing are then done, which is ultimately used to meet the application goals. The communication may be done through a satellite link or a ground-based radio communication system like GSM, depending upon the application, while the final processing may be done either at the server or at the user receiver. Thus, it needs synergic use of

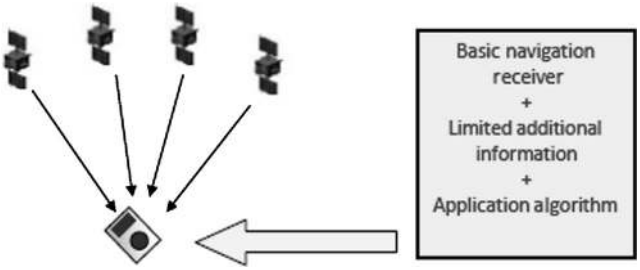

FIGURE 11.1

Schematic for the standalone architecture for global navigation satellite system applications.

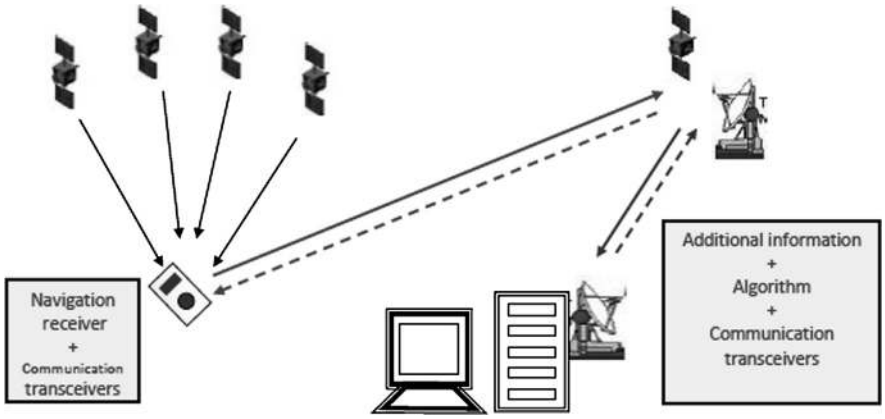

FIGURE 11.2

Basic architecture of extended applications.

navigation and communication systems. The results are finally displayed to the user through a proper GUI (Fig. 11.2).

11.2.2 Applications roundup

Since the 1990s, navigational applications have become immensely popular across the globe. The popularity of GNSS applications can be gauged by their extent of usage. Here, we list some important Sat-Nav applications that are currently being used. However, it is important to understand that, with the ever-widening spectrum of GNSS-based applications, no list can be exhaustive. Further, the descriptions provided here are not comprehensive in terms of technical intricacies, but are only brief mentions of their utilizations (El-Rabbani, 2006; Parkinson & Spilker, 1996).

FIGURE 11.3

Applications for road navigation.

11.2.2.1 Societal applications

Although the initial purpose of the initial GNSS systems, viz., GPS and GLONASS, was military, the versatility of the systems and the societal demands of their applications were the forces that made them available for civilian use. In contrast, civil applications have now become the driving force for further development and advanced research related to these systems. Different societal applications are possible with the systems, which we broadly categorize and describe under the following subheads.

11.2.2.1.1 Vehicular applications

Satellite Navigation solutions, in conjunction with additional information, generate useful navigation products. These products provide general navigational aids to road, water, and air vehicles and are widely used throughout the world today.

- *Road navigation*: Using satellite-based navigation has become a popular option for modern road transit systems. Besides showing one's positions on digital maps in real time and tracking the locus of their progress, it can help motorists find the proper course to their destinations or provide optimal routes to commercial vehicles. This is done by matching the map with the derived positions and is probably the most familiar application of satellite navigation. (Fig. 11.3). When augmented with a communication link, this may be used for vehicle tracking, fleet monitoring, and management. It is done by transmitting the individual positions of individual vehicles, or those in a fleet, with time stamps to a server through a preferred communication channel, updated at regular intervals. Subsequently, all the positions received at a server are collated and can be observed through a consolidated display at the server with additional information like average

speed, expected time to reach destination, etc. The same information, with or without filtering, may also be sent to any specific user. Tracking, tracing, and scheduling of vehicles has become very popular, particularly for booking cabs online. GNSS positions are now being utilized for e-tolling. Here, any vehicle using a taxable highway does not have to wait at the toll booths to pay the charges. The amount is automatically deducted from the subscribed users' account, depending on the length of the taxable road used by them, as derived from their GNSS data. This increases the average speed over the highway, in addition to convenience to the user. GNSS also helps in general traffic management, enabling appropriate supervision and decision-making options for traffic routing and guidance.

- *Rail navigation*: The basic navigation service may be provided on trains to make the passengers aware of the exact locations of the trains, relative position over the entire route, speed, heading, time, next station, expected time to reach, etc. In addition, the tracking of the individual trains can be done and disseminated through a central server in a manner similar to the fleet monitoring described above. This can serve to generate data for the real-time rail information service and also to derive the statistics of the rail movement and related statistics, as well. This data can also be used for an intelligent rail guidance system that can automatically recommend varying train speeds, re-route traffic, thus increasing the efficiency of the rail track capacity.
- *Marine navigation:* A wide variety of vessels move on water bodies each day. Irrespective of the purposes and size of the vessels, which may vary from the commercial giant ships to entertainment sea liners or small fishing boats, the safety and route optimization of marine transportation is a vital need. Therefore, it is important for the sea goers to stay on the "correct trail" or return to the best identified spot for entertainment or reaching the potential fishing zone, etc. This is a part of waypoint planning and management, which includes risk assessment, too. This may also help define international water boundaries and access rights to areas. Resident applications can raise alarms in a receiver whenever the boundaries are crossed. Monitoring and identification of registered vessels may be done when positions derived from these vehicles are transmitted to the monitoring system through a satellite link (Sennott et al., 1996). The accuracy, integrity, continuity, and availability that the GNSS position fixes provide can establish its need for critical maritime movements.
- *Air navigation*: Reliance on satellite navigation is the future of air navigation and air traffic management systems. Precising of the position estimation en-route is done through the integration of INS or other systems (Eschenbach, 1996) with the GNSS system, while the augmentation system provides enough accuracy and integrity for aircraft landing as well as during the en-route phase. Augmentation enables the aircraft to carry out a precision approach for landing with different categories of precision, satisfying the specified accuracy, continuity, and integrity levels (Parkinson et al., 1996). GNSS features complying with tight requirements enhance the reliability of the system. The air traffic controlling scenario has

Table 11.1 Supplementary list of vehicular GNSS applications.

Road navigation	Rail navigation	Maritime navigation
• Remote monitoring of road traffic conditions. • Design and control of an intelligent city transport system. • Road safety and security with Accidental reporting. • E-insurance (pay insurance for the vehicle as per use).	• Train control and signaling. • Traffic information. • Passenger information system. • Safety at UMLC. • Real-time track and other asset monitoring. • Prevention of collision, derailments, and rail switch errors.	• Observing sea level changes. • Dredging operation. • Laying pipelines/cables. • Positioning of oil rigs. • Prevention of piracy. • Automatic identification system and Vessel monitoring system. • Coastal surveillance. • Potential fishing zone.

*(*UMLC*, Unmanned level crossing)*

changed with the advent of ADS-B type of system. In this system, the individual aircrafts and the Air traffic controller, can both identify and visualize the locations of other aircraft in their vicinity as the aircrafts share their precise mutual positions derived through the GNSS positioning systems. This provides added awareness to the pilots of their surroundings (Braff et al., 1996).

The use of GNSS provides precision positions in road, rain, maritime, and air traffic and thus reduces the necessary minimum separation between the adjacent vehicles. This increases the capacity, and the increased capacity enhances the efficiency. Other Road, Rail, Maritime, and Air Navigation applications utilizing GNSS are listed in Table 11.1.

- *UAV Navigation:* Unmanned Aerial Vehicles (UAVs), commonly known as drones, rely heavily on GNSS for accurate navigation and positioning. GNSS provides essential data that enables UAVs to perform a wide range of tasks with precision and reliability, including self-navigation. The accurate position fixes provided by the GNSS in both urban canyon and open conditions help the UAV to carry out autonomous operations, such as surveying, mapping, and inspection, without human intervention.
- *Space navigation*: Considering the geo-directive nature of the GNSS signals, the service may be used for providing navigation solutions to satellites in LEO. This may provide high precision orbit determination with minimum ground control. It may also support attitude determination of the spacecrafts, replacing expensive onboard attitude sensors with low-cost multiple antennae placed on it, along with specialized algorithms (Lightsey, 1996). It may also provide timing solutions to the low-earth remote sensing satellites for time tagging and other timing purposes, replacing expensive spacecraft clocks with low-cost, precise time receivers. Details of the utilization of GNSS signals in LEO orbits and even at much higher altitudes are discussed later in this chapter.

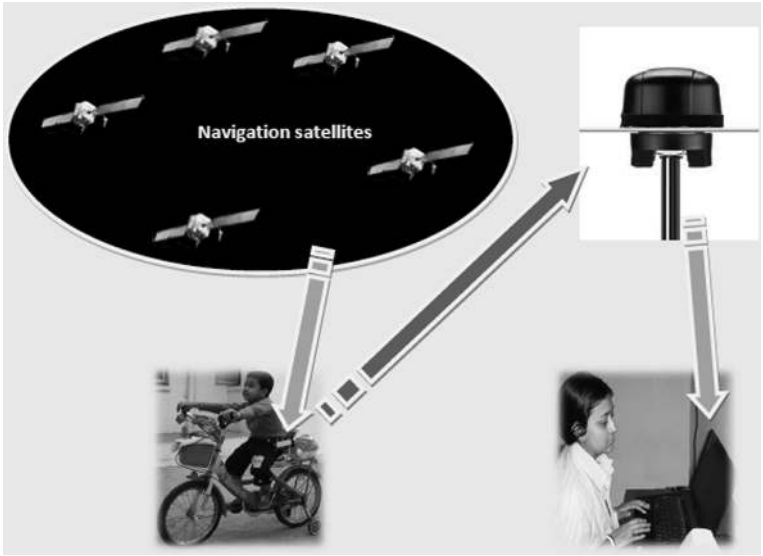

FIGURE 11.4

Applications for child tracking.

11.2.2.1.2 Tracking-based applications

- *Child tracking*: Today's parents can benefit from the advancements of the modern navigational technology. They can identify and follow the locations of their children from their home or workplace. This addresses the major concern of tracking the children's locations when the parents are away from them. This can be implemented by using GNSS receivers estimating positions and equipped with a communication channel like GSM or Wi-Fi to to transfer this position and display it the parents' phone or website at regular intervals. Thus, a child's movement can be monitored easily (Fig. 11.4).
- *Location-based services* (LBS): 'Location Based Service' is a service provided to users giving specific information that is explicit to the position where the user is currently located and which are most relevant to the user at that location. These information services are generally offered to users on their mobile phones, websites, etc. to meet specific requirements or demands. LBS may be either a Push or a Pull type of service. In the former case, the service provider spontaneously disseminates information to the user, while in the latter case, the user fetches information based on their query. The services are mostly driven by commercial benefits or may also be due to social welfare and specific information dissemination.

The popular form of LBS is a query-based service, in which the user, on estimating their positions, raises different queries and asks for a response from a central data

server through a communication channel. The type of queries may vary widely. However, some of the most frequently used queries belong to the following types (Wikipedia, 2024).

Amenities: Closest hospital, hotels, ATM, petrol filling station, restaurant, shopping mall
Weather: Current weather at the location, temperature, and possibility of rain
Topology: Landform, height from sea level, nearest river, lakes, mountains, etc.
Entertainment: Any event near the location on the date, movies, theatres, places of interest, etc.
Agriculture and Industry: Soil type, crops, agro-industrial products, etc.

The user query, tagged with its current location, is served by the centralized database. The server containing the geo-specific and relevant geoinformatic or remote sensing database returns the response to the query to the user through the same return channel. Thus, a strong convergence and synergy of navigation, communication, remote sensing and Geographical Information System (GIS) is what makes a worthwhile LBS system.

- *Sports and entertainment:* Satellite Navigation is also significantly used in sports and entertainment. Primarily, for outdoor exploration, it can eliminate many hazards associated by providing precise location and timing. Activities, like mountain trekking, hiking, etc., carry with them many intrinsic dangers, including getting lost in unfamiliar or unsafe territory. The only form of reliable navigation available here is from satellites. In addition to its all-weather ability to provide position, these digital data may be stored to record and return to waypoints or even to retrace suitable routes. GNSS technology is used to track athletes' performance in real-time, providing precise data on speed, distance, and location. Therefore, it is used by the trainers to improve techniques and strategies. This is particularly useful in sports like running, cycling, skiing, etc. Other applications include motor racing, recreational aviation, yachting, boating etc. GNSS technology has also generated entirely new sports and outdoor activities. An example of this is 'Geocaching', a sport in which the goal is to seek containers, called "geocaches," at specific locations marked by coordinates and provided to the participants. It rolls a pleasurable day's outing and a treasure hunt into one. Another new sport is 'Geo dashing', a cross-country race to a predefined coordinate. Fig. 11.5.

11.2.2.1.3 Disaster management

Giving a timely warning and providing quick assistance are two major concerns of civilian administrative authorities during and after a disaster. Satellite-based navigation, providing signals from space, can continue services even in the case of disasters when other land-based services are likely to fail. These signals can be used efficiently for both, before the occurrence of any event to take preemptive actions based on predictions, or postfacto for relief and management activities.

FIGURE 11.5

Geocatching.

From www.pexels.com.

- *Disaster warning*

Several human and animal habitats are located in earthquake-prone areas. Navigation can play a prominent role in generating seismological warnings. This requires a wide network of very accurate receivers with robust algorithms that can help to quickly identify earthquakes and generate prediction flags. The major criticality in the system is the correct identification of the quakes without missed detection or false alarm (Allen & Ziv, 2011). In a similar manner, activities like landslides can also be identified. River floods and tsunamis can also be identified and warned of by monitoring the river and sea surface heights, respectively, typically done using buoys

equipped with the GNSS receivers. The warning messages can also be transmitted using the unused capacity of the navigation channel itself to reach the users in a geotagged and geofenced manner.

- *Search and rescue*

  Locating stranded people, animals, and assets and helping to save them are very important in operations after any disaster. This can be efficiently done through a centralized monitoring and crisis management platform, which can be established in conjunction with the navigation system. On one hand, Sat-Nav users, additionally enabled with a communication channel like GSM, WiFi, can indicate their specific locations using the preferred channel, if still available. These identifications can be observed centrally to make prompt decisions and rush aid. From the rescuers' perspective, once their receivers are registered in the system, their locations may automatically be tracked for efficient coordination, possibly carrying out exchange of information and instructions. This allows improved planning and optimization of resource allocation from a central location and permits prompt responses.

- *Emergency/medical services*

  About a billion of emergency calls are generated worldwide every year. In many cases, emergency vehicles cannot be dispatched on time due to the absence of sufficient location information. A pivotal component of any successful emergency operation is time. The dispatcher, in most cases, has either to ask for the exact location or to map the calling telephone number, each of which consumes much critical time. With satellite navigation, the precise location of the event can be tagged with the call, reducing the approach time of the assistance and thus saving lives. The use of GNSS for fire positioning and detection, guided fire-fighting and logistic support, and damage assessment is very common nowadays.

11.2.2.1.4 Precision farming

The use of precise positioning in different farming activities is referred to as Precision farming. These activities include farm planning, field mapping, and activity control. GNSS-based field mapping is used for precise applications like precise sowing, watering, and administering fertilizers. These precise activities produce a higher yield and reduce expenses by creating a more environmentally friendly farm. Many modern farms use UAVs to carry out the above farming activities like dropping seeds for sowing, spraying pesticides, delineation of crop areas, etc., in which GNSS is used for precise control and navigation of the UAVs. This requires submeter level accuracy, which is achievable using a DGNSS or real-time kinematics (RTK) receiver or Precise Point Positioning (PPP). It also allows farmers to work during low visibility field conditions such as rain, dust, fog, and darkness (Fig. 11.6).

11.2.2.2 Scientific and technological applications

Satellite-based navigation may also serve many scientific applications where absolute precision is necessary. In experimental physics or in different applications of technology, precise position and timing requirements need to be complied with. This also

FIGURE 11.6

Precision farming.

calls for the integrity of information in addition to an enhanced level of accuracy and precision.

11.2.2.2.1 Surveying, geodesy, and geographical information system

Surveying estimates locations of points on the Earth. As technology is evolving and expanding throughout the world, the surveying and mapping community is resorting more to GNSS-based techniques. It significantly reduces the amount of equipment and effort that are normally required for other conventional surveying techniques. Moreover, GNSS-based surveying does not need a line-of-sight requirement between

two stations, which other typical surveying mechanisms do. Therefore, it can be done in all-weather conditions with ease. Surveying needs sophisticated receivers capable of carrier phase measurements to provide RTK or postprocessing with submetric accuracy. GNSS-based surveying can be done over land for cadastral, construction, mapping, mine surveying, etc. While over the marine and coastal region, hydrographic and offshore surveying can be done.

Geodesy is the scientific study of finding the shape of the Earth. This is carried out using the relative positioning techniques of satellite navigation systems to find the baseline between the points under survey. GNSS techniques do not require mutual visibility and thus allow large baselines. Further, the coincidence of the GNSS reference origin with the geocentre, which is also the origin of all survey measurements, gives the added advantage of having no requirement for relative transformation of the coordinates (Larson, 1996; Leick, 1995; Torge, 2001).

GIS is used to record geographical data and digitally map the geographical distributions of different parameters and assets. For example, GIS maps may represent natural and man-made features like transportation routes, political boundaries, forest contours, building footprints, land parcels, etc. GIS digital maps can be accurately created with centimetric accuracy using delineation through GNSS based positioning.

11.2.2.2.2 Earth and atmospheric studies

Apart from obtaining the position solutions and time, the signals from the navigation satellites may be ingeniously used for earth and atmospheric studies. Propagation features like the delay, bending, reflections, and signal fluctuations, experienced by the traversing radio waves of the navigation signal, may be utilized for deriving the required parameters for the studies. The most common areas involve earth and atmospheric studies, including the ionosphere, some of which are described below.

- *Meteorological studies:* Meteorologists are using GNSS signals for atmospheric sounding using the Radio occultation technique. This is done by receiving and measuring the atmospheric bending of the signals received from the navigation satellite when the direct beam is occluded by the Earth. The bent signal is typically received by a navigation receiver onboard a LEO satellite from a navigation satellite on the other side of the Earth, such that without bending the signal would be shadowed by the Earth. The amount of bending is estimated from the derived absolute positions of the GPS transmitter and the receiver. The bending is used for profiling of the tropospheric meteorological parameters like density, pressure, temperature, and humidity. The derived distribution can be used for the characterization of the atmosphere Fig. 11.7
- *Ionospheric studies***:** The dual-frequency receivers can measure the slant ionospheric TEC. Hence, they can act as a device for time-stamped measurements of ionospheric TEC. Moreover, wherever available, the SBAS message also contains the near-real-time ionospheric delay data at specified grid points transmitted to the user. Thus, the current state of the vertical Total Electron Content over the whole area covered by the grids can be simultaneously obtained at a single or

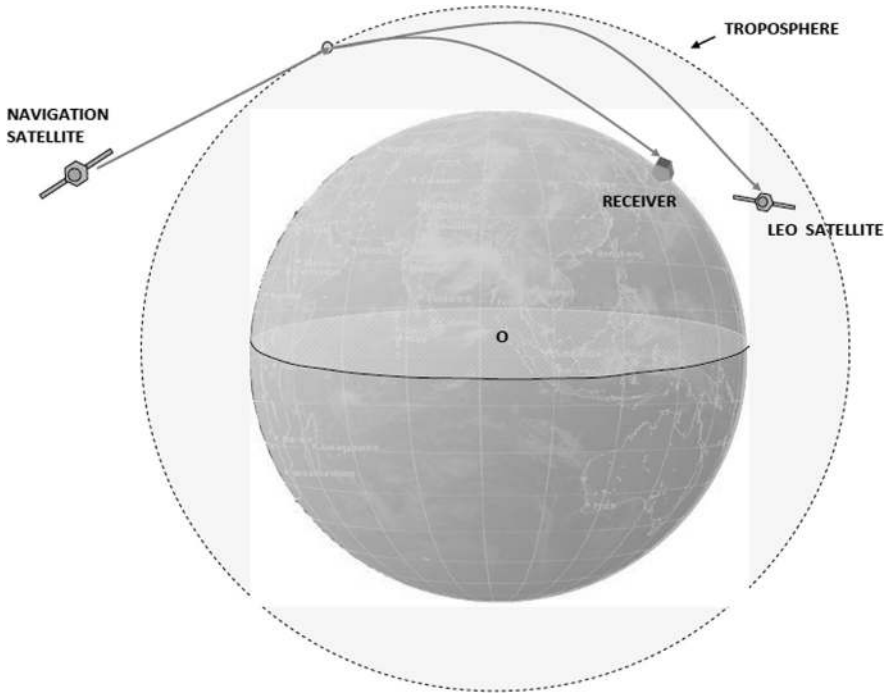

FIGURE 11.7

Applications in radio occultation.

multiple locations. Additionally, from the discrete TEC measurements, the whole spatial profile of the electron density may be derived using Tomography (Acharya et al., 2004; Brown & Ganguly, 2001; Hansen, 2002). This provides great value for ionospheric research. Simultaneously, the ionospheric irregularity parameter ROTI, etc., can be obtained from the GNSS measurements.

11.2.2.2.3 Environmental studies

The satellite navigation system can be used to obtain accurate and timely information related to the environmental elements. This empowers authorities to make better decisions needed to sustain the Earth's environment while balancing human needs. Precision positions derived using GNSS can be used to delineate and measure the coverage of forests and estimate their canopy size. This helps to prevent illegal deforestation or human encroachment into forest areas. It can also be used for monitoring extensive natural physical features like coasts, river basins, riverine extensions, lakes, mines, etc. Their temporal contour variations, which link to critical environmental changes, can be monitored very easily with GNSS. The positions derived using satellite navigation can be used for animal and livestock tracking. Endangered species of animals may also be tracked and mapped, helping to preserve and enhance declining

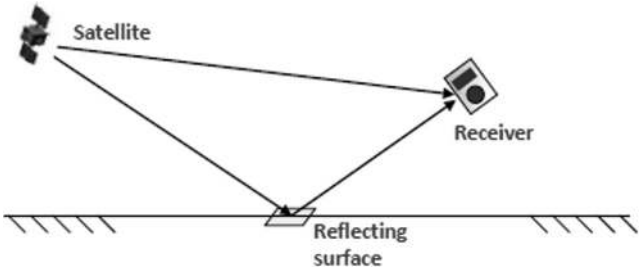

FIGURE 11.8

Reflectometric applications.

populations. The animals can be easily traced or spotted for required medication and other aids whenever necessary.

GNSS-based reflectometry can be used for ocean heights and for soil moisture studies. Reflectometric measurements of the navigation signals in terms of the delay and power are used to estimate the sea surface height and salinity using interferometric approaches with direct signal. In addition to proper algorithms, this needs the receiver to be capable of handling very low power signals as expected from the reflected waves from the sea surfaces (Camps, 2008; Garrison et al., 2011) (Fig. 11.8).

11.2.2.3 Precision timing service

Precise time, like precise position, is crucial to a variety of activities. Systems like terrestrial and satellite communication, electrical power grids, and electronic networks, etc., all rely on precision timing for synchronization and operational efficiency. GNSS can be used to provide precise time by synchronizing the user receiver with the system clocks. It does so by disciplining the receiver clock with the satellite clocks. When locked to satellites, the receiver's time stability becomes as good as the onboard atomic clocks. This enables users to determine the time to an accuracy of the order of nanoseconds, without the cost of owning and operating expensive atomic clocks. By locking two or more clocks to the GNSS system time, they can be brought to synchronization with the same order of precision. Therefore, GNSS provides cost-effective solutions to meet precise time requirements even when the devices of the infrastructure or network are spread over a wide geographic area. For most of the typical requirements, the timekeepers are in fixed locations and know their precise position; they only need one satellite to get the offset of their local clock from the navigation system time. Precise Time synchronization finds its uses in various critical infrastructures and applications, including the electric power distribution, communication networks, satellite earth stations, national timekeeping, metrology, scientific research, and many more.

11.2.2.3.1 Synchronizing laboratory events

GNSS-based time and frequency synchronization is used by many laboratories for calibration and metrology. Synchronized activities at remotely located laboratories or

experiment locations are carried out using GNSS-based time transfer and synchronization. This may be achieved using GNSS through time transfer using the Common View (CV) technique. This method is described later in this chapter. Distributed networks of instruments that must work together to precisely measure common events require precision timing sources that can guarantee accuracy at several points. GNSS-based timing works exceptionally well for any such distributed timing application dispersed over wide geographic areas.

11.2.2.3.2 Electric power grid

A power grid is a complex and interconnected system. What happens in one part of the grid affects the operation elsewhere. Precise time and high-speed communications of encoded '*event identities*' in the substation are the enabling technologies that make it feasible to understand and control the activities at one place, depending upon what is happening at the other. This inevitably requires accurate time stamps, with event flag data being communicated. Further, combining powers generated from different generation stations on the same grid requires the component electric sinusoids' parameters to be in the same phase. Synchronized phasors (synchrophasors) are used to measure the phasors and communicate them to a common monitoring station with a precise time stamp, the time being obtained using the GNSS. The different phasors are then time-synchronized for accuracy. Transmission line frequency decreases as load increases and vice versa. The synchrophasor measurements can be used to speed up or slow down of generators. Apart from this, fault location over a transmission line is done by analyzing the precise timing of the traveling wave as it propagates through a grid. This is derived by measuring the difference in arrival times of fault artifacts at the two ends of a faulted line. These time measurements require extensive precision, which is obtained and maintained with GNSS-based timing systems.

11.2.2.3.3 Communication system

In Communication systems, different time-based apportionment of the resources to users is devised. The time division multiple access (TDMA) is one of them, in which a particular channel is allotted to other users in a time-sharing mode, and each user transmits and receives their data in their portions of time. Unless a very precise time is kept, along with synchronizations between different users, there is a probability of one user dumping data into a different user's segment, resulting in interference. Both satellite and terrestrial communication links use this type of multiple access technique. Cellular networks use GNSS time to keep all of their remotely located base stations in perfect synchronization with the Master Station and other parts of the network. GNSS is used for the synchronization of user traffic and control timeslots and for handovers between base stations. Precise time synchronization is also necessary for IP-based applications like streaming audio and video. Time and frequency synchronization is done using GNSS, which leads to a more efficient utilization of the limited radio spectrum used in these networks.

Similar synchronization in enterprise networks, business, and banking transactions is also necessary, which is achieved using the GNSS timing applications.

11.3 Specific applications

In this section, we shall discuss a couple of important applications in detail that use satellite navigation. The rationale for separating out select applications for detailing is to be aware of the intricacies involved in harnessing the technology for applications. So, we have chosen applications from two separate categories, one for precise position while the other for precise estimation of time. We shall begin with the details of one which is actually a service generating precise position that involves augmentation. We have, however, chosen to incorporate it in this section to highlight the close dependency of the applications requiring precise positioning on augmentation system services.

11.3.1 Precise point positioning (PPP)

The errors in the GNSS positioning arise from the inaccuracies in estimation of parameters and other measurements. These errors are caused primarily by satellite clock errors, deviations of the satellites from the predicted orbits, or by delays incurred during signal propagation. Out of these, in any standalone GNSS receiver, errors like the satellite clock deviations are corrected using the clock correction parameters in the navigation data, while the lower-order ionospheric delays are corrected using dual-frequency measurements. However, the errors due to the use of inaccurate satellite positions, residual ionospheric errors, including their higher-order delays, residual clock errors, etc., are still retained in the measurements. Overall, around 1-2 m residual error is common in the range measurements in normal receivers, which limits achievable position accuracies to several meters. To achieve centimetric accuracy, all these remaining errors are required to be factored in and reduced to negligible terms before using them for positioning.

PPP is a GNSS positioning method in which highly accurate positions, with centimetric accuracies, are estimated using a single standalone receiver. This is done by precisely correcting each individual error in the receiver measurements, the knowledge of the errors being obtained from an external independent system. This independent system derives the errors in advance using measurements from its own network of reference receivers and using different physical models.

PPP differs from the differential approaches for precise positioning, like RTK, in the way the errors are eliminated. It does not eliminate the errors in the measurements by differencing it from any reference measurements. This removes the necessity for the user receiver to remain connected to any reference station. Hence, no reference station is needed in the vicinity of the user. The corrections are derived separately by the system, including an independent network of reference stations and are communicated to the users through separate channels.

11.3.1.1 Precise point positioning architecture and functionalities

In a PPP, there are two different entities, viz. (1) the user, who seeks the precise position, and (2) the service provider, who delivers the user receiver with the

information for correcting the errors. The service provider derives the GNSS corrections and delivers them to the user using different delivery mechanisms. The user, on the other hand, subscribes to the services and requests for obtaining corrections in his measurements and estimations.

Amongst the errors, those that contribute heavily to the error budget of a standalone receiver, the clock error for a given satellite is global, and the ephemeris errors are also almost spatially invariant. So, once these errors are estimated, they can be applied globally. The first-order ionospheric errors are typically corrected by the users. Tropospheric errors are modelled and mitigated. But it is to be remembered that, to achieve centimeter-level accuracy, these corrections need to be accurate to the same order. Further, the errors, which otherwise look insignificant, have also to be estimated and corrected. These errors may include the following

- *Antenna phase-center errors:* difference between the electrical phase center of the antenna to the antenna tip.
- *Earth tides:* vertical movements of the Earth's surface by astronomical gravitational forces.
- *Receiver errors:* The receiver noise and its intrinsic errors, like interfrequency bias, etc.

To derive the errors, the PPP service providers carry out the following activities:

1. Establishing a GNSS reference network at well-surveyed locations to provide raw data of carrier phase measurements from which the ranges are derived by removing the ambiguity.
2. Processing the raw observations, measured in carrier phase by the monitoring stations to derive the highly precise GNSS satellite orbit ephemerides, clock biases, etc., and generate other necessary corrections that can be delivered globally to any receiver.
3. The accuracies of these estimated parameters or corrections are much better than those obtained through navigation signals and thus improve positioning accuracy. These products are then made available in real-time or postprocessing mode to the user.
4. Delivery of the products through terrestrial or satellite-based networks. Geostationary satellites are also sometimes used for the dissemination of errors, to cover a wider area of services.

From the above, it is evident that basically PPP is an augmentation system. A certain form of PPP is similar to the carrier phase version of the SBAS system.

At the user's end, the ionospheric errors are derived using the dual-frequency receivers. However, the dual-frequency receivers can estimate and correct the first-order errors only. The higher-order corrections can be done using triple and more frequencies. Tropospheric errors are derived using atmospheric models. In order to achieve centimetric accuracy, it is essential that the random errors in the receiver are also alleviated. Toward this, longer static measurements are done that provide better precision, since the zero-mean random thermal noise components in the

measurements get removed in the effect. Thus, the user receiver, upon using these corrections or estimated parameters with improved accuracy than those obtained through navigation signals, improves its positional estimation accuracy.

For PPP with postprocessing, satellite orbit and clock corrections are made available online in standard file formats. Corrections and improved parameters for multiple systems are also now being made available. This aids users using multiconstellation receivers to achieve even better availability and accuracy.

For real-time PPP (RT-PPP), the data is required to reach the user within a stipulated time interval. For this, streams of correction data with minimum latency are provided to the users. The position estimation errors, however, increase with increasing latency introduced. Therefore, while relaying correction messages to end-users, the efficiencies in computing and messaging are critical components in the process.

At the receiver, it takes a certain amount of time to achieve a stable state of a consistent, high-precision solution by resolving the ambiguities. This time is called the Convergence Time. This is dependent upon various factors like the number of satellites visible, their geometry, receiver quality, correction data quality, etc. The convergence time is of the essence in PPP. PPP solutions need a relatively longer convergence time compared to differential methods. However, recently, some methods have been developed to accelerate integer ambiguity resolution in PPP. At the current state of technology, accuracy up to a few centimeters can be obtained within a few minutes. For centimetric accuracies or better, the convergence time will increase and may take few tens of minutes.

11.3.1.2 Applications of precise point positioning

PPP is basically used in applications where precise positioning is needed, yet without the constraint of arranging and remaining connected to a reference station or a network, as in RTK. Currently, there are many available commercial PPP services. These services are availed by users for a wide variety of applications. The application areas include mining, forestry, survey, automobiles and aviation, unmanned aerial vehicle (UAV) guidance and control, agriculture, construction, and a lot many more. However, many of these applications can well use RTK for their purposes.

In mining, precise delineation of the mines is necessary for planning and taking necessary steps for environmental protection, taxation, resource management, safety, etc. Similarly, precise forest demarcation is necessary for taking suitable actions for conservation, maintaining biodiversity, sustainable management, etc. In addition, they are also useful for maintaining legal and regulatory compliance and conflict resolution. PPP-derived positions are also used for seismic surveys and oil and gas exploration. Unmanned vehicles such as UAVs require precise automated trajectories, quick convergence of location data, and accurate geo-tagging. Assignments such as delivery or dock station landing must be precise, at a specific address, and therefore require PPP-like precise services. Automated driving needs very precise and reliable location data. Cars with advanced driving assistance systems may use the PPP positioning with centimetric accuracy for controlling and steering the cars. The use

of robotic machines in industries has now become common. Robotic applications are now also used in vogue in construction, particularly at locations with increased human safety hazards. In such cases, PPP-based positioning with enhanced accuracy plays a vital role. Precision agriculture relies on high-accuracy PPP to guide tractors, sprayers, and other agricultural vehicles. Increased accuracy in such activities ensures complete and precise coverage on the one hand and minimizes the damage to the environment on the other.

11.3.2 Attitude determination

An extended rigid body has six degrees of freedom. These degrees of freedom determine the position and also define the orientation of the body. The orientation of the body with respect to a fixed reference frame is called the attitude. The relative positioning of some fixed points on any moving body enables us to find the attitude of the body with respect to any standard frame on the Earth. We shall learn only the fundamental ideas of attitude determination in this section.

For attitude determination, it requires a reference frame to be defined and fixed on the moving body. The relative orientation of this body's fixed frame with respect to a standard local or geocentric reference frame is the attitude of the body. For convenience, we shall consider the moving body to be a vehicle and will be referred to accordingly henceforth.

Relative orientation of a frame with respect to the other is determined by the angles that the coordinate axes of a frame make with those of the other. So, we may say that the complete set of direction cosines of the axes of the body frame of the vehicle with respect to the standard reference frame determines its attitude. Now, any vector has three directional cosines with respect to the frame. Directional cosines are the cosines of the angle that the vector makes with the axes of the frame. As each of the individual axes of the body fixed frame is a vector, each of these three axes will make three angles with the three axes of the standard frame, making a total of nine. This may be represented as a tensor matrix.

However, these nine directional cosines are not independent. Let the body frame defined by three axes be denoted by F' = [X' Y' Z'] while the axes of the standard reference frame are denoted by F = [X Y Z]. These are shown in Fig. 11.9.

So, once two of the directional cosines, say α and β of the X' axis, are fixed in the F frame, the third cosine γ is automatically fixed as they maintain the relation $\alpha^2 + \beta^2 + \gamma^2 = 1$. So, we require only two independent parameters to fix X' in F.

After X' is defined in F, the plane perpendicular to X' containing Y' and Z' is also automatically fixed. However, to fix the direction of Y' in this plane, we need two more such directional cosines. They will define its relative orientation with respect to two axes of F on this plane. Once the X' and Y' axes are defined in F, the other axis Z' is automatically fixed in this frame. So, totally, we have only four independent relative directions that define the orientation of one frame in the other. If we know these four independent elements, we can derive the complete set of nine directional

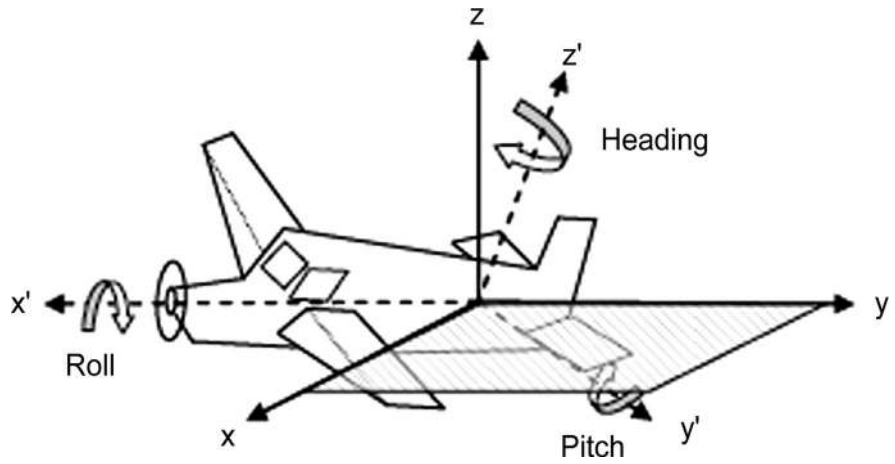

FIGURE 11.9

Attitude determination.

cosines. Then, any vector defined in the F' frame can be well converted to the F frame and vice versa. Further, the attitude of the vehicle containing the frame F' can be defined.

The matrix that transforms the vectors from one frame to the other is called the *Attitude Matrix* or the *Directional Cosine Matrix* (Cohen 1992, Cohen 1996). The most convenient way to represent the cosine elements of the matrix is by representing its elements as the dot products of the unit vectors of the two frames. So, for F (X, Y, Z) and F' (X', Y', Z') frames, the attitude matrix is

$$A = \begin{pmatrix} X' \cdot X & X' \cdot Y & X' \cdot Z \\ Y' \cdot X & Y' \cdot Y & Y' \cdot Z \\ Z' \cdot X & Z' \cdot Y & Z' \cdot Z \end{pmatrix} \tag{11.1}$$

The reference frame, with respect to which the attitude is to be defined, may be chosen appropriately for the application. We have already learnt in chapter 1 that for vehicles like aircraft, land, or sea vehicles, local frames like ENU and NED are very suitable, while the geocentric ECEF is a more convenient reference for spacecraft attitude. Further, nonconventional application-specific frames may also be used for this purpose.

The body frame is also a right-handed Cartesian that remains fixed with the moving vehicle. From an origin located at the centre of the body, the X' axis may be defined in the forward direction along the main axis of the body, which is also the direction of its true motion, while the Y' axis is normal to it but on the plane containing the vehicle body. The Z–axis remains normal to both as shown in Fig. 11.6. The X–axis is called the Roll Axis, as a rotational motion about this axis is called a ***Roll***. A Roll is manifested by a change in the orientation of the Y' & Z' axes with respect to the

reference frame and is represented by the angle f. The Y–axis is called the ***Pitch*** axis. A change in the orientation X' & Z' axes with respect to the reference frame marks a variation in the Pitch angle θ of the vehicle. Finally, the Z–axis is called the Heading axis, as rotation about this axis is termed as a ***Heading***. The orientation of the X' & Y' axes changes with respect to the reference when the Heading angle Ψ changes.

When the body frame is aligned with the reference frame, the heading, pitch, and roll angles are all taken as zero. It makes A an identity matrix. For definite Roll, Pitch, and Heading angles of the vehicle, the Attitude matrix becomes (Cohen, 1996)

$$A = \begin{pmatrix} \cos\theta\cos\psi & \cos\theta\sin\psi & \sin\theta \\ -\cos\varphi\sin\psi + \sin\varphi\sin\theta\cos\psi & \cos\varphi\cos\psi + \sin\varphi\sin\theta\sin\psi & \sin\varphi\cos\theta \\ \sin\varphi\sin\psi + \cos\varphi\sin\theta\cos\psi & -\sin\varphi\cos\psi + \cos\varphi\sin\theta\sin\psi & \cos\varphi\cos\theta \end{pmatrix} \tag{11.2}$$

Here, the element A_{ij} represents the projection factor of the i^{th} coordinate in the body frame F' on the j^{th} axis of the reference, F.

11.3.2.1 Measurements and estimations

Now consider that two navigation receivers, R1 and R2, are placed on the body of the vehicle, separated by a distance b', which forms the baseline on the body-fixed frame. These receivers measure the carrier phase of the signal transmitted by the same satellite. Recall that we learnt in chapter 8 that for short baselines, the single difference phase equation at receiver 1 and 2 from satellite s can be written as

$$\Delta\varphi^s_{12} = \left(-e^s_1 \cdot b\right) + N^s_{12}\lambda + c\Delta\delta t_{12} + \varepsilon^s_{12} \tag{11.3}$$

where, φ^s_{12} is the difference between the measured phases at the two receivers. b is the baseline in the reference frame F,e^s_1 is the unit vector from the reference receiver R1 to the satellite s. For any moving vehicle, the distance between the receivers R1 and R2 is small enough to assume that the same unit vector holds good for receiver R2 to satellite 1, that is, $e^s_1 = e^s_2$. Here ε^s_{12} is the differential error between the two receivers, encompassing the receiver noise and all other differential residual errors between the two receivers. Since the baseline is small, all the errors may be considered to be identical, but the receiver noise. So, ε^s_{12} is mostly contributed by the difference in the receiver noise. $N^s{}_{12}$ is the difference between the integer ambiguities in the two receivers and dt_{12} is their differential clock error. c and λ are the velocity and wavelength of the signal, respectively.

Considering the two receivers are driven by either the same clock or two clocks that are synchronized, $c\Delta\delta t_{12} = 0$. Since the positional difference of the receivers is negligible, the ionospheric and tropospheric errors are assumed to be eliminated on differencing. Hence, the equation turns into

$$\Delta\varphi^s_{12} = \left(-e^s_1 \cdot b\right) + N^s_{12}\lambda + \varepsilon^s_{12} \tag{11.4}$$

The difference integer ambiguity $N^s{}_{12}$ is required to be resolved first. We have briefly discussed in Chapter 8 how the integer ambiguity is resolved. On resolving

$N^s{}_{12}$, we have

$$\Delta\varphi^s_{12} - N^s_{12}\lambda = \left(-e^s_1 \cdot b\right) + \varepsilon^s_{12} \tag{11.5}$$

The left hand side of eq. 11.5 is the differential geometric range of the two receivers to the satellite s, denoted by $Dr^s{}_{12}$. So, expanding b and e in terms of their components along the standard reference axes, we get

$$\Delta\rho^s_{12} = -\left(b_x e_x + b_y e_y + b_z e_z + \varepsilon^s_{12}\right) \tag{11.6}$$

Now, if at any instant A is defined by eq. 11.2, then the corresponding baseline b in the reference frame may be expressed in terms of the baseline b' in the body frame by the relation

$$b = A^T b' \tag{11.7}$$

So we may write

$$\Delta\rho^s_{12} = -A^T\left(b' \cdot e^s_1\right) + \varepsilon^s_{12} \tag{11.8}$$

In this equation, $\Delta\rho^s_{12} = \Delta\varphi^s_{12} - N^s_{12}\lambda$, is completely known, where the term $\Delta\varphi^s_{12}$is measured by the receivers while $N^s_{12}$is estimated. Unit vector e^s_1 can be estimated from the relative position of the satellite and the antenna. b' in the body frame is prefixed and hence known a-priori. Only the elements of the matrix A are unknown. This matrix contains the elements of the attitude of the vehicle, that is, orientation of the body-fixed axes. These values are nonlinear trigonometric functions but remain unchanged for a definite orientation of the vehicle, irrespective of any baseline chosen on the body-fixed frame. Therefore, to obtain the attitude parameters for different elements of A, the equation can be solved by using similar phase measurements from different pairs of receivers on the vehicle and for different satellites visible.

The solution is obtained by minimizing the quadratic attitude determination cost function for the m baselines and n satellites from any arbitrary receiver k in the body frame.

$$J(A) = \sum_{i=1}^{m}\sum_{j=1}^{n}\left\{\Delta\rho^j_{ki} - A^T(b'_i \cdot e^j_k)\right\}^2 \tag{11.9}$$

where b'_i is the i^{th} baseline defined in the body frame with respect to reference receiver R_k and receiver R_i, and $\Delta\rho^j_{ki}$is the differential geometric range between the same receivers toward the satellite j.

Since the elements of A are nonlinear in nature, first a trial solution A_0 is obtained, and a better estimate is obtained by linearizing the cost function about the trial solution and solving for the correction matrix δA, so that $A + \delta A$ becomes the revised and improved solution after the correction. This process is iterated, and the final solution is assumed when the corrections δA does negligible alterations to the solution. Intrinsically, we have assumed the baselines to be all coplanar (Cohen, 1992; Cohen & Parkinson, 1992; Cohen, 1996).

11.3.3 Frequency and time transfer

Navigation solutions derived in a receiver enables it to determine the difference between the clock the user receiver and the reference time for GNSS. The clock contained within a user's receiver is usually a quartz crystal clock. Only in a few specific cases, an external clock such as a rubidium or a cesium frequency standard can be the local reference for a GNSS receiver. The accuracy of the GNSS system clocks can be exploited to obtain precise time at one location or to disseminate the same timing accuracy to two or more different locations.

When the precise time information obtained and maintained by a clock at a certain location is made available to clocks at other locations, time transfer is said to have occurred. It is to be noted here that the time transfer is different from synchronizing two clocks with a GNSS clock. The basic architecture of such a time transfer system contains two clocks separated by distance, in which at least one of them has the capability of steering its own time. There is a calibration channel through which the calibration information is communicated between the two clocks. The free-running stability of the clocks and the characteristics of the calibration channel are the parameters that determine the overall performance of the total system in terms of accuracy and precision. If the purpose of the comparison is to calibrate the time of the local device, which we are discussing here, then the delay through the channel must be known or derived, and any uncertainty in this delay will enter into the error budget for the overall calibration procedure.

There are three general methods that are commonly used to transmit time and frequency information, viz. ***one way time transfer***, ***two-way time transfer***, and ***the Common View (CV) method***. One way time transfer is the same as synchronizing the receiver clock to the satellite clock using the navigation signal, which we are already acquainted with. So, here we shall discuss the other two methods (Klepczynski, 1996; Levine, 2008; Miranian et al., 1991) with obvious relation to satellite-based transfers. We shall describe the advantages and limitations of the methods, including their uncertainty estimates. Schelatic layout of different time transfer methods is shown in Fig. 11.10.

11.3.3.1 Two-way time transfer

Two-way time transfer is the method involving two clocks and in which both the peer clocks transmit and receive time data sent by the other. The calibration value is derived from the delays observed in two opposite directions. We call the clock the "precision clock," with which the other clock at any other location is required to be synchronized, as the 'reference'. The other clock which needs to be synchronized with the reference is called the "user clock."

This method has the inherent assumption that, unlike one-way time transfer, where the user clock is a receive-only terminal, here both the clock units are able to communicate between them in a duplex manner. Moreover, it assumes that the time for a message to travel between the two stations is the same in both directions. However, the absolute time required to transmit the message from one end to the other is not

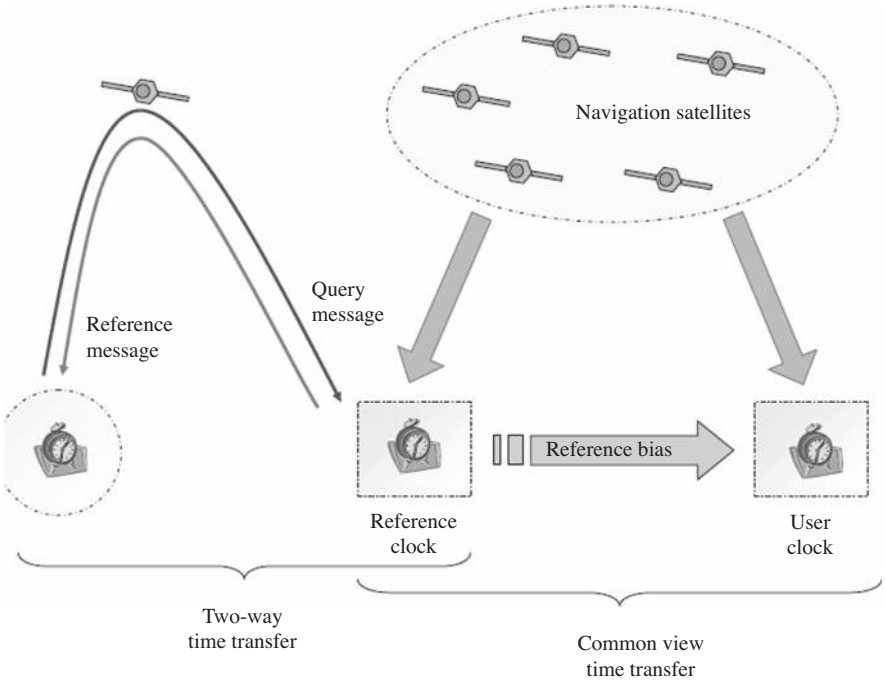

FIGURE 11.10

Different time transfer methods.

important, but should be considerably small, such that within the round-trip time, the characteristics of the clock do not change.

Let the user clock C_u have a positive bias of δt_{ur} with respect to the reference clock C_r. Now, to derive this delay, the user clock transmits a message at a time T_{us} toward the reference clock, with a time stamp in it. T_{us} is measured by the clock at the user station. Since this time is δt_{ur} ahead of the reference time, the true time at that instant in the reference clock was $T_{us} - \delta t_{ur}$.

Note, the subscript appears with the time T. The first suffix will either be "u" or "r," representing whether it is the user or the reference that is measuring it. The second represents whether it is during the sending or during the receiving process, and will be represented by "s" and "r" respectively. The message is received at the reference station at time T_{rr}, where T_{rr} is measured by the clock at the reference station. Since the reference clock is accurate, Trr is the true time. The time for the message movement from the user to the reference clock in terms of the reference clock is

$$\begin{aligned} \Delta_r &= T_{rr} - (T_{us} - \delta t_{ur}) \\ &= T_{rr} - T_{us} + \delta t_{ur} \end{aligned} \tag{11.10}$$

However, the measured time of message transfer, as obtained by using the local time of the receiving reference station and the time stamp marked on the message, is

$$\begin{aligned}\Delta_m &= T_{rr} - T_{us} \\ &= \Delta_r - \delta t_{ur}\end{aligned} \tag{11.11}$$

At any subsequent time, the reference station sends a message to the user station, also marked with a time stamp. It also sends D_m as measured at the reference along with it. This message is transmitted at time T_{rs} measured by the clock at the reference station and is received at the user station at time T_{ur}, measured by the clock at the latter station. Similarly, the true reference time and the measured time of travel are respectively

$$\nabla_r = T_{ur} - \delta t_{ur} - T_{rs} \tag{11.12}$$

and

$$\begin{aligned}\nabla_m &= T_{ur} - T_{rs} \\ &= \nabla_r + \delta t_{ur}\end{aligned} \tag{11.13}$$

However, the stations have the measured values only and need to derive the bias δt_{ur} from them. So, differencing Δ_m and D_m and halving them, we obtain

$$\begin{aligned}&\tfrac{1}{2}(+\nabla_m - \Delta_m) \\ &= \tfrac{1}{2}\left[+\left(T_{ur} - T_{rs}\right) - \left(T_{rr} - T_{us}\right)\right] \\ &= \tfrac{1}{2}\left(\nabla_r + \delta t_{ur} - \Delta_r + \delta t_{ur}\right) \\ &= \tfrac{1}{2}\left(2\delta t_{ur} + \nabla_r - \Delta_r\right) \\ &= \delta t_{ur} + \tfrac{1}{2}(\nabla_r - \Delta_r)\end{aligned} \tag{11.14}$$

If the path delays are symmetric, then $(\Delta_r - \nabla_r)$ is zero, and thus the user clock can obtain its own delay and can correct the same.

However, if the message takes different times for the forward and the reverse journey, and if the difference is ε, then the result becomes $\delta t_{ur} + \frac{1}{2}\varepsilon$, and it is necessary to eliminate or reduce this error to a minimum. In many cases, this error remains proportional to the absolute path delay, and in such cases, the effect of any asymmetry can be minimized by keeping the path delay itself small.

The protocol does not require any constraint relationship among the transmit times at the user and the reference. So, the reference clock may simply echo the message from the user station with a time stamp, or otherwise can reply to the received message at any later time. The delay between the receiving at the reference and its response does not affect the estimates provided that it is measured accurately and that both clocks are well behaved during this interval. Therefore, if we have a GNSS receiver at any definite location with the facility of communicating with other stations, then the accuracy of the clock derived at this station may be disseminated to all other user clocks, which thus enjoy almost similar precision even without requiring GNSS connectivity.

The role of the navigation system here is not in synchronizing the clocks but in providing accuracy and precision to one of them, such that it can behave as a reference. So, with this method, a reference station located within the service area of a satellite navigation system can provide precise timing to one that can even be beyond the service area or located at a place where the TDOP is constantly poor to provide a precision timing service. The calibration channel, through which the synchronization is obtained, may be any other communication channel. If the two clocks are far apart, this may be implemented through a duplex satellite channel where the propagation and the transponder delay remain almost the same for both the forward and reverse path. This is, however, achieved at the expense of the station being capable of duplex satellite communication with the reference. This mandatory requirement makes the hardware at the user stations more complicated and expensive than the one-way method. Moreover, the messages must maintain a prescribed format assigned a-priori, and no anonymous association is possible. So, two-way time transfer is possible only in closed groups.

This technique can be used in a differential positioning system like DGNSS or RTK, where the users fix their position and synchronize their clocks with respect to the remotely located reference stations. When the positions of the users are fixed, synchronization of the clocks at these two places removes one of the unknown parameters, the relative clock bias. With one of the unknowns being now alternatively estimated, it eases the estimation process and also reduces the requirement for visibility of satellites. The precise clock can be any independent precision clock, synchronized to the GNSS system time while the user clock is synchronized to the reference by this method. Another example of this is the application in Very Long Baseline Interferometry (VLBI), where remotely located receivers need synchronous clocks.

11.3.3.3 Common view (CV) time transfer

In the CV time Transfer techniques, the two clock sites require time transfer exchange measurements taken from a common GNSS satellite. It is the time transfer method in which several stations with their respective clocks, including the station with a reference clock, receive data from a common source over paths whose delays are approximately equal and then exchange data mutually to derive the calibration information.

Here, in this method, the time transmission from the navigation satellite is utilized. So, all the stations mentioned here are equipped with GNSS receivers. Further, their stations receive this timing signal and derive their respective clock bias with that of the satellite. One of the receivers of this timing signal may be a reference atomic clock, while the clocks at other locations in the CV are required to be synchronized with the reference. The term "*Common View*" itself suggests that in such a method, the path for the reference and for the users should have common characteristics in all respects.

On receiving the time signals transmitted from a single common satellite, each clock measures the time at which a particular signal arrives at its location using its

own clock. The time measured at the jth user clock will be

$$T_{uj} = T^s + \delta t^s_{uj} + d^s_{uj} \tag{11.15}$$

where u_j represents the j^{th} user station, T_{uj} is the measured time at the jth station, T^s is the transmit time at the satellite measured with the satellite clock, $\delta t^s_{uj}$is the bias of the clock at the j^{th} station with respect to this satellite clock, and $d^s_{uj}$is the path-traversing time taken by the signal to reach from the satellite to the j^{th} station. The stations then compare these measurements and use them to get their mutual timing bias, as described below.

The reference clock station keeping a highly precise time while the user station wants to achieve similar precision in timekeeping using a nominal clock. The reference clock receiver receives the same timing signals from the same satellite in the system. The reference station measures the receive time as

$$T_r = T^s + \delta t^s_r + d^s_r \tag{11.16}$$

where T_r is the measured time at the reference station in his own clock on receiving the satellite signal, T^s is the transmission time of the signal measured with the satellite clock, $\delta t^s_r$is the positive bias of the reference station's clock with respect to the satellite clock and d^s_r is the path delay between the satellite and the reference station. T^s can be derived from the time stamp marked on the message. Hence, the time difference can be obtained as

$$\begin{aligned} \Delta^s_r &= T_r - T^s \\ &= \delta t^s_r + d^s_r \end{aligned} \tag{11.17}$$

Similarly, differencing at the j^{th} user station provides us with

$$\begin{aligned} \Delta^s_{uj} &= T_{uj} - T^s \\ &= \delta t^s_{uj} + d^s_{uj} \end{aligned} \tag{11.18}$$

Note here that the transmission times T^s and the reception time Tr for the user and the reference, respectively, need not be the same. However, the satellite clock transmitting the time needs to be stable enough such that it does not drift considerably within this time. This difference derived at the reference clock receiver, that is, the reference bias, is communicated to the user station, and on further differencing these two derived differences, we get,

$$\begin{aligned} \Delta^s_{r\_uj} &= \Delta^s_r - \Delta^s_{uj} \\ &= \delta t^s_r + d^s_r - \delta t^s_{uj} - d^s_{uj} \\ &= \delta t^s_r - \delta t^s_{uj} + d^s_r - d^s_{uj} \end{aligned} \tag{11.19}$$

Now, if the one-way path delays from the transmitter to the two stations are equal, then both the path delays cancel out, and the difference becomes

$$\Delta^s_{r\_uj} = \delta t^s_r - \delta t^s_{uj} \tag{11.20}$$

So, the time bias between the user and the reference clocks can be computed without knowing anything about the source or the path delay. Any change in the path delay that occurs with time gets cancelled and does not affect the process to the extent that it remains common to the paths to the two stations. So, if one of the stations has a precise clock, the same precision may be exploited at the other station.

However, in practice, it is difficult to find such a situation such that the path delays to both locations are exactly equal. This problem can be eliminated if the receivers can obtain their precise range from the satellite. This enables the receivers to estimate the traversing time of the signal. This can be used in eqs. 11.17 and 11.18, to replace the d_r^s and d_{uj}^s values respectively in the left-hand side of the equation. As a result, the exact clock biases are obtained through these two equations at these two locations, both with respect to the satellite clock. So, when this information is exchanged, the user clock can derive its relative bias with respect to the reference clock and correct it.

This method may also be extended to even antipodal locations, that is, even without seeing the same set of satellites, if the satellite sources are all synchronized to a common reference system clock or their relative time skews are precisely known. This is true for satellite navigation.

Once the receiver clocks are synchronized, the user clock issues time markers in a definite format for use in different applications. 1 pulse per second (PPS) signals are used for precise timekeeping and time measurement. 1PPS is commonly used in standards laboratories to compare time and frequency sources at the highest level of precision. The pulses are aligned to integer seconds of GNSS system time or UTC within a precision of a few nanoseconds.

11.3.4 Applications in space service volume

Space service volume (SSV) of GNSS is a relatively new concept that refers to the region of space where GNSS signals can be used for positioning, navigation, and timing beyond the terrestrial service volume.

The GNSS was originally designed for terrestrial and near-terrestrial uses. Consequently, the navigation satellites transmit signals focused toward the Earth with the main lobes of the antennas also directed toward the Earth. GNSS satellites are in MEO or GEO orbits. Therefore, the signal from the navigation satellites fills the volume of space from its orbital sphere up to the Earth's surface, that is, the space below the satellite toward the Earth, enclosing the Earth and the surrounding area. Out of these, the space enclosed by the volume consisting of the Earth and the surrounding space up to a height of 3000 km comprises the terrestrial service volume.

However, the transmitted signal does not remain strictly confined to the terrestrial volume. A portion of the signal extends beyond the terrestrial volume into space. These signals can be utilized as opportunities for positioning beyond the Earth's surface. It is interesting to note that the signal does not remain enclosed within the volume below the orbital sphere of the navigation satellites but also spills out beyond it in space.

Therefore, the SSV is defined within the region of space between 3000 km to 36,000 km above the Earth's surface. That is, it comprises the outer sphere of the volume containing the navigation signals. SSV is divided into two distinct regions: lower SSV (3000–8000 km) and upper SSV (8000–36,000 km).

Currently, the satellites in LEO, GTO, HEO, GEO, etc., which are present in the SSV of the GNSS, carry receivers and utilize GNSS for their positioning in space. The main lobe signals are available in LEO, MEO, GEO, and in some cases in portions of HEO. These signals can be used for onboard position determination of these satellite orbits, provided the necessary number of satellites are visible.

Even beyond 36,000 km, interesting applications of SSV have been envisaged and implemented in the HEO and even in the trans-lunar orbits. The satellites beyond the GEO orbital heights also receive signals either from the direct lobes of the satellites across the Earth or from the side lobes of the satellite antennas. It is obvious, though, that the received signal strength is extremely low, and it needs highly sensitive receivers to utilize these signals for positioning purposes. Such use of the GNSS signals outside the terrestrial service volume has the direct benefits of precise positioning in space, which in turn provides better control, maneuvering, and navigating abilities to the satellites, even sometimes without the intervention of the ground control.

The benefits offered in the SSV applications are not without challenges. There are different constraining requirements for utilizing the GNSS in the SSV. One important aspect of them is handling very low power, as mentioned before. Under certain situations, the SSV receivers receive only an insignificant portion of the main transmission, resulting in very low power to work with. Therefore, these receivers need to be specialized with the capability of very low power acquisition. Constant research in this area has developed new algorithms that enable the receivers to acquire signals even at very low Carrier-to-Noise density ratio (C/N_0). Utilizing this capability, the receiver can continue positioning activities up to several times the normal terrestrial distance from the navigation satellites.

The other very important aspect is the reduced number of visible satellites. At greater height from the Earth's surface, although more numbers of satellites are visible, their look angles span more than 180 degree in elevation, requiring receiver antenna with wider beamwidth. In contrast, at heights beyond the sphere of the navigation satellite's orbit, the numbers of effective visible satellites drop. However, the current inception of the interoperable signal upon modernization of the different GNSS systems alleviates the issue to a certain extent. The receiver does not have to depend solely on one system and consequently has the freedom to choose from all the compatible satellites visible to it. So, even at extraterrestrial locations, the receiver can use measurements from a good number of satellites resulting in comparatively better dilution of precision (DOP).

The benefits of SSV are evident. Applications have been devised utilizing GNSS in lower orbit and high-altitude platforms. However, its usage is limited due to conditional challenges, as discussed in the previous section, like the poor DOP, less visibility, and feeble power. Despite these challenges, the benefits derived from

the SSV are enormous, and that drives different space-based applications to use the GNSS-based positioning in the SSV. The SSV, providing precise positioning capabilities in Earth's outer sphere and further in space, enables new mission concepts, such as GNSS-assisted lunar missions, agile and close colocation of satellites, reduced ground interceptions, lower mission costs, onboard autonomy, and operational robustness.

For low Earth orbit satellites, particularly remote sensing satellites, precise orbit determination is important for various reasons. These satellites revolve around the Earth at heights from 300 km to a few thousand kilometers. Those satellites orbiting in the SSV have better visibility of the navigation satellites than their terrestrial counterparts. But, at the same time, these satellites have high spatial dynamics due to their orbital speed and hence experience large Doppler. Due to their rapid change in constellation geometry, very agile receiver processing is required. The precise positions thus obtained help these satellites in better time tagging and geotagging of the data.

For the satellites in GEO, the MEO-based satellite constellation placed at lower altitudes and transmitting toward the Earth barely provides any signal. However, signals from the navigation satellites located on the other side of the Earth can be received at these locations. These satellites have main lobes of their antenna directed toward the Earth. Although the locations radially opposite to the navigation satellites and large areas around them are entirely shadowed. Some amount of radiation from the side lobes may also reach across the limb of the Earth to these GEO satellites. In such a situation, in addition to the very low reception of power, the number of visible satellites, however, is also very less. Therefore, such receivers need a highly sensitive reception system with strong onboard processing capabilities.

Many satellites in highly elliptical orbits (HEO) have their perigeal and near perigeal locus within the SSV. During these periods, when the GNSS signals are accessible, the satellite-based navigation services are availed for positioning and to fully utilize them for precision. For example, in the Magnetospheric Multiscale (MMS) satellite mission, which revolves around the Earth in the magnetosphere to identify and capture the time sequence of the magnetospheric reconnection process, GNSS plays a crucial role in its positioning and navigation. The MMS mission operates in HEOs and has reached nearly halfway to the Moon while at apogee, aided by the GNSS-based navigation. At these distances, the received signal power is about 20 dB below the typical power received on the Earth's surface. Hence, this requires advanced GNSS receivers capable of acquiring and tracking weak signals. GNSS has helped these four spacecraft executing formation flying to navigate autonomously, reducing the need for ground-based tracking and increasing mission efficiency. Further, the dual Proba-3 spacecraft, which also carry out formation flying in space in HEOs for the coronagraphy of the Sun, also use the GNSS over a certain portion of their orbital period for positioning that aids in their precision flying.

Now, here comes the question: how far can the GNSS signals be utilized beyond the GEO sphere? GNSS experts have suggested using the GNSS signals as a navigation aid for lunar missions. At the lunar distance, the cone angle of the typical

GNSS satellites in MEO is about 7.5°. Therefore, it is evident that the DOP provided by the satellites is extremely poor. The degraded accuracy due to the poor DOP is acceptable for en-route navigation of spacecrafts, unless it is executing any critical maneuvers. Added to this, the insignificant reception power, this proposition has no dearth of challenges for implementation. SSV applications, therefore, present an exciting opportunity for spacecraft operation with challenges still to overcome (Parker et al., 2018).

References

Acharya, R., Sivaraman, M. R., & Bandyopadhyay, K. (2004). Tomographic estimation of ionosphere over Indian region. In *2004 Proceedings of ADCOM, Ahmedabad, ACCS, 564-567*.

Allen, R. M., & Ziv, A. (2011). Application of real-time GPS to earthquake early warning. *Geophysical Research Letters, 38*(16). doi:10.1029/2011GL047947.

Braff, R., Powell, J. D., & Dorfler, J. D. (1996). Applications of the GPS to air traffic control 1. *Global Positioning System: Theory and Applications*. AIAA.

Brown, A., & Ganguly, S. (2001). Ionospheric tomography: Issues, sensitivities, and uniqueness. *Radio Science, 36*(4), 745–755. doi:10.1029/1999rs002414.

Camps, A. (2008). A hybrid radiometer/GPS reflectometer to improve sea surface salinity estimates from space. *Microwave radiometry and remote sensing of environment*. MICRORAD 2008, Florence, Italy.

Cohen, C. E. (1996). Attitude determination II. *Global positioning systems: Theory and applications*. AIAA.

Cohen, C.E. (1992). *Attitude Determination using GPS*. Ph.D Thesis, Stanford University. Available at: https://web.stanford.edu/group/scpnt/gpslab/pubs/theses/ClarkCohenThesis92.pdf. (Retrieved on 17th February 2014).

Cohen, C. E., & Parkinson, B. W. (1992). Institute of navigation aircraft applications of GPS-based attitude determination: Test flights on a Piper Dakota. In *1992 Proceedings of ION-GPS-92, Institute of Navigation, San Diego, CA, USA*.

Parkinson, B. W., O'Conner, M. L., & Fitzgibbon, K. T. (1996). Aircraft automatic approach and landing using GPS I. *Global positioning systems: Theory and applications*. AIAA.

El-Rabbani (2006). Introduction to GPS (2nd ed.), Artech House, Boston, MA, USA.

Eschenbach. (1996). GPS applications in general aviation II. *Global positioning systems: Theory and applications*. AIAA.

Garrison, J. L., Voo, J. K., Yueh, S. H., Grant, M. S., Fore, A. G., & Haase, J. S. (2011). Estimation of sea surface roughness effects in microwave radiometric measurements of salinity using reflected global navigation satellite system signals. *IEEE Geoscience and Remote Sensing Letters, 8*(6), 1170–1174. doi:10.1109/LGRS.2011.2159323.

Hansen, A. (2002) *Tomographic estimation of the ionosphere using terrestrial GPS Sensors*. Ph. D Thesis, Stanford University, Available at http://web.stanford.edu/group/scpnt/gpslab/pubs/theses/AndrewHansenThesis02.pdf. (Retrieved on 22 May, 2013).

Klepczynski, W. J. (1996). GPS for precise Time and time interval measurements II. *Global positioning systems: Theory and applications*. AIAA.

Larson, K. M. (1996). Geodesy II. *Global positioning systems: Theory and applications*. AIAA.
Leick, A. (1995). *GPS satellite surveying* (2nd ed). John Wiley and Sons.
Levine, J. (2008). A review of time and frequency transfer methods. *Metrologia, 45*(6), S162. doi:10.1088/0026-1394/45/6/s22.
Lightsey, E. G. (1996). Spacecraft attitude control using GPS carrier phase II. *Global positioning systems: Theory and applications*. AIAA.
Miranian, M., & Klepczynski, W. J. (1991). Time Transfer via GPS at USN0. In *1991 Proceedings of the 4th international technical meeting of the satellite division of the institute of navigation (ION GPS)*.
Parker, J. J. K., Bauer, F. H., Ashman, B. W., Miller, J. J., Enderle, W., & Blonski, D. (2018). The multi-GNSS space service volume. In *Proceedings of the international astronautical congress, IAC*. International Astronautical Federation, IAF, Bremen, Germany. http://conference.researchbib.com/?action=viewEventDetails&eventid=17342&uid=re90b8. 2018.
Parkinson, J. J., Spilker, B. W., Global positioning system: Theory and applications. Vol I & II. (1996).
Sennott, J., Ahn, I. S., & Pietraszewski, D. (1996). Marine applications II. *Global positioning systems: Theory and applications*. AIAA.
Torge, G. (2001). *Geodesy* (3rd ed.). Water de Gruyter, New York, USA.
Wikipedia. (2024). Location-based services Retrieved from: https://en.wikipedia.org/wiki/Location-based_service. (Retrieved on 23 December, 2024).

Appendix 1

Satellite Navigation Systems

There are many major primary satellite navigation systems as of today. Some of them are global, while others are regional. Many more new systems are about to come up very soon. The existing operational systems are:

1. Global Positioning System (GPS) of the United States;
2. Global Navigation Satellite System (GLONASS) of Russia;
3. GALILEO of the European Union;
4. Quazi Zenith Satellite System (QZSS) of Japan
5. BeiDou of China; and
6. Navigation using Indian Constellation (NavIC) of India

Out of these, NavIC is a regional systems, while QZSS is a regional complementary system to GPS. All other systems are global. The important features of a few of these systems are mentioned below.

A1.1 Global Positioning System

The GPS was developed by the United States a part of the satellite-based military navigation system. The US Department of Defense (DoD) planned to use the constellation of artificial satellites and find the position of any location high accuracy through radio-based ranging. Accordingly, the satellites started being launched from 1978 under the NavStar program. The system acquired its initial operational capability in 1993 while the full operational capability was achieved in 1995.

GPS, like any typical system, has the architectural components that can be divided into three segments, viz. ground segment, space segment, and the user segment, as mentioned in Chapter 2 (El-Rabbani, 2006; Parkinson & Jr, 1996).

A1.1.1 Ground Segment

The GPS ground segment consists of the ground monitoring stations distributed across the world. There are six monitoring stations in Hawaii and Kwajalein in the Pacific Ocean, Diego Garcia in the Indian Ocean, Ascension Island, and Cape Canaveral, Florida, in the Atlantic Ocean. One master station is located in Colorado Springs, Colorado. At these stations, signals from satellites are monitored and their orbits tracked. These are used to predict the near-future satellite orbit and correct their clock as described in Chapter 2. The uplink antennas are collocated with most of the monitoring stations.

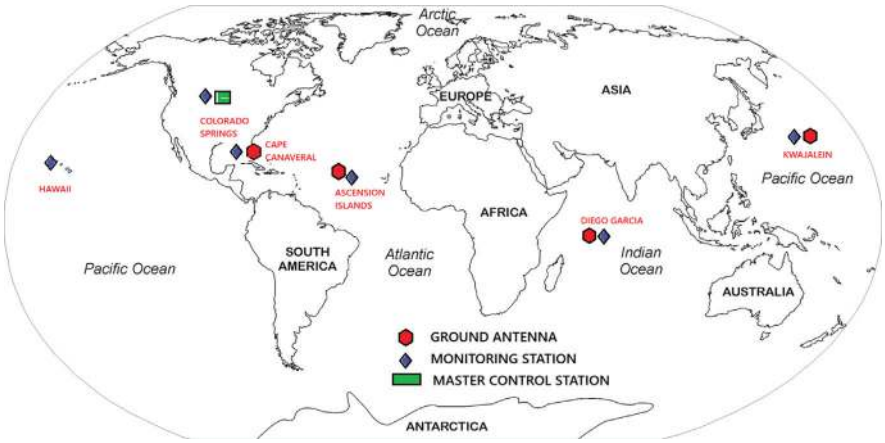

FIGURE A1.1

Ground Stations of GPS.

A1.1.2 Space Segment

The space segment of GPS consists of the satellite constellation. This constellation, placed in MEO, has 24 satellites in almost circular orbits. The satellites are distributed in six equispaced orbital planes with four satellites in one plane, which are unevenly phased as shown in Fig. A1.1. The semimajor axis of the orbits is about 26,500 km, with almost zero eccentricity. This keeps the satellites about 20,000 km above the Earth's surface. The corresponding period is 11 h 58 min. The inclination of 55 degrees makes the satellites visible overhead up to 55 degrees on both Northern and Southern Hemispheres of the Earth. The constellation is designed in a way that users across the globe can see at least four satellites at all times, with few exceptions. Typically six to eight satellites are visible at a time.

The most recent set of satellites has the provisions of laser ranging for better ephemeris predictions, and also has a search and rescue payload along with navigation.

A1.1.3 User Segment

Users employ the receive-only terminals to receive the navigation data transmitted by the satellites and compute their position. Receivers of different capabilities and accuracies are used. The dual-frequency receivers with highly stable clocks are costly, whereas the single-frequency receivers with less accurate clocks are available at low prices. Receivers with differential capabilities are used for civilian precise applications like surveying.

A1.1.4 GPS Services

GPS provides two categories of services, viz., precise positioning services (PPS) and standard positioning services (SPS). The PPS is a high-accuracy, single-receiver GPS positioning service available only to the US military and other selected agencies. The SPS provides uninterrupted positioning service to any civilian user on a global scale; however it is less accurate than the PPS.

A1.1.5 GPS Signal Structure

A1.1.5.1 Carrier Signal

GPS employs a sinusoidal signal with frequencies 1575.42 and 1227.60 MHz as its two carriers. These signals are designated as L1 and L2, respectively. The satellites transmit the same navigation signal at these two frequencies. They are coherently selected multiples of a 10.23 MHz master clock, derived from an atomic standard.

GPS uses code division multiplexing that enables its different satellites to use the same carrier frequency simultaneously without interference. Each carrier frequency is BPSK modulated by a "spreading code," which remains multiplied over the navigation data as described in Chapter 3. These ranging codes are different for different satellites and are orthogonal to each other.

A1.1.6 Ranging Code

GPS uses pseudorandom orthogonal Gold codes for ranging with suitable correlation characteristics. There are two kinds of such codes. The C/A code of length 1023 chips is issued at a 1.023 Mchips/s rate. It is used for the standard positioning service. The other code is called the P code. It is of much larger length and has a rate of 10.23 Mchips/s. L1 is modulated with both P code and C/A code in phase quadrature, while L2 is modulated only by the P code. The faster and longer P codes result in better accuracy and reliability. It is accessible only to the PPS service users, whereas common SPS users can access only the C/A codes with lesser accuracy.

At times P code is encrypted into a secure antispoof Y code, also called the P(Y) code. The C/A Code & P code epochs & navigation data are perfectly synchronized. The salient features of C/A and P codes are mentioned below.

A1.1.6.1 C/A Code

- The C/A ranging codes are meant for civil users.
- These are short codes with a period of 1023 bits.
- The chip rate is 1.023 MHz, so the sequence is of 1 ms duration.
- Short code permits rapid acquisition.
- C/A Codes are Gold codes formed by the products of select equal-period 1023 bits PN codes.

A1.1.6.2 P code

- It is meant for use by DoD authorized users only.
- It is a long code.
- Chip rate is 10.23 MHz, that is, 10 times faster than C/A.
- It is a product of two pseudorandom codes, X_1 and X_2.
- X_1 has a sequence of 15,345,000 chips, and X_2 has a sequence of 15,345,037 chips.
- The P code has a period of around 38 weeks.
- In GPS, the P code is reset every Saturday/Sunday midnight, so that the period of truncated sequence is one week.
- The P code is difficult to acquire without acquisition aids.

A1.1.7 Data

The GPS satellites transmit navigation and other data, like bias and health data, formatted in a definite manner in a contiguous fashion. A description of the navigation data structure is given below:

- It consists of ephemeris data, clock bias, almanac, and health data.
- Subframes 1, 2, and 3 are specific to transmitting satellite, and 4 and 5 are common to all satellites.

The GPS navigation data is a bipolar NRZ signal issuing bits at the rate of 50 bits per second in a fixed framed format. The satellites transmit one data frame of 1500 bits in 30 s. Each frame is divided into five subframes of 6 s each. Out of these, subframes 1, 2, and 3 are specific to the transmitting satellite. Each subframe is of length 300 bits and starts with a definite preamble followed by data and parity bits.

Every subframe consists of few words. Words 1 and 2 have the same format in every subframe. Word 1 is the telemetry word. Its first 8 bits constitute the preamble 10,001,011 ($8B_H$), and the rest is the telemetry data. Word 2 is the handover word and contains the truncated Z count that indicates the time of the end of the subframe in quantum of 1.5 s. The rest of the words are navigation data.

The navigation data of subframes 1,2, and 3 are specific to the transmitting satellite while those of subframes 4 and 5 are common for all satellites. Subframe 1 contains 2nd order polynomial coefficients to calculate satellite clock offset in addition to its time-of-applicability. Subframes 2 and 3 contain the ephemeris, consisting of the orbital parameters. The ephemeris time-of-applicability is also transmitted along with it. The same data content continues for consecutive frames until a new update. New data sets of subframes 1, 2, and 3 usually begin to be transmitted precisely at the start of the hour.

Subframes 4 and 5 contain the almanac data of all satellites and some related health and configuration data. Due to the large volume of the data, it is subcommutated in a contiguous manner as the last two subframes in every frame. It takes 25 such frames to complete one set of this data. So, the data repeats after 25 consecutive frames, which

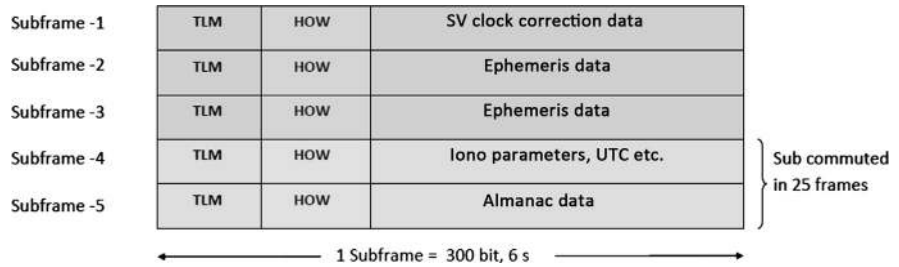

FIGURE A1.2

GPS navigation data format.

take 12.5 min for the same. The same data is transmitted until the next upload (Global Positioning System Directorate, 2012; Kaplan & Hegarty, 2006; Misra & Enge, 2001). The structure of the GPS data is shown in Fig. A1.2.

Elements of the navigation data

- *TLM*: Telemetry data
- *HOW*: Handover word containing Z count
- *CC*: Clock correction data
- *EPM*: Ephemeris parameters
- *IONO*: Ionospheric correction data (Klobuchar coefficients)
- *UTC*: Universal coordinated time
- *ALM*: Almanac data

Navigation data parameters like the ephemeris, almanacs, clock-offset coefficients, etc., are updated every 2 h. The beginning of transmitting new data is called a cutover, which occurs at hour boundaries. Coefficients for ionospheric delay change at a slower rate. These data, however, are uploaded by the ground stations in advance, once every 24 h. The coordinate datum used by the GPS is WGS-84 (Parkinson & Spilker 1996).

A1.1.8 Modernization of GPS

In order to meet the growing demands of the users in both segments of the services, major upgradations have been done to improve the GPS service quality. Upgradation has been done in both the GPS space and control segments as well as in its signal structure. New signals have been introduced, with new features to improve the performance. The new signals are serving both civilian and military services (http://www.gps.gov).

In addition to establishing monitoring stations outside USA, one important step forward for the modernization of the GPS is to switch from the fixed frame-based data format to the flexible message type. This will enable it to transmit different navigation parameters in the data on a priority basis at variable intervals (Kovach et al., 2013).

The new signals include the L2C, L5, and L1C. The legacy civil signal L1 C/A will also be continued, making a total of four signals for civilian use.

L2C is the second civilian GPS signal, which, when combined with L1 C/A, enables ionospheric correction. It also has a dedicated channel for codeless tracking. Therefore, it will deliver faster signal acquisition, enhanced reliability, and greater operating range. The higher effective transition power of L2C also makes it easier to receive under foliage and indoor conditions.

L5 is the third civilian GPS signal, primarily conceived for the safety-of-life transportation and other high-performance applications. In addition to higher power, it offers greater bandwidth for improved immunity to jamming and an advanced signal design, including multiple message types and forward error correction.

L1C is the fourth civilian GPS signal, designed to enable interoperability between GPS and other systems. It has both the data and pilot channels. The pilot channel uses TMBOC modulation of BOC(6,1) and BOC(1.1) for interoperability, while the data channel uses normal BOC modulation. The design also includes forward error correction in addition to the multiplexed binary offset carrier modulation. This has improved mobile GPS reception in cities and other challenging environments.

More than one civil frequency in GPS will obviate the need for a codeless or semi-codeless approach for ionospheric error corrections.

As an endeavor to improve the performance, the satellite slots in the space segment have been expanded. The GPS constellation is a mix of new and legacy satellites. There are still satellites from Block II-A with advanced technology compared to the Block II satellites. Some of them, whose life has expired, have been replaced by the Block II-R. Block II-R(M) satellites have been put in place, which replaced the older ones and also have modernized the signal L2C. The follow-on series of satellites in Block II-F carries both L2C and L5 signals with a longer life expectancy. The most recent of the satellites, comprising Block III /IIIF, are already in space and consist of all three civilian signals, including L1C. They also carry the search and rescue payload (Kovach et al., 2013).

A1.2 Global'naya Navigatsionnaya Sputnikovaya Sistema

The Global'naya Navigatsionnaya Sputnikovaya Sistema (GLONASS) was also developed as a military navigation system by the then USSR in the early part of the 1970s.

The GLONASS space segment is comprised of 28 satellites, out of which 24 are in operational phase, 3 are spares, and 1 is in in-flight test phase. The satellites are distributed in three orbital planes separated by 120 degrees, with eight evenly spaced satellites in each plane. Different frequency channels are allocated to each of these satellites with an appropriate frequency reuse plan. The orbits of these satellites have a radius of about 25,500 Km. This is slightly less than that of the GPS, and consequently, the period of rotation is 11 h 15 min, which is also obviously less than GPS. The inclination of the orbital planes is 64.8 degrees. This increased inclination

helps in obtaining the satellites evenly distributed across the sky for even places at higher latitudes.

Starting the development in 1976, the launching of the GLONASS satellites began from 1982. The system was formally declared operational in 1993, while in December 1995, the full constellation was achieved. But, due to no further launches, the system was left with only six operational satellites in 2001. However, GLONASS recovered from this stage very quickly, and in October 2011, the full constellation was again restored. Apart from the first generation satellites, the active satellites now have representations from both the second and third generations. The second generation satellites are of type GLONASS-M with increased lifetime. The current version of the satellites is of type GLONASS-K and K2 series, which has reduced mass and hence further improved lifetime.

The ground stations for monitoring the GLONASS satellites are almost entirely located within the former USSR. The System Control Centre (SCC) is at Krasnoznamensk, and the Central Clock is located at Schelkovo, near Moscow. The network of five Telemetry, Tracking and Command (TT&C) stations is at Schelkovo, Komsomoisk, St. Petersburg, Ussuriysk and Yenisseisk. Some of these stations also have the Laser Ranging capability. Although most of the monitoring stations are all within the Russian territory, new stations are being installed outside this region, in Brazil (GPS World, 2013) and South Africa (GPS World, 2017).

GLONASS offers both standard precision and high precision services for civilians and the military, respectively. So, the GLONASS satellites transmit two types of signal, viz. the standard precision (S) signal and the high precision (P) signal.

S signals use the direct sequence spread spectrum (DSSS) technique with a single ranging code at a rate of 0.511 Mcps. Each satellite transmits on a different frequency using a 15-channel frequency division multiple access (FDMA). The carrier frequencies span either side from 1602.0 MHz (L1) and are given by GLONASS (2005).

$$f1(n) = 1602\,\text{MHz} + n \times 0.5625\,\text{MHz}.$$

where, n represents the index and n = −7,−6,−5, …0, …, 6, 7. These signals are then BPSK-modulated and transmitted using right-handed circular polarization (RHCP).

P signal uses the same DSSS with ranging codes 5.11 Mcps. It is transmitted in FDMA in the L1 band signals with the same center frequencies but with phase orthogonality. It is also broadcasted in L2, with the center frequency f2, where,

$$f2(n) = 1246\,\text{MHz} + n \times 0.4375\,\text{MHz}.$$

Aiming to provide better accuracy, multipath resistance, and especially, greater interoperability with other GNSS Systems, new GLONASS satellites transmit CDMA signals in addition to the traditional FDMA. GLONASS CDMA open signals L1OC and L2OC are transmitted at frequencies around 1600 MHz and 1248 MHz. and are BPSK modulated. The corresponding restricted signals are in the same frequencies but in phase quadrature and use BOC modulation. The GLONASS L3 signal is centered at

1202 MHz. The open L5 signal is also available at 1176.45 MHz, the same frequency as the Galileo/BeiDou signal E5b. The modulation is BPSK for both data and pilot with chip rate of 10.23 MHz. These bands are especially suitable for safety-of-life applications because no other users are allowed to interfere with their signals.

The signal uses a truncated Kasami code of length 10230 transmitted with a period of 1 ms. The navigation data frames are of 1500 bits transmitted at 50 bits per second rate. Each frame carries 15 strings of data of 100 bits each. 5 such frames constitute a superframe. The ephemerides are updated every 30 minutes. GLONASS uses a coordinate datum named "PZ-90.11" in contrast to the GPS's WGS-84.

A1.3 GALILEO

GALILEO is the global primary satellite navigation system by the European Union, a project managed by the European Commission with support from the European Space Agency. In addition, this system is also compatible and interoperable with GPS.

With the endeavor for such a navigation system starting in around 1999, the Galileo project was supposed to be completed in three phases. However, unlike GPS and GLONASS, this was fully controlled by the civilian authority from its beginning. The first phase for characterizing the critical technologies for this system was completed with the GIOVE-A and GIOVE-B experimental satellites, launched in 2005 and 2008, respectively. The launching of Galileo satellites began in 2011. The full operational capability with initial services was available from December 2016.

In addition to the typical navigation services, namely the open service (OS) and public regulated service (PRS), GALILEO will also offer commercial and search and rescue services.

Galileo is designed for 30 satellites in 3 orbital planes. The active constellation comprises 24 satellites, including 6 spare satellites. The orbital radius is about 30,000 km, that is, at about 24,000 km above the Earth's surface. The corresponding period of revolution is 14 h 22 min with the orbital inclination of 56 degrees. Currently, there are 26 operational satellites in orbit with 2 other satellites being used for search and rescue purposes. Galileo used the L1 (1559–1591 MHz) and the L5 (1164–1300 MHz) frequencies for the purpose of code division multiplexing access (CDMA) mode and with both BPSK and BOC modulation (Margaria et al., 2007; Shivaramaiah & Dempster, 2009).

The Galileo ground segment is a vast and intricate system comprising two Galileo control centres (GCC) located in Italy (GCC-I) and Germany (GCC-D), ensuring redundancy. There are also two Galileo security monitoring centres (GSMC) based in Spain (GSMC-E) and France (GSMC-F). A global network of uplink (ULS) and Galileo sensor stations (GSS) provides provisions for round-the-clock data collection and uploading. In addition, the Galileo data dissemination network (GDDN), a dedicated network controlled and managed end-to-end by the Galileo program, which gives continuous availability. There are seven external entities (EE), including the Galileo service centre (GSC) for service monitoring and the return link service

provider (RLSP), which supports Galileo's search and rescue (SAR) service, connected via the external data distribution network (EDDN) (Upgrading Galileo, 2024).

The free OS provides positioning and time information intended mainly for high-volume satellite navigation applications. The commercial service (CS) for the development of applications for professional or commercial use by means of improved performance and data with greater added value than those obtained through the OS.

The PRS is restricted to government-authorized users for sensitive applications that require a high level of service continuity. The PRS uses strong, encrypted signals.

The search and rescue support service (SAR) works by detecting distress signals transmitted by beacons, locating these beacons, and relaying messages to them.

References

El-Rabbani. (2006). *Introduction to GPS* (2nd ed). Artech House.

Global Positioning System Directorate GPS. (2012). *Space segment/navigation user interfaces: IS-GPS-200G*. Global Positioning System Directorate.

GPS World, 2013. First GLONASS Station Outside Russia Opens in Brazil. Available at: https://www.gpsworld.com/first-glonass-station-outside-russia-opens-brazil/. Accessed on 10.01.2025.

GPS World, 2017. GLONASS ground stations go live in South Africa. Available at: https://www.gpsworld.com/glonass-ground-station-goes-live-in-south-africa/. Accessed on: 12.01.2025

Kaplan, E. D., & Hegarty, C. J. (2006). *Understanding GPS principles and applications* (2nd ed). Artech House.

Kovach, K., Haddad, R., & Chaudhri, G. (2013). LNAV Vs. CNAV: More than Just NICE Improvements, ION-gnss+—2013 . Nashville.

Margaria, D., Dovis, F., Mulassano, P., (2007). An Innovative Data Demodulation Technique for Galileo AltBOC Receivers, Journal of Global Positioning system, 6(1), 89-96.

Misra, P., & Enge, P. (2001). *Global positioning system: Signals, measurements and performance*. Ganga Jamuna Press.

Parkinson, B. W. (1996). *Global positioning systems, theory and applications*. AIAA.

Shivaramaiah, N. C., & Dempster, A. G. (2009). *The Galileo E5 AltBOC: Understanding the signal structure, IGNSS symposium 2009—Australia*. International Global Navigation Satellite Systems Society.

Upgrading Galileo, 2024. Inside GNSS, Available at: https://insidegnss.com/working-papers-upgrading-galileo/. Retrieved on 12 January, 2025.

Index

Page numbers followed by "*f*" and "*t*" indicate, figures and tables respectively.

F

G

H

I

J

S

T

U

V

W

Understanding Satellite Navigation

Second Edition

Rajat Acharaya

Understanding Satellite Navigation, Second Edition presents the foundational principles of satellite navigation technology with the bare minimum of mathematics and without resorting to complex equations. By emphasizing first principles, the book guides readers through each concept using practical demonstrations and fully worked examples, allowing theory to emerge organically. A comprehensive suite of MATLAB simulations illuminates how signals and systems respond to different configurations, transforming abstract ideas into visible, interactive models. Implementation strategies and real-world applications are woven throughout, alongside in-depth treatments of special topics such as Space Weather, the Kalman Filter, and ionospheric dynamics.

New in This Edition: compatibility and interoperability of GNSS systems, reflecting the modern trend of integrating multiple constellations for enhanced performance; analysis of impairments like jamming and spoofing, addressing integrity requirements for critical applications, exploration of Space Service Volume applications, anticipating future uses beyond Earth's surface; and detailed examination of space weather effects on GNSS, covering macro- and mesoscale variations

Key Features

- Lucidly explains the fundamentals of satellite navigation systems, using MATLAB as a visualization and problem-solving tool
- Worked-out numerical problems are provided to aid practical understanding
- Online support provides MATLAB scripts for simulation exercises and MATLAB-based solutions, standard algorithms, and PowerPoint slides

About the Author

Dr. Rajat Acharya is a Senior Scientist at the Space Applications Centre, a key unit of the Indian Space Research Organisation (ISRO). With over two decades of involvement in India's satellite navigation programs—GAGAN and NavIC—he has significant contributions in ionospheric modelling and space weather research. Dr. Acharya serves as Course Director for GNSS and SATCOM at the UN-affiliated Centre for Space Science and Technology Education in Asia and the Pacific (CSSTEAP). He has also been a Visiting Professor at Gujarat University, where he taught postgraduate courses in Geo-informatics and Satellite Navigation. Dr. Rajat Acharya regularly teaches Space Weather at the postgraduate level and has written extensively, authoring other popular books on the subject. He also represented India as Co-Chair of Working Group-C during the sessions of the International Committee on Global Navigation Satellite Systems (ICG).

ELSEVIER

ACADEMIC PRESS
An imprint of Elsevier
shop.elsevier.com

ISBN 978-0-443-36432-7